

2013 RSNA (Filtered Schedule)

**Sunday, December 01, 2013**

10:30-12:00 PM • **VSPD11** • Room: S100AB • Pediatric Radiology Series: Pediatric Neuroimaging I  
01:30-06:00 PM • **VSIO11** • Room: S405AB • Interventional Oncology Series: Controversies and Emerging Questions in the Management of Renal Tumors  
02:00-03:30 PM • **VSPD12** • Room: S102AB • Pediatric Radiology Series: Pediatric Musculoskeletal

**Monday, December 02, 2013**

08:30-12:00 PM • **VSBR21** • Arie Crown Theater • Breast Series: Breast MR Imaging  
08:30-12:00 PM • **VSER21** • Room: E350 • Emergency Radiology Series: Advanced Concepts in Imaging of Trauma  
08:30-12:00 PM • **VSGI21** • Room: N227 • Gastrointestinal Series: Emerging Issues in Abdominal CT  
08:30-12:00 PM • **VSIN21** • Room: S404CD • Radiology Informatics Series: Mobile Computing Devices  
08:30-12:00 PM • **VSIR21** • Room: E352 • Interventional Radiology Series: Peripheral and Visceral Occlusive Disease  
08:30-12:00 PM • **VSMK21** • Room: E451B • Musculoskeletal Radiology Series: Knee Imaging  
08:30-12:00 PM • **VSNM21** • Room: S505AB • Nuclear Medicine Series: Assessment of Cancer Treatment Response: Updates  
08:30-12:00 PM • **VSNR21** • Room: N230 • Neuroradiology Series: Spine  
08:30-12:00 PM • **VSPD21** • Room: S102AB • Pediatric Radiology Series: Fetal - Neonatal Imaging  
01:30-06:00 PM • **VSIO21** • Room: S405AB • Interventional Oncology Series: Hepatocellular Carcinoma

**Tuesday, December 03, 2013**

08:30-12:00 PM • **VSBR31** • Arie Crown Theater • Breast Series: Emerging Technologies in Breast Imaging  
08:30-12:00 PM • **VSER31** • Room: E352 • Emergency Radiology Series: Leveraging Technology for State-of-the-Art Practice  
08:30-12:00 PM • **VSGI31** • Room: N230 • Gastrointestinal Series: Pancreas - Inflammation and Neoplasm  
08:30-12:00 PM • **VSGU31** • Room: N228 • Genitourinary Series: Prostate Cancer 2013-Review of the Disease and the Role of MR in Staging and Surveillance  
08:30-12:00 PM • **VSIN31** • Room: S502AB • Radiology Informatics Series: Natural Language Processing: Extracting Information from Text Radiology Reports ...  
08:30-12:00 PM • **VSIR31** • Room: E351 • Interventional Radiology Series: Venous Disease  
08:30-12:00 PM • **VSMK31** • Room: E451B • Musculoskeletal Radiology Series: Ultrasound  
08:30-12:00 PM • **VSNM31** • Room: S505AB • Nuclear Medicine Series: Non-FDG PET Radiotracers in Oncology  
08:30-12:00 PM • **VSNR31** • Room: N227 • Neuroradiology Series: Brain Tumors  
08:30-12:00 PM • **VSPD31** • Room: S102AB • Pediatric Radiology Series: Chest/Cardiovascular Imaging I  
01:30-06:00 PM • **VSIO31** • Room: S405AB • Interventional Oncology Series: Lung  
03:00-06:00 PM • **VSPD32** • Room: S102AB • Pediatric Radiology Series: Advanced Pediatric Abdominal Imaging

**Wednesday, December 04, 2013**

08:30-12:00 PM • **VSCA41** • Room: S502AB • Cardiac Radiology Series: Transcatheter Aortic Valve Replacement (TAVR)  
08:30-12:00 PM • **VSIR41** • Room: E352 • Interventional Radiology Series: Embolotherapy  
08:30-12:00 PM • **VSNR41** • Room: E451B • Neuroradiology Series: Stroke  
01:30-06:00 PM • **VSIO41** • Room: S405AB • Interventional Oncology Series: Progress, Challenges and Opportunities

**Thursday, December 05, 2013**

08:30-12:00 PM • **VSCA51** • Room: S404CD • Cardiac Radiology Series: Cardiac Dual Energy CT  
08:30-12:00 PM • **VSCH51** • Room: E351 • Chest Series: Hot Topics in Chest Imaging: Emerging Technologies and Clinical Applications  
08:30-12:00 PM • **VSIR51** • Room: E352 • Interventional Radiology Series: Non-Vascular Interventions  
08:30-12:00 PM • **VSMK51** • Room: E451B • Musculoskeletal Radiology Series: Pelvis and Hip Imaging  
08:30-12:00 PM • **VVA51** • Room: S502AB • Vascular Imaging Series: CT Angiography-New Techniques and Their Application  
01:30-06:00 PM • **VSIO51** • Room: S405AB • Interventional Oncology Series: Liver Metastases and Bone

**Friday, December 06, 2013**

08:30-12:00 PM • **VSIR61** • Room: E451A • Interventional Radiology Series: Top 5 Complications in Interventional Oncology - Avoidance, Recognition and M...  
08:30-12:00 PM • **VSMK61** • Room: N228 • Musculoskeletal Radiology Series: Elbow, Hand and Wrist Imaging  
08:30-12:00 PM • **VVA61** • Room: E352 • Vascular Imaging Series: MR Angiography-Principles and Technique Optimization

**Pediatric Radiology Series: Pediatric Neuroimaging I**

**Sunday, 10:30 AM - 12:00 PM • S100AB**

PD MR NR

[Back to Top](#)

**VSPD11** • AMA PRA Category 1 Credit™:3.75 • ARRT Category A+ Credit:4

**Moderator**  
**Marvin D Nelson**, MD  
**Moderator**  
**Sanjay P Prabhu**, MBBS

**VSPD11-01 • MR Imaging of the Neonatal Brain**

**Marvin D Nelson** MD (Presenter)

**LEARNING OBJECTIVES**

1) To review the common adversities and reactions to such in the fetal and neonatal brain. 2) To demonstrate the use of various imaging techniques for assessing acquired fetal and neonatal brain lesions. 3) To highlight the importance of the placenta on normal brain development.

**VSPD11-02 • Impaired Preoperative Global and Regional Cerebral Perfusion in Newborns with Complex Congenital Heart Disease**

**Usha D Nagaraj** MD (Presenter) ; **Iordanis Evangelou** DPhil ; **Mary Donofrio** ; **Gilbert Vezina** MD ; **Catherine Limperopoulos** PhD

**PURPOSE**

To compare global and regional cerebral perfusion in neonates with congenital heart disease (CHD) versus healthy controls using arterial spin labelling (ASL) MRI.

#### METHOD AND MATERIALS

ASL is a non-invasive technique for evaluating cerebral perfusion without the use of an exogenous contrast agent. We performed brain MRIs in 73 newborns (30 with complex CHD, 43 controls) prior to open heart surgery on a 3T scanner. 3D FSE Pseudo-continuous ASL sequence was utilized. Post-acquisition image processing was undertaken on a Linux workstation using FSL software. All cases were reviewed by a board certified radiologist (UN) who was blinded to clinical parameters and case/control status. Mean whole brain cerebral blood flow (CBF) was calculated using the scanner software and recorded in mL/100g/min. CBF ASL images were linearly co-registered to the axial T2 images for anatomic delineation and selection of regions of interest to further evaluate regional blood flow using ITK-SNAP software. Areas studied included the frontal white matter, posterior white matter, thalami and basal ganglia.

#### RESULTS

Mean gestational age at MRI of the neonates studied was 40.9 weeks. Mean birth weight in reported neonates was 3174 grams. Affected newborns represented a variety of CHD diagnoses including hypoplastic left heart syndrome, tetralogy of Fallot, transposition of the great vessels, and ventricular septal defects. Average whole brain CBF in the controls (20.1 +/-4.6 mL/100g/min,) was significantly higher than in the newborns with CHD (17.4 +/- 4.1 mL/100g/min, p=0.01). Average regional perfusion in the occipital white matter of the controls (13.9 +/- 5.1 mL/100g/min) was also significantly higher than in the patients with CHD (11.3 +/- 3.8 mL/100g/min, p=0.02). Regional CBF in the frontal white matter, thalamus and basal ganglia did not demonstrate a statistically significant difference between the controls and CHD newborns.

#### CONCLUSION

ASL MRI demonstrates differences in cerebral perfusion between newborns with CHD versus normal healthy controls. Our data suggests that newborns with CHD may have decreased whole brain perfusion and a regional vulnerability in the occipital white matter prior to open heart surgery.

#### CLINICAL RELEVANCE/APPLICATION

ASL MRI is a promising non-invasive tool for evaluating changes in cerebral perfusion resulting from abnormal hemodynamics in neonates with complex congenital heart disease.

### VSPD11-03 • Abnormal Glutamatergic Metabolism during Cooling Correlates with Poor Outcome in Neonates Undergoing Hypothermia Therapy

**Jessica L Wisnowski** PhD (Presenter) ; **Tai-Wei Wu** ; **Ida Ashoori** ; **Marvin D Nelson** MD ; **Istvan Seri** MD, PhD \* ; **Ashok Panigrahy** MD ; **Stefan Bluml** PhD

#### PURPOSE

To study glutamatergic metabolism in neonates undergoing hypothermia therapy (HT) for suspected hypoxic-ischemic injury (HII)

#### METHOD AND MATERIALS

#### RESULTS

Neonates with poor outcome had lower creatine (? 24%), N-acetyl-aspartate (? 27%) and myo-inositol (? 11%) and higher lactate (Lac; ? 285%) and glutamine (Gln; ? 184%) during HT (see Figure). Glutamate (Glu) concentration during HT did not distinguish outcome groups; however, after HT, Glu was lower in neonates with poor outcome. Finally, as predicted from models, Glu concentration was lower (? 20%) during HT compared to after.

#### CONCLUSION

HII affects 3-5/1000 neonates and nearly half face death or severe disability despite therapy. Glutamate excitotoxicity in the setting of energy failure is widely hypothesized to be a key mechanism of cell death following HII. We found elevated glutamine in the neonates with poor outcome, and it is possible that this is indicative of excitotoxic injury as well as some ongoing capacity for astrocytes to detoxify excessive glutamate, albeit ultimately at a level insufficient to prevent poor outcome. However, it is important to consider that glutamine is not only synthesized from glutamate in astrocytes, but also that glutamine can be used as an energy metabolite. More research is needed to map the metabolic fate of glutamate and glutamine in neonates with HII.

#### CLINICAL RELEVANCE/APPLICATION

MR examinations during HT may not only aid clinical management but also the development of adjuvant therapies that aim to alleviate glutamate excitotoxicity.

### VSPD11-04 • Longitudinal Changes in Diffusion Properties in White Matter Pathways in Patients with Tuberous Sclerosis Complex

**Jae W Song** MD, MS (Presenter) ; **Fiona Baumer** MD ; **Paul D Mitchell** MS ; **Rudolph Pienaar** PhD ; **Mustafa Sahin** MD, PhD ; **Ellen Grant** MD ; **Emi Takahashi** PhD

#### PURPOSE

The purpose of this study was to identify predictors of longitudinal changes in diffusion properties of white matter tracts of projection, association and commissural fibers in patients diagnosed with Tuberous Sclerosis Complex.

#### METHOD AND MATERIALS

Structural and diffusion magnetic resonance imaging was carried out in 17 subjects diagnosed with Tuberous Sclerosis Complex (TSC) (mean age, 7.2 ± 4.4 years, range: 2 - 17.5 years) and with at least 2 scans (mean number of days between the 2 scans 419.4 days ± 105.4 days, range: 309 - 741 days). There were 10 males and 7 females; 5 of whom had autism spectrum disorder (ASD); and 10 of whom had seizure disorder. A coordinate-based tractography atlas was used to guide ROI placement to delineate the internal capsule/corona radiata, cingulum, and corpus callosum. These ROIs were then co-registered using FLIRT to each subject's second scan. The outcomes were mean change in apparent diffusion coefficient (ADC) and the mean change in fractional anisotropy (FA).

#### RESULTS

Multiple linear regression analyses showed gender to be a significant predictor of mean change in ADC in TSC subjects in the left internal capsule, right and left cingulum, and corpus callosum, adjusting for initial ADC scan measures. Gender was only a significant predictor of mean change in FA in the corpus callosum. Adjusting for initial ADC or FA scan measures, seizure disorder also emerged as a significant predictor of mean change in ADC, but not for mean change in FA, in the left internal capsule. ASD did not emerge as a significant predictor in either the mean change in ADC or FA in the studied white matter tract pathways.

#### CONCLUSION

Gender and seizure disorder were independent predictors of mean change in ADC or FA in some white matter tract pathways in TSC subjects. White matter microstructural integrity was more affected in males than in females in the left internal capsule, right and left cingulum, and corpus callosum and more affected in TSC subjects with seizure disorder in the left internal capsule than in subjects without seizure disorder.

#### CLINICAL RELEVANCE/APPLICATION

Effects of new therapies for TSC are being evaluated by changes seen on neuroimaging. Thus, understanding how specific patient characteristics differentially affects neuroimaging in TSC is recommended.

### VSPD11-05 • Posterior Fossa Morphometry and Volumetric Analysis in Three Different Groups of Pediatric Patients: Congenital Chiari Type 1 Malformation, Posterior Craniosynostosis and Costello Syndrome

**Rosalinda Calandrelli** ; **Gabriella D'Apolito** MD (Presenter) ; **Mariavalentina Tumino** ; **Luigi M Pedone** MD ; **Simona Gaudino** MD ; **Cesare Colosimo** MD

#### PURPOSE

Cerebellar tonsils herniation is caused by heterogeneous group of disorders with different pathogenic origins and it may occur early or late in childhood. In order to better evaluate the mechanism of herniation we performed a morphometric and volumetric analysis of the posterior cranial fossa in three different groups of pediatric patients in which cerebellar tonsil herniation occurs: children with congenital Chiari I malformation, children with posterior craniosynostosis and children with Costello Syndrome.

#### METHOD AND MATERIALS

Volumes of the posterior cranial fossa (PCFV) and cerebellum (CV) were assessed on axial T2-weighted MR images in 26 children with congenital Chiari I malformation (average 60 + 24 months), 6 children with Costello Syndrome (average 32+ 22 months) and 10 children with posterior craniosynostosis (average 12+ 11 months). The ratio of PCFV and CV was calculated to obtain the proportion of the PCFV occupied by the CV and to reduce the variability among the different groups. Each group was compared with an age matched control group. Volumetric measurements were correlated with diameter of the foramen magnum, tentorial angle, supraocciput and basiocciput lengths.

#### RESULTS

In children with congenital Chiari type I malformation, PCFV/CV ratio, antero-posterior diameter of the foramen magnum, supraocciput and basiocciput lengths were found significantly reduced (p < 0.05). In children with Costello Syndrome, PCFV/CV ratio, PCFV, antero-posterior and latero-lateral diameters of the foramen magnum and basiocciput length were found significantly reduced, while tentorial angle was found significantly increased (p < 0.05). In children with posterior craniosynostosis, PCFV, CV, latero-lateral diameter of the foramen magnum, supraocciput and basiocciput lengths were found significantly reduced (p < 0.05).

#### CONCLUSION

Our findings support the theory that reduction of PCFV plays an important role in developing cerebellar tonsillar herniation but other factors like foramen magnum diameters, supraocciput and basiocciput lengths and tentorial angle, contribute to explain the mechanism of cerebellar tonsils herniation.

#### CLINICAL RELEVANCE/APPLICATION

Morphometry and volumetric analysis of the posterior fossa are helpful to understand cerebellar tonsillar herniation mechanism guiding clinical or surgical approach.

### VSPD11-06 • MRI Findings of Hypertrophic Olivary Degeneration after Surgery for Posterior Fossa Tumors in Children

**Tommaso Tartaglione MD (Presenter) ; Annibale Botto ; Andrea M Alexandre MD ; Giana Izzo MD ; Mariacarmela Sciandra MD ; Simona Gaudino MD ; Cesare Colosimo MD**

#### PURPOSE

Hypertrophic olivary degeneration (HOD) is a possible consequence of injuries along dento-rubro-olivary pathway. The purpose of our study was: 1) To evaluate the incidence of HOD after surgery for posterior fossa pediatric tumors. 2) To show the typical MRI findings of HOD. 3) To analyze time correlation between surgery and MRI evidence of HOD.

#### METHOD AND MATERIALS

We based our study on a retrospective evaluation of 57 patients surgically treated for posterior fossa tumors in our institution between 2007 and 2012. For each patient Magnetic Resonance (MR) examination was performed before surgery. Every patient underwent clinical and radiological follow-up by serial MR examinations with variable time interval from surgery date (from 1 week to 5 years). All examinations included conventional MRI sequences before and after gadolinium injection and DWI images. For each exam we evaluated: 1) signal intensity of inferior olivary nucleus (ION) 2) dimensions of ION (normal, enlarged, atrophic) 3) signal intensity along the dento-rubro-olivary pathway (red nucleus, dentate nucleus, central tegmental tract, inferior and superior cerebellar peduncles) that could explain HOD. 4) evidence of haemorrhagic lesions. Findings were correlate with time interval between surgery and MR examination

#### RESULTS

HOD was diagnosed in 18/57 patients (31 %). In all the 18 patients, MRI showed high signal intensity on T2w images in ION and lesions in dentate nuclei (mono- or bilaterally), with subsequent contralateral or bilateral HOD. Enlargement of ION (hypertrophy) was found in only 3/18 cases, with variable time delay from surgery (from 1 to 5 months). In 2 cases of bilateral HOD we observed hyperintensity on T2w images in both superior cerebellar peduncles. DWI and contrast enhanced T1w images did not show alterations of ION.

#### CONCLUSION

1) Hyperintensity on T2w MRI images in the ION was the most common finding in HOD, and was often associated to lesions in contralateral dentate nucleus. 2) Enlargement of ION was not always present and time interval between surgery and its MRI evidence was variable. 3) The low incidence of ION enlargement could be related to the absence of hemorrhagic lesions in our population

#### CLINICAL RELEVANCE/APPLICATION

MRI changes in HOD were frequently assessed after posterior fossa surgery for pediatric tumors.

### VSPD11-07 • MRI of Pediatric White Matter Disease

**Sanjay P Prabhu MBBS (Presenter)**

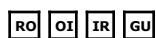
#### LEARNING OBJECTIVES

1) To become familiar with the spectrum of white matter disease in children including demyelination, dysmyelination and neurometabolic disorders. 2) To provide a step-wise algorithm for approaching imaging studies with white matter abnormality and use a pattern-recognition approach to narrow the differential diagnosis. 3) To illustrate examples of conditions with characteristic imaging findings and elaborate use of advanced imaging techniques in refining the diagnosis.

#### ABSTRACT

## Interventional Oncology Series: Controversies and Emerging Questions in the Management of Renal Tumors

**Sunday, 01:30 PM - 06:00 PM • S405AB**



[Back to Top](#)

**VSI011 • AMA PRA Category 1 Credit™:4.25 • ARRT Category A+ Credit:5**

#### Moderator

**Debra A Gervais, MD \***

#### LEARNING OBJECTIVES

1) To review management options for small renal masses as well as indications for each. 2) To review the data supporting the energy based thermal ablation modalities for ablation of renal masses. 3) To describe the role and limitations of biopsy of renal masses. 4) To review the management of benign solid renal masses. 5) To describe the evidence for ablation of T1b renal masses.

### VSI011-01 • Controversy 1-T1a Renal Tumor: Resect, Ablate, or Follow

#### LEARNING OBJECTIVES

View learning objectives under main course title.

## VSI011-02 • Small Renal Mass (T1a): The Case for Resection

**Adam S Feldman MD** (Presenter)

### LEARNING OBJECTIVES

View learning objectives under main course title.

## VSI011-03 • Long-term Results of Renal RFA Based on a Single-center 203 Cases Experience: Better than Surgery for Early RCC?

**Irene Garetto MD ; Carlo Gazzera ; Marco Busso MD ; Gianluca Amadore ; Federica Solitro MD ; Andrea Veltri MD** (Presenter) \*

### PURPOSE

To evaluate the long-term effects of RFA of renal masses (RM), assessing safety, technique effectiveness and survival, in order to compare the best results with surgical series.

### METHOD AND MATERIALS

203 RM (12-75 mm, m 30; 193 malignant; 123 exophytic, 67 parenchymal, 13 central) in 137 patients (95 males; 20-88 y, m 64; 13 with hereditary tumors, 31 with solitary kidney) underwent RFA in our center in the last decade (196 US-guided, 7 CT-guided). The treatment sessions have been 220 (17 retreatments for partial ablation or early recurrence). More recently, complications were prevented with additional techniques (namely, 10 hydrodissection and 3 pyeloperfusion). Adverse Events (including major complications) and technique effectiveness (Complete Ablation) were evaluated, as well as predictors for adverse AE and CA. Overall (OS), Disease-Free (DFS) and Cancer-Specific Survival (CSS) were calculated (follow-up 1-109 months, m 39). Predictors for survival (solitary kidney, previous cancer disease, tumor type, site and size, etc.) were specifically investigated.

### RESULTS

17 (8.4%) AE were recorded, including 4 (2%) major complications (all before using preventing techniques). Exophytic extension and smaller diameter were protective against AE at the uni/multivariate analysis. CA was obtained in 85% RM overall and in 115/124 with a diameter

### CONCLUSION

RFA of not central small RM is safe and effective and provide high long-term survival rates. Early stage RCC should be considered for RCT comparing RFA with surgical resection.

### CLINICAL RELEVANCE/APPLICATION

RFA of not central T1a RCC is safe and successful. Thus, RFA offers an optional choice as a first-line therapy. RCTs are still necessary to assess if RFA is better than surgery for early RCC.

## VSI011-04 • Small Renal Mass (T1a): The Case for Ablation

**Jeremy C Durack MD** (Presenter)

### LEARNING OBJECTIVES

1) Understand and compare treatment alternatives for small renal masses. 2) Recognize imaging features of small renal masses that impact treatment alternatives. 3) Understand the risks and benefits of image guided renal mass ablation.

## VSI011-05 • Small Renal Mass (T1a): Both Cases for Intervention are Weak. Active Surveillance Will Do Just as Well

**Stuart G Silverman MD** (Presenter) \*

### LEARNING OBJECTIVES

View learning objectives under main course title.

## VSI011-06 • Controversy 2-Small Renal Mass (T1a) Ablation is Chosen. Heat or Cold?

### LEARNING OBJECTIVES

View learning objectives under main course title.

## VSI011-07 • Small Renal Mass (T1a): The Case for Heat Based Ablation

**Debra A Gervais MD** (Presenter) \*

### LEARNING OBJECTIVES

View learning objectives under main course title.

## VSI011-08 • 5-year Outcomes of Percutaneous Radiofrequency Ablation of 100 Renal Cell Carcinomas

**Timothy D McClure MD** (Presenter) ; **Nelly Tan MD** ; **Daniel S Chow MD** ; **Allan Pantuck MD** ; **James Sayre PhD** ; **Steven S Raman MD**

### PURPOSE

Determine intermediate term oncological outcomes and determine predictors of primary efficacy in the percutaneous radiofrequency ablation (RFA) of pathologically proven renal cell carcinomas (RCC).

### METHOD AND MATERIALS

After IRB approval we performed a HIPAA compliant study of all patients who underwent RFA for pathologically proven RCC. Technical success, local tumor progression, primary and secondary technique effectiveness were defined per the Working Group of Image Guided Tumor Ablation. Univariate and multivariate logistic regression analysis was performed to determine predictors of primary technique effectiveness and complications. Kaplan-Meier local tumor progression-free, metastasis-free, and overall survival were calculated. All analyses were done using the statistical software STATA/SE 11.2. Alpha of 0.05 was considered significant.

### RESULTS

115 RFA sessions for 100 RCC lesions in 84 patients were identified. Mean age was 70.3 years (range 35-93). 51/84 (61%) patients were men and 33/84 patients (39%) were women. The median ASA score was 3 (range 2-3). The median(mean) lesion size was 2.3(2.6) cm (range 0.7-6cm). The median(mean) follow up was 24(27) months (range 1-106 months). Total technique effectiveness was 95%. Primary technique effectiveness was 86% (86/100 lesions). Secondary technique effectiveness was 9% (9/100 lesions). Treatment failure was 5%(5/100). Technical success was 99.1%. Using logistic regression statistical analysis, predictors of primary efficacy were: location, size, proximity to collecting system, R.E.N.A.L nephrometry sum, and number of ablation zones. Complications occurred in 15 of 115 RFA sessions (13%) with no deaths. The median 2.1year local progression free, metastasis free, disease specific survival, and overall survival was 86%, 98.7%, 100%, and 97.6% respectively.

### CONCLUSION

Percutaneous RFA for RCC is safe and effective with excellent intermediate oncologic control. Location, size, lesion nearness to the collecting system, R.E.N.A.L Nephrometry sum, and number of ablation zones predicts primary efficacy.

### CLINICAL RELEVANCE/APPLICATION

### VSI011-09 • Percutaneous Microwave Ablation of Renal Tumors: Multicenter Evaluation of Safety and Efficacy

**Anna Moreland** (Presenter) ; **Timothy J Ziemlewicz** MD ; **Aaron M Fischman** MD \* ; **J. Louis Hinshaw** MD \* ; **Jason Abel** ; **Meghan G Lubner** MD ; **Sarah Best** ; **Marci Center** ; **Christopher L Brace** PhD \* ; **Fred T Lee** MD \*

#### PURPOSE

To evaluate the feasibility, safety, and efficacy of a high-powered, gas-cooled microwave ablation system for treatment of renal tumors.

#### METHOD AND MATERIALS

Between 1/2011 and 4/2013, 45 renal tumors were treated at 2 medical centers using ultrasound and CT-guided microwave ablation with a high-powered, gas-cooled microwave ablation system (NeuWave Medical, Madison, WI). Tumors included biopsy-proven renal cell carcinoma (n=36), angiomyolipoma (n=4), oncocytoma (n=2), and other (n=3). Mean patient age was 64 years. Post-procedure imaging was performed by CECT or MRI to evaluate for enhancement in the ablation zone.

#### RESULTS

Mean pre-treatment tumor diameter was 2.7 cm (range: 1.0-5.4). Tumor diameter decreased by a mean of 11% on immediate post-ablation CT. Mean duration of power application was 6.5 minutes, and mean generator power was 73.7 W. Technical effectiveness was 100%. There was one major complication: a retroperitoneal hematoma on post ablation day 11. This coincided with restarting anticoagulation for suspected pulmonary embolus in a patient with a thrombotic history, and required readmission and transfusion of PRBCs. Median hospital stay was 1 day, and median length of clinical follow-up was 11 months. All patients are alive and without evidence of metastatic disease, with the exception of 1 death occurring 6 months post ablation and unrelated to either the procedure or the malignancy. 28 patients have had follow-up imaging at a mean of 6.3 months status post ablation, with local tumor progression noted at the ablation zone in 1 case. Overall, the procedure demonstrated 95% primary treatment effectiveness and a 98% secondary treatment effectiveness, with 1 tumor yet to be retreated.

#### CONCLUSION

Use of a high-powered, gas-cooled percutaneous microwave ablation system for the treatment of small renal masses demonstrates safety and technical success in the short term.

#### CLINICAL RELEVANCE/APPLICATION

Preliminary experience treating renal tumors with a high-powered, gas-cooled microwave system suggests that the procedure is technically feasible, safe, and efficacious at early time points.

### VSI011-10 • Small Renal Mass (T1a): The Case for Cold Ablation

**Peter J Littrup** MD (Presenter) \*

#### LEARNING OBJECTIVES

1) Understand the different approaches and techniques of thorough renal mass cryoablation that produces very low recurrence rates, even for larger central tumors. 2) Understand the appropriate settings to utilize protective techniques (i.e., hydrodissection, balloon interposition, ureteral stent, etc..) for adjacent calyces, bowel and ureter to avoid complications. 3) Identify major imaging follow-up criteria for ablation success and any early failures. 4) Describe the overall cost-efficacy trade-offs for cryo vs. heat-based renal ablations vs. partial nephrectomy, in relation to tumor location, complications and recurrence rates.

#### ABSTRACT

Cryoablation of smaller renal cancers (i.e., T1a, or For safety, cases will be considered for avoidance of direct calyceal puncture, selection of hydrodissection or balloon interposition for bowel protection, and protection of the uretero-pelvic junction by stent placement. Imaging outcomes of complications and their avoidance will be shown. For optimal efficacy, tumor size in relation to number and size of cryoprobes emphasize the 1-2 Rule of at least 1 cryoprobe per cm of tumor diameter and no further than 1 cm from tumor margin, as well as cryoprobe spacing of

### VSI011-11 • Percutaneous Renal Cryoablation in Obese and Morbidly Obese Patients

**Grant D Schmit** MD (Presenter) ; **Anil N Kurup** MD ; **Adam J Weisbrod** MD ; **Robert J McDonald** MD, PhD ; **Matthew R Callstrom** MD, PhD \* ; **Thomas D Atwell** MD ; **Robert Thompson** MD ; **Stephen Boorjian**

#### PURPOSE

To compare percutaneous renal cryoablation complications and outcomes in obese and morbidly obese versus nonobese patients.

#### METHOD AND MATERIALS

389 percutaneous cryoablation procedures were performed in 367 patients for treatment of 421 renal masses at our institution between 2003 and 2012. Patients were categorized into three groups based on body mass index (BMI): nonobese (BMI < 30.0kg/m<sup>2</sup>), obese (BMI 30.0-39.9kg/m<sup>2</sup>) and morbidly obese (BMI > 40.0kg/m<sup>2</sup>). Each group was retrospectively analyzed for major complications (Clavien > Grade 2) and oncologic outcomes.

#### RESULTS

189 (48.6%) renal cryoablation procedures were performed on nonobese patients, 161 (41.4%) on obese patients and 39 (10.0%) on morbidly obese patients. Eleven (5.8%) major complications occurred in nonobese patients, 15 (9.3%) in obese patients and 3 (7.7%) in morbidly obese patients. As such, there was no significant difference in the rate of major complications in obese (p=0.23) or morbidly obese (p=0.67) compared to nonobese patients. There was one ablation-related death from complications of urosepsis. A total of 13 local treatment failures were identified, including 5 technical failures and 8 local tumor recurrences during median imaging follow-up of 18 months (interquartile range: 8-36). Six (3.2%) local treatment failures occurred in nonobese patients, 5 (2.9%) in obese patients and 2 (4.8%) in morbidly obese patients. Again, no significant difference was noted in local treatment failure rate between obese (p=0.96) or morbidly obese (p=0.57) compared to nonobese patients.

#### CONCLUSION

Percutaneous renal cryoablation complication rates and outcomes in obese and morbidly obese patients are similar to those in nonobese patients.

#### CLINICAL RELEVANCE/APPLICATION

To our knowledge, this is the first paper to evaluate percutaneous renal cryoablation complications and outcomes based on patient body mass index (BMI).

### VSI011-12 • Controversy 3-Biopsy or No Biopsy Before Ablation

#### LEARNING OBJECTIVES

View learning objectives under main course title.

### VSI011-13 • Renal Cell Cancer Subtype as a Predictor of Efficacy in Radiofrequency Ablation

**Timothy D McClure** MD (Presenter) ; **Allan Pantuck** MD ; **James Sayre** PhD ; **Steven S Raman** MD

#### PURPOSE

To determine if renal cell cancer (RCC) subtype predicts efficacy in the percutaneous radiofrequency ablation (RFA) of RCC.

#### METHOD AND MATERIALS

With IRB approval we performed a HIPAA compliant retrospective study of patients who underwent RFA for RCC and determined subtype pathology that included clear cell, chromophobe, papillary, oncocytic neoplasm, and RCC not otherwise specified. Pathology was determined by biopsy or post resection surgical pathology. Group comparisons were done using univariate and multivariate logistic regression analysis to determine factors impacting primary efficacy, secondary efficacy, and technique effectiveness. All analyses were done using the statistical software STATA/SE 11.2. Alpha of 0.05 was considered significant. Technical success, local tumor progression, primary and secondary technique effectiveness were defined per the Working Group of Image Guided Tumor Ablation.

#### RESULTS

100 pathologically proven RCC masses were identified in 84 patients with the following subtypes: clear cell: 55/100 (55%), oncocytic neoplasms: 19/100 (19%), papillary: 13/100 (13%), RCC not otherwise specified 10/100 (10%), and chromophobe: 3/100 (3%). Median post ablation follow up was up to 106 months (mean 24 months). Non clear cell RCC subtypes had more favorable outcome compared to clear cell RCC for primary, secondary and total technique 44/45(97.8%), 1/45 (2.2%), 45/45 (100%) versus 42/55 (76.4%), 8/55 (14.5%), 50/55 (90.9%) respectively(p=0.002). Overall primary, secondary and total technique effectiveness was 86%, 9%, and 95% respectively.

#### CONCLUSION

Non-clear cell RCC subtypes have more favorable ablation outcomes compared to clear cell RCC after percutaneous RFA.

#### CLINICAL RELEVANCE/APPLICATION

Pathology predicts efficacy in the percutaneous RFA of renal masses. Pre-procedure biopsy should be done prior to percutaneous RFA of renal masses to better predict outcomes.

### **VSI011-14 • Biopsy or No Biopsy Before Ablation? Don't Trouble Yourself or the Patient with the Renal Mass Biopsy - Go Ahead and Ablate**

**Steven S Raman MD** (Presenter)

#### LEARNING OBJECTIVES

1) Understand how to image renal masses prior to ablation. 2) Understand how to use appropriate CT and MR protocols to enable renal mass characterization. 3) Describe the most common CT and MRI enhancement signatures of common RCC subtypes, oncocytoma and lipid poor AML.

#### ABSTRACT

Characterization of small renal masses has proven challenging. However, with appropriate CT and MR protocols, the majority of these lesions can now be characterized pre procedurally, enabling a confident diagnosis. In this lecture, we will describe renal mass characterization protocols and describe the common imaging signatures of RCC subtypes and their common mimics including lipid poor AML and oncocytoma. This may eliminate need for preprocedural biopsy.

### **VSI011-15 • Biopsy or No Biopsy Before Ablation? Biopsy Every Renal Tumor before Percutaneous Ablation**

**William W Mayo-Smith MD** (Presenter) \*

#### LEARNING OBJECTIVES

1) Explain the expanding role of renal mass biopsy. 2) Explain why biopsy is necessary before all renal tumor ablations. 3) Demonstrate biopsy techniques.

### **VSI011-16 • Emerging Questions in Renal Tumor IR Management**

#### LEARNING OBJECTIVES

View learning objectives under main course title.

### **VSI011-17 • Benign Disease: Leave Alone, Ablate or Suggest Something Else?**

**S. William Stavropoulos MD** (Presenter) \*

#### LEARNING OBJECTIVES

1) Understand and compare treatment alternatives for benign renal masses. 2) Recognize imaging features of benign renal masses that impact treatment alternatives. 3) Understand the risks and benefits of image guided treatment of benign renal masses.

### **VSI011-18 • Large Renal Masses (T1b): Does Ablation Have a Seat at the Table?**

**Thomas D Atwell MD** (Presenter)

#### LEARNING OBJECTIVES

1) Appreciate the strengths and limitations of percutaneous ablation in treating renal tumors measuring larger than 4cm.

#### ABSTRACT

### **VSI011-19 • Outcomes Following Percutaneous Cryoablation of Renal Masses 4.1-7.0cm**

**Jay J Vlainck MD** (Presenter) ; **Grant D Schmit MD** ; **Anil N Kurup MD** ; **Adam J Weisbrod MD** ; **Matthew R Callstrom MD**, PhD \* ; **Thomas D Atwell MD** ; **Stephen Boorjian** ; **Robert Thompson MD**

#### PURPOSE

To describe safety and oncologic outcomes following percutaneous cryoablation of renal masses measuring 4.1-7.0cm.

#### METHOD AND MATERIALS

Retrospective review of 71 renal tumors measuring 4.1-7.0cm in 70 consecutive patients treated with percutaneous cryoablation between 2003 and 2011. Local recurrence, cancer-specific survival and overall survival rates were recorded. Complication rates (Clavien Dindo) were also documented.

#### RESULTS

Mean tumor size was 4.8 cm. A single (1.4%) technical failure was observed at the time of ablation. Of the 58 (82%) tumors that were followed for at least three months, there was a single (1.7%) recurrence. The mean duration of follow-up for the 57 tumors that did not recur was 2.2 years (range 0.3 - 7.1). Estimated recurrence-free survival rates at 1, 3, and 5 years following cryoablation were 97.9%, 97.9%, and 97.9%, respectively.

Among the 58 tumors that were followed for at least three months, 36 (62%) were RCC at biopsy, including the single recurrence. Mean duration of follow-up for the 35 RCC tumors that did not recur was 2.0 years (range 0.3 - 6.1). Estimated recurrence-free survival rates at 1, 3, and 5 years for these biopsy-confirmed RCC tumors were 96.4%, 96.4%, and 96.4%, respectively. Of the 36 (51%) patients with sporadic RCC, estimated cancer-specific survival rates at 1, 3, and 5 years were 100%, 94%, and 94%, respectively. Of the 71 cryoablation procedures, there were 5 (7.0%) complications of grade 3 or greater.

#### CONCLUSION

Cryoablation represents a safe treatment alternative for patients with renal masses, with intermediate-term oncologic efficacy for T1b tumors.

#### CLINICAL RELEVANCE/APPLICATION

Outcomes in this study suggest that cryoablation of T1b renal cell carcinoma may be more efficacious than previously considered, particularly when considering the AUA guidelines.

## Pediatric Radiology Series: Pediatric Musculoskeletal

Sunday, 02:00 PM - 03:30 PM • S102AB



[Back to Top](#)

**VSPD12** • AMA PRA Category 1 Credit™:3.75 • ARRT Category A+ Credit:4

#### Moderator

**Paul K Kleinman**, MD

#### Moderator

**John D MacKenzie**, MD

**VSPD12-01 • Pediatric Hip Conditions Predisposing to FAI**

**Sarah D Bixby** MD (Presenter)

#### LEARNING OBJECTIVES

1) Understand the difference between 'cam,' 'pincer,' and 'mixed' femoroacetabular impingement (FAI) syndromes. 2) Become familiar with accepted imaging parameters that help to establish the diagnosis of FAI in pediatric and adolescent patients. 3) Become familiar with pediatric hip conditions that may lead to FAI in patients, and understand the natural progression of these diseases. 4) Understand how imaging studies impact clinical management of patients with FAI.

#### ABSTRACT

Femoroacetabular impingement (FAI) may be considered cam-type, pincer-type, or mixed-type depending on whether the primary morphologic abnormality exists in the femur, acetabulum, or both. FAI has generated attention in the literature given its association with osteoarthritis of the hip as well as debilitating hip pain. Children and adolescents may develop FAI, which can lead to devastating joint damage at a relatively early age if left undetected and/or untreated. Certain populations of pediatric patients, such as those with slipped capital femoral epiphysis (SCFE) or Legg-Calvé-Perthes disease (LCP) will almost certainly develop FAI even after their primary disease has been treated. Radiologists will assist their clinical colleagues by suggesting the diagnosis on imaging examinations based on certain imaging parameters, which will be reviewed. In patients with confirmed FAI based on history, physical exam findings, and imaging, MRI examinations of the hip with radial sequences and cartilage sensitive sequences may be helpful to orthopedists as they consider surgical versus nonsurgical options. These techniques will be discussed.

**VSPD12-02 • MR Findings of Femoroacetabular Impingement (FAI) in Healed Perthes Stulberg Class 3, 4 and 5 Hips. Does MR Have a Role in Preoperative Evaluation?**

**Siddharth P Jadhav** MD (Presenter) ; **J. H Kan** MD ; **Scott B Rosenfeld** MD

#### PURPOSE

To evaluate the use of MRI as a complement to the Stulberg classification in the pre-operative work-up of FAI secondary to healed Perthes and its impact on orthopaedic management

#### METHOD AND MATERIALS

We performed retrospective evaluation of MR arthrography (MRA) findings in patients with healed Perthes disease. Patients presented over a period of 6 years (2008-2013) with hip pain and clinical signs of FAI. We included patients with hip radiographs and pre-operative dedicated MRA of the hip joint. A total of 16 hips in 15 patients were included. The radiographic findings were classified according to the Stulberg classification. The MRA was evaluated for abnormal alpha angles using radial imaging to evaluate the degree and location of CAM-type circumferential abnormality with alpha angle threshold of 55 degrees. MRA was also reviewed for presence and extent of labral tears and articular cartilage damage. These findings were correlated with the Stulberg classification

#### RESULTS

Mean age was 14.9 years (range: 10.5 to 21.8 years; 40% female). Nine hips were Stulberg Class III, six hips were Stulberg class 4 and 1 hip was Stulberg class V. 3 hips had 50% circumferential CAM deformity. For the 8 with >50% CAM deformity, 5 (56%) were class III, 2 (33%) were class IV hips and 1 (100%) was class 5 hips. 13 hips (81%) had labral tears which most commonly involved the anterior and superior labrum. 11 hips (69%) had abnormal femoral articular cartilage and 6 hips (37.5%) had abnormal acetabular cartilage. The femoral head cartilage abnormalities were most severe posteriorly and centrally. Full thickness cartilage loss was present in 2 class III hips (22%) and 4 class IV hips (67%). The labrum was torn in 8 class III hips (89%) and 5 class IV hips (83%)

#### CONCLUSION

MRA provides additional information about the exact location of the aspherical portion of the femoral head and neck, the size and location of a cam lesion, as well as the status of the labrum and articular cartilage in patients with healed Perthes disease. From an orthopaedic perspective, this can assist in making treatment decisions, planning surgery, and counseling the patient about the likelihood of success of hip preservation surgery

#### CLINICAL RELEVANCE/APPLICATION

Routine use of MRA can provide information in addition to that derived from the radiographic Stulberg classification. This facilitates the orthopaedic management of patients with healed Perthes

**VSPD12-03 • Normative Shape Analysis of the Developing Piglet Femur in Forming a Metric for Characterizing Femoral Head Deformation Following Experimentally Induced AVN**

**Andy Tsai** MD (Presenter) ; **Susan A Connolly** MD ; **Arthur Nedder** ; **Frederic Shapiro**

#### PURPOSE

Childhood idiopathic AVN of the hip (Legg-Calvé-Perthes disease) results in considerable morbidity. To simulate this disease for laboratory study, we used an AVN model in a skeletally immature piglet hip created by placement of a tight silk ligature around the base of the femoral neck and sectioning of the ligamentum teres, rendering the femoral head completely avascular. The temporal characterization of this piglet's deforming femur, based on the metric established from a normative shape database we derived from a population of normal piglet femurs, forms the basis for this paper.

#### METHOD AND MATERIALS

Normative piglet femur developmental data was generated via serial CT images of bilateral femurs from 3 normal piglets at regular time intervals. We applied a shape analysis technique to this data set using level set method as the shape descriptor and principal component analysis as the feature selector in deriving a shape subspace that compactly describes the normal development of the piglet femur. This parametric subspace efficiently captures the major temporal changes of the femurs, and can be used as an effective metric in quantifying how much a query femur deviates from the norm. We applied this shape metric to the experimental femur data generated via serial CT images of a piglet following experimental unilateral induction of femoral head AVN. The contralateral femur served as the control.

## RESULTS

The application of this shape metric to the experimental data traces out a deformation trajectory over time of the diseased femur that progressively differs from the trajectory of the same piglet's contralateral normal femur. Hence, this computational framework can objectively indicate the time point when the shape of the femur starts to deviate from the norm, and the amount of deviation. As a by-product, this technique's intuitive 3D visualization of the shape changes (via variations of selected eigenmodes and surface distance-difference colormaps) reveals patterns of changes in the normal and abnormal development of the femur that solidifies widely-accepted clinical observations.

## CONCLUSION

The clinical application of this analysis tool is expected to play an important tool in (1) assessing disease progression; (2) directing clinical intervention; and (3) gauging the effectiveness of treatment.

## CLINICAL RELEVANCE/APPLICATION

This methodology may potentially revolutionize the diagnosis and treatment protocol of pediatric hip AVN.

### VSPD12-04 • Symptomatic Pediatric Developmental Osseous Variants

**Paul K Kleinman MD** (Presenter)

#### LEARNING OBJECTIVES

1) Learn the important normal anatomic variants that may cause disease. 2) Learn the important normal anatomic variants that may simulate disease. 3) Learn the problematic variants that are indeterminate and require further imaging and follow up.

#### ABSTRACT

A wide range of normal variants may be encountered in the pediatric skeleton. Differentiation of innocent variants from those with superimposed acute/chronic trauma may pose a challenge radiographically. Opposite comparison views may be helpful. MRI usually resolves the issue...but not always. Correlation with clinical findings is essential.

### VSPD12-05 • Apophyseal Joint Inflammation in Patients with Enthesitis Related Arthritis; Serial Observations and Correlation with Sacroiliitis

**Tom Amies MBBS, BSc** (Presenter) ; **Kanimozhi Vendhan MBBS, DMRD** ; **Debajit Sen** ; **Corinne Fisher** ; **Yiannakis Ioannou** ; **Margaret A Hall-Craggs MD**

#### PURPOSE

To observe changes in apophyseal joint inflammation on serial scans in patients with enthesitis related arthritis (ERA), and to correlate this with sacroiliitis.

#### METHOD AND MATERIALS

We performed a retrospective review of serial MRI lumbar spine scans of ERA patients attending the adolescent rheumatology clinic at our institution. The duration of follow up ranged from 3 months to 4yrs 10 months. Scan protocol consisted of sagittal T1, sagittal STIR and sagittal T1 contrast enhanced images of the lumbar spine along with contrast-enhanced coronal and axial imaging of the sacroiliac joints. Images were reviewed by an expert MR reader. As there is no universally accepted grading criteria to assess apophyseal joint inflammation in adolescents, we adapted and modified a grading system used in adults. Sacroiliitis was graded as stable, improved, worse or as mixed response when some regions showed improvement with other parts of the joint showing worsening inflammation.

#### RESULTS

A total of 70 scans were available in 29 ERA patients. Apophyseal joint inflammation was present in 15 of 29 patients. Amongst these 9 were on disease modifying anti-rheumatic drugs, 3 on anti-TNF therapy and the other 3 on NSAIDS. In 6 of 15 the apophyseal joint synovitis and sacroiliitis moved in the same direction i.e they either became worse or better together. However in 9 of 15 the apophyseal joint synovitis and sacroiliitis behaved differently, i.e with worsening apophyseal joint inflammation on serial scans the sacroiliitis either stayed stable or showed improvement.

#### CONCLUSION

We have shown that apophyseal joint synovitis and sacroiliitis can respond independent of one another. This is a novel finding.

#### CLINICAL RELEVANCE/APPLICATION

Concurrent sacroiliitis and apophyseal joint synovitis in patients with enthesitis related arthritis can respond differentially with therapy. This could account for persistent pain.

### VSPD12-06 • A Description of Inflammatory Changes of the Lumbar Spine in Patients with Enthesitis-related Arthritis

**Kanimozhi Vendhan MBBS, DMRD** ; **Tom Amies MBBS, BSc** (Presenter) ; **Corinne Fisher** ; **Debajit Sen** ; **Yiannakis Ioannou** ; **Margaret A Hall-Craggs MD**

#### PURPOSE

To assess inflammatory changes in the lumbar spine in a cohort of patients with enthesitis-related arthritis (ERA) as compared to a control group of adolescents with mechanical back pain.

#### METHOD AND MATERIALS

We performed a retrospective case control study and reviewed MRI lumbar spine scans of a total of 83 patients (62 cases;21 controls). Images were reviewed by an expert MR reader who was blinded to clinical details. The presence or absence of morphological features of enthesitis (oedema of corners of vertebral endplates), facet joint synovitis (articular process oedema,enhancing synovitis) and inflammation of the posterior elements (enhancement of interspinous ligaments and spinous process) was assessed at each lumbar vertebral level. Facet joint synovitis was subjectively graded from 0 to 3 (0 being normal and 3 being severe). As there is no universally accepted grading criteria to assess facet joint inflammation in adolescents, we adapted and modified a grading system used in adults. The presence or absence of sacroiliitis (erosions of articular surface, bone marrow oedema and enhancement) was also recorded. STATA software was used for data analysis.

#### RESULTS

One or more abnormalities of the lumbar spine were found in 47 (76%) of 62 ERA cases. MR evidence of facet joint synovitis was seen in 24 (39%) of cases and in 1 patient (5%) in the control group. This difference was highly significant (p value = 0.003). Amongst patients with abnormal facet joints (n=24), grade 1 synovitis was present in 9 (37%) , grade 2 lesions in 10 cases (42%) and grade 3 synovitis in 5 cases (21%) . Overall 47 of the 62 cases showed evidence of sacroiliitis. None of the patients in the control group had sacroiliitis. Inflammatory changes in the SIJs were accompanied by abnormalities of the lumbar spine in 36 cases (58%). In 5 of 24 ERA cases with facet joint synovitis there was no MR evidence of sacroiliitis. This is a novel observation. There was no statistically significant difference between the cases and controls in the prevalence of disc changes, end plate oedema and inflammation of the posterior elements.

#### CONCLUSION

Facet joint inflammation was seen in 39% of ERA patients. This is a previously undescribed finding and could contribute to back pain in these children.

#### CLINICAL RELEVANCE/APPLICATION



Lumbar spine inflammatory disease should be considered as a cause of back pain in patients with ERA, independent of the presence of sacroiliitis.

## VSPD12-07 • ACL Reconstruction in the Skeletally Immature Patient: Current Concepts in Diagnosis and Treatment

**Craig Finlayson MD (Presenter) \***

### LEARNING OBJECTIVES

1) Participants will identify anatomic and neuromuscular risk factors for ACL injury in the young patient. 2) Participants will work through the differential diagnosis of acute ACL tear and identify associated injury patterns in the young patient. 3) Participants will understand the risks of ACL reconstruction unique to the young patient.

### ABSTRACT

Although once thought to be rare, anterior cruciate ligament injuries are being diagnosed with increasing frequency. Controversy exists regarding the management of ACL injuries in patients with open physes. Nonoperative management of complete tears in skeletally immature patients generally has a poor prognosis in terms of knee function and is associated with progressive intra-articular injury. Conventional surgical techniques for ACL reconstruction risk iatrogenic growth disturbance because of physal violation, and cases of growth disturbances have been reported in several studies. This module will discuss the pathophysiology, diagnosis and prevention of ACL injuries in the skeletally immature as well as some of the risks and controversy regarding surgical treatment.

## Breast Series: Breast MR Imaging

**Monday, 08:30 AM - 12:00 PM • Arie Crown Theater**



[Back to Top](#)

**VSBR21 • AMA PRA Category 1 Credit™:3.25 • ARRT Category A+ Credit:4**

**Moderator**

**Christopher E Comstock, MD**

**Moderator**

**Linda Moy, MD**

### VSBR21-01 • MR Image Acquisition

**Mitchell D Schnall MD, PhD (Presenter)**

### LEARNING OBJECTIVES

1) To describe the technical elements needed to perform high-quality breast MRI. 2) To describe and illustrate the pulse sequences needed for high-quality breast MRI. 3) To describe and illustrate the importance of simultaneously achieving high in-plane spatial resolution, thin slices, adequate temporal resolution, adequate signal-to-noise ratios, and full coverage of both breasts in breast MRI. 4) To show examples of high-quality and sub-standard breast MRI exams.

### VSBR21-02 • Breast MRI at 7 Tesla: Image Evaluation and Comparison to 3 Tesla

**Ryan Brown (Presenter) ; Pippa Storey PhD ; Christian Geppert \* ; Ana Claudia Leite ; James S Babb PhD ; Daniel Sodikson MD, PhD ; Graham Wiggins ; Linda Moy MD**

### PURPOSE

To evaluate the image quality of T1-weighted fat suppressed breast MRI at 7T, with 3T images in the same subjects serving as a baseline reference.

### METHOD AND MATERIALS

3D T1w images were acquired in 17 subjects using a bilateral transmit-receive coil and adiabatic inversion-based fat suppression (FS) at 7T, and a seven channel receive array and saturation-based FS at 3T. Images were qualitatively graded on a five-point scale by two radiologists and quantitatively assessed through fibroglandular/fat contrast, and signal uniformity measurements. Acquisition time and voxel size for the four unilateral sequences were: 1. 7T standard resolution, 119s, 1.1x1.1x1.6mm<sup>3</sup>; 2. 7T high resolution, 390s, 0.6mm isotropic; 3. 3T standard resolution, 71s, 1.1x1.1x1.6mm<sup>3</sup>; 4. 3T high resolution, 324s, 0.6mm isotropic.

### RESULTS

Image quality scores at 7T and 3T were similar (4.3 at 7T vs 4.1 at 3T, p=0.27) in standard-resolution images, indicating that breast imaging with clinical protocol parameters can be performed with high image quality at 7T. The 7T SNR advantage was underscored in high-resolution images, where image quality was significantly greater than at 3T (4.2 at 7T vs 3.1 at 3T, ppp

### CONCLUSION

The 7T bilateral transmit-receive coil and adiabatic inversion-based FS technique produce image quality that is as good as or better than 3T. The improved SNR can be exploited for high-resolution imaging to improve fibroglandular tissue detail.

### CLINICAL RELEVANCE/APPLICATION

High breast image quality and uniformity was achieved with clinical parameters at 7T. 7T SNR improves delineation of small structures that may be beneficial for lesion classification.

### VSBR21-03 • Determining Breast Cancer Grade with 3T-TWIST MRI

**Roel D Mus MD (Presenter) ; Ritse M Mann MD, PhD \* ; Jelle O Barentsz MD, PhD ; Peter Bult MD, PhD ; Nico Karssemeijer PhD \* ; Bram Platel PhD**

### PURPOSE

To assess the correlation between time to enhancement (TTE) and tumor grade using an ultrafast DCE MR Mammography protocol.

### METHOD AND MATERIALS

1031 patients underwent contrast enhanced breast MRI at 3.0T (Siemens, Magnetom Trio and Skyra) using a 16 channel bilateral breast coil. A bi-temporal protocol was employed, interleaving a TWIST (Time-resolved angiography With Stochastic Trajectories) sequence during and immediately after IV administration of 0.1mmol/kg Gd-DOTA (20 time points, spatial resolution 1\*0.9\*2.5 mm, temporal resolution 4.32 seconds). 102 consecutive patients with invasive ductal (IDC) or lobular (ILC) carcinoma were included in this analysis. The TTE was determined on maximum intensity projections from the TWIST acquisitions as displayed on a dedicated DynaCAD breast MRI workstation (InVivo). TTE was defined as "the timepoint where the lesion started to enhance" minus "the time point where the aorta started to enhance". For different tumor histology and grade categories the mode TTE was calculated and TTE distribution was compared using one way anova.

### RESULTS

Mode TTE was 4.3 sec for 32 grade III IDC, 8.6 sec for 40 grade II IDC and 18 ILC and 12.9 sec for 12 grade I IDC. There was no significant difference in TTE between IDC and ILC (p=0.465). In IDC TTE distribution was significantly different between tumor grade categories (p

### CONCLUSION

TTE provides a non-invasive method to predict histological grade. Lesions that enhance very rapidly are more likely high grade than lesions that enhance relatively slow.

#### CLINICAL RELEVANCE/APPLICATION

Breast cancer therapy is dictated by pathological features of the tumor with the poorest prognosis. Because pathology is subject to sampling errors, TTE can be used to ascertain sampling of the most relevant part of the tumor.

### **VBSR21-04 • Dynamic Contrast-enhanced (DCE) Breast MR of DCIS: A Comparison of Same-patient Quantitative Features at 3T and 1.5T**

**Amie Y Lee MD (Presenter) ; Habib Rahbar MD ; Wendy B Demartini MD \* ; Savannah C Partridge PhD \* ; Matthew L Olson ; Sue Peacock MSC ; Constance D Lehman MD, PhD \***

#### PURPOSE

Breast MR is increasingly performed at 3T, which is hypothesized to improve lesion characterization over 1.5T due to higher spatial and contrast resolution. More accurate depiction of extent with 3T may be especially important for DCIS as surgical re-excision is often required due to imaging-occult components. Our purpose was to assess same patient MR features of DCIS at 3T and 1.5T.

#### METHOD AND MATERIALS

This IRB-approved prospective study included 20 patients (6/2010 to 5/2012) with newly diagnosed pure DCIS who underwent preoperative MR at both 3T and 1.5T. Both examinations had 3D T1-weighted fast gradient echo protocols with one pre- and three post-contrast series of approximately 180 seconds each. 3T (Philips Achieva TX) spatial resolution was 0.5 x 0.5 x 0.65 mm and 1.5T (GE LX) was 0.85 x 0.85 x 1.6 mm. 3T and 1.5T MR examinations were interpreted by different radiologists blinded to results of the second MR. Radiologist-assessed maximum lesion sizes were recorded, and whole-lesion kinetic synopses were computed using in-house automated software for 90 seconds initial and 450 seconds delayed phase enhancement. Sizes at 3T and 1.5T were correlated to final surgical pathology and differences in MR kinetics at 3T and 1.5T were evaluated (Spearman correlation, Wilcoxon signed-rank test).

#### RESULTS

DCIS mean sizes were 18.2 mm (0-67) on 3T, 18.2 mm (0-60) on 1.5T, and 14.1 mm (0-55) on pathology. Size correlation between imaging and pathology was higher for 3T (0.66, p=0.002), mean difference 7.5 (0-35) mm, compared to 1.5T (0.36, p=0.13), mean difference 11.5 (0-50) mm. Initial phase mean peak and % rapid enhancement were higher at 3T, but overall there were no statistically significant differences in initial or delayed phase kinetics at 3T compared to 1.5T, with mean peak enhancement 173.8 vs. 118.2 (p = 0.08), % medium 66.7 vs. 80.2 (p = 0.12), % rapid 33.3 vs. 19.8 (p = 0.12), % persistent 54.6 vs. 62.8 (p = 0.29), % plateau 23.2 vs. 21.0 (p = 0.05) and % washout 22.2 vs. 16.1 (p = 0.22).

#### CONCLUSION

In patients with newly diagnosed DCIS, lesion size at 3T MR had higher correlation than 1.5T with final pathology. Initial and delayed phase kinetics did not differ significantly between field strengths.

#### CLINICAL RELEVANCE/APPLICATION

3T may be more accurate than 1.5T in preoperative assessment of DCIS extent. Despite a hypothesized improved contrast resolution at 3T, DCIS kinetics did not differ significantly between 3T and 1.5T.

### **VBSR21-05 • Time-resolved Gadolinium-enhanced MR Imaging of the Breast**

**Hanan Sherif MD (Presenter) ; Ahmed-Emad Mahfouz MD ; Amal Alobadly MD ; Issam Albozom MD**

#### PURPOSE

To evaluate the very early onset of lesion enhancement on time-resolved ultrafast gadolinium-enhanced MR imaging as a differentiating sign between benign and malignant breast lesions.

#### METHOD AND MATERIALS

100 women with breast lesions were examined at 1.5 T (Siemens, Erlangen, Germany), by ultrafast T1-weighted GRE images every 5 s for 30 s after injection of Gd-DOTA (Dotarem, Guerbet, France), followed by 5 spacially-resolved MR image series every 30 s. Images were subtracted; maximum-intensity-projection images were obtained, and images were randomized and reviewed by two blinded readers, who reviewed only the spacially-resolved MR images and gave BIRADS diagnosis. After one month, they evaluated only the time-resolved MR images and noted the time of first appearance of enhancement.

#### RESULTS

The patients had 249 enhancing lesions: 66 malignant on histopathology and 183 benign on basis of histopathology or 1-year imaging follow-up. On time-resolved MR imaging, the onset of enhancement occurred 5-10 s after injection in 15 lesions (all malignant), 10-15 s in 23 lesions (21 malignant, 2 benign), 15-20 s in 34 lesions (28 malignant, 6 benign), and 20-25 s in 117 lesions (2 malignant, 115 benign). All malignant lesions enhanced before 25 s. Taking 20 s as the cut-off point, early enhancement had sensitivity of 96.9%, specificity of 95.6%, positive predictive value of 88.8%, negative predictive value of 98.8%, and accuracy of 95.9% for diagnosis of carcinoma. Based on the onset-of-enhancement sign the diagnosis of the spacially-resolved MR imaging has been corrected in 14 lesions (5.6%).

#### CONCLUSION

Time-resolved ultrafast gadolinium-enhanced MR imaging of the breast demonstrates earlier enhancement of malignant lesions compared to benign lesions. Lesion enhancement within the first 20 s is an accurate sign of breast carcinoma.

#### CLINICAL RELEVANCE/APPLICATION

Time-resolved imaging after injection of contrast agent increases accuracy of diagnosis of breast carcinoma. It is a useful addition to the protocol of gadolinium-enhanced MR imaging of the breast.

### **VBSR21-06 • Sensitivity of an Abridged Breast MRI Protocol to Detect a Known Breast Cancer**

**Laura Heacock MS, MD (Presenter) ; Amy N Melsaether MD ; Kristine M Pysarenko MD ; James S Babb PhD ; Hildegard B Toth MD ; Linda Moy MD**

#### PURPOSE

A shorter MRI may be cheaper, better tolerated by patients and faster for the radiologist to interpret. These changes may lead to wider access to Breast MRI. We evaluated the ability of an abridged MRI protocol to detect a known breast cancer.

#### METHOD AND MATERIALS

An IRB approved retrospective review of 100 breast MRI exams at 3T; with a unifocal biopsy-proven carcinoma was performed by two radiologists. Initially they evaluated the precontrast T1, first post-contrast T1 and first subtraction T1 post-contrast images blinded to the clinical history and prior films. Then they assessed the images given the above information and once more with the addition of the pre-contrast T2 images. The scan time for the 3 T1-sequences was 4 mins; the scan time for the T2-sequence was 4 mins. The time to interpret the study and the confidence score was assessed for each study. Comparison was made to the original diagnostic interpretation.

#### RESULTS

Of 100 cancers, 58 were masses, 25 were nonmass enhancement (NME) and 17 were categorized in the original report as both masses and NME. Sixty-two were invasive carcinomas, 29 were ductal carcinoma in situ (DCIS), and 9 were invasive carcinomas and DCIS. The mean size was 1.8 cm (range 0.6 - 10 cm). The sensitivity for both readers was 98% (CI 93.4% - 99.6%). Mean time for interpretation for reader 1 (R1) was 24secs (range 1 - 55 secs) for reader 2 (R2) was 14secs (range 3-77secs). R1 took an additional 10 secs to read and correlate the T2 image and R2 took 4.2 secs. R1 showed a significant increase in confidence (p 0.1) with the addition of either priors or T2 images. There was no significant correlation (r) between lesion size and either evaluation time (|r|0.5) or reader confidence (|r|0.35). Also, there was no significant difference (p>0.25) between lesion types in terms of evaluation time or reader confidence. Two

cases of DCIS were missed; both were seen on the 2nd post-contrast scan.

#### CONCLUSION

An abridged protocol has a high sensitivity for detecting known DCIS and invasive carcinoma and significantly reduced the interpretation time.

#### CLINICAL RELEVANCE/APPLICATION

Almost all cancers are detected with an abridged MRI protocol. The specificity and recall rates of a shorter exam should be examined to determine if this change may lead to wider access to breast MRI.

### **VSB21-07 • DCE MRI of the Breast: The Effect of Breast Compression on the Diagnosis and Staging of Breast Cancer**

**Riham H El Khouli MD, PhD (Presenter) ; Katarzyna J Macura MD, PhD \* ; Ihab R Kamel MD, PhD \* ; David A Bluemke MD, PhD \* ; Michael A Jacobs PhD**

#### PURPOSE

Breast compression stabilizes the breast to reduce motion and is used in conjunction with MRI guided breast biopsy. Our study aim was to evaluate the effect of breast compression on A) enhancement of both breast cancer and glandular tissue (GT) B) DCE MRI performance

#### METHOD AND MATERIALS

For this IRB approved retrospective study, we reviewed 425/210 studies/cases. Each patient had 2 or more MRI studies, 1 with and at least 1 without breast compression. We included 302 studies in total divided in 3 groups: 1) Biopsy proven breast cancer (102/59 studies/lesions), 2) Breast lesion detected on one MRI study and not the other (18/9 studies/lesions), 3) Cases with 1 study with unilateral compression (for GT enhancement difference, 90), and a noncompressed study (control, 92). %Enhancement difference between noncompressed and compressed studies for early and delayed post-contrast phases was calculated. Breast density, type of lesion (mass versus NMLE), lesion size, %Compression and kinetic curve type were evaluated

#### RESULTS

%Compression varied between 0 and 61%. Among 59 cancer cases, 39% were DCIS and 61% invasive. %Enhancement was higher in noncompressed versus compressed studies in both early and delayed phases (p-value 0.1)

#### CONCLUSION

Breast compression affected cancer detection, lesion size, and DCE MRI interpretation and performance. We recommend limiting the application of breast compression except when clinically necessary

#### CLINICAL RELEVANCE/APPLICATION

Many breast coils are capable of applying compression with a patient dependent degree. Compression significantly affected enhancement characteristics of breast cancer and DCE MRI diagnostic accuracy

### **VSB21-08 • Diffusion-weighted Imaging and Advanced Techniques**

**Savannah C Partridge PhD (Presenter) \***

#### LEARNING OBJECTIVES

1) Understand the physical basis of diffusion imaging and methods used to acquire diffusion-weighted data. 2) Understand the clinical applications of diffusion-weighted imaging for cancer diagnosis and assessment of response to therapy. 3) Be familiar with the challenges of breast diffusion imaging and technical considerations for protocol optimization. 4) Future directions.

#### ABSTRACT

### **VSB21-09 • Diffusion Weighted Imaging and Dynamic Contrast Enhanced Imaging in Breast Cancer at 7 Tesla**

**Stephan Gruber MD (Presenter) ; Olgica Zaric ; Katja Pinker-Domenig MD ; Lenka Minarikova ; Thomas H Helbich MD \* ; Siegfried Trattnig MD ; Pascal A Baltzer MD ; Wolfgang Bogner MSC**

#### PURPOSE

To assess the feasibility and diagnostic value of diffusion weighted imaging (DWI) in addition to contrast-enhanced imaging (DCE-MRI) with high spatial and/or temporal resolution in breast cancer at 7 Tesla. DWI has been shown to add important diagnostic value at lower field strengths (

#### METHOD AND MATERIALS

#### RESULTS

Both DWI and DCE-MRI provided excellent data quality with sub-milimeter spatial resolution approving great feasibility of these techniques in morphological evaluations. Based on the ADC threshold of  $1.35 \times 10^{-3} \text{mm}^2/\text{s}$ , DWI showed a 100% sensitivity and 100% specificity to distinguish between malignant and benign lesions. DCE-MRI, based on contrast enhancement kinetics and morphologic features, had a sensitivity and a specificity of 100%, 96%, respectively in breast lesions diagnostics.

#### CONCLUSION

This study shows that DWI and DCE-MRI at 7T are feasible in patients with breast cancer. In our pilot data we could demonstrate high sensitivity and specificity at 7T for both methods. At 7T, DWI automatically provides high-quality T2-weighted reference images ( $b=0 \text{ s/mm}^2$ ) that can replace additional T2-weighted MRI and, thereby, save valuable measurement time.

#### CLINICAL RELEVANCE/APPLICATION

Ultra high-field MR at 7T has the potential to improve sensitivity and specificity of DWI and DCE-MRI in the differential diagnosis between benign and malignant breast tumors.

### **VSB21-10 • Apparent Diffusion Coefficient in Invasive Ductal Breast Carcinoma: Correlation with the Tumor-stroma Ratio of Breast Cancer and Detailed Histologic Features**

**Eun Sook Ko MD (Presenter) ; Boo-Kyung Han MD, PhD ; Eun Young Ko MD, PhD ; Jung Hee Shin MD ; Soo Yeon Hahn MD**

#### PURPOSE

The purpose of this study was to determine whether ADC values vary according to tumor-stroma ratio, dominant stroma type or presence of central fibrosis.

#### METHOD AND MATERIALS

61 patients with invasive ductal carcinoma not otherwise specified (IDC NOS) who underwent breast MRI with diffusion-weighted imaging (DWI) were included in this study. Apparent diffusion coefficient (ADC) values of lesions were measured. Two pathologists evaluated the tumor-stroma ratio, dominant stroma type (collagen, fibroblast, lymphocyte), and central fibrosis. Detectability on DWI was compared according to tumor-stroma ratio. Mean ADC values were compared with tumor-stroma ratio, dominant stroma type, presence of central scar. Multiple linear regression analysis was also performed to determine variables independently associated with ADC values.

#### RESULTS

On DWI, detectability was not significantly different between two groups ( $P = 0.244$ ). ADC values were significantly lower in stroma-poor group ( $P < 0.001$ ). There was statistically significant difference of mean ADC values according to dominant stroma type ( $P = 0.021$ ). Mean ADC values in collagen dominant type were lower than fibroblast dominant or lymphocyte dominant type. At multiple linear regression analysis, tumor-stroma ratio ( $P = 0.007$ ), tumor size ( $P = 0.007$ ) and dominant stroma type (fibroblast dominant,  $P = 0.029$ )

were independently correlated with ADC values.

#### CONCLUSION

ADC values showed significant difference according to tumor-stroma ratio and dominant stroma type.

#### CLINICAL RELEVANCE/APPLICATION

Tumor-stroma ratio is known as independent prognostic factor of breast carcinoma. We hypothesized that these histopathologic features affect ADC values.

### **VSB21-11 • Dynamic Contrast Enhanced (DCE) and Diffusion Weighted Imaging (DWI) Breast MRI at 3T: A Road Map of MRI Characteristics for Breast Cancer Histological Subtypes Characterization**

**Riham H El Khouli** MD, PhD (Presenter) ; **Katarzyna J Macura** MD, PhD \* ; **Ihab R Kamel** MD, PhD \* ; **David A Bluemke** MD, PhD \* ; **Michael A Jacobs** PhD

#### PURPOSE

To evaluate the value of multiparametric breast MRI data at 3T (including morphology, DCE MRI and DWI with Apparent Diffusion Coefficient (ADC) mapping) in distinguishing between different breast cancer histological subtypes of pure Ductal Carcinoma In-Situ (pDCIS), Invasive Ductal and Invasive Lobular Carcinoma (IDC, ILC)

#### METHOD AND MATERIALS

Our institutional review board approved the study. Out of 1405 consecutive patients who underwent bilateral breast MRI at 3T, 219 patients with 234 lesions were included in the study (mean age 53+11.5 year). Both high temporal (15 sec) DCE and high spatial resolution (0.5 mm<sup>2</sup> voxel size) MRI were acquired along with DWI. Regions of interest were drawn on the ADC maps of breast lesions and normal appearing glandular tissue (GT). Morphologic features, DCE-MRI results (kinetic curve type), GT and lesion absolute and normalized ADC values were included in multivariate models for prediction of breast cancer histological subtypes. Area under ROC curve analysis was performed

#### RESULTS

Of 234 breast cancer lesions, 13.3% of were pDCIS, 31.6% IDC, 31.2% mixed DCIS and IDC, 13.7% ILC, 9% mixed IDC and ILC, and 1.3% were of miscellaneous . Lesion morphology (combining type of lesion with margin/distribution), Kinetic curve type, time to peak enhancement, and GT and lesion absolute and normalized ADC value were univariate predictors of breast cancer histological subtypes with an AUC 0.65-0.78. The multivariate diagnostic model combining lesion morphology, kinetic curve type, and normalized ADC value showed the best diagnostic accuracy (AUC 0.83). Using optimum cutoff value analysis, we developed a 3 category diagnostic model (AUC=0.83) consisting of 2 steps; 1) Differentiating pDCIS rather than invasive cancer if NMLE or smooth mass with a normalized ADC value >0.55. 2) Differentiating ILC rather than IDC for age of patient >59 and GT ADC value

#### CONCLUSION

DWI with normalized ADC map value assessment improves characterization of breast cancer histological subtypes beyond conventional morphological and DCE-MRI at 3T. Therefore, a 3 category Multiparametric Multi-steps MRI diagnostic model provides the potential for breast cancer histological subtypes characterization

#### CLINICAL RELEVANCE/APPLICATION

Different breast cancer subtypes have different MRI characteristics. We developed multivariate diagnostic model combining morphology, DCE, and DWI to distinguish different breast cancer subtype

### **VSB21-12 • Is Unenhanced Breast MRI Using Diffusion Weighted Imaging at 3 Tesla an Alternative to Dynamic Contrast Enhanced Breast MRI?**

**Pascal A Baltzer** MD (Presenter) ; **Hubert Bickel** MD ; **Wolfgang Bogner** MSC ; **Thomas H Helbich** MD \* ; **Stephan Gruber** MD ; **Katja Pinker-Domenig** MD

#### PURPOSE

Contrast enhanced breast MRI (ceMRI) is the most sensitive method for detection of breast cancer. Limiting factors for a broader availability of this method are costs caused by magnet time and the contrast agent. Diffusion Weighted Imaging (DWI) is increasingly used in clinical practice. It has shown its value for lesion detection and differentiation and has been used together with T2w TSE images as an unenhanced alternative (ueMRI) to ceMRI in mass lesions. The purpose of this study was to apply DWI only to a non-selected group of MRI patients referred during routine clinical practice and to compare the results to ceMRI in a multi-reader study.

#### METHOD AND MATERIALS

Patients from routine breast MRI at 3 Tesla referred due to conventional BI-RADS 3-5 ratings were eligible for this retrospective study and retrieved from our prospectively populated database. No dropouts due to incomplete examinations occurred. Two radiologists with >5 years experience in breast MRI (O1, O2) independently read ueMRI and ceMRI examinations and gave them a BI-RADS rating (1=no lesion, 2=benign lesion, 3=probably benign lesion, 4=suspected malignancy, 5= definite malignancy). Furthermore, lesion size, ADC values and BI-RADS criteria were assessed. Reference standard for radiological ratings was histopathology or imaging follow up. Statistical analysis included Receiver Operating Characteristics (ROC) analysis and kappa statistics.

#### RESULTS

67 malignant and 56 benign findings were identified in 119 patients (mean age 54+/-14y). Area under the ROC curve was 0.901 (O1) and 0.905 (O2) for ceMRI and 0.882 (O1) and 0.854 (O2) for ueMRI. The differences between observers and techniques were not statistically significant (P>0.05). However, specificity was 75% (O1) and 71% (O2) in ueMRI and 80% (O1) and 77% (O2) in ceMRI. Kappa agreement was high with 0.968 (ceMRI) and 0.893 (ueMRI).

#### CONCLUSION

Unenhanced MRI of the breast is feasible in clinical practice. While invasive cancers can be detected with equal sensitivity compared to ceMRI, ueMRI showed lower specificity and reproducibility.

#### CLINICAL RELEVANCE/APPLICATION

Due to equal sensitivity, ueMRI has potential to be applied as a screening sequence before ceMRI. Further studies are needed in order to clarify whether it could be a cost effective alternative.

### **VSB21-13 • MR Spectroscopy**

**Michael S Middleton** MD, PhD (Presenter) \*

#### LEARNING OBJECTIVES

1) Understand spectroscopy techniques. 2) Learn the biochemical basis for breast spectroscopy. 3) Interpret spectroscopy. 4) Understand potential applications of breast spectroscopy.

#### ABSTRACT

### **VSB21-14 • Role of 1H MRS Metabolic Profiling in Assessing Breast Cancer Recurrence**

**Dania Daye** BS (Presenter) ; **Suzanne L Wehrli** PhD ; **Dhruv Pant** ; **Christopher Sterner** ; **Mitchell D Schnall** MD, PhD ; **Lewis Chodosh** MD, PhD

#### PURPOSE

While dysregulated metabolism has long been recognized as a key feature of cancer development, the metabolic changes accompanying

cancer recurrence are largely unexplored. The goal of this study was to identify key metabolic differences between primary and recurrent mammary tumors using 1H MRS in combination with expression analysis of key metabolic enzymes and to assess the role of those findings in predicting human breast cancer recurrence.

#### METHOD AND MATERIALS

Our lab has developed an inducible bitransgenic mouse model which accurately reproduces key features of the natural history of human breast cancer progression: primary tumor development, tumor dormancy and recurrence. 9 primary and 9 recurrent mammary gland tumors were dissected from a cohort of 18 MMTV-rtTa;TetO-NeuNT mice in which Her2/neu is overexpressed specifically in the mammary glands. 1H MRS was performed at 400 MHz on a Bruker Avance DMX 400 wide-bore spectrometer. Gene expression levels of associated metabolic enzymes were obtained using qRT-PCR. A tumor metabolism gene expression signature was generated based on these results and used for human association analysis in five microarray datasets from patients with HER2-positive breast cancer.

#### RESULTS

Recurrent mammary tumors displayed higher levels of lactate ( $p=0.009$ ) and glycine ( $p=0.001$ ), lower levels of succinate ( $p=0.009$ ) and phosphocholine (PC) ( $p=0.013$ ), and a higher glutamate:glutamine ratio (glu/gln) ( $p$

#### CONCLUSION

Our results suggest that tumor metabolism evolves during breast cancer progression and raise the possibility that tumor metabolic changes may be useful for predicting clinical outcomes in breast cancer patients.

#### CLINICAL RELEVANCE/APPLICATION

1H MRS could potentially aid in predicting risk of relapse in patients diagnosed with HER2-positive breast cancer. More studies are needed to assess the role of MRS in breast cancer prognostication.

### **VSBR21-15 • Three Dimensional MR Spectroscopic Imaging Using DIXON Imaging for Water Content Correction and Improved Cho Quantification in Breast Cancer**

**Stephan Gruber MD (Presenter) ; Lenka Minarikova ; Katja Pinker-Domenig MD ; Thomas H Helbich MD \* ; Wolfgang Bogner MSC ; Siegfried Trattng MD ; Marek Chmelik MS**

#### PURPOSE

Fat contamination in breast tissue alters measured Cho SNR and consequently, the estimated Cho concentration measured by three dimensional MR spectroscopy (3D-MRSI). We propose a semi-quantitative Cho signal estimation with additional correction to tissue water content for each voxel, using information extracted from Dixon imaging.

#### METHOD AND MATERIALS

#### RESULTS

Average variance of initial Cho signal amplitude from selected voxels was 16.1 and 5.72 before and after correction. In vivo results showed a variance for Cho SNR of 2.05 and 0.256 before and after correction.

#### CONCLUSION

Variations of Cho concentrations in the phantom and in vivo were reduced after correction for fat/water content by a factor of ~3 and ~8, respectively. Furthermore, the influence of the CSI matrix position on Cho SNR in patient's data is minimized. Our method is able to compensate for deviations in matrix positioning (i.e. partial volume effects), which improves quantification of Cho. In this study we have shown that information deriving from Dixon images can be used as a partial water reference for Cho SNR in 3D-MRSI.

#### CLINICAL RELEVANCE/APPLICATION

Semi-quantitative 3D-MRSI based on fat/water-Dixon imaging reduces the variance of Cho signal. This is important for therapy monitoring and to distinguish between malignant and benign lesions.

### **VSBR21-16 • Quantitative Imaging of Breast Cancer: Association between Receptor Status, 18FDG-PET and 3 Tesla MRI Using DWI and 3D-MR-spectroscopy**

**Katja Pinker-Domenig MD (Presenter) ; Pascal A Baltzer MD ; Heinrich Magometschnigg ; Michael Weber ; Wolfgang Bogner MSC ; Stephan Gruber MD ; Georgios Karanikas MD ; Zsuzsanna Bago-Horvath ; Thomas H Helbich MD \***

#### PURPOSE

Expression of specific molecular markers such as estrogen receptor (ER), progesterone receptor (PR), and HER2 status assessed by invasive tissue sampling, has direct prognostic and therapeutic implications in breast cancer (BC) patient management. The aim of this study was to determine whether correlations exist between imaging biomarkers such maximum standardized up-take value (SUVmax) with 18FDG breast PET-CT or apparent diffusion coefficient (ADC) with diffusion weighted imaging and signal-to-noise ratio with 1H MR spectroscopy (MRSI) of the primary breast cancer lesions and IHC derived receptor status.

#### METHOD AND MATERIALS

In this IRB approved prospective study 249 patients with primary BC were included. Before surgery all patients underwent 3T MRI including DWI with ADC measurements in all patients. Cho-SNR obtained by 3D-1H-MRSI was available in 62 cancers. 134 patients underwent 18FDG breast PET-CT and SUVmax of tumors was calculated. Standard immunohistochemistry was performed on a surgical specimen. Appropriate statistical tests were used to test for possible associations among ER, PR, HER2 and imaging biomarkers.

#### RESULTS

#### CONCLUSION

#### CLINICAL RELEVANCE/APPLICATION

Assessment of the non-invasive imaging biomarker SUVmax with 18FDG breast PET-CT can provide valuable information about the state of ER, PR, and HER2 receptors of BC.

### **VSBR21-17 • MR Spectroscopy of the Breast at 3 Tesla: A Clinical Experience**

**Stefania Montemezzi MD (Presenter) ; Francesca Caumo MD ; Iliaria Baglio ; Lucia Camera ; Gabriele Meliado ; Carlo Cavedon DPhil**

#### PURPOSE

The study was aimed at improving the feasibility of total choline (tCho) detection in breast lesions and at estimating sensitivity and specificity of breast 3T-MR spectroscopy (MRS) to aid MR-based diagnosis of malignancy.

#### METHOD AND MATERIALS

141 patients (157 lesions, range 0.05-108.86 cm<sup>3</sup>, mean 6.62 cm<sup>3</sup>) were enrolled (21-84 yrs, mean 58.5 yrs). All patients had breast abnormalities on mammography or sonography, confirmed by cytology and/or micro-biopsy. Single-voxel MRS was performed by means of a Philips Achieva STx 3.0T scanner. First-order pencil-beam shimming was used on a 15.6 cm<sup>3</sup> volume centred on the region of interest (ROI), which ranged 0.34-8.0 cm<sup>3</sup> (mean 1.33 cm<sup>3</sup>). MRS used TE=135ms, TR=3000ms, 128 samples, water (window 140Hz) and fat (SPAIR, offset 80Hz) suppression. When possible, MRS was performed before contrast agent injection and repeated thereafter. Pre-saturation was used to suppress signal from nearby regions. Local field homogeneity was evaluated by means of the FWHM of the unsuppressed water peak. A threshold was placed at 45Hz, above which MRS was not performed due to insufficient field homogeneity. tCho was estimated by means of the signal-to-noise ratio (SNR) of the peak at 3.2 ppm.

#### RESULTS

MRS was feasible in 89.5% of the lesions using pencil-beam shimming (mean FWHM of water peak 34Hz), compared to 54.2% (29Hz) when standard iterative shimming was used (first 80 patients). 59 lesions (52.2% of reliable spectra) showed detectable tCho (SNR 1.4-53.7, mean 8.5). Comparison with available histopathological examination of surgical specimens (or micro-biopsy for benign lesions) showed 87.5% sensitivity and 86.0% specificity. No correlation between lesion volume and SNR of the tCho peak was observed. Malignant lesions that showed no tCho had a volume of 0.7cc or less.

#### CONCLUSION

High-field MR spectroscopy is expected to improve SNR of the investigated metabolites, however field homogeneity is more difficult to achieve compared to 1.5T. The adjustment of the shimming process improved the fraction of cases for which high-field MRS resulted feasible. Further research is warranted to improve choline detectability and to confirm the observed sensitivity and specificity of the method.

#### CLINICAL RELEVANCE/APPLICATION

MRS at 3T could improve the specificity of breast MR. Improving its feasibility is a key factor, however the possible correlation between tCho concentration and malignancy needs further investigation.

## Emergency Radiology Series: Advanced Concepts in Imaging of Trauma

Monday, 08:30 AM - 12:00 PM • E350



[Back to Top](#)

**VSER21** • AMA PRA Category 1 Credit™:3.75 • ARRT Category A+ Credit:4

#### Moderator

**Mariano Scaglione**, MD

#### Moderator

**Clint W Sliker**, MD

### VSER21-01 • Penetrating Wounds to the Torso: Evaluation with Multi-Detector CT

**Felipe Munera** MD (Presenter)

#### LEARNING OBJECTIVES

1) To discuss the role of MDCT in patients with penetrating torso trauma. 2) Describe MDCT protocol for penetrating torso injuries. 3) Review the MDCT findings of selected penetrating abdominal injuries.

#### ABSTRACT

Penetrating injuries account for a large percentage of visits to emergency departments and trauma centers worldwide. Emergency laparotomy is the accepted standard of care in patients with a penetrating torso injury who are not hemodynamically stable and have a clinical indication for exploratory laparotomy, such as evisceration or gastrointestinal bleeding. Continuous advances in technology have made MDCT an indispensable tool in the evaluation of many patients who are hemodynamically stable, have no clinical indication for exploratory laparotomy, and are candidates for conservative treatment. Multidetector CT may depict the trajectory of a penetrating injury and help determine what type of intervention is necessary on the basis of findings such as active arterial extravasation and major vascular, hollow viscus, or diaphragmatic injuries. Because multidetector CT plays an increasing role in the evaluation of patients with penetrating wounds to the torso, the radiologists who interpret these studies should be familiar with the CT findings that mandate intervention.

### VSER21-02 • Value of Contrast-enhanced CT in Detecting Active Hemorrhage Associated to Major Pelvic Trauma and Guiding Angiographic Treatment

**Ilenia Di Giampietro** (Presenter); **Grazia Loretta Buquicchio**; **Vincenza Di Giacomo**; **Guendalina Menichini** MD; **Michele Galluzzo** MD; **Margherita Trinci** MD; **Stefano Pieri** MD; **Vittorio Miele** MD

#### PURPOSE

In patients with major abdominal trauma, pelvic fractures associated to active hemorrhage are a common cause of hemodynamic instability. Therapeutic option depends on source and entity of bleeding: arterial hemorrhage requires angiographic embolization; the venous one or that from bone ends is treated conservatively with pelvic packing or external fixator. Our purpose is to establish the role of CT in the detection of active hemorrhage after major pelvic trauma compared to angiography.

#### METHOD AND MATERIALS

Between 9/2010 and 12/2012, 773 patients with major trauma underwent a CT examination in emergency department. Pelvic fractures were present in 180/773 patients. In all patient affected by pelvic fracture the presence of pelvic hematoma, intra- or retroperitoneal and/or in the soft tissue (glutes, adductors muscles), was searched. Authors look also for the presence of active contrast blush during the early arterial, the portal phase and near the stumps of bone fracture. Angiography was performed in 67 patients after CT detection of active bleeding or in case of not explained hemodynamic instability.

#### RESULTS

Among 180 patients with pelvic injury, 163 showed a pelvic hematoma; 27 a soft tissue hematoma. At CT active hemorrhage was identified in 47/180 cases (29 bleedings were visible in the arterial phase; 9 in the venous one; 2 in both of them; 11 near bone ends). All 47 patients underwent arteriography who showed hemorrhage in 22/29 cases of arterial bleeding, 3/9 case of venous phase bleeding, 2/11 cases of bleeding near bone ends. 20 patients underwent arteriography without evidence of active bleeding at CT; 4/20 showed active extravasation of contrast material. 2/20 underwent internal iliac embolization even in absence of extravasation.

#### CONCLUSION

CT has high sensitivity to detect active bleeding and to establish its origin, thus guiding the optimal therapeutic option. Our experience suggest to perform arteriography even in case of bleeding from bone ends or of venous origin, and when there is an hemodynamic instability without relevant CT findings.

#### CLINICAL RELEVANCE/APPLICATION

Our study highlights a new flow chart to follow in bleeding trauma of the pelvis in the polytrauma patient

### VSER21-03 • Trauma Whole Body MDCT: An Assessment of Image Quality in Conventional Dual Phase and Modified Triphasic Injection

**Raghavendra Kamanahalli** MD, FRCR; **Nishat Bharwani** MBBS; **Elizabeth A Dick** MD, FRCR; **Shirley Fetherston** BS; **Elika Kashef** FRCR (Presenter) \*

#### PURPOSE

To compare image quality of conventional arterial and portal venous (PV) phase CT with 2 modified triphasic injection protocols in trauma patients.

#### METHOD AND MATERIALS

60 whole body trauma MDCT were included. 20 consecutive MDCT were reviewed in each group. Group A arterial (30s) and PV (60s) phase acquisitions; Group B ♦triphasic♦ contrast injection with acquisition at 60s and Group C ♦modified triphasic♦ injection with

acquisition at 70s delay. All patients were imaged on a 256-slice scanner using IV Iomeron 400.

Images were analysed for arterial, venous and parenchymal attenuation profiles with regions of interest in the major arteries, veins and solid abdominal organs.

A 5-point scoring system was used to assess image quality: excellent studies with optimal arterial, venous and parenchymal opacification scored 5 while studies scoring

#### RESULTS

In 57 of 60 patients (95%) image quality was scored as good or excellent (=4). 1 study from each group scored 3, however all studies were considered to be of diagnostic quality.

With the exception of the common iliac arteries in group C ( $p = 0.03$ ), no statistically significant difference was demonstrated in the vascular attenuation using triphasic or conventional protocols. The average HU of the portal vein was significantly higher in group B and C ( $p = 0.0001$ ).

Attenuation profiles in the solid abdominal viscera were significantly higher ( $p = 0.002$ ) using both triphasic protocols than with conventional protocols.

Triphasic injection scans at 60s delay provided better arterial opacification than at 70s with comparable venous and parenchymal opacification.

#### CONCLUSION

In polytrauma, comparable image quality can be achieved using a triphasic IV contrast injection protocol with single MDCT acquisition as with conventional trauma MDCT using arterial and PV phase acquisitions.

#### CLINICAL RELEVANCE/APPLICATION

The use of a triphasic injection protocol with 256-slice MDCT results in dose reduction over conventional arterial followed by PV phase CT in polytrauma patients with no compromise in image quality.

### VSER21-04 • Thoracic Spine Fractures in Patients with Minor Trauma: Is the Conventional X-ray Necessary?

**Murat Karul MD (Presenter) ; Peter Bannas MD ; Amelie Hoffmann ; Bjorn P Schonngel ; Gerhard B Adam MD ; Jin Yamamura MD**

#### PURPOSE

To investigate the accuracy of biplane radiography in detection of thoracic spine fractures in patients (pts) with minor trauma using multidetector computed tomography (MDCT) as reference and to compare the mean effective dose of both techniques.

#### METHOD AND MATERIALS

107 consecutive pts (age  $67 \pm 20$ y) with minor trauma of the thoracic spine and low to moderate back pain on physical examination were included retrospectively. All had undergone biplane radiography first, followed by MDCT in a time frame of 10 days because of aggravation of their symptoms. Contingency table was used for classification of screening test results. Both Chi-square test ( $\chi^2$ ) and mean effective dose were used to compare diagnostic methods.

#### RESULTS

MDCT revealed 77 fractures in 65/107 pts (60.7%). Biplane radiography was true positive in 32 pts (29.9%), false positive in 19 pts (17.8%), true negative in 23 pts (21.5%), and false negative in 33 pts (30.8%), showing a sensitivity of 49.2%, a specificity of 54.7%, a positive predictive value of 62.7%, a negative predictive value of 41.1%, and an accuracy of 51.4%. Most fractures were diagnosed in the thoracolumbar junction (39/77; 50.6%). None of the fractures missed on biplane radiography was unstable. Presence of a fracture on biplane radiography was highly statistical significant, if this was simultaneously proven by MDCT ( $\chi^2 = 7.6$ ;  $p = 0.01$ ). Mean effective dose on biplane radiography was 0.7mSv, and on MDCT was 7.5mSv.

#### CONCLUSION

Sensitivity and specificity of biplane radiography in diagnosis of thoracic spine fractures in pts with minor trauma are low. The mean effective dose of MDCT was more than 10 times as high as on biplane radiography.

#### CLINICAL RELEVANCE/APPLICATION

Considering the wide availability of MDCT that is usually necessary for taking significant therapeutic steps, indication for biplane radiography in minor trauma pts should be very restrictive.

### VSER21-05 • Solid Organ Injury: What's New?

**Kathirkamanathan Shanmuganathan MD (Presenter)**

#### LEARNING OBJECTIVES

1) Demonstrate common and uncommon solid organ injuries. 2) Discuss the performance and utility of arterial phase imaging the solid organs. 3) Compare liver and splenic injury.

#### ABSTRACT

### VSER21-06 • Hyperdense Adrenal Glands on Contrast-enhanced CT Scans: Evaluation of the Clinical Impact in Polytrauma Patients

**Julia Schek MD ; Patric Kroepil MD ; Janina Klasen ; Philipp Heusch MD ; Gerald Antoch MD \* ; Rotem S Lanzman MD (Presenter)**

#### PURPOSE

The purpose of this study was to evaluate the clinical impact of hyperdense adrenal glands seen on contrast-enhanced CT scans of polytraumatized patients.

#### METHOD AND MATERIALS

292 trauma patients (195 male, 97 female, mean age  $45.3 \pm 23.3$  years) undergoing major trauma management in our Level I Trauma Center were included in this retrospective study. Standardized trauma management included CT scans of the brain, cervical spine, chest and abdomen, which were performed on a 6-row scanner (Emotion 6, Siemens, Erlangen, Germany). CT scans of the chest and abdomen were performed 60 s after the injection of 120 ml of iodated contrast material (Accupaque 300, GE Healthcare) at 110 kV. CT scans were retrospectively reviewed by two radiologists blinded to clinical data in consensus mode. ROIs were drawn in both adrenal glands and the inferior vena cava (IVC) in order to assess Hounsfield Units (HU). Patients were assigned to two groups; Group A (positive group), patients with hyperattenuating adrenal glands (HU adrenal gland > IVC) and Group B (negative group), patients without hyperattenuating adrenal glands (HU adrenal gland < IVC). The severity of injury was determined using the Injury Severity Score (ISS). The clinical outcome was analyzed using the electronic patient record.

#### RESULTS

18 patients (9 men and 9 women, mean age  $42.2 \pm 24.2$  years) were assigned to Group A (positive group) and 274 patients (186 men and 88 women, mean age  $48.4 \pm 22.4$  years) were assigned to Group B (negative group). Average signal intensity of the adrenal glands was  $150.8 \pm 36.1$  HU in group A as compared to  $83.7 \pm 23.6$  in group B ( $p < 0.0001$ ). 8 of 18 (44.4%) patients in group A and 33 of 274 (12.4%) patients in group B died during hospitalization ( $p < 0.05$ ). Patients in group A deceased  $2.1 \pm 3.7$  days following trauma as compared to  $6.4 \pm 11.8$  days in group B. Mean ISS did not differ significantly between both group A and B ( $26.2 \pm 24.0$  and  $18.06 \pm 16.72$ , respectively) ( $p > 0.05$ ).

#### CONCLUSION

Polytrauma patients with hyperdense adrenal glands on contrast-enhanced CT scans have a higher mortality rate as compared to patients

with regular attenuation of the adrenal glands.

#### CLINICAL RELEVANCE/APPLICATION

The presence of hyperdense adrenal glands on contrast-enhanced CT scans seems to be a predictor of poor clinical outcome.

### **VSER21-07 • Can MDCT Features of Mesenteric Injuries Be Used to Predict the Presence of a Surgical Bowel Injury?**

**Scott D Steenburg MD (Presenter) ; Matthew J Petersen MD**

#### PURPOSE

The purpose of this study was to determine if 64 slice MDCT imaging features of blunt mesenteric injuries can be used to predict the presence of a surgical bowel injury.

#### METHOD AND MATERIALS

The radiology archives at a Level 1 trauma center were searched over a 5 year period to identify patients with mesenteric injuries seen on admission 64 slice MDCT.

Two board certified emergency radiologists, blinded to clinical outcomes and surgical findings, independently reviewed each case. The size and number of each mesenteric contusion and/or hematoma, the presence or absence of active mesenteric bleeding, bowel wall thickening, free fluid, extraluminal gas, mesenteric vessel termination, mesenteric vessel beading, focal bowel wall defect, bowel wall perfusion abnormality, and bowel wall thickening >3mm were recorded. The radiologists subsequently assessed, based on the imaging findings, if they thought the patient had a surgical bowel injury requiring definitive therapy.

#### RESULTS

A total of 131 patients with MDCT diagnosis of mesenteric injury were identified. Mean age was 48.7 years (range 18-86) and 66.4% (n=87) were male.

Active bleeding was seen in 14.5% (n=19), bowel wall thickening in 92.3% (n=112) free fluid in 54.2% (n=71), mesenteric vessel termination in 10.7% (n=14), mesenteric vessel beading in 9.9% (n=13), focal bowel wall defect in 3.0% (n=4), and bowel wall perfusion abnormality in 12.2% (n=16) of patients. No patients had extraluminal gas. No patients received oral contrast medium per institutional trauma protocol.

A total of 18 patients underwent laparotomy based on imaging findings and/or clinical exam. Surgical bowel injuries were confirmed in 15 / 18 patients (83.3%). The remaining 113 patients were successfully managed non-operatively with no delayed diagnosis of bowel injury with a mean follow up interval of 527 days (range 1-2012 days).

Active bleeding, free fluid and mesenteric vessel beading were more common in patients with surgical bowel injuries. The accuracy, sensitivity, specificity, PPV and NPV of 64 slice MDCT in predicting the presence of a surgical bowel injury were 74.8%, 80.8%, 74.4%, 28.6% and 96.6%, respectively.

#### CONCLUSION

MDCT has only modest accuracy and sensitivity for predicting the presence of surgical bowel injuries.

#### CLINICAL RELEVANCE/APPLICATION

The diagnosis of surgical bowel injuries remains challenging despite 64-slice MDCT technology.

### **VSER21-08 • QandA/Break**

### **VSER21-09 • CT of Cardiac Trauma in the ED**

**Sanjeev Bhalla MD (Presenter)**

#### LEARNING OBJECTIVES

1) Understand the spectrum of cardiac injury in the setting of blunt and penetrating trauma mainly on CT. The role of cardiac MR will also be discussed.

### **VSER21-10 • Radiological Findings and Severity of Injuries in Patients with Acute Alcohol Intoxication**

**Yuka Morita MD (Presenter) ; Taiki Nozaki MD ; Jay Starkey MD ; Masaki Matsusako MD, PhD ; Hiroshi Yoshioka MD ; Yukihiisa Saida MD ; Yoshinao Sato MD ; Saya Horiuchi MD ; Makoto Goto ; Takaharu Suzuki**

#### PURPOSE

To review the radiological findings of fractures with acute alcohol intoxication and discuss their characteristic features.

#### METHOD AND MATERIALS

The institutional review board approved this retrospective study with a waiver of informed consent. A total of 1286 adult patients (median age 57.0 years, range 20-102 years; male 748 (58.2%), female 538 (41.8%)) who visited our emergency department (ED) and presented with fractures during July 2010 and December 2011 were retrospectively reviewed. Patients were divided into 2 groups: the intoxicated group and non-intoxicated group before the injury by chart review. Differences of the clinical features and radiological findings were compared between the two groups.

#### RESULTS

One-hundred and eighty one (14%) patients were grouped into the intoxicated group (median age 51.0 years, range 20-85 years; male 148 (81.8%) and female 33 (18.2%)) and 1105 (86%) were grouped into the non-intoxicated group (median age 58.0 years, range 20-102 years; male 600 (54.3%) and female 505 (45.7%)). The intoxicated group showed higher rate of head/neck fractures and lower rate of extremities than the non-intoxicated group with statistical significance (skull 23.2% vs 5.8%; p

#### CONCLUSION

The alcohol-intoxicated patients who visit the emergency department are at higher risk of head/neck fractures than non-intoxicated patients.

#### CLINICAL RELEVANCE/APPLICATION

To understand the characteristic patterns of fractures in alcohol intoxicated patients and the differences from non-intoxicated patients is essential for our radiological assessments.

### **VSER21-11 • Relevance of Incidental Findings in Seriously Injured Patients - The Necessity of Appropriate Management Procedures**

**Thomas Lehnert MD (Presenter) ; Josef Matthias Kerl MD \* ; Julian L Wichmann MD ; Ralf W Bauer MD \* ; Claudia Frellesen ; Thomas J Vogl MD, PhD**

#### PURPOSE

The multislice computed tomography (MSCT) is the gold standard in the initial evaluation of trauma patients. Besides providing information regarding the presence or absence of acute trauma-related injuries, MSCT scans also reveal pathologies unrelated to the trauma which may be clinically significant. The aim of the present study was to determine the frequency and clinical importance of incidental findings in multiple injured patients at a level one trauma centre.

#### METHOD AND MATERIALS

This is a retrospective analysis of prospectively collected data on 2242 multiple injured patients at a level I trauma centre from 2006 to 2010. A total 2,036 patients (91%) underwent an initial MSCT. The MSCT reports were retrospectively reviewed regarding unexpected findings not related to trauma. These incidental findings were rated on a 4-point level scoring system regarding clinical importance and urgency of initiation of further steps.



## RESULTS

1142 (49.9%) of the patients had one or more incidental findings. A total of 2844 incidental findings were detected. Overall 349 tumor findings were noted (12.3% of all incidental findings). 113 findings were suspicious for malignant processes or metastasis. Regarding the clinical importance, 168 (5.9%) of the incidental findings required urgent follow-up (Level 4) and 527 (18.5%) of the incidental findings required a follow-up prior to discharge (Level 3).

## CONCLUSION

MSCT in multiple injured patients reveals one or more incidental findings in more than one out of two patients. A scoring system classifying the actual relevance of each incidental finding applicable in daily routine of patient care could be introduced.

## CLINICAL RELEVANCE/APPLICATION

The consequent handling of incidental findings may burden trauma surgeons and emergency physicians additionally, but should lead to a responsible health care for the patients.

### **VSER21-12 • Simplified Approach to Midface Trauma**

**O. Clark West MD (Presenter) \***

#### LEARNING OBJECTIVES

1) Apply a simplified approach to midface trauma CT as described by James T. Rhea, MD. 2) Identify major patterns of midface injury. 3) Incorporate **◆**butress**◆** terminology into facial CT reports.

### **VSER21-13 • Comparison of MRI, CT Scan and Plain Hip Radiograph for the Early Diagnosis of Hip Fracture in Emergency Patients**

**Laleh Daftaribesheli MD (Presenter) ; Shima Aran MD ; Hani H Abujudeh MD, MBA \***

#### PURPOSE

Comparison of hip MRI results with plain hip radiograph and CT, and evaluating their role in diagnosis of patients with suspected hip fracture in emergency room

#### METHOD AND MATERIALS

The medical records of 314 patients who had MRI in emergency room of Massachusetts General Hospital from January 2008 to January 2013 with a suspected hip fracture were retrospectively reviewed. Patients **◆** mean age was 63 years old and 70% of patients were female. 281/314 had hip x-ray and 18/314 had both MRI and CT in addition to x-ray

#### RESULTS

MRI could diagnose 96/314 patients with hip fracture, 6/96 reports were non definitive. X-ray reported 27/281 positive cases with 16/27 being non definitive. CT was positive in 9/18, with 1/9 being non definitive. In patients with all 3 examinations, according to MRI 9/18 patients had fractures and 9/18 were negative. In 12/18 cases MRI and CT report were completely consistent with each other. In 2/18 patients both CT and x-ray were negative for the fractures reported in MRI. In one case (1/18) with positive CT and negative x-ray happened to be negative by MRI.

Of 90/314 definite cases with MRI, 88/90 patients had plain hip x-ray which was positive in 9/88 patients. In 3/9 its diagnosis was ruled out by MRI. 7/88 of x-ray reports were non definitive for fracture. X-ray reported the wrong site of fracture in 3/88 cases and in 2/88 cases it diagnosed fractures which were ruled out by MRI. Our results showed that plain hip radiograph in addition to being negative in nondisplaced fractures was reported negative in patients with minimally displaced to displaced fractures, and in patients with both types of displaced and nondisplaced. Plain hip radiograph could not detect the fracture in 75/88 (85%) of patients with definite fractures on MRI and in 5/88 (5.6%) of all patients with both examinations it reported false positive fractures or wrong location of the fracture. The sensitivity of plain film in these patients after deleting suspicious cases was found to be only 7.6%.

#### CONCLUSION

These results favor the advantage of immediate MRI imaging specially in female elderly patients with suspected hip fracture

#### CLINICAL RELEVANCE/APPLICATION

Use of MRI instead of CT and routine use of plain hip radiograph as a first step in diagnosis of patients with suspected hip fracture in emergency room eliminates the unnecessary exposure to radiation

### **VSER21-14 • The Degree of Articular Depression as a Predictor of Soft-tissue Injuries in Tibial Plateau Fracture**

**Marc Regier (Presenter) ; Frank Oliver G Henes MD ; Azien Laqmani ; Gerhard B Adam MD ; Alexander Spiro**

#### PURPOSE

Magnetic resonance imaging (MRI) provides sufficient information with regard to specific soft-tissue injuries in the knee, but in daily clinical routine it is not generally used to evaluate acute tibial plateau fractures. The aim of the present study was to intraindividually evaluate whether the amount of tibial plateau fracture depression at multi-detector computed tomography (MDCT) scans correlates with the incidence of associated soft-tissue injuries determined at MRI.

#### METHOD AND MATERIALS

A total of 54 consecutive patients with a mean age of 51.2 years (range, 33 **◆** 69 years) were included in this intraindividual comparative study. All patients were admitted to the emergency department of a university medical center with acute tibial plateau fracture. Within the emergency department a 256 slice MDCT was conducted in each patient (Voltage, 120 kVp; current-time product, 110 mAs). Within a mean time interval of 2.8 days (range, 0 **◆** 5 days) MR imaging was performed using standard T1w and T2w sequences at 3 Tesla. Image readout was consensually performed by an experienced musculoskeletal radiologist and an orthopedic traumatologist, who assigned the Schatzker classification and measured the articular depression. Statistical analysis included ANCOVA and logistic regressions.

#### RESULTS

#### CONCLUSION

Articular depression assessed by MDCT seems to be a potential predictor of specific meniscal and ligamentous injuries in acute tibial plateau fractures. Therefore, if articular depression is observed at MDCT, MR imaging should generally be recommended in addition with respect to associated soft-tissue lesions.

#### CLINICAL RELEVANCE/APPLICATION

If articular depression due to acute tibial plateau fracture is detected at MDCT, MRI should be considered indispensable in order to prevent missing concomitant soft-tissue injuries.

### **VSER21-15 • Panel/QandA**

---

## **Gastrointestinal Series: Emerging Issues in Abdominal CT**

**Monday, 08:30 AM - 12:00 PM • N227**

**Moderator**

**Giles W Boland**, MD

**Moderator**

**Jonathan B Kruskal**, MD, PhD \*

### **VSGI21-01 • Oral Contrast Issues**

**Perry J Pickhardt** MD (Presenter) \*

#### LEARNING OBJECTIVES

1) Understand the relative advantages and disadvantages of the use of positive oral contrast in abdominal CT imaging for a wide variety of clinical scenarios.

### **VSGI21-02 • Discontinuation of Positive Oral Contrast for Routine CT Scans Does Not Result in Substantial Repeat Scans**

**Wilbur Wang** BA (Presenter) ; **Nikita Shah** ; **Michael A Ohliger** MD, PhD ; **Yanjun Fu** PhD ; **Zhen J Wang** MD ; **Benjamin M Yeh** MD \*

#### PURPOSE

To evaluate the rate of repeat scans after an institution-wide policy to discontinue the routine administration of positive oral contrast in favor of oral tap water for routine abdominal CT examinations.

#### METHOD AND MATERIALS

From a total of 12,370 abdominal CT scans performed at our institution from March 9, 2009 to June 26, 2012, we identified all repeat abdominal CT scans occurring between 2 hours and 14 days after an initial abdominal CT scan. On March 9, 2009 our department discontinued the routine administration of positive oral (iodinated) contrast in favor of oral tap water for such scans. Readers recorded the presence of oral and IV contrast in both initial and repeat abdominal CT scans images. For scans in which positive oral contrast was given, the reason for administering oral contrast was given..

#### RESULTS

From a total of 12,370 abdominal CT examinations, 439 (3.5%) were repeat scans, and of these, 47 scans (10.7%) used oral contrast on the repeat CT scan but not the initial. The most common reasons for administration of oral contrast were for evaluation of abscess (40.0%), evaluation for perforation (33.1%), and obstruction (13.1%). Only 11 out of the 439 repeat scans (2.5%) were explicitly performed due to a need for oral contrast in the repeat scan (0.09% of all scans). Significantly fewer repeat scans used oral contrast (either on the initial study or repeated study) in 2012 (5 of 60 scans, or 8.3%) compared with 2009 (76 of 215 scans, or 35.3%,  $P < .01$ ). Overall, the frequency of repeat abdominal CT scans significantly decreased from 4.7% in 2009 to 2.8% in 2012 ( $P < .001$ ).

#### CONCLUSION

The discontinuation of positive oral contrast from routine abdominal CT protocols at our institution led to a miniscule frequency of repeat examinations (0.09% of all scans) which diminished over 3 years. Our findings support the continuation of this policy, especially when weighed against the inconvenience, expense, and potential complications of administering oral contrast to every patient.

#### CLINICAL RELEVANCE/APPLICATION

Discontinuation of positive oral contrast from routine abdominal CT exams does not result in a substantial frequency of repeat examinations with oral contrast.

### **VSGI21-03 • Radiation Dose Reduction Techniques**

**Rendon C Nelson** MD (Presenter) \*

#### LEARNING OBJECTIVES

1) To understand the pros and cons of radiation dose reduction in CT. 2) To learn methods for radiation dose reduction that do not impact image quality. 3) To learn methods for radiation dose reduction that do impact image quality. 4) To understand the implications of using iterative reconstruction techniques for CT.

### **VSGI21-04 • Abdominal CT Radiation Doses (Conventional and Organ Doses) from Large Academic Institute with 3 Scan Vendors and Different Iterative Reconstruction Techniques**

**Sarvenaz Pourjabbar** MD (Presenter) ; **Sarabjeet Singh** MD ; **Mannudeep K Kalra** MD \* ; **Atul Padole** MD ; **Ranish D Khawaja** MBBS, MD ; **Diego A Lira** MD ; **Sanjay Saini** MD

#### PURPOSE

To assess and compare radiation doses for abdominal CT examinations performed with different scanning protocols, various scan manufacturers and models, with and without iterative reconstruction in routine clinical settings.

#### METHOD AND MATERIALS

This IRB-approved, HIPAA-compliant study included 8758 consecutive abdomen-pelvis CT exams (mean age: 59.3±16.6 years; M: F=4469:4288). Automatic dose monitoring software (Exposure, Bayer) was used to retrieve patient demographics, including date of birth, gender, weight, patient maximum skin to skin diameters, CTDIvol, DLP, effective doses, Size Specific Dose Estimates (SSDE), as well as organ doses. Selected scan protocols and scanner models with information on Iterative Reconstruction (IR) were also recorded. Analysis of variance was used to evaluate differences across above variables. P-value of 0.05 with 95% confidence interval was considered significant.

#### RESULTS

Distribution of CT examinations per scanner included 16-slice GE (n=3200), 64-slice GE (n=1730), 64-slice Philips (n=176), 128-Siemens (n=221) and 256-Philips (n=724). Abdominal CT were performed with several clinical protocols, including routine abdominal CT (n=2963), stone/hematuria (n=570) and cancer follow up (n=1385). Stone protocols were performed more commonly on 64-GE with mean CTDIvol (n=344, 8.5±3.3 mGy), 16 GE (n=220, 10.5±3.8 mGy), and 256-Philips (n=144, 8.4±5 mGy). Routine abdominal CT were stratified in 4 weight groups, less than 135lbs (n=683, 6±2 mGy), 136-200lbs (n=2257, 9±2.5 mGy), 200-300lbs (n=812, 13 ± 3.2 mGy) and more than 300lbs (n=51, 26±8 mGy). Estimated effective doses for iterative reconstruction scanners were 8 ±3 (n=764, Discovery750HD) 9 ± 3 (n=133, Definition FLASH) and 7± 3 (n=124, Brilliance iCT). Organ doses are summarized in a graphical manner in figure 1.

#### CONCLUSION

Clinical indication, CT scanner, and size based variations in abdominal CT protocols help in optimization of radiation doses. Although CT dose indexes provide good estimates for comparing across CT scanners, organ doses should be used for comparing patient doses.

#### CLINICAL RELEVANCE/APPLICATION

Abdominal CT examinations doses ranged from 6 to 26 mGy and hence it is important to optimize based on clinical indication, weight and iterative reconstruction technique.

### **VSGI21-05 • Observer Performance for Site-specific Detection and Correct Classification of Malignant Liver Lesions for an Image-based Denoising Method and Iterative Reconstruction**

**Joel G Fletcher** MD (Presenter) \* ; **Lifeng Yu** PhD ; **Zhoubo Li** ; **Armando Manduca** PhD \* ; **Daniel J Blezek** PhD ; **David M Hough** MD ; **Sudhakar K Venkatesh** MD, FRCR ; **Gregory C Brickner** MD ; **Joseph G Cernigliaro** MD ; **Amy K Hara** MD \* ;

#### PURPOSE

Noise reduction techniques may improve subjective image quality, but few studies have addressed impact on diagnostic performance. Our purpose was to determine if lower dose (LD) CT images reconstructed with image-based noise reduction (Noise Map; NM) or an IR technique (SAFIRE; Siemens Healthcare) resulted in reduced observer performance for detection of primary or secondary liver tumors (LTs), compared to routine dose filtered back projection (FBP) images.

#### METHOD AND MATERIALS

CT projection data from 60 CT exams were collected (30 abdomen at 16 mGy, 30 liver at 23 mGy; 31 with LTs). Presence of LTs was defined by progression/regression on CT/MR or pathology. Using a validated noise insertion tool, LD NM, LD FBP, and LD SAFIRE images were created corresponding to 12 mGy (abd) or 14 mGy (liver). In each reading session, 3 readers randomly evaluated either routine dose FBP, LD FBP, LD NM, or LD SAFIRE images. 3 mm CT images were reviewed on a dedicated computer workstation, with readers circling all liver lesions, then selecting a diagnosis (LT vs. individual benign diagnoses) and confidence score (0-100), and grading image quality. Reference detections were similarly marked, with automated matching of reference and reader lesions using an overlapping spheres method. JAFROC analysis was performed on a per-lesion basis for LTs, with true positives correctly localized and classified. A limit of non-inferiority of -0.1 was defined a priori.

#### RESULTS

There were 73 LTs with a median size of 1 +/- 1 cm. The JAFROC figure of merit (FOM) overlapped for routine dose FBP, LD FBP, and LD NM (FOM 95% CI = 0.84-0.95, 0.79-0.93, 0.82-0.93, respectively for routine FBP, LD FBP, LD NM), with the estimated differences between routine FBP and LD FBP or NM being non-inferior. Similarly, JAFROC FOMs were similar between routine dose FBP and each LD approach in the subset of 44 cases with SAFIRE (0.97 vs. 0.94, 0.93, 0.94), with LD approaches being non-inferior. Diagnostic image quality was greatest for LD images with noise reduction ( $p < 0.03$  all readers).

#### CONCLUSION

Lower dose CT images reconstructed with FBP, NM and SAFIRE can be interpreted without loss of diagnostic performance despite the improved image quality of NM and SAFIRE.

#### CLINICAL RELEVANCE/APPLICATION

Although perceived quality of LD images was improved with use of noise reduction methods, observer performance was not significantly different than for FBP even for challenging liver tumors.

### **VSGI21-06 • Prospective Evaluation of Prior Image Constrained Compressed Sensing (PICCS) Algorithm in Abdominal CT: Preliminary Results Comparing Reduced Dose with Standard Dose Imaging**

**Meghan G Lubner MD (Presenter) ; David H Kim MD \* ; Jie Tang PhD ; Perry J Pickhardt MD \* ; Alejandro Munoz Del Rio PhD ; Guang-Hong Chen PhD \***

#### PURPOSE

To report preliminary prospective results of an ongoing CT dose reduction trial using Prior Image Constrained Compressed Sensing (PICCS).

#### METHOD AND MATERIALS

50 patients (23 F, 27 M, mean age 57.7 years, mean BMI 28.6) were scanned in this HIPAA compliant, IRB approved study. Immediately following routine contrast-enhanced (n=26) or unenhanced (n=24) abdominal MDCT, a second reduced dose (RD), matched series scan was performed (target dose reduction 70-90%). DLP, CTDI<sub>vol</sub> and SSDE were compared between scans. Multiple reconstruction algorithms (standard filtered back projection (FBP), adaptive statistical iterative reconstruction (ASIR), and Prior Image Constrained Compressed Sensing (PICCS)) were applied to the RD series. Standard dose images (SD) were reconstructed with FBP (reference standard). Two blinded readers evaluated each series for subjective image quality and focal lesion detection. Objective noise and region of interest attenuation (HU) were measured at designated sites.

#### RESULTS

Mean DLP, CTDI<sub>vol</sub>, effective diameter and SSDE for the RD series was 140.3 mGy\*cm (median 79.4, range 15.9-526.6), 3.7 mGy (median 1.8, range 0.4-26.4), 30.1 cm (median 30, range 24.6-38.0), and 4.15 mGy (median 2.31 range 0.59-24.3) compared to 493.7 mGy\*cm (median 345.8, range 57-1453.7), 12.9 mGy (median 7.9 mGy, range 1.43-79.8) and 14.6 mGy (median 10.1, range 2.1-73.4) for the SD series respectively. This is a mean SSDE reduction of 72%. RD PICCS image quality score was 2.8±0.5, improved over the RD FBP and RD ASIR scores (1.7±0.7 and 1.9±0.8 respectively), but less than the SD score of 3.5±0.5 ( $p$

#### CONCLUSION

PICCS allows for marked dose reduction at abdominal CT at the expense of subjective image quality scores and diagnostic performance. Further study is needed to determine optimal dose reduction level to maintain acceptable diagnostic accuracy.

#### CLINICAL RELEVANCE/APPLICATION

PICCS allows for substantial CT dose savings (70-90%), lowering the dose for some applications (urolithiasis, colon ca screening) into the sub-mSv range.

### **VSGI21-08 • Dual Energy CT**

**Alec J Megibow MD, MPH (Presenter) \***

#### LEARNING OBJECTIVES

1) Understand basic physical principles that support Dual Energy CT applications for abdominal imaging. 2) Familiarize audience with radiation dose and image quality as they relate to Dual Energy CT. 3) Demonstrate the value of unique dual energy CT capabilities drawing on examples from abdominal imaging capabilities.

### **VSGI21-09 • Can Multi-material Decomposition Algorithm Generated Virtual Unenhanced (VUE) Images from Single Source Dual-energy CT meet the Qualitative and Quantitative Expectations of True Unenhanced (TUE)?**

**Mukta D Agrawal MBBS, MD (Presenter) \* ; Jorge M Fuentes MD ; Avinash R Kambadakone MD, FRCR ; Yasir Andrabi MD, MPH ; Shaheen Sombans MBBS ; Jannareddy Namrata Reddy MBBS ; Koichi Hayano MD ; Dushyant V Sahani MD**

#### PURPOSE

We investigated the performance of recent commercially available multi-material decomposition (MMD) algorithm rendered VUE images for image quality/texture improvements and attenuation (HU) measurements.

#### METHOD AND MATERIALS

In IRB approved prospective study, 33 consecutive patients had arterial and delayed phase ssDE-CTA (GE discovery CT750 HD) of the abdomen for AAA. The VUE images were generated using MMD algorithm. Each patient also had true unenhanced exam (TUE) for comparison. Three independent readers assessed the image quality and acceptance of VUE for TUE using a four-point scale. Visualization of incidental findings such as renal stones, vascular calcification, fatty liver, and cysts was evaluated. For quantitative measurement, attenuation values (HU) of liver, kidney, muscle and background fat were obtained on TUE and VUE. Pearson correlation coefficient was used for statistical analysis.

#### RESULTS

The MMD-VUE images were rated acceptable in all 33 exams and actually preferred by all three readers over TUE (IQ score 3 vs 2.1). All renal stones (n=17), vascular calcification (n=33) and fatty liver infiltration (n=13) were accurately detected on MMD-VUE images. The

mean HU on MMD-VUE demonstrated good to excellent correlation with TUE values for liver (r=0.85), kidney (r=0.7), muscle (r=0.82) and fat (r=0.9). The mean attenuation difference (HU) between TUE-VUEa, TUE-VUEd and VUEa-VUEd for liver, kidney, muscle and fat was

#### CONCLUSION

The MMD algorithm rendered VUE images meet the clinical expectations of quality and quantitative measurements and therefore a viable replacement of TUE.

#### CLINICAL RELEVANCE/APPLICATION

Virtual unenhanced CT images that are quantitatively and qualitatively comparable to true unenhanced CT images are expected to bring workflow and radiation dose savings benefits.

### VSGI21-10 • The Clinical Impact of Retrospective Analysis in Spectral Detector Dual Energy Body CT

**Michal H Gabbai MD (Presenter) ; Isaac Leichter PhD ; Zimam Romman \* ; Amiaz Altman PhD \* ; Jacob Sosna MD \***

#### PURPOSE

In existing tube-based dual-energy CT (DECT), dual-energy protocols must be prescribed in advance to select tube voltage or operate the two tubes at different kV. Spectral detector-based DECT enables retrospective reconstruction and analysis of data obtained from a single CT acquisition with no requirement to plan a dual-energy protocol in advance. The purpose of this study was to assess the potential added value of retrospective dual-energy reconstruction features.

#### METHOD AND MATERIALS

A total of 43 patients were scanned with a novel Spectral Detector CT (SDCT) prototype (Philips Healthcare, Cleveland, OH, USA). IRB approval and patient consent were obtained. The clinical indication for each case was evaluated, and indications were compared to the final diagnosis by two radiologists in consensus. The number of cases in which retrospective analysis of spectral data could potentially assist in the diagnosis while the indication on the request did not suggest in advance the use of dual-energy reconstruction was analyzed.

#### RESULTS

SDCT data helped to achieve the diagnosis for 19 out of 43 patients (44%). In 8 of the 43 (18.6%), clinical history on the study request indicated potential advantage from use of a dual-energy protocol (4 suspected pulmonary emboli, 2 suspected kidney stones, 1 suspected insulinoma, 1 suspected hepato cellular carcinoma). In the remaining 35 patients, dual-energy reconstruction was not indicated from the referral. In 11 of the 35 patients (31%) retrospective spectral detector reconstruction improved visualization of the following unexpected pathologies: 2 incidental adrenal adenomas (contrast enhanced CT, virtual non-enhanced images), 2 pelvic DVT cases (low KeV images), 3 pancreatic cysts (with low KeV, improved contrast-to-noise), 3 metal implants (reduced artifacts at higher KeV), and one abdominal aortic aneurysm (suboptimal CTA visualized at low KeV).

#### CONCLUSION

Retrospective spectral image reconstruction and analysis may frequently offer clinical advantage in cases where DECT is not indicated based on clinical history.

#### CLINICAL RELEVANCE/APPLICATION

Spectral detector-based dual-layer CT allows retrospective reconstruction and post-processing image analysis that may frequently be useful in clinical practice.

### VSGI21-11 • CT Perfusion

**Benjamin M Yeh MD (Presenter) \***

#### LEARNING OBJECTIVES

1) Understand the potential benefits and drawbacks of imaging contrast material inflow and outflow for improving clinical diagnoses in the abdomen and pelvis, including for the evaluation and monitoring of tumors and fibrosis. 2) Review methods for quantifying different parameters associated with contrast material distribution into abdominopelvic tissues. 3) Show methods to improve consistency and radiation dose with CT perfusion imaging.

#### ABSTRACT

Use of intravenous contrast material is critical to the evaluation of a broad range of abdominopelvic diseases at CT. The rate of inflow and outflow of contrast material relative to arterial flow and intravascular concentrations, as well as distribution of contrast materials into tissues, reflect the underlying vascular and micro vessel physiology of tissues. On a simplistic level, subjective evaluation of enhancement relative to normal tissues is used routinely by radiologists to detect, characterize and monitor tumors and inflammatory processes. More advanced dynamic contrast enhanced imaging can be used to quantify such microvessel parameters as blood volume, blood flow, mean transit time, arterial fraction, extracellular fraction, and permeability surface, and has been studied in particular for monitoring treatment response in tumors. Simple equilibrium imaging can be used to assess relative washout and extracellular fraction, and appears to be a potentially valuable method to quantify and monitor a wide range of disease.

### VSGI21-12 • Role of Perfusion CT in Characterization of Pancreatic Mass Lesions

**Raju Sharma MD (Presenter) ; Ajay K Yadav MBBS ; Devasenathipathy Kandasamy ; Shivanand R Gamanagatti MBBS, MD ; Ashu Seth Bhalla MBBS, MD ; Peush Sahni MBBS, MS ; Arun K Gupta MBBS, MD**

#### PURPOSE

Perfusion CT (PCT) provides quantitative information regarding blood perfusion and permeability in tissues in a noninvasive way. This prospective study was conducted to evaluate the utility of PCT findings in characterization of pancreatic mass lesions

#### METHOD AND MATERIALS

PCT was done in 67 patients with histopathologically proven pancreatic mass. The spectrum of pancreatic pathology included adenocarcinoma (30), cystic neoplasm (21), neuroendocrine tumor (8), mass forming chronic pancreatitis (3), metastatic mass (3) and pancreatic tuberculosis (2). Perfusion parameters evaluated were blood flow (BF) and blood volume (BV). 25 controls with no pancreatic pathology were also studied

#### RESULTS

No significant difference in perfusion parameters was noted in head, neck, body and tail of pancreas in control groups (BF 52-150ml/100ml/min and BV 22-50ml/100ml). Neuroendocrine tumors showed the highest perfusion values (BF 122-260ml/100ml/min and BV 30-40ml/100ml) in comparison to normal pancreas. Cystic pancreatic tumors showed the least perfusion values (BF 0.2-34ml/100ml/min and BV 0.5-15 ml/100ml) followed by adenocarcinoma (BF 2.8-36ml/100ml/min and BV 0.5-18 ml/100ml), metastatic and inflammatory pancreatic masses in increasing order. BF and BV were significantly reduced in the center of pancreatic adenocarcinoma and gradually increased from center to periphery of the lesion, as opposed to cystic tumors which showed homogeneous reduction

#### CONCLUSION

Significant decrease in BF and BV values as compared to normal pancreas was seen in all pancreatic masses except neuroendocrine tumors. PCT may also help to differentiate pancreatic adenocarcinoma from inflammatory masses.

#### CLINICAL RELEVANCE/APPLICATION

Perfusion parameters can be an additional paradigm to characterize pancreatic mass lesions. This may in the future be useful to detect isodense pancreatic tumors which can be missed on conventional CECT.

### VSGI21-13 • Perfusion CT in Patients with Hepatocellular Carcinoma: Comparison with Intravoxel Incoherent Motion Diffusion

## (IVIM)-Diffusion Weighted Imaging (DWI)

Mi Hye Yu MD (Presenter) ; Jeong-Min Lee MD \* ; Joon Koo Han MD ; Byung Ihn Choi MD, PhD \*

### PURPOSE

To determine the value of perfusion parameters from perfusion CT in patients with hepatocellular carcinoma (HCC) and analyze the correlation with those obtained from intravoxel incoherent motion diffusion (IVIM)-diffusion weighted imaging (DWI)

### METHOD AND MATERIALS

A total of 30 patients (M:F=23:7; mean age,  $58.7 \pm 13.27$ ; age range, 20-77) suspected having HCC were prospectively enrolled in this study. They underwent IVIM-DWI (10 b values, 1.5T) and liver perfusion CT (4D spiral mode, scan range 10 cm, 21 scans, cycle time 1.5 seconds) within 2 days before hepatic resection. Following perfusion parameters were calculated: blood flow (BF), blood volume (BV), permeability surface (PS), arterial perfusion (AP), portal perfusion (PP), total liver perfusion (TLP) and hepatic perfusion index (HPI) from perfusion CT; apparent diffusion coefficient (ADC), pseudodiffusion coefficient ( $D^*$ ), diffusion coefficient ( $D$ ) and perfusion fraction ( $f$ ) from IVIM-DWI. Those parameters statistically analyzed comparing HCC and liver parenchyma. Pearson's correlation test was also used to correlate perfusion CT and IVIM-DWI parameters.

### RESULTS

Regarding the perfusion CT, BF, BV, AP, TLP and HPI were significantly higher, whereas PS and PP were significantly lower in HCC than in the liver parenchyma (BF = 39.46 mL/100mL/min, BV = 11.80 ml/100mL, AP = 41.86 mL/min/100mL, TLP = 47.24 mL/min/100mL, HPI = 87.88%, PS = 16.03 ml/100mL/min, PP = 5.37 mL/min/100mL,  $p < 0.05$ ). Among the IVIM-DWI parameters,  $D^*$  was significantly lower, whereas  $f$  was significantly higher in HCC than in the liver parenchyma ( $D^*$ , 4.95 vs.  $9.71 \cdot 10^{-3}$  mm<sup>2</sup>/s;  $f$ , 20.17 vs. 16.37 %;  $p < 0.05$ ). However, no significant correlation found between the perfusion CT and IVIM-DWI parameters.

### CONCLUSION

Perfusion CT and IVIM-DWI can quantitatively assess the hepatic perfusion in patients with HCC, even though there was no significant correlation between the parameter of the two modalities.

### CLINICAL RELEVANCE/APPLICATION

Quantitative assessment of hepatic perfusion using perfusion CT and IVIM-DWI can provide important information about the hepatic perfusion of HCC.

## VSGI21-14 • Panel Discussion

### Radiology Informatics Series: Mobile Computing Devices

Monday, 08:30 AM - 12:00 PM • S404CD



[Back to Top](#)

VSIN21 • AMA PRA Category 1 Credit™:3.25 • ARRT Category A+ Credit:3.5

#### Moderator

David S Hirschorn, MD

#### VSIN21-01 • Introduction

David S Hirschorn MD (Presenter)

#### VSIN21-02 • Platforms and Security

George L Shih MD, MS (Presenter) \*

#### LEARNING OBJECTIVES

1) iOS vs. Android platforms: a. Provide basic understanding of the differences and similarities between the Apple iOS and Google Android operating systems, as it mainly applies to the realm of medical imaging for end-users and developers; b. Introduce other competing platforms. 2) Mobile Security: Provide basic understanding of different security concerns and technologies (VPN, wifi, etc) available on mobile devices.

#### ABSTRACT

The physician dream of replacing the ubiquitous clipboard is now almost a reality. Radiologists and non-radiology clinicians will benefit from the enlarged screen size of the iPad and other mobile devices. The two main platforms for tablet mobile devices are currently the Apple iOS and the Google Android operating systems. While they share many similarities in terms of user interface functionality, they also have differences in the ways applications are created and used. This session will compare and contrast those differences, and also introduce other competing platforms. These devices will need to have the same or enhanced security compared with traditional computers because of increased portability and potential use of devices off the hospital wifi network (eg, iPad), including the use of VPN and other encryption methods (eg, https). Managing and controlling stored content will remain a major challenge for all portable devices. Other issues such as image capture (from the internal camera) and uploading them to the PACS or EMR will also need to be addressed. The recently introduced ability for locating a lost device and performing a remote wipe will hopefully allow for better adoption in medical settings, by alleviating anxiety for hospital IT departments. These devices clearly constitute a fundamental game change for radiology, both for inpatient and outpatient use cases, once security concerns are properly addressed.

#### VSIN21-03 • A Global Market Analysis for Clinical Imaging Mobile Applications

Charles T Lau MD ; Ahmed El-Sherief MD (Presenter)

#### CONCLUSION

A viable market for clinical imaging practice mobile applications exists worldwide, particularly if coupled with formal marketing efforts, augmented user value, and cross-platform development. Although resources for mobile application development can be evenly distributed between smartphone and tablets for mature markets, similar efforts should heavily favor tablet deployment in emerging markets.

#### Background

Smartphones and tablets represent a powerful platform for deployment of clinical tools that can advance the quality of clinical imaging practice worldwide. Effective efforts to leverage mobile technology in the advancement of medical care require an understanding of the global market for thoracic imaging mobile applications.

#### Evaluation

Two radiologists at a major academic medical center in North America created and deployed seven clinical imaging practice mobile applications for the iOS platform addressing anatomy, oncology, differential diagnosis generation, and common practice guidelines. One mobile application was specifically deployed with independent versions for tablets and smartphones in order to assess differences between these subsets of the mobile market. All mobile applications were distributed free of charge and without in-app advertising in over 150 nations. Trends in sales volumes and sales by country were observed during a 4-month period following a 3-month rollout window.

#### Discussion

A total of 6,116 unique sales were observed during a 4-month period. The top 8 national markets for clinical imaging practice mobile applications included the United States, Brazil, Italy, United Kingdom, Spain, Turkey, India, and China. Customers in the U.S. represented

the largest national market, accounting for 27% of all sales. Analysis of mobile application sales with independent smartphone and tablet versions revealed that the ratio of tablet versus smartphone uptake among providers is different in emerging markets than markets in North America and Europe. Whereas the tablet version of one application outsold the smartphone version by 22% in the U.S. and 12% in the U.K., tablet versions outsold smartphone versions by 144% in India, 70% in China, and 300% in Russia.

## **VSIN21-04 • The Process of Creating and Deploying a Mobile Application for iOS: An Introduction for Radiologists**

**Charles T Lau MD (Presenter) ; Ahmed El-Sherief MD**

### **CONCLUSION**

Most radiologists are familiar with the process of publishing in a peer-reviewed journal or speaking at a national conference. Mobile platforms such as iOS will be an important alternative venue of communication, and an understanding of this medium is required for those who hope to take advantage of it.

### **Background**

Mobile applications on platforms such as the iPhone and iPad represent an exciting venue for radiologists seeking to enhance their impact on colleagues' practices. Individuals interested in leveraging the iOS platform can benefit from an understanding of how this process works from beginning to end.

### **Evaluation**

Many smartphone and tablet users are familiar with mobile applications. However, the process that proceeds from the genesis of an idea and results in a mobile app in the iTunes App Store can be complex.

### **Discussion**

Developing a powerful mobile iOS application for health care providers in radiology is a long and multi-step process. The process begins with the identification of a concept or practice guideline that can be enhanced by electronic and mobile media, but underutilized because of the limitations of current media. A convenient user-interface providing a simple and understandable way of supplying user input and displaying answers is designed within Xcode Interface Builder. Software code is written in Objective-C to convert user-supplied input values to appropriate output. The resulting mobile app represents a unification of user interface design and software code tailored for a small screen, an app that must be rigorously tested and subsequently vetted by the App Store. Marketing efforts to communicate user value must be undertaken. User feedback is solicited to guide continued improvement. Many hurdles and pitfalls during these steps may be encountered and are discussed.

## **VSIN21-05 • Digital Improvement of Mobile X-ray Machines Based on Wi-Fi Flat Panel System**

**Jian Guan MD (Presenter) ; Xiao Mei Cheng ; Ling Zhang MD ; Shengwen Deng ; Shao Chun Lin**

### **CONCLUSION**

Digital improvement of mobile X-ray machines based on Wi-Fi flat panel system is practical and proven to have many advantages by clinical application.

### **Background**

There are 5 mobile X-ray machines distributed in different buildings in our hospital. The aging of equipments obviously influence image quality. Medical technologist (MT) have to take a stack of imaging plates and make many times trips between department of radiology and different wards. The cost for replacement with new mobile DR is great and all old machines will be abandoned. So we need to find a simple and available way to improve them.

## **VSIN21-06 • Apps, Bandwidth, and Integration**

**Asim F Choudhri MD (Presenter)**

### **LEARNING OBJECTIVES**

1) To have an understanding of available applications available for mobile medical imaging, including native clients, web clients, and virtual desktop/terminal server approaches. 2) To have an understanding of bandwidth concerns in mobile medical imaging, including device data handling, network speeds, and possible bandwidth cost issues. 3) To have an understanding of possible clinical implementations of mobile medical imaging within radiology departments and in health care networks overall.

### **ABSTRACT**

**Applications:** There are several vastly different approaches to mobile viewing of medical images. Native clients are programs written using a software development kit for a given platform. These clients can retrieve data from remote servers and view locally stored image data. Web clients are web-based programs which are often (but not always) platform independent. They will typically access remotely stored data which may be stored in a local cache but is usually not permanently stored on the mobile device. Virtual desktop/terminal server software allows a mobile device to access a remote computer or server. The remote server handles all higher level processing and data storage, minimizing the processing requirements of the mobile device but possibly straining bandwidth limitations. Examples of several applications using each of these approaches will be presented, with a discussion of pros and cons for each method as it pertains to an individual user and as it pertains to widespread implementation within a healthcare network. **Bandwidth:** Viewing medical images may require transfer of datasets that are tens or hundreds of megabytes in size. This provides a special challenge for mobile devices which typically receive data via wireless communication. If using a cellular network, network bandwidth can be a limiting factor (as can data transfer costs). File compression can reduce the size of files, however requires data processing power and may involve compromises in image quality. Once data is on a device, image processing may overwhelm its processing capabilities compared with dedicated PACS workstations. We will discuss both network and device bandwidth concerns as it relates to mobile medical imaging, and possible solutions for overcoming obstacles. **Integration into a healthcare system:** Mobile review of medical imaging is a tool which has potential to significantly change health care delivery, but the specifics for implementation are unclear. After a device platform has been selected, security protocols established, and bandwidth concerns solved, each institution will need to determine what role this technology will play. Possibilities include radiology residents (or even faculty) consulting with subspecialty faculty, surgeons and interventionalists triaging patients for procedures and for procedure planning, however these approaches are simply extensions of existing practices. New frontiers in consultation will be discussed, including an example involving mobile imaging review in a multidisciplinary stroke team. Guidance will also be provided regarding training and establishing institutional standard operating procedures documents. The current state of medical-legal concerns and risk management strategies will also be discussed.

## **VSIN21-07 • A Secure, Mobile Device-based System for Rapid Consultation and Sharing of Interesting Cases**

**Loyrirk Temiyakarn MD (Presenter) ; Asim F Choudhri MD**

### **CONCLUSION**

Mobile device-based systems show great promise for secure yet rapid consultation and sharing of interesting cases. Such systems have already been deployed on an institutional and cross-institutional basis and have demonstrated great success.

### **Background**

With the wide variety of PACS in use, radiologists in a group covering different hospitals often find communication between different PACS difficult. This is especially cumbersome when quick and informal consultations are desired between colleagues. With the recent improvements in camera optics and sensors in mobile devices, coupled with highly secure text and picture messaging networks, such limitations in communication can be more easily overcome.

### **Evaluation**

Several mobile device-based applications were evaluated for ease of use, fidelity of image capture, security of transmission, and ease of sharing images among a group of colleagues. Applications tested were on different mobile device platforms and deployed across different

mobile service providers. One particular commercially available application/device combination was chosen as a proof of concept at our institution. The chosen device demonstrated the ease with which images could be captured, regardless of PACS used. Captured images retained enough quality for viewing and diagnosis on the device, and could be cropped to exclude protected health information (PHI). In addition, the chosen application for image transmission has recently demonstrated encryption security sophisticated enough to limit court-mandated law enforcement efforts at interception and decryption. Finally, the chosen application allowed for easy yet secure dissemination of images to a group of colleagues for rapid consultation or review.

#### Discussion

As a proof of concept, the chosen device/application combination has proven extremely effective in the dissemination of still images for rapid consultation and sharing. The ubiquity of mobile devices combined with the flexibility in image capture allows for great versatility. However, the ability to share a series of consecutive images (e.g. cin clips) remains somewhat dependent on the user's ability to capture a movie clip of the desired image series.

### **VISIN21-08 • Optimization of Patient and Staff Radiation Protection in X-ray Imaging Procedures Using a Mobile Phone Application**

**Francis R Verdun** PhD (Presenter) ; **Nick Ryckx** MSc ; **Jean-Christophe Stauffer** ; **Jean-Jacques Goy** MD ; **Reto A Meuli** MD, PhD ; **Nicolas Goy**

#### CONCLUSION

The promotion of radiation protection must be done using all available means. The tremendous growth of mobile devices in the recent years called for a gap to be filled. When ready, our mobile application will help the physician to reach the lowest dose possible while still keeping diagnostic accuracy by estimating his/her practice with respect to the local diagnostic reference levels and giving useful working tips.

#### Background

The number and complexity of interventional radiology and cardiology (IR/IC) procedures has been steadily increasing over the last twenty years. This implies an increased risk of stochastic and even deterministic effects (skin burns) to the patient, as well as an increased exposure of IR/IC staff. Radiation protection must thus become of prime importance and should be promoted by all possible means.

#### Evaluation

We are developing a mobile application that will help the physician to evaluate his/her current state of practice regarding radiation protection. The key elements to achieve this goal are:

- Comparing his/her patient delivered doses to the local diagnostic reference levels (DRL).
- Estimate the risk and severity of potential radiation-induced skin burns and the necessity of patient follow-up.
- Estimate one's average personal dose.
- Give advice in order to reduce patient and staff exposure.
- Give general information about radiation protection.

#### Discussion

As radiation-induced erythema occur several days or weeks the X-ray exposure, it can be easily diagnosed as being caused by another factor, such as medication or allergy. Giving the patient more information about his/her personal risk would greatly improve his/her follow-up to minimize negative side effects of a high dose IR/IC procedure. As for the staff, it will help them with their daily practice by giving them useful tips aiming to reduce the dose delivered to the patient and, as a consequence, their own personal dose.

### **VISIN21-09 • The Use of Mobile Devices for Specimen Mammography Interpretation: Feasibility Study**

**Bo La Yun** MD (Presenter) ; **Sun Mi Kim** MD, PhD ; **Mijung Jang** ; **Hye Shin Ahn** MD

#### PURPOSE

To assess feasibility of mobile device in specimen mammography interpretation by using safety margin on pathologic result as reference standard.

#### METHOD AND MATERIALS

This retrospective study was approved by the institutional review board. Patient informed consent was waived. A total of the 79 consecutive breast specimen mammography (52 invasive cancer, 26 DCIS, and 1 mixed DCIS and LCIS) in 79 women (median age, 49 years; age range, 30-76 years) was included. Three radiologists independently reviewed specimen mammography with three different mobile devices (Nexus10, Google, CA; Galaxy note 10.1, Samsung, Korea; New iPad, Apple, CA;). Other two radiologists independently interpreted the same set of specimen mammography on 5megapixel LCD monitor. Margin evaluation on pathologic report was reviewed as the reference standard. Each reader was asked to measure the shortest distance from the lesion to the margin lesion. The interpretation time was also assessed. Absolute measurement discrepancy defined as the difference between measured shortest distance on specimen mammography and pathological safety margin, and interobserver agreement, sensitivity and specificity were analyzed.

#### RESULTS

Intraclass correlation coefficients were 0.546 for LCD monitor, 0.459 for Nexus, 0.508 for Galaxy, and 0.392 for iPad. The mean absolute measurement discrepancy were  $.66 \pm .49$  for LCD monitor,  $.61 \pm .47$ cm for Nexus,  $.59 \pm .47$ cm for Galaxy,  $.60 \pm .48$ cm for iPad without statistical significant difference among devices ( $P = .59$ ). The mean sensitivity and specificity were 66.8% and 35.2% for LCD monitor, 73.3% and 24.5% for Nexus, 77.8% and 30.2% for Galaxy and 73.3% and 26.0% for iPad. The mean assessment time were 44 seconds (sec) for LCD monitor, 42 sec for Nexus, 38 sec for Galaxy, 45 sec for iPad. There were no statistical significant between LCD monitor and mobile devices interpretation time ( $P = .18$ ).

#### CONCLUSION

The mobile devices and 5-megapixel LCD monitors are comparable in terms of surgical margin evaluation of breast cancer in digital mammograms. The mobile devices could be an option to safety margin evaluation on specimen mammography.

#### CLINICAL RELEVANCE/APPLICATION

Mobile devices are comparable in 5-megapixel LCD monitor in evaluation of specimen mammography margin and could be used for display tool of immediate assessment when LCD monitor is unavailable.

### **VISIN21-10 • Displays and Quality Assurance**

**David S Hirschorn** MD (Presenter)

#### LEARNING OBJECTIVES

- 1) Discuss ranges of spatial and contrast resolution for medical imaging.
- 2) Explore options for calibration and quality assurance.
- 3) Understand the impact of ambient light and viewing distance and angle on medical image display.

#### ABSTRACT

Mobile devices have significantly smaller displays than desktop or even laptop computers to make them lighter and more easily transported. They are also designed for shorter viewing distances which require smaller pixels. The smaller total display size tends to reduce the number of pixels, while the smaller pixel size tends to increase the number of pixels. On balance, these displays typically have considerably fewer pixels than their stationary counterparts. Nonetheless, even desktop displays typically have less resolution than the original image size of a radiograph which is typically about 5 megapixel (MP) for a chest radiograph. And both types of displays have more resolution than a single CT image, which is 0.25 MP. Since these devices do allow zooming and panning, they may be suitable for image interpretation under controlled circumstances. The main purpose of the DICOM Part 14 Grayscale Display Function is to ensure that contrast is preserved across the range of shades of gray from black to white, particularly at the edges where uncalibrated displays tend to

fall off. With desktop displays this can be measured with a photometer, either external or built-in, and graphics adapter adjustments can be made to make the display conformant. Mobile devices typically do not offer this degree of adjustability. This requires a different approach to DICOM curve conformance, and a reasonable alternative is to present the user with a visual challenge to identify low contrast targets placed randomly on the display. If the user can find them and tap on them, then the display may be considered compliant, and if not, then the display should not be relied upon.

## **VSIN21-11 • How Good Is the iPad for Detection of Pneumothorax on Chest X-ray? Diagnostic Performance of Radiologists and Emergency Medicine Physicians**

**Rameysh D Mahmood** MBBCh, FRCR (Presenter) ; **Justin Sim Jw** MBBS ; **Angeline, Choo Choo Poh** MBBS ; **C. C. Tchoyson Lim** MBBS

### **PURPOSE**

Tablets like the iPad have been successfully used as remote image review devices for emergency teleconsultation of high contrast studies e.g. CT. However, their utility in the interpretation of radiographs which require higher spatial and contrast resolution displays is less certain. This study aims to compare the accuracy of pneumothorax (PTX) detection on chest x-rays (CXRs) between the iPad and the PACS monitor and the diagnostic performance between radiologists and emergency medicine (EM) physicians.

### **METHOD AND MATERIALS**

Anonymized full DICOM images of 140 CXRs [40 normal, 48 small PTX (2cm)] were retrospectively chosen from the PACS database and uploaded to 3 iPads (3rd gen). Three radiologists and 3 EM physicians of equivalent experience (2 residents, 1 attending physician each) independently read the CXRs on the iPad running iRAS viewing application (ASTAR, Singapore) and a 5MP Barco monitor running Amalga PACS (Microsoft, USA). The sets were randomized and the PACS and iPad reading sessions were separated by 1 month to avoid memory bias. Each reviewer had to indicate the absence or presence and location of the PTX. The percentage of correct diagnosis was calculated for each display and reader. The detection accuracy of small and large PTX between both displays was also compared.

### **RESULTS**

The iPad diagnoses of the 140 CXRs were accurate in 97.4% compared to 97.6% for PACS. In the CXRs that had PTX, the accuracy of the iPad was 95.0% compared to 97.4% for the PACS monitor ( $p=0.03$ ). The diagnostic accuracy of the radiologists with the iPad was 97.8% compared to 94.5% with the EM physicians ( $p=0.002$ ). 8.8% of small and 1.6% of large PTX were missed on the iPad, compared to 4.5% and 0.9% on PACS respectively.

### **CONCLUSION**

Although there is overall high accuracy in diagnosis of PTX on CXR with the iPad, there was a statistically significant difference compared to conventional PACS monitors, and between radiologists and EM physicians, possibly due to small PTX.

### **CLINICAL RELEVANCE/APPLICATION**

Potential clinical applications of 3rd generation iPad in the field of remote emergency diagnostic teleconsultation.

## **VSIN21-12 • The Diagnostic Performance of a Tablet-PC with a High-resolution Display in Emergency MDCT Interpretation as Compared to a Dedicated 3D PACS Workstation**

**Susanne Tewes** MD ; **Thomas Rodt** MD ; **Steffen Marquardt** ; **Evdokia Evangelidou** ; **Frank K Wacker** MD \* ; **Christian Von Falck** MD (Presenter) \*

### **PURPOSE**

To evaluate a potential role of tablet PC with a high-resolution display (iPad 3) for the interpretation of emergency CT examinations in comparison to a dedicated 3D PACS workstation.

### **METHOD AND MATERIALS**

Three readers compared the detectability of early signs of cerebral infarction and subtle pulmonary embolism in 40 CCT and 40 CTPA examinations using both, a tablet PC with a high-resolution display (iPad 3, Apple Inc., USA) running a radiology app (Visage Ease, Visage Imaging GmbH, Berlin, Germany) and a 3D PACS workstation (Visage 7.1, Visage Imaging GmbH, Berlin). Diagnostic confidence was evaluated on a 5-point Likert scale. Wilcoxon rangsum test, Spearman's correlation and Cohen's kappa were calculated for statistical evaluation.

### **RESULTS**

For all readers, there was no significant difference in the median score between the iPad 3 and the PACS for the CCT and the CTPA, respectively ( $p>0.05$ ). The mean Spearman's correlation coefficients were 0.46 ( $\pm 0.2$ ) / 0.69 ( $\pm 0.16$ ) for the comparison between the iPad and the PACS, 0.41 ( $\pm 0.16$ ) / 0.68 ( $\pm 0.06$ ) for observer agreement using the iPad and 0.35 ( $\pm 0.05$ ) / 0.68 ( $\pm 0.10$ ) for observer agreement using the PACS for CCT and CTPA, respectively. Mean kappa values were 0.52 ( $\pm 0.17$ ) / 0.67 ( $\pm 0.19$ ) for the comparison between the iPad and the PACS, 0.33 ( $\pm 0.16$ ) / 0.69 ( $\pm 0.08$ ) for observer agreement using the iPad and 0.32 ( $\pm 0.16$ ) / 0.60 ( $\pm 0.14$ ) for observer agreement using PACS. The differences were not considered statistically significant ( $p>0.05$ ).

### **CONCLUSION**

The agreement in the interpretation of typical emergency CT examinations between the iPad 3 and a dedicated 3D PACS workstation does not differ significantly from interobserver agreement.

### **CLINICAL RELEVANCE/APPLICATION**

The image quality of the iPad 3 with a high-resolution display allows for a preliminary interpretation of typical emergency CT datasets.

## **VSIN21-13 • Can the iPad Be Used in the Diagnosis of Bone Fractures: Preliminary Results**

**Spyros D Yarmenitis** MD ; **Maria T Tzalonikou** MD (Presenter) ; **Socratis Gavriilidis** MD ; **Grigorios Rigas** MD ; **Irene Vraka** MD ; **John Spigos** BS ; **Athanasios D Gouliamos** MD ; **John Andreou** MD ; **Dimitrios G Spigos** MD

### **PURPOSE**

To evaluate the usefulness of tablets in the diagnosis of bone fractures in a general hospital's emergency department.

### **METHOD AND MATERIALS**

Seventy-eight consecutive trauma cases were evaluated retrospectively. Skeletal radiographs and the corresponding diagnostic reports were retrieved from the PACS-RIS database. They included 39 upper extremities, 28 lower extremities, 7 spinal, 3 rib cages and 1 skull x-rays. Of the cases reviewed, 35 had fractures. The images were anonymized and distributed after randomization to two attending radiologists and to two radiology residents. They used diagnostic monitors and a non-retina display iPad2 device. DICOM images were transferred in a compressed 1263x1536 matrix.

### **RESULTS**

On the diagnostic monitors, the attendings made 130 correct and 26 incorrect diagnoses, while the residents made 127 correct and 29 incorrect diagnoses. On the iPad, the attendings made 128 correct and 28 incorrect diagnoses, while the residents made 125 correct and 31 incorrect diagnoses. In the detection of fractures, the iPad had a Sensitivity 70.9%, Specificity 89.4%, Positive Predictive Value 84.7%, and Negative Predictive Value 78.8%. As a group, the attendings and residents made 257 correct and 55 incorrect diagnoses on the monitors and 253 correct and 59 incorrect diagnoses on the iPad. There was no difference in the accuracy of interpretation among attendings and residents and no difference was found in their performance depending on the device used.

### **CONCLUSION**

Based on this study, tablets will play increasingly important role in the radiographic detection of bone fractures. Although the FDA approved monitors will continue as the diagnostic devices in Radiology departments, tablets will play an essential role as they are mobile



and can be used in the Emergency department or for teleradiology purposes.

#### CLINICAL RELEVANCE/APPLICATION

iPads can be used in diagnosis of fractures in the emergency department and for consultation between physicians from afar.

## Interventional Radiology Series: Peripheral and Visceral Occlusive Disease

Monday, 08:30 AM - 12:00 PM • E352

[Back to Top](#)



**VSIR21** • AMA PRA Category 1 Credit™:3.25 • ARRT Category A+ Credit:3.75

#### Moderator

**Albert A Nemcek, MD \***

#### LEARNING OBJECTIVES

1) Describe recent evidence concerning the use of renal denervation for malignant hypertension. 2) Explain the use of stent grafts in vascular disease. 3) Describe three pitfalls of CTA or MRA in peripheral vascular disease. 4) Outline 3 recommendations for endovascular treatment of peripheral vascular disease. 5) List two important studies published on vascular disease in the past year.

### VSIR21-01 • CTA and MRA for PVD: Pitfalls of Peripheral Vascular CTA and MRA -Don't Make These Mistakes!

**Barry Stein MD (Presenter)**

#### LEARNING OBJECTIVES

View learning objectives under main course title.

#### ABSTRACT

CTA and MRA are accepted powerful non invasive vascular imaging modalities to assess for peripheral vascular disease. Both modalities have their niche clinical indications and both have their pitfalls. The presentation will elaborate on how to avoid these pitfalls illustrating the genesis of these with study acquisition, data post processing and image interpretation.

### VSIR21-02 • In Vivo Quantification of Total Atherosclerotic Burden: Prognostic Accuracy of Whole Body CTA in Relation to Traditional Cardiovascular Risk Index and 8-year Follow-up

**Fulvio Zaccagna MD (Presenter) ; Alessandro Napoli MD ; Gaia Cartocci ; Vincenzo Noce MD ; Maurizio Del Monte ; Carlo Catalano MD**

#### PURPOSE

To investigate if mid-term prognostic value of WB-CTA to predict cardiovascular (CV) events in asymptomatic patients with CV risk factors can be superior to traditional method of risk stratification and can more accurately guide primary preventive strategies in asymptomatic patients.

#### METHOD AND MATERIALS

341 patients with CV risk factors (mean age 63.39±10.4[34-89]) underwent WB-CTA (detector configuration: 64x0.6mm) with an adapted contrast injection protocol (Iomeprol-400, 400mgI/ml; 70+50ml@4ml/s). For the evaluation of atherosclerotic burden the coronary arteries were divided into 15 segments and the extra-coronary arteries into 32 segments and detected stenoses were graded using a 5-point scale (0-4 normal-occlusion; 5 aneurysm). An atherosclerosis burden score (ABS) was generated for each individual and correlated to traditional CV risk (Framingham risk index; FRI). ABS and FRI were compared using Kaplan-Meier survival analysis, ROC analysis and stepwise multivariable Cox proportional hazards regression models.

#### RESULTS

At baseline mean ABS was 19.5±20.1 and mean FRI was 12±10.7; 64.5±11.3 months after WB-CTA all patients received an interview to determine health status during this period. According to Kaplan-Meier curves, mean event-free time was of 86.3±6.4m for ABS

#### CONCLUSION

WBCTA-derived ABS reflects real atherosclerotic burden and provides superior risk stratification and event prediction with respect to FRI; hard event prediction was significantly associated to age, ABS and therapy but not to FRI.

#### CLINICAL RELEVANCE/APPLICATION

WB-CTA allows non-invasive and more accurate risk stratification than FRI; thus, ABS could guide primary therapeutic interventions in a more robust and accurate manner than traditional risk methods

### VSIR21-03 • Whole Body Contrast Enhanced Magnetic Resonance Angiography Screening for Sub-clinical Atherosclerotic Disease

**Graeme Houston MD, FRCR (Presenter) \* ; Matthew Lambert MBBCh, MRCP \* ; Jonathan Weir-McCall MBBCh, FRCR ; Stephen Gandy ; Shona Matthew BSc, PhD \* ; Richard D White MBChB, FRCR ; Jil J Belch ; Alan D Struthers ; Frank Sullivan ; Roberta Littleford PhD**

#### PURPOSE

The Tayside Screening for Cardiac Events (TASCFORCE) study assessed the ability of a number of biomarkers to identify subclinical atherosclerosis in individuals free from, and at low risk of cardiovascular (CV) disease. The CV imaging biomarker studied was a whole body atheroma score derived from whole body contrast enhanced magnetic resonance angiography (WBCE-MRA).

#### METHOD AND MATERIALS

5000 volunteers > 45 yrs with no history of CV disease, a 10 year risk of CV disease less than 20% as assessed by the ASSIGN CV risk score and a B-type natriuretic peptide (BNP) greater than their gender specific median were invited. Of 1651 volunteers, 34 were ineligible due to safety issues, 107 were claustrophobic, and 1510 (91.4%) completed the 3T MRI (Siemens Trio, Erlangen, DE) MRI. WBCE-MRA was acquired from skull vertex to feet using following intravenous injection gadolinium gadoterate meglumine (Dotarem, Guerbet, FR). The subtracted WBCE-MRA data comprised 31 anatomical arterial segments. Each segment was scored according to the extent of luminal narrowing: 0 normal, 1

#### RESULTS

277 of 46,810(0.5%) arterial segments were un-interpretable due to poor quality images, or anatomical variation. Only 606 (40.1%) participants had a normal WBAS. The distribution of arterial abnormalities was head, neck and thorax in 403 (26.7%), abdominal 361 (24.0%) and peripheral arteries 366 (24.2%) of volunteers. The number of volunteers with WBAS of 1-267 (18%), 2-204 (13.5%), 3-117 (7.8%), 4-86 (5.7%), 5-68 (4.5%), 6-47 (3.1%), >7 -114 (7.6%) volunteers respectively. Of the affected segments detected 1644 (76%) were < 50% stenosis, 234 (11%) were 50-75% stenosis, 161 (7.5%) were 70-99% stenosis, 80 (3.7%) were occluded and 32 (1.5%) were aneurysmal vessels.

#### CONCLUSION

WBCE-MRA demonstrates the presence of atherosclerosis in 60% of asymptomatic people at low risk of cardiovascular disease based on accepted risk factors. The severity of disease ranged from

#### CLINICAL RELEVANCE/APPLICATION

Cardiovascular events occur in low risk people. WBCE-MRA demonstrates the sites and severity of atherosclerotic lesions in asymptomatic low risk individuals that may allow preventative therapy.

## VSIR21-04 • Recommendations for Endovascular Treatment of PVD in 2013

**Johannes Lammer MD (Presenter) \***

### LEARNING OBJECTIVES

1) To learn the indications for interventions in PAD. 2) To learn the technique and devices for aortoiliac treatment. 3) To learn the technique and devices for femoropopliteal artery treatment. 4) To learn the technique and devices for below the knee (BTK) treatment. 5) To learn the results of most recent trials. 6) To learn the medical treatment after intervention.

### ABSTRACT

To learn the indications for interventions in PAD To learn the technique and devices for aortoiliac treatment To learn the technique and devices for femoropopliteal artery treatment To learn the technique and devices for below the knee (BTK) treatment To learn the results of most recent trials To learn the medical treatment after intervention

## VSIR21-05 • Influence of Tube Voltage Reduction on Image Quality in MDCTA of Arterial Stents Using Model-based Iterative Reconstruction: A Phantom Study

**Jochen M Grimm MD (Presenter) ; Lucas L Geyer MD \* ; Daniel Maxien MD ; Zsuzsanna Deak MD ; Fabian Mueck ; Michael K Scherr MD ; Stefan Wirth MD \***

### PURPOSE

To evaluate dose saving potential and impact on image quality of tube voltage reduction in MDCT imaging of arterial stents using model-based iterative reconstruction (MBIR) compared to adaptive statistical iterative reconstruction (ASIR) in an anthropomorphic phantom.

### METHOD AND MATERIALS

Different coronary stents were filled with iodinated contrast medium, placed in a thoracic Alderson-Rando phantom and scanned at 120, 100 and 80 kVp at fixed tube currents (200, 100, 50mA). Luminal attenuation values (HU) and standard deviation (image noise; IN) were measured, contrast- (CNR) and signal-to-noise ratio (SNR) were calculated for ASIR and MBIR. Image quality (IQ) was assessed by two blinded radiologists using a 4-point scale. Wilcoxon's test was used for statistical evaluation.

### RESULTS

Average IQ using MBIR was superior compared to ASIR at 120 and 100 kVp (p

### CONCLUSION

MBIR performed superior to ASIR at 120 and 100kVp independent of tube current. At 80kVp, ASIR performed slightly better than MBIR, especially at lower tube currents, without reaching statistical significance. Best relation between IQ and CTDI was found using MBIR at 100kVp and 50mA, delivering an image quality superior to the best ASIR image at only 16% of its CTDI.

### CLINICAL RELEVANCE/APPLICATION

MBIR significantly outperforms ASIR at 100 and 120 kVp. Tube current can be greatly reduced without sacrificing image quality while tube voltage should not be reduced below 100 kV.

## VSIR21-06 • Impact of a Novel CT-based Calcium Scoring System of the Lower Extremity Arteries on Primary Patency Rates after Endovascular Interventions for Peripheral Arterial Disease: Preliminary Results

**Holly L Nichols BS (Presenter) ; Stacey Schriber ; Charles Y Kim MD \***

### PURPOSE

For lower extremity artery lesions, the type and extent of associated calcification has been shown to affect immediate post-angioplasty results but the impact on long-term patency is unknown. The purpose of this project is to utilize a novel calcium scoring system to characterize arterial lesions and correlate with the primary patency rate after endovascular interventions.

### METHOD AND MATERIALS

We reviewed our procedural database between 1/2005 ♦ 12/2009 for lower extremity arteriograms that included an intervention on a stenosis or occlusion. Patients were included if there was no more than one lesion per leg and if a CTA of the lower extremities was performed within the preceding 6 months. A total of 66 lesions were identified in 47 patients (22 males, mean age 63 years). Each treated lesion was reviewed on the CTA for calcium scoring. Calcium morphology was described as none, thin linear, thick linear, or bulky. The percent circumference was scored as none, 1-50%, 51-95%, or >95%. Primary patency was determined by recurrence of symptoms in that extremity or development of 50%+ stenosis at the treated site based on CTA or conventional angiography if available. Patency estimation was performed using the Kaplan-Meier method and compared using the log rank test. The cutoff for statistical significance was a p-value = 0.05.

### RESULTS

Of 66 treated lesions, 54 underwent stenting and 12 underwent angioplasty, without significant difference in patency (p=0.76). Overall, no significant difference in patency was identified based on morphology score alone (p=0.74) or circumference score alone (p=0.13). Subanalysis of extensive calcifications (thick linear or bulky morphology with >50% circumference), eccentric calcifications (thick linear or bulky with 1-50% circumference), or bulky eccentric calcifications stratified by arterial distribution revealed that only bulky eccentric calcifications in the SFA distribution resulted in a significantly decreased patency rate (p=0.03).

### CONCLUSION

Our preliminary findings suggest that this proposed calcium scoring system is predictive of post-intervention patency outcomes in the SFA distribution. Additional data is needed to fully evaluate this correlation.

### CLINICAL RELEVANCE/APPLICATION

Calcium scoring of atherosclerotic lesions may be predictive of post-intervention patency rates, which can help determine whether endovascular therapy should be performed for a given lesion.

## VSIR21-07 • Robust 3D MRI Segmentation of Superficial Femoral Artery for Morphological Analysis of Peripheral Arterial Disease Plaque Burden

**Eranga Ukwatta MENG (Presenter) ; Jing Yuan ; Bernard Chiu ; Wu Qiu ; Martin Rajchl ; Aaron Fenster PhD \***

### PURPOSE

Current luminographic techniques have limited utility in the longitudinal assessment of peripheral arterial disease (PAD). With the advent of fast and non-invasive 3D black-blood MRI sequences, such as 3D motion-sensitized driven equilibrium (MSDE) prepared rapid gradient echo sequence (3D MERGE), superficial femoral artery (SFA) vessel wall can be evaluated up to 50 cm coverage for generating morphological measurements of PAD plaque burden. This study aims develop and evaluate a fast and precise algorithm for segmentation of the femoral artery outer wall and lumen from 3D MR images.

### METHOD AND MATERIALS

Using multi-planar reformatting software, the user selects approximate mid-points on transverse cross-sections of the artery 30 mm apart. The user selected points are then connected using the live-wire algorithm to find the rest of the points on the medial axis. The 3D image is then reoriented using the medial axis of the artery. A novel algorithm was then applied to jointly delineate the SFA lumen and outer wall surfaces from 3D black-blood MR images in a global optimization manner, while enforcing the spatial consistency of the reoriented MR slices along the medial axis of the SFA. The accuracy of the algorithm was evaluated with respect to the manual segmentation. Our data set comprised of 355 2D slices extracted from 10 3D MR images from seven subjects. Five of these subjects were symptomatic with intermittent claudication.

## RESULTS

The algorithm required only 1.8 min of total time to segment a 3D MR image compared to 70-80 min of user time for manual segmentation. The algorithm yielded Dice coefficients of  $89.1 \pm 3.7\%$  and  $85.4 \pm 3.4\%$  and mean absolute boundary distances of  $0.44 \pm 0.1$  mm and  $0.40 \pm 0.1$  mm, and maximum absolute boundary distances of  $0.97 \pm 0.23$  mm and  $0.87 \pm 0.13$  mm for the SFA outer wall and lumen. The reproducibility of the algorithm was computed using five repeated segmentations and the algorithm yielded intra-class correlation coefficient of 0.95 and coefficient of variation of 6.69% for generating vessel wall area.

## CONCLUSION

The algorithm requires only 2-3% of the time required for manual segmentation, which significantly alleviates measurement burden while maintaining high accuracy and reproducibility.

## CLINICAL RELEVANCE/APPLICATION

The algorithm is suitable for generating morphological measurements of PAD plaque burden with high accuracy and reproducibility and it requires only 2-3% of time required for manual segmentation.

### VSIR21-08 • Stent Grafts Explained

**Lindsay S Machan MD (Presenter) \***

#### LEARNING OBJECTIVES

View learning objectives under main course title.

### VSIR21-09 • Updates in Vascular Disease

**Albert A Nemcek MD (Presenter) \***

#### LEARNING OBJECTIVES

View learning objectives under main course title.

### VSIR21-10 • Effect of Renal Sympathetic Denervation on Left Ventricular Hypertrophy in Patients with Medication-resistant Hypertension: 1 Year Follow-up with Cardiac Magnetic Resonance Imaging

**Willemien Verloop MD ; Eva Vink MD ; Peter Blankestijn MD, PhD ; Evert-Jan Vonken MD, PhD ; Michiel Voskuil ; Tim Leiner MD, PhD (Presenter) \***

#### PURPOSE

Renal denervation (RDN) is designed to decrease sympathetic activity and has shown to be an effective treatment for hypertension. The effects of RDN on the heart are largely unknown. Aim of the current study was to investigate the effect of RDN on left ventricular hypertrophy, which is an indicator of end organ damage.

#### METHOD AND MATERIALS

#### RESULTS

#### CONCLUSION

Overall, RDN is not associated with a significant decrease in LV myocardial mass at 1 year after the procedure, although there are large differences between individuals. There is no clear linear relationship between change in blood pressure and LV myocardial mass at 1 year after RDN.

#### CLINICAL RELEVANCE/APPLICATION

There are large interindividual differences in the effect of renal denervation on blood pressure. There is no clear linear relationship between blood pressure change and change in LV myocardial mass.

### VSIR21-11 • Wrap Up and Discussion

#### LEARNING OBJECTIVES

View learning objectives under main course title.

## Musculoskeletal Radiology Series: Knee Imaging

Monday, 08:30 AM - 12:00 PM • E451B



[Back to Top](#)

**VSMK21 • AMA PRA Category 1 Credit™:3.25 • ARRT Category A+ Credit:3.5**

#### Moderator

**Lynne S Steinbach , MD**

#### Moderator

**Mark W Anderson , MD**

### VSMK21-01 • MRI of Meniscal Tears

**Lynne S Steinbach MD (Presenter)**

#### LEARNING OBJECTIVES

1) Discuss several meniscal pitfalls. 2) Review types of tears that are frequently missed or overcalled. 2) Provide an update of some recent information and concepts regarding meniscal MR imaging.

#### ABSTRACT

For several decades, radiologists have been evaluating knee menisci for tears using MRI with high sensitivity, specificity, and positive and negative predictive values. The individual radiologist must have the knowledge of the normal anatomic variants, normal meniscal-ligament interfaces, technical and other pitfalls, and appearances of various types of tears in order to keep up with the standards set by our profession, referring clinicians, and patients. This lecture will review some of those issues and provide an update of recent studies that have focused upon the use of MRI for meniscal evaluation.

### VSMK21-02 • MRI Meniscal Tear Morphology Survey: MSK Radiologist Nomenclature and Potential for Implementation of a Validated Standard

**Robert J Ward MD ; Allen Prober MD (Presenter) ; Thomas L Huang MD ; Troy H Maetani MD ; Shreena Brahmhatt ; Marios Loukas MD, PhD**

#### PURPOSE

Purpose: To evaluate the range of meniscal tear morphology nomenclature on MR knee reports utilized by MSK radiologists, determine if

a potential lack of standardization may lead to perceived diminished report clarity, and explore support for potential implementation of a specific validated classification system.

#### METHOD AND MATERIALS

Methods and Materials: 860 surveys were emailed to members of the Society of Skeletal Radiology (SSR). The survey included 14 questions. 2 questions focused on demographics 6 questions on specific tear morphologies with illustrated examples, 1 question on signal classification with an illustrated example, 2 questions on tear localization, 2 questions measuring the frequency of confusion in reading other radiologists reports, and 1 question on whether the participant was willing to utilize a validated arthroscopy classification system.

#### RESULTS

Results: 250 (29%) responded, 40% academic and 60% non-academic. Approximately 95% had completed an MSK fellowship. Results indicated that differing tear morphologies demonstrate differing degrees of consensus regarding nomenclature. Meniscal signal classification was utilized by only 7% of participants. 60% percentage of MSK radiologists reported that when reading outside studies, tear morphology reporting lead to confusion sometimes. The MSK radiologists responding to the study overwhelmingly (95%) agreed to adopt the International Society of Arthroscopists, Knee Surgery, and Orthopedic Sports Medicine Classification System (ISAKOS).

#### CONCLUSION

Conclusion: MSK radiologist reporting varies substantially with respect to meniscal tear nomenclature sometimes leading to ambiguity among radiologists. There was overwhelming support for implementation of the ISAKOS classification system for meniscal tear MR reporting.

#### CLINICAL RELEVANCE/APPLICATION

Non-standardized tear morphology nomenclature creates ambiguity amongst radiologists and potentially clinicians. Implementation of an ISAKOS standard was endorsed by 95% of responding SSR members.

### **VSMK21-03 • Comparison of Fat-suppressed Fast Spin-echo Images with Different TEs in 3T Knee MRI: Diagnosis of Meniscal, Cruciate Ligament Tears and Cartilage Lesions**

**Moon Young Lee** (Presenter) ; **Won-Hee Jee** MD ; **Sungwon Lee** MD ; **Joon-Yong Jung** MD ; **Yong In**

#### PURPOSE

To retrospectively determine if the sagittal fat-suppressed fast spin-echo (FSE) imaging with intermediate echo time (TE) has comparable accuracy with the short TE imaging in detecting not only the cruciate ligament tears but also the meniscal tears and cartilage lesions in 3T magnetic resonance imaging (MRI).

#### METHOD AND MATERIALS

The institutional review board approved this HIPAA-compliant study, and informed consent was waived. The study included 31 patients (21 men and 10 women; mean 41.8 years, range 18-68) who underwent both arthroscopy and 3T knee MRI including sagittal fat-suppressed FSE with a short TE and two different intermediate TEs (17, 38, and 58). MR imaging were retrospectively analyzed by two independent reviewers and correlated with arthroscopic findings. Medial and lateral meniscal (MM, LM) tears and anterior and posterior cruciate ligament (ACL, PCL) tears were assessed with 5-point confidence scale and the cartilage defect of the medial femoral condyle was graded. The sensitivity, specificity, accuracy and interobserver agreement were calculated for each TE and the ROC curve of the confidence scales were compared

#### RESULTS

A total of 28 meniscal tears (17 MM, 11 LM) and 14 ligament tears (12 ACL, 2 PCL) and 20 cartilage lesions were confirmed by arthroscopy. The mean sensitivity, specificity and accuracy for MM tears were 100%, 73%, 89% at TE 17, 100%, 77%, 90% at TE 38, and 94%, 81%, 89% at TE 58; For LM tears 95%, 95%, 95% at TE 17, 95%, 97%, 97% at TE 38, 95%, 97%, 97% at TE 58, For ACL tears 76%, 83%, 79% at TE 17, 76%, 83%, 79% for TE 38, 76%, 89%, 82% at TE 58; For PCL tears 100%, 89%, 89% at TE 17, 100%, 93%, 92% at TE 38, 100%, 96%, 95% at TE 58; For cartilage lesions 100%, 95%, 81% at TE 17, 100%, 95%, 85% at TE 38, 100%, 95%, 84% at TE 58. Interobserver agreements were moderate to almost perfect in the meniscus, ligament and cartilage lesions (? = 0.584 to ? = 0.950). The ROC analyses revealed no significant difference between the TEs (P > .05).

#### CONCLUSION

A single sagittal intermediate-weighted FSE imaging may replace the sagittal short TE FSE imaging in diagnosing all meniscal, ligament and cartilage lesions at 3T.

#### CLINICAL RELEVANCE/APPLICATION

A single sagittal intermediate-weighted FSE imaging may replace the sagittal short TE imaging in diagnosing all meniscal, ligament and cartilage lesions and save scan time at 3T.

### **VSMK21-04 • Measurement of Meniscal Extrusion Using Radial Multiplanar Reconstruction MR Imaging in Osteoarthritic and Non-arthritic Knees**

**Anish Ghodadra** MD (Presenter) ; **Flavia A Sakamoto** MD ; **Faysal Althawhi** MD ; **Carl S Winalski** MD \*

#### PURPOSE

Identify meniscal extrusion and validate measurements made using radially-oriented multiplanar reconstruction (rMPR) images. Determine location-specific extrusion differences between osteoarthritis patients (OA) and healthy controls.

#### METHOD AND MATERIALS

rMPR images of each meniscus were created from 3D-DESS MR images of randomly selected subjects in healthy control (n=40) and progression (n=124) subcohorts from the Osteoarthritis Initiative. Patients with macerated menisci were excluded. Extrusion relative to tibial edge (excluding osteophytes) was measured every 10-degrees for the entirety of each meniscus by one of two trained readers. Medial meniscal extrusion was measured in 10 subjects by both readers for inter-reader agreement. Sixty mid-body rMPR measurements were compared to standard extrusion measurements from mid-coronal IW-FSE images.

#### RESULTS

Inter-reader agreement for rMPR extrusion at all locations was high (r= 0.78). Correlation with mid-body coronal IW-FSE images was r=0.81. Median extrusion in the anterior, middle and posterior thirds of the medial meniscus was 1.2mm, 0.4mm and 0.2mm, respectively, for controls and 2.2mm, 1.8mm, and 0.9mm for OA (p 1mm of extrusion of the mid-body of the medial meniscus vs. only 25% of control menisci. Although greater in OA, mild anterior extrusion was also common in control subjects. There was no lateral meniscal extrusion for any controls or 76% of the OA group.

#### CONCLUSION

Extrusion can be reliably measured for the entire circumference of the meniscus using the rMPR technique. Significant differences in extrusion patterns were found between control and OA subjects with OA subjects generally having a greater degree of meniscal extrusion. Mild anterior extrusion of the medial meniscus may be a normal finding. The rMPR extrusion analysis may prove valuable for studying the influence of patterns of meniscal deformities on OA incidence and progression as well as to help improve our understanding of the biomechanical implications of meniscal tears and partial meniscectomy.

#### CLINICAL RELEVANCE/APPLICATION

Medial meniscal extrusion differences between OA and controls are greatest in the body and posteromedial region. Lateral meniscal extrusion should be considered abnormal as it was not seen in controls

### **VSMK21-05 • Advanced Imaging of Arthritis**

#### LEARNING OBJECTIVES

1) Review target sites at the knee joint affected by different forms of arthritis. 2) Recognise features of enthesitis seen in seronegative arthritis at the knee joint. 3) Identify imaging findings of arthritis that help to make a disease specific diagnosis.

#### ABSTRACT

The knee joint is frequently affected by osteoarthritis and the features of the disease at this joint have been extensively studied. Recently imaging research has started to elucidate information relating to the etiology and symptomatology of the disease. However the knee is also affected by other forms of arthritis, including sero-positive and negative inflammatory arthritis and the crystal arthritides. While certain features of arthritis such as synovitis and cartilage loss are non-specific and seen in arthritis due to a variety of causes, the patterns of knee involvement, along with other more specific features will often allow a specific diagnosis to be made. This lecture will review imaging features of arthritis as they affect the knee joint and discuss how they help in making a diagnosis and what they can tell us about the disease etiology.

### **VSMK21-06 • Diagnosis of Internal Derangement of the Knee: 3D Isotropic Intermediate-weighted Fast Spin-echo with Fat Saturation versus without Fat Saturation**

**Young Cheol Yoon MD ; Ki Jeong Park MD** (Presenter)

#### PURPOSE

To compare three-dimensional (3D) isotropic intermediate-weighted (IW) fast spin-echo (SE) magnetic resonance (MR) imaging with fat saturation (FS) and without fat saturation in regard to evaluation of ligaments, menisci and cartilage.

#### METHOD AND MATERIALS

The institutional review board approval and waiver of informed consent were obtained for this HIPAA-compliant study. Two radiologists retrospectively and independently reviewed one hundred MR studies. Each MR study consists of 3D isotropic IW fast SE with FS and without FS. The presence of cartilaginous defects, anterior cruciate ligament (ACL), posterior cruciate ligament (PCL), medial meniscus (MM), and lateral meniscus (LM) tears were evaluated. Arthroscopic surgery findings are used for the reference standard. Statistical analysis was performed to calculate sensitivities, specificities, and accuracies of the two methods.

#### RESULTS

For cartilaginous defects and MM, specificity and accuracy of 3D isotropic IW fast SE without FS was significantly greater than with FS (cartilaginous defects, sensitivity, 96.2% vs 94.7%, accuracy, 93% vs 91.7%; MM, sensitivity, 84.8% vs 75%, accuracy, 87.5% vs 82%). The accuracy of 3D isotropic IW fast SE without FS for LM was also significantly higher than with FS (88.1% vs 83.5%). There was no significant difference in sensitivity between the two methods.

#### CONCLUSION

The performance of 3D isotropic IW fast SE without FS is better than with FS to evaluation of cartilaginous defects and meniscus.

#### CLINICAL RELEVANCE/APPLICATION

If one or more fat water-sensitivity sequence is included to routine sequence for the evaluation of bone marrow edema, 3D;IW-FSE;would be;better without fat saturation for evaluation of IDK.

### **VSMK21-07 • MR Imaging of Posterolateral Corner Reconstruction of the Knee by Posterolateral Corner Sling Procedure: Review of 15 Patients with Clinical Correlation**

**Woo Young Kang** (Presenter) ; **Kyung-Sik Ahn MD ; Chang Ho Kang MD ; Suk-Joo Hong MD ; Baek Hyun Kim MD ; Dae-Hee Lee**

#### PURPOSE

To describe the postoperative magnetic resonance (MR) appearance of the posterolateral corner (PLC) reconstruction of the knee and to correlate the MR findings with clinical examination.

#### METHOD AND MATERIALS

Postoperative MR examinations of 15 patients who underwent PLC reconstruction by PLC sling through the fibular tunnel using allograft from 1 to 36 months (mean 10 months) after the surgery were retrospectively reviewed. Graft shape, thickness, signal intensity of the anterior and posterior limbs of the sling were recorded. Peroneal nerve thickness and signal intensity were compared with preoperative MR images. The MR findings were correlated with the time since surgery and clinical examination.

#### RESULTS

All 15 grafts were intact without disruption and 1 had biopsy-confirmed foreign body reaction. Five knees were unstable on physical examination at the time of MR imaging. Anterior limb of the sling appeared as elliptical shape (15 of 15) on axial images with mean thickness of 5.86 (SD ± 3.7) mm and posterior limb as crescent shape (11 of 15) with mean thickness of 3.23 (SD ± 1.2) mm. Signal intensity of the overall graft sling was increased in 13 of 15 cases, and posterior limb showed same or higher grade signal increase compared with anterior limb in 10 of 13 cases. Signal increase in posterior limb was more prominent in graft with longer time interval since surgery (p

#### CONCLUSION

In postoperative MR imaging of PLC reconstruction, increased signal intensity in posterior limb of the PLC sling appears to be related with time interval since surgery but not correlated with clinical stability, and peroneal nerve thickening may be an expected postoperative finding irrelevant to symptom.

#### CLINICAL RELEVANCE/APPLICATION

Postoperative MR imaging after the PLC reconstruction can depict the increased signal intensity of the graft and thickening of peroneal nerve.

### **VSMK21-08 • Postoperative Cartilage Imaging**

**Humberto G Rosas MD** (Presenter)

#### LEARNING OBJECTIVES

1) Review the postoperative imaging appearances of articular cartilage repair, with an emphasis on MRI.

### **VSMK21-09 • Pre- and Postoperative ACL Imaging**

**Mark W Anderson MD** (Presenter)

#### LEARNING OBJECTIVES

1) Describe the normal anatomy of the anterior cruciate ligament and its appearance on MR images. 2) List the primary and secondary MR imaging signs of complete and partial tears of the ACL. 3) Discuss the MR imaging appearances of a normal ACL graft and the most common types of graft complications.

#### ABSTRACT

Tears of the anterior cruciate ligament are exceedingly common, and MR imaging plays an important role in demonstrating the degree of ligament damage as well as associated injuries. As such, a solid understanding of ACL anatomy and pathology is essential, and this lecture will review the MR imaging appearances of the normal ACL as well as the spectrum of ligament injury including both complete and partial tears. Surgical options for ligament reconstruction will be reviewed along with the MR appearances of a normal ACL graft and most

common graft complications.

### **VSMK21-10 • Association of ACL and Anterior Horn Lateral Meniscus Root Ligament Anatomy and Pathology: 11.7 T MRI Anatomic Study with Retrospective Review of 500 Knee MRIs**

**Monica Tafur MD (Presenter) ; Guilherme M Cunha MD ; Ja-Young Choi MD ; Eric Y Chang MD ; Tanya Wolfson MS ; Anthony Gamst PhD ; Paul A DiCamillo MD, PhD ; Graeme M Bydder MBChB \* ; Donald L Resnick MD ; Sheronda Statum ; Christine B Chung MD**

#### **PURPOSE**

Anatomic studies have shown that few fibers of the anteromedial and posterolateral bundles of the anterior cruciate ligament (ACL) partially blend with the anterior horn of the lateral meniscus root ligament (AHLMR) fibers. This close relationship between the ACL and the AHLMR through these blended fibers (BF) might be a pathway for spread of lesions affecting the ACL. We sought to systematically evaluate the prevalence and association of ACL degenerative and traumatic lesions with abnormal MR appearance of AHLMR.

#### **METHOD AND MATERIALS**

In a single cadaveric knee, the tibial attachment of the AHLM root ligament and ACL was imaged on an 11.7T MR system with a 3D GRE (TR20ms, TE7ms) sequence (112x112x120mm resolution). Two blinded readers retrospectively reviewed 500 consecutive knee MRI examinations (6 month period). Studies were searched for the presence of ACL lesions (degenerative mucoid lesions or traumatic tears), abnormal appearance of AHLMR (degeneration or tear) and increased signal of the BF. Relationship between ACL and AHLMR lesions was assessed and presence of regional synovitis was also noted. Statistical analysis was performed using chi-square tests and kappa coefficient.

#### **RESULTS**

High-resolution cadaveric MRI showed contribution of ACL fibers to the AHLM root ligament. The study population consisted of 479 patients, mean age 46 years. Review of clinical MRI cases showed ACL abnormalities in 42.1% of cases (Kappa=0.867), which included degenerative mucoid lesions (22.3%), traumatic tears (39.3%), and synovitis around distal ACL (38.3%). Root ligament abnormal appearance seen in 35.8% of the cases (Kappa=0.933) included degeneration (85.3%) and tears (14.6%). 28% of cases shown abnormal MR signal of the BF. There were significant associations between ACL and AHLM root ligament abnormalities (p

#### **CONCLUSION**

Concurrent abnormalities of the AHLM root ligament and ACL are common and likely due their intimate anatomic relationship through the blended fibers.

#### **CLINICAL RELEVANCE/APPLICATION**

Pathology of root ligaments may alter normal biomechanics of menisci, therefore the importance to identify potential patterns for spread of diseases affecting closely related structures such as the AC

### **VSMK21-11 • Single Bundle Anterior Cruciate Ligament ruptures: Can We See It on MRI?**

**Alireza Zavareh MD, FRCR ; Mike Bradley MBChB ; James Robinson MBBS ; Martin Williams MBChB ; Hyeladzira Thahal MBChB, MRCP (Presenter)**

#### **PURPOSE**

To demonstrate the accuracy of MRI in diagnosing the solitary anteromedial (AM) and posterolateral (PL) bundle tears of the anterior cruciate ligament (ACL) ruptures.

#### **METHOD AND MATERIALS**

We selected 35 cases of ACL rupture with arthroscopically proved solitary tear of either AM or PL bundle. The pre-operative MRI of these cases were randomly given to two experienced musculoskeletal radiologists in our institution who were blinded of the actual results. Their diagnosis of the single bundle tear were scrutinised against the arthroscopic findings. The specificity and sensitivity of the MRI findings were also evaluated as well as the inter-observer variability in the radiological diagnosis. We also recorded the other bone and soft tissue injuries seen on the MRI study to evaluate if these injuries are related to a specific torn bundle.

#### **RESULTS**

Both radiologists were able to pinpoint the correct torn bundle of the ACL. The inter-observer variability is more pronounced regarding the PL bundle tear. The other injuries to the distal femur and proximal tibia were of a slightly different pattern in these two types of injury. Hence, this could be of help when evaluating the ACL for single bundle injuries.

#### **CONCLUSION**

The MRI could be a reliable tool in differentiating the AM and PL tears of the ACL and helping with case selection for the single bundle ACL augmentation.

#### **CLINICAL RELEVANCE/APPLICATION**

There is an increasing trend among the knee surgeons to perform single bundle ACL augmentation instead of whole ACL reconstruction. A more detailed MR report is very helpful for optimal case selection

### **VSMK21-12 • Diffusion Tensor Imaging in the Assessment of Double-bundle Structure of Anterior Cruciate Ligament: A Preliminary Feasibility Study**

**Xianfeng Yang MBChB (Presenter)**

#### **PURPOSE**

To evaluate whether double-bundle structure of ACL could be imaged using diffusion tensor imaging (DTI) and tractography with a 3T MRI scanner.

#### **METHOD AND MATERIALS**

#### **RESULTS**

To our best knowledge, we present the first DTI and tractography results of human ACL. The courses of double bundle of ACL were first analyzed quantitatively using fractional anisotropy (FA), and then visualized in 3D with tractography. Tractography illustrated nicely the 3D courses of double-bundle structure of ACL and corresponded well to the known anatomy .

#### **CONCLUSION**

Quantitative DTI and tractography can be used to image and visualize the double-bundle structure of ACL.

#### **CLINICAL RELEVANCE/APPLICATION**

Three-dimensional view of the AMB and PLB could be a powerful tool to aid image interpretation and guide surgical approach.

### **VSMK21-13 • Medial Synovial Fold of Posterior Cruciate Ligament: Cadaveric Investigation with MRI and Histologic Correlation**

**Mimi Kim MD (Presenter) ; Seunghun Lee MD ; Bong Gun Lee ; Doo Jin Paik MD ; Jiyeon Bae**

#### **PURPOSE**

The purposes of our study were to illustrate the MRI and cadaveric findings of medial synovial fold of posterior cruciate ligament (PCL) and to classify the types according to anatomic position.

#### **METHOD AND MATERIALS**

MRI studies of 22 cadaveric knees were performed. Two musculoskeletal radiologists prospectively reviewed MR images to classify medial synovial folding type of PCL in consensus. MRI types were categorized into three groups, a) invisible type, b) inferior and short type, c) inferior and long type. First, Invisible types didn't show definitive medial fold of PCL on MRI. And, inferior and short types showed visible medial fold without impingement. Finally, inferior and long types had long synovial fold, enough for impingement in the medial femorotibial joint. Correlations were made between findings derived from MRI studies and cadaveric dissections. Histologic analyses were also performed.

#### RESULTS

Most common type of medial synovial folding of PCL was inferior and short type, 76.4% (n=13), followed by inferior and long type, 11.8% (n=2), and invisible type, 11.8% (n=2). At the gross inspection, medial folds of both inferior short and long types were projected into the medial femorotibial joint. Moreover, invisible type on MRI had also protruding medial synovial folding at the superior aspect of PCL. Histologic examinations showed collagenous tissues which were surrounded by single layer of synovial cells.

#### CONCLUSION

Medial synovial folding of PCL is thought to be a normal variant and may be shown in the high frequency of populations according to MRI and cadaveric studies

#### CLINICAL RELEVANCE/APPLICATION

The point is that medial synovial fold of PCL from MRI images is normal variant, it is possible to reduce unnecessary examination.

### VSMK21-14 • Posterior Cruciate and Collateral Ligament Injury Patterns

**Joshua M Polster MD** (Presenter)

#### LEARNING OBJECTIVES

1) Understand the anatomy of the posterior cruciate ligament and collateral ligaments. 2) Understand the pathomechanics of injury of these structures. 3) Understand the relevant clinical decisions made in relation to imaging findings.

#### ABSTRACT

Although posterior cruciate ligament injuries are less common than anterior cruciate ligament injuries, they can lead to significant disability, particularly when seen in conjunction with associated collateral ligament/posterolateral corner injuries. We will review the anatomy, mechanics of injury and imaging findings of these injuries with the objective of being able to provide clinically useful information for referring physicians.

### Nuclear Medicine Series: Assessment of Cancer Treatment Response: Updates

**Monday, 08:30 AM - 12:00 PM • S505AB**



[Back to Top](#)

**VSNM21 • AMA PRA Category 1 Credit™:3.25 • ARRT Category A+ Credit:3.75**

#### Moderator

**Lale Kostakoglu**, MD,MPH

#### Moderator

**Terence Z Wong**, MD, PhD \*

#### LEARNING OBJECTIVES

1) Important methods used for evaluation of treatment response. 2) Examine important findings on PET CT using FDG PET and other novel tracers to understand how to avoid potential pitfalls. 3) Interpret relevant finding with FDG PET and other PET tracer to evaluate response in tumors. 4) Compare available novel tracers for evaluation of treatment response.

#### ABSTRACT

The course is designed for nuclear medicine physicians and radiologists involved in the use of PET CT. The audience will gain knowledge on various clinical applications of FDG PET for evaluation of the therapy response in tumors. The audience will become familiar with novel PET tracers and their application for evaluation of the therapy response in tumors. At the end of the course the audience should be able to apply suitable techniques of FDG PET or other novel tracers for evaluation of the therapy response in tumors.

### VSNM21-01 • Response Assessment Recommendations in Hematologic Malignancies

**Lale Kostakoglu MD,MPH** (Presenter)

#### LEARNING OBJECTIVES

1) Recognize the strengths of FDG PET Imaging in evaluation of therapy response in lymphoma. 2) Understand the importance of interim evaluation of therapy response. 3) Recognize the weaknesses of FDG PET Imaging in evaluation of therapy response in lymphoma.

#### ABSTRACT

There remains a need for a valid means to predict the completeness of therapy response and patient outcome, ideally at baseline, or at least early during treatment, to identify a patient subset with a poor-prognosis in whom continuation of ABVD treatment would be ineffective at achieving remission. [18F]-Fluoro-2-Deoxy-D-Glucose positron emission tomography, particularly integrated with computed tomography (PET/CT) imaging yielded promising results as a surrogate for tumour chemosensitivity and response even proving to be a more accurate predictor of prognosis compared with conventional prognostic factors for lymphoma. One of the most relevant hurdles for a full integration of interim PET scan in the overall therapeutic strategy of HL treatment to harness its prognostic value in the daily clinical practice, is the lack of simple, reproducible interpretation rules shared by the medical community. This depends not only on the uncertainty of boundary definition between "weekly" and "frankly" positive scan, but also from the clinical context in which interim PET is planned: for treatment intensification or de-intensification in case of interim positive or negative scan, respectively. It is evident, in fact, that in the first case a very high PPV and specificity are needed, while in the second a very high sensitivity and NPV are essential to avoid under treatment. Various reading schemes have been used however recently more standardized approaches have been adopted. In this session interpretation criteria developed to be used for interim PET studies and also after completion of therapy will be reviewed to emphasize the strengths and weaknesses of PET as a response surrogate.

### VSNM21-02 • Comparative Diagnostic Performance of <sup>18</sup>F-FDG PET/CT versus Whole-body MRI for Determination of Remission Status in Multiple Myeloma after Stem Cell Transplantation

**Christoph Weber MD** (Presenter); **Silvia Muenster**; **Kersten Peldschus MD**; **Peter Bannas MD**; **Christian R Habermann MD**; **Nikolaus Kroger MD, PhD**; **Gerhard B Adam MD**; **Thorsten Derlin**

#### PURPOSE

To compare the diagnostic performance of whole-body magnetic resonance imaging (WBMRI) versus (18)F-fluorodeoxyglucose ((18)F-FDG) positron emission tomography/computed tomography (PET/CT) for determination of remission status in patients with multiple myeloma (MM) after stem cell transplantation (SCT).

#### METHOD AND MATERIALS

Thirty-one patients were examined by both WBMRI and PET/CT after SCT. Imaging results and clinical remission status as determined by the clinical gold standard (Uniform Response Criteria) were compared.

#### RESULTS

One hundred four lesions were detected in 21 patients. PET/CT had a sensitivity of 50.0 %, a specificity of 85.7 %, a positive predictive value of 62.5 %, a negative predictive value of 78.3 %, and an overall accuracy of 74.2 % for determination of remission status. MRI had a sensitivity of 80.0 %, a specificity of 38.1 %, a positive predictive value of 38.1 %, a negative predictive value of 80 %, and an overall accuracy of 51.6 %. Concordant results were observed in only 12 (11.5 %) of the 104 lesions.

#### CONCLUSION

In the post-treatment setting, both FDG PET/CT and WBMRI provide information about the extent of disease, allowing for a more comprehensive evaluation of persisting or recurrent myeloma. MRI may often be false positive because of persistent non-viable lesions. Therefore, PET/CT might be more suitable than MRI for determination of remission status.

#### CLINICAL RELEVANCE/APPLICATION

PET/CT is the method of choice for an imaging based determination of the remission status in multiple myeloma after stem cell transplantation.

### **VSNM21-03 • The PERCIST Assessment of Response to Radioimmunotherapy in Patients with Lymphoma by Measuring a Single, 5 and all Tumor Lesions**

**Joo Hyun O MD (Presenter) ; Heather Jacene MD ; Jeffrey P Leal BA ; Richard L Wahl MD \***

#### PURPOSE

To determine how well the different PET metrics in PET response criteria in solid tumor (PERCIST) correlate to each other for measuring fractional change before and after radioimmunotherapy.

#### METHOD AND MATERIALS

Patients with refractory or relapsed non-Hodgkin's lymphoma received Bexxar (n=35) or Zevalin (n=14) therapy. FDG PET/CT studies were obtained before the radioimmunotherapy and 12 weeks after single dose of radioimmunotherapy. Three different PERCIST metrics were measured from the baseline and the post therapy FDG PET studies: 1.) the peak standard uptake value corrected for lean body mass (SULpeak) of the single hottest tumor, 2.) the sum of up to the 5 hottest SULpeaks, and 3.) the total lesion glycolysis (TLG) of the entire tumor burden. The three PET metrics represent measurement of a single, up to the 5 hottest lesions, or the entire tumor burden. The fractional change for each PET metric was computed. (Percent change=[baseline measurement - follow-up measurement] ÷ baseline measurement.)

#### RESULTS

For patients treated with Bexxar, the percent change in a single SULpeak correlated with the change of up to 5 SULpeaks (r=0.932, p

#### CONCLUSION

Tracking the single hottest SULpeak before and after radioimmunotherapy shows high correlation with both the analysis of up to the 5 hottest lesions and the entire tumor TLG, both for Bexxar and Zevalin.

#### CLINICAL RELEVANCE/APPLICATION

Measuring just the one hottest SULpeak may adequately represent the entire tumor burden, saving the time and effort that goes into measuring multiple lesions.

### **VSNM21-04 • Role of 18F NaF PET-CT in Tumor Response Assessment of Skeletal Metastasis from Prostate Cancer: A Preliminary Analysis**

**Bhushan Desai MD (Presenter) ; Evan Allgood ; Steven Cen PhD ; Hossein Jadvar MD, PhD**

#### PURPOSE

Conventional morphologic (CT) and functional (99m Tc-MDP bone scintigraphy) imaging methods for qualitative treatment response assessment of bone metastases have been inaccurate and poses a challenge in routine oncological practice and clinical trials. We hypothesize that bone-specific imaging with 18F NaF PET-CT might address an urgent need to develop an objective method for assessing tumor response in bone lesions which can clinically help physicians determine the effectiveness of systemic therapy.

#### METHOD AND MATERIALS

Our preliminary analysis included 21 prostate cancer patients who underwent a baseline and a follow-up 18F NaF PET-CT scan. Clinical (treatment), biochemical (PSA) and quantitative imaging (SUVmax) parameters were collected on these patients. Response was assessed using operational Imaging and PSA based treatment response criteria. Percentage change in AVG of SUVmax of all lesions for each patient was compared to changes in PSA and treatment, to assess if these changes correlated and accurately predicted treatment response. Patients were categorized as Progressors (P) vs. Non-Progressors (NP); Responders (R) vs. Non-Responders (NP) and cross-tabulation was done comparing Imaging and PSA-based response criteria.

#### RESULTS

R vs. NR: 14 of the 21 patients showed concordant response (66.67%). Of the 7 cases which were discordant: 3 were NR by Imaging but R by PSA with a change in treatment after the scan and 4 were R by Imaging but NR by PSA with only 1 patient undergoing change in treatment after the scan. P vs. NP: 7 of the 21 patients showed concordant response (33.34%). Of the 13 cases which were discordant: 5 showed P by Imaging but NP by PSA with a change in treatment after the scan and 8 were NP by Imaging but P by PSA with a change in treatment for only 2 patients.

#### CONCLUSION

Imaging based criteria captured progressors earlier than PSA and this was well correlated with the corresponding change in therapy post scan. Results of our preliminary analysis demonstrate that semi-quantitative analysis of 18F NaF PET/CT might serve as an important imaging tool for monitoring tumor response in bone lesions. These preliminary findings need to be validated on a larger cohort of subjects and assessed in a variety of tumor types as it might have a major implication in patient management.

#### CLINICAL RELEVANCE/APPLICATION

18F NaF PET/CT might serve as an important imaging tool for monitoring tumor response in bone lesions.

### **VSNM21-05 • Response Assessment Recommendations in Solid Tumors: RECIST vs PERCIST**

**Heather Jacene MD (Presenter)**

#### LEARNING OBJECTIVES

1) To compare anatomic and metabolic imaging for response assessment in solid tumors. 2) To discuss limitations of current, widely used criteria for assessing response in solid tumors. 3) To discuss the benefits and limitations of metabolic imaging for response assessment in solid tumors.

### **VSNM21-06 • RECIST 1.0, PERCIST 1.0 and PSA Treatment Response Criteria in Metastatic Castrate-resistant Prostate Cancer**

**Hossein Jadvar MD, PhD (Presenter) ; Bhushan Desai MD ; Lingyun Ji MS ; Susan Groshen PhD ; Chung Y Yu BS ; Tanya Dorff MD ; Jacek Pinski MD, PhD ; Peter S Conti MD, PhD ; David I Quinn MD, PhD**

#### PURPOSE

Many novel therapies are under active evaluation for the treatment of men with metastatic castrate-resistant prostate cancer (CRPC). Anatomic (RECIST1.0), metabolic (PERCIST1.0) and PSA-based (PCWG2) criteria have been proposed for assessing treatment response in this clinical setting. We compared these guidelines in assessment of response to treatment and in relationship to overall survival in men with CRPC.



#### METHOD AND MATERIALS

47 men with metastatic CRPC underwent FDG PET-CT before and 4-mo after start of new systemic therapy. Baseline and 4-mo data were compared using published operational RECIST 1.0, PERCIST 1.0 and PCWG2 definitions with some modifications. Patients were categorized as Responders (R) vs. Non-Responders (NR) and cross-tabulation was done comparing any 2 response criteria eliminating patients who were not evaluable based on either of 2 criteria in each combination. Association between overall survival and a specific response criteria status was calculated using the Kaplan-Meier method.

#### RESULTS

Not all 47 patients were evaluable by all 3 criteria. RECIST 1.0 vs. PERCIST 1.0: 28 of 37 evaluable by both with 75.7% concordance and 9 cases discordant; 6 were NR by RECIST 1.0 but R by PERCIST 1.0 with 3 alive and 3 dead after 22 mo; 3 cases were R by RECIST 1.0 but NR by PERCIST 1.0, 2 died within 1.9 mo post 4-mo scan and 1 was alive at 18.1 mo. PCWG2 vs. RECIST1.0: 23 of 39 evaluable by both with 58.9% concordance and 16 cases discordant; 14 were R by PCWG2 but NR by RECIST 1.0 with 9 dead and 5 alive; 2 were NR by PCWG2 but R by RECIST 1.0 and both died within 1.9 m after 4-mo scan. PCWG2 vs. PERCIST 1.0: 31 of 43 evaluable by both PCWG2 and PERCIST 1.0 with 72.1% concordance and 12 cases discordant; 10 were R by PCWG2 but NR by PERCIST 1.0, 6 died and 4 were lost to follow-up, 2 were NR by PCWG2 but R by PERCIST 1.0, 1 died and 1 was alive at last follow-up.

#### CONCLUSION

PERCIST 1.0 was more concordant than RECIST 1.0 with the PCWG2 response criteria and tended to be better associated with overall survival. PERCIST 1.0 may have a competitive advantage over RECIST 1.0 in the assessment of treatment response in metastatic CRPC (Supported by NIH grants R01-111613 and P30-CA014089; Clinical Trial Registration number NCT00282906)

#### CLINICAL RELEVANCE/APPLICATION

Use of an appropriate treatment response criteria is pivotal for comparative effectiveness of various current and novel therapies in metastatic prostate cancer.

### **VSNM21-07 • FDG PET/CT for Early Response Assessment in Patients (pts) with Advanced Melanoma (MEL) Receiving Immune Checkpoint Blockade**

**Steve Cho MD (Presenter) \* ; Evan J Lipson MD ; Alin Chirindel MD ; Suzanne Topalian MD \* ; Drew M Pardoll MD, PhD ; Richard L Wahl MD \***

#### PURPOSE

Immune checkpoint blockade with anti-CTLA-4 (ipilimumab) prolongs survival in ~20% of pts with advanced MEL, and blockade of the PD-1/PD-L1 pathway induces objective responses in some pts with MEL and other cancers. Traditional CT-based response criteria can be insufficient to measure the activity of these therapies, which can produce delayed or mixed tumor regressions preceded by apparent progressive disease (PD). In MEL pts receiving immune checkpoint inhibitors, we compared the ability of FDG PET and CT at 4 and 12 weeks of therapy to predict and evaluate clinical response.

#### METHOD AND MATERIALS

Ten pts with MEL scheduled for treatment with ipilimumab (8 pts) or anti-PD-L1 (2 pts; BMS-936559) were enrolled. FDG PET/CT was performed at baseline (day -28 to 0) (PET1), and 4 wks (PET2) and 12 wks (PET3) after treatment initiation. The CT portion of the PET/CT was used for conventional restaging with RECIST 1.1 (REC) and WHO criteria. FDG PET was used for quantitative assessment with PERCIST 1.0 (PER). One pt was not able to receive PET3 due to rapid PD.

#### RESULTS

At PET3, 9/10 pts demonstrated PD by all criteria; one pt with lymph node < 1.5 cm in short axis was not evaluable by REC, but had stable disease (SD) by WHO and complete response (CR) by PER. However, when evaluating only index lesions and excluding new lesions as PD, the response for these cohort of patients showed varying clinical benefit by REC (4 SD), WHO (3 SD, 1 partial response (PR)), or PER (1 CR, 1 PR, 2 SD). 8/9 pts had increased tumor FDG uptake at PET2 (7.8% to 211% increase from baseline) of whom 2 had CR or PR on PET3 (100% and 49% decrease from baseline). 1/9 pts had decreased tumor FDG uptake at PET2 (28% decrease from baseline). We observed a pattern of increased tumor FDG uptake and dimensions at PET2 with subsequent improvement by PET3, suggesting the presence of tumor inflammation (anti-tumor immune response) on PET2.

#### CONCLUSION

Increased tumor FDG uptake at 4 weeks (PET2) may indicate inflammation preceding lesional response, or actual tumor progression. These preliminary data suggest that early increased FDG uptake may be necessary but not sufficient for tumor regression in pts receiving immune checkpoint blockade, requiring validation in larger trials.

#### CLINICAL RELEVANCE/APPLICATION

Combined FDG PET/CT using an early 4 week and standard 16 week time-point may be used predict melanoma response assessment to immune checkpoint blockade therapy.

### **VSNM21-08 • The Clinical Value of FDG PET/CT in Assessing Therapeutic Efficacy of Non-surgical Ablation Therapy for Radioiodine-negative Recurrent or Metastatic Thyroid Cancer**

**Kunihiro Nakada (Presenter) ; Hiroki Sugie MD ; Keiichi Kamijo MD, PhD ; Masayuki Sakurai**

#### PURPOSE

Percutaneous ethanol injection (PEI) and radiofrequency ablation (RFA) serve as feasible options for local control of radioiodine-ineffective thyroid cancer after surgery. The purpose of the study was to determine clinical value of PET/CT using F-18 fluorodeoxyglucose (FDG) in assessing therapeutic efficacy of PEI or RFA for radioiodine negative metastatic thyroid cancer.

#### METHOD AND MATERIALS

The study consists of 108 metastatic tumors from thyroid cancer (100 metastatic nodes in the neck or mediastinum and 8 metastatic bone tumors) in 76 patients (PCA/FCA 68/8) who had underwent total thyroidectomy and radioiodine ablation. All patients received high dose I-131 therapy. However, I-131 uptake in the metastatic tumor on the post-therapy scan was no or equivocal. Additionally, patients had reluctance to further surgery or were at high risk for surgery due to other complications. Patients underwent FDG PET/CT within 2mos. prior to and between 1 and 2 mos. post completion of ablation therapy. FDG uptake in the tumor was visually assessed as positive or negative. Patients were followed up for 14-66mos. (median 31) to investigate clinical course of the treated tumors. Efficacy of PEI or RFA was determined based upon RECIST 1.1. Achievement of CR or PR was considered as successful.

#### RESULTS

On the pre-treatment PET/CT, all 109 tumors were FDG positive. Then 99 were treated by PEI while 9 were treated by RFA. On the post-treatment PET/CT, FDG uptake was negative in 76 (70%) and was persistently positive in the remaining 33 (30%). In the FDG negative tumors, CR and PR were observed in 55 and 20, respectively. Regrowth of the tumor was seen in 8 (11%). In the FDG positive tumors, PR were seen in 13 while remaining 20 showed SD. Regrowth of the tumor was seen in 15 (45%). The PPV, NPV and accuracy of FDG PET/CT for successful outcome of ablative therapy were 99%, 61% and 88%.

#### CONCLUSION

Almost all tumors with negative FDG uptake after treatment showed good response. In contrast, tumors with persistent FDG uptake were associated with poorer response and the risk of tumor regrowth was 4 times higher than that in FDG negative tumors. FDG PET seems valuable in assessing efficacy of non-surgical ablation therapy for metastatic thyroid cancer.

#### CLINICAL RELEVANCE/APPLICATION

Application of FDG PET/CT may enhance clinical value of non-surgical ablation therapy and may improve management of radioiodine-negative metastatic thyroid cancer.

## VSNM21-09 • Response Assessment Recommendations after Radiation Therapy

**Terence Z Wong** MD, PhD (Presenter) \*

### LEARNING OBJECTIVES

1) Understand the physiology of normal tissue response to radiation therapy. 2) Understand potential limitations of PET/CT imaging following radiation therapy. 3) Suggest potential strategies for evaluating patients following radiation therapy.

### ABSTRACT

FDG-PET/CT imaging following radiation therapy can be complicated, due to the resulting inflammatory response. These post-radiation effects can mimic residual or recurrent tumor, and may preclude accurate determination of response to therapy. The extent to which radiation therapy effects influences interpretation of PET/CT scans is highly dependent on the organ site and time-dependent normal tissue response. Armed with this knowledge, it is often possible to distinguish radiation changes from tumor. Several strategies are available to improve accuracy of post-treatment PET/CT. Waiting for several months following radiation therapy allows the inflammatory response to subside. Alternatively, imaging early in the course of radiation therapy may allow response to be evaluated before the inflammatory response occurs. Alternative PET tracers, such as F-18 fluorothymidine as a marker of cell proliferation, may be less affected by the inflammatory reaction. Therapeutic strategies can be designed to minimize the impact of radiation effects; for example chemotherapy can be initiated prior to combined chemoradiation, allowing PET/CT to measure the response to the chemotherapy prior to starting radiation therapy.

## VSNM21-10 • Early Assessment of Therapeutic Response of Radioimmunotherapy (RIT) in Non-Hodgkin Lymphoma: Comparing Tumor Volume Reduction and Metabolic PET Measurements in Prediction of Progression Free Survival (PFS)

**Ehab H Youssef** MD, FRCR (Presenter) ; **Yuni K Dewaraja** PhD ; **Hatice Savas** MD ; **Matthew Schipper** ; **Shen Jincheng** ; **Mark S Kaminski** \* ; **Anca Avram** MD

### PURPOSE

To evaluate if initial tumor volume reduction and metabolic response predicts progression free survival (PFS) in patients with advanced follicular non-Hodgkin lymphoma (NHL) receiving 131-I Tositumomab therapeutic regimen. Tumor volumes were measured on CT component of SPECT/CT (at 6 days and 2 weeks), and of PET/CT at 2 months post-RIT; qualitative metabolic response (defined as positive or negative complete metabolic response for disease) was assessed on PET/CT at 2 months post-RIT. Clinical and imaging follow-up was continued for all patients until they progress 1-51.5 months (average 9.3).

### METHOD AND MATERIALS

A group of 53 patients (37 males, 16 females), with advanced (stage III or stage IV) chemotherapy-refractory follicular B-cell lymphoma, aged 33-81 years (median age 54) received 131-I Tositumomab therapy based on whole body dosimetry calculations with the goal of delivering 75 cGy whole body radiation absorbed dose for patients with platelets > 150,000/mL, or 65Gy for patients with platelets

### RESULTS

51 patients (96%) had tumor shrinkage, 26 of them (49%) had =30% shrinkage in 2 weeks, and 25 (47%) had = 73% shrinkage at 2 months.

Statistically significant correlation between progression free survival (PFS) and tumor volume reduction of =30% on CT portion of SPECT-CT (at 2 weeks) and = 73% on PET-CT (at 2 months) was observed (p= 0.0013), and (p< 0.0001) respectively.

Statistically significant correlation between PFS and complete metabolic tumor response on post-therapy PET-CT (2 months) (p< 0.0001) was observed.

### CONCLUSION

Initial tumor volume reduction and complete metabolic response (in PET) can be used to predict PFS, hence can potentially be used to customize future treatment protocols for NHL patients.

### CLINICAL RELEVANCE/APPLICATION

Initial tumor volume reduction and complete metabolic response (in PET) can be used to predict PFS, hence can potentially be used to customize future treatment protocols for NHL patients.

## VSNM21-11 • 18F-fluorodeoxyglucose Positron Emission Tomography (PET) Response to Stereotactic Body Radiotherapy (SBRT) in Metastatic Melanoma

**Miran J Blanchard** MD (Presenter) ; **Zachary C Wilson** MD ; **Brandon M Barney** MD ; **Gregory Wiseman** ; **Kenneth R Olivier** MD ; **Sean S Park** MD, PhD ; **Svetomir Markovic** MD, PhD

### PURPOSE

We report our SBRT experience for extracranial melanoma metastases to objectively characterize the PET metabolic response.

### METHOD AND MATERIALS

32 metastatic melanoma patients (pts) treated with SBRT with baseline and post-SBRT PETs were identified in our prospectively maintained database from 2008 to August 2011. PET metabolic response was evaluated per PERCIST 1.0 criteria: Complete response (CR) was a decrease in the maximum standard uptake value corrected for lean body mass (SUL) to 1.5 times the liver mean + 2 standard deviations, partial response (PR) was a 30% decrease in SUL, progressive disease (PD) was > 30% increase in SUL and stable disease (SD) was any lesion not fitting these criteria. Local control (LC) included CR, PR, and SD.

### RESULTS

57 lesions treated with SBRT and 174 pre- and post-SBRT PET scans were analyzed. Median follow-up (f/u) was 1.6 years. Sites of treated lesions were: 15 musculoskeletal, 14 liver, 14 lung, 12 abdominal, 2 extra abdominal lymph nodes. Median single-fraction equivalent dose (SFED) was 43 Gy (range 18-56 Gy). A median of 5 PET scans (range 2-6) were evaluated for each lesion. LC was 92% and 87% and overall survival was 59% and 29% at 1.5 and 3 years, respectively. Median time to CR was 2.8 months (0.7-15 months). CR was achieved in 49 lesions (86%), and 44 lesions maintained CR at last f/u. Median f/u for lesions in continuous CR was 18 months (0.9-36.5). PR, SD, and PD were 9%, 4%, and 10%, respectively. SFED = 24 Gy correlated with PD (HR 17, p=0.01). At initial f/u (median 2 months), CR was 60%, and 9 lesions (16%) had increased SUL. These 9 lesions resolved to 6 CR, 1 SD, and 2 PD with subsequent f/u. One patient is alive with no evidence of disease (NED) and one patient with NED died of other causes. Three patients had NED on PET and died suddenly of CNS metastasis. 28% developed CNS metastases at a median of 5 months (0.2-32 months) after SBRT.

### CONCLUSION

SBRT is highly effective in inducing a complete metabolic response in melanoma. A SFED of > 24 Gy has been validated as a predictor of lesion control. 16% of lesions had a SUL rise at initial f/u with the majority subsequently achieving CR with no additional local therapy. Three pts with NED on PET died suddenly of brain metastases. Screening brain MRI prior to SBRT for oligometastatic melanoma should be considered.

### CLINICAL RELEVANCE/APPLICATION

SBRT leads to a high rate of complete metabolic response in metastatic melanoma.

## VSNM21-12 • Cu-ATSM Uptake May Predict Prognosis after Treatment in Advanced Head-and-Neck Cancers: Evaluation of Resistant Hypoxic Tissue with Tumor-to-Muscle Ratio

**Yoshitaka Sato** MD ; **Myungmi Oh** MD, PhD ; **Tetsuya Mori** PhD ; **Yasushi Kiyono** PhD ; **Shigeharu Fujieda** MD, PhD ; **Hidehiko Okazawa** MD, PhD (Presenter)

### PURPOSE

To delineate hypoxic tissue in head-neck cancers, [<sup>64</sup>Cu]diacetyl-bis(N<sup>4</sup>-methylthiosemicarbazone) (Cu-ATSM) PET was employed and tracer distribution was compared with [<sup>18</sup>F]fluorodeoxyglucose (FDG). Predictability of effectiveness of tumor treatment was compared between the 2 tracers.

#### METHOD AND MATERIALS

Thirty patients with head-and-neck cancer (mean age: 67 ± 13 y.o.) underwent Cu-ATSM-PET and FDG-PET/CT within a week interval. For Cu-ATSM PET images, 20-min dynamic data acquisition was performed after 600-800 MBq tracer injection, and 10 to 20 min data were used for analysis. After co-registration of Cu-ATSM-PET and FDG-PET/CT images, region of interest (ROI) was placed on the tumour mass using the threshold of 40% of maximum value for each PET image to obtain standardized uptake values (SUV) and maximum SUV (SUV<sub>max</sub>) of each tumour. SUV values of the muscles in the head-and-neck region were also obtained and tumour-to-muscle (T/M) ratio for each tracer was calculated. Patients were followed up at least 6 months after the treatment by using CT, MRI or FDG-PET/CT, and progression-free survival (PFS) period was compared using Kaplan-Meier Logrank analysis. The end-point of the follow-up for PFS was set at the time of recurrence or metastasis of the cancer. Relationships between PET parameters and PFS period were analyzed to assess which was the most appropriate parameter to predict prognosis of head-and-neck cancers.

#### RESULTS

Twenty-eight of the patients received chemoradiation therapy and 2 underwent surgical treatment only. The mean PFS period was 12.6 ± 9.5 months, and 14 patients showed recurrence or metastasis. Patients were divided into 2 groups of higher and lower uptake of tracers using SUV<sub>max</sub> and T/M ratio. Threshold was determined by ROC analysis for each PET parameter, and PFS was compared between the 2 groups. The patient groups determined by the T/M ratio of Cu-ATSM showed significantly different PFS; i.e. higher T/M ratio showed poor PFS compared with the lower T/M ratio group. Other PET parameters did not show significant difference in PFS.

#### CONCLUSION

The high Cu-ATSM T/M ratios predicted the poor prognosis after treatment in patients with head-and-neck cancer. SUV<sub>max</sub> and FDG-T/M ratio were not good indicators of prognosis after the cancer treatment.

#### CLINICAL RELEVANCE/APPLICATION

Cu-ATSM PET is expected to be useful for detection of resistant malignant tumours.

---

### Neuroradiology Series: Spine

---

**Monday, 08:30 AM - 12:00 PM • N230**

---

NR

[Back to Top](#)

**VSNR21 • AMA PRA Category 1 Credit™:3.25 • ARRT Category A+ Credit:4**

#### Moderator

**Adam E Flanders, MD**

#### Moderator

**Leon J van Rensburg, MD, DSc \***

**VSNR21-01 • New Spine MR Techniques**

**Lawrence N Tanenbaum MD (Presenter) \***

#### LEARNING OBJECTIVES

1) To become familiar with the role of diffusion imaging in evaluation of the spine. 2) To become familiar with the methods for optimization of diffusion of the spine. 3) To become familiar with the potential role of MR spectroscopy in evaluation of the painful disc.

**VSNR21-02 • The Use of Deformable External Dielectric Pad in 3T Cervical Spinal Cord MR Imaging to Enhance Image Quality**

**Dan T Nguyen MD (Presenter) ; Christopher Sica PhD ; Sebastian Rupprecht BS ; Jeff Vesek MS ; Gary Thomas MD, MBA \* ; Qing X Yang PhD**

#### PURPOSE

Recent development of an external deformable dielectric pad potentially allows regional image intensity enhancement and reduces center-bright artifact for MR Imaging, especially in high field magnet. The purpose of this study is to validate such theoretical advantages of the dielectric pad in applying to cervical spinal cord MR Imaging.

#### METHOD AND MATERIALS

In 5 clinical patients with Multiple Sclerosis, the 3T cervical MRI studies were acquired without and with the application of the dielectric pad, which surrounds the bottom and sides of the neck. Multi-slice sagittal and transverse turbo spin-echo (TSE) image sets (PD, T1W, T2W in 3mm thickness) were acquired, with some additional scans at 1mm and 1.5 mm thickness to better visualize MS lesions. A Neuroradiologist evaluated the images, and signal-to-noise (SNR) measurements were made in several discs (C1-C4) with the TSE images and separate gradient-echo images with noise scans.

#### RESULTS

The images in the figure were acquired without (left) and with (right) the external dielectric pad. Images with the pad demonstrates enhanced clarity, permitting visualization of several intramedullary cord lesions, whereas the lesions are not visible in the image without pads due to insufficient SNR. The SNR enhancement among the 5 patients in C1 - C4 was in the range of 0 to 60%, with typical enhancement around 20 to 40%. The pads reduced scan power in the range of 31 to 50%, with an average reduction of 38.8%.

#### CONCLUSION

The use of the deformable external dielectric pad enhances the visualization of cord lesion while reduces tissue energy deposition. This ability can aid in improved and earlier diagnosis or treatment followup of spinal cord pathologies.

#### CLINICAL RELEVANCE/APPLICATION

The application of an external deformable dielectric pad potentially enhances image quality of the spinal cord in this cervical anatomical region that is well known to have local field inhomogeneity.

**VSNR21-03 • Evaluation of Works-in-Progress Dixon Fat Suppression in Spine, Musculoskeletal and Neck Imaging Compared with Routine Imaging**

**Yair Safriel MBCh (Presenter) \* ; Brian M Dale PhD \***

#### PURPOSE

Homogeneous fat suppression (FS) on T2 and post contrast T1 imaging is challenging in extremity, spine and neck imaging due to field heterogeneity and/or the presence of orthopedic hardware. FS may fail completely, result in paradoxical water suppression or, sometimes worse of all, generate an image with regions of successful and failed FS on the same image. Alternatives to FS are inversion recovery (IR) or gradient, however, these may have different imaging characteristics for certain anatomy or pathology compared to Turbo Spine Echo (TSE). Dixon FS (DFS) is robust to field heterogeneity and does not alter the sequence's imaging characteristics.

#### METHOD AND MATERIALS

Review Board approval was obtained. DFS separately acquires images where the fat and water signals are in- and opposed-phase. Field inhomogeneity changes the overall phase, but does not change the relative phase between fat and water. Therefore, DFS uses the

relative phase information to suppress fat in a manner insensitive to field inhomogeneity. Over a 6 week period the following DFS was applied to: All neck MRs, all spinal post contrast MRs and a random selection of noncontrast spine and musculoskeletal MRs. In all cases the DFS was obtained in addition to routine T1 or T2 FS sequence. Sequences were performed on a variety of 1.5 and 3T (Espree, Avanto and Tim Trio, Siemens, Germany). Each sequence was scored for edge artifact, FS homogeneity, metal artifact and visualization of pathology.

#### RESULTS

34 DFS sequences (11 lumbar, 7 thoracic and 7 cervical spine, 3 joints, 3 pelvis and 3 necks) were scanned. T2 and T1 DFS scored better or equivalent to T2FS and T1FS in 97% and 100% of cases (P

#### CONCLUSION

DFS has potential to improve imaging of implanted hardware, on both 1.5T and 3T. It may also improve diagnostic confidence, possibly obviating additional or invasive procedures. Further work is needed to better define the parameters prior to commercial release.

#### CLINICAL RELEVANCE/APPLICATION

DFS markedly improves FS image quality in T2 and post contrast T1 sequences without altering the expected signal characteristics of anatomy or pathology

### **VSNR21-04 • Iatrogenic Disorders in the Spine**

**Erik H Gaensler MD** (Presenter)

#### LEARNING OBJECTIVES

This presentation will review the wide spectrum of spine imaging findings that can be due to medical intervention, including diagnostic procedures, radiation therapy, chemotherapy, therapeutic spinal injection procedures, and surgery. The pertinent findings, differential diagnosis and pitfalls of such 'Iatrogenic Disorders' will be discussed.

### **VSNR21-05 • Has Utilization of MRI of the Lumbar Spine Decreased in Response to Appropriateness Criteria for Imaging of Low Back Pain?**

**David C Levin MD** (Presenter) \* ; **David P Friedman MD** ; **Laurence Parker PhD** ; **Vijay M Rao MD**

#### PURPOSE

The overuse of MRI for low back pain (LBP) has been a concern. Appropriateness criteria which have long been promulgated by the ACR, radiology benefits management companies, and other organizations have stated that MRI is generally not indicated in LBP without a prior trial of conservative management, unless certain red flags are present. It is unclear to what extent referring clinicians are aware of or have accepted these criteria. Our purpose was to determine if the utilization of lumbar spine MRI has decreased accordingly, using a large population database.

#### METHOD AND MATERIALS

The nationwide Medicare Physician/Supplier Procedure Summary Master Files for 1999 through 2011 were used. They cover the 36.3 million beneficiaries in traditional fee-for-service Medicare. CPT code 72148 (lumbar spine MRI without contrast) was selected and analyzed. The vast majority of these studies are done with LBP as the indication. Procedure volumes each year were determined by tabulating all global and professional component claims. Technical component claims were excluded to avoid double counting. Utilization rates per 1000 beneficiaries were calculated for all provider specialties and all places of service.

#### RESULTS

In 1999, the total utilization rate of code 72148 was 14.7 exams per 1000. The rate increased progressively till it reached 32.2 in 2008, representing a compound annual growth rate of 9.1%. From 2008 through 2011, there was essentially no change in the rate. In 2011, the rate was 32.3.

#### CONCLUSION

Given the general consensus that early MRI of LBP is usually unnecessary, one might expect the utilization of this procedure to be declining to at least some degree. Instead, it grew rapidly through 2008, then remained unchanged through 2011. Several unrelated factors could have contributed to growth, such as patient demand, concern about malpractice liability, etc. However, even taking these into account, it appears that the appropriateness criteria have had no discernible effect on reducing MRI utilization. This represents an opportunity for radiologists to educate their clinical colleagues about the proper indications for use of this widely performed imaging test.

#### CLINICAL RELEVANCE/APPLICATION

Not applicable

### **VSNR21-06 • Does the Preoperative Trans-artery Embolism Decrease the Blood Loss during Spine Tumor Surgery?**

**Ningyang Jia MD, PhD** (Presenter) ; **Zhiqiong Qiao** ; **Qian He**

#### PURPOSE

This paper aimed to evaluate the effect of pre-surgery trans-artery embolism (TAE) on the intra-operative blood loss during surgical excision of the vertebral tumor.

#### METHOD AND MATERIALS

#### RESULTS

#### CONCLUSION

This study showed that the pre-surgery TAE of the spinal tumor had no significant effect on the intra-operative blood loss during the surgical excision of the spinal tumor.

#### CLINICAL RELEVANCE/APPLICATION

View of the risk of embolism, such method should be carefully considered.

### **VSNR21-07 • Evaluation and Treatment of Cerebrospinal Fluid Hypotension**

**William P Dillon MD** (Presenter)

#### LEARNING OBJECTIVES

1) Recognize the clinical and MR features of intracranial hypotension. 2) Understand the workup of a patient with suspected CSF leak in the spine. 3) Understand the elements of safe epidural blood patch technique.

#### ABSTRACT

Intracranial CSF hypotension is a disorder that presents primarily with postural headache and specific MR features. In this presentation, we will discuss the clinical presentation, common pathologic entities, diagnostic workup and therapeutic options and potential complications for these patients with spontaneous intracranial hypotension.

### **VSNR21-08 • Detection of Spontaneous Cerebrospinal Fluid Leak Using Dual-energy CT Myelography**

**Qiaowei Zhang MD, PhD** (Presenter) ; **Dang Wang MD** ; **Xiang-Yang Gong PhD**

#### PURPOSE

To investigate the accuracy of detecting spontaneous cerebrospinal fluid (CSF) leak using dual-energy CT iodine map and virtual non-contrast (VNC) images compared with mixed images.

#### METHOD AND MATERIALS

64 patients (22 men and 42 women, mean age 40.3±9 years ) with suspected spontaneous CSF leak underwent dual-energy CT myelography (CTM). The tube voltages were Sn140 and 100 kVp. The images of two tubes were mixed at the ratio of 0.5 and served as simulated 120 kVp images. The iodine map and VNC images were calculated. Two radiologists independently reviewed the iodine map/VNC images and the mixed images to identify the CSF leaks along the nerve roots, high-cervical retrospinal CSF collections, and other findings.

#### RESULTS

Using iodine map and VNC images, 421 leaks were found in 56 patients. Using mixed images, 454 leaks were found in 56 patients. The accuracy of detecting CSF leak was 92.7% in per-leakage analysis, and was 100% in per-patient analysis. There is no difference in detecting high-cervical retrospinal CSF collections(n=17). Most of the spinal CSF leaks occurred at the lower cervical region and cervicothoracic junction( C4/5-T1/2, 55.7%).

#### CONCLUSION

The dual-energy CTM can detect spontaneous CSF leaks using iodine map/VNC images. With dual-energy CT, the iodine leaked into perispinal area can be confidentially identified. Multiple simultaneous leaks may common.

#### CLINICAL RELEVANCE/APPLICATION

The dual-energy CTM can increase the diagnostic confidence of CSF leakage detection.

### **VSNR21-09 • The Back Pain Outcomes Using Longitudinal Data (BOLD) Project- Baseline Data from a Prospective Cohort of ~5,000 Seniors with Back Pain**

**Jeffrey G Jarvik MD, MPH (Presenter) \* ; Brian W Bresnahan PhD \* ; Bryan A Comstock ; Richard A Deyo MD, MPH ; Janna Friedly ; Patrick Heagerty ; Larry G Kessler \* ; Sean D Rundell MS ; Judith Turner ; Andrew Avins ; Srdjan Nedeljkovic ; David Nerenz ; Zoya Bauer ; Katherine T James**

#### PURPOSE

To describe how pain, functional status and health related quality-of-life vary by demographic factors among seniors presenting to primary care providers with new episodes of low back pain.

#### METHOD AND MATERIALS

We enrolled patients = 65 years old who presented to a primary care provider with a new episode of back pain. We recruited study participants from three integrated health systems (Kaiser-P N CA, Henry Ford-Detroit and Harvard Vanguard Med Assoc -Boston). Baseline measures included: 1) Roland-Morris Disability Questionnaire (RMDQ); 2) 0-10 pain numerical rating scales (NRS); 3) Brief Pain Inventory (BPI); 4) Patient Health Questionnaire (PHQ)-4; 5) EuroQol-5D (EQ5D); 6) Pain duration; 7) Patient expectations. We examined demographic characteristics, comparing the three recruitment sites. We used the chi-square test to compare categorical variables and unpaired t-tests to compare numerical variables and the Mann-Whitney U-test when appropriate.

#### RESULTS

We enrolled 5,288 patients. RMDQ had a small increase with age, from a mean (SD) of 9.1(6.6) at ages 65-69 to a mean of 10.7(6.1) for those greater than 85. The average pain duration also increased with age (32% of those 65-69 having had pain of more than a year compared with 44% >85). The oldest age group had slightly lower confidence (4.9(3.7) vs. 5.6(3.7)) that they would be pain-free or substantially improved by 3 months.

African American (AA) patients were worse on most baseline measures of function and pain. Eg: the mean/median RMDQ scores were 12.1/13 in AAs compared with 8.8/8 for Caucasians. Because over 50% of AAs were at Detroit, confounding by site may be a factor. However, within a given site, AAs had worse scores than Caucasians by more than 1 point on the Roland scale. There were substantial differences between sites with respect to potentially important prognostic demographic factors and baseline reported measures.

#### CONCLUSION

We observed substantial differences of our baseline measures between sites, emphasizing the need for caution when pooling results from a multicenter study. African-Americans appeared to have worse back-related health status in our cohort although confounding by site was present.

#### CLINICAL RELEVANCE/APPLICATION

There is great heterogeneity between sites with respect to baseline characteristics of seniors with back pain. Worse health status among African-Americans may be explained, in part, by site factors.

### **VSNR21-10 • Kyphoplasty vs Vertebroplasty: Economics and Evidence Base**

**David F Kallmes MD (Presenter) \***

#### LEARNING OBJECTIVES

1) To update the community regarding relative costs between the procedures. 2) To update the community regarding recent changes in reimbursement for the procedures. 3) To gain insight into the current practice patterns for both procedures, including procedure volumes and practitioner specialty. 4) To review outcomes in the setting of prospective, controlled trials of vertebroplasty and kyphoplasty.

### **VSNR21-11 • Efficacy of Vertebroplasty for Non Osteoporotic Spinal Compression Fractures. The VOLCANO Study: Vertebroplasty vs. Conservative Treatment in Acute Non Osteoporotic Vertebral Fractures**

**Adrian I Kastler MD, MSc (Presenter) ; Eulalie Huguonnet ; Betty Jean MD ; Jean Gabrillargues ; Bruno Pereira ; Emmanuel Chabert ; Aurelien Coste ; Beatrice Claise ; Viorel Achim ; Toufik Khalil ; Denis Sinardet ; Guillaume Coll ; Bernard Irthum ; Jean Chazal**

#### PURPOSE

Post Traumatic vertebral compression fractures (VCF) are commonly treated with braces. Vertebroplasty may be an alternative treatment. The aim of this prospective study is to assess the effectiveness of vertebroplasty for non osteoporotic compression fractures in the acute setting compared to conservative management

#### METHOD AND MATERIALS

This prospective, randomized, non-blinded, single-center study was carried out in France between 2010 and 2012. Patients aged from 18 to 70 suffering from acute (

#### RESULTS

Intermediate analysis performed after 100 inclusions (52 vertebroplasties and 48 bracing) showed a statistical significance in the primary outcome and lead to premature discontinuation of the study. At one month, mean RDQ was 7.56 in the vertebroplasty group and 11.1 in the brace group (p=0.004). At 6 month the difference decreases, still in favor of vertebroplasty (3.7 vs 2.61, p =0.07). A higher pain reduction at 48h post trauma was significant in the vertebroplasty group (p

#### CONCLUSION

Our study showed a significant improvement in back pain related disability in patients with post traumatic vertebral fractures treated in acute phase by vertebroplasty compared to patients treated by braces. At follow up controls, vertebral height's loss was significantly higher in the bracing group. (ClinicalTrials.gov number, NCT01643395)

#### CLINICAL RELEVANCE/APPLICATION

Acute vertebral compression fracture is a painful condition usually treated with bracing. Vertebroplasty management appears to be safe and effective and should be considered as an alternate treatment

## **VNSR21-12 • Neoplastic Lytic Vertebral Lesions with Erosion of Posterior Wall and Epidural Mass: An Absolute Contraindication to Vertebroplasty?**

**Alessandro Cianfoni** (Presenter) ; **Eytan Raz MD** ; **Emanuele Pravata' MD** ; **Giuseppe Bonaldi MD**

### **PURPOSE**

To assess technical and clinical complications of Percutaneous Vertebroplasty (PV) performed for pain palliation and/or stabilization of neoplastic lytic vertebral body lesions, with cortical erosion of the posterior wall (CE-PW), often associated with soft tissue epidural mass (EM).

### **METHOD AND MATERIALS**

Retrospective assessment of technical and clinical complications of PV on 54 consecutive levels (8 cervical, 28 thoracic, 18 lumbar) with CE-PW, in 38 patients. EM was present in 35/54 levels. Lytic lesions were metastasis from solid tumors at 43 levels, multiple myeloma at 8, and lymphoma at 3. The procedures were variably performed before, during, or after radiation treatment and/or chemotherapy. All procedures were performed under fluoroscopic guidance, combined to CT-guidance for 8 levels. Cavity-creation was performed with plasma-field-activated radiofrequency (coblation) wands in 50/54 levels, prior to cement injection. Post-procedure CT of the treated levels was obtained in all cases. Clinical follow-up was performed at 1 and 4 weeks post-procedure.

### **RESULTS**

In 50/54 levels the PV resulted in satisfactory PMMA filling of the lytic cavity and adjacent trabecular spaces, especially in the weight-bearing anterior half of the vertebral body. An epidural leak of PMMA occurred in 7/54 levels. This resulted in limited cement injection in 2/7 cases, resulting in technically unsatisfactory stabilization. One of these patients presented with a new compression fracture at the same level which required re-treatment. Two patients reported radicular pain after the PV, likely related to the epidural leak, spontaneously resolving within one week. No patients reported worsened pain at one week follow-up. No cases resulted in worsening of neurological function.

### **CONCLUSION**

In our series of PV of neoplastic lytic vertebral lesions we observed an epidural leak of PMMA in only 14 % of patients despite presence of CE-PW and EM, with extremely low rate of transient clinical complication, without major or permanent complications. Our data seem to justify use of PV in such patients with intractable pain or at risk for vertebral collapse.

### **CLINICAL RELEVANCE/APPLICATION**

Cement augmentation of neoplastic lytic spine lesions can be performed with safety also in cases with posterior wall erosion, provided adequate technique and skills level

---

## **Pediatric Radiology Series: Fetal - Neonatal Imaging**

**Monday, 08:30 AM - 12:00 PM • S102AB**

**PD** **OB** **GU**

[Back to Top](#)

**VSPD21 • AMA PRA Category 1 Credit™:3.25 • ARRT Category A+ Credit:4**

### **Moderator**

**Christopher I Cassady**, MD

### **Moderator**

**Beth M Kline-Fath**, MD

### **Moderator**

**Richard A Barth**, MD \*

## **VSPD21-01 • Fetal Neuro Imaging**

**Beth M Kline-Fath MD** (Presenter)

### **LEARNING OBJECTIVES**

1) The participant will briefly review basic prenatal neurosonology and fetal MR imaging sequences. 2) The embryology of the fetal brain will be correlated with important landmarks identified on MR imaging for each gestational age. 3) The learner will be able to utilize the appearance of the germinal matrix, brain parenchymal signal, sulcation and myelination to verify normal fetal brain anatomical milestones.

### **ABSTRACT**

## **VSPD21-02 • Does Fetal MRI Add Clinically Important Information in Cases of Isolated Ventriculomegaly Revealed by Tertiary Antenatal Ultrasound?**

**Stacy K Goergen MBBS** (Presenter) ; **Tejaswi Kandula MBBS** ; **Michael Fahey MBBS, PhD \***

### **PURPOSE**

Antenatal counselling for fetal cerebral ventriculomegaly (VM) is guided by size of the ventricles and the presence and nature of concurrent structural abnormalities. There are limited consensus guidelines regarding the role of fetal magnetic resonance imaging (FMRI) as an adjunct to ultrasound (US) in cases of isolated VM (IVM). The evidence suggests that MRI is indicated when IVM on US is severe (>15mm), but there is less agreement about its role when IVM is mild or moderate (10-15mm). Our aim was to evaluate the incidence of additional findings on FMRI when IVM is identified on tertiary level antenatal US.

### **METHOD AND MATERIALS**

We prospectively analyzed data from a single university affiliated, tertiary referral fetal diagnostic / therapy unit. Inclusion criteria were singleton or twin pregnancies evaluated with antenatal US performed prior to FMRI with a resulting diagnosis of IVM. Amniocentesis was offered prior to FMRI but variably performed depending on maternal preference.

### **RESULTS**

59 pregnancies studied between November 2006 and February 2013 fulfilled inclusion criteria. Median gestational age at US was 26 weeks (21-36) and timing of FMRI was 28 weeks (22-37). Median time elapsed between US and FMRI was 7 days (0-21). In 41/59 cases, there was agreement between ultrasound and MRI regarding severity of VM. Additional findings on FMRI were seen in 5/42 fetuses (11.9%) with US diagnosed mild VM, 0/10 with moderate VM, and 4/7 (57.1%) with severe VM. Of these 9 cases, 2 had amniocentesis both with a normal result. The additional findings were clinically significant in 2/5 cases with mild VM compared with 4/4 cases with severe VM. These included periventricular nodular heterotopia, foramen of Monro subependymal nodule in tuberous sclerosis, absent septum pellucidum with postnatal diagnosis of septo-optic dysplasia, and agenesis of the corpus callosum.

### **CONCLUSION**

Clinically significant cranial abnormalities on FMRI, specifically midline anomalies and malformations of cortical development, were identified in 5% of fetuses with mild to moderate IVM on tertiary antenatal US. The low rate of additional findings in this group is consistent with other recently published data.

#### CLINICAL RELEVANCE/APPLICATION

The low yield of clinically important abnormalities on fMRI when VM is isolated and mild to moderate in severity on high quality antenatal US should inform antenatal counselling and referral pathways.

### VSPD21-03 • Can Prenatal US Stand Alone to Diagnose Microcephaly or Is Fetal Head MRI Needed?

**Gal Yaniv MD, PhD (Presenter); Eldad Katorza; Vered P Tsehmaister Abitbol MD; Gilad Twig; Salim Bader; Eli Konen MD; Chen C Hoffmann MD**

#### PURPOSE

To evaluate the agreement between ultrasound (US) and fetal head magnetic resonance imaging (feMRI) head biometry.

#### METHOD AND MATERIALS

A retrospective analysis was performed on 60 sequential feMRI scans obtained between 2011-2013 following US diagnosis of microcephaly w/o severe intrauterine growth retardation (IUGR: head circumference = -2 standard deviations [SD] and estimated fetal weight [EFW] = 2 SD). Inclusion criteria were single fetus and fewer than 21 days between performance of US and feMRI. The mean gestational age (GA) of fetuses at US and feMRI acquisition was 33±3.3 and 34±3 weeks, respectively. The mean interval between US and feMRI scanning was 7.3±6 days. Biparietal diameter (BPD) and occipitofrontal diameter (OFD) results were converted to percentiles and SD by Chervenak and Hadlock normograms for US and compared to Garel normograms for feMRI. US measurements of OFD were recorded in 36/60 of the scans. Data on GA, EFW and interval between scans were also recorded.

#### RESULTS

Forty-two of the 60 fetuses with US-suspected microcephaly (70%) were IUGR. BPD values were = -2 SD in only 5 (8.3%) according to feMRI (PP

#### CONCLUSION

There is discrepancy between US and feMRI findings in the assessment of fetal head biometry. US measurements are performed only on the skull, while feMRI enables direct measurement of the brain. Abnormal anatomical findings are more predictive for true microcephaly in both US and feMRI. Thus, diagnosis of microcephaly by US alone is not sufficient and should be validated by feMRI before a final diagnosis is established and consultations with the parents are held.

#### CLINICAL RELEVANCE/APPLICATION

The diagnosis of microcephaly can lead to pregnancy termination, and diagnosis by US alone is insufficient and requires confirmation by a feMRI study.

### VSPD21-04 • Evaluation of ADC Values of the Dead Fetus Compared to Fetal Brain Infarct and Normal Siblings in Twin Pregnancies Complicated with TTTS

**Ronen Bercovitz RT, MA (Presenter); Boaz Weisz; Gal Yaniv MD, PhD; Chen C Hoffmann MD; Shlomo Lipitz; Anat Biegon; Eldad Katorza**

#### PURPOSE

To evaluate the ADC values in the dead fetus, compared to brain infarct and to normal sibling in cases of monochorionic diamniotic (MCBA) twins, suffering from complications of twin to twin transfusion syndrome (TTTS).

#### METHOD AND MATERIALS

A retrospective analysis was performed on 70 sequential MRI scans of fetuses in cases of MCBA pregnancies complicated with TTTS between 2009-2012. 15 women with MCBA pregnancies (mean maternal age 31 years, gestational age range 18-32, 1-4 scans/subject) were included. Follow up scans performed 1-72 days after ischemia to monitor the living remaining fetus. Whole brain ADC values (expressed in  $\text{mme}2/\text{sec} \times 10^9$ ) were obtained at 5 weeks after ischemia. In the cases with infarcts ADC was measured in the infarcted zone. All measurements were performed using a GE workstation. The results of the dead fetuses and of the infarcted zones in the living fetuses were compared to the normal siblings

#### RESULTS

The mean (SD) ADC value in the normal fetuses was 1675 (277), compared to 684 (165) in dead fetuses and 1097 (546) in infarcted brains (p

#### CONCLUSION

The ADC value in dead fetuses increases slowly with time, and does not reach normal values even months after death, while the values in the infarcts of the living fetus normalize within 2 weeks, as was reported in early life and in adulthood. The reason for this phenomenon is unclear, and may be due to the unchanged environment of the dead fetus while the pregnancy continues with the second healthy sibling. A second factor may be lack of blood flow in the dead fetus, thus the tissue is 'frozen' and not liquefied.

#### CLINICAL RELEVANCE/APPLICATION

The time of death of a fetus cannot be determined by the low ADC value, which can stay low for more than 5 weeks.

### VSPD21-05 • Congenital Diaphragmatic Hernia: Fetal and Neonatal Correlation

**Christopher I Cassady MD (Presenter)**

#### LEARNING OBJECTIVES

1) Identify the application of basic anatomic, pathologic, and physiologic principles to congenital diaphragmatic hernia. 2) Analyze imaging and therapeutic techniques and apply this knowledge to protocol development, patient management/safety, and cost in the management of CDH. 3) Demonstrate understanding of the influence of socioeconomic issues on current and future practice patterns for this referral. 4) Compare indications for specific imaging strategies in CDH.

### VSPD21-06 • Correlation of the Observed-to-Expected MR Fetal Lung Volume and the Observed-to-Expected US Lung-to-Head Ratio at Different Times of Gestation in Fetuses with Congenital Diaphragmatic Hernia

**Katrin Kastenholtz (Presenter); Anna Walleyo; Christel Weiss; Angelika Debus MD; Claudia Hagelstein MD; Meike Weidner; Thomas Schaible; Stefan O Schoenberg MD, PhD \*; Karen Busing; Sven Kehl MD; Wolfgang Neff MD, PhD**

#### PURPOSE

Determination of the observed-to-expected MR fetal-lung-volume (o/e MR FLV) and observed-to-expected US lung-to-head ratio (o/e US LHR) are both quantitative methods to predict clinical outcome in fetuses with congenital diaphragmatic hernia (CDH). The purpose of this study was to evaluate the potential of the o/e MR FLV and o/e US LHR to evaluate survival, need for extracorporeal membrane oxygenation (ECMO) therapy and development of chronic lung disease (CLD) at different times of gestation (32 weeks gestation (w.g.)) and especially to individually compare the o/e MR FLV and the o/e US LHR for each fetus.

#### METHOD AND MATERIALS

In total 201 fetuses were included in this study and o/e MR FLV and o/e US LHR were calculated for 270 examinations performed within 72 hours (62 examinations 32 w.g.). Prognostic accuracy of o/e MR FLV and o/e US LHR was assessed by performing receiver operating characteristic curve (ROC) analysis and correlation was determined using linear regression analysis.

#### RESULTS

At all times of gestation investigated our results revealed significant differences of both o/e MR FLV and o/e US LHR for neonatal survival or no survival, need for ECMO therapy and development of CLD or not (p-values between

#### CONCLUSION

O/e MR FLV and o/e US LHR are highly valuable prognostic parameters for prenatal prediction of survival, need for ECMO therapy and

development of CLD in fetuses with left sided CDH for all times of gestation. No prognostic significance was obtained in cases of right sided CDH. O/e MR FLV and o/e US LHR correlate significantly for patients with left sided CDH, best when examinations are performed prior to 32 w.g.. No significant correlation of both parameters could be found in fetuses with right sided CDH.

#### CLINICAL RELEVANCE/APPLICATION

O/e MR FLV and o/e US LHR are reliable prognostic parameters and correlate well for prenatal prediction of survival, need for ECMO therapy and development of CLD in fetuses with left sided CDH.

### **VSPD21-07 • Magnetic Resonance Imaging Based Ratio of Fetal Lung Volume to Fetal Body Volume as a New Prognostic Marker in Growth Restricted Fetuses with Congenital Diaphragmatic Hernia**

**Meike Weidner** (Presenter) ; **Claudia Hagelstein** MD ; **Angelika Debus** MD ; **Anna Walleyo** ; **Christel Weiss** ; **Stefan O Schoenberg** MD, PhD \* ; **Thomas Schaible** ; **Karen Busing** ; **Wolfgang Neff** MD, PhD

#### PURPOSE

Several prenatal prognostic parameters for fetuses with congenital diaphragmatic hernia (CDH) exist. Most of them reference to a control group, which can be problematic if individual fetal development differs from expectation. To overcome this, we evaluated the prognostic accuracy of the individually calculated magnetic resonance imaging (MRI) based ratio of fetal lung volume (FLV) to fetal body volume (FBV) concerning survival in congenital diaphragmatic hernia (CDH), especially in fetuses with growth restriction.

#### METHOD AND MATERIALS

#### RESULTS

#### CONCLUSION

The MRI based ratio (FLV/FBV) is a highly reliable prenatal predictor of neonatal survival in children with CDH. Unlike other prognostic parameters (e.g. observed/expected MR-FLV, ultrasound based observed/expected lung-to-head ratio) it is independent of reference to a control group and can also be used in patients whose growth development differs from expectation.

#### CLINICAL RELEVANCE/APPLICATION

The measurement of fetal body volume supplementary to fetal lung volume may enhance prognostic accuracy in cases of congenital diaphragmatic for individuals whose growth development is restricted.

### **VSPD21-08 • Congenital Bronchopulmonary Malformations (BPMs) - Prenatal Sonographic Features with Postnatal Correlations. A Single Institution Experience**

**Juliette Garel** MD (Presenter) ; **Laurent A Garel** MD ; **Dorothee Dal Soglio** MD ; **Francoise F Rypens** MD ; **Chantale Lapierre** MD ; **Josee Dubois** MD ; **Andree Grignon** MD

#### PURPOSE

BPMs include bronchogenic cysts (BC), bronchial atresias (BA) either isolated or associated with intralobar pulmonary sequestrations (ILPS), congenital pulmonary airways malformations (CPAMs) type I and II, and extralobar pulmonary sequestrations (ELPS) - (Claire Langston classification). Recent literature on congenital lung lesions emphasized the lack of correlations between imaging and pathology. Our purpose is to compare the prenatal sonograms of BPMs and postnatal diagnoses in a single institution cohort.

#### METHOD AND MATERIALS

Retrospective study over 10 years. Pre and postnatal imaging performed in same radiology department. Prenatal descriptors = timing of conspicuity, lesion echogenicity, macrocysts, vascular connections (systemic feeder, venous return), bronchocele. Postnatal diagnoses based upon pathology (surgical cases) or postnatal CT (non-operated cases).

#### RESULTS

115 cases, including 56 surgical cases, and 5 upcoming interventions. Postnatal diagnoses = BC (n=5), CPAM (n=33), PS (n=33) including 11 hybrid lesions (coexisting PS and CPAM), trapping (n=32) including 10 BA, suprarenal PS/hybrid (n=12). Non-surgical cases (n=54): suprarenal location (n=12), spontaneous regression (n=17), embolization (n=3), lost to F.U. (n=8), expectant management (n=12), fetal demise (n=2). Prenatal ultrasound and postnatal correlations = all BPMs visible on mid 2nd trimester US; macrocystic BPMs = CPAM type I and II, or hybrid lesions (intrapulmonary BC often considered at pathology as monocystic CPAM type I equivalent); echoic lesions with systemic vascularization = PS; echoic lesions without systemic vascularization = trapping; bronchocele seen in BA.

#### CONCLUSION

- Conspicuity timing = BPMs always visible on 18-22 WGA sonogram, to the contrary of fetal pulmonary tumors (3 cases in our data bank). - PS almost equally made of ELPS and ILPS (value of color Doppler ultrasound for assessing venous return). - Focal echoic lesions without systemic feeder likely to be trapping (no CPAM type III in our series). Fetal bronchocele very suggestive of BA. Overall, excellent ultrasound pathology correlations, resulting in an improved management (investigations and treatment options) postnatally.

#### CLINICAL RELEVANCE/APPLICATION

Routine US has resulted in a marked increase in prenatally recognized BPMs. Salient US features allow for a reliable prenatal diagnosis of the various BPMs and for a better management postnatally.

### **VSPD21-09 • Pediatric Genitourinary Imaging: Fetal and Neonatal Correlation**

**Jeanne S Chow** MD (Presenter)

#### LEARNING OBJECTIVES

The purpose of this presentation is to review typical prenatal imaging findings of congenital anomalies of the genitourinary tract, the typical evaluation and appearance of these findings post-natally, and the management of these anomalies

### **VSPD21-10 • Radiation Dose Reduction at MDCT for the Prenatal Diagnosis of Skeletal Dysplasia**

**Chihiro Tani** MD (Presenter) ; **Yoshinori Funama** PhD ; **Chikako Fujioka** RT ; **Yukiko Honda** MD ; **Yuko Nakamura** MD ; **Kazuo Awai** MD \* ; **Shuji Date** ; **Yoko Kaichi** ; **Daisuke Komoto** MD

#### PURPOSE

To determine the sufficient minimum radiation dose for the prenatal diagnosis by MDCT of skeletal dysplasia using fetal specimens.

#### METHOD AND MATERIALS

This study received institutional review board approval for the use of 15 fetal specimens (gestational age: 24 - 36 weeks). The specimens were immersed in 5% formalin in a plastic container that approximated the abdominal circumference of pregnant women. CT scans were acquired with a 64-detector scanner (VCT, GE). The scanning parameters were: tube voltage 100kVp, tube current 600-, 300-, 150-, 100-, and 50mA, rotation time 0.4 sec, pitch 1.375. Images were subjected to adaptive statistical iterative reconstruction (ASiR $\diamond$ , blending rate: 60%). First, we measured fetal dose in 5 specimens using 4 glass dosimeters attached on the surface of fetus, and calculated the mean of the measured dose. Furthermore, we calculated the mean of the measured dose in 5 specimens in each tube current. Then, in each tube current CT scanning of all 15 specimens, image quality was evaluated as follows. In each scan protocol of each specimen, we generated maximum intensity projection and volume rendering images of the fetal skeleton. Two radiologists recorded the visualization of a metatarsal, metacarpal, the 12th rib, fibula, and femoral metaphysis using a visual score where 3=clear, 2=unclear, 1=not visible. We performed statistical analysis of the diagnostic ability of each scan protocol using Steel $\diamond$ s test. Standard image quality was considered obtainable at 600mA.



## RESULTS

The fetal exposure dose was 10.2 mGy at a tube current of 600mA, 5.3 at 300mA, 2.5 at 150mA, 1.8 at 100mA, and 0.9 at 50mA. In visual evaluation of images, without ASiR there was a statistically significant difference between 50- or 100mA images and 600mA images (50mA:p

## CONCLUSION

At MDCT for the prenatal diagnosis of skeletal dysplasia, the radiation dose for images acquired with ASiR the fetal radiation dose can be reduced to 1.8mGy.

## CLINICAL RELEVANCE/APPLICATION

MDCTscans obtained at 100mA, 100kVp, and ASiR are of sufficient diagnostic quality for the prenatal diagnosis of skeletal dysplasia and their radiation dose is low (1.8 mGy).

### VSPD21-11 • Challenges and Controversies in Imaging Necrotizing Enterocolitis

**Charles M Maxfield MD** (Presenter)

#### LEARNING OBJECTIVES

1) Recognize imaging features of necrotizing enterocolitis. 2) Discuss imaging algorithm to the diagnosis and follow-up of necrotizing enterocolitis. 3) Review clinical features and pathophysiology of necrotizing enterocolitis.

### VSPD21-12 • The Superficial Echogenic Lesions Detected in Neonatal Cranial Ultrasonography: A Possible Indicator of Significant Birth Trauma

**Byoung Hee Han** (Presenter) ; **Sung Bin Park MD** ; **Kyung Sang Lee** ; **Sun Young Ko** ; **Yeon Kyung Lee**

#### PURPOSE

To evaluate the characteristics and the significance of the superficial echogenic lesions(SEL) in neonatal cranial ultrasonography(US).

#### METHOD AND MATERIALS

We retrospectively reviewed the clinical records and neuroimaging studies of forty neonates who showed SEL on neonatal cranial US. MRI was taken in 18 of them within 2 weeks after US. We evaluated the location, number, size and follow-up changes of SEL and the associated lesions to know the clinical significance of SEL.

#### RESULTS

The echogenic lesions were positioned around the sulci in 39 cases and considered as brain parenchymal lesions accompanying with subarachnoid hemorrhage (SAH). Only in one case, the lesion was positioned intraparenchymally. On US, the locations of the lesions were mainly frontal and parietal in 38 cases and occipitotemporal in 5 cases. The lesions were single in 13 and multiple in 27 cases. The maximal size of the lesions were 5 to 30mm(mean 15mm). There were associated other hemorrhagic lesions in subdural(SDH=12), epidural(EDH=4), intraventricular(IVH=2) location. One SDH was accompanied by skull fracture. Three EDH were combined with skull fractures. Cephalhematoma or caudal succedaneum were noted in 15 cases and five(33.3%) of them were associated with EDH and fracture associated SDH. On follow up study, the SELs evolved and disappeared until 3 months on follow-up US.

#### CONCLUSION

The SEL in neonatal cranial US involves brain parenchyma and leptomeningeal space. Although SEL itself is usually not significant clinically, it can be one possible indicator of significant birth trauma such as EDH and SDH with skull fracture especially when it combines with cephalhematoma or caudal succedaneum.

#### CLINICAL RELEVANCE/APPLICATION

Cranial ultrasonography can easily detect the superficial echogenic lesions of neonatal brain and if it is found and scalp hematoma is present, MRI should be recommended to detect intracranial hematoma

### VSPD21-13 • Comparison of Clinical US Measurements of the Ventricles to 3D US Ventricle Volumes in IVH Patients

**Jessica E Kishimoto** (Presenter) ; **Walter M Romano MD** ; **Aaron Fenster PhD \*** ; **David Lee MD, FRCPC** ; **Sandrine De Ribaupierre**

#### PURPOSE

Premature neonates with intraventricular hemorrhage (IVH) are followed with serial 2D US, head circumference (HC) measurement, as well as clinical examination to determine if they require treatment for hydrocephalus. However, accurate volume measurements are impossible with 2D images, and one relies on ratios and width of ventricles to estimate the changes in ventricular volume. 3D ultrasound (US) has been proven feasible in a clinical setting in this population, and ventricular volumes from those images have been comparable to those made in MRI. Since 2D US and HC measurements have historically been used clinically, we aimed to compare those clinical standard measurements against 3D US ventricular volumes.

#### METHOD AND MATERIALS

A Philips HDI 5000 US machine with a C8-5 transducer was used for all 2D US exams. 3D US images were acquired, using the same probe, attached to a system that generated 3D images by mechanically moving the transducer. HC measurements were recorded on the days US images were acquired. Five IVH patients were scanned 1-2 times/week for the duration of their stay in the NICU, for a total of 7-11 scans per patient. Total of 47 scans for all patients investigated. Levene's index (LI), axial horn width (AHW), third ventricle width (3rd) and the thalamo-occipital distance (TOD) were measured on the 2D US images, and ventricle volumes were manually segmented from 3D US images. Pearson correlation between each index and volume as well as the correlations between the change in each index between adjacent time points and corresponding change in volume were performed.

#### RESULTS

Strong, significant correlations ( $r > 0.80$ ,  $p < 0.001$ ) were found for all correlations comparing the change in volumes and the change in 2D measurements. Change in HC was the lowest of all the correlations ( $r = 0.085$ ).

#### CONCLUSION

AHW, 3rd and TOD measurements can be predictive of ventricle volumes, but make poor estimates of changes in volumes of IVH patients.

#### CLINICAL RELEVANCE/APPLICATION

Neither changes in 2D US measurements, nor changes in HC appear to be related to actual ventricle volume changes. This should be taken into account when reviewing standard cranial US exam.

### VSPD21-14 • Doppler Evaluation of Anterior Cerebral Artery in Children on ECMO and Age-matched Controls: Predictive Value in Cerebrovascular Complications

**Eman N Alqahtani MBBS** (Presenter) ; **Carlos A Zamora MD, PhD** ; **Melania Bembea** ; **Ivor Berkowitz** ; **Kathryn A Carson** ; **Thierry Huisman MD** ; **Aylin Tekes MD**

#### PURPOSE

Patients on extracorporeal membrane oxygenation (ECMO) are at high risk of cerebrovascular complications (CVC) due to serious underlying diseases, systemic heparinization and sepsis. Our aims were: 1) To evaluate resistive index (RI) measurements in the anterior cerebral artery (ACA) to predict CVC such as intracranial hemorrhage (ICH) and ischemic events in children on ECMO, 2) To evaluate the differences in RI measurements between children on ECMO and age-matched controls, 3) To evaluate clinical variables to predict CVC.

## METHOD AND MATERIALS

The institutional review board approved this study. A retrospective chart review of patients

## RESULTS

There were a total of 98 children (ECMO n=36, age matched controls n=62). Nine (25%) of the 36 developed CVC (ICH n=6, ischemia n=3). The difference between baseline and compression RI values and percent change on the first day of ECMO was statistically significantly higher for children with CVC compared to no CVC ( $p=0.03$  and  $p=0.02$ , respectively). Median percentage change in the RI value was 5.59% in controls. The median percent change was -20%-78) during the period on ECMO in the no CVC group, while the ICH group showed the widest range of RI percent change until the day of CVC (Fig. 1). Of the clinical variables, only age at initiation of ECMO was statistically significantly associated with increased risk of CVC ( $\geq 2$  days ( $p=0.02$ ).

## CONCLUSION

Children who had ICH had the widest range of percent RI change during the course of ECMO. Minimal RI change can be reassuring for no CVC in children with ECMO. Children younger than 3 days of age at the time of ECMO cannulation are at higher risk for CVC. These results should be validated in larger prospective studies.

## CLINICAL RELEVANCE/APPLICATION

We want to understand the role of cerebral autoregulation in patients on ECMO aiming to predict CVC that affect 30-50% of patients on ECMO.

## Interventional Oncology Series: Hepatocellular Carcinoma

Monday, 01:30 PM - 06:00 PM • S405AB

RO OI IR GI

[Back to Top](#)

**VSI021** • AMA PRA Category 1 Credit™:4.25 • ARRT Category A+ Credit:5

### Moderator

Jean-Francois H Geschwind, MD \*

### LEARNING OBJECTIVES

1) To learn the indications for transcatheter-based therapies for patients with HCC. 2) To understand the potential limitations, pitfalls, side effects and toxicities associated with transcatheter therapies for patients with HCC. 3) To know the results, imaging responses and survival benefit of various transcatheter therapies. 4) To know the future transcatheter therapies and understand their potential. 5) To learn the various combination therapies available and undergoing clinical evaluation for HCC.

### ABSTRACT

**01) Staging Systems, Epidemiology, and Medical** -1) Identify state-of-the art surgical treatment, non-surgical treatment, and transplantation treatment for patients with HCC. 2) Identify the most appropriate treatment for early and advanced stage of HCC. 3) Describe and discuss indications for resection in chronic liver disease. 4) Integrate interventional radiological procedures in the treatment of HCC. **02) HCC mgmt in Europe** -1) To understand how HCC patients are being managed in Europe. 2) To learn the decision making processes driving treatment selection for patients. 3) To review the data from the European point of view. **03) HCC mgmt in Korea** -1) To understand how HCC patients are being managed in Korea. 2) To learn the decision making processes driving treatment selection for patients. 3) To review the data from the Korean point of view. **04) HCC mgmt in HK/China** - 1) To understand how HCC patients are being managed in China. 2) To learn the decision making processes driving treatment selection for patients. 3) To review the data from the Chinese point of view. **05) HCC mgmt in Japan** - 1) To understand how HCC patients are being managed in Japan. 2) To learn the decision making processes driving treatment selection for patients. 3) To review the data from the Japanese point of view. **06) Panel Discussion: HCC in the world** **07) Intraarterial Therapies in the US: Where are we?** - 1) Understand patient selection process 2) Understand the patient indications and complications 3) Understand the rationale for combining anti-angiogenic agent with loco-regional therapies 4) Understand the results of various catheter based intra-arterial therapies for Liver Cancer **08) Assessment of Tumor Response** - 1) review methods of response assessment 2) discuss limitations of current methods 3) describe future imaging concepts in development **09) Tumor Board** - The algorithm by which patients with HCC are worked up and their appropriateness for transplant or resection will be discussed.

## VSI021-01 • Staging Systems, Epidemiology, and Medical Therapy

Alan P Venook MD (Presenter) \*

### LEARNING OBJECTIVES

1) Identify state-of-the art surgical treatment, non-surgical treatment, and transplantation treatment for patients with Hepatocellular Carcinoma. 2) Identify the most appropriate treatment for early and advanced stage of Hepatocellular Carcinoma. 3) Describe and discuss indications for resection in chronic liver disease. 4) Integrate interventional radiological procedures in the treatment of Hepatocellular Carcinoma.

## VSI021-02 • HCC Management in Europe

Riccardo A Lencioni MD (Presenter)

### LEARNING OBJECTIVES

View learning objectives under main course title.

## VSI021-03 • Hepatocellular Carcinoma (HCC) Treated with Transarterial Chemoembolization and Radiofrequency Ablation: Diagnostic Efficacy of Combined Dynamic Perfusion MRI with ADC Mapping in the Assessment of Therapeutic Effects

Daive Ippolito MD (Presenter) ; Pietro A Bonaffini MD ; Davide Fior MD ; Cristina Capraro MD ; Orazio Minutolo MD ; Sandro Sironi MD

### PURPOSE

To determine the additional predictive value obtained by the correlation of kinetic parameters derived from dynamic contrast-enhanced MR perfusion imaging with apparent diffusion coefficient (ADC) value obtained by diffusion weighted MR imaging in the assessment of therapeutic effects of interventional treatment of HCC lesions.

### METHOD AND MATERIALS

A total of 54 patients with biopsy proven diagnosis of HCC lesion, that underwent to TACE or RFA treatment, were prospectively enrolled in our study. MR study was performed, using a 1.5T MRI system (Achieva, Philips), for each patient 4 weeks after the treatment and consist of multiphase standard protocol with T2 and T1 sequences, dynamic contrast enhanced THRIVE, including also diffusion weighted imaging (DWI) with different b-value. Philips workstation was used to generate color permeability maps showing perfusion of enhancing tumors and quantitative ADC maps. After the placing of regions of interests (ROIs) on site of the maps which best corresponded to the enhanced regions of the lesion, the following parameters were calculated: Relative Enhancement, Maximum Enhancement, Maximum Relative Enhancement, Time to Peak and ADC values, and statistical analysis was performed.

### RESULTS

Perfusion parameters and ADC values of treated lesions could be quantitative assessed using parametric imaging analysis. Sixteen out of 54 patients had a residual disease and values of obtained parameters measured within residual tumor tissue were: REA 44.66, RVE 60.50, RLE 52.72, ME 553.21(%), MRE 65.95(%), TTP(s) 140.61, and  $982.21 \pm 103.93 \times 10^{-3} \text{mm}^2/\text{sec}$ . The corresponding values obtained in remaining cases in whom a complete necrosis was achieved were: REA -1.24, RVE 5.93, RLE 16.9, ME 203.24, RE 25.78, TTP 165.87

and  $1682.7 \pm 149.7 \times 10^{-3} \text{ mm}^2/\text{sec}$ . A significant difference (p < 0.05).

#### CONCLUSION

The quantitative multiparametric MR images analysis could offer functional quantitative information about cellular density and tumor blood supply of HCC lesions, useful in predicting and assessing treatment response.

#### CLINICAL RELEVANCE/APPLICATION

Combined parametric analysis of functional MRI represents an vivo marker of biological characteristic of HCC lesion, providing quantitative information useful for assessment of therapeutic response.

### VSIO21-04 • HCC Management in Korea

**Jin Wook Chung MD** (Presenter) \*

#### LEARNING OBJECTIVES

View learning objectives under main course title.

### VSIO21-05 • HCC Management in Hong Kong, China

**Ronnie T Poon** (Presenter)

#### LEARNING OBJECTIVES

View learning objectives under main course title.

### VSIO21-06 • Radiofrequency Ablation of 318 Cases of Hepatocellular Carcinoma as First Line Treatment: 10 Years Survival Result and Prognostic Factors

**Wei Yang** (Presenter) ; **Wei Wu** PhD ; **Jung Chieh Lee** ; **Zhong-Yi Zhang** PhD ; **Min Hua Chen** MD ; **Kun Yan** MA

#### PURPOSE

To our knowledge, the long-term (>5 years) survival results for radiofrequency ablation (RFA) in HCC is few. Our study aimed to investigate the efficacy of RFA for 318 patients with hepatocellular carcinoma (HCC) as first line treatment, and the prognostic factors for post-RFA survival rate.

#### METHOD AND MATERIALS

From 2000 to 2012, 730 patients with HCCs underwent ultrasound guided percutaneous RFA treatment in our department. Among them, 318 consecutive patients received RFA as first treatment and enrolled in this study. They were 251 males and 67 females, average age  $60.3 \pm 11.3$  years (24-87 years). The HCC were 1.0-6.7 cm in diameters (average  $3.3 \pm 1.2$  cm). Univariate and multivariate analysis with 15 potential variables were examined to identify prognostic factors for post-RFA survival rate.

#### RESULTS

The overall post-RFA survival rates at 1, 3, 5, 7, 10 year were 90.2%, 67.3%, 53.6%, 41.2% and 29.1%, respectively. In the 209 patients with stage I of HCC (AJCC staging), the 1, 3, 5, 7, 10 year survival rates were 94.2%, 72.9%, 63.6%, 57.6%, 41.5% , respectively. In the 239 patients with liver function class A (Child-Pugh classification), the 1, 3, 5, 7, 10 year survival rates were 94.4%, 75.8%, 64.3%, 52.3%, 32.4%, respectively. Ten potential factors were found with significant effects on survival rate, and they were AJCC staging, tumor pathological grading, number of tumors, pre-RFA liver function enzymes, pre-RFA AFP level, Child-Pugh classification, portal vein hypertension, using contrast ultrasound in RFA procedure, RFA electrode type and tumor necrosis one month after RFA. After multivariate analysis, 4 factors were identified as independent prognostic factors for survival rate, and they were Child-Pugh classification, number of tumors, pre-RFA AFP level, and portal vein hypertension. Totally, 548 RFA sessions were performed and major complications occurred in 12 sessions (2.1%).

#### CONCLUSION

This long-term follow-up study on a large group of HCC patients confirmed that RFA could achieve favorable outcome on HCC patients as first line treatment, especially for patients with child-Pugh class A, single tumor, low AFP level pre-RFA and without portal vein hypertension.

#### CLINICAL RELEVANCE/APPLICATION

This study provided evidence that RFA for early HCC was effective and safe as a first-line treatment even for patients usually considered good candidates for surgery.

### VSIO21-07 • HCC Management in Japan

**Yasuaki Arai MD** (Presenter) \*

#### LEARNING OBJECTIVES

View learning objectives under main course title.

### VSIO21-08 • A Minimal Ablative Margin Is Acceptable for Radiofrequency Ablation of Small Hepatocellular Carcinoma: A Long-term, Follow-up Study Using Magnetic Resonance Imaging with Impaired Ferucarbotran Clearance

**Kensaku Mori MD** (Presenter) ; **Kuniaki Fukuda MD** ; **Katsuhiko Nasu MD, PhD** ; **Michiko Nagai MD** ; **Tsukasa Saida MD** ; **Manabu Minami MD, PhD**

#### PURPOSE

We aimed to prospectively compare the local recurrence rates after radiofrequency ablation (RFA) for small ( $\leq 3$  cm) hepatocellular carcinomas (HCCs) among different ablative margin (AM) statuses on magnetic resonance imaging (MRI) with impaired ferucarbotran clearance.

#### METHOD AND MATERIALS

Fifty-five patients with 57 HCCs (diameter; 0.8-2.7 cm; mean  $\pm$  SD,  $1.6 \pm 0.5$  cm) underwent RFA 2-7 h after ferucarbotran-enhanced MRI. On unenhanced T2\*-weighted images acquired after 3-5 days, AMs appeared as hypointense rims owing to impaired ferucarbotran clearance. AM status was classified as  $\diamond$ AM-plus,  $\diamond$ AM completely surrounding the tumor;  $\diamond$ AM-zero,  $\diamond$ partly discontinuous AM without tumor protrusion; or  $\diamond$ AM-minus,  $\diamond$  discontinuous AM with tumor protrusion. The minimal AM thicknesses were measured in the AM-plus group. The range of follow-up periods in the patients with and without local recurrence was 0-45 months ( $10 \pm 15$  months) and 7-58 months ( $28 \pm 14$  months), respectively. Local recurrence rates of different AM statuses were compared using the Kaplan-Meier method and log rank test.

#### RESULTS

Of the 57 HCCs, 34 (60%), 16 (28%), and 7 (12%) were classified as AM-plus, AM-zero, and AM-minus groups, respectively. The respective 1-, 2-, 3-, and 4-year local recurrence rates were 3%, 8%, 8%, and 31% for the AM-plus group; 12%, 12%, 20%, and 20% for the AM-zero group; and 71%, 71%, not applicable (NA), and NA for AM-minus group. The local recurrence rates were significantly lower for the AM-plus and AM-zero groups than for the AM-minus group ( $P < 0.001$  and  $P = 0.003$ , respectively). However, the difference of local recurrence rates between AM-plus and AM-zero groups was not significant ( $P = 0.454$ ). In the AM-plus, the local recurrence rates were 22% (2/9), 10% (1/10), 0% (0/5), 0% (0/4), and 0% (0/6) for AMs of 1 mm, 2 mm, 3 mm, 4 mm, and  $\geq 5$  mm, respectively.

#### CONCLUSION

When AMs are assessed after RFA for small HCCs by using MRI with impaired ferucarbotran clearance, the minimal AMs are acceptable to avoid local recurrence in a long-term period, although AMs of  $\geq 3$  mm seems preferable.

#### CLINICAL RELEVANCE/APPLICATION

MRI with impaired ferucarbotran clearance enables precise assessment of AMs after RFA and will contribute to avoid not only insufficient but also overzealous treatment for small HCCs.

### **VSIO21-09 • Panel Discussion: HCC in the World: How Do We Put All this Information Together? New International Staging System? Are Guidelines Really Useful?**

#### LEARNING OBJECTIVES

View learning objectives under main course title.

### **VSIO21-10 • Intraarterial Therapies in the US: Where Are We?**

**Jean-Francois H Geschwind MD (Presenter) \***

#### LEARNING OBJECTIVES

1) Understand patient selection process. 2) Understand the patient indications and complications. 3) Understand the rationale for combining anti-angiogenic agent with loco-regional therapies. 4) Understand the results of various catheter based intra-arterial therapies for Liver Cancer.

### **VSIO21-11 • Final Analysis of GIDEON (Global Investigation of therapeutic DEcisions in hepatocellular carcinoma and Of its treatment with sorafenib): Regional Trends, Safety, and Outcomes in Patients Receiving Concomitant Transarterial Chemoembolization**

**Jean-Francois H Geschwind MD (Presenter) \* ; Masatoshi Kudo ; Jorge Marrero \* ; Alan P Venook MD \* ; Sheng-Long Ye ; Jean-Pierre Bronowicki \* ; Xiao-Ping Chen ; Lucy Dagher ; Junji Furuse ; Laura Ladron De Guevara \* ; Christos Papandreou \* ; Arun J Sanyal ; Tadatoshi Takayama ; Seung Kew Yoon MD, PhD ; Keiko Nakajima \* ; Riccardo A Lencioni MD**

#### PURPOSE

Transarterial chemoembolization (TACE) and sorafenib represent distinct treatment modalities for hepatocellular carcinoma (HCC), and there is a strong rationale and growing evidence supporting the use of TACE and sorafenib combined in unresectable HCC (uHCC) patients. GIDEON is a large, non-interventional study conducted in uHCC patients treated with sorafenib. The study allows for analysis of global treatment patterns in real-life practice, including concomitant TACE use.

#### METHOD AND MATERIALS

Data were collected from >3000 patients in whom the decision to treat with sorafenib had been made in clinical practice. Treatment history and disease characteristics were recorded at study entry; safety and outcomes data were collected during follow-up.

#### RESULTS

3202 patients comprised the final safety population. Of these, 47.2% received prior TACE, 10.1% received concomitant TACE, and 7.3% received TACE both prior to and concomitantly with sorafenib. Regionally, concomitant TACE use was highest in Latin America (14.4%), Asia-Pacific (13.5%), and the US (13.0%), with the lowest use in the EU (4.7%). Overall, of the patients who received concomitant TACE, the greatest number were from the US, China, and Japan (22.5%, 24.6%, and 19.1%, respectively). Patients who received concomitant TACE had a similar incidence of drug-related adverse events (88.6%) to those who did not (84.9%), as well as a similar incidence of serious drug-related adverse events (6.2% and 9.6%, respectively). In the intent-to-treat population (n=3213), median overall survival (months [95% CI]) was longer in patients who received concomitant TACE (21.6 [17.9-upper limit not estimable]) than in those who did not (9.7 [9.2-10.4]). Time to progression was also slightly higher in patients who received concomitant TACE (6.6 [5.8-7.6]) compared with those who did not (4.5 [4.1-4.8]).

#### CONCLUSION

The GIDEON study provides insight into treatment patterns in clinical practice. Data from the GIDEON study suggest that, globally, TACE is used concomitantly with sorafenib and appears to be a valid therapeutic option in patients with uHCC.

#### CLINICAL RELEVANCE/APPLICATION

The optimal role of TACE and sorafenib combined in the HCC treatment pathway is of increasing clinical interest. Data from GIDEON add to the evidence to further evaluate this approach.

### **VSIO21-12 • Assessment of Tumor Response**

**Riad Salem MD, MBA (Presenter) \***

#### LEARNING OBJECTIVES

1) Review methods of response assessment. 2) Discuss limitations of current methods. 3) Describe future imaging concepts in development.

### **VSIO21-13 • Evaluation of Tumor Necrosis in Liver Explants after Chemoembolization or Radiofrequency Ablation as Bridge Therapies for Hepatocellular Carcinoma**

**Carmen Garcia Alba MD (Presenter) ; Julien Cazejust MD ; Fabiano Perdigao ; Bertrand Bessoud MD ; Dominique Wendum MD, PhD ; Yves M Menu MD ; Olivier Soubrane ; Olivier Rosmorduc**

#### PURPOSE

To compare, in liver explants, the tumor necrosis rate of hepatocellular carcinoma (HCC) treated by chemoembolization (TACE) or radiofrequency ablation (RFA) as bridge therapies for patients on the waiting list for liver transplantation.

#### METHOD AND MATERIALS

This monocentric retrospective study included 38 liver transplanted patients between November 2009 and December 2012 with history of HCC treated with bridge therapies while on the waiting list for liver transplantation. All treatments were approved by the Multidisciplinary Tumor Board of our institution following BCLC and EASL guidelines. Treatments were performed by experienced interventional radiologists. Anatomopathologic study of the liver explants was performed by an experienced anatomopathologist. In patients with consecutive treatments, only the last one was taken into consideration in this study.

#### RESULTS

Twelve patients underwent RFA for 14 lesions (mean 1.17 lesions per patient). The mean tumor size was 24mm (SD 7), with a mean necrosis rate of 93% (SD 13). No lesion treated by RFA had a necrosis rate

#### CONCLUSION

Tumor necrosis rate for both treatments was =80% on liver explants. RFA showed a trend toward higher tumor necrosis rate than TACE. TACE allowed treating twice as many lesions per patient as RFA (p

#### CLINICAL RELEVANCE/APPLICATION

The use of bridge therapies for HCC prevents from progression related dropout, with a high necrosis rate for both treatments studied (>80%) demonstrated on liver explants.

### **VSIO21-14 • Tumor Board**

## LEARNING OBJECTIVES

1) The algorithm by which patients with HCC are worked up and their appropriateness for transplant or resection will be discussed.

### **VSIO21-15 • Percutaneous Microwave Ablation of Hepatocellular Carcinoma: Early Clinical Results with 106 Tumors**

**Timothy J Ziemlewicz MD (Presenter) ; J. Louis Hinshaw MD \* ; Meghan G Lubner MD ; Christopher L Brace PhD \* ; Marci Center ; Fred T Lee MD \***

#### PURPOSE

Microwave (MW) ablation is a promising technology that offers several advantages over radiofrequency (RF) ablation. The purpose of this study was to retrospectively review the results in the first 75 patients with hepatocellular carcinoma (HCC) treated with a high-power, gas-cooled MW device at a single center.

#### METHOD AND MATERIALS

Between December 2010 and March 2013 we treated 106 hepatocellular carcinomas in 75 patients via a percutaneous approach utilizing US and/or CT guidance. There were 65 male and 10 female patients with mean age of 61 years (range 44-82). All procedures were performed with a high-powered, gas-cooled microwave system (Certus 140, Neuwave Medical, Madison, WI). Mean power was 77 Watts (range 30-140 Watts) and mean ablation time 5.3 minutes (range 1-11.5 minutes).

#### RESULTS

Tumors ranged in size from 0.5 to 7.0 cm (mean 2.5 cm) and median imaging follow-up was 7 months. All treatments were considered technically successful with no evidence of residual tumor at immediate post-procedure CECT. Primary treatment effectiveness by imaging was 88.7% (94/106), 92.5% (87/94) for tumors < 4 cm and 61.5% (8/13) for tumors > 4 cm. Of the tumor progression in lesions

#### CONCLUSION

Treating hepatocellular carcinoma using microwave ablation is safe with treatment effectiveness equivalent or improved from other percutaneous ablation modalities.

#### CLINICAL RELEVANCE/APPLICATION

Microwave tumor ablation can be safe and effective when compared with more established modalities such as radiofrequency ablation, however more research of effectiveness is needed.

---

### **Breast Series: Emerging Technologies in Breast Imaging**

---

**Tuesday, 08:30 AM - 12:00 PM • Arie Crown Theater**

---



[Back to Top](#)

**VSBR31 • AMA PRA Category 1 Credit™:3.25 • ARRT Category A+ Credit:4**

#### **Moderator**

**Michael A Cohen , MD**

#### **Moderator**

**John M Lewin , MD \***

#### LEARNING OBJECTIVES

#### ABSTRACT

### **VSBR31-01 • Contrast Mammography**

**John M Lewin MD (Presenter) \***

#### LEARNING OBJECTIVES

1) This course will review the use of contrast enhancement in mammography- prior results with temporal evaluation and current results using dual energy technology. 2) Results of trials comparing contrast enhancement with standard breast imaging such as routine mammography, ultrasound and MRI will be discussed.

#### ABSTRACT

Contrast-enhanced digital mammography, now a clinically available product, continues to be a fruitful area of both basic and clinical research. This session will provide an overview of the physics of CEDM, its history, recent research results, current status and potential clinical applications.

### **VSBR31-02 • Contrast-enhanced Spectral Mammography vs. Mammography and MRI - Clinical Performance in a Multi-reader Evaluation**

**Eva M Fallenberg MD (Presenter) \* ; Felix Diekmann MD \* ; Corinne Balleyguier MD ; Diane M Renz MD ; Ritse M Mann MD, PhD \* ; Florian Engelken MD, MBCh ; Alexander Poellinger MD ; Heba A Amer ; Clarisse Dromain MD**

#### PURPOSE

To compare contrast-enhanced digital mammography (CESM) to mammography (MG) and MRI on diagnostic accuracy of histologically proven breast lesions.

#### METHOD AND MATERIALS

The study was approved by Health Authorities and Ethics Committee. 90 consenting patients diagnosed with breast cancer were imaged with MG, CESM and MRI and underwent surgery. CESM was performed as a bi-lateral mammography starting 2 minutes after injection of 1.5ml/kg of an iodinated contrast agent (300 mg/ml) with a flow of 3ml/s. CESM images alone and MG images were interpreted by two blinded independent radiologists with an interval of minimum 4 weeks for memory wash-out. MRI was analyzed by another set of two independent readers. Per lesion sensitivity and specificity were evaluated across readers. BI-RADS 4 was defined as threshold for true positives. Gold standard was post-surgical histology.

#### RESULTS

105 malignant and 10 benign histologically proven lesions were assessed in this dataset. Average sensitivity were 84.1% (reader1) and 67% (reader 2) for MG, 90.2% and 88.8% for CESM and 91.1% and 90% for MRI, respectively. Specificity was 100% (reader 1) and 80% (reader 2) for MG, 81.8% and 90% for CESM and 71.4% and 50% for MRI.

#### CONCLUSION

CESM and MRI showed similar sensitivity for index cancer and multiple foci, both superior to MG. MG and CESM outperformed MRI in specificity.

#### CLINICAL RELEVANCE/APPLICATION

CESM is a reliable imaging technique, which may replace MRI in cases with contraindications and may replace MG due to superior diagnostic accuracy in symptomatic patients.

### **VSBR31-03 • Contrast-enhanced Spectral Digital Mammogram versus Contrast-enhanced MR Mammography in the Assessment of Breast Carcinoma: Initial Clinical Experience**

**Maha Helal MD (Presenter) ; Rasha M Kamal MD ; Radwa Essam MBBS ; Iman Godda MD ; Sahar Mansour MD ; Nelly Alieldin MD ; El-Shaimaa M Sharaf MBCh**

#### PURPOSE

evaluate the diagnostic performance of contrast-enhanced spectral digital mammography versus dynamic contrast-enhanced magnetic resonance imaging in the detection and staging of breast cancer.

#### METHOD AND MATERIALS

In this institutional ethics approved prospective study, we compared the performance of contrast based digital mammography with magnetic resonance imaging on 70 female patients. Standard digital mammogram was done in the mediolateral oblique and craniocaudal projections followed by low (22-33 kVp) and high (44-49 kVp) energy exposures in the same projections. Sequential post contrast magnetic resonance imaging was set in the axial orientation and post processed using maximum intensity projection and multiplanar reconstruction images. Both examinations performed by IV injection of non-ionic contrast agent. Outcomes of the surgical specimen or ultrasound guided core biopsy were the gold standard of reference in all cases.

#### RESULTS

The study included 33 pathologically proved benign (47 %) and 37 (53%) malignant breast lesions. The areas of contrast uptake had been correlated with abnormalities seen on the conventional mammography. Both contrast enhanced digital mammography and magnetic resonance imaging were individually assessed in the same group of cases. Multicentric and multifocal carcinomas were detected by contrast mammograms in 29.7% (n=11) of diagnosed malignant cases, when only unifocal carcinoma was reported on conventional mammograms. In the context of malignancy both modalities stood on the same land. Enhancement detection of some benign lesions (n=5) was limited in digital mammography. Statistical analysis yielded a sensitivity, specificity and accuracy of 93.7%, 66.6% and 80.6% compared to 93.7 %, 86.6% and 90.3% for contrast enhanced mammograms and magnetic resonance imaging respectively

#### CONCLUSION

Contrast-enhanced digital mammogram is non-inferior to breast MRI in the contest of detection and characterization of breast malignancy.

#### CLINICAL RELEVANCE/APPLICATION

Contrast-enhanced mammography is an advanced application of digital mammography that had to be compared with breast MRI as it is more applicable and cost effective.

### **VSB31-04 • Contrast-enhanced Breast Tomosynthesis versus Dynamic Contrast-enhanced Breast MRI in the Diagnosis of Suspicious Breast Lesions on Mammogram**

**Chen-Pin Chou MD (Presenter) \* ; Chia-Ling Chiang ; Tsung-Lung Yang MD**

#### PURPOSE

To compare the diagnostic performance of contrast-enhanced breast tomosynthesis (CEBT) and dynamic contrast-enhanced breast MRI (DCE-MRI) for breast lesions detected on digital mammogram.

#### METHOD AND MATERIALS

The study was approved by institutional review board. Written informed consent was obtained from all patients. A total of 102 consecutive women suspected of having breast lesions on digital mammogram between March 2012 and December 2012 underwent both CEBT and DCE-MRI. For the dual-energy CEBT, a modified Selenia Dimensions (Hologic, Inc.) machine was used. Simultaneously 2D mammogram and 3D tomosynthesis were taken after injection with 1.5 mL iodine contrast agent per kilogram of body weight of and imaged between 2 and 6 minutes after injection. Contrast-enhanced images were taken in the suspicious breast (pre-contrast MLO view, post-contrast CC and MLO view) and contralateral breast (post-contrast MLO view). The lesion classifications on CEBT were finally determined based on findings on 2D mammogram, 3D tomosynthesis and post-contrast subtraction 2D and 3D images. Women were also evaluated at 1.5T (GE) or 3T MRI (Siemens) with dedicated breast coil. CEBT and DCE-MRI were interpreted by different radiologists.

#### RESULTS

Total 90 histological findings were available in 76 women (mean age 50.7 years, range 35-66 years). About 89% women did not have clinical symptoms. Ten women had two breast lesions in unilateral breasts. Four women had bilateral breast lesions. Of the 90 lesions, 67% had microcalcification on mammogram. The pathology revealed 46 benign lesions and 44 breast malignancies (21 carcinoma in situ, and 23 invasive breast cancers). The sensitivity/ specificity for CEBT and DCE-MRI were 97%/63% and 91%/63%, respectively.

#### CONCLUSION

Both CEBT and DCE-MRI showed similar diagnostic efficacy for women with suspicious breast lesions on mammogram, but CEBT was faster and easily accomplished diagnostic tool than breast DCE-MRI.

#### CLINICAL RELEVANCE/APPLICATION

CEBT may be an alternative tool for women who have suspicious breast lesions and cannot tolerate breast DCE-MRI.

### **VSB31-05 • Benign Enhancement on Contrast Enhanced Dual Energy Digital Mammography**

**Maxine S Jochelson MD (Presenter) ; D. David Dershaw MD ; Janice S Sung MD ; Mary Hughes MD ; Elizabeth A Morris MD**

#### PURPOSE

To describe the incidence, appearance and etiologies of non-malignant enhancing lesions depicted on contrast enhanced dual energy digital mammography (CEDM).

#### METHOD AND MATERIALS

In a retrospective HIPAA compliant IRB approved study, images and clinical histories of 100 consecutive women who underwent CEDM for either breast cancer staging or high risk screening were reviewed. The incidence of benign, focally enhancing lesions or diffuse parenchymal enhancement on CEDM, diagnosed by either biopsy, correlation with the clinical history or recent MRI findings, was determined.

#### RESULTS

CEDM was performed for staging of known cancer in 67/100 (67%) and for high risk screening in 33/100 (33%). 95/100 (95%) of patients had a breast MRI within 30 days of CEDM. Focal enhancement, subsequently determined to be the result of a benign process, was detected in 11/100 (11%) of women: 8/67 (12%) of women with cancer and 3/33 (9%) of screening patients. 5 patients demonstrated rim enhancing lesions: 3 corresponded to cysts on MRI (2 simple and 1 inflamed) and 2 to seromas at the site of recent intervention. 1 corresponded to a skin lesion on MRI. 5 other areas of focal enhancement underwent biopsy yielding radial scar, fibroadenoma, adenosis, PASH, and periductal inflammation. Diffuse background parenchymal enhancement was present in 26/100 (26%), all of whom had a similar pattern on MRI.

#### CONCLUSION

Focal non-malignant enhancement occurred in 11% of studies. Etiologies included cysts, seromas, a radial scar and a fibroadenoma among others. Half of them required tissue sampling to exclude malignancy. Appreciating the imaging appearance of these benign lesions may potentially prevent unnecessary biopsies in the future.

#### CLINICAL RELEVANCE/APPLICATION

Both focal and diffuse non malignant enhancement can be seen on CEDM. Recognition of the appearance of these findings may improve the specificity of this exam and limit unnecessary biopsies.

## **VSBR31-06 • Tomosynthesis**

**Mark A Helvie MD (Presenter) \***

### **LEARNING OBJECTIVES**

1) To understand the basic principles used in obtaining digital breast tomosynthesis (DBT) images. 2) To understand experimental and clinical trial data which form the basis for DBT clinical application. 3) To understand the potential benefits and areas of weakness of DBT compared to conventional mammography. 4) To understand the potential clinical applications of DBT and current regulatory status of DBT. 5) To understand future issues related to DBT.

### **ABSTRACT**

DBT clinical trial data is emerging which will form the basis of clinical use. Because DBT has the potential to significantly change the practice of breast imaging, careful review of the results of these trials and implications for clinical practice is essential for informed decision regarding DBT.

## **VSBR31-07 • Implementation of Synthesized 2D Plus Tomosynthesis Images in Breast Cancer Screening: Comparison of Performance Levels with Full Field Digital Mammography Plus Tomosynthesis in a Population-based Screening Program**

**Per Skaane MD, PhD (Presenter) \* ; Randi Gullien RT \* ; Ellen B Eben MD \* ; Ingvild N Jebesen \* ; Unni Haakenaasen MD \* ; Ulrika Ekseth MD \* ; Mona Krager MD \***

### **PURPOSE**

To compare diagnostic performance of combined FFDM plus digital breast tomosynthesis (DBT) with synthesized 2D (C-view) plus DBT in breast cancer screening.

### **METHOD AND MATERIALS**

Eight radiologists prospectively interpreted independently 12,271 screening examinations including FFDM plus DBT and C-View plus DBT. Both reading modes included standard CC and MLO views of each breast. A 5-point rating scale for probability of cancer was used in the image interpretation. All cases with a positive score (defined as 2 or higher) were discussed at an arbitration meeting before decision for final recall. The reconstructed images (C-Views) do not require additional radiation exposure. Using analyses for binary data accounting for correlated interpretations and adjusted for reader-specific volume and performance levels and two-sided significance levels of 0.05, we compared performance levels when using C-view plus DBT with respect to positive scores, recall rates, and cancer detection rates with the corresponding FFDM plus DBT interpretations.

### **RESULTS**

Interpretation of 12,271 independently interpreted examinations under the two modes resulted in 656 (656/12,271=5.3%) and 651 (651/12,271=5.3%) positive scores for the FFDM plus DBT and the C-view plus DBT, respectively. Following arbitration meeting, the recall rates were 297/12,271= 2.4% and 270/12,271=2.2%, respectively. The cancer detection rate was 100/12,271=0.81% and 100/12,271=0.81%, for FFDM plus DBT and C-view plus DBT, respectively. There was no significant difference in the cancer detection between the two modes (McNemar test, p=0.85).

### **CONCLUSION**

Synthetically reconstructed 2D images applied in combination with DBT showed comparable results regarding positive predictive values and cancer detection rates with FFDM plus DBT.

### **CLINICAL RELEVANCE/APPLICATION**

The use of synthetically reconstructed 2D images (C-View) in combination with tomosynthesis resulted in comparable performance to actual exposure generated 2D plus tomosynthesis.

## **VSBR31-08 • Diagnostic Accuracy of Combination Synthetic Mammograms with Tomosynthesis vs. Combination FFDM with Tomosynthesis**

**Margarita L Zuley MD (Presenter) ; Andriy I Bandos PhD ; Jules H Sumkin DO \* ; Victor J Catullo MD ; Amy H Lu MD ; Denise Chough MD ; Marie A Ganott MD ; Grace Y Rathfon MD ; Luisa P Wallace MD**

### **PURPOSE**

To assess the diagnostic performance of combination synthetic mammograms and tomosynthesis (synthetic 2D+Tomo) to combination FFDM and tomosynthesis (FFDM+Tomo)

### **METHOD AND MATERIALS**

IRB approval was obtained. 123 cases deemed challenging by 2 non-participating independent reviewers were chosen from our research database to create a stress test, including 36 biopsy verified cancers, 35 biopsy proven benign lesions and 52 recalled screening exams proven to be normal on recall and 1 year follow up. 5 academic womens imagers performed a retrospective fully crossed and balanced multi case multi reader study where each study was reviewed twice, once with the synthetic mammogram and then tomosynthesis and once with the standard mammogram and then tomosynthesis. Probability of malignancy (POM) on a 100 point scale and BI-RADS scores were recorded for the 2D study and then again with tomosynthesis for each mode. Data analysis was performed using random-reader analysis (DBM MRM, v.2.33) based on the nonparametric area under the ROC curve (AUC).

### **RESULTS**

The reader-averaged AUC for the FFDM+Tomo and synthetic 2D+Tomo modalities were 0.898 and 0.871 correspondingly (p=0.15). Four readers performed somewhat poorer albeit not significantly (p>0.05) with synthetic 2D+Tomo. The average difference of 0.027 was not statistically significant with 95% confidence interval from -0.013 to 0.067.

### **CONCLUSION**

Synthetic 2D mammograms with tomosynthesis allowed similar interpretive performance to standard FFDM in combination with tomosynthesis and, therefore, may be an acceptable alternative for screening.

### **CLINICAL RELEVANCE/APPLICATION**

Lowering radiation dose during tomosynthesis based screening is possible with synthesized 2D images.

## **VSBR31-09 • Features of Additional Breast Cancers Detected by Digital Breast Tomosynthesis after Normal Digital Mammography**

**Paula Martinez Miravete ; Jon Etxano MD (Presenter) ; Pedro Slon MD ; Paula B Garcia MD ; Maite Millor MEd ; Luis Pina MD, PhD**

### **PURPOSE**

To evaluate the radiological presentation and histology of breast cancers detected by digital mammography (DM) and additional cancers detected by complementary Digital Breast Tomosynthesis (DBT).

### **METHOD AND MATERIALS**

From December 2010 to September 2012, we prospectively recruited 9300 consecutive patients with ACR density patterns II, III and IV in an enriched population that underwent both DM and DBT (COMBO mode).165 patients with cancer were detected using the COMBO mode. Out of these 165 breast tumors, 105 were detected by DM and 71 by additional DBT. We retrospectively evaluated the features of the radiological presentation and histology of breast cancers detected by DM and breast cancers detected by DBT. For the statistical analysis we performed a Pearson's Chi Square test with the SPSS 15.0 software.

## RESULTS

Significant differences were found regarding the radiological presentation of both groups ( $p < 0.05$ ) were found in the rate of Invasive Ductal Cancers (DM= 35/105; 33%, DBT=25/61; 41%) and Invasive Lobular Carcinoma (DM= 14/105; 13.3%, DBT=13/61; 21.3%).

## CONCLUSION

The additional breast cancers detected by DBT show different radiological presentation and histology than breast cancers detected with DM, being more common architectural distortions and tubular breast cancers.

## CLINICAL RELEVANCE/APPLICATION

DBT is an emerging imaging technique capable to detect additional cancers not seen in conventional DM. The radiological presentation and histology of these additional cancers are different.

### **VBSR31-10 • Addition of Tomosynthesis to Conventional Digital Mammograms: Effect on Image Interpretation Time of Screening Examinations**

**Pragya A Dang MD (Presenter) ; Phoebe E Freer MD ; Kathryn L Humphrey MD ; Elkan F Halpern PhD \* ; Elizabeth A Rafferty MD \***

#### PURPOSE

To determine the impact of the implementation of a screening tomosynthesis program on real-world clinical performance by quantifying the differences in interpretation times of conventional screening mammography to combined tomosynthesis-mammography screening for multiple participating radiologists with a wide range of experience in a large academic center.

#### METHOD AND MATERIALS

Ten board certified radiologists read digital mammography alone or combined tomosynthesis-mammography screening examinations in batch mode for one hour-long uninterrupted sessions, as a part of routine screening practice. Number of examinations read during each session was recorded for each reader. The experience level for each radiologist was also correlated to the average number of cases read during the hour. The BI-RADS density and BI-RADS assessment category for each examination were collected. Analysis of Variance (ANOVA) test (SAS) was used to determine differences in the number of studies interpreted per hour for different radiologists, different techniques, and different experience levels of radiologists.

#### RESULTS

A total of 3,665 examinations (1,502 combined tomosynthesis-mammography and 2,163 digital mammography) were interpreted by 10 radiologists, with at least 5 sessions per radiologist per modality. An average of  $23.8 \pm 0.55$  (14.4-40.4) and  $34.0 \pm 0.55$ , (20.4-54.3) examinations per hour, were interpreted by combined tomosynthesis-mammography and digital mammography, respectively. The average interpretation time for a combined tomosynthesis-mammography examination was 2.8 (1.5-4.2) minutes and digital mammography was 1.9 (1.1-3.0) minutes. The time taken to read a combined tomosynthesis-mammography examination was on average 0.9 minutes longer (47% longer) compared to the digital mammography alone examination. With the increase in years of breast imaging experience, there was a decrease in the overall additional time required to read combined tomosynthesis-mammography examinations ( $p = 0.03$ ,  $R^2 = 0.52$ ).

#### CONCLUSION

Addition of tomosynthesis to mammography results in increased time to interpret screening examinations when compared to conventional digital mammography alone.

#### CLINICAL RELEVANCE/APPLICATION

Reliable estimation of differential interpretation time with tomosynthesis should prove useful in preparing for its impact on radiologists' workload and resource allocation.

### **VBSR31-11 • Diagnostic Performance of Digital Breast Tomosynthesis: Comparison with Breast Magnetic Resonance Imaging and Conventional Digital Mammography in Women with Known Breast Cancers**

**Won Hwa Kim MD, MS ; Jung Min Chang MD (Presenter) ; Ann Yi MD ; Woo Kyung Moon ; Su Hyun Lee MD ; Nariya Cho MD ; Hye Ryoung Koo MD ; Min Sun Bae MD, PhD ; Seung Ja Kim**

#### PURPOSE

To evaluate the diagnostic performance of digital breast tomosynthesis (DBT) compared with breast magnetic resonance (MR) imaging and conventional digital mammography (DM) in women with known breast cancers.

#### METHOD AND MATERIALS

This study was approved by the institutional review board and informed consent was obtained. Between March and October 2012, 176 consecutive patients with known breast cancer (mean age, 51.3 years; range, 22-78 years) underwent DM, DBT and MR imaging. All 176 index cancers and 12 additional cancer (6 ipsilateral and 6 contralateral) cancers were identified. Two radiologists independently interpreted the images from each examination without clinical information and evaluated probability of cancer (5-point scale) for all findings. Sensitivity, false-positive rates, and area under the alternative free-response receiver operating characteristic curve (AUC) were estimated with histopathology and follow-up data as a reference standard.

#### RESULTS

The mean invasive tumor size was 2.2cm. Sensitivity for index cancers was the highest in MR imaging followed by DBT and DM (all  $P < .05$ ; reader 1, 98%, 93%, and 85%; reader 2, 98%, 92%, and 85%). Sensitivity for additional cancer was the highest in MR imaging followed by DBT and DM (all  $P < .05$ ; reader 1, ipsilateral, 67%, 33%, and 0%; reader 2, ipsilateral, 83%, 50%, and 17%; reader 1, contralateral, 100%, 67%, and 50%; reader 2, contralateral, 100%, 83%, and 67%). False-positive rate was the highest in MR imaging followed by DBT and DM (reader 1, 18%, 9%, and 7%; reader 2, 13%, 8%, and 7%), and was significantly frequent in MR imaging than DBT in one reader ( $P = .033$ ). The AUC for MR imaging, DBT, and DM were 0.946, 0.920, and 0.832 for reader 1; and 0.945, 0.912, and 0.828 for reader 2. The AUCs for DBT and MR imaging were significantly higher than DM ( $P < .05$ ); AUCs were not significantly different between DBT and MR imaging (Reader 1,  $P = .18$ ; Reader 2,  $P = .12$ ).

#### CONCLUSION

DBT showed lower sensitivity than MR imaging in detection of index and additional breast cancers, but false positives were less frequent with DBT than MR imaging.

#### CLINICAL RELEVANCE/APPLICATION

With DBT, comparable diagnostic performance to MR imaging and higher performance than DM was achieved. For additional cancer detection, DBT had limited diagnostic performance compared to MR imaging.

### **VBSR31-12 • Comparison of Visibility and Diagnostic Accuracy of Cone Beam Computed Tomography, Tomosynthesis, MRI and Digital Mammography for Breast Masses**

**Margarita L Zuley MD (Presenter) ; Ben Guo PhD ; Marie A Ganott MD ; Andriy I Bandos PhD ; Victor J Catullo MD ; Amy H Lu MD ; Amy E Kelly MD ; Maria L Anello DO ; Gordon S Abrams MD ; Denise Chough MD**

#### PURPOSE

To compare lesion visibility and diagnostic accuracy of cone beam computed tomography (CBCT) and tomosynthesis (DBT) to MRI and digital mammography (FFDM)

#### METHOD AND MATERIALS

IRB approval was obtained. From 04/16/2009 to 06/21/2011,, 178 mass lesions in 151 consecutively consenting women underwent



FFDM, DBT, CBCT and contrast enhanced MRI prior to percutaneous biopsy. 97 CBCTs were unenhanced (NC-CBCT) and 81 had contrast (CE-CBCT). DBT studies were unenhanced. Histopathology established truth. A nonparticipating radiologist marked each lesion location. A retrospective fully crossed, balanced reader study was performed with 7 MQSA qualified academic breast radiologists who recorded lesion visibility in each mode and if visible provided a probability of malignancy (POM) score on a 100 point scale. For each mode, ROC curves were obtained by a vertical average of the reader specific curves. Statistical analyses accounting for correlation and random reader effects were performed using the MRMC analysis (DBM MRMC, v.3.0) for area under the ROC curve (AUC) and using the generalized linear mixed model (proc glimmix, SAS, v.9.3) for visibility.

## RESULTS

100 benign and 78 malignant masses were included. Average size was 19.7 mm (median 14mm, range 4-100mm). Percentage of visible lesions differed (88% FFDM, 91% DBT, 82% CBCT [81% NC-CBCT sub-set, 84% CE-CBCT sub-set] and 93% MRI). For visualization, MRI was significantly better than CBCT (p

## CONCLUSION

For masses MRI has the highest accuracy and visibility and was significantly better than CBCT but not DBT. CBCT accuracy and visibility improve with use of contrast but further improvements are necessary for use as an alternative to MRI, FFDM or DBT.

## CLINICAL RELEVANCE/APPLICATION

Tomosynthesis may possibly be a viable alternative to MRI for breast mass evaluation.

### VSBR31-13 • Elastography

**A. Thomas Stavros MD (Presenter) \***

#### LEARNING OBJECTIVES

1) To understand the elastic properties of normal and pathologic breast tissues. 2) To get an overview of the different ultrasound methods and technologies. 3) To learn about the clinical results obtained with the different methods. 4) To understand the role of elastography within the imaging protocol.

#### ABSTRACT

Real-time elastography (RTE) of the breast may easily and quickly integrate conventional breast imaging. Excitation is applied to the tissue and sophisticated algorithms are used to estimate their elasticity. Different technologies use direct mechanical or radiation force excitation. Qualitative scores and/or quantitative values are usually derived from the estimate of the effect on the tissue and help to differentiate soft benign lesions from malignancies. These are usually stiffer due to the secretion of collagen and fibronectin, and the surrounding edema. Fluid lesions almost always show a typical three-layered pattern on strain elastography. They have typical patterns even with radiation force technologies (ARFI and shear wave). These last allow a true quantitative evaluation of the acoustic modulus and promise to be the gold standard for the future applications. Clinical reports show a high diagnostic accuracy: increased specificity for atypical carcinomas and a very high specificity in benign lesions, including BI-RADS category 3 lesions. With the best cutoff point between elasticity scores 3 and 4, the true negative predictive value is over 90%. Most mistakes are linked to the histopathology of the lesions. In invasive carcinomas RTE clearly shows the peripheral infiltration improving the volume measurement; 3D elastography and tomographic imaging may help in this respect. RTE scores and values are well reproducible. Indexes of intra-observer and inter-observer agreement are very good. Elastography scores have been introduced into the new BI-RADS edition. They upgrade BI-RADS 3 lesions and downgrade 4a lesions. In daily practice this results into earlier biopsies for cancers and reduced biopsies and longer follow-up intervals for benign lesions. Elastography is easy and quick; it must become part of the evaluation of all focal lesions. Still RTE score is only a complementary descriptor to BI-RADS and its interpretation requires some training.

### VSBR31-14 • BIRADS Classification for Real Time Ultrasound Elastography: More Comprehensive, Accurate and Action Oriented Results

**Mukta D Mahajan MBBS (Presenter) ; Sonal Garg MBBS ; Mukund S Joshi MD ; Chander Lulla MBBS**

#### PURPOSE

1. To devise a BIRADS category of standardized breast reporting for Elastography of focal breast lesions based on the elastography score and distance ratio method of evaluating them. 2. To qualitatively assess the sensitivity, specificity, positive and negative predictive value of preset cutoffs of elastography score and distance ratio in assigning a BIRADS rating to them when compared with BIRADS grey scale ultrasound and histopathology. 3. To evaluate the efficacy of implementing this Elastography BIRADS scheme in the diagnostic pathway of evaluating breast lesions at our institution and thereby generate a protocol based guide to management. 4. To reduce the incidence of biopsies and diagnostic conundrums in assessing indeterminate focal breast lesions.

#### RESULTS

The data was analyzed using 2 cut offs for ES and 4 cut offs for DR to compute the most accurate scheme for BIRADS-EL categorisation. The sensitivity, specificity, PPV and NPV for BIRADS-EL was found to be 71.7%, 90.1%, 68%, 91.5%. This was found to be superior the existing methods of analysis. The area under the receiver operating characteristic (ROC) curve for BIRADS-US, ES, DR and BIRADS-EL was 0.888, 0.928, 0.938 and 0.956 respectively. After implementing BIRADS-EL as a part of diagnostic workflow and protocol, assessment of the number of biopsies that were successfully averted was analyzed. The data collected after its implementation was evaluated after 3 months, 6 months and 1 year and has shown consistent result as the study group.

#### CONCLUSION

The present study suggests that Elastographic BIRADS classification of focal breast lesions is more accurate than BIRADS grey scale ultrasound in differentiating benign and malignant lesions when both methods i.e. ES and DR are combined. This method of reporting can standardize elastography results and make them readily comparable with other modalities. Results obtained are action oriented and leave no ambiguity in inconclusive or indeterminate lesions thereby improving the quality of non-invasive diagnosis and reducing the incidence of ultrasound guided biopsies.

#### METHODS

We studied a total of 215 breast lesions in 112 women by B-mode ultrasonography and real time breast elastography. All the lesions were assigned an ultrasound BIRADS category based on their imaging appearance. An Elastography score (ES) of 1 to 5 and distance ratio (DR) of 1 was assigned to each lesion based on elastographic assessment. BIRADS US category 4 and 5 lesions, ES 4,5 and DR = 1 or >1 lesion were biopsied. BIRADS US 3, ES 3 and DR 0.8 to 1 lesions were either followed up every 6 months for a period of 2 years or biopsied. BIRADS US 2, ES 1,2 and DR

### VSBR31-15 • Added Value of Shear-Wave Elastography in Evaluation of Breast Masses Detected on Screening Ultrasound

**Su Hyun Lee MD ; Jung Min Chang MD (Presenter) ; Nariya Cho MD ; Hye Ryoung Koo MD ; Min Sun Bae MD, PhD ; Won Hwa Kim MD, MS ; Mirinae Seo MD ; Woo Kyung Moon**

#### PURPOSE

To prospectively validate the added value of shear-wave elastography (SWE) in evaluation of breast masses detected on screening ultrasound (US).

#### METHOD AND MATERIALS

This study was conducted with institutional review board approval, and written informed consent was obtained. From April to October 2012, B-mode US and SWE were performed for 207 breast masses detected on screening US (mean size, 1.0 cm) in 207 consecutive women (mean age, 45 years) prior to US-guided core biopsy. Ten radiologists performed the examinations and assessed the likelihood of malignancy and Breast Imaging Reporting and Data System (BI-RADS) category for breast masses using B-mode US alone and a combination of B-mode US and SWE, respectively. Radiologists were allowed to upgrade BI-RADS category 3 masses to 4a when the maximum elasticity color (Ecol) was red and to downgrade category 4a to 3 when Ecol was dark blue or light blue with a maximum elasticity value (Emax) = 65 kPa, a cutoff value determined in a prior study, to achieve the best diagnostic accuracy in differentiating

benign lesions from malignant ones. The areas under the receiver operating characteristics curve (AUC), sensitivities, and specificities of the two datasets were compared.

#### RESULTS

Twelve of the 207 breast masses (5.8%) were malignant and consisted of nine invasive ductal carcinomas, two ductal carcinomas in situ, and one tubular carcinoma. The AUC of B-mode US increased from 0.700 to 0.879 when SWE was added ( $P = .002$ ). Considering category 4a or higher as a positive result for malignancy, the sensitivities were not different between B-mode alone and combined B-mode and SWE (91.7% [11 of 12], both). However, the specificity increased from 17.4% (34 of 195) to 73.8% (144 of 195) when SWE was added ( $P$

#### CONCLUSION

Combined use of SWE and B-mode US can increase both the accuracy and specificity in differentiating benign from malignant breast masses detected on screening US.

#### CLINICAL RELEVANCE/APPLICATION

SWE can be valuable in reducing the considerable false-positive rate of screening breast US examinations.

### **VSBR31-16 • Volume of Peri-tumoural Stromal Stiffness (VPSS) Surrounding Invasive Breast Cancer as Measured by 3D Shearwave Elastography (SWE): An Imaging Biomarker for Risk of Systemic Spread?**

**Andrew Evans** MRCP, FRCR (Presenter) ; **Patsy Whelehan** MSc \* ; **Sarah J Vinnicombe** MRCP, FRCR ; **Kim Thomson** ; **Lee Jordan** ; **Caroline Mitchie** ; **Colin Puride** ; **Alistair M Thompson**

#### PURPOSE

3D SWE allows the VPSS around breast cancers to be measured. Vascular invasion (VI) is most commonly detected at the tumour/stromal interface and is strongly associated with nodal involvement. We hypothesised that the likelihood of VI and nodal involvement may vary with the VPSS and that these relationships may be stronger than those seen between these risk factors for systemic spread and other ultrasound (US) parameters such as mean stiffness on 2D SWE, grey scale diameter and grey scale volume.

#### METHOD AND MATERIALS

2 and 3D grey scale US and SWE were carried out on a series of 62 consecutive breast cancers treated by immediate surgery. The VPSS and other US features were measured prior to surgery and then correlated with the presence of vascular invasion and nodal status at histologic examination. Statistical significance was ascertained using chi square and chi square test for trend.

#### RESULTS

VPSS has a strong relationship to VI status ( $p=0.003$ ) with none of the 17 patients with 3 of VPSS having VI, 13 of 36(36%) with a VPSS between 0.5 and 3cm<sup>3</sup> having VI and 5 of 9(56%) with a VPSS >3cm<sup>3</sup> having VI. Grey scale diameter and grey scale volume had significant but weaker relationships with VI ( $p=0.02$  and  $0.03$  respectively). A significant relationship was also found between VPSS and nodal status ( $p=0.04$ ). Nodal positivity rates using the above VPSS cut offs were 12%, 33% and 44% respectively. None of the other US parameters had statistically significant associations with nodal status

#### CONCLUSION

VPSS has stronger associations with markers of systemic spread than other US parameters and may be helpful in patient selection for neoadjuvant chemotherapy.

#### CLINICAL RELEVANCE/APPLICATION

In women with breast cancer the volume of peritumoral stiffness seen on 3D shearwave elastography may help patient selection for neoadjuvant chemotherapy

### **VSBR31-17 • Shear-wave Elastography in Detection of Residual Breast Cancer after Neoadjuvant Chemotherapy**

**Su Hyun Lee** MD ; **Jung Min Chang** MD (Presenter) ; **Nariya Cho** MD ; **Hye Ryoung Koo** MD ; **Min Sun Bae** MD, PhD ; **Won Hwa Kim** MD, MS ; **Mirinae Seo** MD ; **Woo Kyung Moon**

#### PURPOSE

To evaluate the accuracy of shear-wave elastography (SWE) in detecting residual cancer after neoadjuvant chemotherapy (NAC).

#### METHOD AND MATERIALS

This retrospective study was approved by our institutional review board and the requirement for written informed consent was waived. From January 2012 to February 2013, 71 women with stage II-III invasive breast cancers who received NAC and were imaged with B-mode ultrasonography (US), SWE, and magnetic resonance imaging (MRI) before surgery were included. Clinical tumor response was assessed using image findings from B-mode US and MRI and classified into two groups (0: no residual tumor, 1: residual tumor). Quantitative elasticity values (maximum kPa) were acquired for primary lesions depicted on US. Pathological complete response (pCR) was defined as no residual invasive cancer cells. The quantitative SWE values were compared between the pCR and non-pCR group using independent samples t-test. The areas under the receiver operating characteristics curve (AUC), sensitivities, and specificities of B-mode US, MRI, and SWE for detecting residual tumor were compared, with histopathologic examination as the reference standard.

#### RESULTS

Of the 71 women, 15 (21.1%) achieved pCR. The mean size of residual invasive cancers was 2.1 cm (range 0.1-6.4 cm). The maximum SWE value was significantly higher in the non-pCR group (mean, 122.9 kPa) than in the pCR group (30.6 kPa) ( $P$

#### CONCLUSION

SWE was accurate in the detection of residual cancer after NAC. When combined with B-mode US, the accuracy improved to a level similar to breast MRI.

#### CLINICAL RELEVANCE/APPLICATION

In predicting pCR after NAC, SWE can offer valuable information. Addition of SWE to conventional imaging can be useful for surgical planning in breast cancer patients.

## **Emergency Radiology Series: Leveraging Technology for State-of-the-Art Practice**

**Tuesday, 08:30 AM - 12:00 PM • E352**



[Back to Top](#)

**VSER31 • AMA PRA Category 1 Credit™:3.75 • ARRT Category A+ Credit:4**

**Moderator**  
**Suzanne T Chong**, MD  
**Moderator**  
**Savvas Nicolaou**, MD

### **VSER31-01 • Information Technology Solutions for Managing Emergency Radiology**

**Robert A Novelline** MD (Presenter)

#### LEARNING OBJECTIVES

1) Learners will be able to introduce technology solutions for improving the management of Emergency Radiology facilities. 2) Learners

will be able to identify technologies for optimizing Emergency Radiology patient scheduling, procedure protocoling, routine reporting, managing important and urgent communications, expediting workflow and satisfying requirements for peer review.

### **VSER31-02 • Is the Teleradiology Consultation Using a Smartphone with Mobile PACS Helpful When an On-call Radiology Resident Is Not Confident about the Presence of Appendicitis?**

**Nak Jong Seong MD (Presenter) ; Bohyoung Kim PhD ; Kyoung Ho Lee MD ; Seung Chan Lee MD**

#### **PURPOSE**

To discover whether the teleradiology consultation using a smartphone with mobile PACS (Picture Archiving and Communication System) can improve diagnostic performance of preoperative CT when an on-call radiology resident cannot make confident CT interpretation in regard to the presence of acute appendicitis

#### **METHOD AND MATERIALS**

From a previous randomized controlled trials associating with the acute appendicitis, we collected 68 patients' CT scans for which on-call radiologists scored the presence of acute appendicitis as grades 2, 3, and 4 in the 5-grade Likert scale. Two off-site abdominal radiologists retrospectively interpreted CT scans with suspected appendicitis, using iPhone 4 and a commercially available mobile PACS under a wireless network. Inter-observer agreement was measured using kappa statistics for two iPhone readers. Regarding the diagnosis of acute appendicitis as the reference standard, receiver operating characteristic (ROC) analysis was performed to compare the diagnostic performance of four readers: on-call radiologist, in-house attending abdominal radiologist, and two iPhone readers. The confidence grades for the presence of acute appendicitis were compared among four readers by using the Wilcoxon signed rank test for appendicitis and non-appendicitis cases, respectively, along with the heat maps combined with a dendrogram

#### **RESULTS**

The kappa statistic for the two iPhone readers was 0.90. The areas under the curve (AUCs) of two iPhone readers (AUC=0.97, 0.91) tended to be higher than that of on-call radiologist (AUC=0.85). For the appendicitis (or non-appendicitis) case, the in-house attending radiologist and two iPhone readers showed significantly higher (or lower) grades for the presence of acute appendicitis than on-call radiologist (P

#### **CONCLUSION**

Teleradiology consultation using a smartphone with mobile PACS is acceptable in the diagnosis of inconflident acute appendicitis by on-call radiologist.

#### **CLINICAL RELEVANCE/APPLICATION**

Smartphone reading using a mobile PACS could be helpful as a teleradiology consultation in the diagnosis of acute appendicitis, especially inconflident CT reading by on-call radiologist.

### **VSER31-03 • Value of Automated 3D-rendering and Rib Labeling for Evaluation of Rib Fractures in Whole-body CT Data Sets of Polytrauma Patients - Preliminary Results**

**Stefan Puig MD, MSc (Presenter) ; Daniel Ott MD ; Jennifer L Cullmann ; Tomas Dobrocky MD ; Johannes T Heverhagen MD, PhD \* ; Hendrik Von Tengg-Kobligh MD \***

#### **PURPOSE**

Aim was to evaluate accuracy and efficiency of a new CT image processing tool, which enables an automated 3D-rendering of whole body CT data sets including an unfolded display of the rib cage and the spine as well as an automated rib and spine labeling.

#### **METHOD AND MATERIALS**

Two readers (senior physicians) independently evaluated randomly selected whole-body-CTs of polytrauma patients for rib fractures. All CTs have been performed with a 128-slice-scanner. Axial reconstructions (slice-thickness: 1mm) were used as primary data to be retrospectively analyzed with the syngo.CT Bone-Reading client (syngo.via VA 20; Siemens, Germany). We evaluated numbers and location of fractures and compared the results with previously written reports. A final consensus read served as reference standard for rib fractures. Accuracy of the rib and spine labeling was recorded. In addition, time for reading was measured. Reader satisfaction with the software client was assessed using a 4-point Likert scale (1 = very useful for reporting; 2 = useful; 3 = undetermined; 4 = impedes reporting).

#### **RESULTS**

Up to now, 15 whole-body-CT-scans from 15 patients (mean age = 55.3 years; range 21 - 84 years) have been included in the analysis. 6/15 (40.0%) patients had rib fractures, 4/6 (16.67%) showed multiple fractures. Based on patients with rib fractures, sensitivity for reader 1 and reader 2 was 83.3% (5/6) and 100%, respectively. A non-displaced fracture of the first rib was detected by only one reader. According to the prior written reports 4/6 (66.67%) patients were reported as positive for rib fracture based on conventional reading. Time for reading was 2min 38s and 2min 20s, respectively. In 7/15 (46.7%) rib and spine segmentation as well as labeling was correct. Reasons for incorrect segmentation and/or labeling were: congenital anomaly (n=1), severe kyphosis (n=1), no segmentation of first rib (n=5). Both readers rated the software client as useful for reporting (mean rating: 1.8 and 1.6). In no case the software client was rated as to interfere with reporting.

#### **CONCLUSION**

Using the syngo.CT Bone-Reading client we could achieve a higher detection rate of rib fractures compared to conventional reading in a relatively short reading time.

#### **CLINICAL RELEVANCE/APPLICATION**

Automated 3D-rendering of whole body CTs allows a time-saving evaluation of the ribs and spine and enables a higher detection rate of rib fractures than conventional reading in polytrauma patients.

### **VSER31-04 • Enhancing Your CT Practice with Dual Energy in the ER**

**Aaron D Sodickson MD, PhD (Presenter)**

#### **LEARNING OBJECTIVES**

1) Summarize key concepts of dual energy CT. 2) Describe protocol building, workflow and postprocessing of dual energy scanning. 3) Highlight a variety of game-changing dual energy applications for emergency radiology practice that have the potential to enhance information content, reduce radiation dose, or both.

### **VSER31-05 • Use of Dual-energy CT and Virtual Non-calcium Techniques to Evaluate the Time to Resolution of MRI-proven Bone Bruises**

**Song-Tao Ai ; Mingliang Qu MD (Presenter) ; Katrina N Glazebrook MBChB ; Peter Rhee DO ; Shuai Leng PhD ; Maria Shiung ; Cynthia H McCollough PhD \***

#### **PURPOSE**

The purpose of this study was to investigate the short-term status of post-traumatic bone bruises using dual-energy CT (DECT) and virtual non-calcium (VNCa) techniques in a cohort of patients with MRI-proven bone bruising lesions subsequent to unilateral knee injury.

#### **METHOD AND MATERIALS**

Patients with unilateral knee injury occurring between March 2009 and July 2011 resulting in bone bruises confirmed by MRI and who had bilateral DECT scanning of the knee performed within six months of the injury were identified from chart review. DECT examinations were performed using a clinical protocol. Two radiologists evaluated VNCa images without knowledge of MRI results for the presence of increased soft tissue attenuation in four anatomic regions, and DECT findings were compared to the prior MRI and contralateral DECT

images.

## RESULTS

14 patients with MRI-proven bone bruises were identified by chart review to have undergone DECT subsequent to the MRI exam, with a total of 36 out of 56 (64%) lesion-positive anatomical regions by MRI. DECT detected lesions in 10 out of 14 patients (71%) and identified 22 out of the 36 (61%) lesion-positive regions identified by MRI. The mean CT numbers in VNCa images for positive and negative bone bruising regions were  $-7.6 \pm 24.9$  HU (22 regions) and  $-58.2 \pm 19.5$  HU (34 regions) (p-value < 0.001), respectively. The number of days between injury and DECT ranged 11 to 99. At 2, 4, 6, and 8 weeks post-injury, 14 (38.9%), 18 (50.0%), 23 (63.9%) and 34 (94.4%) lesion-positive regions by MRI were negative by DECT, respectively.

## CONCLUSION

This study confirmed the feasibility of using DECT and a VNCa technique to evaluate the short-term status of post-traumatic bone bruises and found that over 90% of MRI-proven bone bruise regions had resolved by 8 weeks post-injury.

## CLINICAL RELEVANCE/APPLICATION

DECT exam provided reliable assessment of the presence or absence of bone bruising and allowed assessment of the time to resolution of bone bruising in this small patient cohort.

## **VSER31-06 • Lung Perfused Blood Volume (Lung PBV) Imaging on Dual-energy CT: Quantitative Capability for Disease Severity Assessment in Patients with Acute Pulmonary Thromboembolism**

**Sachiko Miura MD (Presenter) ; Yoshiharu Ohno MD, PhD \* ; Yuko Nishimoto MD ; Kimihiko Kichikawa MD**

## PURPOSE

To determine the capability of lung perfused blood volume (PBV) imaging on dual-energy CT (DECT) for disease severity assessment in acute pulmonary thromboembolism (APTE) patients.

## METHOD AND MATERIALS

Twenty-one consecutive APTE patients underwent contrast-enhanced DECT and echocardiography at the onset. A normalized lung PBV (nLung PBV) image was generated by pixel analysis in each patient. In each patient, the overall perfusion (OP) and heterogeneity (H) indexes were assessed as averages of mean and standard deviation of the nLung PBV value within ROIs placed over each lung field in both lungs. In this study, the disease severity of APTE was determined as CT angiographic clot burden score (CBS) according to past literatures and tricuspid regurgitation pressure gradient (?P). Then, all patients were divided into right heart (n=13) and non-right heart (n=8) dysfunction groups. To determine the capability of DECT indexes for disease severity assessment, CBS and ?P were statistically correlated with both DECT indexes. To assess difference of each index between the two groups, all indexes were compared by Student's t-test. To determine the capability for differentiating the two groups, feasible threshold values of CBS and the DECT indexes as having significant differences between the two groups were determined using ROC-based positive test. Finally, sensitivity, specificity and accuracy were compared to each other by using McNemar's test.

## RESULTS

CBS had significant correlation with OP index ( $r=-0.82$ , p

## CONCLUSION

The Lung PBV imaging on DECT has a potential for disease severity assessment in APTE patients, and it is considered at least as valuable as clot burden score in routine clinical practice.

## CLINICAL RELEVANCE/APPLICATION

The Lung PBV imaging on DECT has a potential for disease severity assessment in APTE patients, and it is considered at least as valuable as clot burden score in routine clinical practice.

## **VSER31-07 • Comparison of the Image Quality between Virtual Non Contrast Scans Obtained on Solid State Detectors and on the New Fully Integrated Digital Chip Detector that were Generated from Abdominal Dual Energy CT Exams in the Emergency Department**

**Adrian Reagan MD (Presenter) ; Patrick McLaughlin FFRCSEI ; Savvas Nicolaou MD ; Luck J Louis MD ; Ana-Maria Bilawich MD ; Sharon Gershony MD**

## PURPOSE

To determine the effect on noise reduction in VNC studies generated on solid state detector (SSD) and on the new fully integrated digital chip detector (FICD) and to determine whether virtual non contrast images provide similar quality to standard NC studies with the aim of eliminating the need for NC scans effectively reducing radiation dose in the acute setting.

## METHOD AND MATERIALS

10 DECT studies were imaged on the SSDs and 10 on the new FICD using the 128 slice DS Definition scanner. Protocol parameters included: 64 by 0.6 mm col. reconstructed to 1.5mm axial DE 100 and 140 kv tin filter data sets. D30 1.5 mm axial DECT images were loaded into the multimodality station within the liver VNC DE application class. 3mm axial VNC images were exported to pacs for analysis. Routine NCIs were obtained using 64 by 0.6 mm col., reconstructed to a thickness of 3mm axial slices using B30 kernel keeping CTDI vol the same as the DECT protocol. Noise was calculated via SD of ROIs in 5 tissues. Two Radiologists graded the quality of the NC and VNC image sets using a 5-point Likert scale. SNR was then averaged and the means were compared between the VNC data set imaged on the SSD and the VNC data set imaged on the new FICD. Analysis between VNC images and standard NC studies obtained on the FICD was also performed. A Mann-Whitney U test was used to compare the level of noise between VNC images done on SSD and VNC images done on the FICD. VNC images obtained on the FICDs were also compared with regular NCIs from the same detector. VNCIs performed on the FICD revealed a U value of 25 (p 0.05). The new VNC data when compared to the regular NC data obtained on the FICD revealed a U-value of 40 (p > 0.05).

## RESULTS

VNC images obtained on the FICD demonstrated lower noise values compared to VNC data sets obtained on the SSD. No difference in noise values was found between the standard NC studies and the new VNC images. Subjectively VNC abdomen sets provided equal diagnostic quality compared to standard NC studies.

## CONCLUSION

Findings suggest VNC image noise levels are reduced on the new FICDs. New VNC studies provide diagnostic images comparable to standard NC protocols.

## CLINICAL RELEVANCE/APPLICATION

The new FICDs resulted in diagnostic VNC studies and thus represent a future dose reduction strategy in the elimination of non contrast studies in abdominal ED protocols.

## **VSER31-08 • QandA/Break**

## **VSER31-09 • Multi-detector CT: One Stop Shop for the Assessment of Acute Chest Pain**

**Savvas Nicolaou MD (Presenter)**

## LEARNING OBJECTIVES

1) Discuss diagnostic imaging algorithm for the assessment of acute chest pain. 2) Discuss the benefits and Limitations of cardiac CT in the acute setting. 3) Review the optimization of the Cardiac CT in the emergency department. 4) Assess literature evidence of MDCT in diagnosis of acute coronary syndrome (ACS) with regards to cost, time to diagnosis and outcomes. 5) Discuss the role of a

Triple-Rule-Out Protocol in evaluation of acute chest pain. 6) Discuss the characteristics of coronary lesions on MDCT that are associated with ACS. 7) Review new dose reduction techniques which maintain diagnostic quality available including prospective ECG gating, BMI-based tube voltage reduction and iterative reconstruction.

#### ABSTRACT

Chest pain is a very common presentation in the emergency department (ED), accounting up to 5.8 million visits a year and as the second leading complaint in the ED. It is important to properly diagnose acute coronary syndrome (ACS) in these patients; 2-8% of patients with ACS are misdiagnosed and inappropriately discharged home which has been demonstrated to be associated with a doubling of mortality rate. It is vital to differentiate ACS from other serious causes of chest pain including pulmonary embolism and aortic dissection. Multidetector CT (MDCT) has been proposed to be a one-stop shop as it allows quicker time, low costs, and easy access, the ability to rule out ACS confidently using non-invasive visualization, and visualization of extracardiac findings.

### **VSER31-10 • Are Cardiac Risk Factors and Risk Scores Useful to Triage Patients Presenting to the Emergency Department with Chest Pain among Those Judged to Be at Low to Intermediate Risk of Acute Coronary Syndrome?**

**Jacob P Deutsch ; Maria M Hannaway ; Adrian T Estepa ; Anand I Kenia ; David C Levin MD \* ; Ethan J Halpern MD**  
(Presenter)

#### PURPOSE

To evaluate the predictive value of cardiac risk factors and risk scores for coronary artery disease (CAD) and adverse outcomes in an emergency department (ED) population judged to be at low to intermediate risk for acute coronary syndrome (ACS).

#### METHOD AND MATERIALS

IRB approval was obtained for this HIPPA compliant, prospective cohort study. The study cohort included consecutive patients who presented to the ED with chest pain over a 36 month period, were admitted to the observation unit, evaluated with coronary CTA (cCTA) and agreed to provide written informed consent. Cardiac risk factors, clinical presentation, ECG and laboratory studies were recorded with a standard template; TIMI and GRACE scores were tabulated. cCTA findings were reviewed by two experienced cardiac radiologists, rated on a 6 level plaque burden scale, and classified for presence/absence of significant CAD (stenosis = 50%). Adverse cardiovascular outcomes were recorded after 30 days.

#### RESULTS

Among 250 patients evaluated by cCTA, 143 (57%) had no CAD, 64 (26%) demonstrated minimal plaque (70% stenosis). Six patients developed adverse cardiovascular outcomes. Among traditional cardiac risk factors, only age (older) and sex (male) were significant independent predictors of CAD. Correlation with CAD was poor for TIMI ( $r=0.12$ ) and GRACE ( $r=0.09-0.23$ ) risk scores. Although risk factors, patient presentation, and risk scores were poor predictors of CAD and adverse outcomes, cCTA identified severe CAD in all subjects with adverse outcomes.

#### CONCLUSION

Among patients who present to the ED with chest pain and are judged to be at low to intermediate risk of ACS, traditional risk factors, TIMI and GRACE scores are not useful to stratify patient risk for CAD and adverse outcomes. cCTA is an excellent predictor of outcome.

#### CLINICAL RELEVANCE/APPLICATION

Coronary CTA is superior to traditional risk factors for triage of patients presenting to the ED with chest pain and who are judged to be at low to intermediate risk of acute coronary syndrome.

### **VSER31-11 • MRI in Abdominal Emergencies**

**Stephan W Anderson MD** (Presenter)

#### LEARNING OBJECTIVES

1) To understand the appropriate use of MRI in the abdominal emergency setting. 2) To discuss the protocol considerations for maximizing the diagnostic yield of MRI in imaging abdominal emergencies. 3) To illustrate relevant imaging findings for a range of abdominal emergencies to which MRI may be appropriately applied.

### **VSER31-12 • Efficacy of MR Sequences in the Optimal Visualization of the Appendix**

**Ajay K Singh MD** (Presenter) ; **Garry Choy MD, MS** ; **Mukesh G Harisinghani MD**

#### PURPOSE

The aim of this study was to determine the frequency of visualization of appendix on different MR sequences.

#### METHOD AND MATERIALS

The MR sequences obtained in 61 patients for the evaluation of pelvis and right lower quadrant were included in this study. Two board certified radiologists independently evaluated the different MR sequences for the visualization of the appendix. The frequency of visualization of the normal or abnormal appendix was documented for single shot fast spin-echo (SSFSE), T2 fast spin echo (FSE), T1 weighted gradient-echo (GRE) and inversion recovery sequences (STIR).

#### RESULTS

SSFSE without fat saturation in 3 planes was able to visualize the appendix in 90.9% of the cases (50/55). Amongst the 3 planes (axial, coronal and sagittal) of image acquisition with SSFSE, the coronal image acquisition was considered to be the best in the visualization of the appendix, followed by acquisition in axial plane. The frequency of visualization of appendix on T2 FSE sequences was 62.5% (10/16) without fat saturation and 26.6% (4/15) with fat saturation. In phase T1-weighted GRE (39.2%) sequence was found to be more likely to visualize the normal appendix, compared to out of phase T1-weighted GRE sequence (12.5%). Of the MR sequences evaluated in this study short tau inversion recovery (8.3%) and fat saturated SSFSE (4.7%) sequences were least likely to visualize the appendix.

#### CONCLUSION

All imaging protocols in patient with suspected appendicitis should include 3 planes SSFSE without fat saturation, T2 FSE sequence without fat saturation and T1 in-phase sequence. Fat saturated SSFSE, STIR and T2 FSE sequences are least effective in visualization of the normal appendix.

#### CLINICAL RELEVANCE/APPLICATION

This study allows a radiologist to choose the most optimal sequences in the visualization of the appendix in patients with suspected acute appendicitis.

### **VSER31-13 • Diagnostic Performance of Noncontrast Abdominopelvic MRI for the Evaluation of Suspected Acute Appendicitis in Patients < 40 Years Old**

**Matthew Covington MD** (Presenter) ; **Shannon Urbina** ; **Lori Stolz MD** ; **Diego R Martin MD, PhD** ; **Dorothy L Gilbertson-Dahdal MD** ; **Sarah M Desoky MD** ; **Hina Arif** ; **Bobby T Kalb MD**

#### PURPOSE

Evaluate the sensitivity and specificity of MRI for the detection of acute appendicitis in patients = 40 years old presenting to the ED with right lower quadrant pain

#### METHOD AND MATERIALS

Study was IRB-approved, HIPPA compliant. Inclusion criteria selected total of 59 patients = 40 years old presenting to emergency room with possible acute appendicitis and evaluated with MRI as the primary imaging test between 8-2012 and 3-2013. Exclusion criteria

excluded patients > 40 years old and patients without symptoms of acute appendicitis. All MR exams were performed with a fast, no oral/no intravenous contrast protocol, utilizing a combination of multiplanar, non-breath-hold, T2-weighted HASTE sequences without and with spectral adiabatic inversion recovery (SPAIR) fat suppression. The acquisition time for each exam was recorded. The MRI was interpreted the same day in a prospective fashion by the radiologist assigned to the clinical service that day. The results were classified as a) positive, b) negative or c) indeterminate for acute appendicitis. MRI results were also categorized for additional pathology or sources of pain. Each patient was followed up by either a) surgical findings or b) phone call follow-up at 1 week and 6 months after the ED visit and interrogation of medical records for subsequent clinical work-up. Statistical analysis included calculation of sensitivity, specificity, positive and negative predictive values.

#### RESULTS

59 patients received MRI for evaluation of right lower quadrant pain and 5 exams were positive for acute appendicitis (8.5%). When compared with gold standards of surgery (5/59) and phone call follow-up with medical records review (54/59), MRI demonstrated a sensitivity of 100%, specificity of 100%, negative predictive value of 100% and positive predictive value of 100%. Out of the 54 patients with negative MRI for acute appendicitis, an alternate diagnosis was offered in 22/54 (40.7%). The average exam time for each MRI was 15 minutes (range 12-22 minutes).

#### CONCLUSION

MRI is a highly accurate test for the diagnosis of acute appendicitis in patients = 40 years old, with sensitivity and specificity of 100% in our study, utilizing a rapid imaging protocol without oral or IV contrast.

#### CLINICAL RELEVANCE/APPLICATION

MRI is highly accurate for diagnosing acute appendicitis in patients = 40 years old, providing a rapid, non-radiation based exam for evaluation of right lower quadrant pain in the emergency setting.

### VSER31-14 • Panel/QandA

## Gastrointestinal Series: Pancreas - Inflammation and Neoplasm

Tuesday, 08:30 AM - 12:00 PM • N230



[Back to Top](#)

VSGI31 • AMA PRA Category 1 Credit™:3.25 • ARRT Category A+ Credit:4

#### Moderator

Eric P Tamm, MD

#### Moderator

Naoki Takahashi, MD \*

### VSGI31-01 • Cutting-edge Imaging of the Pancreas

Riccardo Manfredi MD (Presenter)

#### LEARNING OBJECTIVES

1) Describe state of the art imaging modalities in diagnostic imaging of pancreatic diseases. 2) Illustrate diagnostic imaging findings useful for the differential diagnosis between pancreatic adenocarcinoma and non-neoplastic mimickers such as autoimmune pancreatitis and para-duodenal pancreatitis. 3) Understand the physiology of secretin and its application during secretin-enhanced Magnetic Resonance Cholangiopancreatography (MRCP). 4) Indication to secretin-enhanced MRCP its role in different clinical settings.

#### ABSTRACT

New diagnostic imaging modalities are applied in pancreatic diseases such as contrast-enhanced ultrasound, computed tomography (CT) perfusion, diffusion-weighted imaging and secretin-enhanced Magnetic Resonance (MR) imaging. These new diagnostic imaging modalities are helpful in different medical needs in pancreatic imaging such as the early diagnosis of pancreatic adenocarcinoma, differential diagnosis between pancreatic adenocarcinoma and non-neoplastic mimickers such as focal autoimmune pancreatitis and para-duodenal pancreatitis. MR imaging and MR cholangiopancreatography (MRCP) are useful in the diagnosis of cystic pancreatic neoplasms and in their characterization, by depicting internal features and the relationship between the neoplasm and the pancreatic duct system. Furthermore secretin-enhanced MR cholangiopancreatography (S-MRCP) is able to investigate ductal system abnormalities, such as those occurring in recurrent acute pancreatitis, chronic pancreatitis and acute pancreatitis. S-MRCP is also able to determine pancreatic exocrine reserve in severe chronic pancreatitis or in post-operative patients.

### VSGI31-02 • Does Model Based Iterative Reconstruction (MBIR with VEO) Improve State-of-the-Art CT of the Pancreas at 80 kVp and 8 mL/s?

Wendy L Stiles MD (Presenter) ; Joseph M Collins MD \* ; Alvin C Silva MD ; Amy K Hara MD \* ; Marina E Giurescu MD ; Robert G Paden ; Donna Sterns RN ; Qing Wu ; Deborah Unger RN

#### PURPOSE

Improve CT imaging of pancreatic neoplasm, utilizing reduced acquisition energy (80 kVp), maximized iodine flux at 8 mL/s injection rate and a novel MBIR reconstruction algorithm.

#### METHOD AND MATERIALS

23 patients with known pancreatic neoplasm underwent multi-phase CT (15M, 8F; ages: 42-82 yrs). Radiation exposure parameters (kVp, noise index, mA, pitch) customized to body size; width of patient's body on AP scout: Sm. =30 cm, Med. 31-40 cm, Lg. 41-50 cm, XL =51 cm. By altering pitch, 83% of patients were imaged at 80 kVp to take advantage of iodine's k-edge (33 keV). Maximum iodine flux (i.e. 8 mL/s) obtained by simultaneous injection of IV contrast (150 mL or 200 mL Omnipaque 350) at 4 mL/s in each arm with 18 or 20 gauge needles. Images were reconstructed with 3 different algorithms: filtered back projection (FBP), adaptive statistical iterative reconstruction (ASIR), and model based iterative reconstruction (MBIR with VEO, GE Healthcare). Signal-to-noise (SNR) and contrast-to-noise (CNR) compared on images processed with FBP, ASIR, and MBIR. Three experienced (> 7 yrs) abdominal radiologists independently compared overall image quality and lesion conspicuity (key finding) between FBP, ASIR, and MBIR on a scale from 0-4 (0 = worst, 4 = best).

#### RESULTS

Density of normal pancreas on arterial phase averaged 222.2 HU using 80 kVp acquisition energy at 8 mL/s IV contrast injection rate.

MBIR statistically improved SNR and CNR compared to ASIR and FBP (p

#### CONCLUSION

**MBIR significantly improved quantitative and qualitative measures of overall image quality and key findings related to pancreatic neoplasm. We achieved substantially greater enhancement of the pancreas than what has been reported previously by combining the advantages of a reduced acquisition energy 80 kVp and maximized iodine flux from injecting at 8 mL/s. Coupled with MBIR, this CT technique provides better images to evaluate pancreatic neoplasm.**

#### CLINICAL RELEVANCE/APPLICATION

MBIR on images acquired at 80 kVp at maximized iodine flux sets a new standard for state-of-the-art pancreatic imaging, providing better images to discern pancreatic neoplasm.

### VSGI31-03 • Studies of Multi B-values DWI in Assessing Chronic Pancreatitis at 3.0T MR

**Chunshu Pan MD (Presenter) ; Li Wang ; Jianping Lu MD ; Chao Ma**

#### PURPOSE

To assess the value of multi b-values DWI using biexponential model for diagnosis chronic pancreatitis. To investigate the value of parameters derived by biexponential model and monoexponential model in evaluating the atrophy of chronic pancreatitis.

#### METHOD AND MATERIALS

48 patients with chronic pancreatitis and 36 healthy volunteers underwent DWI with 9 b-values up to 1000 s/mm<sup>2</sup> on 3.0T MR system. ADC<sub>tot</sub> and D\*, D, f was calculated by monoexponential model and biexponential model respectively. Atrophy rate was determined by the maximum diameter of the duct divided by the average diameter of the pancreas. Mann-Whitney U test was used for comparing the difference of ADC<sub>tot</sub>, D\*, D, f between chronic pancreatitis and normal pancreas. Dependency of D\*, D, f on atrophy rate was characterized by using a Spearman rank-order correlation test.

#### RESULTS

#### CONCLUSION

#### CLINICAL RELEVANCE/APPLICATION

Multi b-values DWI could be helpful to assess the degree of fibrosis of chronic pancreatitis and pancreatic blood supply.

### VSGI31-04 • Pancreatic Cancer

**Koenraad J Morteel MD (Presenter)**

#### LEARNING OBJECTIVES

1) To review the imaging features that allow diagnosis, staging, and management of pancreatic cancer.

#### ABSTRACT

Ductal pancreatic adenocarcinoma accounts for nearly 95% of all malignant pancreatic neoplasms and is the ninth most common malignancy. Prognosis is poor with a 5-year survival rate ranging from 1% to 5%. The majority of tumors are located in the pancreatic head and because of the involvement of the common bile duct, they present earlier than tumors arising in the body or tail of pancreas. MDCT is the imaging modality of choice for the detection and preoperative staging of pancreatic cancer. On contrast-enhanced MDCT images, adenocarcinomas present as hypoattenuating lesions with respect to the surrounding normal pancreatic parenchyma. There are also some indirect signs for the presence of a tumor on CT without identification of the tumor itself. Maximum tumor conspicuity can be achieved during either the pancreatic parenchymal (40 seconds) or portal venous phases (70 seconds) of a dynamic contrast enhanced CT exam. The detection of hepatic metastases is critical in the preoperative staging of the patients since presence of metastatic foci within the liver makes the tumor unresectable. In the absence of obvious liver metastases, tumor respectability depends on the presence of local invasion or vascular involvement. In the absence of obvious liver metastases, tumor respectability depends on the presence of local invasion or vascular involvement. In a recent prospective study comparing EUS, CT, MRI and angiography in preoperative staging and tumor resectability assessment of pancreatic cancer, Soriano et al. reported that CT is the mainstay for pancreatic cancer staging, with the best figures in the evaluation of extent of primary tumor, locoregional extension, vascular invasion, and metastatic spread (with accuracies 73%, 74%, 83% and 88%, respectively).

### VSGI31-05 • Post-Whipple Imaging Surveillance in Patients with Pancreatic Ductal Adenocarcinoma: Association with Overall Survival in Multivariate Analysis

**Azadeh Elmi MD (Presenter) ; Janet E Murphy MD, MPH ; Seyed Mahdi Abtahi MD ; Shaunagh McDermott FFRCSI ; Elkan F Halpern PhD \* ; Mukesh G Harisinghani MD**

#### PURPOSE

While it is common clinical practice to routinely image patients with pancreatic ductal adenocarcinoma (PDAC) after Whipple procedure, there is no consensus that close imaging follow-up improves overall survival (OS). We evaluated the role of routine imaging in patients with PDAC following Whipple.

#### METHOD AND MATERIALS

We identified 1007 patients, who underwent Whipple for PDAC between 2005 and 2011, of whom 229 (105 F; median age 68 years) had regular postoperative clinical follow-up at our hospital. Patients were assigned to two follow-up groups based on clinical chart review; imaging-surveillance (IS) group defined as routine imaging at scheduled intervals, vs. clinical (C) group who had imaging only triggered by either change in clinical status or change in CA19-9. Follow-up was obtained through hospital and Cancer Data Registry records. Survival was calculated from date of surgery to death or last follow-up, with data censored as of March 13, 2013. Kaplan-Meier survival curves were compared using the log-rank test, and Cox regression models were used for multivariate analysis.

#### RESULTS

Patients were followed for a mean period of 24.35 months and visited every 2.44 months on average. Patients in IS group underwent significantly more imaging (4.41 vs. 2.08 scans per year, p=0.0083) but not more frequent follow-up visits. The most frequent imaging was CT of chest and abdomen at 3-4 months interval. In univariate analysis, age, gender, neoadjuvant or adjuvant treatment did not show significant association with OS. Univariate associations with OS were detected with post-Whipple ECOG status, T-stage, N-stage, chemotherapy for metastatic disease, disease recurrence, new metastasis, and IS. In multivariate analysis, ECOG status, recurrence, and new metastasis were independent predictor of survival. Also, our predictor of interest, IS, was highly associated with longer survival in multivariate modeling, with a median OS of 30.4 vs.17.1 months for IS and C groups (log-rank p=0.002). The survival probability was 41.1% and 27.3%, respectively.

#### CONCLUSION

Routine imaging surveillance was associated with prolonged OS post-Whipple in this retrospective analysis of patients with PDAC in a multivariate model.

#### CLINICAL RELEVANCE/APPLICATION

Routine imaging follow-up after Whipple is associated with prolonged survival, a hypothesis-generating finding that should be studied prospectively and could ultimately impact surveillance guidelines.

### VSGI31-06 • Diffusion-weighted Imaging of Advanced Pancreatic Adenocarcinoma: Can Apparent Diffusion Coefficient Values Predict the Response to Chemotherapy?

**Marcello A Orsi MD (Presenter) ; Claudio Losio MD ; Francesco A De Cobelli MD ; Francesco Giganti MD ; Michele Reni ; Alessandro Del Maschio MD**

#### PURPOSE

Chemotherapy is the only option to improve survival and quality of life of patients affected by advanced Pancreatic Adenocarcinoma (PA). Response to treatment is difficult to assess, as tumor regression is not usually measurable earlier than 2-3 months and markers early kinetics are not reliable. We investigated the role of diffusion-weighted imaging (DWI) in predicting PA response to chemotherapy

#### METHOD AND MATERIALS

We studied 22 patients with unresectable PA (stage III and IV) candidate to a six-months multidrug gemcitabine-based regimen. All patients underwent baseline magnetic resonance imaging (MRI) of upper abdomen including respiratory triggered echo-planar DWI (b value: 0,600 s/mm<sup>2</sup>); 12 patients of this group were also studied with the same MRI protocol after one month of treatment. On axial images, mean Apparent Diffusion Coefficient (ADC) of the lesions were measured independently by two radiologists. Response was

assessed using CT, PET-CT (Recist Criteria) performed at 6-8 months after treatment; patients who achieved partial response and stable disease were considered as Responders (R), the ones who developed progressive disease as Non-Responders (NR)

## RESULTS

In our population we obtained 15 Rs and 7 NRs. Baseline lesional ADC was significantly lower in R group than in NR group ( $1,35 \pm 0.23$  vs  $1,68 \pm 0,17 \times 10^{-3} \text{mm}^2/\text{s}$ ; p

## CONCLUSION

Our preliminary results indicate that a higher baseline ADC, probably linked with the pre-treatment intratumoral amount of necrosis, is associated with worst response to treatment. Increase of ADC after one month, probably linked with chemotherapy direct effects like membrane disruption and cytolysis, positively correlates with subsequent tumor reduction

## CLINICAL RELEVANCE/APPLICATION

Quantitative DWI could probably early identify patients affected by PA not responding to chemotherapy and be a promising tool in developing new therapies and guiding therapeutic strategies

### VSGI31-07 • Cystic Pancreatic Tumors

**Douglas S Katz** MD (Presenter)

#### LEARNING OBJECTIVES

1) To overview the differential diagnosis of cystic lesions of the pancreas. 2) To demonstrate examples of multiple types of cystic lesions of the pancreas with an emphasis on CT and MR, but with some US correlation. 3) To review the current literature of cystic pancreatic lesions, with an emphasis on areas of controversy as well as management issues.

### VSGI31-08 • Incidental Pancreatic Cystic Lesions: Relationship with All-cause Mortality and Incidence of Pancreatic Neoplasm

**Victoria Chernyak** MD (Presenter) \* ; **Milana Flusberg** MD ; **Linda B Haramati** MD, MS \* ; **Alla M Rozenblit** MD ; **Eran Bellin**

#### PURPOSE

To assess relationship of incidental pancreatic cysts found on CT/MR and all-cause mortality, incidence of all pancreatic cancers and incidence of pancreatic adenocarcinoma (AdenoCA) and pancreatic ductal carcinoma (DCA).

#### METHOD AND MATERIALS

Cyst cohort included cases with CT/MR reports done between 11/1/01-11/1/11 and describing incidental pancreatic cysts. No-cyst cohort was frequency-matched on age decade, modality and year of initial study from a pool of patients without reported pancreatic cysts. Cases with diagnosis of any pancreatic cancer within 5 years of initial CT/MR were excluded. 10-year cumulative mortality, 10 year cumulative incidences of any pancreatic cancer and incidences of AdenoCA/ DCA were compared between cohorts. Reports in Cyst cohort were reviewed for number of cysts, size and location of largest cyst, presence of calcification, septations, enhancing component, main pancreatic duct (MPD) dilatation, regional lymphadenopathy (LAN).

#### RESULTS

There were 1,343 cases in Cyst cohort and 4,015 cases in No-cyst cohort with mean age of 70.1 ( $\pm 15.3$ ) and 69.6 ( $\pm 15.6$ ) years, respectively ( $p=0.32$ ). 10 year cumulative all-cause mortality was 19.1% (95% CI 13.1-24.7) in Cyst cohort and 19.1% (95% CI 15.1-22.9) in No-cyst cohort ( $p=0.42$ ). 10 year cumulative incidences of all pancreatic cancers were 1.7% (95% CI 0.6-2.7) in Cyst cohort and 0.3% (95% CI 0.1-0.5) in No-cyst cohort (p

#### CONCLUSION

Incidental pancreatic cysts on CT/MR are associated with 5.2 times higher risk of pancreatic AdenoCA/DCA but not with increased all-cause mortality.

#### CLINICAL RELEVANCE/APPLICATION

Incidental pancreatic cysts do not affect all-cause mortality, but are markers of increased risk of pancreatic adenocarcinoma and ductal carcinoma.

### VSGI31-09 • Is Mural Nodule a Predictor for Malignancy in Patients with Intraductal Papillary Mucinous Neoplasms of the Pancreas?

**Seo-Youn Choi** MD (Presenter) ; **Seong Hyun Kim** ; **Kyung Mi Jang**

#### PURPOSE

To evaluate whether the location and the distribution of mural nodules were important for prediction of malignancy in patients with intraductal papillary mucinous neoplasms (IPMNs) of pancreas

#### METHOD AND MATERIALS

: This retrospective study was approved by the institutional review board and informed consent was waived. This study included 44 patients with surgically resected 44 IPMNs (23 malignancy and 21 benignancy) which had mural nodules on pathology and CT or MRI. Qualitative (morphologic type of IPMNs, location and distribution of mural nodules, presence of solid lesion, pancreatitis, irregular thick septum, and additional cystic lesion) and quantitative (maximal diameter of main pancreatic duct, the size of the largest cystic lesion and solitary mural nodule) parameters were compared between malignant and benign IPMNs using univariate and multivariate logistic regression analyses.

#### RESULTS

Of 23 malignant IPMNs, 17 (73.9%) lesions had mural nodules in main duct or both main and branch duct on location, whereas 15 of 21 (71.4%) benign IPMNs had mural nodule in branch duct on location ( $p=0.008$ ). Multiple or diffuse mural nodules were more frequently observed in malignant IPMNs (16/23, 69.6%) than benign IPMNs (6/21, 28.6%) ( $p < 0.01$ ). The presence of pancreatitis and additional cystic lesion, maximal diameter of main pancreatic duct, size of the largest cystic lesion and solitary mural nodule were not significantly different between malignant IPMNs and benign IPMNs ( $p > 0.05$ ). On multivariate analysis, mural nodules in main duct type on location (odds ratio [OR] = 41.18), and multiple (OR= 34.0) or diffuse mural nodules (OR= 27.0) on distribution were identified as significant factors for prediction of malignancy in IPMNs with mural nodules.

#### CONCLUSION

Mural nodules in main duct and multiple or diffuse distribution of mural nodules were independent predictors of malignancy in IPMNs with mural nodules.

#### CLINICAL RELEVANCE/APPLICATION

Mural nodules in main duct and multiple or diffuse distribution of mural nodules were independent predictors of malignancy in IPMNs with mural nodules.

### VSGI31-10 • Acute Pancreatitis

**Desiree E Morgan** MD (Presenter) \*

#### LEARNING OBJECTIVES

1) Discuss the imaging findings in patients with acute pancreatitis using the preferred nomenclature of the revised Atlanta Criteria. 2) Identify the various retroperitoneal collections associated with acute pancreatitis.

### VSGI31-11 • Is CT Useful in Patients with Acute Pancreatitis Presenting to Emergency Department?



**PURPOSE**

To assess the use of CT in patients with acute pancreatitis (AP) presenting to the emergency department (ED).

**METHOD AND MATERIALS**

In this IRB-approved HIPAA-compliant retrospective study, we identified all patients with AP presenting from March 2012 through February 2013 to ED of an academic teaching hospital with approximately 60,000 annual visits. Patients were initially identified using ICD-9 code for AP (577.0) and diagnosis was then confirmed using clinical criteria from chart reviews. Based on existing literature, AP was confirmed when two of the following three were present: typical abdominal pain, elevated lipase/amylase >3 times normal and CT findings of pancreatitis. Abdominal CT scans obtained in ED or within 24 hours of admission were reviewed by a fellowship-trained abdominal radiologist.

**RESULTS**

**CONCLUSION**

CT is frequently obtained in patients with AP presenting to ED even if diagnosis can be made based on established clinical criteria of typical abdominal pain and markedly elevated labs. CT is unlikely to be useful in these patients in the acute setting, as complications of AP in this setting may be rare.

**CLINICAL RELEVANCE/APPLICATION**

Abdominal CT rarely shows complications of acute pancreatitis in the acute phase, and it may not be necessary if diagnosis can be confidently made based on typical abdominal pain and elevated labs.

**VSGI31-12 • Perfusion CT- Can It Predict the Development of Pancreatic Necrosis in Early Stage of Severe Acute Pancreatitis**

**Ajay K Yadav** MBBS (Presenter) ; **Raju Sharma** MD ; **Devasenathipathy Kandasamy** ; **Shivanand R Gamanagatti** MBBS, MD ; **Ashu Seth Bhalla** MBBS, MD ; **Deep N Srivastava** MD, MBA ; **Pramod Garg** MBBS, MD ; **Ankur Goyal** MBBS, MD ; **Sreenivas V ; Arun K Gupta** MBBS, MD

**PURPOSE**

Pancreatic necrosis is among the most important factors which determine the outcome of patients with severe acute pancreatitis (SAP). This prospective study was conducted to evaluate if perfusion CT can detect pancreatic ischemia at an early stage of SAP and predict the development of necrosis.

**METHOD AND MATERIALS**

Perfusion CT (PCT) was performed in 42 consecutive patients of acute pancreatitis admitted within 72 hours from the onset of abdominal pain. Twenty-two patients were classified as having SAP on the basis of APACHE II (score >8) or SIRS criteria. All patients underwent a follow-up portal venous phase CECT after 2-3 weeks to see the progression of disease and look for pancreatic necrosis. Twenty five controls with no pancreatic pathology were also studied.

**RESULTS**

Out of 22 patients of SAP, 12 patients showed severe pancreatic perfusion defects (blood flow

**CONCLUSION**

Perfusion CT is a reliable tool for the detection of pancreatic ischemia at an early stage of SAP and can be used to predict the development of necrosis.

**CLINICAL RELEVANCE/APPLICATION**

Perfusion CT can predict pancreatic necrosis in SAP which opens up the scope for early intervention to prevent this ominous complication.

**VSGI31-13 • Autoimmune Pancreatitis**

**Joel G Fletcher** MD (Presenter) \*

**LEARNING OBJECTIVES**

1) To review the diagnostic criteria for autoimmune pancreatitis. 2) To discuss the differences between Type 1 and Type 2 autoimmune pancreatitis. 3) To emphasize the need to maximize visualization of pancreatic and intrahepatic ducts and understand temporal changes in contrast enhancement in autoimmune pancreatitis. 4) To describe the diagnostic and other frequently seen imaging findings of autoimmune pancreatitis. 5) To describe imaging findings demonstrating response to treatment and recurrence of autoimmune pancreatitis after remission. 6) To describe useful imaging features in the differential diagnosis of pancreatitis versus neoplasms and other inflammatory conditions.

**VSGI31-14 • Differentiation of Focal-type Autoimmune Pancreatitis from Pancreatic Carcinoma: Assessment by Multiphase Contrast-enhanced CT**

**Naohiro Furuhashi** (Presenter) ; **Kojiro Suzuki** MD ; **Yusuke Sakurai** ; **Mitsuru Ikeda** MD ; **Yuichi Kawai** ; **Shinji Naganawa** MD

**PURPOSE**

To assess the utility of multiphase contrast-enhanced computed tomography (CT) for differentiating focal-type autoimmune pancreatitis (AIP) from pancreatic carcinoma (PC).

**METHOD AND MATERIALS**

Subjects in this retrospective study comprised 21 patients (20 men, 1 woman; mean age, 66.7 years; range, 55-79 years) with 22 focal-type AIP lesions who fulfilled International Consensus Diagnostic Criteria and/or Revised Japanese Pancreas Society criteria and 60 patients (36 men, 24 women; mean age, 65.8 years; range, 38-82 years) with 61 PC lesions who were pathologically diagnosed from surgically resected specimens. Two radiologists blinded to the final diagnosis and other examination findings independently evaluated findings from multiphase contrast-enhanced CT in each patient. Along with pancreatic findings, extrapancreatic findings for the bile duct, kidneys and lymph nodes were also evaluated. Frequencies of each finding were compared between AIP and PC. Interobserver agreement was evaluated by kappa statistic.

**RESULTS**

Homogeneous enhancement during the delayed phase (AIP, 86% vs. PC, 41%;  $p < 0.001$ ,  $\chi^2 = 0.64$ ) were more frequently observed in PC. Presence of four of seven CT findings, that is, i) homogeneous enhancement during the delayed phase, ii) dot enhancement during the pancreatic phase, iii) duct penetrating sign, iv) main pancreatic duct wall enhancement, v) capsule-like rim, vi) absence of ring-like enhancement during the delayed phase and vii) absence of peripancreatic strand, offered 82% sensitivity and 95% specificity for identifying focal-type AIP.

**CONCLUSION**

The combination of CT findings can be helpful for differentiating focal-type AIP from PC.

**CLINICAL RELEVANCE/APPLICATION**

Focal-type AIP can mimic PC and responds to steroid therapy. Differentiation of these two entities might contribute to improvements in patient management.

**VSGI31-15 • Autoimmunpancreatitis: Therapy Monitoring Using IVIM-diffusion MRI**

**Miriam Klauss MD (Presenter) ; Klaus Maier-Hein ; Jens Werner MD, PhD \* ; Hans-Ulrich Kauczor MD \* ; Lars Grenacher MD ; Bram Stieltjes MD**

#### PURPOSE

To evaluate diffusion imaging in autoimmune pancreatitis (AIP) before and after steroid treatment using IVIM-derived parameters.

#### METHOD AND MATERIALS

To date, 17 patients suspected of having an AIP underwent diffusion-MRI (1.5 T). Diffusion-weighted images were acquired using a single-shot echo-planar imaging sequence in breath-hold with the following imaging parameters: TR = 1300 ms, TE = 60 ms, FOV = 350 x 273 mm<sup>2</sup>, 14 slices, b-values = 0, 50, 100, 150, 200, 300, 400, 600 and 800 s/mm<sup>2</sup>. DW-data were post-processed using an in-house developed software. Eight patients had an AIP (n=2 resection, n=6 clinical consensus). Six patients had follow-up examinations during steroid treatment. IVIM-parameters (perfusion fraction f and perfusion free diffusion coefficient D) were extracted from manually drawn ROIs for patients with and without AIP for initial and follow-up examinations. ROIs were anatomically matched between initial and follow-up examinations. The derived parameters were tested for significant differences between healthy tissue and AIP and between initial and follow-up examinations in AIP patients using an unpaired and paired t-test respectively.

#### RESULTS

#### CONCLUSION

The diffusion-derived IVIM-perfusion fraction f is significant lower in patients with AIP, normalizes at the first follow-up examination during steroid treatment and remains constant in the second follow-up examination.

#### CLINICAL RELEVANCE/APPLICATION

IVIM-diffusion MRI could serve as an imaging biomarker during steroid treatment in patients with AIP.

## Genitourinary Series: Prostate Cancer 2013-Review of the Disease and the Role of MR in Staging and Surveillance

Tuesday, 08:30 AM - 12:00 PM • N228

[OI](#) [MR](#) [GU](#)

[Back to Top](#)

**VSGU31 • AMA PRA Category 1 Credit™:3.25 • ARRT Category A+ Credit:3.5**

#### Co-Moderator

**Peter L Choyke**, MD \*

#### Co-Moderator

**Anwar R Padhani**, MD \*

### VSGU31-01 • Introduction: Prostate Cancer: Why We Need Imaging

**Peter L Choyke** MD (Presenter) \*

#### ABSTRACT

There have been exciting recent developments in new PET/SPECT tracers for oncology. It is now possible to examine all of the major hallmarks of cancer using PET tracers including proliferation (18F-FLT), angiogenesis (18F-Fluciclitide), apoptosis (18F-CP18) and hypoxia (18F-VM4). These agents, among others, will be introduced in the context of targeted molecular therapy of cancer.

### VSGU31-02 • Basics of Prostate MRI: Detection

**Masoom A Haider** MD (Presenter) \*

#### LEARNING OBJECTIVES

1) Have a systematic approach to the interpretation of multiparametric MRI for prostate cancer localization prostate. 2) Appreciate the strengths and limitations of multiparametric MRI in cancer localization. 3) Understand the requirements for performing a state of the art prostate MRI protocol for cancer localization.

### VSGU31-03 • Role of Repeat 3T Multiparametric MR Imaging and MR-guided Biopsy versus Repeat TRUS-guided Biopsies after 1 Year Follow-up in Low-risk Prostate Cancer Patients in an Active Surveillance Protocol

**E. H. J. Hamoen** MD (Presenter) ; **Caroline M Hoeks** MD ; **Rik Somford** MD ; **Henk Vergunst** ; **J. Oddens** ; **Christina A Hulsbergen-Van De Kaa** MD, PhD ; **Inge Van Oort** MD, PhD ; **Fred Witjes** MD, PhD ; **Chris Bangma** ; **Jelle O Barentsz** MD, PhD

#### PURPOSE

To evaluate reclassification rates after 1 year follow-up of repeat 3T multiparametric MR imaging (mp-MRI) and MR guided biopsy (MRGB) versus repeat TRUS-guided biopsy (TRUSGB) for men with prostate cancer within the Prostate Cancer Research International Active Surveillance (PRIAS) study.

#### METHOD AND MATERIALS

From September 2009 to February 2013, 93 prostate cancer patients from 4 referral centers were included in the MR-PRIAS protocol. Inclusion criteria were: PSA =10 ng/ml, PSA density < 0,2 ng/ml/ml, clinical stage = cT2, Gleason score = 6, and = 2 positive biopsy cores. Patients underwent mp-MRI and MRGB within 3 months after diagnosis, and mp-MRI, MRGB and TRUSGB after 1 year follow-up. Reclassification was defined as more than two positive cores at repeat TRUSGB, Gleason > 6 at repeat TRUSGB or MRGB, presence of prostate cancer in = 3 separate cancer foci upon both MRGB and TRUSGB, or suspicion on T3 tumor on mp-MRI. Results of combined repeat mp-MRI and MRGB were compared with standard repeat TRUSGB at 1 year follow-up.

#### RESULTS

With mp-MRI + MRGB, 24/93 (26%) patients were initially reclassified. In the first year, 9/93 (10%) patients were excluded on patient request or because of other reasons. Repeat examinations at 1 year follow-up were thus far performed in 41 patients, of whom 17/41 (41%) showed reclassification and were advised to undergo radical treatment. The other 24/41 (59%) patients remained on active surveillance. Reclassification at 1 year was due to both TRUSGB and MRGB results in 6/17 patients (35%), due to TRUSGB results only in 7/17 patients (41%), and due to mp-MRI or MRGB results only in 4/17 patients (24%). Combined with standard repeat TRUSGB, performing repeat mp-MRI and MRGB after 1 year led to an additional reclassification of 10% (4/41) of the patients.

#### CONCLUSION

Repeat mp-MRI and MRGB after 1 year follow-up are of additional value in prostate cancer patients in an active surveillance protocol, as combining mp-MRI and MRGB with repeat TRUSGB leads to an additional reclassification of 10% of the patients.

#### CLINICAL RELEVANCE/APPLICATION

mp-MRI and MRGB are of added value in low-risk prostate cancer patients on active surveillance, especially shortly after the initial diagnosis. However, TRUSGB cannot be omitted at 1 year follow-up.

### VSGU31-04 • Multi-parametric MR Imaging Characteristics of Missed Prostate Cancer: Correlation with Histopathology

**Nelly Tan** MD (Presenter) ; **Daniel J Margolis** MD \* ; **David Y Lu** MD ; **Kevin G King** MD ; **Steven S Raman** MD ; **Robert E Reiter** MD ; **Jiaoti Huang**

## PURPOSE

To determine the characteristics of prostate cancer foci missed by multi-parametric MRI.

## METHOD AND MATERIALS

A HIPAA-compliant, IRB-approved retrospective study of 122 patients with multi-parametric prostate MRI were compared to whole mount prostate obtained after a radical prostatectomy was performed between October 2010 and January 2013 was performed. Clinical (age, PSA, biopsy), MR imaging (T2, DWI, DCE and MRSI), and pathologic features (Gleason Score, size of tumor, pathological stage, extracapsular extension) were obtained. A GU radiologist and pathologist collectively reviewed each case and matched the MR lesion to whole-mount pathology lesion. A standardized classification system (PI-RADS) was used to characterize the multi-parametric MR features based on Linkert scale (1-5). Chi-square analysis was performed for categorical variable and t-test for continuous variable. A p-value of 0.05 was considered significant.

## RESULTS

122 patients had 284 unique prostate tumor foci. 149 (52.5%) prostate cancer foci in 74 patients were missed by MRI. 111 (74.5%) were GS6 followed by 23 (15.4%) GS 3+4, 9 (6.0%) GS4+3, 6 (4.0%) GS 8-10. Missed CaP foci were smaller in size (0.8 vs 1.8 cm,  $p=0.001$ ), had higher proportion of GS6 (74 vs 28%) and lower proportion of GS3+4 (15 vs 40%), GS4+3 (6 vs 21%), GS8-10 (4 vs 10%), compared to CaP that were detected by MR. Missed CaP had higher proportion localized to one segment of the prostate-- apex (30 v 10%), mid (37 v 18%), base(9 v 5%)-- and lower proportion of foci crossing multiple segments--apex to base (3 v 20%), apex to mid (11 vs 26%), mid to base (10 v 22%)-- compared to detected CaP lesions ( $p=0.0001$ ). There was no difference in use of endorectal coil (87 vs 86%,  $p=0.86$ ), PSA (7.7 v 7.1,  $p=0.44$ ) or prostate volume (41 vs 45,  $p=0.12$ ) between detected and missed CaP.

## CONCLUSION

Prostate CaP foci missed on MRI were smaller in maximal diameter, higher in proportion of low-grade tumors (GS6), were localized to one segment of the prostate instead of crossing multiple segments compared to prostate foci detected by MR.

## CLINICAL RELEVANCE/APPLICATION

Our findings has implications for the use of standard systematic prostate biopsies in addition to MR-based targeted biopsy for full characterization of tumor burden.

### VSGU31-05 • Staging Prostate Cancer with MRI

Neil M Rofsky MD (Presenter)

### VSGU31-06 • Identification of Apparent-diffusion-coefficient (ADC) Cut-off Values for the Detection of Lymph Node Metastasis During DWI-MRI in High-risk Prostate Cancer Patients: Implication for Daily Clinical Practice

Marc Regier (Presenter) ; Christian Seiwerts ; Frank Oliver G Henes MD ; Hendrik Kooijman \* ; Hendrik Isbarn ; Markus Graefen ; Guido Sauter ; Gerhard B Adam MD ; Lars Budaus

## PURPOSE

Recent investigations have outlined a remarkable potential of diffusion-weighted MRI (DWI) to detect lymph node metastases in various tumour entities. Therefore, the purpose of this study was to determine apparent-diffusion-coefficient (ADC) cut-off values for the differentiation of benign and malignant lymph nodes in patients suffering from prostate cancer in a high-risk constellation.

## METHOD AND MATERIALS

In 59 consecutive patients classified as high-risk following the D'Amico criteria, pelvic MRI was performed one day prior to radical prostatectomy. A standardized T2-STIR and DWI sequence were applied to all patients (b-values: 0, 25, 75, 100, 200, 500 and 900). Monoexponential ADC calculation and mapping was performed for all lymph nodes within the small pelvis which had been identified reading the T2-STIR and DWI data. Overall, 1393 lymph nodes were removed during radical prostatectomy and level based drawings were used to record their location. Histopathologic analysis was performed for all dissected nodes using standard techniques. Finally, lymph nodes were dichotomized into benign and malignant and ADC cut-off values were determined using ROC, Wilcoxon and chi-square test.

## RESULTS

Histopathologic analysis revealed nodal metastases in 35.6% (21/59) of all patients. The mean number of lymph nodes removed was 26 in node negative and 24 in node positive patients ( $p=0.35$ ). In all patients, lymph nodes >4mm were successfully identified at MRI. In malignant lymph nodes the mean ADC was  $0.76 \times 10^{-3} \text{mm}^2/\text{s}$ , whereas in benign nodes the mean ADC was  $1.43 \times 10^{-3} \text{mm}^2/\text{s}$  ( $p=0.99$ ) for the differentiation of benign and malignant lymph nodes.

## CONCLUSION

In a high-risk collective, DWI with ADC mapping can be used to assess lymph node metastases prior to prostatectomy. Mean and minimum ADC cut-off values of  $0.98 \times 10^{-3} \text{mm}^2/\text{s}$  and  $0.74 \times 10^{-3} \text{mm}^2/\text{s}$  allow for the discrimination of benign and malignant lymph nodes with high accuracy.

## CLINICAL RELEVANCE/APPLICATION

The application of DWI with ADC cut-off values determined can help to assess nodal metastases in prostate cancer prior to surgery and should therefore be implemented into preoperative routine imaging.

### VSGU31-07 • The Role of PI-RADS Scoring System in Increasing Radiologist's Performance in Detecting Prostate Cancer with a Multiparametric-MRI Examination

Flavio Barchetti ; Valeria Panebianco MD ; Valerio Forte ; Damiano Caruso MD ; Maria Giulia Bernieri ; Chiara Zini MD (Presenter) ; Carlo Catalano MD

## PURPOSE

To evaluate the gain of radiologist's performance in assessing suspected areas of prostate cancer (PC) by assessing the increase of sensitivity and specificity employing PI-RADS scoring system in a Multiparametric-MRI (Mp-MRI).

## METHOD AND MATERIALS

400 patients who underwent from June 2010 to January 2013 a Mp-MRI examination of the prostate gland for raising PSA serum levels and who were positive for PC at histology, were independently retrospectively evaluated by the same 2 readers who together previously observed the exams. Reader A (R.A) was an experienced radiologist in uro-genital field with 10 years of experience, and reader B (R.B) was a radiology resident with 3 years of experience. In the previous reading session the suspected lesions were assessed without using PI-RADS scoring system, while in the second reading session PI-RADS was employed.

## RESULTS

58 patients out of 400 were originally assessed negative for the presence of morpho-functional changes both in peripheral zone (PZ) and central zone (CZ). In the second reading session R.A identified 25 PI-RADS 1, 21 PI-RADS 2 and 12 PI-RADS 3, while R.B 34 PI-RADS 1, 14 PI-RADS 2 and 10 PI-RADS 3 ( $K = 0.765$ ,  $P = 0.134$ ).

145 patients out of 400 were originally assessed doubtful for the presence of PC. R.A in 94 out of 145 patients subsequently considered the lesions PI-RADS 4, in 8 men PI-RADS 5 and in 43 PI-RADS 3, while R.B in 84 patients assumed the altered areas PI-RADS 4, in 5 men PI-RADS 5 and in 56 PI-RADS 3 ( $K = 0.754$ ,  $P = 0.254$ ).

In the remaining 197 patients the lesions were esteemed simply as suspicious PC in the previous reading session. In the second reading session R.A deemed 156 altered zones as PI-RADS 5 and the other 41 as PI-RADS 4, on the other hand R.B accounted 141 lesions as PI-RADS 5 and 56 as PI-RADS 4 ( $K = 0.862$ ,  $P = 0.383$ ).

All in all the sensitivity and specificity of R.A in evaluating the foci of morpho-functional changes increased respectively from 59% to 94% and from 52% to 94% ( $P = 0.025$ ) and for R.B respectively from 47% to 86% and from 41% to 92% ( $P = 0.038$ ).

## CONCLUSION

the sensitivity and specificity of radiologists performance in assessing suspected areas of PC by employing PI-RADS scoring system in a Mp-MRI examination seems to increase substantially reaching statistically significant results ( $P < 0.05$ ).

## CLINICAL RELEVANCE/APPLICATION

We highlight the importance of PI-RADS in evaluation of prostate cancer

## VSGU31-08 • The Role of Imaging in Active Surveillance

**Anwar R Padhani MD (Presenter) \***

### LEARNING OBJECTIVES

1) To provide an overview of the concepts underpinning active surveillance (AS) strategies for low risk prostate cancer patients. 2) To illustrate the ability of multiparametric (mp) MRI (diffusion weighted, dynamic contrast enhanced and spectroscopy) to assess tumor location, volume and grade. 3) To discuss the role of mpMRI for confirming clinical patient selection criteria for AS. 4) Highlight the benefits of mpMRI for detecting cases at higher risk and thus unsuited for AS. 5) Demonstrate changing imaging phenotype during AS period.

### ABSTRACT

Active surveillance is a widely accepted treatment strategy for men diagnosed with low-risk prostate cancer. However, follow up studies show that up to one third of suitable patients eventually undergo radical therapy. Early conversion to radical therapy is likely to be due to imperfect initial selection methods resulting in inclusion of higher-risk cases. Large anterior-apical lesions of higher grades constitute these cases. This MRI overview will provide radiologists with the necessary knowledge on how to best inform clinicians of the suitability of cases for AS and to identify those at higher risk requiring earlier intervention. Multiparametric MRI assessments enable the location, grading and volumetry of index prostatic lesions to be undertaken. Reviews of mpMRI of index lesions suspicious of high grade and high-risk, unsuitable for AS and requiring earlier intervention will be shown. Challenges facing mpMRI in this area of clinical application will be discussed

## VSGU31-09 • Prospective Comparative Study of Targeted Prostate Biopsy Directed to MRI-suspicious Regions vs. Artemis™ Computerized 12 Core Template Biopsy

**James Wysock (Presenter) ; Andrew B Rosenkrantz MD ; Fang-Ming Deng MD, PhD ; Samir S Taneja MD \***

### PURPOSE

Artemis™ computerized 12 core template biopsy (ARTEMIS 12 core) standardizes prostate sampling through template construction from 3D ultrasound (US) modeling of 2D transrectal ultrasound. MRI-targeted biopsy aims to optimize diagnostic yield via targeted sampling of MRI-suspicious regions (mSR). This study describes results of an IRB-approved prospective study of men undergoing MRI-targeted biopsy of mSR followed by ARTEMIS 12 core in order to prospectively compare mSR targeted biopsy to 12 core biopsy.

### METHOD AND MATERIALS

125 men enrolled in a prospective clinical trial underwent biopsy that included 4 cores to each mSR (2 cores via MRI-US fusion guidance and 2 cores via visual guidance) followed by ARTEMIS 12 Core. All mSR were localized by a single radiologist and reviewed by two urologists prior to biopsy. Biopsy yield was compared between the two techniques.

### RESULTS

Mean age of the study cohort was  $64.0 \pm 8.15$  yrs with a mean PSA  $5.91 \pm 4.37$  ng/mL. The cohort was composed of 67 (53.6%) men undergoing initial biopsy and 34 (27.2%) undergoing repeat biopsy without a prior diagnosis of cancer and 24 (19.2%) men on active surveillance. Overall, cancer was detected in 71 (56.8%) men on targeted biopsy and 61 (48.8%) by ARTEMIS 12 core biopsy ( $p = 0.254$ ). MRI-targeted biopsy detected Gleason 7 or higher in 34 (27.2%) men, equal to the detection rate with ARTEMIS 12 core 34 (27.2%), ( $p = 0.789$ ). MRI-targeted biopsy detected Gleason 6 cancer in 37 (29.6%) as compared to 47 (37.6%) detected on ARTEMIS 12 core ( $p = 0.185$ ). Mean cancer core length per positive core and percent positive cores were significantly greater in MRI-targeted than ARTEMIS 12 core among all cancers detected, ( $p = 0.014$ ,  $p = 0.0001$ , respectively).

### CONCLUSION

MRI-targeted biopsy with 4 cores per mSR provided equivalent detection of Gleason 7 or greater cancer as ARTEMIS 12 core biopsy while significantly reducing the number of cores to obtain this information and providing significantly greater cancer core length per core.

### CLINICAL RELEVANCE/APPLICATION

Targeted biopsy of mSR improves diagnostic efficiency over 12 core biopsy. Future work may prove targeted biopsy alone sufficient for prostate cancer evaluation.

## VSGU31-10 • Initial Prospective Evaluation of the Prostate Imaging Reporting and Data Standard (PI-RADS)

**Geert Litjens MSc (Presenter) ; Nico Karssemeijer PhD \* ; Jelle O Barentsz MD, PhD ; Henkjan Huisman PhD \***

### PURPOSE

To evaluate the performance of the prostate imaging reporting and data standard (PI-RADS) proposed by the European Society of Urogenital Radiology and the effect of reader experience on this performance.

### METHOD AND MATERIALS

A consecutive cohort of 254 patients who underwent a detection MRI in 2012 and a subsequent MR guided biopsy were included. All patients were prospectively reported by 1 out of the 10 reporting radiologists according to the PI-RADS guidelines. Two radiologists are experts (20 and 15 years of experience) and 8 are inexperienced (3 years of experience or less). The inexperienced and experienced readers reported 146 and 108 cases respectively. The radiologists reported 436 lesions in these patients of which 339 were biopsied. 190 of these 339 were prostate cancer. 127 tumors had a Gleason 4 or higher component and were considered high-grade cancer, all others were considered low grade. Each lesion received an overall PI-RADS score between 1 and 5. The sensitivity, specificity, positive predictive value (PPV) and negative predictive value (NPV) were calculated by thresholding at each of the PI-RADS scores with the biopsy results as ground truth. High-grade cancers with a PI-RADS score above or equal to the threshold are true positives. Non-cancers below the threshold were considered true negatives.

### RESULTS

In total 19, 67, 112 and 141 lesions were biopsied for PI-RADS 2, 3, 4 and 5. The inexperienced reader sensitivities for PI-RADS 2, 3, 4 and 5 are: 1, 1, 0.96 and 0.69 respectively. The experienced readers obtained 1, 1, 0.98 and 0.71. The specificities were 0, 0.16, 0.48 and 0.76 for the inexperienced and 0, 0.07, 0.36 and 0.89 for the experienced readers. The PPV and NPV were 0.46, 0.50, 0.61, 0.71 and 1, 1, 0.93, 0.74 for the inexperienced readers. For the experienced readers we obtained 0.46, 0.48, 0.57, 0.84 and 1, 1, 0.96, 0.78 respectively.

### CONCLUSION

Only PI-RADS 4 and 5 lesions require biopsy; inexperienced and experienced readers have sensitivities of 0.96 and 0.98 at this threshold. Experience matters: the number of unnecessary biopsies in PI-RADS 5 lesions is reduced by almost half, according to the PPV change from 0.71 to 0.84 between inexperienced and experienced readers.

### CLINICAL RELEVANCE/APPLICATION

PI-RADS reported lesions may help reduce the number of unnecessary biopsies. The strong effect of experience emphasizes the need for adequately trained radiologists for reporting prostate MR.

## VSGU31-11 • Negative Predictive Value of Multiparametric MRI for Prostate Cancer Detection: Outcomes of 5-year Follow Up for Men with Negative Findings on Initial MRI

**Ryo Itatani** (Presenter) ; **Tomohiro Namimoto** MD ; **Shutaro Atsuji** ; **Kazuhiro Katahira** ; **Shoji Morishita** MD ; **Kousuke Kitani** ; **Yasuyuki Hamada** ; **Mitsuhiko Kitaoka** ; **Takeshi Nakaura** MD ; **Yasuyuki Yamashita** MD \*

### PURPOSE

Prostate cancer is currently screened by PSA and digital rectal examinations (DRE), and diagnosed by random biopsy resulting in the discovery of multiple insignificant cancers that often lead to overtreatment. MRI may be used to triage patients who require invasive treatment, if its negative predictive value (NPV) is sufficiently high. The purpose of our study was to assess NPV of multiparametric MRI and evaluate its clinical utility as an optimal tool to rule out significant prostate cancer to investigate outcomes of 5-year follow up for men with negative findings on initial MRI.

### METHOD AND MATERIALS

Between November 2004 and August 2007, there were 622 men who were suspected of harboring prostate cancer and underwent MRI followed by transrectal ultrasound (TRUS)-guided biopsy in our institution. Among them, 255 men with negative findings on MRI were included in our study and their 5-year outcomes were retrospectively assessed. A positive finding by TRUS-guided biopsy was considered as false negative. Patients with neither increase in PSA value nor positive finding on DRE, MRI and TRUS-guided biopsy for 5-year follow up were considered to be true negative. NPV of multiparametric MRI were calculated. For patients undergone radical prostatectomy who had positive finding in biopsy, mean signal intensity (SI) on T2 weighted imaging and mean apparent diffusion coefficient (ADC) value on ADC map of initial MRI were compared between peripheral-zone cancer and normal peripheral zone based on pathologic maps.

### RESULTS

For 5-year follow up, 49/255 patients had positive findings of TRUS-guided biopsy. Among them, 27/49 cases proved to be clinical insignificant cancer. The other 206/255 patients had no clinical evidence of prostate cancer. NPV was 80.8% for total prostate cancer detection and was 91.4% for significant prostate cancer detection. With respect to SI and ADC value, there was no significant difference between peripheral-zone cancer and normal peripheral zone.

### CONCLUSION

Our study showed that negative findings on multiparametric MRI were associated with either negative TRUS-guided biopsy or insignificant prostate cancer. The risk of harboring significant prostate cancer is considered to be relative low in such patients.

### CLINICAL RELEVANCE/APPLICATION

Multiparametric MRI shows great NPV for prostate cancer detection and is a useful tool to rule out clinical significant prostate cancer before biopsy.

## VSGU31-12 • A Global Standard for Prostate MRI Reporting

**Jelle O Barentsz** MD, PhD (Presenter)

### LEARNING OBJECTIVES

1) After this course the participants will have guidelines for magnetic resonance imaging (MRI) in prostate cancer. 2) They will know clinical indications, and minimal and optimal imaging acquisition protocols. 3) The participants will have an introduction in a structured reporting system (PI-RADS).

### ABSTRACT

The aim is to show clinical guidelines, developed for multi-parametric MRI of the prostate by a group of prostate MRI experts from the European Society of Urogenital Radiology (ESUR), based on literature evidence and consensus expert opinion. True evidence-based guidelines cannot not be formulated, but a compromise, reflected by "minimal" and "optimal" requirements will be made. The scope of these ESUR guidelines is to promulgate high quality MRI in acquisition and evaluation with the correct indications for prostate cancer across the whole of Europe and eventually outside Europe. The guidelines for the optimal technique and three protocols for "detection", "staging" and "node and bone" will be presented. The use of endorectal coil vs. pelvic phased array coil and 1.5 vs. 3 T discussed. Clinical indications and a PI-RADS classification for structured reporting are shown. This presentation provides guidelines for magnetic resonance imaging (MRI) in prostate cancer. Clinical indications, and minimal and optimal imaging acquisition protocols shown. A structured reporting system (PI-RADS) will be introduced and described.

## VSGU31-13 • Discussion and Concluding Comments

### Radiology Informatics Series: Natural Language Processing: Extracting Information from Text Radiology Reports to Improve Quality

Tuesday, 08:30 AM - 12:00 PM • S502AB



[Back to Top](#)

**VSIN31** • AMA PRA Category 1 Credit™:3.25 • ARRT Category A+ Credit:3.5

### Moderator

**Curtis P Langlotz**, MD, PhD \*

### LEARNING OBJECTIVES

1) Learn how natural language processing (NLP) can be used to extract information from radiology reports. 2) Understand the basic NLP methods and their strengths and weaknesses. 3) Examine examples of how NLP can be used to automate quality improvement processes in radiology practices. 4) Assess the synergy between NLP and standardized reporting practices.

### ABSTRACT

Natural Language Processing (NLP) refers to the automated extraction of meaningful information from narrative text. Some NLP systems use simple rules to categorize text according to whether a particular concept may be present. More sophisticated systems use part-of-speech tagging and grammatical parsing to extract concepts and relationships from text. Some NLP systems use statistical approaches that can learn to categorize text automatically based on a test set of positive and negative examples. When applied to radiology reports, NLP systems are most frequently used to identify and retrieve reports of interest, such as reports containing a critical result, an incidental finding, or a recommendation for follow up. NLP systems are simpler to construct and more accurate when the structure of the analyzed text is constrained in some manner. Several real-world examples of both simple and sophisticated NLP systems in radiology will illustrate the spectrum of applicable techniques and the potential benefit to radiology practice.

## VSIN31-01 • Natural Language Processing: Motivations and Overview

**Curtis P Langlotz** MD, PhD (Presenter) \*

### LEARNING OBJECTIVES

1) Learn how natural language processing (NLP) can be used to extract information from radiology reports. 2) Understand the basic NLP methods and their strengths and weaknesses. 3) Examine examples of how NLP can be used to automate quality improvement processes in radiology practices. 4) Assess the synergy between NLP and standardized reporting practices.

### ABSTRACT

Natural Language Processing (NLP) refers to the automated extraction of meaningful information from narrative text. Some NLP systems

use simple rules to categorize text according to whether a particular concept may be present. More sophisticated systems use part-of-speech tagging and grammatical parsing to extract concepts and relationships from text. Some NLP systems use statistical approaches that can learn to categorize text automatically based on a test set of positive and negative examples. When applied to radiology reports, NLP systems are most frequently used to identify and retrieve reports of interest, such as reports containing a critical result, an incidental finding, or a recommendation for follow up. NLP systems are simpler to construct and more accurate when the structure of the analyzed text is constrained in some manner. Several real-world examples of both simple and sophisticated NLP systems in radiology will illustrate the spectrum of applicable techniques and the potential benefit to radiology practice.

### **VIN31-02 • Enhancing Provided Patient Clinical Information by Automated Review of Prior Radiology Reports Using the Clinical Context Indicator (CCI): A NLP Based Data Extraction and Presentation PACS-integrated Tool**

**Adam R Travis MD (Presenter) ; Paul J Chang MD \* ; Yuechen Qian ; Merlijn Sevenster PhD \* ; Gabriel Mankovich BSC ; Johannes Buurman PhD \***

#### **PURPOSE**

Physicians do not always provide adequate histories when ordering imaging studies; this may be due to Computerized Physician Order Entry (CPOE) systems that allow limited codified indications (♦drop down menus♦) as input parameters. Lack of history may result in suboptimal or even incorrect interpretation by radiologists. We test the hypothesis that a PACS-integrated view of patient history automatically synthesized from prior radiology reports improves the quality of clinical history sections in radiology reports.

#### **METHOD AND MATERIALS**

CCI functions as a PACS plugin that extracts pertinent information from prior radiology reports and displays it along three ♦axes♦ for each exam: history, acute indication, and follow-up recommendations. CCI uses natural language processing (NLP) to populate the history and follow-up axes by extracting and filtering unique sentences from relevant sections in prior reports. The acute indication axis is populated with the Reason For Exam (RFE) from the CPOE system. Prospective evaluation was conducted by a team of senior residents in normal workflow. First, the reader viewed the CCI summary and dictated the history based only on this information. Then, the reader reviewed all pertinent patient data (e.g., pathology, labs) from the EHR and modified the dictated history, if necessary. Later, for each dictated study an attending radiologist compared the quality of the initial CCI-only history to the final dictated history and to the RFE, which were each used as baselines.

#### **RESULTS**

Preliminary data on 32 neuro CT cases shows that 34.4% of CCI-only histories were rated significantly more complete than RFE histories. However, CCI-only histories were significantly augmented with pathology (18.8%) and/or other data (9.4%) derived from the EHR.

#### **CONCLUSION**

Patient clinical context derived from CPOE exam indications alone were enhanced by the automated extraction and PACS-integrated presentation of information derived from prior radiology reports. However, additional important patient information was derived from the EHR. Therefore, automated PACS-integrated tools designed to present patient context should extract data from both prior radiology reports and the EHR.

#### **CLINICAL RELEVANCE/APPLICATION**

Automated PACS-integrated tools designed to present patient context should extract data from both prior radiology reports and the EHR. These tools can enhance information provided by CPOE alone.

### **VIN31-03 • Facilitate Mammography Quality Standards Act (MQSA) with Automatically Correlating Radiology Reports of Breast Cancer Patients Containing Biopsy Recommendations with Subsequent Pathology Reports**

**Ye Xu PhD (Presenter) ; Thusitha Mabotuwana ; Yuechen Qian ; Merlijn Sevenster PhD \***

#### **PURPOSE**

MQSA mandates for quality control of breast radiology reports suggesting a biopsy follow-up (BIRADS scores 3, 4 and 5) are correlated with pathology outcome. This is typically done manually, which is time consuming and error prone. Our purpose is to develop and evaluate a natural language processing system (NLP) that 1) automatically recognizes if a breast radiology report contains a biopsy recommendations and, if so, 2) finds the pathology reports that discusses biopsy outcome from a stack of pathology reports.

#### **METHOD AND MATERIALS**

Our NLP system includes two components: 1) recommendation detector; 2) pathology report finder. Annotation guidelines were created in an iterative fashion for creating recommendation detection ground truth by four researchers, including one radiologist. Ground truth was created based on 5,200 radiology reports, from a deidentified corpus of breast radiology report obtained from a hospital in the Midwest. From a test set of 300 reports, we selected all reports that contain a recommendation of any type (not necessarily biopsy recommendations), yielding a final test set of 110 reports. The pathology report finder utilizes laterality, interval and reason for exam information to determine if a pathology report is the follow-up of a give radiology report. We conducted a preliminary evaluation on the full radiology-pathology histories of 21 breast cancer patients with at least one radiology report with a biopsy recommendation.

#### **RESULTS**

Evaluated on the 110 reports, the recommendation detector achieves precision, recall and F-measure scores of 0.97, 0.99, and 0.98 respectively. Among 18 of 21 patients (86%), the pathology report finder successfully finds matches between pathology reports and radiology reports containing biopsy recommendation. Among those 18 patients (20 reports), there are 4 breast image studies with BIRADS 4, but their pathology diagnosis identified as benign.

#### **CONCLUSION**

This study demonstrates the potential of using NLP technologies to facilitate the quality assurance of MQSA. Our algorithms reliably identify studies that contain biopsy recommendation and can support automatic correlation with biopsy reports. Adequately integrated in a workflow support tool, healthcare providers can use it to get instant feedback on false positive rates of imaging diagnosis based on biopsies.

#### **CLINICAL RELEVANCE/APPLICATION**

Facilitate the quality assurance of MQSA

### **VIN31-04 • Using an Enterprise Cloud-based NLP Platform to Convert Unstructured Reports into Structured Clinical Data for Analytics**

**James Maisel (Presenter) \***

#### **CONCLUSION**

Natural language processing was demonstrated to extract structured codes from unstructured data sources such as transcription. The structured codes could be queried with a basic analytic tool to provide subsets of patients based upon structured data with typical stratifications required for clinical studies and practice management issues.

#### **Background**

Analytics is a tool to extract and use meaning from data and facilitates screening, outcomes analysis, evidence-based decision support, audit protection, research, cross-system communication, and reporting. In our study, an enterprise cloud-based platform was designed to accept unstructured clinical documentation from diverse sources. With Natural Language Processing (NLP), data can be structured and coded for analytics. The study evaluated the potential of the platform to structure data and make it available for secondary use with analytic reporting . Study results and implications will be discussed.

#### Evaluation

Assorted types of data including over 500,000 records from dictation, scanned records and semi-structured EHR text were evaluated as potential sources for analytics. Dictation was converted to text with backend speech recognition and edited. Transcribed, scanned OCR documents and semi-structured EHR messages were preprocessed and passed through natural language processing (NLP). The output was post-processed and coded into standardized terminologies including SNOMED CT, ICD-9, ICD-10, RxNorm, LOINC and CPT-4 codes derived from postprocessing and stored within a MS SQL database to serve as a clinical data repository. A front end application was designed to allow physicians to query the database for analytic output based on these codes and terms.

#### Discussion

The NLP platform successfully processed all forms of unstructured text and semi-structured data and output structured codes. The analytic form worked well at extracting subsets of records based on their codes. The analytics reporting application successfully extracted records that contained one or more structured terminologies or exact text searches. Combinations of terms and exclusions and nested searches could be performed in live-time. Record names could be de-identified.

### **VSIN31-05 • An NLP-based, Data-driven Paradigm for Clinical Documentation Improvement and Analytics**

**James Maisel** (Presenter) \*

#### CONCLUSION

Not only does natural language processing increase the effectiveness and efficiency of clinical documentation (by reducing physician time required and increasing documentation quality), but it makes possible a variety of secondary data uses.

#### Background

A clinical documentation workflow utilizing dictation and natural language processing can make the documentation process faster and produce structured data required for software-based clinical documentation improvement, analytics, and reporting. The workflow involves a physician dictating a note, the dictation's conversion to text by speech recognition, natural language processing generating structured data from the text, entry of the structured data and text into the EHR, processing of the structured data by clinical documentation improvement application, manual documentation improvement using the documentation improvement application's output, and making available the note's structured data in a data repository for analytics and reporting.

#### Evaluation

Integrating Natural Language Processing (NLP) into the clinical workflow can enable increased documentation efficiency, clinical documentation improvement, and various analytics that take advantage of the structured data generated by NLP.

#### Discussion

Because free (unstructured) dictation is a faster method of documentation than standard EHR data entry, free text will continue to be an important part of electronic health records. Natural Language Processing (NLP) can be used to structure free text contained in the physician's documentation. The following is an example of a clinical documentation improvement analytics application that would use structured, codes generated by NLP. An ICD-10 specificity application could prompt the physician to enter more details about a medical problem in order to generate a more specific ICD-10 code, which might be beneficial for billing. The structured data stored in the data repository can be used for a variety of analytical and reporting purposes, including for outcomes analysis, value-based medicine, surveillance of high-risk populations, PQRS measure reporting, research, case management, quality informatics, and public health analytics.

### **VSIN31-06 • Natural Language Processing to Solve Problems in Clinical Practice**

**Michael E Zalis MD** (Presenter) \*

#### LEARNING OBJECTIVES

1) Describe salient features of electronic health record data and Radiology workflow that create obstacles for efficient, high quality care delivery. 2) Describe and demonstrate essential aspects of natural language processing and related aspects of computer science and show how these tools can begin to improve Radiology work-flow and care delivery. 3) Describe future directions for natural language processing tools in Imaging.

#### ABSTRACT

Electronic health record data, whether in discretized (structured field) or unstructured forms presents a potentially overwhelming amount of information for a Radiologist to consume at the time of clinical encounter. This applies for both in- and out-patient settings, and spans a broad range of sub-specialty and acuity scenarios. Consuming and understanding this data in an efficient way is essential for efficient, high quality care delivery, especially since most Radiologists have little prior familiarity with their patients. Several natural language processing techniques are available to filter the EHR data to permit a Radiologist or affiliated support staff the ability to ascertain essential information for their care. In addition, related techniques of knowledge management and machine learning can combine to form powerful tools that can assist the Radiologist in rapidly gleaning essential contextual and safety information contained in the EHR. We will show several examples of these techniques at work in clinical settings. Coupled to industry market trends as well as mandates related to Meaningful Use 2, these tools are becoming increasingly powerful and pervasive. Improved automation and accuracy of filtration will make these tools all the more useful, widespread and value-adding to the practice of Radiology.

### **VSIN31-07 • Follow-up Imaging of Pulmonary Nodules**

**Cara L Morin MD** (Presenter) ; **Scott Shimp BS** ; **William W Olmsted MD** ; **Amy Kunce ARRT** ; **Eliot L Siegel MD** \*

#### PURPOSE

Initial imaging studies often include findings that cannot be completely evaluated, and radiologists often make recommendations for additional imaging. For pulmonary nodules, well-known guidelines address such recommendations. In routine practice, however, the rates of radiologists' recommendations for follow-up and of referring physicians' compliance are not well documented. Data are limited on whether clinicians follow the advice of radiologists.

#### METHOD AND MATERIALS

A retrospective analysis on a sample of 10,000 radiology records from 2006 to 2010 from our institution that included pulmonary nodule findings was performed using statistical and pattern matching methods. Analysis was performed for follow-up recommendations and adherence. If the term 'follow up' was detected in a record, all records were analyzed to determine if there was a subsequent record with a later date and the same patient ID. If such a record was found, it was assumed that a follow up did occur. Analysis was also performed on a subsample of patients with at least 2 reports (5,954 records). Results for the full sample and subsample provided a range of values to be refined in subsequent analysis.

#### RESULTS

Within the sample of patients obtaining an initial XR (radiograph), CT, or PET study (9,863), ~48% of reports contained a recommendation for follow-up. The recommendation rate varied between 41% and 57% across all sample years. Of reports recommending follow-up, 53%~71% resulted in a subsequent study within 2 yr. CT and XR accounted for ~73% and ~23% of all studies, respectively, whereas CT and XR accounted for 83% and 13%, respectively, of follow-up studies. CT and PT studies resulted in follow-up recommendations in ~55% of cases, whereas only ~28% of XR studies resulted in follow-up recommendations. With respect to timing, 38% of follow-up reports occurred within 3 mo, 22% within 3~6 mo, and 22% within 6~12 mo.

#### CONCLUSION

Our data on a large sample set of imaging records indicate that follow-up imaging for pulmonary nodule is recommended for ~48% of XR, CT, or PET studies. In those cases where follow-up imaging is recommended, approximately 53%~71% are actually obtained.

#### CLINICAL RELEVANCE/APPLICATION

Recommendations for additional imaging are common in radiology reports. Our initial analysis demonstrates suboptimal adherence and

these cases should be tracked.

## VSIN31-08 • Measuring Expressions of Uncertainty in Radiology Texts for Natural Language Processing Applications

**Brian E Chapman** PhD (Presenter) ; **Amilcare Gentili** MD ; **James Y Chen** MD \* ; **Asako Miyakoshi** MD ; **Wendy Chapman** PhD

### CONCLUSION

Our results showed that radiologist had high overall consistency in where they centered probabilities but that their probability mappings had high variability. We observed inconsistency in our NLP cue categorization, particularly the overlap between the definitely and probably negated categories. Further, the results indicate our model of uncertainty could be improved by adding a fifth category of **ambivalent** to capture the highly uncertain existence cues with probabilities near 0.5.

### Background

Natural language processing (NLP) is an important tool for extracting structured information from radiology texts. pyConTextNLP uses linguistic cues to determine whether a finding is negated, asserted, or uncertain. We compared probabilities assigned by radiologists against categories defined in pyConTextNLP.

### Evaluation

A set of linguistic cues describing negated and asserted existence with and without uncertainty was created by combining (a) 133 pyConTextNLP cues categorized as **definitely negated**, **probably negated**, **probably existent**, and **definitely existent** and (b) 108 cues translated from Swedish clinical texts. Three radiologists separately reviewed the cues in random order and assigned single-point probabilities to each cue followed by probability ranges (blinded to single-point responses).

### Discussion

Pairwise comparisons of single-point probabilities showed very small differences in the mean values (mean difference of 0.012) but large variability (mean standard deviations of 0.21). Similarly range mappings showed small but somewhat differences in the mean location (-0.0035) and widths (0.0008) of the assigned probability ranges but large variability in these measures (mean standard deviation of 0.21 and 0.30). Examining mean range width versus the mean point mapping showed that cues with point mappings near the extremes (0 and 1.0) had much smaller range widths than cues with point mappings near 0.5. Radiologist discordance showed a similar pattern. For the categorized cues, the mean (standard deviation) of the assigned point probabilities were as follows: definitely negated 0.078 (0.11), probably negated 0.17 (0.16), probably existent 0.71 (0.11), definitely existent 0.91 (0.083).

## VSIN31-09 • Unlocking Information from Text: Pulmonary Embolism, Pneumonia, and Report Clarity

**Wendy Chapman** PhD (Presenter)

### LEARNING OBJECTIVES

1) Be able to define natural language processing (NLP) and describe some of the tasks accomplished through this technique. 2) Understand how NLP could be used to help identify patient cohorts for imaging/radiology studies. 3) Know how well NLP performs at extracting and reasoning with findings described in radiology reports. 4) Be able to describe some of the challenges in developing and applying NLP to radiology reports.

## VSIN31-10 • Natural Language Processing of CT Pulmonary Angiography Reports for the Detection of Pulmonary Embolism Chronicity and Location of Filling Defects

**Sheng Yu** ; **Ruth M Dunne** MBBCh (Presenter) ; **Andetta R Hunsaker** MD ; **Elizabeth George** MBBS ; **Frank J Rybicki** MD, PhD \* ; **Kanako K Kumamaru** MD, PhD ; **Cai Tianxi** ; **Matey Neykov** ; **Arash Bedayat** MD ; **Karin E Dill** MD

### PURPOSE

To develop and test a Natural Language Processing (NLP) algorithm that analyzes clinical reports of CT Pulmonary Angiography (CTPA) for the diagnoses of pulmonary embolism (PE), the chronicity of PE when present, and the location of the most proximal filling defect considered positive for PE.

### METHOD AND MATERIALS

The final CTPA reports for 10,330 CTPA examinations performed at our academic institution from 8/1/03 and 3/31/10 were manually, independently reviewed by at least two physicians for the diagnosis of PE. For patients with PE, chronicity subtype information (acute, subacute, chronic, acute on chronic, and other) and the most proximal embolus location (central, lobar, segmental, or subsegmental pulmonary artery) were also recorded. A NLP program was developed to analyze the content of the reports and to convert the semantics to numeric features as the counts on the occurrences of relevant concepts related to PE status and subtypes. Statistical models were built to classify the diagnoses of PE, the chronicity, and the most proximal locations by aggregating information from all informative features.

### RESULTS

The prevalence of PE was 19.3% (1996/10330), determined from manual review of the reports and considered **truth**. The classification algorithm based on the NLP extracted features was highly accurate in the detection of PE with a cross-validated AUC of 0.995. Among patients with PE, the **true** fraction of acute, subacute, chronic, acute on chronic, and other PE were 82.7%, 2.1%, 8.3%, 3.9%, and 3.0%, respectively. Proximal extension of the embolus was classified as central in 24.3%, lobar in 23.2%, segmental in 39.4%, and subsegmental in 13.1% of patients. The current classification models for acute versus non-acute and central versus non-central PE based on the NLP extraction achieved an AUC of 0.897 and 0.936 respectively.

### CONCLUSION

Natural language processing is a promising automated tool to identify patients with a positive CTPA report, and provides data regarding chronicity and the proximal embolus location.

### CLINICAL RELEVANCE/APPLICATION

Given the relatively standard terminology, range of findings, and low positivity rate, NLP for automated extraction of PE-related information has the potential to creation of large research cohorts.

## VSIN31-11 • Natural Language Processing Enabled Capturing of BI-RADS Data from Unstructured Radiology Reports

**V J Jagannathan** PhD ; **Claudine Martin** BS ; **Juergen Fritsch** PhD (Presenter) \*

### CONCLUSION

The proposed BI-RADS information identification approach allows for more efficient mammography reporting workflows (see diagram). Furthermore, it can be used to notify the radiologist in real-time about any missing, relevant information needed for reporting purposes. The recommendation captured in structured form can drive reminders and follow-ups and the assessment captured can be used for patient communication.

### Background

Breast Imaging Reporting and Database System (BI-RADS) is a quality assurance guide developed by the American College of Radiology (ACR) to standardize breast imaging reporting<sup>1</sup>. In this work, we review an approach to capture the standard BI-RADS data elements directly from narrative mammography reports. The data elements include:

- 1) Breast Density
- 2) BI-RADS Assessment
- 3) Recommendation for Follow-Up
- 4) Laterality The proposed workflow supports processing of unstructured (typed or dictated) Radiology reports via a Natural Language Understanding (NLU) engine to automatically identify and then validate the correctness of the above data elements. Radiology reports are converted into standard HL7 Clinical Document Architecture (CDA) format, which also allows for encoding the discovered BI-RADS data



#### Evaluation

Users review and validate the correctness and completeness of the data and thereby provide implicit feedback that is being used to continuously improve system performance, which is being measured via precision and recall on a manually annotated gold standard data set.

#### Discussion

We present an approach that allows identifying and validating structured BI-RADS data from unstructured, narrative reports. Diagnostic mammograms, MRIs and Ultrasound reports will contain explicit BI-RADS assessments but not typically explicit breast density values as found in screening mammograms. Also, laterality identification in the presence of multiple tumors is non-trivial. Yet, Radiologists prefer narrative reporting systems over structured reporting tools for efficiency and expressivity reasons.

### VSIN31-12 • Error Bot: Improving Radiology Report Quality by Notifying Radiologists of Report Errors in Real-time

**Matthew J Minn MD (Presenter) ; Arash R Zandieh MD ; Ross W Filice MD**

#### CONCLUSION

Radiology report errors inevitably occur and may impact patient management. Our project not only documents error rates, but shows that automated intervention can positively impact patient management by both prospectively decreasing error rates and correcting substantial numbers of errors that do occur.

#### Background

Radiology report errors occur due to inaccurate speech recognition, report macros, and other human error. We created a system that detects report errors in real-time and sends immediate notifications to the reporting radiologists by page and email. Our goal is to improve report quality by two main mechanisms: correct errors that do occur quickly and provide continuous feedback in hopes of decreasing future error rates.

#### Evaluation

We receive a real-time Health Level 7 (HL7) feed from our Radiology Information System (RIS) (Siemens). Our Mirth Connect HL7 engine (Mirth Corporation) filters report messages and checks for errors using custom JavaScript algorithms. If a potential error is detected, a call is made to custom Bash (GNU) scripts that page and email the associated radiologists. All related information is tracked in a MySQL (Oracle) database.

We focused on two error types. Laterality errors were flagged on discrepancy between laterality in the procedure name and the report conclusion. Gender errors were flagged on discrepancy between patient sex and descriptors in the report. Error rates were determined for 4 months before (Pre) and 7 months after (Post) the notification system was implemented. Flagged reports were curated to determine true positive detections. These were then followed to see if they were ultimately corrected.

#### Discussion

We found significant improvement in potential errors detected (Pre: 198/149,537; 0.13%, Post: 290/277,531; 0.10%, p-value 0.01) and true positive rates (Pre: 116/149,537; 0.08%, Post: 147/277,531; 0.05%, p-value 0.002) after the detection and notification system was implemented. Most importantly, the number of true positive reports ultimately corrected improved dramatically after our notification system started (Pre: 17/116; 15%, Post: 133/147; 90%, p-value

### VSIN31-13 • Automated Structuring of Radiology Reports using Natural Language Processing

**Paras Lakhani MD (Presenter)**

#### LEARNING OBJECTIVES

1) Learn about the differences between and structured, standardized, and free-text reporting. 2) Learn about basic natural language processing (NLP) techniques, and how they can be applied to transform free-text narrative radiology reports into standardized reports. 3) Learn about the pros and cons of such automated systems. 4) Provide real-life examples of the natural language processing system with various reporting styles. 5) Discuss future directions of NLP and its applicability to structured reporting.

## Interventional Radiology Series: Venous Disease

**Tuesday, 08:30 AM - 12:00 PM • E351**



[Back to Top](#)

**VSIR31 • AMA PRA Category 1 Credit™:3.25 • ARRT Category A+ Credit:3.75**

#### Moderator

**Scott O Trerotola, MD \***

#### LEARNING OBJECTIVES

1) Describe the use of radiofrequency wire in central venous occlusion. 2) Explain the current role of inferior vena caval filtration in venous disease. 3) Describe the steps involved in creating a quality improvement project related to inferior vena cava filter follow-up. 4) Outline the current approach to diagnosis and treatment of central venous stenosis. 5) Describe the rationale for adrenal vein sampling. 6) List 3 differences between the US and Europe in fistula use and how Fistula First has narrowed that gap.

### VSIR31-01 • Central Venous Stenosis - Why Does It Occur? How Can We Prevent It? Treatment With Conventional Tools

**Dheeraj K Rajan MD (Presenter) \***

#### LEARNING OBJECTIVES

1) Describe common causes of central venous stenosis (CVS). 2) Describe preventative measures that may be undertaken to avoid CVS. 3) Describe common tools and techniques for treatment of CVS available to radiologists.

### VSIR31-02 • Central Venous Occlusion Treatment with RF Wire

**Marcelo Guimaraes (Presenter) \***

#### LEARNING OBJECTIVES

1) Describe the radio-frequency wire technique in the recanalization of chronic and benign central venous occlusions.

#### ABSTRACT

Purpose: Central venous occlusion is not an infrequent problem in patients who had long-term venous catheters. The recanalization of CVOs using conventional techniques may fail in up to 24% of cases. The radiofrequency wire puncture technique was utilized in symptomatic patients. MandM: Between 2008-2013, 58 patients, ages 26-78 years, presented with swollen arm and/or face secondary to benign CVOs related to tunneled catheters. Coronal chest CTA was used to evaluate the central venous anatomy. First, a pericardium window is selected for potential cardiac tamponade drainage. Simultaneous upper extremity (brachial) and central venograms (femoral approach) are performed to define the CVO. Typically, the RF wire was advanced within a 5-Fr KMP catheter from the cranial venous stump towards a 10 mm snare placed in the caudal stump. The RF wire tip and the snare alignment was checked PA, RAO, LAO. If the RF wire puncture was inadequate, a new location was pursued. Pre-stent 4mm balloon PTA was followed by 9-12mm stent placement. Self-expandable stents were used in the subclavian-brachiocephalic transition and balloon-expandable stents were used in brachiocephalic

or SVC lesions. Clinical and venogram F/U's were scheduled at 3, 6, 9 and 12 months. Results: 56 patients were successfully treated with RF wire technique. One hemothorax and one cardiac tamponade were successfully treated with drain catheter placement without clinical repercussions. Resolution of symptoms was obtained in 51/56 patients treated in mean follow-up of 16 months. 5/56 patients had stent occluded at 3 months that required balloon angioplasty for successful recanalization and all had improvement of symptoms following the second intervention. Conclusion: RF wire technique is a good alternative in benign CVO's when conventional techniques have failed. It is an alternative in the management of symptomatic patients. Thorough technique must be used in the order to minimize potential complications.

#### **VSIR31-04 • Prophylactic Placement of an Inferior Vena Cava Filter during Endovenous Intervention for Acute Deep Venous Thrombosis of the Lower Extremity**

**So Hyun Park** (Presenter) ; **Se Hwan Kwon MD** ; **Joo Hyeong Oh MD** ; **Tae-Seok Seo** ; **Myung Gyu Song MD**

##### **PURPOSE**

To evaluate the usefulness of an inferior vena cava (IVC) filter during endovenous intervention for acute deep vein thrombosis (DVT) in the lower extremity.

##### **METHOD AND MATERIALS**

We performed endovenous intervention in 106 patients (M:F =30:76; mean age, 59.8 years) with acute DVT in the lower extremity after placement of an IVC filter between July 2004 and December 2012. In all patients, aspiration thrombectomy was performed, and percutaneous transluminal angioplasty (PTA) or additional stent placement was carried out in six and 88 patients, respectively. We evaluated presence of a trapped thrombus in the IVC filter on final venograms obtained during the procedure (n=106) or on follow-up CT (n=55), respectively. The transverse length of the trapped thrombus was defined as four grades (1-4) divided by the IVC filter diameter for each 25%. We also evaluated the relationship between thrombus trapping, stenosis of the iliac vein, extended thrombus in the IVC.

##### **RESULTS**

A trapped thrombus in the IVC filter was detected in 46/106 patients (43%) on final venograms or on follow-up CT. A trapped thrombus in the IVC filter was detected in 8/12 patients (75%) after aspiration thrombectomy only, in 4/6 patients after additional PTA (67%), and 34/88 patients after additional stent placement (39%). A trapped thrombus in the IVC filter was observed on venograms in 35/106 patients (33%) and on follow-up CT in 25/55 patients (45%). In 25 trapped thrombi observed on CT images, 11 were not shown on final venograms and were newly detected on CT images. Thrombus sizes were grade 1 in four patients (8.7%), grade 2 in eight patients (17.4%), grade 3 in 22 patients (47.8%), and grade 4 in 12 patients (26.1%). Among 67 patients in whom DVT was detected on CT before the procedure, the incidences of a trapped thrombus in cases with or without an extended thrombus into the IVC on CT images were 13/17 (76.5%) and 18/50 (36.0%), respectively.

##### **CONCLUSION**

Thrombus migration developed frequently during endovenous intervention in patients with DVT in the lower extremity, and IVC filter placement may be useful for prevention of pulmonary thromboembolism.

##### **CLINICAL RELEVANCE/APPLICATION**

IVC filter placement may be useful for prevention of pulmonary thromboembolism.

#### **VSIR31-05 • IVC Filter Update**

**John A Kaufman MD** (Presenter) \*

##### **LEARNING OBJECTIVES**

View learning objectives under main course title.

#### **VSIR31-06 • Debate - When Should We Be Placing Permanent Filters?**

**John A Kaufman MD** (Presenter) \* ; **Steven M Zangan MD** (Presenter)

##### **LEARNING OBJECTIVES**

View learning objectives under main course title.

#### **VSIR31-07 • Filter Follow-Up - PQI**

**Steven M Zangan MD** (Presenter)

##### **LEARNING OBJECTIVES**

View learning objectives under main course title.

#### **VSIR31-08 • Utility of Preoperative Vascular Mapping to Select Patients at High Risk for Early Thigh Hemodialysis Graft Failure**

**Mark D Little MD** (Presenter) ; **Michael Allon** ; **Michelle M McNamara MD** ; **Song Ong** ; **Mark E Lockhart MD** ; **Carlton Young** ; **Michelle L Robbin MD** \*

##### **PURPOSE**

To determine whether noninvasive preoperative evaluation of vascular diameters and calcification can identify patients in whom arteriovenous thigh graft survival is likely to be impaired.

##### **METHOD AND MATERIALS**

Institutional review board approval was obtained and informed consent was waived. Retrospective analysis, including a qualitative assessment of calcification burden, was performed on 143 chronic hemodialysis patients who received ultrasound vascular mapping prior to thigh graft placement. Severity of pelvic arterial calcification was scored in 80 patients who received peri-operative computed tomography, using a semi-quantitative 5-point scale. Patient characteristics and graft outcomes were examined. Statistical analysis was performed on each group.

##### **RESULTS**

Preoperative ultrasound screening identified no or mild arterial calcification in 113 of 143 patients (79%) and moderate to severe calcification in 30 of 143 patients (21%). Patients with moderate to severe arterial calcification had significantly increased technical graft failure (hazard ratio=6.59; 95% CI, 2.06-21.05; p=0.002 by Fisher's exact test) and decreased cumulative graft survival (hazard ratio=2.32; 95% CI, 1.48-6.69, p= 0.003 by log rank test) compared to patients with no or mild disease. Cumulative graft survival was not associated with venous diameters (HR 1.06; 95% CI, 0.63-1.80, p=0.82) or arterial diameters (HR 1.19; 95% CI, 0.70-2.03, p=0.43). Low CT calcification score was seen in 74 of 80 hemodialysis patients (93%). Primary technical failure occurred in 3 of 6 patients (50%) with high versus 5 of 74 patients (6.8%) with low calcification score (hazard ratio=7.4; 95% CI, 2.31-23.72, p=0.01). US was more sensitive (64% versus 38%) but less specific (83% versus 96%) than CT in predicting immediate technical graft failure. Positive predictive value of CT and US was 50% and 23%, respectively.

##### **CONCLUSION**

Preoperative sonographic assessment of thigh vessel diameter and calcification can select patients who need further CT assessment of pelvic calcifications to identify those at higher risk for primary technical graft failure and decreased cumulative graft survival.

##### **CLINICAL RELEVANCE/APPLICATION**

US can identify moderate or severe arterial calcification where pelvic CT may aid site selection to lessen early technical failure, thereby improving long term hemodialysis thigh graft survival.

## VSIR31-09 • Updates in Dialysis

**Luc A Turmel-Rodrigues MD (Presenter)**

### LEARNING OBJECTIVES

1) Explain the role of fistula maturation procedures in access intervention and their results. 2) Outline the arguments for and against prophylactic PTA of failing access. 3) Describe recent evidence concerning the use of stent-grafts in failing hemodialysis grafts. 4) Describe three methods of fistula declotting. 5) Describe differences between the US and Europe in fistula use and how Fistula First has narrowed that gap. 6) Explain why many believe a ♦Catheter Last♦ approach may be even more important than ♦Fistula First♦.

### ABSTRACT

Purpose: to provide information about new radiologic techniques and concepts in the management of dialysis access complications.

Materials and Methods: review of the recent international literature.

Results: In the field of pre-op mapping, non CE-MRA of upper limb vessels is feasible and might be helpful. Anatomy: high origin of forearm arteries is evidenced in 12.8% of patients. In the area of nonmaturing fistulas, cannulation of the elbow artery for angiographic evaluation is safe and effective, dilation of the radial artery gives way to durable results, embolization of venous ♦competing vessels♦ and ♦collaterals♦ is controversial. Dilation: the value of prophylactic dilations is controversial in prosthetic grafts and less controversial in autogenous fistulas. Minimally symptomatic and asymptomatic central vein stenoses/occlusions should not be treated. The value of coated balloons has to be confirmed. Stents: PTFE covered stents are helpful at the venous anastomosis of grafts although their value is controversial in the cephalic arch. Hand ischemia: look at the ulnar artery in forearm fistulas. Excess flow: the reliability and reproducibility of percutaneous banding has to be confirmed. Plugs can be used to occlude arteries, veins and fistulas. Thrombosis: percutaneous thrombectomy is cost-effective, surgical results are improving in autogenous fistulas. Central catheters: several reports of arterial damages confirm that imaging guidance should be mandatory for insertion.

Conclusion: recent publications show that our everyday practice is changing and that very few concepts are not subjects to controversy.

## VSIR31-10 • Excellent Success Rate of Adrenal Venous Sampling after Simple Modification of Routine Protocol

**Sadahiro Yamamura (Presenter) ; Yoshinori Shigematsu ; Koichi Yokoyama ; Osamu Ikeda MD ; Toshinori Hirai MD ; Yasuyuki Yamashita MD \***

### PURPOSE

To evaluate efficacy of the modification of adrenal venous sampling (AVS) protocol in comparison with our previous results.

### METHOD AND MATERIALS

Since 2009, 114 patients with primary aldosteronism were subjected to AVS conducted by a single radiologist. From the retrospective reviews of the first 72 patients, AVS protocol was modified and applied prospectively for the latter 42 patients. The criterion for biochemical successful catheterization was cortisol value of more than 200 $\mu$ g/dl and/or an adrenal vein/inferior vena cava cortisol ratio of greater than 5. The blood was drawn at the central adrenal veins with use of ACTH.

### RESULTS

The biochemical success rate (BSR) for the first 72 patients was 91.7 % (66/72), and the causes of the failure in these 6 patients were analyzed. In all six patients, the procedures were unsuccessful on the right side. For 3 patients, the catheter tip slippage was seen during the sampling. Adrenal hemorrhage occurred in 8 patients and AVS was biochemically unsuccessful in 2.

For the latter patients, our routine AVS protocol was modified in two points. First, to avoid catheter tip slippage, the way of catheter tip settlement was changed. Before the modification, in case that the catheter tip was too deep into the adrenal vein, we had moved the tip of the 4F catheter by pulling the catheter. After modification, we moved the 4F catheter tip by pushing the adrenal venous wall with microguidewire through the 4F catheter. The blood was drawn through the space between the microguidewire and 4F catheter by using a Y-shape connector. Second, to avoid adrenal hemorrhage, we used a 5mm cylinder instead of a 10 ml cylinder when fumbling and injecting to the right adrenal vein.

In the latter 42 patients, the BSR was perfect. The incidence of the right adrenal hemorrhage decreased to 2.4 %.

### CONCLUSION

Use of microguidewire, Y-shape connector and smaller cylinder of 5ml improved BSR of AVS with a low risk of right adrenal hemorrhage.

### CLINICAL RELEVANCE/APPLICATION

AVS collecting whole adrenal venous blood with our method will improve the cure rate of the operated patients because it can also guarantee the normal adrenal function of the non-operated side.

## VSIR31-11 • Non-contrast-Enhanced MR Imaging of Right Adrenal Vein for Adrenal Venous Sampling: Comparison with Multidetector CT Angiography

**Hideki Ota MD, PhD (Presenter) ; Kei Takase ; Kazumasa Seiji MD, PhD ; Ryo Morimoto ; Fumitoshi Satoh MD, PhD ; Shoki Takahashi MD**

### PURPOSE

Primary aldosteronism is the main cause of secondary hypertension in younger population and induces renal dysfunction. Adrenal venous sampling (AVS) is essential to localize unilateral or bilateral lesions causing primary aldosteronism. However, catheterization to the right adrenal vein is technically challenging due to its small size and anatomical variations. Identification of the right adrenal vein prior to AVS is important to achieve successful procedure. This study aims to compare detectability of the right adrenal vein by non-contrast-enhanced MR imaging at 3T and multidetector CT angiography.

### METHOD AND MATERIALS

Consecutive 65 patients (mean age, 54.5, range 33-77) scheduled for AVS were included. Sixty-three patients underwent both MR and CT imaging. The remaining two underwent only MR imaging due to high risk of contrast-induced nephropathy. Three-dimensional respiratory-triggered true fast imaging with steady-state precession imaging was acquired in transverse section for MR imaging. Contrast-enhanced four-phase scanning was performed for CT imaging. On both modalities, image quality of the right adrenal vein was evaluated on a five-point scale (1=invisible, 5=excellent). Detectability and image quality were compared using McNemar♦s test or Wilcoxon signed ranks test.

### RESULTS

Non-contrast enhanced MR imaging demonstrated right adrenal veins in 59 of the 65 patients (91%). In the 63 patients who underwent both examinations, the detectability of the right adrenal vein was significantly higher for CT than MR imaging (100% vs. 90%,  $p=0.04$ ). When all the patients scheduled for AVS were included, the detectability was not significantly different between both modalities ( $p=0.28$ ). CT demonstrated significantly higher image quality than MR imaging ( $p$

### CONCLUSION

CT angiography is a reliable tool for detection of the right adrenal vein. When risks of radiation and contrast-induced complication were taken into account, non-invasive MR imaging becomes a first choice for planning of AVS.

### CLINICAL RELEVANCE/APPLICATION

Non-contrast-enhanced MR as well as CT can demonstrate the right adrenal vein. MR exam is recommended for planning of AVS when risks of radiation and contrast-induced complication was taken into account

## VSIR31-12 • Adrenal Vein Sampling: You Can Do This (Maybe)

**Scott O Trerotola MD (Presenter) \***

## LEARNING OBJECTIVES

1) Describe the laboratory profile of candidates for adrenal vein sampling in aldosteronism. 2) List characteristic features and tip-offs for identifying the adrenal veins. 3) Describe the catheter shapes that work most commonly for AVS. 4) Interpret a straightforward set of AVS results. 5) Explain the roles of lateralization index, selectivity index, and contralateral suppression in AVS.

## ABSTRACT

Adrenal vein sampling, by far most commonly performed for aldosteronism, is experiencing a resurgence with recognition that the poor results of the past, particularly with right sided sampling, can be markedly improved with new techniques and materials. This presentation will focus on the technical aspects of AVS, with a strong focus on correct identification of the right and left adrenal veins as well as mimics which can undermine success. Recent advances aimed at improving results even for inexperienced operators will be discussed, including the roles of cone beam CT, preoperative CT, anatomic clues, rapid cortisol assays, and catheter optimization. Typical patient selection, patient preparation and results interpretation will be covered using a case presentation format. Strategies for developing an AVS program will be reviewed. The presentation will focus exclusively on aldosteronism, since other indications for AVS are rare.

## VSIR31-13 • Wrap Up and Discussion

### LEARNING OBJECTIVES

View learning objectives under main course title.

## Musculoskeletal Radiology Series: Ultrasound

Tuesday, 08:30 AM - 12:00 PM • E451B



[Back to Top](#)

**VSMK31 • AMA PRA Category 1 Credit™:3.25 • ARRT Category A+ Credit:3.5**

### Moderator

**Marnix T Van Holsbeeck, MD \***

### Moderator

**Kenneth S Lee, MD \***

## VSMK31-01 • Shoulder Ultrasound (Demonstration)

**Jon A Jacobson MD (Presenter) \***

### LEARNING OBJECTIVES

1) Be familiar with ultrasound examination and anatomy of the shoulder and common pathology.

## VSMK31-02 • Ultrasound Assessment of the Rotator Cable and Correlation with Functional Outcome, Tear Size and Muscle Fatty Atrophy

**Etienne Blain Pare MD, FRCPC (Presenter) ; Karim Basile MD ; Nicola Hagemester \* ; Patrice Tetreault MD, MSc ; Dominique Rouleau MD, MSc ; Nathalie J Bureau MD**

### PURPOSE

To investigate the relationship between visualization of the rotator cable (RC) on ultrasound (US) and functional outcome, tear size and muscle fatty atrophy in subjects with full-thickness rotator cuff tears (RCT) and asymptomatic volunteers (AV).

### METHOD AND MATERIALS

In this cross-sectional study, 52 subjects with full-thickness RCT (32 men; age range 39-67 years; mean 57 years) and 20 (AV) (11 men; age range 35-64 years; mean 54 years) were examined prospectively with US by a musculoskeletal radiologist with 17 years of experience. A RC was defined as an articular-sided bundle of fibers perpendicular to the rotator cuff tendons. The length and width of the full-thickness RCT were measured in the frontal and sagittal planes and tear area was calculated. Supraspinatus (SS) muscle atrophy was assessed by calculating the occupation ratio of the SS fossa (Thomazeau 1997). SS and infraspinatus (IS) fatty atrophy was graded by comparing the echogenicity and pennate pattern with that of the trapezius muscle (Khoury 2008). A physiotherapist used the Constant score to measure functional outcome. Statistical analysis was performed using the Student t test and the Fisher exact test.

### RESULTS

The RC was visualized in 75% of AV and in 25% of RCT subjects. Non-visualization of the RC in RCT subjects correlated significantly with a larger tear area (612.12 mm<sup>2</sup> vs 247.24 mm<sup>2</sup>),  $p < 0.0001$ , 95% CI (145.83; 528.6). The mean Constant score was significantly higher in AV than in RCT subjects (87.5 vs 51.3),  $p < 0.0001$ , 95% CI (31.6; 40.7) but it did not correlate with RC visualization in the RCT group ( $p = 0.3$ ) nor in the AV group ( $p = 0.11$ ). There was a significant difference in the severity of muscle fatty replacement of the SS ( $p = 0.03$ ) and the IS ( $p = 0.014$ ), as well as in the severity of SS muscle atrophy ( $p = 0.04$ ) in RCT subjects without a visible RC as compared to those with a visible RC.

### CONCLUSION

Non-visualization of the RC on US correlates with larger RCT, higher grades of SS and IS muscle fatty replacement and with SS muscle atrophy. Visualization of the RC in subject with RCT does not appear to correlate with better functional outcomes.

### CLINICAL RELEVANCE/APPLICATION

RC visualization on US in subjects with full-thickness RCT may assist orthopedic surgeons in choosing the optimal treatment for their patients (conservative vs surgery).

## VSMK31-03 • Dynamic Ultrasonography of the Shoulder: Availability to Diagnose Combined Adhesive Capsulitis with Full-thickness Tear of the Supraspinatus Tendon

**Hoseok Lee (Presenter) ; Jae Hyuck Yi MD**

### PURPOSE

To determine the availability of dynamic ultrasonography of the shoulder to diagnose combined adhesive capsulitis with full-thickness tear of the supraspinatus tendon.

### METHOD AND MATERIALS

Since 2010, total 80 patients (M:F = 37:43, mean age: 61.56, age range: 36-82) with full-thickness tear of supraspinatus tendon (SSPT) who performed both dynamic ultrasonography (dUS) and MRI of the shoulder (32 cases of conventional MRI and 48 cases of indirect MR arthroscopy) were included in this retrospective study. 35 patients who showed subacromial gliding limitation (SGL) of the SSPT during dUS were classified into group I, 45 patients who did not show SGL of the SSPT were classified into group II. The dUS score was estimated by severity of SGL (0: none, 1: mild, 2: moderate, 3: severe). MRI was assessed for following 3 findings suggesting adhesive capsulitis; 1)maximal capsular thickness in axillary recess (AR) =4mm, 2)maximal capsular thickness in rotator cuff interval (RI) =7mm, 3)presence of bright signal change of capsule in AR and RI on fat-suppressed T2-weighted image of conventional MRI or capsular enhancement in AR on indirect MR arthroscopy. Each of these findings was given 1 score, and total MRI score of each patients was calculated. Statistic analysis was performed by using Pearson correlation coefficient and Fischer exact test.

## RESULTS

The mean value of dUS score and MRI score of total patients were  $0.59 \pm 0.77$  and  $1.42 \pm 1.13$ . The mean thickness in AR and RI were  $5.45 \pm 1.37$  mm and  $6.81 \pm 1.37$  mm in group I, and  $3.20 \pm 0.86$  mm and  $6.08 \pm 1.39$  mm in group II. dUS score was significantly correlated with capsular thickness in AR ( $r=0.742$ ,  $p$

## CONCLUSION

Subacromial gliding limitation of the supraspinatus tendon during dynamic ultrasonography was significantly correlated with MR findings suggesting adhesive capsulitis. Therefore, dynamic ultrasonography of the shoulder may be useful to diagnose combined adhesive capsulitis with full-thickness tear of the supraspinatus tendon.

## CLINICAL RELEVANCE/APPLICATION

Dynamic ultrasonography can demonstrate subacromial gliding limitation of the supraspinatus tendon and this exam is recommended in the evaluation of suspected adhesive capsulitis.

### VSMK31-04 • Diagnostic Performance of Conventional Ultrasonography Combined with US Strain Elastography for Differentiation between Benign and Malignant Subcutaneous Soft Tissue Mass Lesions

**Tharakeswara Kumar Bathala** MD (Presenter) ; **Gaiane M Rauch** MD, PhD ; **Melanie Bass** ; **Deborah Borst** ; **Brian Hobbs** PhD ; **Deepak G Bedi** MBBCh \*

## PURPOSE

To evaluate diagnostic performance of conventional ultrasonography (US) combined with US Strain Elastography (USE) for differentiation between benign and malignant subcutaneous soft tissue mass lesions, with the pathology as reference standard.

## METHOD AND MATERIALS

After Institutional IRB approval, we identified 74 patients with a subcutaneous soft tissue mass who had US and USE from January 2009 to May 2012. Three radiologists retrospectively reviewed US and USE images in consensus. Gray scale US imaging features were classified as benign, malignant and indeterminate. USE images were assessed according to tissue elasticity based on color scale and classified as soft, intermediate and hard. Pathological diagnosis obtained either by percutaneous biopsy or surgical excision was used as reference standard. The statistical analysis included evaluation of sensitivity and specificity for US and USE separately, as well as a composite evaluation of US + USE; Bowker's test was used for evaluation of matched US and USE outcomes for symmetry.

## RESULTS

Out of 74 lesions, US 37 were classified as benign, 8 indeterminate, 29 malignant. USE found 35 benign, 14 indeterminate, 25 malignant lesions. US+USE classified 40 as benign, 4 indeterminate and 30 malignant. The estimated sensitivity and 95% CI for US, USE and US+USE was 100% (82-100%), 95% (75-100%), and 100% (82-100%) respectively. The specificity for US, USE and US+USE was 71% (57-82%), 67% (53-79%), and 77% (63-87%) respectively. Significant evidence for the lack of agreement among the matched US and Elastography results was not found ( $p=0.51$ ). The data suggest US alone is highly sensitive for detecting and characterization of subcutaneous soft tissue lesions. Only 8 patients resulted in an indeterminate US, all of which had benign lesions on pathology. Among these 8, USE was determinate for only 4, of which 3 were correctly classified as benign and 1 was incorrectly classified as malignant. Thus, estimated specificity is improved for the US+USE.

## CONCLUSION

In the presence of an indeterminate result on conventional US, USE may improve specificity for diagnosing subcutaneous soft tissue lesions. Combination of US and USE could provide a better diagnostic performance than conventional US alone.

## CLINICAL RELEVANCE/APPLICATION

Addition of USE evaluation to conventional gray scale US imaging improves imaging-based diagnostic information for soft tissue nodule work up.

### VSMK31-05 • Value of Real-time Sharewave Elastography in Achilles Tendinopathy: Is the Abnormal Tendon Softer?

**Jean-Philippe Nueffer** MD (Presenter) ; **Fabio Becce** MD ; **Fabrice Michel** MD, PhD ; **Benoit Barbier-Brion** MD ; **Adrian I Kastler** MD, MSc ; **Sebastien L Aubry** MD, PhD

## PURPOSE

To determine if the viscoelastic properties of Achilles tendon assessed by real-time sharewave elastography (SWE) are modified in tendinopathy

## METHOD AND MATERIALS

Twenty-six abnormal tendons (16 unilateral and 5 bilateral tendinopathies) from 21 patients with Achilles tendinopathy and 176 normal tendons (from 16 patients and 80 healthy volunteers) were prospectively included and compared. Mean sharewave velocity ( $V_{mean}$ ) was measured on axial and sagittal SWE images at two degrees of passive ankle flexion (position 1: complete plantar flexion; and position 2: 0 degree flexion). Tendon maximum anteroposterior and lateral diameters, cross sectional area and the presence of tears were also noted

## RESULTS

In position 1, the abnormal tendons  $V_{mean}$  was significantly lower than for contralateral normal tendons on sagittal ( $\Delta=-1.23$ m/s,  $p=0.004$ ) and axial elastograms ( $\Delta=-0.68$ m/s,  $p=0.03$ ); and significantly lower than for normal tendons only on axial images ( $\Delta=-0.49$ m/s,  $p=0.01$ ). In position 2 and on axial elastograms, the abnormal tendons  $V_{mean}$  was 1.14m/s lower than for contralateral normal tendons however without reaching statistical significance ( $p=0.07$ ). In position 2, the abnormal tendons  $V_{mean}$  was significantly lower than for normal tendons on sagittal ( $\Delta=-1.26$  m/s,  $p$

## CONCLUSION

Abnormal Achilles tendons have lower  $V_{mean}$  and are therefore softer than normal tendons. There is no SWE signal into tendon tears

## CLINICAL RELEVANCE/APPLICATION

Tendon softening, assessed by real-time SWE, is a new helpful tool in the evaluation of Achilles tendinopathy. SWE may also provide quantitative parameters to assess the severity of tendinopathy

### VSMK31-06 • Ultrasound-guided Shoulder Injection

**Etienne Cardinal** MD (Presenter)

## LEARNING OBJECTIVES

1) Be familiar with ultrasound examination and anatomy of the hip and common pathology.

### VSMK31-07 • Ultrasound-guided (US) Percutaneous Treatment of Rotator Cuff Calcific Tendinitis (RCCT): Randomized Comparison between One- and Two-needle Procedure

**Davide Orlandi** MD (Presenter) ; **Giulio Ferrero** ; **Francesca Lacelli** MD ; **Enzo Silvestri** MD ; **Giovanni Serafini** MD ; **Luca Maria Sconfienza** MD, PhD

## PURPOSE

US-Guided percutaneous treatment of RCCT has been widely demonstrated to be effective using one or two needles, but direct comparison between the two methods has never been performed. Our aim was to compare the technical and one-year clinical outcome of these two different approaches.

## METHOD AND MATERIALS

IRB approval and patients' informed consent were obtained. One hundred patients to be treated for RCCT diagnosed with ultrasound (77

females, mean age 46y, range 32-70 years) were randomized into two groups. Group A (50 patients; mean visual analogue scale [VAS]=7.8) was treated using an US-guided 16G double-needle technique (local anesthesia, washing with warm saline, intrabursal steroid), while group B (50 patients; mean VAS=7.4) was treated using a 16G single-needle technique. Calcification appearance at US (fluid, soft, hard), procedure time and ease of calcium dissolution (subjectively scored as easy=1, intermediate=2, difficult=3) were recorded. VAS follow-up was performed at 1,3,6 and 12 months. Complication rate was noted. Mann-Whitney U and Chi-square statistics were used.

## RESULTS

### CONCLUSION

One- and two-needle procedures are equally effective in treating RCCT with no major complications. Two-needle procedure allows for significantly reducing treatment time and appears to be much easier when dealing with soft and hard calcium deposits.

### CLINICAL RELEVANCE/APPLICATION

Two needles US-guided percutaneous treatment of RCCT seems to be the treatment of choice in patients affected by soft and hard calcifications, compared to one needle technique.

## VSMK31-08 • Postoperative Monitoring of Local and Free Flaps with Contrast Enhances Ultrasound (CEUS)- Analysis

**Ernst Michael Jung MD (Presenter) ; Janine Rennert MD ; Lukas Prantl MD**

### PURPOSE

Tissue defects are a common problem in trauma surgery or oncology. Flap transplantation is often the only therapy to cover these extensive wound defects. To date several monitoring systems exist but none has made it to clinical day work. Objective: Aim of this study was to assess perfusion disturbances of local and free flaps using contrast enhanced ultrasound (CEUS).

### METHOD AND MATERIALS

112 patients were examined after local or free flap transplantation during the first 72 hours after operation. CEUS was performed by one experienced examiner with a linear transducer (6-9 MHz, LOGIQ E9/GE) after a bolus injection of 2.4 ml sufohexa-fluoride microbubbles (SonoVue, Bracco, Italy). Retrospective vascular perfusion was quantified by evaluating the stored DICOM cine loops using the perfusion software QONTRAST (Bracco, Italy). Over a total penetration depth of 3 cm every centimetre was analysed separately. 27 complications were observed. Complete flap loss was only seen in 4 cases whereas 23 flaps had to undergo minor revisions and survived.

### RESULTS

Regarding the complete flap size quantitative analysis showed significant higher perfusion values in patients without complications compared to patients with complications: PEAK 16.5 vs. 10.0 (p=0.001), TTP 32.6 vs. 22.2 (p=0.001), RBV: 738.8 vs. 246.2 (p

### CONCLUSION

CEUS was capable of detecting vascular disturbances after flap transplantation. TTP, RBV and MTT seem to be the most accurately parameters and are very unsusceptible to malfunction during measurement.

### CLINICAL RELEVANCE/APPLICATION

CEUS offers an excellent imaging method to detect early reduction of the tissue transplants microvascularization also if MRI is not available or not realizable.

## VSMK31-09 • The Effects of US-guided Injection of Platelet-rich-Plasma (PRP) on the Degenerative Disease of the Achilles and Patellar Tendon in Athletes

**Alice La Marra MD (Presenter) ; Lorenzo Maria Gregori ; Silvia Mariani MD ; Luigi Zugaro ; Antonio Barile ; Carlo Masciocchi**

### PURPOSE

To evaluate and show the result of injection with Platelet Rich Plasma (PRP) of tendinosis of Achilles and Patellar tendon in athletes.

### METHOD AND MATERIALS

In the last three years we evaluated 50 athletes with degenerative tendinosis of Achilles tendon and 30 athletes with degenerative tendinosis of patellar tendon. All the patients were first evaluated through diagnostic testing (MRI and US guided) and then through clinical observations (VAS for pain and VISA-A and VISA-P for functionality). The patients underwent a cycle of platelet rich plasma US-guided infiltrations every 21 days for a total of three treatments. Another MRI was performed 30 days and one year after the last infiltration.

### RESULTS

In the patients with tendinosis of Achilles tendon we have found an improved overall by 80% (VAS) and 53%(VISA-A). Relatively to the patellar tendon, the VAS value is increased of 75% (VAS) and 50% (VISA P). We observed partial or complete morphological recovery and normalization of MRI signal in 90%. We observed a reduction of sectional area in the Achilles tendon in 39/50 cases and in the patellar tendon in 18/30 cases. Eight patients with tendinosis of Achilles tendon presented an area increased by 10% and five patients with tendinosis of patellar tendon presented an area increased by 15%. The mean VAS at one year of treatment improved in all cases overall by 70%.

### CONCLUSION

Our study showed that in patients who underwent PRP treatments there was an improvement of the functionality, a decrease in pain and a normalization of the signal intensity seen on MRI. Therefore, our experience proves that PRP infiltration may be a good therapeutic alternative for the treatment of Achilles and patellar tendinopathy in athletes.

### CLINICAL RELEVANCE/APPLICATION

The US-guided PRP treatment in case of degenerative tendon diseases may increase Achille's and Patellar tendons functionality and reduce recovery times in athletes.

## VSMK31-10 • Wrist and Hand Ultrasound (Demonstration)

**Marnix T Van Holsbeeck MD (Presenter) \***

### LEARNING OBJECTIVES

1) Be familiar with ultrasound examination and anatomy of upper extremity nerves and common pathology.

## VSMK31-11 • High-resolution Ultrasonography of the Dorsal and Palmar Extrinsic Wrist Ligaments in Correlation with 3T Magnetic Resonance Imaging in 40 Normal Volunteers and 10 Cadaveric Specimens with Surgical Correlation

**Mihra S Taljanovic MD (Presenter) ; Dean Holden MD, FRCPC ; Elizabeth A Krupinski PhD ; Joseph E Sheppard MD**

### PURPOSE

To confirm that high-resolution ultrasonography (HRUS) has comparable results with 3T Magnetic Resonance Imaging (MRI) in visualization of the extrinsic wrist ligaments.

### METHOD AND MATERIALS

HRUS and 3T MRI of the extrinsic wrist ligaments were performed on 10 fresh frozen cadaveric wrist specimens and on 40 wrists in normal volunteers. Dorsal radiocarpal-DRCL, dorsal intercarpal-DICL and dorsal ulnotriquetral-DUTL, radioscapocapitate-RSCL, long radiolunate-LRLL, short radiolunate-SRLL, radioscapolunate-RSLL, palmar ulnolunate-PULL, palmar ulnotriquetral-PUTL,

ulnocapitate-UCL, and palmar scaphotriquetral-PSTL ligaments were evaluated. The ligaments were graded by two examiners in consensus, using the following grading system: Grade 1- ligament completely seen, Grade 2- ligament partially seen (< 100 % but > 50% of the ligament clearly seen) and Grade 3- ligament not seen (< 50% of the ligament clearly seen). Visibility on US and 3T MRI was compared using the following grading system: A- ligament equally well seen on US and MRI, B- ligament better seen on MRI, and C- ligament better seen on US. All cadaveric wrists were dissected by an orthopaedic hand surgeon. The results for each of the ligaments were shown in percentages. Differences between the distributions of percentages were tested for significance using the X2 test.

#### RESULTS

None of the examined 550 ligaments received grade 3. For MRI there was a significant difference in visualization of the ligaments ( $X^2 = 143.04$ ,  $p < 0.0001$ ) with DUTL, RSCL and UCL receiving significantly more scores of Grade 2 than the other ligaments. For US, there was a significant difference in visualization of the ligaments ( $X^2 = 143.83$ ,  $p < 0.0001$ ) with DUTL, PUTL, and PSTL receiving significantly more scores of Grade 2 than the other ligaments. There was a significant difference ( $X^2 = 335.72$ ,  $p < 0.0001$ ) with DUTL, PUTL, and PSTL receiving significantly more B scores than the other ligaments and the other 8 ligaments receiving more C scores. On surgical dissections in 10 cadavers all dorsal and palmar extrinsic wrist ligaments were intact.

#### CONCLUSION

HRUS enables satisfactory visualization of the extrinsic wrist ligaments with results that are at least comparable to 3T MRI.

#### CLINICAL RELEVANCE/APPLICATION

High-resolution ultrasonography enables good visualization of the extrinsic wrist ligaments and can be utilized in evaluation of these structures in routine clinical practice and sports medicine.

### VSMK31-12 • Ultrasound-guided Percutaneous Injection for De Quervain's Disease Using Three Different Techniques: Preliminary Results of a Randomized Controlled Trial

**Luca Maria Sconfienza MD, PhD (Presenter) ; Davide Orlandi MD ; Emanuele Fabbro MD ; Giovanni Mauri MD ; Giovanni Serafini MD ; Francesco Sardanelli MD \***

#### PURPOSE

De Quervain's disease is a painful stenosing tenosynovitis of the first dorsal compartment of the wrist, caused by a thickening of the retinaculum. Ultrasound-guided intracompartmental steroid injections reported pain relief in up to 97% of patients at 6 months follow-up with a rate of symptoms recurrence up to 20%. We compared the efficacy and the outcome at 6 months follow-up of three different ultrasound-guided treatment options for De Quervain's disease.

#### METHOD AND MATERIALS

#### RESULTS

No adverse reactions occurred. At 1-month follow-up we found: group 1, mean thickness=0.5mm, mean VAS=1.5, mean quickDASH=22; group 2,0.6,1.4,23; group 3,0.5,1.2,21. At 3-month follow-up: 0.5,1.1,21;0.6,1.2,21;0.4,1.1,21. At 6-month follow-up: 0.8,3.4,32;0.6,2.1,26;0.5,1.0,19. VAS and quickDASH are graphically represented in Figure 1.

#### CONCLUSION

Ultrasound-guided intracompartment injection of triamcinolone acetonide+sodium hyaluronate seems to represent a promising approach to treat De Quervain's disease, reducing symptoms recurrence up to six months.

#### CLINICAL RELEVANCE/APPLICATION

Combined injection of steroid and hyaluronic acid is effective to treat De Quervain's disease and prevents symptoms recurrence up to six months.

### VSMK31-13 • Ultrasonography of the Radial and Ulnar Collateral Ligaments of the Wrist with Surgical Correlation

**Mihra S Taljanovic MD (Presenter) ; Stephen Johnston ; Wynter N Phoenix MD ; Joseph E Sheppard MD**

#### PURPOSE

To re-evaluate the utility of high-resolution sonography (HRUS) in the assessment of collateral ligaments of the wrist.

#### METHOD AND MATERIALS

HRUS of the radial (RCL) and ulnar (UCL) collateral ligaments of the wrist was performed on 56 cadaveric wrists on the General Electric Logiq 9 ultrasound machine, with a 9-12 MHz linear hockey stick transducer. Both ligaments were primarily scanned in the longitudinal axis using the anatomic landmarks. The visibility of these ligaments was assessed during the sonographic examination by the examiner and additional 3 observers (surgery resident, medical student and ultrasound technologist). The ligaments were classified as well seen, adequately seen or not seen on sonography. Surgical dissections of 12 RCLs and 12 UCLs in 6 cadavers with their surrounding relationships to the extensor tendons and dorsal compartments of the wrist were subsequently performed. The ligaments were classified as present or absent and graded I or II depending on the surgeon's subjective assessment of ligamentous thickness (I- thick, II- thin). HRUS and dissection results were then compared.

#### RESULTS

The RCLs were seen on sonography in all cadaveric wrists in their anatomic locations between the radial styloid and radial aspect of the scaphoid, dorsal to the radial artery and deep and somewhat dorsal to the 1st extensor compartment. They had an echogenic fibrillar appearance. All UCLs had an appearance of a thick echogenic band and were seen between the ulnar styloid and triquetrum abutting the deep aspect of the 6th extensor compartment. In 9 cadavers, 18 right and left RCLs were well seen and in the remaining 19 cadavers they were adequately seen. In 8 cadavers, 16 right and left UCLs were well seen and in the remaining 20 cadavers they were adequately seen. On sonography, the investigators were uncertain if what they called UCLs represent true ligaments or thickening of the joint capsule. On surgical dissections all RCLs and UCLs were proven to be true ligaments. On dissections, 9 of 12 RCLs were graded I and 3 were graded II. All UCLs were graded I on dissections. All of the dissected ligaments were well seen on sonography.

#### CONCLUSION

The RCL and UCL of the wrist are true ligaments that can be well seen on HRUS.

#### CLINICAL RELEVANCE/APPLICATION

The collateral ligaments of the wrist are true ligaments and can be well seen on HRUS which can be utilized in clinical practice in evaluation of these structures.

### VSMK31-14 • Prognosis Value of Ultrasonographic Assessment in Muscle Strain Injuries: Longitudinal Study of a 70 Elite Athletes Cohort

**Jerome Renoux MD (Presenter) ; Jean-Louis Brasseur ; Philippe Thelen ; Christian Dibie**

#### PURPOSE

To evaluate prognosis value of ultrasonography performed in the first days of muscle strain injuries.

#### METHOD AND MATERIALS

A prospective cohort study was lead between 2010 and 2012 in the French National Sport Institute. Ultrasonographic assessment of muscle strain lesions was performed between the 2nd and the 8th day. Return to play (total or best clinical recovery) was evaluated with a benefit of a six months hindsight. Correlation between ultrasonographic signs and clinical prognosis was statistically evaluated. Echographic signs included the local semiology (Rodineau and Durey's 5 grades classification system was used) , lesion size, lesion type (myofascial vs. pure fascial), and location of the lesion (muscular group, centromuscular vs. perimuscular, proximal vs. distal).

Echographic and clinical follow-up were performed until return to play.

## RESULTS

70 patients were recruited. 67% of the lesions were located at the lower limbs, 20% at the upper limbs and 13% at the abdominal or thoracic walls. Mean delay between trauma and ultrasonography was 4,5 days. 3 percents were grade 0 injuries, 33% grade 1, 42% of grade 2, 20% of grade 3 and 2% of grade 4. Return to play time differed between the 5 grades of injuries (respectively 1,2±0,8 ; 3,1±1,2 ; 4,8±1,6 ; 8,5±3,8 ; 18 ± 10 weeks ; p = 0.03). Myofascial lesions were correlated with a better lay-off time compared to pure fascial lesions (4,7 vs. 5,8 weeks ; p= 0.02). Proximal lesions had a poorer prognosis compared to distal lesions (5,2 vs. 3,9 weeks ; p = 0.009). Recurrence occurred in 16%.

## CONCLUSION

Ultrasonography has a good prognosis value for muscle strain lesions. For this purpose, ultrasonography has to describe precisely the grade, the lesion type and its precise location.

## CLINICAL RELEVANCE/APPLICATION

Ultrasonography can help clinicians to determine prognosis of muscle strain lesions. It helps to distinguish two types of lesions (pure fascial and myofascial) with different treatments.

### VSMK31-15 • Interesting Musculoskeletal Ultrasound Cases

**Jon A Jacobson MD** (Presenter) \*

#### LEARNING OBJECTIVES

1) Be familiar with important topics in musculoskeletal ultrasound.

## Nuclear Medicine Series: Non-FDG PET Radiotracers in Oncology

**Tuesday, 08:30 AM - 12:00 PM • S505AB**



[Back to Top](#)

**VSNM31 • AMA PRA Category 1 Credit™:3.25 • ARRT Category A+ Credit:4**

#### Moderator

**Jonathan E McConathy**, MD, PhD \*

#### Moderator

**Hossein Jadvar**, MD, PhD

### VSNM31-01 • Proliferation Imaging: FLT/PET in Oncology

**David A Mankoff MD, PhD** (Presenter)

#### LEARNING OBJECTIVES

1) Describe the kinetics of thymidine relevant to FLT PET imaging. 2) Discuss approaches to FLT image interpretation. 3) Describe studies that have tested FLT PET as a marker cancer response to treatment.

### VSNM31-02 • Quantitative Study of 18F-fluorodeoxyglucose and 18F-fluorothymidine PET Characteristics in Esophageal Squamous Cell Carcinoma Staging

**Changsheng Ma MS** (Presenter) ; **Yong Yin**

#### PURPOSE

To quantitatively evaluate the value of diagnostic information provided by both 18F-FDG and 18F-FLT PET and quantitatively investigated whether 18F-FLT PET had a better performance compared with 18F-FDG PET in esophageal squamous cell carcinoma (ESCC) staging and delineation.

#### METHOD AND MATERIALS

26 patients with newly diagnosed ESCC and underwent pretreatment 18F-FDG and 18F-FLT PET were included in this study. The indices such as the standardized uptake value (SUV), gross tumor length and extracted texture parameters between 18F-FDG and 18F-FLT PET were compared, respectively. Moreover, the indices relationship between 18F-FDG and 18F-FLT PET mentioned above, were analyzed using Spearman's correlation coefficient and Paired T-test. Subsequently all patients received esophagectomy and the extracted PET indices capability in ESCC pathological staging were assessed by Kruskal-Wallis test and Mann-Whitney test. In addition, tumor delineation length on 18F-FDG (SUV threshold 2.5) and 18F-FLT (SUV threshold 1.4) PET were validated by pathologic gross tumor length.

#### RESULTS

#### CONCLUSION

The 18F-FDG and 18F-FLT PET scans have their own advantages in ESCC staging and tumors were well identified as the nonphysiologic distribution of radiotracers intensity typically higher than normal tissues on either PET scans. Delineation on the two types of PET with proper threshold can both provide accuracy estimation of pathologic tumor length. Those different indices extracted from PET scans can be potentially employed to differentiate AJCC and TNM in ESCC stage.

#### CLINICAL RELEVANCE/APPLICATION

No

### VSNM31-03 • Diagnostic and Prognostic Value of Nodal Staging by 4'-[Methyl-11C]-Thiothymidine (4DST) PET/CT in Non Small Cell Lung Cancer

**Ryogo Minamimoto MD, PhD** (Presenter) ; **Jun Toyohara** ; **Miyako Morooka MD** ; **Yoko Miyata** ; **Momoko Okazaki** ; **Kazuhiko Nakajima** ; **Kiichi Ishiwata** ; **Kazuo Kubota MD**

#### PURPOSE

4'-[methyl-11C]-thiothymidine (4DST) is a novel PET tracer available for evaluating proliferation of malignancy. We prospectively compared the diagnostic ability of 4DST PET/CT and FDG PET/CT for detection of regional lymph node metastasis of non-small cell lung cancer (NSCLC). In addition, we surveyed the relation between these PET results and prognosis of NSCLC patients.

#### METHOD AND MATERIALS

A total of 31 patients with NSCLC underwent 4DST PET/CT and FDG-PET/CT. PET imaging was obtained from 40 min for 4DST and 60 min for FDG after injection. The PET/CT images were evaluated qualitatively and quantitatively for focal uptake of each PET tracers, according to American Joint Committee on Cancer staging system. Surgical and histologic results were regarded as reference standards. Patients were followed up 2 years after surgery for survey of recurrence. A multivariate analysis was performed to assess the prognostic significance of T stage, N stage and maximum SUV of 4DST and FDG for primary lung tumor.

#### RESULTS

Four patients were inoperable by being proved dissemination during surgery. In 27 patients with 156 resected lymph nodes, metastasis



was pathologically proved in 9 patients with 17 lesions. On a per-lesion basis, sensitivity, specificity, positive predictive value, negative predictive value and accuracy for lymph node staging were 82, 73, 33, 96 and 74 % respectively for 4DST, 29, 86, 25, 88 and 78% respectively for FDG. Statistical significant difference was confirmed in the sensitivity between 4DST and FDG. The cases with positive nodal findings by 4DST showed higher rate (91%) of lesion extent or recurrence within 2 years, compared to FDG (45%). Multivariate analysis showed that N stage by 4DST was most influential prognostic factor for recurrence or lesion extent.

#### CONCLUSION

4DST PET/CT showed high sensitivity for the detection of lymph node metastasis, and it was independent prognostic value for recurrence or lesion extent in NSCLC.

#### CLINICAL RELEVANCE/APPLICATION

4DST PET/CT can contribute to detect lymph node metastasis, and 4DST PET/CT can predict prognosis for recurrence or lesion extent in NSCLC.

### VSNM31-04 • Bone PET Imaging: NaF PET in Oncology

**Baris Turkbey MD** (Presenter)

#### LEARNING OBJECTIVES

1) To identify the advantages of F-18 NaF PET/CT imaging in oncology. 2) To understand the importance of a standardized imaging protocol. 3) To become comfortable differentiating benign from malignant lesions on F-18 NaF PET/CT.

#### ABSTRACT

F-18 NaF PET/CT has been shown to have higher sensitivity and specificity than planar <sup>99m</sup>Tc-MDP bone scanning in several small studies. The concomitant acquisition of anatomic images permits immediate correlation of any abnormal findings. Additionally, F-18 NaF PET/CT bone imaging can be quantitated, allowing bone disease to be  $\diamond$ measurable $\diamond$ , increasing its utility therapy monitoring. When a consistent F-18 NaF uptake period is used, the SUV values are highly reproducible, and due to the high extraction fraction, high quality images can be obtained with a radiation dose exposure similar to that of Tc-99m MDP (including the low dose CT scan). This presentation will discuss the benefits and challenges of F-18 NaF PET/CT in oncology.

### VSNM31-05 • Prospective Evaluation of Planar Bone Scintigraphy, SPECT/CT, <sup>18</sup>F NaF PET/CT and Whole Body 1.5T MRI for Detection of Bone Metastases in High Risk Breast and Prostate Cancer Patients

**Ivan Jambor MD** (Presenter) ; **Anna Kuisma** ; **Riikka Huovinen** ; **Minna Sandell** ; **Joakim Auren** ; **Sami A Kajander MD** ; **Jukka Kemppainen** ; **Jani Saunavaara** ; **Tommi Noponen** ; **Heikki R Minn MD, PhD \*** ; **Hannu J Aronen MD, PhD** ; **Marko Seppanen**

#### PURPOSE

The aim of the study was to compare the diagnostic accuracy of <sup>99m</sup>Tc-methylene-diphosphonate planar bone scintigraphy (<sup>99m</sup>Tc-MDP BS), <sup>99m</sup>Tc-methylene-diphosphonate single photon emission tomography/computed tomography (<sup>99m</sup>Tc-MDP SPECT/CT), <sup>18</sup>F NaF PET/CT and whole body 1.5 Tesla MRI (wbMRI) for the detection of bone metastases in high risk breast cancer and prostate cancer patients.

#### METHOD AND MATERIALS

Twenty-five breast cancer and twenty-six prostate cancer patients at high risk of bone metastases prospectively underwent <sup>99m</sup>Tc-MDP BS, <sup>99m</sup>Tc-MDP SPECT/CT, <sup>18</sup>F NaF PET/CT and wbMRI. Coronal T1-weighted, T2-weighted STIR, axial diffusion weighted images (b-values: 0, 150, 1000 s/mm<sup>2</sup>) covering whole body were acquired. Four independent reviewers interpreted each individual modality, grading lesions as suspicious, equivocal and benign, without the knowledge of other imaging findings. The final metastatic status was based on the consensus reading of all imaging modalities. The bone findings were compared on patient and region basis. In the region based analysis, the skeleton was divided into five regions.

#### RESULTS

Based on the consensus reading, 18 (35%) patients and 54 (21%) regions had presence of bone metastases while 33 patients and 201 regions were free of bone metastases. <sup>99m</sup>Tc-MDP BS was false negative in 4 patients. In the region based analysis, the sensitivity for <sup>99m</sup>Tc-MDP BS, <sup>99m</sup>Tc-MDP SPECT/CT, <sup>18</sup>F NaF PET/CT and wbMRI was 70%, 87%, 98% and 90%, respectively. The number of equivocal findings for <sup>99m</sup>Tc-MDP BS, <sup>99m</sup>Tc-MDP SPECT/CT, <sup>18</sup>F NaF PET/CT and wbMRI was 30, 6, 8, 2, respectively. wbMRI provided clinically useful information concerning soft tissues in 6 patients while CT in 4 patients.

#### CONCLUSION

Whole body 1.5T MRI, including diffusion weighted imaging, had similar diagnostic accuracy for detecting bone metastases in high risk breast and prostate cancer patients as <sup>99m</sup>Tc-MDP SPECT/CT, <sup>18</sup>F NaF PET/CT. These modalities were significantly more sensitive in region based analysis than <sup>99m</sup>Tc-MDP BS and provided increased diagnostic confidence. Additional soft tissues information provided by whole body 1.5T MRI has potential to affect the patient management.

#### CLINICAL RELEVANCE/APPLICATION

Whole body MRI showed similar sensitivity for detecting bone metastases in high risk breast and prostate cancer patients as <sup>99m</sup>Tc-MDP SPECT/CT, <sup>18</sup>F NaF PET/CT and was superior to bone scintigraphy.

### VSNM31-06 • Quantitative Imaging Biomarkers in Whole Body <sup>18</sup>F-Sodium Fluoride (<sup>18</sup>F-NaF) PET-MRI to Evaluate Prostate Cancer Bone Metastases

**Luis S Beltran MD** (Presenter) ; **Christopher Glielmi PhD \*** ; **Fabio Ponzo MD** ; **Andrew B Rosenkrantz MD** ; **Rajan Rakheja** ; **Anna Ferrari MD** ; **Marc H Schiffman MD** ; **Scott Tagawa MD** ; **David Nanus MD** ; **Himisha Beltran MD** ; **Michael P Recht MD**

#### PURPOSE

To correlate quantitative PET and MR diffusion weighted imaging parameters in prostate cancer (PC) bone metastases utilizing whole body <sup>18</sup>F-Sodium Fluoride (<sup>18</sup>F-NaF) PET-MRI

#### METHOD AND MATERIALS

6 men (median age 73, range 63-83) with advanced PC and known bone metastases underwent whole body PET-MRI (Siemens Biograph mMR) 45 minutes after the intravenous administration of 9 mCi of <sup>18</sup>F-Sodium Fluoride (<sup>18</sup>F-NaF). The maximum Standardized Uptake Value (SUVmax), mean Apparent Diffusion Coefficient (ADCmean), and Intravoxel Incoherent Motion (IVIM) parameters including fast component of diffusion (Dfast), slow component of diffusion (Dslow), and Perfusion Fraction (PF) from multi-b value diffusion weighted imaging were calculated in dominant bone lesions (diameter > 1.5 cm). Correlation between SUVmax and ADCmean, Dfast, Dslow, and PF were evaluated using Spearman rank correlation (r). Two patients underwent biopsy of metastatic lesions.

#### RESULTS

15 metastatic bone lesions were evaluated. The average value for SUVmax was 28.6 (5.9-61.7, SD 27). The average value (10<sup>-3</sup> mm<sup>2</sup>/sec) for ADCmean was 0.93 (0.47-1.8, SD 0.38), for Dfast was 18.2 (11-28, SD 4.5), and for Dslow was 0.98 (0.4-1.7, SD 0.39). The average PF (%) was 10.3 (3.2-18.5, SD 5.1). There was a significant negative correlation between SUVmax and ADCmean (r=-0.75; p=0.001). There were weak to moderate negative correlations between SUVmax and IVIM parameters (p>0.14): Dfast: r=-0.11; Dslow: r=-0.38; PF: r=-0.17. In both patients who had biopsies of metastatic lesions, the biopsy site was determined after reviewing the PET-MRI images. One patient had a biopsy of a bone lesion with a high SUVmax of 48.9 in the L5 vertebral body. Another patient had a biopsy of a metastatic supraclavicular lymph node rather than a bone lesion due to a low SUVmax value of 5.9 of the dominant bone lesion. Both patients with biopsies of metastatic lesions, were positive for metastatic PC.

#### CONCLUSION

ADCmean and SUVmax show a significant negative correlation in 18F-NaF PET-MRI. IVIM parameters showed weak to moderate negative correlations with SUVmax and may provide complementary information to ADC and SUV, thus warranting further attention in future larger studies.

#### CLINICAL RELEVANCE/APPLICATION

Our pilot data shows feasibility of 18F-NaF PET-MRI in providing quantitative metrics (SUV,ADC,IVIM) of PC bone metastases, which warrant study as biomarkers for biopsy planning and treatment response

### **VSNM31-07 • Prostate Cancer Choline PET Imaging and Other PET Tracers**

**Hossein Jadvar MD, PhD (Presenter)**

#### LEARNING OBJECTIVES

1) Review the major biological targets that may be useful for imaging in prostate cancer. 2) Understand the need for tailoring the imaging technique to the particular clinical phase of disease. 3) Analyze the current evidence with the potential utility of PET with various radiotracers in the imaging evaluation of prostate cancer.

#### ABSTRACT

Recent advances in the fundamental understanding of the complex biology of prostate cancer have provided increasing number of potential targets for imaging and treatment. In this presentation, I review the experience with a number of major PET radiotracers for potential use in the imaging evaluation of men with prostate cancer.

### **VSNM31-08 • [Cu-62]-ATSM PET-CT Study as Hypoxic Imaging in Patients with Gliomas: Comparison with Multitracer Approach Using [F-18]-FDG and [C-11]-Methionine**

**Ukihide Tateishi MD, PhD (Presenter) ; Kensuke Tateishi ; Ayako Shishikura ; Tomohiro Yoneyama ; Ikuo Torii ; Tomio Inoue MD, PhD ; Nobutaka Kawahara**

#### PURPOSE

The purpose of study was to investigate multitracer approach by [Cu-62]-diacetyl bis (N4-methylthiosemicarbazone) ([Cu-62]-ATSM) PET-CT as hypoxic imaging comparing with [F-18]-FDG PET-CT and [C-11]-Methionine PET-CT for differentiation of tumor grade in patients with glioma.

#### METHOD AND MATERIALS

Multitracer PET-CT studies using [Cu-62]-ATSM, [F-18]-FDG and [C-11]-Methionine were performed in 32 patients with glioma prior to surgery. The maximum standardized uptake value (SUV max), tumor/ background ratio (TBR), and volumetric analysis were quantitatively assessed. Distribution of trace uptake was qualitatively evaluated in comparison with MR images. To confirm tissue hypoxia, the transcription factor hypoxia inducible factor-1alpha (HIF-1alpha) utilized as a hypoxic marker was also assessed.

#### RESULTS

There were 17 glioblastoma multiformes (GBM) and 15 grade II or grade III gliomas. Of these, 19 (59.4%) patients were newly diagnosed. The SUVmax and TBR of [Cu-62]-ATSM were significantly higher in GBM than in non-GBM gliomas (p = 0.003 and 0.0001, respectively); however, there were no significant differences when assessed by [F-18]-FDG and [C-11]-Methionine. At a TBR cutoff threshold of 1.9, [Cu-62]-ATSM was the most predictive of GBM, with 94.1% sensitivity and 80.0% specificity. The mean TBR was significantly higher in HIF-1alpha positive tumors than those with HIF-1? negative tumors (p

#### CONCLUSION

Our results demonstrated that [Cu-62]-ATSM PET-CT provides the valuable information to discriminate GBM. [Cu-62]-ATSM appears to be a suitable tracer establishing attractive therapeutic strategies for hypoxic imaging in GBM.

#### CLINICAL RELEVANCE/APPLICATION

[Cu-62]-ATSM is a suitable biomarker establishing attractive therapeutic strategies for hypoxic imaging in GBM.

### **VSNM31-09 • Diagnostic Performance of Synthetic Amino Acid Anti-3-[18F] FACBC PET in Recurrent Prostate Carcinoma Detection**

**Oluwaseun Odewole MBBS, MPH (Presenter) ; Pooneh Taleghani MD ; Ashesh B Jani MD ; Bitai Savir-Baruch MD ; Leah M Bellamy ; Adeboye Osunkoya MD ; Weiping Yu PhD ; Raghuvveer K Halkar MD \* ; Peter Nieh MD ; Viraj Master MD ; Mark M Goodman PhD \* ; David M Schuster MD**

#### PURPOSE

anti-3-[18F] FACBC is a synthetic amino acid PET radiotracer with utility in detection of prostate cancer (Radiology 2011; 259:852). Following full accrual in a clinical trial, we investigate the diagnostic performance of anti-3-[18F] FACBC PET/CT in the detection of both prostatic and extraprostatic recurrence of prostate cancer.

#### METHOD AND MATERIALS

115 patients with suspected recurrent prostate carcinoma after definitive therapy for localized disease and negative bone scan underwent anti-3-[18F] FACBC. Studies were interpreted blindly to other imaging using established dual time point criteria. Correlation was made to histology and clinical followup by a multidisciplinary board.

#### RESULTS

109 out of 115 patients and 86 out of 115 patients had a reference standard sufficient to determine the presence of prostatic or extraprostatic disease respectively. Mean PSA ( $\pm$ SD) was 7.1( $\pm$ 7.7) ng/ml. Average follow-up after imaging was 41.5( $\pm$ 13.4) months. 94 of 115 (81.7%) examinations were positive. In the prostate bed, anti-3-[18F] FACBC had a sensitivity of 89.0%, specificity of 35.1%, accuracy of 70.6%, positive predictive value of 72.7% and a negative predictive value of 61.9% while for extra-prostatic disease detection, anti-3-[18F] FACBC had a sensitivity of 58.3%, specificity of 94.7%, accuracy of 74.4% positive predictive value of 93.3%, and a negative predictive value of 64.3%. All prostatic true positive lesions (100%) on FACBC and 89.3% of extra-prostatic lesions had histological confirmation of disease. On a whole body basis, true positive lesion detection rate was 16.7, 72.7, 85.2 and 84.3 at PSA (ng/ml) of 0-1, 1.1-2, 2.1-5 and >5.1 respectively.

#### CONCLUSION

anti-3-[18F] FACBC has favorable diagnostic performance in the detection of recurrent prostate cancer and can delineate prostatic from extra-prostatic recurrence.

#### CLINICAL RELEVANCE/APPLICATION

anti-3-[18F] FACBC is useful for restaging of patients with suspected prostate cancer recurrence.

### **VSNM31-10 • Hypoxia Imaging: FMISO PET Imaging in Oncology**

**Joseph G Rajendran MBBS (Presenter)**

#### LEARNING OBJECTIVES

1) Understand the evolution of tumor hypoxia and its biological implications. 2) Identify the mechanistic changes in tumor biology that will result in tumor resistance and poor patient outcome. 3) Learn novel ways to image tumor hypoxia with focus on FMISO PET imaging. 4) Understand the potential approaches to overcoming the negative impact of hypoxia.

#### ABSTRACT

The physiological microenvironment for a tumor is largely dictated by abnormal vasculature and metabolism. Many solid tumors develop

areas of hypoxia during their evolution caused by unregulated cellular growth, resulting in greater demand on oxygen for energy metabolism. Hypoxia induces a cascade of changes that reflects the homeostatic attempts (highly conserved evolutionally) to maintain adequate oxygenation that may result in tumor cells to adapt by developing more aggressive survival traits; mediated by Hypoxia Inducible Factor (HIF1a) part of the cellular oxygen sensing mechanism. Hypoxic tumors are not effectively eradicated with conventional doses of radiation and show resistance to several chemotherapy drugs. Hypoxia may also result in angiogenesis (itself a marker of tumor aggressiveness) mediated by Vascular endothelial growth factor (VEGF). While angiogenesis is a frequent consequence of hypoxia, some tumors develop extensive angiogenesis without the presence of hypoxia and vice versa. Advances in PET imaging instrumentation, coupled with the development of an increasing array of novel molecular probes, provide opportunities for imaging and selection of appropriate therapies to overcome the cure limiting effects of these two fundamental aspects of tumor microenvironment. The biology of tumor microenvironment related to hypoxia and its effect on patient outcome and developments in imaging technology and novel radiotracers for hypoxia imaging with a focus on F-18 FMISO would be reviewed. Challenges and novel treatments to overcome the cure limiting ability of hypoxia will be discussed.

### **VSNM31-11 • Correlation of F-18 Fluoromisonidazole PET Findings with HIF-1A and p53 Expressions in Head and Neck Cancer: Comparison with F-18 FDG PET**

**Takashi Norikane** (Presenter) ; **Yuka Yamamoto** MD, PhD ; **Yukito Maeda** ; **Nobuyuki Kudomi** ; **Yoshihiro Nishiyama** MD

#### **PURPOSE**

We evaluated tumor hypoxia using F-18 fluoromisonidazole (FMISO) positron emission tomography (PET) in relation to the expression of hypoxia-inducible factor-1? (HIF-1?) and p53 in patients with head and neck cancer and compared with 2-deoxy-2-F-18-fluoro-D-glucose (FDG) PET.

#### **METHOD AND MATERIALS**

A total of 28 tumors (23 primary tumors and 5 metastatic lymph nodes) from 24 patients with newly diagnosed head and neck cancer were examined with FMISO PET and FDG PET. The FMISO PET images were scaled to the venous blood concentration of FMISO activity to produce tumor-to-blood (T/B) values. Hypoxia was defined as a region with a T/B ratio of  $\geq 1.2$ . The maximum T/B ( $T/B_{max}$ ) and hypoxic volume were calculated by region-of-interest (ROI) analysis. For FDG PET, the maximum standardized uptake value ( $SUV_{max}$ ) and hypermetabolic volume were calculated by ROI analysis. The expressions of HIF-1? and p53 using immunohistochemistry were estimated in tumor tissue samples.

#### **RESULTS**

There was a significant correlation between hypoxic volume and  $T/B_{max}$  ( $r=0.53$ ,  $P=0.003$ ) using FMISO PET and between hypermetabolic volume and  $SUV_{max}$  ( $r=0.38$ ,  $P=0.046$ ) using FDG PET. The hypoxic volume using FMISO PET and hypermetabolic volume using FDG PET also showed a significant correlation ( $r=0.44$ ,  $P=0.020$ ). The values of FMISO hypoxic volume was significantly correlated with HIF-1? ( $r=0.40$ ,  $P=0.037$ ) and p53 ( $r=0.47$ ,  $P=0.012$ ) obtained on immunohistochemical examination.

#### **CONCLUSION**

These preliminary results suggest that hypoxic volume measured by FMISO PET may be a potential noninvasive biomarker for predicting tissue hypoxia in patients with head and neck cancer.

#### **CLINICAL RELEVANCE/APPLICATION**

Hypoxic volume measured by FMISO PET may be a potential noninvasive biomarker for predicting tissue hypoxia in patients with head and neck cancer.

### **VSNM31-12 • 18F-fluoroethylcholine (18F-Cho) PET/MRI Functional Parameters in Paediatric Brain Tumors**

**Francesco Fraioli** MD (Presenter) ; **Ashley M Groves** MBBS \* ; **Jamshed Bomanji** ; **Rizwan Syed** MBBS, FRCR ; **Asim Afaq** FRCR

#### **PURPOSE**

This study tested the principle that simultaneous 18F-fluoroethylcholine PET/MRI along with functional parameters ( $SUV_{max}/mean$  and  $ADC_{mean}$ ) is a valuable option for diagnosis, and response assessment, in children and adolescents with histological confirmed gliomas and intra-cranial germ cell tumors.

#### **METHOD AND MATERIALS**

18F-Cho PET MRI scans were performed in 10 children with biopsy proven intra-cranial tumours detected on MRI imaging. Five patients also underwent a second PET MR scan after chemotherapy. PET data were acquired simultaneously with the MR sequences. The standardized uptake values (SUVs) ratios between the lesion and normal brain tissue greater than background was indicative of a positive scan. Maximal Standardized Uptake Value ( $SUV_{max}$ ) and mean SUV ( $SUV_{mean}$ ) and apparent diffusion coefficient (ADC) Mean of the whole tumor ROI were recorded. For all tumors the association between the ADC mean and to SUV mean and max was assessed using the non-parametric Spearman correlation coefficient

#### **RESULTS**

In all the patients the ratio between 18F-cho lesion and normal brain tissue were significantly elevated and were shown to be independent predictors of the presence of gliomas. The areas of 18F-Cho uptake matched to areas of contrast enhancement and of restricted diffusion.

There was a negative correlation between  $SUV_{max}$  and  $ADC_{mean}$ .

Five patients had response assessment scans 6 weeks after chemo-radiotherapy; in four patients there was an agreement between volume changes, 18F-Cho and ADC values. In one patient there was a minimal reduction of  $SUV_{max}$  and mean and  $ADC_{mean}$ . In this patient the tumor volumetric dimensions were stable.

#### **CONCLUSION**

PET MR allows simultaneous acquisition of morphological and molecular images. ADC maps may provide additional information in staging and follow up brain tumors.

#### **CLINICAL RELEVANCE/APPLICATION**

PET MR allows simultaneous acquisition of morphological and molecular images. ADC maps may provide additional information in staging and follow up brain tumors.

---

## **Neuroradiology Series: Brain Tumors**

**Tuesday, 08:30 AM - 12:00 PM • N227**



[Back to Top](#)

**VSNR31 • AMA PRA Category 1 Credit™:3.25 • ARRT Category A+ Credit:4**

**Moderator**

**Soonmee Cha**, MD

**Moderator**

**Edmond A Knopp**, MD

**VSNR31-01 • Pre-op fMRI: Protocols and Pearls**

**Andrei I Holodny** MD (Presenter) \*

## **VSNR31-02 • Language Mapping with 3T Functional MRI: Application to Preoperative Planning of Patients with Diffuse Gliomas**

**Gregory Kuchcinski** (Presenter) ; **Charles Mellerio** ; **Johan Pallud** ; **Edouard Dezamis** ; **Guillaume Turc** ; **Raphaelle Souillard-Scemama** ; **Caroline Malherbe** DSc ; **Jean-Francois Meder** MD, PhD ; **Catherine Oppenheim** MD, PhD

### **PURPOSE**

To evaluate the accuracy of 3Tesla functional MRI (fMRI) for preoperative language mapping, compared to direct electric cortical stimulations (DCS) during awake surgery in adult patients with diffuse gliomas. To identify clinical and tumor factors associated with fMRI accuracy.

### **METHOD AND MATERIALS**

Language mapping with fMRI and DCS of 31 consecutive patients with diffuse gliomas (low-grade n=19, high-grade n=12) since January 2010 was analyzed. Three block-design paradigms were performed during fMRI (letter fluency, category fluency, semantic association). During awake surgery, the entire exposed cortex was stimulated to identify essential language areas. A site-by-site comparison between fMRI and intraoperative DCS mapping was performed, using a cortical grid (1 cm<sup>3</sup> voxels), with calculation of sensitivity and specificity. Influence of gender, age, previous oncological treatment and tumor features (volume, malignancy grade, contrast enhancement, perfusion) on fMRI accuracy (match vs. mismatch sites) was tested in uni- and multivariate analyses.

### **RESULTS**

Among 1637 tested cortical sites, 90 (5%) were positive for language during DCS. Sensitivity and specificity of the 3 language paradigms ranged from 29 to 41% and 89 to 90%, respectively. Higher sensitivity was achieved by combining the 3 tasks (60% [95%CI=49-70]); p

### **CONCLUSION**

Preoperative language mapping with fMRI, even at 3T, cannot replace intraoperative DCS in patients with diffuse gliomas. Combining the language tasks may improve its reliability. Tumor grade is associated with fMRI/DCS discrepancy.

### **CLINICAL RELEVANCE/APPLICATION**

fMRI is recommended as part of the presurgical planning of gliomas to assess language hemispheric dominance, though its reliability in localizing essential language cortical areas is insufficient.

## **VSNR31-03 • Usage of fMRI for Pre-surgical Planning in Tumor and Vascular Lesion Patients: Task and Statistical Threshold Effects on Language Lateralization**

**Matthew Andreoli** (Presenter) ; **Tanvi Nadkarni** ; **Veena A Nair** PhD ; **Bornali Kundu** ; **Peng Yin** ; **Brittany Young** ; **Chad H Moritz** RT ; **M. Elizabeth Meyerand** PhD ; **Vivek Prabhakaran** MD, PhD

### **PURPOSE**

Functional magnetic resonance imaging (fMRI) is a non-invasive pre-surgical tool that may be used to measure lateralization of language function in brain tumor and vascular lesion patients, and guide neurosurgeons to devise a surgical approach to treat lesions. We investigated the effect of varying the statistical thresholds as well as the type of language task on functional activation patterns and language lateralization. We hypothesized that language lateralization indices (LIs) would be threshold- and task-dependent.

### **METHOD AND MATERIALS**

Braining data were collected from brain tumor patients (n=67, average age 48 years) and vascular lesion patients (n=25, average age 43 years) who received pre-operative fMRI scanning. Both patient groups performed expressive (antonym and letter word generation) and receptive (text-reading, text-listening) language tasks. A control group (n=25, average age 45 years) performed the letter-word generation task.

### **RESULTS**

Brain tumor patients showed left-lateralization during antonym-word generation and text-reading tasks at high threshold values and bilateral activation during letter-word generation task, irrespective of varying the threshold values. Vascular lesion patients showed left-lateralization during the antonym and letter-word generation, and text-listening task at high threshold values.

### **CONCLUSION**

Our results suggest that the type of task and the applied statistical threshold influence LI and that the threshold effects on LI may be task-specific. Thus identifying critical functional regions and computing LIs should be done on an individual subject basis, using a continuum of threshold values with different tasks to provide the most accurate information for pre-surgical planning of lesion resections.

### **CLINICAL RELEVANCE/APPLICATION**

Examining lateralization index (LI) using a variable statistical threshold and different tasks may maximize retention of language activity in tumor and vascular lesion patients, post-surgically.

## **VSNR31-04 • Diffusion Applications in Brain Tumors**

**Aaron S Field** MD, PhD (Presenter)

### **LEARNING OBJECTIVES**

1) Review the fundamental mechanisms by which diffusion imaging can address problems of tissue characterization in brain tumor patients. 2) Examine the role of diffusion imaging in differential diagnosis of the most common brain tumors including meningioma, glioma, lymphoma, and pediatric tumors of the posterior fossa. 3) Understand the potential but also the limitations of diffusion tensor imaging in defining tumor margins and planning tumor resections. 4) Understand the role of diffusion imaging in evaluating brain tumor treatment-related effects, including cytoreductive therapeutic response, radiation necrosis, and treatment-related white matter injury.

## **VSNR31-05 • Diffusion Repeatability Evaluation And Measurement (DREAM)-MRI: A New Technique for Quantifying the Voxel-wise ADC Probability Density Function for Brain Tumor Characterization and Response Measurement**

**Benjamin M Ellingson** MS, PhD (Presenter) \* ; **Timothy F Cloughesy** MD \* ; **Whitney B Pope** MD, PhD \*

### **PURPOSE**

Diffusion MRI has been shown to be valuable for characterizing brain tumor cellularity and response to therapy; however, measurements of ADC can often be prone to noise contamination and other artifacts that lead to inaccurate measurement. We have developed a new method termed "diffusion repeatability evaluation and measurement" (DREAM)-MRI for repeatedly acquiring ADC measurements in a short period of time in order to construct the voxel-wise ADC probability density function (ADC PDF) and provide a measure of uncertainty in ADC estimation. In the current study we have examined this technique in phantoms, normal volunteers, and patients with glioblastoma.

### **METHOD AND MATERIALS**

All scans were performed on a 3T MR system (Siemens Trio; Erlangen, Germany). The ACR and ADNI phantoms were used to test ADC PDF dependence on pulse sequence parameters. A total of 10 healthy volunteers and 5 patients with glioblastoma were enrolled in the current study. DREAM-MRI consisted of a total of 100 diffusion measurements in the x, y, and z direction were obtained within 8 minutes for 10 slices using optimized partial Fourier encoding, parallel imaging, and echoplanar acquisition. ADC PDFs were constructed from the different samples and compared across sequence parameters and tissue types.

### **RESULTS**

ADC PDF variability was lowest using a b-value of 500s/mm<sup>2</sup>, but did not change appreciably across TR, TE, number of acquisitions, shimming technique, or T1 characteristics of the material (from ADNI phantom). Mean ADC and variability in ADC appeared correlated. As expected, normal white matter had a lower mean ADC and lower ADC variability compared with gray matter. Serial ADC PDFs showed no appreciable difference when volunteers were rescanned at a later time point. Glioblastoma patients showed low ADC PDF characteristics in

tumor regions, which changed serially as a result of radiation therapy.

#### CONCLUSION

DREAM-MRI is a novel technique for quantifying the voxel-wise ADC PDF and may be useful for evaluation of brain tumor response to therapy.

#### CLINICAL RELEVANCE/APPLICATION

Diffusion MRI is useful for brain tumor treatment evaluation, but ADC measurement uncertainty is a concern. The DREAM-MRI sequence overcomes this limitation.

### VSNR31-06 • Potential Use of Mean Apparent Diffusion Coefficient Values in Defining the Portal for Radiotherapy

**Daniel Jeong MD (Presenter) ; Sharon E Byrd MD ; Shalini Garg MD ; Mehmet Kocak MD**

#### PURPOSE

A major challenge in treating Glioblastoma Multiforme (GBM) is distinguishing the extent of tumor from surrounding inflammation and edema on conventional MRI sequences. The T1 post contrast and T2/FLAIR sequences are widely utilized to assess tumor extent and define the radiation portal for radiotherapy, but Apparent Diffusion Coefficient (ADC) maps are not as widely used. Multiple authors have shown a significant difference in ADC values for tumor, edema, and normal white matter. However, few studies have evaluated ADC values at sites of future tumor recurrence using pre and post treatment MRI exams. The aim of this study is to evaluate pre treatment mean ADC values at sites that gave rise to future tumor recurrence compared to similar background tissue that did not progress to tumor.

#### METHOD AND MATERIALS

Out of 110 consecutive patients with pathology proven GBM at our institution from 1/1/2009 to 5/31/2012, 20 had definitive post radiotherapy recurrence after 3 months and had received treatment and follow-up imaging at our institution. These 20 patients were included in this single-center retrospective cohort study. Pre and post radiotherapy MRI exams were evaluated, and the sites of tumor recurrence on post treatment exams were correlated with corresponding tissue on pretreatment exams and the type of background surrounding tissue was noted (edema, normal white or gray matter). Mean ADC values were compared for sites of future tumor recurrence and background tissue that did not progress to tumor recurrence.

#### RESULTS

The mean ADC value of brain tissue on pre-radiotherapy MRI exams in regions of future tumor recurrence was significantly lower than the mean ADC values in regions of surrounding tissue not progressing to tumor ( $p = 0.002$ ), without noticeable abnormalities seen on conventional T1 post contrast and T2/FLAIR MR sequences.

#### CONCLUSION

Mean ADC values may help predict sites of future tumor recurrence in GBM, and could be helpful in pre-radiation planning and identifying microscopic tumor prior to gross tumor recurrence on conventional MR imaging.

#### CLINICAL RELEVANCE/APPLICATION

Mean ADC values may help identify microscopic tumor prior to gross recurrence and should be considered during radiation planning.

### VSNR31-07 • Perfusion Methods in CNS Tumors

**Daniel P Barboriak MD (Presenter) \***

#### LEARNING OBJECTIVES

1) To gain familiarity with the basic principles used to derive imaging measurements of blood volume, blood flow and capillary permeability in brain tumors. 2) To learn the potential utility of perfusion imaging for providing insight into the processes of neoangiogenesis and into the methods of action of brain tumor therapies. 3) To understand how the challenges of lack of standardization in both image acquisition and analysis are being addressed by national research and cooperative groups.

#### ABSTRACT

In the context of brain tumors, perfusion imaging is a broad term referring to a variety of techniques measuring delivery of blood to tumors, the intrinsic vascularity of tumors, and the permeability of the blood brain barrier. The most commonly used techniques are dynamic susceptibility contrast-enhanced MRI (DSC-MRI), dynamic contrast-enhanced MRI (DCE-MRI) and arterial spin labeling (ASL). The most commonly used figures of merit corresponding to these techniques are relative cerebral blood volume and blood flow (rCBV, rCBF) for DSC-MRI, volume transfer coefficient and initial area under the gadolinium concentration curve ( $K_{trans}$ , IAUGC) for DCE-MRI and cerebral blood flow (CBF) for ASL. There is considerable interest in using these techniques to grade tumors by predicting either tumor pathology or patient survival, to distinguish between true progression and pseudoprogression / radiation necrosis in patients with recurrent enhancement after treatment, and to provide an earlier or more reliable indicator of patient response to treatment. Without question, perfusion imaging has provided insight into the brain tumor vascular microenvironment, which could be considered a phenotypic characteristic of tumors with important implications for tumor genomics, tumor pathophysiology and drug development. Although these techniques have been shown to influence therapy decisions for individual patients, multicenter clinical trials demonstrating the added value of perfusion imaging have yet to be successfully concluded. In this talk, four questions will be addressed. First, how are figures of merit derived from perfusion imaging related to underlying tumor pathophysiology? Second, how can these figures of merit be derived? Third, why have these techniques not yet been being integrated into routine clinical practice? Finally, what is the future outlook for these techniques?

### VSNR31-08 • Baseline Spin-Echo Echo-Planar Perfusion nCBV > 2.0 prior to Chemoradiation Is a Strong Independent Predictor of Poor Progression-free and Overall Survival in Patients with Newly Diagnosed Glioblastoma

**Ayca Akgoz MD (Presenter) ; Rifaquat Rahman ; Hui You ; Alhafidz Hamdan ; Ravi T Seethamraju PhD \* ; Patrick Y Wen MD \* ; Geoffrey S Young MD \***

#### PURPOSE

Prior studies have indicated that gradient-echo echo-planar (GE-EPI) perfusion weighted imaging (PWI) may be helpful in prognosis and treatment assessment in newly diagnosed glioblastoma (GBM) patients. While both animal and limited human data suggest that SE-EPI PWI data is more closely correlated with the presence of neovascularity and survival in GBM than GE-EPI PWI, no large series has assessed this. We assessed whether SE-PWI before and after initiating chemoradiation can stratify patients with respect to progression free survival (PFS) and overall survival (OS).

#### METHOD AND MATERIALS

Sixty-eight glioblastoma patients with interpretable pre and post-treatment SE-PWI were identified. In each study, normalized cerebral blood volume (SE-nCBV) was calculated by hot-spot method from 3 regions of interest (ROI) selected within the areas of maximal cerebral blood volume (CBV) in enhancing and/or non-enhancing tumor and 1 ROI selected within the contralateral normal appearing white matter. Univariate and multivariate Cox proportional hazards model was utilized to identify perfusion parameters predictive for PFS and OS. Receiver operator curve characteristic analysis was used to identify thresholds optimized for 15-month survival, and Kaplan-Meier estimates of PFS and OS were calculated.

#### RESULTS

In multivariate analysis, baseline mean SE-nCBV was predictive of PFS ( $p=0.038$ ) and OS ( $p=0.004$ ). Patients with a baseline mean SE-nCBV < 2.0 had a PFS (median 47.0 weeks,  $p < 2.0$ ) (median PFS 25.3, median OS 56.0 weeks). Exploratory multi-group stratification demonstrated that survival was inversely proportional to baseline mean SE-nCBV over a range from 2.0 - 4.0 ( $p=0.025$ ) suggesting a 'dose dependency' for SE-nCBV as a survival marker.

#### CONCLUSION

Baseline mean SE-nCBV prior to chemoradiation promises to be strongly predictive of poor chemoradiation response and poor survival in the subgroup of GBM patients with SE-nCBV >2.0. Prospective evaluation of SE-nCBV as a marker to select patients for more frequent monitoring and possibly early initiation of adjunctive therapy is indicated.

#### CLINICAL RELEVANCE/APPLICATION

Glioblastoma patients with high SE nCBV prior to adjuvant radiochemotherapy should be monitored particularly carefully and strongly considered for adjuvant therapy when indicated.

### VSNR31-09 • Intravoxel Incoherent Motion of Malignant Brain Tumors: A Validation Study with Pathologic Correlation and Normalized Cerebral Blood Volume

**Chong Hyun Suh MD (Presenter) ; Ho Sung Kim ; Ji-Won Kang MD ; Seung Soo Lee MD ; Namkug Kim PhD ; Choong Gon Choi MD ; Sang Joon Kim MD**

#### PURPOSE

To validate the perfusion (f) and true diffusion (D) parameters derived from intravoxel incoherent motion (IVIM) MR imaging with pathologic correlation of hypervascular tumor (glioblastoma) and hypovascular tumor (primary CNS lymphoma, PCNSL) and normalized cerebral blood volume (nCBV) derived from dynamic susceptibility contrast MR perfusion imaging.

#### METHOD AND MATERIALS

Our institutional review board approved this study. Fifty-nine consecutive patients (33 men, 26 women, mean age 54.5 years) who had pathologically confirmed glioblastoma (n=38) or PCNSL (n=21) prior to any treatment were assessed using maximum f ( $f_{max}$ ) and minimum D ( $D_{min}$ ) derived from IVIM MR imaging. We acquired 16, different b-values. The best predictor for differentiating glioblastoma from PCNSL was determined by receiver operating characteristic (ROC) curve analyses. A corresponding nCBV was used for validation of the  $f_{max}$  using partial correlation analysis.

#### RESULTS

The mean  $f_{max}$  was significantly higher in the glioblastoma group ( $0.101 \pm 0.016$ ) than in the PCNSL group ( $0.021 \pm 0.010$ ) ( $p < 0.0001$ ). The mean  $D_{min}$  did not significantly differ between the two groups ( $P = 0.190$ ).  $f_{max}$  was an excellent predictor for differentiating glioblastoma from PCNSL (area under the curve, 0.987; 95% confidence interval (CI): 0.916, 0.996; cut-off value, 0.025), with a sensitivity of 97.4% and a specificity of 90.5%. There was a significant positive correlation between  $f_{max}$  and corresponding nCBV for all cases ( $r = 0.651$ ;  $P < 0.0001$ ).

#### CONCLUSION

IVIM MR imaging can be used as a non-contrast, noninvasive imaging method to assess the diffusion and perfusion characteristics of malignant brain tumors.

#### CLINICAL RELEVANCE/APPLICATION

Intravoxel incoherent motion (IVIM) MR imaging allows noninvasive, reliable distinction as part of the diagnostic workup for patients who are suspected of having malignant brain tumors.

### VSNR31-10 • Imaging the Post Therapy Brain

**Eu-Meng Law MBBS (Presenter) \***

#### LEARNING OBJECTIVES

1) To understand the challenges with current and novel therapeutics for brain tumors, particularly with regard to conventional imaging of the post therapeutic brain. 2) To understand the challenges with defining and characterizing pseudoprogression and the application of advanced MRI methods. 3) To understand pseudo response with anti-angiogenic agents therapy and the application of advanced MRI methods in characterizing pseudo response.

#### ABSTRACT

#### REFERENCES:

1. L.C. Hygino da Cruz Jr, Gasparetto E et al AJNR April 2011 2. Sanghera et al., Clin Oncol (R Coll Radiol). 2011 24:216-27 3. Shiroishi M, Law M et al MRI Clinics 2013

### VSNR31-11 • Proliferation Rate Estimates Derived from Serial Diffusion MR Scans Correlate with [18F]-FLT PET SUV Values in Recurrent Glioblastoma Treated with Bevacizumab

**Benjamin M Ellingson MS, PhD (Presenter) \* ; Timothy F Cloughesy MD \* ; Johannes Czernin MD \* ; Whitney B Pope MD, PhD \***

#### PURPOSE

Proliferation rate estimates from cell invasion, motility, and proliferation level estimate (CIMPLE) maps derived from fitting a novel spatiotemporal mathematical model to serial diffusion MR data have been shown to correlate with choline-to-NAA ratio using NMR spectroscopy, glioma grade, and PFS/OS during bevacizumab. These maps predict future contrast enhancement in approximately 30% of patients on bevacizumab, as suggested in a recent pilot study. Proliferation rates based on the time-rate-of-change in ADC values within a voxel may reflect proliferative potential. The current study examined the relationship between CIMPLE map estimates of proliferation rate and 18F-FLT PET SUV, a molecular marker of DNA synthesis, in order to test whether CIMPLE maps could spatially localize regions of proliferative tumor.

#### METHOD AND MATERIALS

Fourteen patients were enrolled in the current pilot study. All patients had at least three MRI scans and one 18F-FLT PET scan during bevacizumab therapy. MR scans consisted of at least a T2w, post-contrast T1w, and diffusion MR scan with  $b=0$  and  $1000s/mm^2$ . Diffusion MR scans were distortion corrected, then all follow-up MR scans were registered to the first post-treatment MR scans. CIMPLE maps were generated by fitting a voxel-wise spatiotemporal model of cell invasion and proliferation, assuming ADC a surrogate for cell density. A new matrix solution to the CIMPLE map algorithm was implemented for patients with >3 scans. 18F-FLT PET scans were acquired during the period of MR evaluation. PET SUV scans were co-registered to MR space for subsequent analyses.

#### RESULTS

Regions with high proliferation rate on CIMPLE maps appeared generally colocalized to regions of 18F-FLT PET. Average proliferation rate within contrast-enhancing regions was highly correlated with average 18F-FLT PET SUV (Pearson's correlation coefficient,  $R^2 = 0.79$ ,  $P$

#### CONCLUSION

Regions with elevated proliferation rate on CIMPLE maps derived from serial diffusion MR data appear to reflect regions undergoing rapid DNA synthesis as suggested by 18F-FLT PET.

#### CLINICAL RELEVANCE/APPLICATION

CIMPLE maps provide a non-invasive method for estimating tumor growth dynamics, which may be useful for treatment monitoring and predicting tumor progression.

### VSNR31-12 • Change in ADC of High Grade Glioma Infiltrative Component during Radiotherapy Predicts Treatment Response and Time-to-Progression

**Jin Rong Qu MD, PhD ; Jian-Ping Dai MD ; Tao Jiang ; Ayca Akgoz MD (Presenter) ; Ravi T Seethamraju PhD \* ; Qifeng Wang ; Shao-Wu Li ; Lin Ai ; Tianzi Jiang PhD ; Geoffrey S Young MD \***

## PURPOSE

Apparent diffusion coefficient (ADC) derived from diffusion-weighted imaging (DWI) is a promising marker for cellularity in a wide range of tumors. While change in ADC during chemoradiation is a rational marker for prediction of high grade glioma (HGG) patient response and prognosis, mixed success has been reported to date. This may be because temozolamide chemotherapy and angiogenesis inhibition induce changes in vascular permeability and edema that confound the correlation of ADC with cellularity. As such, we hypothesize that ADC should perform well as a marker of survival in a cohort of patients treated with radiotherapy (RT) alone.

## METHOD AND MATERIALS

In 25 patients who had undergone resection of HGG, ADC was measured in ROI placed in residual solid and infiltrative tumor before and after 30Gy RT. RT response during radiation was classified as complete resolution (CR), partial response (PR), stable disease (SD), or progressive disease (PD) based on conventional anatomic MRI images. Change in ADC during RT was correlated with treatment response, TTP and OS.

## RESULTS

As predicted, RT response correlated significantly with TTP (0.59;  $p=0.002$ ). Median TTP was 49.9 days for patients with PD compared with 202.7 days for SD, 208.0 days for PR, 234.5 days for CR. The ADC of the residual solid tumor increased during RT in the CR group but did not significantly change in the PD group. ADC of infiltrative tumor increased during RT in PD. Increase in infiltrative tumor ADC correlated significantly with shorter TTP (0.545;  $p=0.005$ ). Correlation between increase in solid tumor ADC and longer TTP (0.286;  $p=0.249$ ) did not reach statistical significance but showed a trend consistent with the prior literature.

## CONCLUSION

Decrease in non-enhancing infiltrative tumor ADC correlates with better RT response and longer progression free survival of HGG patients treated with radiation alone. This supports our hypothesis that temozolamide chemotherapy and angiogenesis inhibition effects on vascular permeability may significantly confound the use of ADC for detection of HGG response.

## CLINICAL RELEVANCE/APPLICATION

Increase in ADC of infiltrative tumor during RT of HGG correlates with worse treatment response, shorter time to progression and decreased overall survival.

## Pediatric Radiology Series: Chest/Cardiovascular Imaging I

Tuesday, 08:30 AM - 12:00 PM • S102AB

PD VA CH CA

[Back to Top](#)

**VSPD31** • AMA PRA Category 1 Credit™:3.25 • ARRT Category A+ Credit:3.5

### Moderator

**Shreyas S Vasanawala**, MD, PhD \*

### Moderator

**Taylor Chung**, MD

### Moderator

**Daniel W Young**, MD

**VSPD31-01** • State of the Art MRI and MRI of Congenital Heart Disease

**Frandics P Chan** MD, PhD (Presenter) \*

### LEARNING OBJECTIVES

1) To review the MRI environment and anesthesia requirements for pediatric patients with congenital heart disease. 2) To understand what MRI can do that echocardiography or catheter angiography cannot, and how this is used to advantage in congenital heart disease. 3) To explore advanced techniques, such as four-dimensional phase contrast imaging, real-time imaging, and non-contrast coronary angiography, that can expedite and increase the capability of cardiac MRI studies.

### ABSTRACT

Cardiac MRI is an established imaging tool for the assessment of congenital heart disease in children and adults. The lack of oncogenic radiation makes MRI the preferred tool over CT. However, in young patients who require general anesthesia, the imager should be familiar with the risks involved. While usually safe, general anesthesia has heightened risk in patients with aortic obstruction, pulmonary hypertension, arrhythmia, and ventricular failure. In current clinical practice, the three-dimensional capability of cardiac MRI is used to accurately assess ventricular volume and function. Flow measurement by two-dimensional phase contrast is used to assess shunt ratio, cardiac output, and valvular regurgitation. Comprehensive cardiac MRI examination for a patient with complex congenital heart disease can be time-consuming, and it requires an MRI operator with considerable skill and knowledge of cardiac anatomy. Four-dimensional phase contrast imaging capture a volume of the cardiac anatomy and flow physiology, which can be analyzed by post-processing, thereby simplifying the scan protocol and shortening the study time. Other advanced MRI techniques include real-time and pseudo-gated imaging for fetal studies, delayed-enhancement of myocardium for endocardial fibroelastosis, and MR coronary angiography for coronary anomalies.

**VSPD31-02** • Clinical Validation of Free Breathing Navigator Triggered Retrospectively Cardiac Gated Cine Steady-state Free Precession (NAV-SSFP) Imaging in Sedated Children

**Lamya A Atweh** MD (Presenter) ; **Amol Pednekar** PhD \* ; **Siddharth P Jadhav** MD ; **Esbén S Vogelius** MD ; **Raja Muthupillai** PhD \* ; **Rajesh Krishnamurthy** MD \*

### PURPOSE

The cine steady-state free precession (SSFP) is the preferred sequence for ventricular function evaluation, however it requires suspended respiration which is difficult in sedated children. Many groups perform multi-NSA acquisitions (MN) during free breathing. In this work, we validate a navigator triggered SSFP (NAV-SSFP) sequence that drives the magnetization to steady-state before cardiac gated cine acquisition in the sedated free-breathing pediatric population.

### METHOD AND MATERIALS

This prospective study was performed with IRB approval on 20 sedated children with congenital heart disease (age:  $7\pm 6$  yrs, HR:  $97\pm 22$  bpm, RespR:  $22\pm 9$  bpm). The cine SSFP sequence was modified to include respiratory triggering with Navigator [1]. Imaging was performed on a 1.5T MR scanner. Identical imaging parameters were used for MN (4 NSA) and NAV sequences, covering both ventricles in short-axis orientation (TR/TE/flip angle:  $3/1.5/60^\circ$ ; acquired voxel size:  $1.3\text{-}1.6 \times 1.3\text{-}1.8 \times 4\text{-}9.5$  mm<sup>3</sup>; SENSE acceleration factor: 2; temporal resolution: 30-45 ms). Image quality assessment (Figure 1) and quantitative volumetric analysis was performed by a single blinded user. One-sided Wilcoxon signed rank test and Box plot analysis were performed to compare the clinical scores. Bland-Altman (BA) analysis was performed on LV and RV volumes.

### RESULTS

The clinical scores for NAV-SSFP were consistently better than MN-SSFP (Table 1). Total score with equal weights to each clinical score category was significantly better for NAV compared to MN. EDef scores were significantly better for NAV-SSFP than MN-SSFP. ISA scores were identical. The BMC scores were not significantly different. BA analysis for LV volumes indicates that variability between NAV and MN acquisitions is comparable to inter and intra-observer variability reported in the literature (Table 2) [2]. Total scan duration for NAV-SSFP ( $4.1\pm 1.6$  min) was shorter than MN-SSFP ( $5.2\pm 0.8$  min).

#### CONCLUSION

Modifying the cardiac gated cine SSFP sequence for free-breathing and navigator triggering allows clinically diagnostic images in sedated patients without penalty for contrast, spatio-temporal resolution, or total scan time while significantly decreasing RF duty cycle and improving spatial detail. 1 ISMRM 3938, 2012 2 JMRI 28(39-50), 2008

#### CLINICAL RELEVANCE/APPLICATION

Free-breathing navigator triggered cine SSFP allows diagnostic images in sedated patients with improved spatial resolution and shorter scan times.

### VSPD31-03 • Noninvasive 4D Pressure Difference Mapping Derived from 4D Flow MRI in Patients with Repaired Aortic Coarctation: Comparison with Young Healthy Volunteers

**Fabian Rengier MD (Presenter) ; Michael Delles DiplEng ; Joachim Eichhorn MD ; Hendrik Von Tengg-Kobligh MD \* ; Hans-Ulrich Kauczor MD \* ; Roland Unterhinninghofen PhD ; Sebastian Ley MD**

#### PURPOSE

In patients with aortic coarctation, pressure measurements before and after repair currently are obtained by invasive catheterization or by echocardiography using the Bernoulli equation. Purpose of this study was to assess spatial and temporal pressure changes in patients with repaired aortic coarctation compared to young healthy volunteers using 4D flow MRI and derived 4D pressure difference maps.

#### METHOD AND MATERIALS

4D flow MRI of the thoracic aorta was performed at 1.5T in 13 patients after aortic coarctation repair without recoarctation (mean age 18.8 years, 5 female, 8 male) and 13 healthy volunteers (mean age 22.9 years, 4 female, 9 male). Spatial/temporal resolution was 1.6x1.6x2.1mm<sup>3</sup>/28ms. Using published algorithms and in-house developed image processing software, 4D pressure difference maps relative to the proximal ascending aorta were computed based on the Navier-Stokes equation. The thoracic aorta was divided into four segments: ascending aorta, aortic arch, proximal descending aorta and distal descending aorta. For each segment, spatial pressure range at mid systole and maximum slope of local pressure amplitudes were calculated.

#### RESULTS

Mean spatial pressure range at mid systole for patients/volunteers was (in mmHg): ascending aorta 1.8/1.6 (p=ns), arch 4.8/1.7 (p=0.02), proximal descending 8.9/1.6 (p

#### CONCLUSION

Noninvasive 4D pressure difference mapping derived from 4D flow MRI showed significant spatial and temporal changes in patients with repaired aortic coarctation compared to young healthy volunteers, particularly affecting aortic arch and proximal descending aorta, but also distal descending aorta. The technique can characterize such changes not only noninvasively but also in greater detail than echocardiographic pressure gradient measurements.

#### CLINICAL RELEVANCE/APPLICATION

4D pressure difference mapping can characterize spatial and temporal changes of intraluminal aortic pressure and may evolve into a noninvasive alternative to catheterization in coarctation follow-up.

### VSPD31-04 • Assessment of Conduit Size prior to Percutaneous Pulmonary Valve Replacement: Which MR Sequence Is Best?

**Ladonna J Malone MD (Presenter) ; Jane Gralla ; Uyen Truong ; Brian Fonseca ; Thomas Fagan MD ; Lorna Browne MD, FRCR**

#### PURPOSE

The advent of percutaneous pulmonary valve replacement (PVR), providing a nonsurgical approach to the management of severe pulmonary regurgitation in patients with right ventricle to pulmonary artery (RV-PA) conduits, has transformed treatment of patients with repaired congenital heart disease. Cardiac MRI (CMR) is increasingly relied upon to determine candidacy for percutaneous PVR using angiographic size criteria. In order to optimize the CMR assessment, our goal was to determine which pulse sequence had the best agreement with conventional angiographic measurement of the right ventricle to pulmonary artery (RV-PA) conduit obtained during percutaneous PVR.

#### METHOD AND MATERIALS

15 patients had CMR performed prior to percutaneous PVR procedure. Measurements of the narrowest diameter of the RV-PA conduit were obtained on the following sequences: cine gradient echo (GE) at end-systole and at end-diastole, T1 TSE obtained in systole, 3D gadolinium enhanced MRA, and 3D SSFP. Multiplanar reformats using 3D reconstruction software were used to measure both AP and transverse dimensions on 3D sequences, but only AP diameters if an RVOT plane was obtained (cine GE and T1 TSE). These were compared to angiographic measurements using Bland Altman plots and Intraclass Correlation Coefficient (ICC).

#### RESULTS

Cine GE measurements at end-systole had the best agreement with angiogram with a mean difference of 0.8 mm (95% limits of agreement -3.86 to 5.46 and ICC 0.75). The AP dimension on 3D MRA also had a high ICC (0.85) and a relatively narrow 95% limits of agreement (-0.89-5.67), but demonstrated a consistent over-measurement bias with a mean difference from angiogram of 2.39 mm. The 3D SSFP measurements demonstrated the worst agreement, likely due to inherent artifacts in stenosed conduits. Slow flow artifact on T1 TSE impaired accurate measurement in irregularly calcified conduits.

#### CONCLUSION

RV-PA conduit measurements obtained from cine GE at end-systole and 3D MRA demonstrate strongest agreement with conventional angiographic measurements in evaluating percutaneous PVR candidacy.

#### CLINICAL RELEVANCE/APPLICATION

Standardization of RV-PA conduit measurements with improved angiographic agreement should decrease incidence of unsuccessful percutaneous PVR procedures related to failure to meet size criteria.

### VSPD31-05 • Noninvasive Quantification of Aortopulmonary Collateral Flow and Intracardiac Shunt Flow for the Patients who Underwent Bidirectional Glenn Shunting

**Rongpin Wang MD (Presenter) ; Qiping Deng MD ; Meiping Huang MD**

#### PURPOSE

To explore the feasibility of calculating aortopulmonary collateral flow (APCF) and intracardiac shunt flow (ICSF) in patients underwent bidirectional Glenn shunt (BGS) by using phase-contrast MRI (PC-MRI) sequence.

#### METHOD AND MATERIALS

Twenty-two BGS patients (patient group) and 15 healthy volunteers (control group) were performed at 3.0 tesla MR system by using PC-MRI sequence to measure the flow of great vessels of right pulmonary artery (RPA), left pulmonary artery (LPA), ascending aorta (AA), superior vena cava (SVC) and inferior vena cava (IVC). The quantity of AA (Q<sub>AA</sub>), pulmonary (Q<sub>p</sub>) and venous return (Q<sub>v</sub>) per minute were calculated by using Report Card software. APCF and ICSF was calculated as the formula: APCF= Q<sub>S</sub>-Q<sub>v</sub>, ICSF= 2Q<sub>S</sub>- (Q<sub>v</sub>+Q<sub>p</sub>). The end-diastolic volume index (EDVI) of major ventricle were performed with cine-MRI sequence, and the regurgitation area of atrioventricular valve were measured with ultrasound cardiography. The difference of Q<sub>p</sub>, Q<sub>S</sub> and Q<sub>v</sub> and blood flow of great vessels intragroup were assessed by using paired samples t-test. The relationship of ICSF with EDVI of major ventricle and with the regurgitation area of atrioventricular valve was evaluated with correlation and regression analysis.

#### RESULTS

In control group, Q<sub>p</sub>: Q<sub>S</sub>: Q<sub>v</sub> were found to be 1: 1.009: 0.974. In patient group, Q<sub>S</sub> was found significantly higher than Q<sub>v</sub>, and Q<sub>v</sub> was



significantly higher than Qp. The blood flow of great vessels in patient group were found to be significantly lower than that of in control group except the flow of AA, while the regurgitation fraction of great vessels in patient group were found to be significantly higher than that of in control group. The APCF ranged from 0.23 to 1.63 l/min/m<sup>2</sup> (mean 0.88 l/min/m<sup>2</sup>), and the ICSF ranged from 0.22 to 1.29 l/min/m<sup>2</sup> (mean 0.61 l/min/m<sup>2</sup>). A positive relationship between ICSF and EDVI and the regurgitation area of atrioventricular valve were found ( $r=0.685$ , and  $r=0.806$ ).

#### CONCLUSION

The parameters of blood flow of great vessels can be reliably measured with PC-MRI sequence on 3.0 tesla MR system. And then, the SPCF and ICSF can be calculated.

#### CLINICAL RELEVANCE/APPLICATION

The APCF and ICSF can be calculated simultaneously in BGS patients by using phase-contrast MRI sequence, which may play an important role for therapeutic decision-making and evaluating prognosis.

### VSPD31-06 • Evaluation of the Pulmonary Vasculature in Mouse Models of Congenital Diaphragmatic Hernias

**Michael Phillips ; Daku Siewe BS (Presenter) ; Joshua C Tan ; Scott Moore ; Sean McLean ; Yueh Z Lee MD, PhD \***

#### PURPOSE

Congenital diaphragmatic hernia (CDH) is a common birth defect that leads to pulmonary hypertension. Decreased arterial development in the lung contributes to the pulmonary hypertension observed in CDH. The Slit3 knockout mouse is a viable mouse model for CDH that develops pulmonary hypertension (PHtn). We sought to quantitatively assess pulmonary artery blood vessel development using specimen CT scanning of the perfused pulmonary vasculature of mouse models of CDH.

#### METHOD AND MATERIALS

We perfused the pulmonary vasculature of 3 month old Slit3 wild type mice (no hernia) to Slit 3 knock mice (CDH/PHtn) using a radio-opaque material (microfil) with density tailored to minimize venous contamination. Vessel overfill was determined through examination by microscope. The mouse lungs with the filled vasculature were excised and scanned on a specimen scanner (Scanco microCT 40) at 8 micron resolution. The data was transferred for offline analysis using iNtuition (Terarecon). Vessel branching, length and diameter were measured.

#### RESULTS

5 wildtype (Slit3) and 5 CDH (Slit3 KO) were scanned. Severe hypoplasia was evident in the lungs from the CDH mice. Total lung volume was decreased in the knockout mice, consistent with the presence of a CDH. Vessel overfill The pulmonary vasculature was also altered, reflecting the abnormal development. Branch by branch vessel quantitation analysis is ongoing.

#### CONCLUSION

Quantitative analysis of pulmonary vasculature specimens from mice is readily feasible, providing a powerful new tool for the evaluation of mouse models of disease that effect the lung and lung development. We hope to combine our novel methods of in-vivo and ex-vivo imaging of these mouse models of CDH to add to the armamentum of pediatric radiologists. Though the imaging and analysis approaches are demonstrated in mice, the techniques may be readily translatable to clinically relevant imaging.

#### CLINICAL RELEVANCE/APPLICATION

Quantitative measures of the pulmonary vasculature are possible in mouse models of CDH, enabling a powerful tool for the evaluation of treatment effects that may be translated into children with CDH.

### VSPD31-07 • High Temporal versus High Spatial Resolution in MR Quantitative Pulmonary Perfusion Imaging of 2-year Old Children after Congenital Diaphragmatic Hernia Repair

**Meike Weidner (Presenter) ; Frank G Zoellner ; Claudia Hagelstein MD ; Stefan O Schoenberg MD, PhD \* ; Katrin Zahn ; Thomas Schaible ; Lothar R Schad PhD ; Wolfgang Neff MD, PhD**

#### PURPOSE

Congenital diaphragmatic hernia (CDH) leads to lung hypoplasia. Using dynamic contrast enhanced (DCE) MR imaging, lung perfusion can be quantified. As according to simulations absolute MR perfusion values depend on temporal resolution, we compared two different MR protocols to investigate firstly if impaired ipsilateral lung perfusion is present with both protocols in 2-year old children after CDH repair, secondly if simulation results can be confirmed and thirdly which protocol should be preferred.

#### METHOD AND MATERIALS

DCE-MRI was performed in 36 children after CDH repair using a 3D TWIST sequence. Two MR protocols were applied: protocol A (n=18) based on a high spatial (3.0sec;voxel size:1.25x1.25x1.25mm<sup>3</sup>) and protocol B (n=18) on a high temporal resolution (1.5sec;voxel size:2x2x2mm<sup>3</sup>). 0.05mmol/kg body weight of contrast agent (Dotarem, Guerbet, France) was administered. Pulmonary blood flow (PBF) was calculated for both lung sides by placing 6 cylindrical regions of interest (ROI), apical, middle and basal, in the ventral and the dorsal lung, respectively. Peak signal to noise ratio (PSNR) was calculated.

#### RESULTS

#### CONCLUSION

In 2-year old children after CDH repair ipsilateral lung perfusion is significantly reduced. Higher temporal resolution and increased voxel size show a gain of PSNR and significantly decrease the underestimation of PBF. Protocol B should therefore be preferred, as a 2 mm<sup>3</sup> isotropic voxel resolution is sufficient to detect side-differences of lung perfusion.

#### CLINICAL RELEVANCE/APPLICATION

In the long-term follow up of children after CDH, MR-perfusion imaging can help to quantify lung impairment without ionizing radiation. A temporal resolution of 1.5 sec is advisable.

### VSPD31-08 • Translational Experience in the Treatment of Duchenne Muscular Dystrophy (DMD) by Intra-arterial Transplantation of Mesoangioblasts (MABs): From a Toxicity Study in 10 Beagle Dogs to the First, Phase-1 Study in 3 Dystrophic Children

**Massimo Venturini MD (Presenter) ; Giulio Cossu ; Letterio S Politi MD ; Michele Colombo ; Giulia Agostini ; Alessandro Del Maschio MD**

#### PURPOSE

Literature lacks of complete, single-center translational studies. DMD, a genetic syndrome characterized by progressive absence of dystrophin protein, causes progressive muscle degeneration, paralysis and death. Corticosteroids are not effective, while novel therapies (gene/stem cells) are on work. Our aim was to assess MABs intra-arterial infusion in Beagle dogs and, subsequently, in 3 dystrophic children, at escalating dose, to preliminarily assess the safety.

#### METHOD AND MATERIALS

Every 3 weeks, 10 dogs, under immunosuppressive treatment (cyclosporine-A), were submitted to 4 intra-arterial infusions each (2 in one lower limb, 2 in aorta), of either MABs (n=6) or placebo (n=4). Dogs were sacrificed to assess toxicity after 251 days. One year later, after the approval on behalf of the institutional ethical committee and obtaining written informed consent from the children's parents, every 2 months 3 DMD children (mean age=10 years) under immunosuppressive treatment (tacrolimus) were submitted to 4 allogeneic MABs intra-arterial infusions each (2 in one lower limb, 2 multidistrict) using a 4-Fr introducer/catheter. Efficacy was assessed every 2 months by quantitative strength measurements (Kin-Com-test) and thighs/legs fibro-fatty degeneration/quantification (MRI), and after 8 months by gastrocnemius biopsies.

## RESULTS

No mortality related to MABs in Beagle dogs was recorded. The 12 intra-arterial MABs infusions were regularly performed with no peri-procedural complications, except for one successfully treated vasospasm. The only relevant complication was 1 focal thalamic ischemia of 1-cm (MRI) that occurred 5 hours after the fourth infusion, after sporadic atrial fibrillation (ECG) (Atrial-fibrillation-related-thrombosis? Late vasospasm?), without consequences. Relative stabilization/decrease in disease progression was observed. At MRI, a stabilization of fibro-fatty degeneration was more evident in the child treated at an earlier disease stage.

## CONCLUSION

Our translational experience about MABs intra-arterial transplantation in DMD, showed no signs of toxicity in beagle dogs and a relative safe and partial effective in dystrophic children, with encouraging future perspectives.

## CLINICAL RELEVANCE/APPLICATION

In DMD, a major MABs intra-arterial concentration, transplanted exclusively in the lower limbs, at an early disease stage, could determine an improvement of dystrophin restoration and clinical impact.

### VSPD31-09 • Coronary Artery Imaging in Children

**Cynthia K Rigsby MD** (Presenter)

#### LEARNING OBJECTIVES

1) To provide an overview of the imaging modalities used to image coronary arteries in children. 2) To show examples of anomalies of coronary artery origin, course, and termination. 3) To illustrate coronary artery anomalies associated with congenital heart disease. 4) To demonstrate coronary artery findings in Kawasaki disease.

#### ABSTRACT

Coronary artery anomalies can be classified as anomalies of origin and course, anomalies of coronary termination, coronary anatomy with congenital heart disease and acquired coronary abnormalities. Normal coronary artery anatomy and an imaging focused discussion of each of the different type of coronary abnormalities will be presented.

### VSPD31-10 • Correlation of CT and MR findings with Surgery for Anomalous Aortic Origin of Coronary Arteries (AAOCA)

**Lamya A Atweh MD** (Presenter) ; **Carlos M Mery MD** ; **Prakash M Masand MD** ; **Silvana M Lawrence MD, PhD** ; **Dean E McKenzie** ; **Rajesh Krishnamurthy MD** \*

#### PURPOSE

Anomalous aortic origin of the coronary artery (AAOCA) is commonly evaluated with magnetic resonance imaging (MRI) or computed tomography (CT) prior to surgery. Imaging targets include ostial location and morphology, intramurality, and presence of proximal stenosis. Precise description of the AAOCA morphology is important for surgical planning. Our objective is to correlate CT and or MRI with surgical findings in this high-risk population.

#### METHOD AND MATERIALS

IRB approval was obtained for our retrospective study. We identified all patients with AAOCA who were operated at our institution from 2003-2013. Patients who had no imaging available for review were excluded. Imaging was reviewed by a pediatric radiologist with 13 years of experience in cardiac imaging who was blinded to the results of the surgeries. Studies were assessed for the type of AAOCA, location and morphology of the anomalous ostium, right-left ostial relationship, and presence and length of intramural course. Surgical findings were reviewed for the same variables. The imaging interpretations were compared to the surgical data for concordance.

#### RESULTS

The patient population consisted of 16 patients (M:F = 10:6; age: 10 years ± 5), with 8 CT and 10 MR exams. 2 patients had both MRI and CT. CT was more accurate than MRI for all imaging targets (Table). MRI accurately predicted the type of coronary artery anomaly (90%) and ostial location (80%), but fared poorly in predicting type of R-L ostial relationship (60%), ostial morphology (10%) and intramurality (30%). Apart from its high accuracy for imaging targets, CT also provided virtual angioscopic views of the ostia that simulated surgical exposure.

#### CONCLUSION

CT is more accurate than MRI for characterization of critical imaging targets of AAOCA.

#### CLINICAL RELEVANCE/APPLICATION

CT is more accurate than MRI in defining ostial morphology, ostial relationship and intramural course and should be the imaging method of choice for AAOCA.

### VSPD31-11 • Compression of the Left Anterior Descending Artery during Percutaneous Pulmonary Valve Replacement: The Protective Role of Epicardial Fat?

**Ladonna J Malone MD** (Presenter) ; **Uyen Truong** ; **Brian Fonseca** ; **Thomas Fagan MD** ; **Lorna Browne MD, FRCR**

#### PURPOSE

The advent of percutaneous pulmonary valve replacement (PVR), providing a nonsurgical approach to the management of severe pulmonary regurgitation in patients with right ventricle to pulmonary artery (RV-PA) conduits, has transformed treatment of patients with repaired congenital heart disease. Extrinsic compression of the left anterior descending artery (LAD) during percutaneous PVR is a rare but potentially catastrophic complication, necessitating preoperative selective coronary angiogram with test balloon inflation to assess risk. If LAD occlusion is demonstrated, the percutaneous PVR is aborted. Cardiac MRI (CMR) is the gold standard in measuring RV size and optimal timing of PVR. Although LAD anatomy is well delineated on CMR, the minimum separation between the RV-PA conduit and LAD that would prevent LAD compression is unknown.

#### METHOD AND MATERIALS

16 patients underwent CMR prior to percutaneous PVR. Prior to PVR, 2 patients demonstrated extrinsic compression of the LAD during test balloon inflation while the other 14 did not. CMRs in both groups were retrospectively reviewed and the following data recorded in each: i) shortest distance between LAD and RV- PA conduit, ii) presence of circumferential epicardial fat surrounding the LAD, iii) thickness of conduit calcification, iv) proximal LAD course and v) relative position of the great vessels. Mean distance and minimum distance between LAD and RV-PA conduit were calculated in all patients and parameters in both patient groups compared.

#### RESULTS

In patients without extrinsic LAD compression, the mean distance from LAD to RV-PA conduit was 6.8 mm. The minimum distance was 1.6 mm. All these patients demonstrated a circumferential cuff of epicardial fat between the LAD and RV-PA conduit. Both patients with LAD compression had no measureable distance (0 mm) between the conduit wall and LAD, and a circumferential cuff of epicardial fat was absent. There was no significant difference in conduit calcification thickness between the two groups.

#### CONCLUSION

A circumferential cuff of epicardial fat between the LAD and RV-PA conduit decreases risk of extrinsic LAD compression during percutaneous PVR.

#### CLINICAL RELEVANCE/APPLICATION

The absence of a circumferential cuff of epicardial fat between the LAD and RV-PA conduit on a pre PVR CMR should raise concern for potential LAD compression during percutaneous PVR.

## VSPD31-12 • Cardiovascular CT in Neonates and Infants: Comparison of Effective Radiation Dose between Target-mode Prospective EKG-gated Volumetric CT Using 320 Detector Scanner and Ungated CT Using 64-slice Scanner

Siddharth P Jadhav MD (Presenter) ; Prakash M Masand MD ; Rajesh Krishnamurthy MD \*

### PURPOSE

The target mode of prospective EKG gating with the volumetric 320 detector scanner provides cardiac pulsation-related motion compensation for cardiovascular imaging without increasing radiation exposure when compared to ungated volumetric studies. The objective of this study is to compare target mode volumetric imaging (320) to ungated 64 slice imaging (64) for cardiovascular studies in neonates and infants for image quality, diagnostic efficacy and radiation exposure.

### METHOD AND MATERIALS

Following IRB approval, a retrospective evaluation of our experience with CTA for cardiovascular indications in neonates and infants aged 0-6 months was performed. 29 patients who underwent ungated imaging with 64 slice scanner from 2010-2012, and 22 patients who underwent volumetric imaging with the target protocol on the 320 detector scanner in 2012-2013 were included. Parameters collected included clinical history, indication for CT, qualitative assessment of image noise and pulsation related blurring, diagnostic efficacy, and radiation dose parameters (CTDI and DLP). Comparison was made to catheterization data and surgical reports for diagnostic accuracy.

### RESULTS

The distribution of clinical indications was comparable between the 64 and 320 groups, and included status of branch pulmonary arteries in Tetralogy of Fallot, evaluation of aortopulmonary collaterals or ductal dependent pulmonary flow in pulmonary atresia, anomalous pulmonary venous return, pulmonary vein stenosis, coarctation, heterotaxy, and vascular mediated airway compromise. All studies were diagnostic for the main clinical indication. Average DLP for target 320 studies was 11.6, with average effective dose of 0.75 mSv using conversion tables from ICRP publication 103. Average DLP for 64 slice studies was 63.88, with average effective dose of 4.31 mSv. The 320 studies resulted in higher image quality related to less pulsation artifact, with visualization of coronary origins in all but one case.

### CONCLUSION

Volumetric imaging with the target mode offers several advantages over previous generation scanners for cardiovascular indications in infants, including a 82% reduction in effective dose, ability to perform free-breathing studies, and improved image quality.

### CLINICAL RELEVANCE/APPLICATION

Volumetric imaging with target-mode of EKG gating offers improved image quality and reduced radiation dose when compared to 64 slice CT for cardiovascular imaging in neonates and infants.

## VSPD31-13 • Radiation Dose and Image Quality Comparison of Three Scan Schemes in Retrospective ECG-gated Coronary CT Angiography for Pediatric Patients

Zhiming Liu MD (Presenter) ; Yong Li Cao ; Yun Peng MD

### PURPOSE

Retrospective ECG-gated coronary CT angiography (CCTA) is often used in children because of their higher heart rates. In this study, we assessed the image quality and radiation dose of three scan schemes in order to select an optimal retrospective CCTA technique for maximum dose reduction.

### METHOD AND MATERIALS

60 consecutive patients (ages: 2months - 13years) were randomly assigned to three groups (20 in each group) for retrospectively ECG-gated CCTA with different tube current (mA) selection schemes. The tube voltage was 80kV, gantry rotation speed was 0.35s and helical pitches were between 0.16 and 0.20 based on patient heart rates for all groups. Group A used a fixed 350mA, group B used ECG modulated mA (350mA for 40-80% cardiac phases and 70mA for other phases), and group C also applied patient-dependent mA selection scheme for ECG modulation. The patient-dependent mA selection method was based on the CT value measurement in the scout view for individual patients. Image quality was assessed and image noise and CTDI value were measured for the three groups, and statistically compared with SPSS13.0.

### RESULTS

Image noises and their standard deviations were  $25.5 \pm 4.3$  HU,  $25.0 \pm 4.8$  HU and  $24.8 \pm 1.2$  HU, respectively, with no difference among the three groups ( $p > 0.05$ ). Group C had much less deviation in image noise than groups A and B. There were no statistical difference between image quality scores among the three groups ( $4.3 \pm 0.4$ ,  $4.4 \pm 0.3$  and  $4.5 \pm 0.4$ , all  $p > 0.05$ ). The effective doses were 4.39mSv, 3.23mSv and 2.34mSv for groups A, B and C, respectively. Dose reductions of 26% and 47% were achieved for groups B and C, respectively, compared with group A with the use of a fixed mA. Group C with the patient-dependent mA for ECG modulation had the lowest effective dose.

### CONCLUSION

Patient-dependent tube current scheme in retrospective CCTA for pediatric patients allows us to achieve a desired and consistent image quality across patient population, with the lowest radiation dose to patients.

### CLINICAL RELEVANCE/APPLICATION

Low kVp and patient-dependent mA in retrospective CCTA for pediatric patients allows us to achieve a consistent image quality across patient population, with the lowest radiation dose to patients.

## VSPD31-14 • Head Tracked Stereoscopic Pre-surgical Evaluation of Major Aortopulmonary Collateral Arteries in the Newborns

Francis P Chan MD, PhD (Presenter) \* ; Sergio Aguirre \* ; Holly Bauser-Heaton MD, PhD ; Frank Hanley MD ; Stanton B Perry MD

### PURPOSE

Children born with pulmonary atresia (PA) with major aortopulmonary collateral arteries (MAPCA) undergo early surgery to reconstruct their central pulmonary arteries. This surgery, unifocalization, requires precise mapping of all native vessels supplying the lungs and this is currently accomplished by catheter angiography (CA), with supplemental 3D information from CTA. As each patient has his unique vascular anatomy, visual comprehension can be extremely challenging. A recently developed head tracked stereoscopic system, True 3D, helps user manipulate and inspect holographic objects in free space. We test the hypotheses that interpretation of CTA in MAPCA cases using True 3D is faster than and as accurate as traditional tomographic readout.

### METHOD AND MATERIALS

With IRB approval, newborns less than 10-days old diagnosed with PA and MAPCA, who had CA and CTA of the chest within 2 weeks, were identified between 2007 and 2011. The CA images were evaluated by an experienced cardiologist for the origins and destinations of each native pulmonary artery and MAPCA to the lung segments. The CTA images were similarly scored by a cardiac radiologist using traditional tomographic readout and True 3D in two sessions separated by 4 weeks. Using CA as the reference standard, sensitivity, specificity, accuracy, these two approaches were calculated. Interpretation times were compared using paired Student's t-test.

### RESULTS

9 newborns (mean weight 3.2kg) produced 25 traceable MAPCAs in addition to native pulmonary arteries. Using an 18-segments lung model, 774 distinct vessel-segment combinations were compared. The sensitivity, specificity, and accuracy of tomographic readout are 81%, 93% and 91% respectively. For True 3D, they are 90%, 91% and 91% respectively. The average time for interpretation is significantly shorter with True 3D, 13 +/- 4 min, than with tomographic readout, 22 +/- 7 min ( $P = 0.0004$ ).

### CONCLUSION

This preliminary study demonstrates that head tracked stereoscopic interpretation of complex, minute pulmonary vessels in the newborn

is accurate as compared to traditional readout. The interpretation time is significantly faster with True 3D, and this is likely due to enhanced visual cognition using the stereoscopic approach.

#### CLINICAL RELEVANCE/APPLICATION

Advanced digital stereoscopy enhances visual cognition of complex anatomic relationship and is recommended for the evaluation of congenital anomalies of the pulmonary vasculature.

### VSPD31-15 • Determining the Normal Aorta Size in Infants and Children

**S. Bruce Greenberg MD ; Shilpa Hegde MD (Presenter) ; Shelly Lensing**

#### PURPOSE

No adequate standards for determining the normal range of effective diameters of the aorta or iliac arteries in children using CT or MRI exist. Our purpose is to establish normal standards for the effective diameter of the aorta at multiple levels and of the iliac artery origins.

#### METHOD AND MATERIALS

Chest, abdomen and pelvis computed tomography examinations with intravenous contrast performed in children without cardiovascular disease provided the data sets. Body surface area (BSA) was calculated from patient height and weight for each patient. Children age ranged from 0 to 20 years (mean 9.5 years, sd 5.7). Body surface area ranged from 0.2 to 2.5 meter<sup>2</sup> (mean 1.23 meter<sup>2</sup>, sd 0.59). Chest measurements were performed on 88 children and abdomen measurements on 110 children. Double-oblique 1 mm reconstructions were used to measure aorta and iliac artery effective diameter at multiple locations by two pediatric radiologists. Pearson correlation and linear regression compared the body surface area and effective diameter measurements.

#### RESULTS

The results are summarized in the table. Very strong correlation between BSA and effective diameter were present at all measured levels of the aorta and the iliac arteries. The derived linear regression equations and beta standard error are included in the table. **Aorta or iliac artery level Pearson correlation Effective diameter (mm) Beta S.E.** aorta annulus 0.94 10 + (7.8) BSA 0.30 sinus of Valsalva 0.93 11.8 + (9.5) BSA 0.41 STJ 0.90 8.9 + (8.2) BSA 0.43 Ascending aorta 0.91 9.1 + (8.6) BSA 0.43 Aorta arch 0.93 6.8 + (8.2) BSA 0.35 Isthmus 0.94 6.5 + (7.1) BSA 0.29 Prox desc aorta 0.93 6.5 + (6.6) BSA 0.29 Aorta at diaphragm 0.93 6.2 + (5.2) BSA 0.24 Superior to celiac axis 0.92 5.8 + (5.2) BSA 0.22 Renal artery level 0.91 4.2 + (5.0) BSA 0.22 Distal abdominal aorta 0.91 4.0 + (4.6) BSA 0.21 Right iliac artery 0.88 2.8 + (3.2) BSA 0.17 Left iliac artery 0.89 2.9 + (3.1) BSA 0.16

#### CONCLUSION

The expected effective diameter for children of any expected body surface area can be calculated from the equations at 8 levels in the chest and three levels in the abdomen. The common iliac artery effective diameters can also be calculated.

#### CLINICAL RELEVANCE/APPLICATION

The linear regression analysis equations allow radiologists to quantitatively determine if the aorta is hypoplastic or aneurysmal in children rather than rely on subjective impression.

### VSPD31-16 • Imaging of Adolescents and Young Adults with Congenital Heart Disease

**Lorna Browne MD, FRCR (Presenter)**

#### LEARNING OBJECTIVES

1) Describe the relevant complex cardiac anatomy encountered in CHD adolescents and young adults, many of whom have undergone prior surgical repairs. 2) Describe the most likely lesions encountered in CHD adolescents and young adults. 3) Discuss some common surgical repairs and encountered complications. 4) Determine appropriate MR protocols for evaluating congenital heart disease according to the anatomic, pathologic, and hemodynamic characteristics of the defect and type of previous surgical repair. 5) Discuss the main clinical questions that are specifically posed in individual cases of pre and post operative CHD in adolescents and young adults.

---

### Interventional Oncology Series: Lung

**Tuesday, 01:30 PM - 06:00 PM • S405AB**

**RO** **OI** **IR** **CH**

[Back to Top](#)

**VSI031 • AMA PRA Category 1 Credit™:4.25 • ARRT Category A+ Credit:5**

#### Moderator

**Alison R Gillams , MBChB \***

#### LEARNING OBJECTIVES

1) To learn the latest results of ablation in primary and secondary lung tumours. 2) To understand how to use the different ablation technologies (RF, MW and cryotherapy). 3) To learn optimal patient selection for lung ablation. 4) To understand the imaging appearances following ablation. 5) To know how to diagnose and manage possible complications following ablation.

### VSI031-01 • Primary Lung Cancer

**Robert D Suh MD (Presenter)**

#### LEARNING OBJECTIVES

1) Discuss long term outcomes of image-guided ablation for early stage lung cancer. 2) Discuss local control rates of image-guided ablation for early stage lung cancer. 3) Understand the factors in image-guided ablation influencing survival and local control. 4) Understand treatment options and relative outcomes of image-guided ablation compared to alternative therapies for early stage lung cancer.

#### ABSTRACT

Thermal ablation is a safe therapeutic and effective option to provide local control for 1♦ lung malignancies. Thermal ablation confers survival benefits in carefully selected patients: RF ablation with encouraging mid- and long-term results. Microwave and cryoablation remain promising techniques, requiring future studies for validation.

### VSI031-02 • Colorectal Lung Metastases

**Stephen B Solomon MD (Presenter) \***

#### LEARNING OBJECTIVES

View learning objectives under main course title.

### VSI031-03 • Sarcoma and Other Non-CR Lung Metastases

**Jean Palussiere MD (Presenter)**

#### LEARNING OBJECTIVES

View learning objective under main course title.

## **VSI031-04 • Irreversible Electroporation of Lung Metastases: Initial Experience**

**Thierry J De Baere MD (Presenter) \* ; Julien Joskin ; Antoine Hakime MD ; Geoffroy Farouil ; Lambros C Tselikas MD ; Frederic Deschamps**

### **PURPOSE**

Because recurrence rate of lung RFA has been reported higher when tumor are in contact with large vessels we used Irreversible Electroporation (IRE) used to treat such located lung metastases and reported herein our initial experience

### **METHOD AND MATERIALS**

### **RESULTS**

### **CONCLUSION**

IRE is well tolerated, induces a rapid decrease in size of the treated tumor but tumor regrowth is frequent within the first year of follow-up.

### **CLINICAL RELEVANCE/APPLICATION**

IRE of lung metastases, although inducing rapid decrease of the tumor size does not prevent later growth of the tumor. Consequently, the technique must be improved before routine clinical use.

## **VSI031-05 • What Does SBRT Contribute to the Management of Primary or Metastatic Lung Cancer?**

**Brian T Collins MD (Presenter) \***

### **LEARNING OBJECTIVES**

1) Review SBRT technology. 2) Review SBRT patient selection. 3) Discuss mature locoregional outcomes of SBRT for stage I NSCLC and pulmonary metastases. 4) Discuss mature survival outcomes of SBRT for stage I NSCLC and pulmonary metastases. 5) Review expected chronic toxicities of thoracic SBRT.

## **VSI031-06 • Clinical Tumour Board**

**Robert D Suh MD (Presenter) ; Stephen B Solomon MD (Presenter) \* ; Brian T Collins MD (Presenter) \* ; Jean Palussiere MD (Presenter)**

### **LEARNING OBJECTIVES**

1) Understand case-based information. 2) Identify treatment strategies. 3) Evaluate thoracic interventional procedures.

## **VSI031-07 • Interpretation of Follow-up Imaging**

**William H Moore MD (Presenter) \***

### **LEARNING OBJECTIVES**

1) Identify the findings on follow up imaging that are characteristic of post-ablation zones. 2) Identify the findings on follow up imaging that are characteristic of recurrence. 3) Compare the post ablation imaging findings between RFA, Microwave, Cryoablation and Nanoknife.

### **ABSTRACT**

## **VSI031-08 • Why, When and How I Perform RF Ablation of Lung Tumours**

**Jo-Anne O Shepard MD (Presenter) \***

### **LEARNING OBJECTIVES**

1) Understand multidisciplinary patient selection and describe the indications and contraindications to RFA of the lung. 2) Outline the RFA procedure including sedation, appropriate approach and positioning, equipment setup and treatment and followup protocols.

## **VSI031-09 • Why, When and How I Perform MW Ablation of Lung Tumours**

**Thomas J Vogl MD, PhD (Presenter)**

### **LEARNING OBJECTIVES**

1) Identify indications for MWA of lung tumors. 2) Identify procedure-related risk factors. 3) Learn about tips and tricks.

### **ABSTRACT**

Thermal ablation techniques have increasingly expanded their role in minimal invasive destruction of tumor tissue beyond the liver, especially in the lung. Both primary and secondary lung cancers are currently of interest among thermal ablation techniques such as laser therapy, radiofrequency ablation, and others. With its introduction microwave ablation (MWA) has rapidly gained its role as a precise, excellently controllable ablation technique.

In the following course different techniques of MWA of lung cancers will be presented. This includes techniques on the access, protocols for the ablation and preventive management of complications. Special focus is directed towards the daily management of risk factors at our institute in Frankfurt based on the up-to-date experience.

In the second part the indications for thermal ablation among other technologies such as radiooncology, surgery and systemic chemo-immunotherapy will be presented.

In summary, MWA of neoplastic diseases of the lung rapidly gains acceptance and provides excellent treatment results with a low rate of complications and side effects. Its current role among an armamentarium of other treatment techniques has to be searched for, documented, consolidated and expanded.

## **VSI031-10 • Evaluation of a Combined Protocol of Microwave Ablation (MWA) and Transpulmonary Chemoembolization (TPCE) versus MWA Only Protocol: Treatment of Primary and Secondary Nonresectable Lung Tumors**

**Thomas J Vogl MD, PhD (Presenter) ; Thomas Dauda BS ; Stefan Zangos MD ; Emmanuel C Mbalisike MD ; Nour-Eldin A Nour-Eldin MD, MSc**

### **PURPOSE**

To evaluate tumor response with volumetric assessment of tumor sizes after treating nonresectable primary and secondary lung tumors with transpulmonary chemoembolization (TPCE) combined with microwave ablation (MWA) versus MWA only protocol in palliative intention.

### **METHOD AND MATERIALS**

Between 2007 and 2012, 23 patients (10 males, 13 females; average, 61.2 years; range, 29-83) suffering from unresectable primary (n=3) and secondary lung tumors (n=20) were treated with TPCE (average, 4.3 sessions) followed by MWA. Another 13 patients (8 males, 5 females; average, 60.2 years; range, 28-83) suffering from unresectable primary (n=2) and secondary lung tumors (n=11) were only treated with MWA. Patients treated with a combined therapy suffered from primary lung tumors (n=3) and metastases of different origins such as colorectal carcinomas (n=6), breast cancer (n=5), urothel carcinoma (n=3), and others (n=6). Patients treated only with MWA suffered from primary lung tumors (n=2) and metastases of different origins such as colorectal carcinomas (n=6), and others (n=5). Follow-up was between 4 months and 3.7 years for primary and secondary lung tumors.

## RESULTS

All patients tolerated the combined treatment and the MWA only well and without adverse effects. The rate of spontaneously resolving pneumothoraces was 5.3% in the combined protocol and 4.1% in the MWA only protocol. According to the retrospective study data, in the combined treatment protocol complete response was documented in 30.4% (n=7) of lesions, while in 21.7% (n=5) stable disease was documented and in another 47.8% (n=11) a progressive disease situation. In the group of patients treated only with MWA (n=13), complete response was documented in 38.5% (n=5), stable disease in 7.7% (n=1) and progress in 53.8% (n=7).

## CONCLUSION

According to the first evaluated data the additional use of TPCE results in a slight improvement of the local response rate and a reduction of the rate of progression. Further prospective studies are, however, necessary.

## CLINICAL RELEVANCE/APPLICATION

Transpulmonary chemoembolization (TPCE) and microwave ablation (MWA) are relevant palliative treatment options in patients with primary and secondary nonresectable lung tumors

### VSI031-11 • Why, When and How I Perform Cryoablation of Lung Tumours

**Peter J Littrup MD (Presenter) \***

#### LEARNING OBJECTIVES

1) Understand the different approaches and techniques for thorough cryoablation of lung tumors (e.g., the ♦1-2 Rule♦), emphasizing unique benefits for chest wall, pleural-based, central and para-esophageal locations. 2) Understand techniques to minimize morbidity, assessing tumor location and approach. 3) Identify major imaging follow-up criteria for ablation success and any early failures. 4) Describe the overall cost-efficacy trade-offs for cryo vs. heat-based renal ablations vs. stereotactic body radiation therapy, in relation to tumor location, complications and recurrence rates.

#### ABSTRACT

Cryoablation of lung tumors offers a lower pain alternative than heat-based modalities, especially for pleural and/or chest wall locations. Central locations near major bronchi locations also have low rates of pneumothorax or broncho-pleural fistulas, while paraesophageal locations are readily protected by esophageal warming balloons. Major cryoablation benefits include its excellent visualization of ablation zone extent, low procedure pain and flexible hydrodissection of chest wall ablation sites near skin. CT-guidance is the cryoablation guidance modality of choice due to circumferential visualization and ready availability. MR-guidance has little clinical benefit or cost-efficacy.

For safety, cases will be considered for choosing the most avascular approach, extent of peri-bronchial contact and chest wall involvement. Imaging outcomes of complications and their avoidance will be shown. For optimal efficacy, tumor size in relation to number and size of cryoprobes emphasize the ♦1-2 Rule♦ of at least 1 cryoprobe per cm of tumor diameter and no further than 1 cm from tumor margin, as well as cryoprobe spacing of

### VSI031-12 • Thoracic Cryoablation: A Major Benefit for More Central and Chest Wall Locations?

**Peter J Littrup MD (Presenter) \* ; Hussein D Aoun MD ; Barbara A Adam MSN ; Evan N Fletcher MS, BA ; Mark J Krycia BS**

#### PURPOSE

To assess recurrence factors for percutaneous thoracic cryoablation. Tumor and ablation size, complications, location and vessel proximity were assessed for patients with primary thoracic and metastatic tumors.

#### METHOD AND MATERIALS

CT and/or CT-US fluoroscopic-guided percutaneous cryoablation was used in 222 procedures on 283 tumors (75 primary, 208 metastatic tumors) in 133 patients, noting tumor and ablation volumes, location, abutting vessels >3mm, recurrences, complications, and tumor type. Primary thoracic included all lung cancer types (n=70) and pleural tumors (n=5). Complications were graded by the National Institutes of Health, Common Terminology of Complications and Adverse Events (CTCAE). Hydrodissection and esophageal warming balloon were used for tissue separation as needed (20 and 9 respectively). A minimum of 2 cryoprobes were used on all patients and for larger tumors, tumor diameter plus one was used for probe number.

#### RESULTS

All patients required only conscious sedation. Overall tumor and ablation median size was 2.2cm and 4.2cm, respectively. Major complication rates were significantly lower in tumors =3 cm as opposed to >3cm, 1.5% (2/134) vs. 11.8% (9/76) (p

#### CONCLUSION

CT guided percutaneous cryoablation in the lung provides a low morbidity alternative for complex patients, particularly for pleural/chest wall and more central tumors. Complication rates are significantly lower for tumors

#### CLINICAL RELEVANCE/APPLICATION

Thoracic cryoablation is not affected by vessel proximity and produces low recurrence and complication rates. Cryoablation appears superior for central and chest wall locations.

### VSI031-13 • Complications of Lung Ablation, Preventing Them and When They Occur - Their Management

**Kamran Ahrar MD (Presenter)**

#### LEARNING OBJECTIVES

1) List potential complications of lung tumor ablation. 2) Outline steps to avoid potential complications. 3) Outline steps to manage complications.

### VSI031-14 • Evaluating Cryoablation of Metastatic Lung/Pleura Tumors in Patients - Safety and Efficacy (ECLIPSE)

**David A Woodrum MD, PhD (Presenter) ; Thierry Debaere ; Fereidoun G Abtin MD ; Peter J Littrup MD \* ; Frederic Deschamps ; Robert D Suh MD ; Hussein D Aoun MD ; Matthew R Callstrom MD, PhD \***

#### PURPOSE

To evaluate safety and preliminary efficacy of CT guided lung cryoablation for lung metastases =3.5cm in patients with pulmonary metastatic disease.

#### METHOD AND MATERIALS

Forty patients (24 males, 16 females; mean age 63 years) were enrolled in a prospective single arm study to evaluate CT guided lung cryoablation (Galil Medical, Arden Hills, MN) for patients with lung metastases. Inclusion criteria were up to 3 unilaterally or a maximum of 5 metastases bilaterally. Patients were followed with serial CT imaging at 1 week, 3, 6, and 12 months. The primary endpoint for the study is local tumor control assessed by a modified RECIST. Complications were assessed using the CTCAE 4.0

#### RESULTS

A total of 62 tumors (40 patients) underwent 48 cryoablation procedures. The mean tumor size was 1.4 cm (range 0.3 to 3.2 cm), and 80% (n=32) of patients had unilateral disease. Sedation was general (67%; n=32), conscious/sedation in 31% (n=15), and 2% regional sedation (n=1). Treatment time ranged from 32-272 minutes (mean=101). Nine chest tubes (18%) were placed for pneumothorax but removed in 1 day or less. With the exception of three grade 3 events (non-cardiac chest pain, pneumothorax requiring VATS, and dialysis fistula thrombosis), all other reported adverse events (95.2%) were classified as CTCAE grade 1 or 2. The most common events (48 procedures) occurring within 30 days of the procedure were pneumothorax 50% (n=24), hemorrhage 8% (n=4). All resolved with minimal to no intervention. We did not encounter major hemorrhage to the lung or the pleura. At 3 months, 28 patients (75%) followed up with 100% response rate defined as either stable disease, partial response, or complete response. At 6 months, 15 patients

(38%) followed up with a 95% response rate due to one patient having a local failure.

#### CONCLUSION

Cryoablation of metastatic lung tumors =3.5 cm appears to be a safe. Our preliminary results demonstrate promising local tumor control within the lung.

#### CLINICAL RELEVANCE/APPLICATION

CT guided lung cryoablation demonstrates safety and preliminary efficacy in treating metastatic lung disease.

### VSI031-15 • Percutaneous Cryoablation in Management of Recurrent Mesothelioma after Surgical Pleurectomy and Decortication: Efficacy and Predictors of Local Recurrence

**Fereidoun G Abtin MD (Presenter) ; Jesse K Sandberg MD ; Robert D Suh MD ; William Hsu PhD ; James Sayre PhD ; Robert Cameron MD**

#### PURPOSE

Percutaneous cryoablation (PCT) is an ablative technique, used to manage recurrent mesothelioma in patients following surgical lung sparing decortication and pleurectomy. The purpose of this study was to evaluate the efficacy and clinical and ablation variables that are predictive of tumor recurrence following PCT.

#### METHOD AND MATERIALS

IRB obtained. From a database containing surgical and radiological information, patients with recurrent mesothelioma following lung sparing pleurectomy and decortication with at least one PCT were identified. Patients were followed after PCT using CT and PET/CT scans for at least 6 months. Clinical variables included: stage at diagnosis, chemotherapy, radiation, recurrence time lag following surgery, and number of lesions at time of recurrence presentation. PCT variables included: size of the lesion, edge of ice ball beyond the tumor, number of probes, size of probes, number of cryo cycles, maximum and total freeze and thaw time. A stepwise multiple logistic regression model was used to assess predictors of local recurrence after ablation; local recurrence determined by increased regional metabolic activity or increased size of post ablation zone.

#### RESULTS

17 patients were identified who underwent a total of 75 outpatient cryoablations (range of 1-25). Lesions measured a mean of 37 mm (range 14-113) by 22.0 mm (range 12-55) in diameter. At 6 months 68/75 (90.7%) ablations showed no recurrence. No major, but minor complications including hematoma, small pneumothorax and hemoptysis in one patient each and erythema in 3 chest wall subcutaneous lesions (5/75 =6.6%). Late complications in 4/75 (5.3%) ablations. Considering the clinical and ablation variables, iceball beyond tumor edge less than 6.52 mm detected on CT scan during ablation was the only statistically significant predictor of recurrence (p

#### CONCLUSION

PCT can be used for management of recurrent mesothelioma following surgery with low recurrence rate of 9.3%, and limited early complications of 6.6%. When performing PCT, at least 6.52 mm of the edge of iceball is needed to extend beyond the edge of tumor to limit local recurrence.

#### CLINICAL RELEVANCE/APPLICATION

Percutaneous Cryoablation can be used in local control of recurrent mesothelioma after surgery with low recurrence rate and limited early complications.

### VSI031-16 • Can a Biopsy Performed after Lung Radiofrequency Ablation Be Contributive?

**Lambros C Tselikas MD (Presenter) ; Julien Adam ; Frederic Deschamps ; Geoffroy Farouil ; Julien Joskin ; Christophe Teritehau ; Antoine Hakime MD ; Thierry J De Baere MD \***

#### PURPOSE

To evaluate the effectiveness of a biopsy performed after lung radiofrequency ablation (RFA).

#### METHOD AND MATERIALS

Institutional review board approval was obtained. Eighteen patients with lung tumors, including 72% of metastases (14/18) (8 colorectal, 1 renal, 1 parathyroid, 1 melanoma, 1 osteosarcoma, 1 cholangiocarcinoma and 1 breast cancer) and 23 % of primary lung cancers (1 epidermoid and 3 adenocarcinomas) were treated with lung RFA. A biopsy was performed immediately after RFA. The biopsy was obtained through the canula used to insert the RFA probe without need for additional puncture. Pathological results including diagnostic of malignancy and morphological characteristics of tumor have been analyzed. Effectiveness was defined by ability to obtain a diagnosis of malignancy. The ability to diagnose tumor subtype, and primitive tumor location (if applicable) was determined. Procedures characteristics, recurrences and complications were also registered.

#### RESULTS

Mean tumor size was 17.9mm (SD: 1.5mm) at CT immediately before RFA. 89% (16/18) of biopsies were able to diagnose malignancy. Cancer subtype and origin for malignant tumors was determine in 72% (13/18) of tumors. During one-year follow-up, 1 tumor demonstrate local progression (5.5%), 5 patients presented distant lung disease progression (33%) and 11 were lung disease free (61%). Thirteen complications occurred (72%), including 5 pneumothoraxes requiring chest tube placement (27%), and 7 minor pneumothoraxes without treatment (34%), and 1 intrapulmonary hemorrhage (5%) not requiring any specific treatment. No fatal complication occurred.

#### CONCLUSION

A biopsy performed after RFA of lung tumor can confirm malignancy in close to 90% of cases. This diagnosis is obtained without the need for additional puncture. Such post RFA biopsy avoids the need for immediately pre-RFA biopsy, which are at risk of alveolar hemorrhage, then blurring the tumor for subsequent targeting with RFA.

#### CLINICAL RELEVANCE/APPLICATION

Biopsy performed after RFA through the guiding canula has a high success rate, limits the number of transthoracic punctures, and preserves the best puncture path for RFA probe placement in lung tumor.

### VSI031-17 • IR Tumour Board

**William H Moore MD (Presenter) \* ; Jo-Anne O Shepard MD (Presenter) \* ; Thomas J Vogl MD, PhD (Presenter) ; Peter J Littrup MD (Presenter) \* ; Kamran Ahrar MD (Presenter)**

#### LEARNING OBJECTIVES

1) Understand case-based information. 2) Identify treatment strategies. 3) Evaluate interventional procedures.

---

### Pediatric Radiology Series: Advanced Pediatric Abdominal Imaging

**Tuesday, 03:00 PM - 06:00 PM • S102AB**



[Back to Top](#)

**VSPD32 • AMA PRA Category 1 Credit™:1.5 • ARRT Category A+ Credit:1.5**

**Moderator**

**Daniel J Podberesky, MD \***

### VSPD32-01 • Advanced Pediatric Liver MR Imaging Techniques: Elastography and Liver Iron Quantification

Daniel J Podberesky MD (Presenter) \*

#### LEARNING OBJECTIVES

1) Learn the basic principles of MR elastography. 2) Understand how to apply liver MR elastography techniques to a pediatric population. 3) Understand the role that liver MR elastography plays in the clinical evaluation and surveillance of liver fibrosis and inflammation. 4) Review the physiology of iron homeostasis and the pathophysiology of iron overload. 5) Learn the basic principles of liver iron concentration determination using MRI. 6) Learn how liver iron concentration determination by MRI is clinically used in the pediatric population.

#### ABSTRACT

### VSPD32-02 • Liver Stiffness Evaluation Using Acoustic Radiation Force Impulse (ARFI) Measurement in Children: Biliary Atresia Patients vs. Healthy Children

Mi-Jung Lee (Presenter) ; Myung-Joon Kim ; Hye Kyung Chang ; Seok Joo Han

#### PURPOSE

To evaluate stiffness of liver and spleen in children using acoustic radiation force impulse (ARFI) imaging, to correlate shear wave velocity (SWV) of liver with transient elastography (TE) and aspartate aminotransferase-to-platelet ratio index (APRI), and to correlate SWVs of liver and spleen with the presence of esophageal varices.

#### METHOD AND MATERIALS

Children with biliary atresia (BA group) and sex- and age-matched healthy children (control group) underwent abdominal ultrasonography and ARFI. SWVs were measured using a 4-9 MHz linear probe for children under 5 years old and a 1-4 MHz convex probe for older children. Three valid SWV measurements were acquired for liver and spleen in each patient. SWVs of liver and spleen, spleen size, TE scores, APRI, and the presence of esophageal varices were evaluated. Linear mixed model with random effects were used to analyze SWVs.

#### RESULTS

Both group included thirty-two patients (M:F=10:22; age 0.3-15, mean 4 years old). Height, weight, and body mass index were not different between two groups. The mean SWVs of liver was 2.45 m/s in BA group and 1.14 m/s in the control group (p

#### CONCLUSION

SWVs of liver and spleen increased in children with biliary atresia compared with healthy children. And the SWVs of liver correlated with TE scores. However, SWVs of liver and spleen was not helpful to predict the presence of esophageal varices.

#### CLINICAL RELEVANCE/APPLICATION

SWVs of liver increased in children with biliary atresia and correlated with TE scores. However, SWVs of liver and spleen was not helpful to predict the presence of esophageal varices.

### VSPD32-03 • Diagnostic Accuracy of Ultrasonography (US) Examination for the Evaluation of Nutcracker Syndrome (NS): Comparison with Multidetector-row Computed Tomography (MDCT) as a Reference Standard

Minho Park MD (Presenter) ; Sung Kyoung Moon ; Seong Jin Park MD, PhD ; Joo Won Lim ; Dong Ho Lee MD ; Young Tae Ko MD, PhD

#### PURPOSE

To assess the diagnostic accuracy of US for the evaluation of pediatric NS patients with urinalysis abnormality (UA) compared with MDCT as a reference standard.

#### METHOD AND MATERIALS

This study included 66 pediatric patients with UA who underwent MDCT and US for the past 7 years. Eighteen patients with other biopsy-proven or clinically diagnosed renal diseases were excluded. MDCT and US images of 48 patients were reviewed retrospectively. By CT, AP diameters of the left renal vein (LRV) at the hilum (CDh) and aortomesenteric space (AMS, CDa) and the diameter ratio (CDh/a) were assessed. The presence of a beak sign of LRV at AMS and corticomedullary enhancement difference between both kidneys (CMD) in the portal phase were assessed. Patients were grouped as Gr 1 (high NS probability) and Gr 2 (low NS probability) according to the following CT criteria: 1) CDh/a>4; 2) presence of beak sign; and 3) presence of CMD. Patients with two or more criteria were categorized as Gr 1. By US, the AP diameters of LRV at the hilum (UDh) and AMS (UDa), diameter ratio (UDh/a), flow velocity at the hilum (Vh) and AMS (Va), and flow velocity ratio (Vh/a) were assessed. Twenty-four-hour urine proteinuria tests and US parameters were compared using an independent t-test.

#### RESULTS

Gr 1 and 2 comprised 30 and 18 patients, respectively. The mean CDh, CDa, and CDh/a in Gr 1 were 9.9±1.2 mm, 1.9±0.5 mm, and 5.9±3.2 mm, respectively. The mean CDh, CDa, and CDh/a in Gr 2 were 9.0±1.5 mm, 2.9±0.8 mm, and 3.4±1.1 mm, respectively. A significant difference existed in the 24-h urine proteinuria level between the groups (216.3±49.0 mg/d in Gr 1 vs. 133.4±58.8 mg/d in Gr 2; P<0.05). Vh, Va, and Vh/a showed no significant difference (Gr 1 vs. Gr 2: 22.5±7.6 cm/s vs. 22.0±6.7 cm/s, 135.0±30.4 cm/s vs. 122.1±37.7 cm/s, and 7.8±9.0 cm/s vs. 5.9±2.3 cm/s, respectively; P>0.05).

#### CONCLUSION

Based on MDCT, precise diagnosis of NS by US is difficult. Thus, US should be performed with care in patients who may have NS.

#### CLINICAL RELEVANCE/APPLICATION

When NS is doubtful in US, MDCT should be considered for a more accurate diagnosis, even in pediatric patients.

### VSPD32-04 • Quantification of Liver Fat Content in Adolescents with Non-alcoholic Fatty Liver Disease: Comparison of Triple-Echo Chemical Shift Gradient-Echo Imaging and in Vivo Proton MR Spectroscopy

Rossella Di Miscio ; Lucia Pacifico ; Michele Di Martino (Presenter) ; Concetta V Lombardo ; Flavio Ferraro ; Claudio Chiesa ; Carlo Catalano MD

#### PURPOSE

To compare a triple-echo gradient-echo sequence for measuring the fat content of the liver with using hydrogen 1 (1H) magnetic resonance (MR) spectroscopy and liver biopsy as the reference standard.

#### METHOD AND MATERIALS

In 74 pediatric patients with (42 men, 34 women; mean age, 11 years), 3.0-T single-voxel point-resolved 1H MR spectroscopy of the liver (Couinaud segment VII) was performed to calculate the liver fat fraction from the water (4.7 ppm) and methylene (1.3 ppm) peaks, corrected for T1 and T2 decay. Liver fat fraction was also computed from triple-echo (consecutive in-phase, opposed-phase, and in-phase echo times) breathhold spoiled gradient-echo sequence (flip angle, 20°), by



estimating T2\* and relative signal intensity loss between in- and opposed-phase values, corrected for T2\* decay. Pearson correlation coefficient, Bland-Altman 95% limit of agreement.

#### RESULTS

Mean fat fractions calculated from the triple-echo sequence and 1H MR spectroscopy were 6% (range, 0.9%–24.4%) and 14% (range, 3%–43%), respectively. Mean T2\* time was 14.7 msec (range, 5.4–25.4 msec). Pearson correlation coefficient was 0.89 (P .0001). With the Bland-Altman method, all data points were within the limits of agreement.

#### CONCLUSION

A breath-hold triple-echo gradient-echo sequence with a low flip angle and correction for T2\* decay is accurate for quantifying fat in segment VII of the liver. Given its good correlation and concordance with 1H MR spectroscopy, this triple-echo sequence could replace 1HMR spectroscopy in longitudinal studies.

#### CLINICAL RELEVANCE/APPLICATION

A breath-hold triple-echo gradient-echo sequence with a low flip angle and correction for T2\* decay is a reliable tool for the quantification of liver steatosis in adolescents with NAFLD

### VSPD32-05 • Vitamin E Effect Monitoring with Hepatic Fat Quantification MR in Pediatric Nonalcoholic Steatohepatitis

**Mi-Jung Lee** (Presenter) ; **Myung-Joon Kim** ; **Hong Koh**

#### PURPOSE

To evaluate the possibility of Vitamin E effect monitoring with hepatic fat quantification MR in pediatric nonalcoholic steatohepatitis.

#### METHOD AND MATERIALS

We retrospectively reviewed pediatric patients who received Vitamin E for nonalcoholic steatohepatitis and underwent hepatic fat quantification MR in last three years. Hepatic fat fraction (%) was measured using dual- and triple-echo gradient-recalled-echo sequences at 3T. Compliance group and non-compliance group for Vitamin E medication were compared clinically, biochemically, and radiologically. Continuous variables were analyzed with Mann-Whitney U test and categorical variables were analyzed with Fisher's exact test.

#### RESULTS

Twenty-seven patients (M:F=24:3, age 12 ± 2.3 years) were included with 22 in compliance group and five in non-compliance group. Baseline findings on all parameters were not different between two groups except triglycerides level (compliance vs. non-compliance group, 167.7 mg/dl vs. 74.2 mg/dl; p=0.001). In compliance group, high-density lipoprotein increased and all the other parameters decreased after medication. However, there were variable changes in non-compliance group. On comparing compliance and non-compliance group, there were significantly different change in dual fat fraction (-19.2% vs. 4.6%; p

#### CONCLUSION

Hepatic fat quantification MR is a useful tool for monitoring Vitamin E effect in pediatric nonalcoholic steatohepatitis. It can also help to avoid unnecessary biopsies in these patients.

#### CLINICAL RELEVANCE/APPLICATION

Hepatic fat quantification MR is a useful tool for monitoring Vitamin E effect in pediatric nonalcoholic steatohepatitis. It can also help to avoid unnecessary biopsies in these patients.

### VSPD32-06 • Systematic Approach to Imaging Pediatric Liver Masses

**Sudha A Anupindi** MD (Presenter)

#### LEARNING OBJECTIVES

1) Identify the common and developing imaging techniques to evaluate liver masses in children. 2) Demonstrate an understanding of the clinical presentation, laboratory findings and imaging features of the most common pediatric liver tumors. 3) Apply these principles to distinguish benign from malignant hepatic tumors.

#### ABSTRACT

1. Identify the common and developing imaging techniques to evaluate liver masses in children.  
2. Demonstrate an understanding of the clinical presentation, laboratory findings and imaging features of the most common pediatric liver tumors.  
3. Apply these principles to distinguish benign from malignant hepatic tumors.

### VSPD32-07 • Correlation between Bowel Ultrasound and Magnetic Resonance Enterography in Children

**Tahani M Ahmad** MD (Presenter) ; **Oscar M Navarro** MD ; **Mary-Louise C Greer** MBBS, FRANZCR

#### PURPOSE

*Introduction:* Inflammatory bowel disease (IBD) is one of the most common gastrointestinal diseases affecting pediatric population in developed countries. Imaging is a crucial component of disease evaluation. Magnetic resonance enterography (MRE) is becoming the most widely accepted imaging modality in current practice although with some drawbacks including high cost, limited availability and long scan times *Aim:* To compare the diagnostic yield and concordance of bowel ultrasound (US) with MRE in children

#### METHOD AND MATERIALS

Prospective study in 33 children undergoing clinically indicated MRE. A dedicated bowel US was performed within 2 hours prior to MRE. Each of the US and MRE images were analyzed blindly by two pediatric radiologists. Inter-reader agreements of nine inflammatory markers for each modality and for each bowel segment were calculated as well as the coefficient of concordance between the consensus US and consensus MRE

#### RESULTS

US showed substantial inter-reader agreement on large bowel and distal ileum but no agreement in the remainder of small bowel. MRE also showed excellent agreement on all bowel segments but moderate on the proximal small bowel. When consensus US was compared to MRE, US showed excellent diagnostic performance in replicating MRE results in most of the large bowel and distal ileum and showed moderate concordance in the remainder of the small bowel and transverse colon.

#### CONCLUSION

US is a reliable tool and showed substantial correlation with MRE in detecting inflammatory changes in the colon, terminal ileum and distal ileum. US remains inferior to MRE for the remainder of the small bowel with less reliability but moderate concordance. Therefore, US can be an excellent complement to MRE particularly for follow-up of disease activity in patients with known IBD and as a primary imaging method for those with nonspecific symptoms or with low-suspicion for having IBD at initial presentation.. MRE remains the preferred method for evaluating disease involvement at presentation.

#### CLINICAL RELEVANCE/APPLICATION

Ultrasound is an excellent complement to MRE in evaluation of IBD in children and is recommended for follow-up of disease activity in patients with known IBD

### VSPD32-08 • Diffusion-weighted MR Imaging (DWI) for Detection of Bowel Inflammation in Pediatric Patients with Inflammatory Bowel Disease

#### PURPOSE

1. To determine the feasibility of diffusion weighted magnetic resonance imaging (DWI) in the detection of bowel inflammation in patients with inflammatory bowel disease. 2. To evaluate the changes in apparent diffusion coefficient (ADC) values in the inflamed bowel in patients with inflammatory bowel disease.

#### METHOD AND MATERIALS

We retrospectively analyzed 44 pediatric patients (ages between 10 to 17 years) with either known or clinically suspicious diagnosis of inflammatory bowel disease who underwent MR Enterography (including free breathing DWI). All of these 44 patients had colonoscopy and biopsy within 4 weeks of MR examination. Two radiologists reviewed DWI and ADC maps to evaluate for inflammation in each bowel segment (terminal ileum, cecum, ascending colon, transverse colon, descending colon, and rectosigmoid colon) and measured the ADC values of each bowel segment. Endoscopic and pathologic results were correlated with DWI findings.

#### RESULTS

Out of 44 patients 7 patients had normal results on endoscopy , pathology and DWI, 27 patients had Crohn's disease (CD) and 10 patients had ulcerative colitis (UC). Among 27 patients with CD, 5 patients had negative endoscopy and pathology and negative DWI. In remaining 22 patients with CD who had positive endoscopy and pathology, DWI detected involved segments of bowel in 19 (86 %) . Out of 10 patients with UC, 2 patients had negative endoscopy and pathology as well as negative DWI. Among 8 patients with UC who had positive endoscopy and pathology, DWI detected inflammation in 6 patients (75 %) . On DWI, bowel segments with inflammation revealed higher signal . On quantitative analysis, ADC values of inflamed and normal bowel were measured and ADC values in inflamed bowel were significantly decreased as compared with normal bowel. The mean ADC value of proven inflamed bowel was  $1.13 \times 10^{-3}$  mm<sup>2</sup>/s (range,  $0.81 \times 10^{-3}$  to  $1.41 \times 10^{-3}$  mm<sup>2</sup>/s), compared to  $2.74 \times 10^{-3}$  mm<sup>2</sup>/s (range,  $1.5 \times 10^{-3}$  to  $4.03 \times 10^{-3}$  mm<sup>2</sup>/s) in normal bowel segments (P < .0001).

#### CONCLUSION

DWI is a valuable imaging tool for detection of bowel inflammation in pediatric inflammatory bowel disease. Sensitivity of DWI is better in CD than UC. ADC values are significantly low in inflamed bowel segments than normal bowel segments.

#### CLINICAL RELEVANCE/APPLICATION

DWI facilitates fast, accurate and comprehensive workup in pediatric inflammatory bowel disease; without the need for IV contrast administration and eliminating risk of radiation.

### **VSPD32-09 • MR Colonography including Diffusion Weighted Imaging (DWI) in Children with Inflammatory Bowel Disease (IBD): Do We Really Need Intravenous Contrast?**

**Sonja Kinner** MD (Presenter) ; **Maria L Hahnemann** MD ; **Bernd Schweiger** \* ; **Thomas C Lauenstein** MD ; **Selma Sirin** MD

#### PURPOSE

MR colonography (MRC) is a well-accepted, non-invasive imaging modality for the depiction of inflammatory bowel disease. Diffusion weighted Imaging (DWI) has been shown to show lesions in abdominal MRI as good as contrast enhanced imaging and can also be used for bowel imaging. The aim of this study therefore was to assess if contrast enhancement is really needed to depict inflammatory lesions in bowel MRI if DWI is available.

#### METHOD AND MATERIALS

38 patients (18 girls, 20 boys, mean age 14.6 years) underwent MRC on a 1.5T (Magnetom Avanto, Siemens). In addition to T2-weighted and contrast-enhanced T1-weighted (ce-T1-w) data, DWI sequences in axial and coronal plane (b = 50, 500, 1000) were acquired and ADC maps were calculated. Two reviewers evaluated i) DWI, ii) ce-T1-w MRC as well as iii) DWI and ce-T1-w MRC concerning lesions (1=none, 2=one/continuous lesion(s), 3= multiple, discontinuous lesions). Furthermore, bowel distension (1=good, 2=moderate, 3=poor distension) and the preferred b-value (0, 500, 1000) were assessed and correlated. Colonoscopy was performed in the following 48 hours and served as reference standard.

#### RESULTS

Ce-T1-w MRC showed lesions correctly in 32 of 38 patients. All 38 patients were diagnosed correctly with the DWI data set and with a combination of DWI and ce-T1-w MRC. In 4 patients DWI presented multiple, discontinuous lesions, while ce-T1-w MRC only showed one continuous lesion. Inflammatory bowel parts were detectable even if bowel distension was suboptimal: The missed lesions in ce-T1-w MRC were found in patients with only poor or moderate distension. Kappa values for the two readers were excellent (k=0.82). A combination of the two higher b-values (b=500 and 1000) was preferred for DWI.

#### CONCLUSION

DWI of the bowel shows inflammatory lesions with high accuracy and proved to show lesions that were not seen with ce-T1-w imaging. DWI can be used even in moderately or poorly distended bowel segments and is able to discriminate between one or more continuous or discontinuous lesions. B-values of 500 and 1000 should be used.

#### CLINICAL RELEVANCE/APPLICATION

DWI seems to be able to replace, in any case complement ce-T1-w MRC. This could be used for short examinations for therapy response assessments and has to be evaluated in future trials.

### **VSPD32-10 • Relationship of the Detection Rate of Active Pediatric Ulcerative Colitis (PUC) and the Time Interval between MR Enterography (MRE) and Endoscopy**

**Mohamed A Aggag** MD (Presenter) ; **Jorge H Davila Acosta** MD ; **Carmen Rotaru** PhD ; **Ericc Benchimol** MD ; **David Mack** MD

#### PURPOSE

1. To correlate DWI and post gadolinium enhancement (PGE) findings with endoscopy findings in PUC  
2. To evaluate the relationship of detection of active PUC and time interval between the MRE and endoscopy

#### METHOD AND MATERIALS

Retrospective study. Inclusion criteria: Newly diagnosed patients with PUC who underwent MRE and endoscopy between Feb 2010 and Dec 2012. Exclusion criteria: Interval time between studies > 31 days. Bowel was divided in 6 segments: Cecum (Ce), ascending colon (AC), transverse colon (TC), descending colon (DC), sigmoid colon (SC) and rectum (Re). MRE was performed in a 1.5 T Magnet. 3 planes SSFSE, axial 2D FIESTA, coronal multiphase 2D FIESTA, coronal and axial DWI b=1000, pre and post gadolinium coronal Dynamic multiphase LAVA fat sat and Axial LAVA fat sat were acquired. DWI was positive if high SI in DWI and low SI in ADC map. PGE was positive if there was avid mucosal enhancement in comparison with the remainder of the small bowel. Endoscopy was positive if ulceration, inflammation or edema were documented. Sensitivity (Se) and specificity (Sp) were calculated in 2 phases. Phase 1 included patients with interval < 15 days and phase 2 included all the patients. Regression logistic analysis for the detection of active PUC and time interval between DWI and endoscopy was calculated in Odds ratios for each segment per week.

#### RESULTS

18 cases in total, 10 in phase 1. Endoscopy was positive in all Re, SC, DC and TC. Decreased Se between phase 1 and 2 for DWI were: Ce 1.0 to 0.67, AC 0.78 to 0.59, TC 0.90 to 0.56, DC 1.0 to 0.72, SC 0.8 to 0.61 and Re 0.8 to 0.6. And for PGE were Ce 0.57 to 0.33, AC 0.44 to 0.29, TC 0.5 to 0.33; DC 0.6 to 0.5, SC 0.4 to 0.33 and Re 0.4 to 0.33. Sp for PGE and DWI were 1.0 in both phases in Ce and AC. Decreased Odds ratios per week for detection of active PUC by DWI were seen as follows: Ce: 0.25 (p=0.04), AC: 0.56 (p=0.12), TC: 0.21 (p=0.02), DC: 0.12 (p=0.03), SC: 0.42 (p=0.04), Re: 0.42 (p=0.04).

## CONCLUSION

1. The longer the interval between MRE and endoscopy, the lower the detection ratio of active PUC by MRE, this is likely due to treatment response.
2. DWI has better sensitivity than PGE in the detection of active PUC.

## CLINICAL RELEVANCE/APPLICATION

These results support that treatment contributes to mucosal healing; therefore, correlation value of endoscopy and MRE is lower in longer time interval, for being considered during MRE interpretation.

### VSPD32-11 • IR of Challenging Pediatric Liver Conditions

**Philip R John** MBBCh, FRCR (Presenter)

#### LEARNING OBJECTIVES

1) To understand the range of hepatobiliary disorders where invasive imaging is required (using vascular and nonvascular interventional techniques). 2) To describe the spectrum of hepatobiliary disorders where IR plays an important role in patient management (hepatic vascular malformations, vascular shunts, transplant issues and the utilization of the liver as a window for cardiac intervention). 3) To emphasize the need for close collaboration and communication between diagnostic and interventional radiology in managing children with hepatobilia.

#### ABSTRACT

### VSPD32-12 • Long-term Outcome of Percutaneous Transhepatic Balloon Dilatation for Anastomotic Stricture at Roux-en-Y Hepaticojejunostomy after Pediatric Living Donor Liver Transplantation

**Minoru Yabuta** MD (Presenter) ; **Toshiya Shibata** MD ; **Ken Shinozuka** ; **Toyomichi Shibata** MD ; **Hiroyoshi Isoda** MD ; **Kaori Togashi** MD, PhD \*

#### PURPOSE

Living donor liver transplantation (LDLT) has been an established treatment for an end-stage liver disease because of shortage of liver graft. Compared with deceased donor liver transplantation, biliary complications more frequently occur in LDLT. Of biliary complications, anastomotic stricture is most common and might sometimes lead to graft loss. The aim of this study is to evaluate the long-term outcome of balloon dilatation and inner drainage following percutaneous transhepatic biliary drainage (PTBD) for anastomotic stricture at Roux-en-Y hepaticojejunostomy after pediatric LDLT.

#### METHOD AND MATERIALS

Between April 1997 and December 2012, consecutive 39 patients (15 men and 24 women, age, 0 - 18 years, median 4 years) who underwent LDLT with Roux-en-Y hepaticojejunostomy developed anastomotic stricture 1 - 218 months (median 8 months) after LDLT. They underwent PTBD, balloon dilatation across the anastomotic stenosis, and inner drainage. After serial exchange with larger diameter tube, drainage tube was removed when biliary stricture was improved on the cholangiography and symptom and biochemical findings were improved clinically. We evaluated tube independent rate, the rate of primary patency, primary assisted patency and secondary patency.

#### RESULTS

In 38 of 39 patients, a drainage tube could be removed. Tube independent rate was 97%. The rate of primary, primary assisted, and secondary patency at 1-, 3-, 5-, 10-years after the initial PTBD were 0.85, 0.77, 0.74, and 0.74 respectively, 0.97, 0.97, 0.97, and 0.86 respectively, and 1.00, 1.00, 1.00, and 1.00 respectively.

#### CONCLUSION

Balloon dilatation and inner drainage following PTBD was an effective treatment for anastomotic biliary stricture at Roux-en-Y hepaticojejunostomy after LDLT.

#### CLINICAL RELEVANCE/APPLICATION

Balloon dilatation and inner drainage following PTBD was an effective in pediatric patients with anastomotic biliary stricture at Roux-en-Y hepaticojejunostomy after LDLT.

### VSPD32-13 • Evaluation of the Difference in Radiation Exposure Levels between Image Intensifier and Flat Panel Detector-based Systems in Pediatric Patients with Biliary Strictures Post-liver Transplantation Treated with Interventional Radiological Procedures

**Roberto Miraglia** MD ; **Luigi Maruzzelli** MD ; **Kelvin Cortis** MD, MRCS, FRCR (Presenter) ; **Fabio Tuzzolino** ; **Roberta Gerasia** ; **Angelo Luca** MD

#### PURPOSE

The aim of this study was to compare radiation exposure levels between biliary interventional procedures performed using an image intensifier and a flat panel detector-based system in liver transplant pediatric patients with biliary strictures (BS).

#### METHOD AND MATERIALS

We enrolled 34 consecutive pediatric liver transplant recipients with BS who underwent a total of 170 image-guided procedures in the period between January 2008 and March 2013. The Dose Area Product (DAP) and fluoroscopy time was recorded for each procedure. Mean age was 61 months (range 4 - 192) and mean weight 17 kg (range 4 - 41). The procedures were classified into 3 categories: percutaneous trans-hepatic cholangiography and biliary catheter placement (n=40), cholangiography and balloon dilatation (n=55), cholangiography and biliary catheter change or removal (n=75). Ninety two procedures were performed in an image intensifier-based angiographic system. All of the 78 procedures performed after July 2010 were performed in a flat panel detector-based interventional suite. The difference between the two angiographic systems was compared using the Wilcoxon rank-sum test, using both DAP and fluoroscopy time. The estimates of the differences of DAP adjusted for the fluoroscopy time were assessed with a multiple generalized linear regression model.

#### RESULTS

Mean DAP in the 3 categories was significantly higher in the group of procedures performed in the image intensifier-based system, as compared to the procedures performed in the flat panel detector-based suite. Statistical analysis revealed a p value of 0.001 in percutaneous transhepatic cholangiogram and biliary catheter placement, 0.0002 in the cholangiogram and balloon dilatation, and 0.00001 in the cholangiogram and biliary catheter change or removal group.

#### CONCLUSION

In our experience, the use of flat panel angiographic equipment reduces radiation exposure in pediatric biliary interventional radiology procedures in children with liver transplantation.

#### CLINICAL RELEVANCE/APPLICATION

The use of flat panel angiographic equipment should be considered for pediatric interventional radiology procedures.

### VSPD32-14 • Free Breathing Radial 3D VIBE- A Possibility to Perform Dynamic Contrast Enhanced Abdominal MRI Examinations of Children under General Anesthesia with an Improved Image Quality

**Maya C Larson** (Presenter) ; **Philipp Weisser** MD ; **Renate M Hammerstingl** MD ; **Martin Beeres** MD ; **Kai T Block** ; **Thomas J Vogl** MD, PhD

## PURPOSE

To show that a MRI protocol including a free-breathing 3D VIBE sequence with radial k-space sampling allows dynamic contrast enhanced abdominal imaging in sedated and ventilated children undergoing MR scans with improved image quality.

## METHOD AND MATERIALS

12 pediatric patients, aged from 2 months to 5 years, referred for clinically indicated contrast enhanced abdominal MRI scans underwent imaging at 1.5T under general anesthesia. The protocol included a free breathing T1 weighted GRE-sequence with radial k-space sampling that was used to acquire three dynamic image series including arterial, portal-venous and hepato-venous phases. Additionally a breath-gated fat suppressed T1 weighted FLASH 2D sequence with rectilinear k-space sampling was performed. All Image series were evaluated by two independent radiologists using a 3-point scale (1 excellent - 2 fully diagnostic - 3 non-diagnostic) regarding overall image quality, special focus was on vessel clarity, distinction of organ parenchyma, artifacts, and- if present- lesions.

## RESULTS

The short acquisition time of the free-breathing T1 weighted 3D VIBE Sequence allowed dynamic contrast enhanced imaging in all examined sedated and ventilated patients without ventilation stop. Furthermore the image quality of all three dynamic image series of the free-breathing T1 weighted 3D VIBE sequence was rated with an average of 1.3 and is therefore considered by both radiologists in consensus as superior to the breath-gated T1 weighted FLASH 2D sequence which was rated with an average of 2.2 on a scale of 1-3 (1 excellent 2- diagnostic - 3 non diagnostic).

## CONCLUSION

The free breathing T1 weighted radial VIBE sequence allows dynamic contrast enhanced imaging of pediatric patients undergoing MRI examination in general anesthesia and in deep sedation. This kind of examination cannot be performed with a standard breath gated T1-FLASH 2 D sequence without ventilation stop or in deep sedation without intubation. Furthermore as the acquisition times are very short and the radial VIBE proves to be very resistant to motion artifacts, the free-breathing 3D VIBE sequence provides improved image quality compared to the T1 FLASH 2D sequence.

## CLINICAL RELEVANCE/APPLICATION

The radial VIBE MRI sequence allows dynamic contrast enhanced imaging of sedated and ventilated children in general anesthesia with an improved image quality and should be therefore recommended.

## VSPD32-15 • Free Breathing Fast Pediatric MRI: Quantitative Analysis of View Sharing vs. Locally Low Rank Motion Weighted Reconstructions

**Shaun V Mohan MD (Presenter) ; Tao Zhang ; Richard A Barth MD \* ; Shreyas S Vasanawala MD, PhD \***

## PURPOSE

Dynamic contrast enhanced functional renal MRI requires well-registered kidneys over all temporal phases as well as high temporal resolution. Fast MR methods, such as compressed sensing and parallel imaging can significantly shorten scan time. Combined with respiratory motion correction, a locally low rank motion weighted (LLRMW) method may enable free breathing fast multi-phase MRI, potentially decreasing the depth and duration of anesthesia. Here we compare LLRMW and the commonly used view sharing (VS) reconstruction to assess motion artifacts quantitatively through measurements of kidney movement for free breathing MRI.

## METHOD AND MATERIALS

With IRB approval, informed consent and HIPAA compliance, 25 pediatric MRI cases (14 male, 11 female, mean age 6) were obtained at our institution for 3T multi-phase DCE MRI with a free breathing acquisition accelerated approximately 6-fold. VS and LLRMW reconstruction were performed. To assess kidney movement, TeraRecon V4.4 was utilized to draw signal profiles across the inferior pole of each renal cortex and adjacent fat. Two patients only had one native functional kidney on which measurements were performed (N=48). The resulting curve indicated the transition in signal strength between the kidney and fat, correlating with the margin of the kidney, and was captured across all 18 temporal phases of the study to assess kidney movement over time. The greatest change between profile transition points indicated the greatest movement for each kidney for both reconstructions.

## RESULTS

A paired t-test was performed on the measurements for the left and right kidneys respectively, comparing VS and LLRMW reconstructions. The mean difference calculated greater overall motion in the VS than LLRMW reconstruction, with 0.5067 mm (95% CI: 0.2719 to 0.7415) for the left kidney and 0.5688 mm (95% CI: 0.3050 to 0.8325) for the right kidney with p values < 0.005.

## CONCLUSION

LLRMW reconstruction of fast MRI on free breathing patients results in significantly reduced kidney movement as perceived on MRI than a VS reconstruction. Further analysis would include an expert review of the two reconstructions to assess for subjective viewer preference of quality and clinical utility.

## CLINICAL RELEVANCE/APPLICATION

Determining the optimal reconstruction for under sampled MRI capture data would help establish a protocol for fast MRI of free breathing children, and facilitate quantitative DCE analysis.

## Cardiac Radiology Series: Transcatheter Aortic Valve Replacement (TAVR)

Wednesday, 08:30 AM - 12:00 PM • S502AB

**IR** **VA** **CA**

[Back to Top](#)

**VSCA41 • AMA PRA Category 1 Credit™:3.75 • ARRT Category A+ Credit:4**

### Moderator

**Dominik Fleischmann , MD \***

### Moderator

**Jonathan A Leipsic , MD \***

## VSCA41-01 • The Emerging Role of TAVR

**James Min MD (Presenter) \***

### LEARNING OBJECTIVES

1) To understand the use of cardiac CT in the setting of transcatheter aortic valve replacement.

## VSCA41-02 • CT-angiography Based Evaluation of the Aortic Valve Annulus for Prosthesis Sizing in Transcatheter Aortic Valve Implantation (TAVI) - Predictive Value and Optimal Thresholds for Major Anatomic Parameters

**Florian Schwarz MD (Presenter) ; Dominik Zinsser BS ; Philipp Lange MD ; Martin Greif ; Maximilian F Reiser MD ; Hans-Christoph R Becker MD ; Alexander Sterzik ; Christian Kupatt MD, PhD ; David Jochheim MD**

## PURPOSE

To evaluate the predictive value of CT-measurements of the aortic annulus for prosthesis sizing in transcatheter aortic valve implantation (TAVI) and to calculate optimal cutoff values for the selection of the small, medium and large valve size for two manufacturers.

#### METHOD AND MATERIALS

In 351 TAVI-patients, optimal prosthesis size was determined during TAVI by inflation of a balloon catheter at the aortic annulus. The Corevalve Valve System (Medtronic; CV) and the Edward Sapien XT valve (Edwards Life Sciences; ES) were used in 235 and 116 patients, respectively. All patients had undergone CT-angiography of the bodytrunc prior to TAVI. Using the CT datasets, the length of the long and short axis as well as circumference and area of the aortic annulus were measured by two experienced observers. A 10-fold nested cross-validation approach was used to estimate the predictive power of different anatomical parameters for the prosthesis size ultimately implanted and to define optimal cut-off points.

#### RESULTS

There was excellent interobserver agreement (ICC's > 0.85), so average values were used for further analysis. Differences between patients who underwent implantation of the small, medium or large prosthesis were significant for all evaluated aortic root parameters and both manufactures (p < .05).

#### CONCLUSION

CT-based aortic root measurements permit good prediction of the prosthesis size considered optimal during TAVI. Applying the proposed parameter ranges, prosthesis size would have been chosen correctly in 87% of cases. Inclusion of the degree of calcification and/or the dimensions of the sinus of Valsalva into our model might further increase its predictive potential.

#### CLINICAL RELEVANCE/APPLICATION

The proposed cutoff-values for major anatomic parameters of the aortic annulus can serve as a guide for non-invasive prosthesis sizing for the most widely used TAVI prosthesis models

### **VSCA41-03 • C-arm CT has Higher Interobserver Variability Compared to Multidetector CT (MDCT) for Transcatheter Aortic Valve Implantation/Replacement (TAVI/R) Planning**

**Suhny Abbara MD (Presenter) \*** ; **Lorenzo Azzalini** ; **Umesh C Sharma MD, DPhil** ; **Ignacio Inglessis** ; **Igor F Palacios** ; **Brian B Ghoshhajra MD**

#### PURPOSE

Accurate characterization of the aortic annulus and root is critical for guidance of prosthesis diameter choice in TAVI/R planning, and to accurately deploy the valve, and is usually performed by transesophageal echocardiography or MDCT. The same C-arm used for fluoroscopy during the procedure may also be utilized to acquire 3-D datasets that are similar to MDCT. However, this C-arm CT (CACT) is not currently used to perform measurements of the aortic root to guide the procedure. We aim to evaluate the interobserver variability of CACT aortic root measurements, as compared to MDCT.

#### METHOD AND MATERIALS

CACT and MDCT were performed in 20 patients. Multiplanar reconstructions were performed to determine aortic annulus area, circumference and diameters, sinus of Valsalva diameters and height, leaflet length, distance of the coronary ostia to annulus plane, sinotubular junction, ascending aortic diameters, and predicted perpendicular projection to annulus plane (Figure 1). Each parameter was determined by two independent blinded cardiac imagers. Interobserver variability for CACT- and MDCT-derived measurements was determined using the intraclass correlation coefficient (ICC).

#### RESULTS

No significant interobserver variability was found for all variables derived from MDCT (ICC 0.45 to 0.93). However, there was significant disagreement for the following measurements derived from CACT: aortic annulus short and long axis diameters, area and circumference (ICC

#### CONCLUSION

No significant interobserver variability was found with MDCT. Although, good agreement was found for the measurements above the aortic annulus with CACT, the measurements of the aortic annulus demonstrate greater variability compared to MDCT, possibly due to absence of contrast within the left ventricular outflow tract. Therefore sizing of TAVI/R valves may not reliably performed based on CACT measurements alone.

#### CLINICAL RELEVANCE/APPLICATION

CACT provides MDCT-like images, but measurements of aortic annulus are not reliable. Sizing of TAVI/R valves therefore continues to require MDCT or echocardiography.

### **VSCA41-04 • Assessment of the Aortic Annulus with TransEsophageal Echocardiography, Multidetector Computed Tomography and Magnetic Resonance to Direct Surgical Sizing: Can We Rely on Imaging?**

**Leonardo Capitulo MD (Presenter)** ; **Marco Gatti MD** ; **Claudio Maria Berzovini** ; **Riccardo Faletti** ; **Stefano Salizzoni** ; **Paolo Fonio** ; **Mauro Rinaldi** ; **Giovanni Gandini MD**

#### PURPOSE

Precise sizing of the aortic annulus is crucial in order to properly select type and size prosthesis to avoid complication during TAVI procedures. We Evaluate aortic annulus sizing performed by TransEsophageal Echocardiography (TEE), MultiDetector Computed Tomography (MDCT) and Magnetic Resonance (MR) and compares the results to direct intra-operative sizing.

#### METHOD AND MATERIALS

#### RESULTS

All imaging techniques yield results in satisfactory agreement with one another and with the Hegar (R=0.70 for TEE; R=0.81 for MDCT and R=0.81 for MR), even if with different behaviors: MDCT and TEE suffer from overestimation for smaller diameters changing into underestimation for larger ones; MR overestimate over the whole diameter range. The measurements within ±2 mm around the Hegar sizing result in 71% for TEE, 76% for MR and 80% for MDCT.

#### CONCLUSION

MDCT and MR seem to be more accurate in annulus measurements, with different advantages and drawbacks, than TEE.

#### CLINICAL RELEVANCE/APPLICATION

The imaging and the assessment of ♦virtual tube♦ could accurately size the aortic annulus in order to properly select the most appropriate valve size for transcatheter aortic valve implantation (TAVI)

### **VSCA41-05 • Functional Anatomy and Measurements of the Aortic Root**

**Jonathan A Leipsic MD (Presenter) \***

#### LEARNING OBJECTIVES

1) Discuss the most reproducible and accurate methods for annular assessment with CT with a focus on the dynamic changes throughout the cardiac cycle. 2) Provide a deeper understanding of proposed annular sizing strategies with MDCT with focus on recently published multicenter trial data. 3) Discuss the role of MDCT to identify potential adverse root features to help reduce the risk of annular injury.

### **VSCA41-06 • Intentional Computed Tomography-based Oversizing in Balloon-expandable Transcatheter Aortic Valve Replacement - Incidence of Paravalvular Regurgitation and Post-deployment Geometry**

**Philipp Blanke MD (Presenter)** ; **Eva Maria Spira** ; **Gregor Pache MD** ; **Mathias F Langer MD, PhD**

#### PURPOSE

To evaluate the incidence of paravalvular regurgitation and post-deployment geometry of intentional computed tomography (CT)-based oversizing of Transcatheter Heart Valves (THV) in Transcatheter Aortic Valve Replacement (TAVR) using pre- and post-deployment dual-source CT.

#### METHOD AND MATERIALS

115 patients with severe aortic stenosis (mean age  $81 \pm 7$  years, mean aortic valve area  $0.68 \pm 0.18 \text{ cm}^2$ ) underwent retrospectively gated dual source CT for THV sizing prior to TAVR. Aortic annulus dimensions were quantified by means of planimetry and area-derived diameter calculation ( $D = 2 \times \sqrt{\text{area}/\pi}$ ) at the level of the basal attachment points of the aortic cusps during systole. THV selection was CT-diameter-based (EdwardSAPIEN XT 23mm THV for D 25mm). Post-deployment CT was performed in 95 patients. Stent-expansion was assessed planimetrically at the inlet, outlet and level of the native annulus. Relative oversizing and relative changes in annulus dimensions were calculated.

#### RESULTS

Average pre-deployment annulus diameter was  $24.1 \pm 1.8 \text{ mm}$ , average post-deployment diameter was  $23.9 \pm 1.5 \text{ mm}$  ( $p = \text{n.s.}$ ). Average relative change in annulus diameter was  $-0.5 \pm 3.6\%$ . Mean relative oversizing was  $9.1 \pm 4.7\%$ . Mean diameter at the THV outlet was significantly larger than at the THV inlet ( $24.3 \pm 1.8 \text{ mm}$  vs.  $23.8 \pm 1.7 \text{ mm}$ ,  $p$

#### CONCLUSION

Intentional oversizing of the THV based on an area-derived annulus diameter in CT and an adapted incremental sizing scheme appears safe and is associated with a lower incidence of relevant paravalvular regurgitation, as compared to published landmark trial with echocardiography-based THV-sizing

#### CLINICAL RELEVANCE/APPLICATION

Planimetric assessment of the aortic annulus by CT allows for intentional prosthesis oversizing in transcatheter aortic valve replacement to reduce the occurrence of paravalvular regurgitation.

### **VSCA41-07 • CT Angiography for Aortic Root Measurements in TAVR Patients: Comparison of High-pitch Dual-source CT Image Acquisition versus Retrospective ECG-Gating**

**Felix G Meinel MD (Presenter) ; U. Joseph Schoepf MD \* ; Carlo Nicola De Cecco MD ; Aleksander Krazinski ; Maximilian F Reiser MD ; Lucas L Geyer MD \* ; Daniel H Steinberg MD**

#### PURPOSE

To compare the diagnostic value and robustness of high-pitch dual-source CT angiography versus retrospectively ECG-gated data acquisition for aortic root measurement during pre-procedural planning of transcatheter aortic valve replacement (TAVR).

#### METHOD AND MATERIALS

With IRB approval and in HIPAA compliance, data of 20 patients ( $77.5 \pm 12.8$  years, 11 male, heart rate  $69.4 \pm 15.5 \text{ bpm}$ ) considered for TAVR were retrospectively analyzed. All patients had undergone both retrospectively ECG-gated cardiac CT (scan 1) as well as high-pitch dual-source CT angiography (scan 2) of the aorta. Scan 2 targeted the end-systolic phase at 35% of the RR-cycle. A BMI-based contrast medium (CM) injection protocol was used with 70-144mL volume, injected at 3.0-5.5mL/s. For consistency, both scans were reconstructed with a section thickness of 1.5mm with 0.7mm increment. Image quality (IQ) was subjectively assessed. Aortic annulus dimensions were measured as area-derived diameters. Based on effective diameter, agreement for prosthesis selection between the high-pitch image acquisition (FLASH) was compared with standard reconstructions at 30%-80% (D<sub>30</sub>-D<sub>80</sub>) of the RR-cycle.

#### RESULTS

All patient studies had at least 150 HU CM attenuation at the level of the aortic root. In scan group 1, aortic annulus measurements could be successfully performed in all patients. Scan 2 resulted in 7 studies with non-diagnostic IQ. Patients with non-diagnostic IQ had a significantly higher body-mass index ( $38.5 \pm 10.1 \text{ kg/m}^2$  versus  $27.4 \pm 4.2 \text{ kg/m}^2$ , pFLASH  $24.1 \pm 2.0 \text{ mm}$ , D<sub>30</sub>  $24.6 \pm 2.2 \text{ mm}$ , D<sub>40</sub>  $24.2 \pm 2.1 \text{ mm}$ , D<sub>50</sub>  $24.1 \pm 2.2 \text{ mm}$ , D<sub>60</sub>  $23.9 \pm 1.99 \text{ mm}$ , D<sub>70</sub>  $23.8 \pm 1.98 \text{ mm}$ , D<sub>80</sub>  $24.2 \pm 2.3 \text{ mm}$ . In patients with diagnostic IQ, the highest agreement in prosthesis sizing was found in 11 of 13 patients by D<sub>30</sub> ( $\kappa = 0.65$ ) and 13 of 13 patients by D<sub>70</sub> ( $\kappa = 1.00$ ) compared with FLASH.

#### CONCLUSION

For TAVR planning, the use of high-pitch dual-source CT angiography is feasible in the majority of patients. However, retrospectively ECG-gated cardiac CT should be considered in problematic scenarios, such as obese patients or cardiac arrhythmia.

#### CLINICAL RELEVANCE/APPLICATION

High-pitch dual-source CTA requires appropriate patient selection for reliable measurements of the aortic annulus in TAVR patients compared with the more robust retrospectively ECG-gated approach.

### **VSCA41-08 • Accuracy of Aortic Root Annulus Assessment with Cardiac Magnetic Resonance in Patients referred for Transcatheter Aortic Valve Implantation: A Comparison with Multi-detector Computed Tomography**

**Gianluca Pontone MD (Presenter) ; Daniele Andreini MD ; Erika Bertella ; Saima Mushtaq ; Paola Gripari ; Monica Loguercio ; Sarah Cortinovis ; Andrea Baggiano ; Edoardo Conte ; Andrea Daniele Annoni MD ; Alberto Formenti ; Mauro Pepi**

#### PURPOSE

Cardiac magnetic resonance (CMR) has distinct advantages over 2D echocardiography such as exceptional spatial resolution and does not need administration of contrast agents, provides similar 3D multi-slice images of the aortic root, so that it may be a valid alternative to MDCT. The aim of this study is to compare the accuracy of CMR evaluation of AoA as compared to MDCT in patients referred for TAVI.

#### METHOD AND MATERIALS

50 patients were studied with a 1.5-T scanner (Discovery MR450, GE Healthcare, Milwaukee, WI). Steady-state free precession cine acquisitions were acquired with following parameters: echo time 1.57 ms, repetition time 46 ms, slice thickness 8 mm, field of view 350mmx263mm, and pixel size 1.4mmx2.2 mm. Two long-axis view of the aortic root and ascending aorta were obtained. Thus, serial short-axis cines orthogonal to the AoA (3-mm thickness with 1.5-mm overlapping) were imaged. The following parameters were assessed with CMR and compared with those obtained with MDCT: AoA maximum diameter (AoA-Dmax), minimum diameter (AoA-Dmin), and area (AoA-A), length of the left coronary, right coronary, and non-coronary aortic leaflets, degree (grades 1 to 4) of aortic leaflet calcification and distance between AoA and coronary artery ostia.

#### RESULTS

AoA-Dmax, AoA-Dmin and AoA-A were  $26.45 \pm 2.83 \text{ mm}$ ,  $20.17 \pm 2.20 \text{ mm}$ ,  $444.88 \pm 84.61 \text{ mm}^2$  and  $26.45 \pm 2.76 \text{ mm}$ ,  $20.59 \pm 2.35 \text{ mm}$  and  $449.78 \pm 86.22 \text{ mm}^2$  by MDCT and CMR, respectively. The length of left coronary, right coronary, and non-coronary leaflets were  $14.02 \pm 2.27 \text{ mm}$ ,  $13.33 \pm 2.33 \text{ mm}$ ,  $13.39 \pm 1.97 \text{ mm}$ , and  $13.95 \pm 2.18 \text{ mm}$ ,  $13.30 \pm 2.14 \text{ mm}$ ,  $13.46 \pm 1.80 \text{ mm}$  by MDCT and CMR, respectively, while the scores of aortic leaflet calcifications were  $3.4 \pm 0.7$  vs.  $2.97 \pm 0.77$ . Finally, the distance between AoA and left main and right coronary artery ostia was  $16.21 \pm 3.07 \text{ mm}$ ,  $16.02 \pm 4.29 \text{ mm}$  and  $16.14 \pm 2.83 \text{ mm}$ ,  $16.14 \pm 4.36 \text{ mm}$  by MDCT and CMR, respectively. There was close agreement between CMR and MDCT measurements, whereas aortic leaflet calcifications were underestimated by CMR.

#### CONCLUSION

Aortic root assessment with CMR including AoA size, aortic leaflet length and coronary artery ostia height is accurate in comparison to MDCT.

#### CLINICAL RELEVANCE/APPLICATION

CMR may be a valid imaging alternative in patients unsuitable for MDCT.

### **VSCA41-09 • Access Vessel Assessment**

**LEARNING OBJECTIVES**

1) Review the possible percutaneous access sites for patients undergoing TAVR: femoral, transapical, transaortic, subclavian/axillary. 2) Explain the techniques for accurate vessel visualization, diameter measurements and curvature assessment. 3) Present the current recommendations for minimum access vessel diameters with clinical examples.

**ABSTRACT**

Treatment planning for TAVR requires meticulous assessment of access vessels to assure safe device delivery. A high-quality CTA dataset with 0.6-1.25mm section thickness is a prerequisite for accurate vessel visualization and measurement. While transverse source images provide a reasonably good 'first look', most patients require dedicated postprocessing with curved planar reformations and orthogonal images through the access vessels to determine the minimal vessel diameter, to assess for the presence of calcifications, and display the degree of tortuosity. The minimum arterial diameter necessary for TAVR depends on the valve type and size, as well as on the outer diameter of the delivery system. The outer diameter of the delivery system should not exceed 1.05 times the inner arterial diameter. If heavy calcifications are present, particularly circumferential or horse-shoe shaped, the delivery system should be smaller. If peripheral arterial access is inadequate, a direct transaortic route can be chosen through a mini-sternotomy, or right mini-thoracotomy (2nd interspace). It is important to exclude heavy calcifications at a potential aortic access site (e.g. plaque of porcelain aorta), and to determine the distance between the aortic access and the valve plane to assure enough length for device delivery. Transapical access can be gained through a left lateral mini-thoracotomy (5th or 6th interspace).

**VSCA41-10 • Low Volume, Low Iodine Concentration Contrast Medium Protocol for Comprehensive CT Planning of Transcatheter Aortic Valve Replacement**

**Aleksander Krazinski ; Philipp Blanke MD ; U. Joseph Schoepf MD \* ; Justin R Silverman ; Carlo Nicola De Cecco MD ; Lucas L Geyer MD (Presenter) \* ; Fabian Bamberg MD, MPH \* ; Daniel H Steinberg MD**

**PURPOSE**

To investigate the feasibility of a dual-source CT angiography (CTA) protocol with a low volume of low iodine concentration contrast medium (CM) for comprehensive planning of transcatheter aortic valve replacement (TAVR) in a patient group with a high prevalence of chronic renal failure and atrial fibrillation.

**METHOD AND MATERIALS**

44 patients, considered for TAVR, underwent retrospectively ECG-gated CTA of the heart, immediately followed by high-pitch CTA of the femoro-ilio-aortic access route using two different injection protocols of low iodine concentration (320mgI/mL) iodixanol: group A, iodine delivery rate (IDR)-based (target, 1.28gI/s), CM volume 60mL, flow rate 4.0mL/s; group B, BMI-based (routine protocol), CM volume range 70-144mL, flow rate range 3.0-5.5mL/s. All injections were followed by a 50mL saline chaser. Aortic root complex and iliofemoral dimensions were measured. Mean arterial attenuation, signal-to-noise ratio (SNR), and contrast-to-noise ratio (CNR) were calculated. Subjective image quality was assessed at the level of the aortic root complex and the aortoiliac vasculature.

**RESULTS**

Gender distribution (12 female, 8 male, p=0.226), age (82.1±9.8 years, 80.0±11.5 years, p=0.520), body mass index (26.8±4.1kg/m<sup>2</sup>, 29.1±4.7kg/m<sup>2</sup>, p=0.098), and heart rate (69.3±10.3bpm, 70.0±14.5bpm, p=0.849) showed no significant differences between groups. Aortic root complex and iliofemoral dimensions could be analyzed in all cases. Mean attenuation at the level of the aortic root (272.5±100.3HU, 318.9±67.3HU, p=0.097), the aorta (214.7±70.0HU, 251.2±82.4HU, p=0.140), and the iliofemoral access route (264.1±87.2, 287.7±64.9, p=0.337) was non-significantly lower in group A. SNR and CNR were non-significantly higher in group B. Qualitative assessment of image quality did not result in significant differences.

**CONCLUSION**

The performance of a combined CTA protocol consisting of a retrospectively ECG-gated cardiac CTA immediately followed by a high-pitch scan of the femoro-ilio-aortic access route is feasible. With this approach, the amount of CM can be considerably reduced by using a single low volume CM bolus without substantial loss of image quality in fragile, multimorbid patients who are considered for the TAVR procedure.

**CLINICAL RELEVANCE/APPLICATION**

This comprehensive protocol facilitates the use of a low volume, low iodine concentration CM protocol, which is essential in this patient group who often presents with significant comorbidities.

**VSCA41-11 • Influence of Left Ventricular Geometry and Body-surface Area on Aortic Annulus Dimensions in Patients prior to Transcatheter Aortic Valve Implantation - Assessment by Computed Tomography**

**Philipp Blanke MD (Presenter) ; Eva Maria Spira ; Tobias Baumann MD ; Gregor Pache MD ; Mathias F Langer MD, PhD**

**PURPOSE**

To investigate the influence of left ventricular geometry, left ventricular function, body surface area (BSA), and gender on aortic annulus dimensions by computed tomography (CT) in patients with severe aortic stenosis.

**METHOD AND MATERIALS**

ECG-gated cardiac dual-source CT data of 289 consecutive patients with severe aortic stenosis (mean age 81±7 years, 121 males, mean aortic valve area 0.68±0.18cm<sup>2</sup>) was included. Aortic annulus dimensions were quantified by means of planimetry and area-derived diameter calculation ( $D = 2 \times \sqrt{\text{area}/\pi}$ ) at the level of the basal attachment points of the aortic cusps during systole. End-diastolic left ventricular volume (LVEDV), left ventricular ejection fraction (LVEF) and left ventricular myocardial mass (LVM) were assessed by multiphasic cine image reconstructions. Pearson correlation analysis and a step-wise multi-linear regression model were performed.

**RESULTS**

Mean aortic annulus diameter was 24.4±2.4mm, mean LVEF 59.1±16.1%, mean LVEDV 145.6±51.5ml, mean LVM 181.8±54.2g, and mean BSA 1.8±0.2m<sup>2</sup>. A positive and significant correlation (p

**CONCLUSION**

In patients with aortic stenosis, aortic annulus dimensions are influenced by gender, BSA and left ventricular geometry. A larger end-diastolic left ventricular volume, as present in left ventricular dilation, is associated with a larger annulus diameter.

**CLINICAL RELEVANCE/APPLICATION**

In patients undergoing transcatheter aortic valve replacement, aortic annulus dimensions are critical for prosthesis sizing. This study aids in understanding predictors of annulus dimension.

**VSCA41-12 • Anatomical and Procedural Features Associated with Annular Injury in Balloon Expandable Transcatheter Aortic Valve Replacement**

**Jonathan A Leipsic MD (Presenter) \* ; Marco Barbanti MD ; Philipp Blanke MD ; Gudrun Feuchtner MD \* ; David Wood MD, FRCPC \* ; James Min MD \* ; John Webb MD, FRCPC \***

**PURPOSE**

Aortic root rupture is a major concern with balloon expandable TAVR. We sought to identify predictors of aortic root rupture during balloon-expandable TAVR using MDCT.

**METHOD AND MATERIALS**

Thirty seven consecutive patients with left ventricular outflow tract (LVOT)/annular rupture complicating balloon expandable TAVR were

collected from 17 centers and 10 countries. Analysis was performed on an historical cohort of 150 consecutive TAVR patients without aortic root rupture who underwent pre-procedure MDCT at St Paul's Hospital, Vancouver, to identify a comparable group. Matched case-control analysis was conducted where random 1 to 1 matching datasets were constructed on confounders which include gender, baseline aortic valve area, baseline mean transaortic gradient and annular area on CT. Conditional logistic regression was used on the matched data to assess study variables' association with root rupture. MDCT assessment included short and long axis diameters and cross sectional area of the sinotubular junction, annulus and LVOT, as well as the presence, location, and extent of LVOT calcification.

#### RESULTS

Mean age was 82.4±8.5 years and 74% of patients were females. There were no significant differences between the two groups in any preoperative clinical and echocardiographic variables. Aortic root rupture was identified in 20 patients and periaortic hematoma in 11. Patients with root rupture had a higher degree of LVOT calcification quantified by Agatston score (181.2±211.0 vs. 22.5±37.6, p < 0.001).

#### CONCLUSION

This study demonstrates that LVOT calcification and aggressive annular area oversizing are associated with an increased risk of aortic root rupture during TAVR with balloon-expandable prostheses. Larger studies are warranted to confirm these findings.

#### CLINICAL RELEVANCE/APPLICATION

We have identified an important anatomical factor and two procedural variables strongly associated with annular rupture which will allow for a deeper understanding of this important complication.

### VSCA41-13 • Complications and Incidental Findings

**Gudrun Feuchtner MD (Presenter) \***

#### LEARNING OBJECTIVES

1) To learn which imaging features are associated with complications related to TAVI procedure. 2) To understand TAVR morphology of aortic valve, annulus, calcifications and implications for procedure success. 3) To learn which incidental findings have impact on pre-procedural patient management and intraoperative complications.

#### ABSTRACT

Transcatheter aortic valve implantation (TAVI) is a modern innovative minimal invasive approach to treat patients with severe aortic stenosis effectively. Imaging plays a key role to ensure procedure success and to avoid complications. During this course, imaging features associated with complications will be discussed: 1) Major vascular complications occur at 15%. This rate can be cut when selecting patients carefully taking into account high-risk features on CT. 2) Aortic annular calcification are related to intraoperative complications, and high-risk characteristics will be shown. 3) Incidental findings having impact on patients' managements will be identified.

### VSCA41-14 • The Impact of Post-implant SAPIEN XT Geometry on Conduction Disturbances, Hemodynamic Performance and Paravalvular Regurgitation

**Cameron J Hague MD (Presenter) ; Jonathan A Leipsic MD \* ; John Webb MD, FRCPC \* ; Stefan Toggweiler ; Melanie Freeman ; Ronald Binder ; David Wood MD, FRCPC \* ; Marco Barbanti MD ; Donya A Al-Hassan MD**

#### PURPOSE

To examine the relationship between post valve placement geometry and position of a percutaneously placed Edwards Sapien XT balloon expandable aortic valve and the presence of prosthetic valve dysfunction and post-implant conduction abnormalities.

#### METHOD AND MATERIALS

89 consecutive patients with symptomatic aortic stenosis undergoing transcatheter aortic valve replacement (TAVR) with a balloon expandable Sapien XT valve had pre and post valve assessments with multidetector computed tomography (MDCT), transthoracic echocardiography (TTE) and pre and post procedure 12 lead ECG. MDCT measures included valve circularity, percent expansion, inflow/outflow valve areas, and implantation height. Chart review assessed for placement of a permanent pacemaker (PPM) in subjects post TAVR. Statistical analyses were performed using SPSS statistics software. A p-value below 0.05 was considered significant. IRB approval was obtained for this study. All subjects provided consent.

#### RESULTS

89 patients (age 82±8 years, 54 male, 35 female) undergoing TAVR with an Edwards Sapien XT THV were analyzed. Analysis of post implant MDCTs demonstrate average THV stent frame placement as follows: outflow 0.3mm +/- 2.6mm below the left main ostium, and inflow (inferior aspect of stent) was 3.6 +/- 2.2mm below the aortic annulus (basal insertion of the native aortic leaflets). Paravalvular regurgitation (PAR) as assessed by TTE was absent in 24.7%, mild in 67.4%, moderate in 5.6% and moderate to severe in 2.2%. As assessed by MDCT stent frame inflow area in relation to the native annular area, and the difference of the stent frame long-axis diameter to native annulus long axis diameter were the only measured parameters predictive of PAR (p=0.03 and p=0.023 respectively). 5.1% of subjects required a new PPM following TAVR. The MDCT derived THV inflow level to annular distance was the strongest predictor of PPM placement post TAVR. (3.5 +/- 2.0mm versus 7.1 +/- 2.5mm, p=0.001).

#### CONCLUSION

MDCT measures of THV implantation depth and relationship of inflow stent area to native annulus area are strong predictors of new onset conduction disturbances/PPM placement and PAR respectively, both important causes of morbidity and mortality post TAVR.

#### CLINICAL RELEVANCE/APPLICATION

MDCT measures of implantation depth and stent inflow area versus native annular area provide important predictors of complications TAVR (PPM placement and PAR respectively).

### VSCA41-15 • Contrast Induced Nephropathy after Contrast Enhanced Computed Tomography prior to Transcatheter Aortic Valve Implantation

**Vera S Schneider BS (Presenter) ; Florian Schwarz MD ; David Jochheim MD ; Christian Kupatt MD, PhD ; Maximilian F Reiser MD ; Hans-Christoph R Becker MD ; Philipp Lange MD ; Julinda Mehilli MD ; Frederik F Strobl MD**

#### PURPOSE

Contrast induced nephropathy (CIN) is a common complication after contrast enhanced computed tomography (CT). Particularly, patients with aortic valve stenosis (AS) are at increased risk for CIN due to their high prevalence of chronic kidney disease. The aim of this analysis is to determine the rate of CIN in patients with AS following contrast enhanced CT scans prior to transcatheter aortic valve implantation (TAVI).

#### METHOD AND MATERIALS

#### RESULTS

Rates for CIN in patients with GFR under 30, 30 to 60 and over 60 ml/min, were 13.6 %, 10.9 %, 6.8 %, respectively. Average contrast volume in patients who developed CIN was 101 ml vs. 92 ml in those who did not (p < 0.05), supporting a strong relation between the development of CIN and the volume of contrast administered.

#### CONCLUSION

The incidence of CIN in high risk patients with AS undergoing contrast enhanced CT depends on the baseline GFR. We found a close relation between the amount of administered contrast media and the development of CIN.

#### CLINICAL RELEVANCE/APPLICATION

Low dose contrast protocols for CT angiography may help reduce the risk of CIN particularly in high risk patients with AS in whom baseline renal function frequently is impaired.



## VSCA41-16 • Fusion of Cardiac Computed Tomography Angiography and 18F-Fluorodesoxyglucose Positron Emission Tomography for the Detection of Prosthetic Heart Valve Endocarditis

**Wilco Tanis** (Presenter) ; **Asbjorn Scholtens** MD ; **Jesse Habets** MD ; **Renee B Van Den Brink** MD, PhD ; **Lex Van Herwerden** \* ; **Steven Chamuleau** MD, PhD ; **Ricardo P Budde** MD, PhD

### PURPOSE

In prosthetic heart valve (PHV) endocarditis transthoracic and transesophageal echocardiography (TTE and TEE) may fail to recognize vegetations and peri-annular extensions, which is an indication for urgent surgery. Moreover, abnormal peri-annular anatomy after PHV implantation is not uncommon and differentiation between active or absent inflammation is difficult. The purpose of this study is to investigate the additional value of imaging with fused Computed Tomography Angiography (CTA) and 18F Fluorodesoxyglucose Positron Emission Tomography including low dose CT (FDG-PET/CT) providing high resolution anatomical and functional information.

### METHOD AND MATERIALS

In our hospital PHV patients suspected for endocarditis undergo additional CTA and sometimes also FDG-PET/CT imaging when TTE and TEE are inconclusive. All PHV patients that underwent FDG-PET/CT were selected from the hospital database and assigned as cases or controls. Surgical inspection was the reference standard for cases.

### RESULTS

Twelve PHV endocarditis cases and six normal functioning PHV controls were identified, which all underwent TTE, TEE, CTA and FDG-PET/CT. On surgical inspection 11/12 cases had peri-annular extension and 4/12 had a vegetation. CTA alone detected all vegetations but missed one peri-annular extension. FDG-PET/CT alone missed all vegetations, however all peri-annular extensions were detected correctly. Combined FDG-PET/CT and CTA detected all peri-annular extensions and vegetations correctly. Controls were all free of significant FDG uptake. SUV ratios around the PHV ring were significantly (p

### CONCLUSION

Fused FDG-PET and CTA imaging is a promising tool to correctly diagnose PHV endocarditis in patients with an inconclusive echocardiography. SUV ratios may be of additional help for correct detection of peri-annular extensions.

### CLINICAL RELEVANCE/APPLICATION

PHV endocarditis sometimes remains difficult to diagnose with echocardiography due to acoustic shadowing of mechanical valves. In those cases hybrid imaging with CTA and FDG-PET/CT may guide treatment.

## VSCA41-17 • Characteristics of Aortic Valvular Function and Ascending Aorta Dimensions According to Bicuspid Aortic Valve Morphology Using Dual-source Computed Tomography

**Tae Hyung Kim** (Presenter) ; **Sung Min Ko** ; **Meong Gun Song** ; **Hweung Gon Hwang** ; **Jung Ah Park**

### PURPOSE

The bicuspid aortic valve (BAV) is associated with aortic valve dysfunction and ascending aorta dilatation. The relationship between BAV morphology and ascending aorta dimensions remains unclear. We sought to characterize the aortic valve function and the ascending aorta dimensions according to valve morphology using dual-source computed tomography (DSCT).

### METHOD AND MATERIALS

Two hundred nine BAV patients who underwent DSCT and transthoracic echocardiography were retrospectively included. BAV was classified into type I (anterior-posterior orientation of cusps or raphe) and type II (lateral orientation of cusps or raphe), and divided into raphe + (presence of raphe) and raphe - (absence of raphe) using DSCT.

### RESULTS

Type I was present in 129 patients (61.7%) and raphe + in 120 (57.4%) patients. BAV type I and II was more commonly in patients with raphe + (84%) and raphe - (69%), respectively. Aortic regurgitation was more common in patients with type I (45%) and raphe + (53%), and aortic stenosis in patients with type II (46%) and raphe - (56%). Type I patients had a larger aortic annulus and smaller tubular portion of ascending aorta (29.9±4.7 mm and 41.7±7.3 mm, respectively) compared to type II patients (26.7±3.5 mm and 44.3±8.3 mm, respectively), P

### CONCLUSION

BAV morphology is helpful in predicting the type of aortic valve dysfunction and the location of ascending aorta dilatation

### CLINICAL RELEVANCE/APPLICATION

BAV morphology is helpful in predicting the type of aortic valve dysfunction and the location of ascending aorta dilatation.

## Interventional Radiology Series: Embolotherapy

Wednesday, 08:30 AM - 12:00 PM • E352



[Back to Top](#)

**VSIR41** • AMA PRA Category 1 Credit™:3.25 • ARRT Category A+ Credit:4

### Moderator

**Jafar Golzarian**, MD

### LEARNING OBJECTIVES

1) Describe recent evidence concerning the use of embolization for symptomatic prostatic hypertrophy. 2) Explain the use of liquid embolic agents. 3) Describe treatment of complex visceral aneurysms using embolization. 4) Describe two obstetrical or gynecologic emergencies requiring embolization. 5) List two techniques to prevent non-target embolization.

## VSIR41-01 • Non-Target Embolization: How To Prevent or Minimize?

**Christoph A Binkert** MD (Presenter) \*

### LEARNING OBJECTIVES

1) To learn about functional anatomy and flow changes during embolization. 2) To learn about the appropriate use of different materials. 3) To learn about technical tricks to minimize non-target embolization.

## VSIR41-02 • Liquid Embolic Agents

**Robert A Morgan** MD (Presenter) \*

### LEARNING OBJECTIVES

1) To learn about the indications, properties and techniques for the use of the different embolic agents.

### ABSTRACT

## VSIR41-03 • Incidence and Clinical Management of Ruptured and Incidentally Diagnosed Visceral Aneurysms

**Sebastian Schotten** MD (Presenter) ; **Evelyn Dappa** ; **Roman Kloeckner** MD ; **Jens Schneider** ; **Christoph Dueber** MD ;

## Michael B Pitton MD

### PURPOSE

Visceral arterial aneurysms (VAA) are a rare entity with a prevalence between 0.1 – 2% and have a high risk for rupture with mortality rates between 20-75%. We therefore reviewed and analyzed the institutional data base for diagnosis and management of VAA over a period of 10 years.

### METHOD AND MATERIALS

An automatic analysis of the institutional database using the word "aneurysm" resulted in identification of 12,588 reports (CT, MRI, and Angiography). 239 of these patients could be identified suffering from VAA (mean age 65 years ± 12.5 years). VAA were analyzed with respect to location, size, true aneurysm or false aneurysms after surgery/intervention, rupture status, management, and clinical follow-up.

### RESULTS

Diagnosis included VAA of the splenic artery (n=81), celiac trunk (n=46), renal artery (n=42), hepatic artery (n=37), superior mesenteric artery (n=15), gastroduodenal artery (n=10) and others (8). The overall size of the aneurysms was  $17.8 \pm 10.2$ mm; min. 4 mm, max. 112 mm). 44 VAA were rated as false aneurysms (18%), 25 of them after surgery and 11 after percutaneous interventions like biopsies or drainages. 58 of 239 cases were treated with transarterial intervention (n=47) or surgery (n=11). Interventions included embolization with coils (n=35) or glue (n=4), implantations of covered stents (n=4), and combinations of these (n=4). 40 patients were diagnosed at rupture and were treated on an emergency basis (hemoglobin  $8.6 \pm 1.7$ mg/dl). There was no significant difference in size between ruptured and non-ruptured VAA ( $15.2 \pm 8.4$ mm vs.  $16.3 \pm 10.1$ mm). The 30-day mortality in ruptured cases was 8.3% (12 of 36) after interventional treatment compared to 25% after surgery (1 of 4). No fatality occurred after interventional treatment of non-ruptured aneurysms (n=11). The conservatively treated patients presented a 30-day mortality of 6.1% (11 of 181).

### CONCLUSION

The clinical impact of accidentally diagnosed VAA still remains unclear. However, symptomatic or ruptured VAA might be associated with a high mortality rate. There was no difference in size in ruptured and non-ruptured aneurysms. Interventional treatment seems to offer a beneficial approach in emergency cases compared to surgery.

### CLINICAL RELEVANCE/APPLICATION

False aneurysms seem to have a considerably higher risk of rupture and should be promptly treated irrespective of the diameter.

## VSIR41-04 • Complex Visceral Aneurysms

Michael D Darcy MD (Presenter) \*

### LEARNING OBJECTIVES

View learning objectives under main course title.

## VSIR41-05 • A Comparison of the Results of Arterial Embolization for Bleeding and Non-bleeding Gastroduodenal Ulcers

Denis Krause MD (Presenter) ; Louis Estivalet ; Pierre Thouant ; Violaine Capitan ; Jean P Cercueil MD ; Romaric Loffroy

### PURPOSE

Although some authors have advocated the practice of arterial embolization for angiographically negative acute hemorrhage from gastroduodenal ulcers, this technique remains controversial. The goal of our study was to compare the results of arterial embolization for bleeding (BU) and non-bleeding (NBU) gastroduodenal ulcers.

### METHOD AND MATERIALS

Transcatheter embolization was performed in 57 patients (39 men, 18 women, mean age 69.8 years) who experienced acute bleeding from gastroduodenal ulcers. At the time of embolization active contrast extravasation was seen in 36 of 57 patients, while in the remaining 21 patients embolization was based on endoscopic findings. Patient demographics, clinical success, need for re-intervention secondary to re-bleeding, and 30-day complication and mortality rates were reviewed and compared between the two groups by using statistical analyses.

### RESULTS

In the BU group, the gastroduodenal artery (GDA) was embolized in 31 patients (86.1%), the left gastric artery (LGA) in three patients (8.3%), and the left gastroepiploic artery (LGEA) in two patients (5.6%). In the NBU group, the GDA was embolized in 18 patients (85.7%), and the LGA in three patients (14.3%). Clinical success (61.9 vs. 75.0%,  $P = 0.30$ ), need for re-intervention (38.1 vs. 27.8%,  $P = 0.42$ ), and 30-day complication (9.5 vs. 5.6%,  $P = 0.57$ ), and mortality (28.6 vs. 25%,  $P = 0.77$ ) rates were not statistically different between the two groups. Embolization in patients in NBU group did not have impact on clinical success (Odds Ratio, 0.54; 95%CI, 0.17–1.72;  $P = 0.30$ ).

### CONCLUSION

Arterial embolization in patients with angiographically NBU is as safe and effective as embolization in patients with BU.

### CLINICAL RELEVANCE/APPLICATION

The practice of empiric arterial embolization for angiographically negative acute hemorrhage from gastroduodenal ulcers should be systematically used as it is efficient.

## VSIR41-06 • Embolization of Obstetrical and Gynecologic Emergencies

Sue E Hanks MD (Presenter)

### LEARNING OBJECTIVES

1) Identify appropriate patients for transcatheter embolization following gynecologic or obstetric procedures. 2) Choose effective embolic agents to treat hemorrhage from gynecologic malignancies. 3) Define angiographic approach to identification of hemorrhage from gynecologic and obstetric emergencies.

## VSIR41-07 • Medium and Long Term Outcome of Prostatic Arterial Embolization to Treat Benign Prostatic Hyperplasia

Joao M Pisco MD (Presenter) ; Hugo A Rio Tinto MD \* ; Tiago Bilhim MD \* ; Lucia C Fernandes MD ; Jose A Pereira MD ; Luis C Pinheiro ; Antonio Oliveira ; Marisa Duarte MD

### PURPOSE

To evaluate the medium and long term outcome of prostatic arterial embolization (PAE) to treat lower urinary tract symptoms associated with benign prostatic hyperplasia (BPH).

### METHOD AND MATERIALS

Two hundred forty patients (age range, 62 – 82 years; mean age, 74.1 y) with BPH and moderate to severe lower urinary tract symptoms after failure of medical treatment underwent PAE between March 2009 and March 2012. Patients were followed between 1 and 4 years after PAE (mean 18 months). International Prostate Symptom Score (IPSS), quality of life improved (QoL), international Index of Erectile Function (IIEF), peak urinary flow (Qmax), prostate-specific antigen (PSA), prostate volume were evaluated every 6 months. Technical success is defined as embolization of at least one prostatic artery. Clinical success is considered when there is a reduction of the IPSS at least 25% of the total score and = 15, a reduction of the QoL at least 1 point of the total or = 3 and no need of medical or any other treatment.

## RESULTS

There were 4 technical failures. From the 236 evaluated patients there were 39 (16.5%) short term clinical failure up to 1 year. Therefore there are 197 evaluated at medium term between 1 and 3 years. From this group of patients evaluated at medium term there were 17 clinical failures. The cumulative rate at 3 years was 23.7%. There are 17 patients followed at long term between 3 and 4 years, with 2 clinical failures. The cumulative rate at 4 years is 75.4%.

There was a major complication a small area of bladder wall base ischemia. Surgery was required to treat that ischemia.

## CONCLUSION

PAE is safe procedure with low morbidity as well as good short, medium and long term results.

## CLINICAL RELEVANCE/APPLICATION

Prostatic Artery Embolization can have a future place in urologic guidelines and it is important to report technical and clinical outcomes.

### VSIR41-09 • Prostate Embolization

**Jafar Golzarian MD** (Presenter)

#### LEARNING OBJECTIVES

View learning objectives under main course title.

### VSIR41-10 • Coil Embolization of the Splenic Artery: Impact on Splenic Volume and Factors Contributing to Volume Preservation

**Stephen R Preece MD** (Presenter) ; **Paul V Suhocki MD** ; **John Yoo** ; **Tony P Smith MD** ; **Charles Y Kim MD \***

#### PURPOSE

Splenic artery embolization can be performed as an alternative to splenectomy in the setting of splenic injury or splenic artery pathology. However, the impact on splenic function is not well understood. The purpose of this study is to determine the impact of coil embolization of the splenic artery on splenic volume based pre- and post-embolization CT imaging as well as hemofiltration function.

#### METHOD AND MATERIALS

Splenic artery embolization was performed on 148 consecutive patients over an 8 year period for various indications in this IRB approved retrospective study. Sixty patients (36 males, mean age 49 years) had contrast-enhanced CT before and after coil embolization of the splenic artery. The mean time between embolization and last follow up CT was 355 days. Pre and post-embolization splenic volumes were calculated with volume rendering software. The presence of Howell-Jolly bodies was ascertained on lab tests.

#### RESULTS

Splenic artery embolization resulted in a mean decrease in splenic volume by 15% (range -88% to +158%). Splenic volumes on CT scans performed within 30 days of embolization did not change significantly after embolization but after 30 days the mean percentage reduction was 21% ( $p=0.004$ ). Embolization of the distal splenic artery resulted in a 30% splenic volume reduction ( $p=0.003$ ) whereas splenic volumes did not change significantly after proximal embolization. Both traumatic and nontraumatic indications resulted in similar degree of volume loss, although pre-embolization splenic volumes were significantly smaller in trauma patients ( $p=0.029$ ), and more trauma patients underwent distal embolization ( $p=0.005$ ). Multivariate analysis revealed that only coil location significantly impacted splenic volume reduction. Three patients transiently had Howell-Jolly bodies after embolization. No patients required repeat embolization or splenectomy.

#### CONCLUSION

Coil embolization of the main splenic artery results in only a modest degree of splenic volume loss with retention of hemofiltration function. These findings support the growing body of literature that some degree of splenic function is maintained after splenic artery embolization.

#### CLINICAL RELEVANCE/APPLICATION

Splenic artery embolization for trauma and splenic artery pathology is likely preferable to splenectomy when feasible considering that at least some degree of splenic function is retained.

### VSIR41-11 • Prostatic Arterial Embolization as an Alternative Treatment for Patients with Benign Prostatic Hyperplasia for Patients with Benign Prostatic Hyperplasia and Acute Urinary Retention with Bladder Catheter

**Lucia C Fernandes MD** (Presenter) ; **Joao M Pisco MD** ; **Luis C Pinheiro** ; **Tiago Bilhim MD \*** ; **Hugo A Rio Tinto MD \*** ; **Marisa Duarte MD** ; **Jose A Pereira MD** ; **Antonio Oliveira**

#### PURPOSE

To Access the results of prostatic arterial embolization (PAE) for patients with benign prostatic hyperplasia (BPH) and acute urinary retention (AUR) with bladder catheter.

#### METHOD AND MATERIALS

Fifty-three patients aged 48 to 82 years with BPH, AUR and bladder catheter underwent PAE. Prostate volume and Prostatic Specific Antigen (PSA) were evaluated before PAE. The prostate volume ranged between 44cc and 210cc (mean 95cc). Twenty-six patients had prostates larger than 100cc. PVA particles sized 100 $\mu$ m and 200 $\mu$ m were used as embolic material. International prostate symptom score (IPSS), Quality of life (QoL), International Index Erectile Function (IIEF), uroflowmetry, (Qmax - peak urinary flow and PVR - post voiding residual volume), Prostatic Specific Antigen (PSA) and prostate volume, were assessed after successful removal of bladder catheter, at 1, 3, 6 and every 6 months thereafter to assess the clinical outcome. Patients were evaluated between 3 and 48 months (mean 15 months). It was considered clinical success if the patient could urinate easily after removal of the prostate catheter, the IPSS lower than to 15 and the QoL reduced at least 1 point and no need of medical treatment or any other treatment.

#### RESULTS

All patients were treated as outpatients. There was one technical failure (1.9%) and one patient was lost to follow-up. There was short-term clinical success at 3 months in 45/51 (88.2%). There were 46 (11.8%) patients which bladder catheter could not be removed and were considered short term clinical failures and PAE was repeated. In 4 of them the bladder catheter could be removed, therefore the secondary clinical success was shown in 49/51 (95.1%) patients. The 2 patients which catheter could not be removed were treated by TURP and open prostatectomy, respectively. At 18 months there were 4/51 (7.8%) mid-term clinical failures. Three of them were successfully treated with repeated PAE. The third was treated by open prostatectomy. In 5 patients controlled at long term between 3 and 4 years there was not any recurrence. There was not any major complication.

#### CONCLUSION

PAE in patients with BPH and AUR with bladder catheter is a safe procedure with successful removal of the bladder catheter and good short mid and long-term results.

#### CLINICAL RELEVANCE/APPLICATION

Applying a new technique (PAE) in patients with BPH and AUR and with bladder catheter

### VSIR41-12 • Panel Discussion: Unknown Cases and/or Complications. What Would You Do?

#### LEARNING OBJECTIVES

View learning objectives under main course title.

### VSIR41-13 • Wrap Up and Discussion

## Neuroradiology Series: Stroke

Wednesday, 08:30 AM - 12:00 PM • E451B

[Back to Top](#)

NR

**VSNR41** • AMA PRA Category 1 Credit™:3.25 • ARRT Category A+ Credit:4

**Moderator**

**Allan L Brook**, MD \*

**Moderator**

**Padraig P Morris**, MBChB

### **VSNR41-01 • Stroke CT Protocols: Extracting Maximal Data in Minimal Time**

**Mayank Goyal** MD, FRCPC (Presenter) \*

#### LEARNING OBJECTIVES

1) Understand the importance of quick and efficient stroke imaging, post processing and decision making. 2) Discuss the pros and cons of various modalities for acute stroke imaging. 3) Discuss and understand the pros and cons of non-contrast CT, CTA and CT perfusion.

#### ABSTRACT

Given all the recent literature in acute stroke including the recent publications from IMS3, it is clear that Time is brain. This means that very part of the process in the work up and treatment of an acute stroke patient needs to be speeded up. This includes the time taken for image acquisition, post processing and interpretation. There has been a recent move towards moving away from a plain and simple 'Non contrast CT' to rule out a bleed and extensive ischemic changes towards doing more extensive imaging. This talk discussed these options and weighs in the pros and cons of using various techniques and modalities. The limitations and advantages of various techniques would be discussed. In addition, there have been dramatic recent advances in the field of endovascular treatment of stroke. Using newer devices like stentrievers, our ability to achieve fast, robust recanalization has significantly improved. However, the rate of good clinical outcomes has not improved to the same degree. This aspect will be further discussed and would be broadly broken down into two components: imaging based patient selection and the need for speed and efficiency without compromising patient safety.

### **VSNR41-02 • Spot Sign Presence on 90 Second Delayed MDCTA Improves Sensitivity for Hematoma Expansion and In-hospital Mortality: A Prospective Study**

**Viesha A Ciura** (Presenter) ; **H. Bart Brouwers** MD ; **Raffaella Pizzolato** MD ; **Jonathan Rosand** MD ; **Joshua Goldstein** MD \* ; **Stuart R Pomerantz** MD \* ; **Ramon G Gonzalez** MD, PhD ; **Javier M Romero** MD

#### PURPOSE

To determine whether 90 second delayed multidetector computed tomography angiography (MDCTA), in addition to routine first-pass MDCTA in patients with spontaneous intracerebral hemorrhage (ICH) improves detection of the spot sign and increases sensitivity for predicting hematoma expansion and in-hospital mortality.

#### METHOD AND MATERIALS

We performed a prospective study of consecutive patients enrolled over 13 months at a single academic center. Uni- and multivariate logistic regression were performed to assess clinical and neuroimaging covariates for relationship with hematoma expansion and mortality. Accuracy measures were calculated, using standard methods, to compare first pass and delayed CTA performance.

#### RESULTS

Of 86 consecutive patients, 25 (29%) had a positive spot sign on either first pass or delayed CTA (14/25 on first pass and 24/25 on delayed CTA). Median baseline hematoma volume was 29.6 mL (interquartile range 5.9 ♦ 72.8 mL). Sensitivity for predicting hematoma expansion increased from 0.60 to 0.70 with addition of delayed CTA. The odds ratio (OR) of hematoma expansion if a spot sign was present on either first pass or delayed CTA was 13.67 (95% CI 2.84 ♦ 65.83, p=0.0009). 18/25 (72%) of all patients with a spot sign died in hospital, versus 17/61 (28%) patients without a spot sign. Addition of delayed CTA improved sensitivity for predicting in-hospital mortality from 0.26 to 0.51. In multivariate analysis, baseline ICH volume and the spot sign were predictive of in-hospital mortality, however, the effect of the spot sign was only significant if present on first pass CTA.

#### CONCLUSION

Addition of 90 second delayed CTA to the imaging workup of patients with spontaneous ICH captures additional patients with the spot sign and increases sensitivity for predicting hematoma expansion and in-hospital mortality, making it an attractive selection tool for targeting patients that may benefit from early surgical or medical intervention.

#### CLINICAL RELEVANCE/APPLICATION

Addition of 90 second delayed CTA to the imaging workup of patients with spontaneous intracerebral hemorrhage captures additional patients at risk for hematoma expansion and in-hospital mortality.

### **VSNR41-03 • CTA-doped Perfusion-CT (PCT): An Original Method to Increase Signal-to-noise, Contrast-to-noise and Reduce Noise in Ultra-low-dose PCT**

**Elizabeth Tong** MD (Presenter) ; **Max Wintermark** MD \*

#### PURPOSE

To use the information contained in CT-angiography data to improve the image quality of ultra-low-dose PCT.

#### METHOD AND MATERIALS

Dynamic PCT datasets were obtained at 80 kVp and decreasing mAs (100,75, 50, 25, 10) in patients suspected of ischemic stroke, concurrently with static CTA of the cervical and intracranial arteries. Fast-Fourier transforms (FFT) of both the PCT and CTA datasets were calculated. High spatial frequencies of the CTA FFT were combined with low spatial frequencies of the PCT FFT, and an inverse FFT was then applied to the combination to create a virtual PCT dataset. The real and virtual PCT datasets were compared at different mAs by assessing contrast-to-noise ratio (CNR), signal-to-noise ratio (SNR) and image noise, and by visual inspection of the processed real and virtual PCT parametric maps.

#### RESULTS

Virtual PCT attained CNR and SNR two- to three-fold superior to real PCT, and noise reduction by a factor 2-3 (p

#### CONCLUSION

We propose a new method to enhance PCT data by rectifying it with CTA. This method yields diagnostic PCT parametric maps from PCT acquired at 50 mAs.

#### CLINICAL RELEVANCE/APPLICATION

Using this new method and settings of 80 kVp and 50 mAs, the effective dose of a PCT study is approximately 1 mSv, which is less than half of a noncontrast head CT dose.

## VSNR41-04 • Stroke MRI: Diffusion, Perfusion, and Beyond

**Greg Zaharchuk MD, PhD (Presenter) \***

### LEARNING OBJECTIVES

1) Understand the concept of the diffusion-perfusion (DWI-PWI) mismatch concept in acute stroke. 2) Review the recent results of stroke trials using the DWI-PWI concept. 3) Appreciate the potential role of other markers, such as collateral flow, oxygenation, pH, and resting-state fMRI for assessing the ischemic brain.

### ABSTRACT

Diffusion-weighted imaging (DWI) is an valuable part of the workup of acute ischemic stroke, as it can be used to define tissue that is irreversibly infarcted, thus setting a lower bound on patient outcome. Often, the region outside of this **core** will demonstrate reduced perfusion, which can be measured with perfusion-weighted imaging (PWI). Typically, PWI is performed with contrast agents injected in a bolus, yielding multiple hemodynamic parameters, including relative CBF, relative CBV, mean transit time, and time-to-peak or Tmax. Earlier studies have suggested that tissue with prolonged Tmax > 6 sec is incorporated into the final infarct in the absence of early reperfusion. Based on this, the idea of the DWI-PWI mismatch has arisen, which posits that patients with small DWI and large PWI lesions will benefit from early reperfusion, and that aggressive methods, including intra-arterial therapy, may be indicated. Several clinical trials have examined this hypothesis, including EPITHET, DEFUSE and DEFUSE-2, and MR-RESCUE. These studies have had variable outcomes, and it has been suggested that the DWI-PWI mismatch, while a useful concept, may be an oversimplification of the situation. Other biomarkers have been tested in exploratory studies, including the use of ASL, a non-contrast measurement that can measure quantitative CBF as well as collaterals. PET studies have suggested that elevated oxygen extraction fraction (OEF) is specific for identifying tissue at risk of infarction, and MRI-based measurements are being developed to assess tissue oxygenation. Finally, the use of resting-state fMRI (rs-fMRI), including both its use to identify core and penumbra as well as arterial arrival delays without contrast, and its ability to identify distant effects of focal ischemia upon larger brain connectivity networks will be discussed.

## VSNR41-05 • Percent Insula Infarction at Admission Improves Prediction of Poor Clinical Outcome-Over That of DWI Lesion Volume Alone-in Anterior Circulation Occlusive Stroke Patients

**Vincent M Timpone MD (Presenter) ; Michael H Lev MD \* ; Livia T Morais MD ; Leticia C Souza MD ; Shervin Kamalian MD, MMedSc \* ; Pamela W Schaefer MD**

### PURPOSE

Large admission DWI infarct volume (>70ml) is an established biomarker for poor clinical outcome in acute stroke. Outcome is more variable in patients with small infarcts (< 70ml). It has been shown that percent insula ribbon infarct (PIRI) at admission can predict penumbral loss (poor tissue outcome). We hypothesized that PIRI can also help identify stroke patients likely to have poor clinical outcome, despite small admission DWI lesion volumes.

### METHOD AND MATERIALS

We analyzed the admission NCCT, CTP, and DWI scans of 55 patients with proximal anterior circulation occlusion on CTA. The following parameters were determined: Percent insula ribbon infarct (PIRI, >50%, 2/3) were also recorded. Statistical analyses were performed to determine accuracy in predicting poor outcome (mRS>2 at 90 days). Covariates in our multivariate regression model were admission NIHSS score, DWI-PIRI, motor strip score, and NCCT-PIRI.

### RESULTS

Admission DWI >70ml (p= 50% (p = 0.045) and NIHSS (p= 50%, were not significant predictors of poor outcome. In patients with admission DWI infarct 50% (n=31, median mRS 5, 95%CI=2-5) compared to those with DWI-PIRI < 50% (n=9, median mRS 2, 95% CI=1-3; p= 0.036). In patients with admission DWI infarct >70ml, DWI-PIRI did not have added predictive value for poor outcome (p=0.9308).

### CONCLUSION

DWI-PIRI >50% predicts poor clinical outcome, and can help identify stroke patients likely to have poor outcome despite small admission DWI lesion volumes. Because it facilitates direct visual estimation of the likelihood of poor outcome, the PIRI-score may help more accurately weigh the potential risks versus benefits of advanced stroke treatments than clinical assessment by NIHSS score alone.

### CLINICAL RELEVANCE/APPLICATION

Consideration of DWI insula infarct involvement may be an additional tool for risk-benefit stratification and patient selection for reperfusion therapy.

## VSNR41-06 • The Configuration of Willis Circle Influences Leptomeningeal Collaterals and Regional Perfusion Patterns in Acute Ischemic Stroke. A Standardized Approach

**Georg Homann (Presenter) ; Uta Hanning ; Ludger Feyen ; Volker Hesselmann MD ; Thomas Niederstadt MD ; Andre Kemmling MD**

### PURPOSE

In proximal (M1) middle cerebral artery (MCA) occlusive stroke the primary feeding artery that supplies posterior leptomeningeal collaterals may arise from the ipsilateral anterior or posterior circulation depending of the configuration of the circle of Willis and presence of fetal variants. Aim of this study was to assess regional brain perfusion parameters and patterns of final tissue outcome subject to Willis **circle** variants.

### METHOD AND MATERIALS

Prospectively, stroke imaging (native CT, CTA and dynamic CTP) was performed in 97 acute strokes. Type of vessel occlusion was matched in all cases (distal M1-occlusive strokes). The configuration of the Willis **circle** was rated according to a pattern favoring leptomeningeal supply from the anterior (Pcom > P1-PCA) or posterior (P1-PCA > Pcom) circulation. CTP-parameter maps were transformed to MNI-152 standardized space to calculate regional brain perfusion using a probabilistic atlas (Harvard-Oxford structural atlas). Final tissue outcome was segmented on follow up imaging targeted at 48h after onset.

### RESULTS

Depending on Willis **circle** variants, the perfusion (blood flow) pattern of ischemia was different in fetal (P1-PCA > Pcom) versus normal (Pcom > P1-PCA) variants (ml/100mg/min): temporal pole (41.2 vs. 31.0), inferior temporal gyrus (36.5 vs. 31.0), subcallosal cortex (54.8 vs. 43.8), orbitofrontal cortex (42.6 vs. 36.9), mediofrontal cortex (54.9 vs. 47.8), cingulate gyrus (58.6 vs. 53.9). Final infarct volume was 14% lower in fetal variant (85.2 vs. 98.2 ml)

### CONCLUSION

In acute MCA-occlusion the effectiveness of leptomeningeal collateralization to curb ischemia depends on the source of the primary feeding artery subject to Willis **circle** variants.

### CLINICAL RELEVANCE/APPLICATION

Willis **circle** configuration contributes to leptomeningeal collaterals. This may be relevant for outcome prediction in the acute stroke setting and therapeutic decision making.

## VSNR41-07 • T2\* "Susceptibility Vessel Sign" Demonstrates Clot Location and Length in Acute Ischemic Stroke

**Olivier Naggara MD (Presenter) ; Jean Raymond MD ; Montserrat Domingo Ayllon MD ; Myriam Edjlali ; Sophie Gerber ; Emmanuel Touze ; Matthieu Zuber ; Jean-Francois Meder MD, PhD ; Jean-Louis Mas ; Catherine Oppenheim MD, PhD**

#### PURPOSE

The purpose of this study was to evaluate, in acute stroke patients, the diagnostic accuracy of MR susceptibility vessel sign (SVS) against catheter angiography (DSA) for the detection of the clot and its value in predicting clot length.

#### METHOD AND MATERIALS

The study was approved by the local ethics committee. Informed consent was waived. The manuscript was prepared in accordance with STARD guidelines. We retrospectively identified consecutive patients (2006-2012) with: (1) pre-treatment T2\* sequence; (2) delay from MRI-to-DSA < 3-hrs; (3) no fibrinolysis between MRI and DSA. The presence and length of SVS on T2\* was independently assessed by three readers, and compared per patient, per artery and per segment, to DSA findings, obtained by two different readers. Clot length measured on T2\* and DSA were compared using intra-class correlation coefficient (ICC) and a Passing & Bablok regression analysis.

#### RESULTS

On DSA, a clot was present in all 85 included stroke patients, in 126 arteries and 175 segments. Sensitivity of SVS was 81.1% (69/85 patients), higher in anterior (55/63, 87.3%), than in posterior circulation stroke (14/22, 63.6%, p=0.02). Sensitivity/specificity were 69.8/99.6% (per artery) and 76.6/99.7% (per segment). PPV, NPV and accuracy were >94%. Correlation between T2\* and DSA for clot length was excellent (ICC: 0.88, 95%CI: 0.81-0.92; Passing & Bablok : 0.91).

#### CONCLUSION

SVS is a specific marker of acute clot in the anterior and posterior circulation. Clot length can be measured reliably on T2\*. SVS could serve as a selection criteria for intra-arterial therapy in future randomized control trial.

#### CLINICAL RELEVANCE/APPLICATION

T2\* sequence may allow the non-invasive assessment of the clot burden in acute ischemic stroke, a finding that may help the triage of patients for intravenous or intra-arterial therapy.

### **VSNR41-08 • Stroke Trials: Update and Perspective**

**Steven Warach** MD, PhD (Presenter)

### **VSNR41-09 • Perfusion-based Selection Leads to Improved Outcomes Compared with Time-based Selection for Endovascular Reperfusion Therapy in Acute Ischemic Stroke**

**Maryam Soltanolkotabi** MD (Presenter) ; **Shyam Prabhakaran** MD, MS ; **Farnoosh Feiz** MD ; **Michael C Hurley** MBBCh ; **Ali Shaibani** MD ; **Richard Bernstein** ; **James Connors** MD, MS ; **Sameer A Ansari** MD, PhD ; **Yvonne Curran** MD

#### PURPOSE

Controversy exists on the role of perfusion imaging based selection of patients with AIS for endovascular therapy. Our hypothesis was that perfusion imaging based selection would improve functional outcomes at 3 months compared to time based selection alone.

#### METHOD AND MATERIALS

We reviewed data from consecutive AIS patients treated with ERT at 4 centers from 2006-2011. We excluded patients with initial NIHSS

#### RESULTS

185 patients (mean age 66.7 y; median NIHSS 19; MCA occlusion 73% and ICA occlusion 27%) were included. TICI 2b/3 reperfusion grade was achieved in 49.7% while symptomatic hemorrhage (PH1/PH2/perforation) occurred in 10.8%. Good outcome at 3 months was seen in 41.7%. Perfusion imaging was used in 69 (37.3%) patients (45 CT and 24 MRI) and was associated with increased onset to groin puncture time (359 vs. 298 minutes, P=0.019). Patients who underwent perfusion imaging were also older (73 vs. 63 years, P

#### CONCLUSION

In this multicenter study, AIS patients who underwent perfusion imaging were over 2fold more likely to have good outcome following ERT despite a delay in time to treatment and age imbalance between groups. Further studies should continue to address the optimal perfusion imaging thresholds for patient selection for ERT.

#### CLINICAL RELEVANCE/APPLICATION

Controversy exists on the role of perfusion imaging based selection of patients with acute ischemic stroke (AIS) for endovascular reperfusion therapy (ERT).

### **VSNR41-10 • Endovascular Stroke Device Update**

**Aquilla S Turk** DO (Presenter) \*

### **VSNR41-11 • Socioeconomic Disparities in the Utilization of Mechanical Thrombectomy for Acute Ischemic Stroke**

**Waleed Brinjikji** (Presenter) ; **Alejandro A Rabinstein** MD ; **Harry J Cloft** MD, PhD \*

#### PURPOSE

Previous studies have demonstrated that socioeconomic disparities in access to treatment for cerebrovascular diseases exist. We studied the Nationwide Inpatient Sample (NIS) to determine if disparities exist in utilization of mechanical thrombectomy for acute ischemic stroke.

#### METHOD AND MATERIALS

Using the NIS for the years 2006-2010, we selected all discharges with a primary diagnosis of acute ischemic stroke. Patients who received mechanical thrombectomy for acute ischemic stroke were identified by using the ICD-9 procedure code 39.74. We examined the utilization rates of mechanical thrombectomy by race/ethnicity (white, black, Hispanic, and Asian/Pacific Islander), income quartile (1st, 2nd-3rd, and 4th) and insurance status (Medicare, Medicaid, self-pay and Private). We also studied thrombectomy utilization rates at hospitals which performed thrombectomy.

#### RESULTS

From 2006-2010, 2087017 patients were hospitalized with a primary diagnosis of acute ischemic stroke. 8946 patients (0.4%) received mechanical thrombectomy. When compared to white patients, Black patients had significantly lower rates of overall mechanical thrombectomy utilization (OR=0.59, 95%CI=0.55-0.64, P

#### CONCLUSION

Our study demonstrated that significant socioeconomic disparities exist in the utilization of mechanical thrombectomy for the treatment of acute ischemic stroke. Further studies are needed to study the underlying causes of these disparities and provide solutions to improve equitable access to mechanical thrombectomy, when appropriate, amongst all segments of the population.

#### CLINICAL RELEVANCE/APPLICATION

Minority patients as well as patients of lower socioeconomic status are less likely to receive mechanical thrombectomy for treatment of acute ischemic stroke.

### **VSNR41-12 • Carotid Artery Plaque Characterization on MRI and Stroke Risk: A Systematic Review and Meta-analysis**

**Hediyeh Baradaran** MD (Presenter) ; **Andrew D Schweitzer** MD ; **Allison Dunning** ; **Diana Delgado** MS ; **Ankur Pandya** PhD, MPH ; **Hooman Kamel** MD ; **Pina C Sanelli** MD ; **Ajay Gupta** MD

#### PURPOSE

MRI-based characterization of carotid plaque composition has high accuracy compared to histopathology and has been recently studied as a potential tool to predict ischemic events in carotid atherosclerotic disease. Intraplaque hemorrhage (IPH), lipid-rich necrotic core (LRNC) and thinning/rupture of the fibrous cap (FC) are the three most studied plaque characteristics. We performed a systematic review and meta-analysis to summarize the association between these three plaque characteristics and future ischemic events in patients with

carotid atherosclerotic disease.

#### METHOD AND MATERIALS

We performed a comprehensive literature search evaluating the association of MRI-based characterization of carotid plaque composition with stroke. The included studies were prospective or retrospective studies examining IPH, LRNC, or FC with mean follow-up of at least 1 month assessing for development of ipsilateral ischemic event (stroke or transient ischemic attack [TIA]). A meta-analysis using random and fixed-effects models with assessment of study heterogeneity and publication bias was performed.

#### RESULTS

Of the 3436 manuscripts screened, 10 met eligibility for systematic review including a total of 832 patients. 6 of the manuscripts studied IPH, 4 studied LRNC, and 3 studied thinning/ruptured FC. The hazard ratio (HR) for IPH, LRNC, and thinning/rupture of the FC as predictors of future stroke/TIA are 4.61 (95% CI 3.02-7.02), 3.00 (95% CI 1.51-5.95) and 7.39 (95% CI 3.26- 16.75), respectively. There was significant heterogeneity in the degree of stenosis, presence of prior symptoms, and MRI techniques amongst the included studies. Measures of heterogeneity showed mild heterogeneity only in the IPH meta-analysis and no statistically significant publication bias in any of the three meta-analyses.

#### CONCLUSION

The presence of IPH, LRNC, and thinning/rupture of the FC in carotid plaque increases the risk of future ipsilateral ischemic event in patients with carotid atherosclerotic disease.

#### CLINICAL RELEVANCE/APPLICATION

Dedicated imaging to characterize plaque composition may offer information beyond luminal stenosis to further risk stratify patients with carotid atherosclerotic disease.

---

## Interventional Oncology Series: Progress, Challenges and Opportunities

---

Wednesday, 01:30 PM - 06:00 PM • S405AB

---

[Back to Top](#)

[RO](#) [OI](#) [IR](#)

**VSIO41** • AMA PRA Category 1 Credit™:3.75 • ARRT Category A+ Credit:4

#### Moderator

**S. Nahum Goldberg**, MD \*

#### LEARNING OBJECTIVES

1) Characterize and appreciate the most important advances of interventional oncology over the last two decades within a well-defined optimization model. 2) Identify key challenges, and greatest opportunities facing the interventional oncology community. 3) Determine under which particular clinical scenarios specific ablation energy sources will have particular benefits over their clinically-available competitors.

#### ABSTRACT

From a practical perspective, six main basic research areas in which interventional oncology has made substantial progress over the last two decades have been identified including: Ablation devices, Transcatheter therapy, Combination Therapy (including nano-technologies), Understanding local and systemic ablation biology, Procedural Image-guidance, and Post-Ablation Follow-up. Along these lines, for the first half of the session speakers will initially present the 3 - 5 most important advances that have occurred over the last decade for each of these areas. For each topic, this will be followed by a critical assessment of the most pressing current challenges facing and the greatest opportunities presented to advance these key components of current interventional oncologic practice. An additional presentation on 'Future directions for IO' and a panel discussion 'which factors will most drive future progress' will complement these discussions. The second half of the session will be dedicated to addressing another hotly debated key issue facing the IO community that is becoming ever more relevant with the proliferation of new ablation devices namely: 'When should I be using that specialized device?' Speakers will sequentially present the benefits and limitations of various ablation energy sources for given clinical scenarios including: microwave, cryotherapy, irreversible electroporation, HIFU, and radiofrequency.

### VSIO41-01 • Ablation Devices

**Christopher L Brace** PhD (Presenter) \*

#### LEARNING OBJECTIVES

1) Identify the most common ablation modalities. 2) Compare each modality in terms of energy delivery physics and clinical utility. 3) Analyze common devices for each modality. 4) Evaluate each device's potential clinical value.

#### ABSTRACT

Thermal ablation devices continue to evolve at a rapid pace. While more established modalities such as radiofrequency (RF) and cryoablation have seen less technological growth in recent years, much is still to be gained from their respective devices. Microwave ablation and irreversible electroporation (IRE) device are now expanding into the clinical marketplace. Six microwave systems are cleared by the FDA, leading to some confusion about how to differentiate those systems from a clinical perspective. IRE as a treatment modality has been slower to emerge as many users await further scientific evaluation of existing systems. The objective of this presentation will be to provide an overview of the basic underlying physics of each treatment modality, present the systems and devices available for clinical use, and elucidate some of the important features of each system to help physician's decide which may be right for their practice.

### VSIO41-02 • Transcatheter Therapies

**Jean-Francois H Geschwind** MD (Presenter) \*

#### LEARNING OBJECTIVES

View learning objectives under main course title.

### VSIO41-03 • Novel Navigation Technique for Superselective TACE to Obtain 3D-safety Margin for HCC

**Toshihiro Tanaka** MD (Presenter) ; **Hideyuki Nishiofuku** ; **Hiroshi Anai** MD, PhD ; **Shinsaku Maeda** ; **Hiroshi Sakaguchi** MD ; **Kimihiko Kichikawa** MD

#### PURPOSE

Our previous report presented at RSNA 2012 demonstrated the importance of the 3-dimensional embolization margin (3D-safety margin) in superselective transcatheter arterial chemoembolization (TACE), which could significantly prolong disease free survival. We developed novel navigation TACE using hybrid CT/Angio with a workstation to obtain 3D-safety margin, and prospectively evaluated the feasibility of this technique.

#### METHOD AND MATERIALS

Fifteen patients with small HCC (size: 1.2-2.9cm, mean 1.8cm) and good liver function (Child-Pugh score: 5-7, mean 5.5) were enrolled in this pilot study. Firstly, a maximum intensity projection (MIP) imaging of the hepatic arteriography was created using CT during hepatic arteriography (CTHA) via the common hepatic artery (CHA). Secondly, a catheter was superselectively inserted into the tumor feeding artery, and presence or absence of the 3D-safety margin was evaluated by the 3D-fusion images reconstructed using whole liver CTHA via CHA and superselective CTHA via the targeted artery. Thirdly, in the cases without 3D-safety margins, the regions, which lacked safety margins, were marked by a workstation (ZIOSTATION<sup>®</sup>). These markings automatically appeared on the MIP images, which showed the arterial branches supplying the tumor surrounding areas.

## RESULTS

In 13 of 15 patients, 3D-safety margins were absent in the initial fusion images. In all 13 cases, the MIP images of the hepatic arteriography clearly showed the supplying branches into the marginal areas. Superselective TACE using lipiodol (mean volume 2.7ml) mixed with epirubicin (mean volume 23mg) were conducted via both the tumor feeding arteries and the marginal branches. 3D-safety margins were obtained in all 15 patients. No severe complications including liver dysfunction were observed. The mean Child-Pugh score after TACE was 5.5, and no local recurrence was seen during follow-up periods (mean 233 days, range: 171-344 days).

## CONCLUSION

Superselective TACE using this novel navigation technique can achieve 3D-safety margin for HCC patients. Currently, a phase II study using this technique is ongoing to evaluate the local tumor recurrence rate for long term period.

## CLINICAL RELEVANCE/APPLICATION

Superselective TACE using this navigation technique can achieve 3D-safety margin, which could prevent local recurrence.

### **VSIO41-04 • Combination Therapy**

**Muneeb Ahmed** MD (Presenter)

#### LEARNING OBJECTIVES

1) Demonstrate how understanding tissue responses in and around the ablation zone can be used to develop mechanism-based approaches to combination therapy. 2) Demonstrate how combination strategies for IO using nanoagents offer significant promise for improving minimally-invasive thermal therapy.

#### ABSTRACT

### **VSIO41-05 • Comparison of Transarterial Administration of Survivin siRNA Combined with Transarterial Chemoembolization (TACE) and TACE Alone in the Treatment of Rats with Hepatocellular Carcinoma (HCC): Experimental Study**

**Thomas J Vogl** MD, PhD (Presenter) ; **Jun Qian** MD ; **Andreas Tran** ; **Elsie Oppermann** ; **Ulli Imlau** ; **Yousef Hamidavi** ; **Huedayi Korkusuz** MD ; **Wolf-Otto Bechstein**

#### PURPOSE

To evaluate the effects of transarterial administration of survivin siRNA combined with transarterial chemoembolization (TACE) vs. TACE alone for treating hepatocellular carcinoma (HCC) in rats.

#### METHOD AND MATERIALS

Subcapsular implantation of a solid Morris hepatoma 3924A in the liver was carried out in 20 male ACI rats (day 0). Tumor volume (V1) was measured by MRI (day 12). After laparotomy and retrograde placement of a catheter into the gastroduodenal artery (day 13), the following different agents were injected into the hepatic artery: TACE (0.1mg of mitomycin + 0.1ml of lipiodol + 5.0mg of degradable starch microspheres) + 2.5nmol survivin siRNA (group A, n=10) or TACE alone (group B, n=10). Tumor volume (V2) was assessed by MRI (day 25), tumor growth ratio (V2/V1) was calculated. Western blot analysis was performed to assess the protein expression level of survivin in each treatment. The progressional potential of the tumors was assessed for quantification of positive VEGF tumor cells via immunohistochemical analysis.

#### RESULTS

Mean tumor growth ratio (V2/V1) was  $1.1313 \pm 0.1381$  in group A, and  $3.1911 \pm 0.1393$  in group B. Compared with group B, group A showed significant inhibition of tumor growth (p

#### CONCLUSION

Combined TACE and transarterial administration of survivin siRNA is more effective than TACE alone for inhibiting the growth of HCC in rats.

#### CLINICAL RELEVANCE/APPLICATION

Combined TACE and transarterial administration of survivin siRNA may be a relevant treatment option in hepatocellular carcinoma.

### **VSIO41-06 • Understanding Local and Systemic Ablation Biology**

**Joseph P Erinjeri** MD, PhD (Presenter)

#### LEARNING OBJECTIVES

View learning objectives under main course title.

### **VSIO41-07 • Adoptive Immunotherapy for Hepatocellular Carcinoma with MRI-monitored Transcatheter Delivery of Ferumoxylol Nanocomplexes-labeled Natural Killer Lymphocytes**

**Kangan Li** MD (Presenter) ; **Zhuoli Zhang** MD, PhD ; **Andrew C Gordon** BA ; **Alexander Y Sheu** BS ; **Weiguo Li** ; **Reed A Omary** MD \* ; **Gui-Xiang Zhang** MD ; **Andrew C Larson** PhD \*

#### PURPOSE

Natural killer (NK)-lymphocytes adoptive immunotherapy (AIT) has advantages over other immunotherapy approaches in being non-MHC-restricted, non-immunogenic and highly cytotoxic for Hepatocellular Carcinoma (HCC). To improve the AIT efficiency, it is essential to visualize and quantify both the biodistribution of NK cells and the AIT responses. The purpose of this study was to test the hypotheses that: a) Magnetic resonance imaging (MRI) will allow quantitative visualization of transcatheter infusion for targeted delivery of ferumoxylol-heparin-protamine (HPF) nanocomplexes-labeled NK cells to HCC; 2) NK cell AIT responses may be predicted based upon MRI measurements.

#### METHOD AND MATERIALS

NK-92MIs were labeled with HPF. 24 Sprague Dawley rats were implanted with McA-RH7777 tumors; 6 rats each comprised intra-arterial (IA)NK, intraportal (IP)NK, IA+IP NK, and IA saline groups. Catheter was placed in hepatic artery or/and portal vein for IA NK/saline or/and IP NK infusions. MRI tumor size, T2\*, apparent diffusion coefficient (ADC) and volume transfer constant (Ktrans) measurements were compared pre and 12 days post infusion. Tumor size changes, T2\*, ADC, and Ktrans were compared; Prussian blue staining was used for histological identification of labeled NK cells; CD56 and CD34 staining qualitatively confirmed NK cells delivery and tumor angiogenesis. ANOVA and Pearson correlation coefficients were used for statistical analyses.

#### RESULTS

Initial tumor diameters were not different between groups (p=0.23), but final tumor diameters were different between all groups (p

#### CONCLUSION

The IA or/and IP distribution of HPF-labeled NK cells were quantitatively visualized with MRI, and labeled NK cell delivery as measured by histology and T2\* were well-correlated with tumor response as determined by change in tumor size, ADC, and Ktrans, with IA+IP NKs demonstrating the strongest response.

#### CLINICAL RELEVANCE/APPLICATION

This technique has potential for in-vivo evaluation of the distribution of NK-cells and AIT responses which can help adjust the patient-specific therapeutic regimens during the clinical application.

### **VSIO41-08 • Radiofrequency (RF) Ablation: Does the Primary Site of Ablation Affect Distant Tumor Growth?**



#### PURPOSE

To determine the effect of primary target site of radiofrequency ablation (RFA) on growth rates of distant subcutaneous tumors in two small animal models.

#### METHOD AND MATERIALS

This study was performed in two different tumor models in Fisher 344 rats. Firstly, R3230 single subcutaneous adenocarcinoma tumors were randomized at 10-11 mm to receive standardized RFA (21g electrode, 1cm active tip, tip temperature 70°Cx5min) or sham procedure (electrode placement without RF) to normal liver or normal kidney (4 groups, n=6 each, total n = 24). Next, two subcutaneous R3230 tumors were implanted, and animals were randomized to either RFA or sham arms (2 groups, n=6 each, total 12 animals). Finally, RFA or sham of normal liver or kidney was performed in animals with a single MATIIB subcutaneous tumor (4 groups, n=6 each, total 24 animals). Animals were sacrificed and tumors harvested at 3.5d (MATIIB) or 7d (R3230) post-treatment. Tumor growth analysis and proliferative indices (Ki67 staining) was performed.

#### RESULTS

RFA of liver and kidney increased distant R3230 tumor size at 7d compared to sham (17.1±2.2mm and 19.6±1.8mm vs. 14.0±1.1mm, p

#### CONCLUSION

RF ablation of various tissues, including liver, kidney, and tumor, can increase the growth rate of distant untreated tumors in two different animal models. RFA of certain organs (such as kidney or tumor) exhibit a stronger growth stimulatory effect. Further study of underlying mechanisms will be critical to minimizing these potentially negative effects.

#### CLINICAL RELEVANCE/APPLICATION

RFA is applied in many tumors and organs. Our study suggests that potentially harmful tumor stimulatory effects likely need to be characterized in an organ-specific manner.

### **VSI041-09 • Procedural Image-Guidance**

**Bradford J Wood** MD (Presenter) \*

#### LEARNING OBJECTIVES

View learning objectives under main course title.

### **VSI041-10 • Imaging Follow-up**

**Riccardo A Lencioni** MD (Presenter)

#### LEARNING OBJECTIVES

View learning objectives under main course title.

### **VSI041-11 • Radiologic-pathologic Correlation of Three-dimensional Shear-wave Elastographic Findings after Radiofrequency Ablation**

**Katsutoshi Sugimoto** MD, PhD (Presenter) ; **Saori Ogawa** ; **Hisashi Oshiro** ; **Takeshi Hara** PhD ; **Yasuharu Imai** ; **Fuminori Moriyasu** MD, PhD

#### PURPOSE

To characterize the findings of three-dimensional (3D) shear-wave elastography (SWE) after radiofrequency (RF) ablation to determine the utility of these findings in the accurate assessment of ablation margins and volumes.

#### METHOD AND MATERIALS

RF ablation (n = 10) was performed in vivo in 10 rat livers using a 15-gauge expandable RF needle. 3D SWE including B-mode ultrasound (US) was performed 15 minutes after the ablation. The acquired 3D volume data were rendered as multislice images (interslice distance, 1.10 mm), and estimated ablation volumes were computed. We compared the 3D SWE findings with digitized gross pathologic and histopathologic photographs obtained in the same image planes as those of the 3D SWE multislice images. Ablation volumes were also estimated by gross pathologic assessment. These measurements were compared with each other.

#### RESULTS

In B-mode US, the ablation zone appeared as a hypoechoic area with a peripheral hyperechoic rim 15 minutes after RF ablation; however, the findings were largely obscure for estimating the ablation area. 3D SWE depicted ablation area and volume more clearly. At the largest ablation area, the mean kPa values of the peripheral rim, central zone, and non-ablated zone were 13.1 kPa ± 1.5, 59.1 kPa ± 21.9, and 4.3 kPa ± 0.8, respectively. The ablation volumes obtained by 3D SWE showed the highest correlation (r = 0.9646; p < 0.00001) with those estimated from gross pathologic assessment. Infiltration of red blood cells observed by histopathologic examination was greater in the peripheral rim of the ablation zone than in the central zone.

#### CONCLUSION

These findings suggest that SWE outperformed B-mode US. 3D SWE can be a reliable technique for spatially delineating thermal lesions resulting from RF ablation.

#### CLINICAL RELEVANCE/APPLICATION

3D SWE could potentially be used for routine assessment of thermal therapies.

### **VSI041-12 • Future Directions for IO**

**S. Nahum Goldberg** MD (Presenter) \*

#### LEARNING OBJECTIVES

View learning objectives under main course title.

### **VSI041-13 • Panel: Which Factors Will Most Drive Future Progress?**

#### LEARNING OBJECTIVES

View learning objectives under main course title.

### **VSI041-14 • When Should I Be Using that Specialized Device: MW Systems**

**Fred T Lee** MD (Presenter) \*

#### LEARNING OBJECTIVES

1) Explain basic microwave physics. 2) Demonstrate the differences between radiofrequency and microwave devices. 3) Show illustrative cases where microwave was either useful or contraindicated.

### **VSI041-15 • Development of New Materials for Tissue Hydrodissection: An Analysis of Heat Transfer in Liquids and Gels**

**Alexander Johnson** BS (Presenter) ; **Christopher L Brace** PhD \*

## PURPOSE

Hydrodissection is used during image-guided interventions to protect critical tissues from damage collateral to the treatment site. Liquids such as normal saline and 5% dextrose in water (D5W) have been used during thermal ablation, but thermoreversible poloxamer 407 (P407) gels may offer greater stability and robustness. The goal of this study was to evaluate the relative importance of conductive and convective heat dissipation in liquid P407, gel P407, and liquid D5W.

## METHOD AND MATERIALS

Radiofrequency (RF) and microwave (MW) ablations were created in ex vivo bovine liver for 10 minutes adjacent to an 11 mm barrier of either gel P407, liquid P407 or liquid D5W. Temperatures were recorded at multiple locations inside the barrier using fiberoptic probes. All experiments were performed in triplicate. Temperature increases at each position within each setup was compared using two-tailed, unpaired Student's t-tests.

## RESULTS

All materials adequately protected the adjacent tissue during RF and MW ablation (mean temperature increase .05). Gel P407 reduced heat flow compared to liquids as indicated by a greater range in mean temperature elevation within the barrier ( $10.2 \pm 0.5^\circ\text{C}$  for gel P407,  $1.3 \pm 0.8^\circ\text{C}$  and  $1.1 \pm 0.9^\circ\text{C}$  for liquid P407 and D5W, respectively; P

## CONCLUSION

Both P407 and D5W provided adequate thermal protection during RF and MW ablation. Heat dissipation in gel P407 was conduction dominated, but was convection domination in D5W and liquid P407. Additionally, P407 switches its primary mode of heat dissipation from convection to conduction after gelation. Thus, fluids convectively dissipate heat and may require a large reservoir for adequate protection while gel materials may need a greater thickness but provide more thermal protection due to lower heat dissipation rates. Further in vivo evaluation seems warranted.

## CLINICAL RELEVANCE/APPLICATION

The clinical use of novel hydrodissection materials can now be educated by empirical evidence of protective ability and general guidelines for barrier creation.

### VSI041-16 • When Should I Be Using that Specialized Device: Cryo

**Peter J Littrup MD (Presenter) \***

#### LEARNING OBJECTIVES

1) Understand the different approaches and techniques for thorough cryoablation of nearly any tumor location (e.g., the 1-2 Rule). 2) Understand unique benefits of cryoablation for soft tissue locations of head and neck, bone, intra/retroperitoneum and superficial locations (i.e., chest/abdominal wall), as well as more central locations for chest liver and renal ablations. 3) Understand techniques to minimize morbidity, assessing tumor location and approach. 4) Identify major imaging follow-up criteria for ablation success and any early failures. 5) Describe the overall cost-efficacy trade-offs for cryo vs. heat-based renal ablations vs. stereotactic body radiation therapy, in relation to tumor location, complications and recurrence rates.

#### ABSTRACT

Cryoablation of tumors in difficult-to-treat locations offers a lower pain alternative than heat-based modalities, especially for multiple soft tissue and central organ locations. Major cryoablation benefits include its excellent visualization of ablation zone extent, low procedure pain and flexible hydrodissection very close to skin surface and adjacent crucial structures. CT-guidance is the cryoablation guidance modality of choice due to circumferential visualization and ready availability. US-guidance can augment cryoablation, especially for smaller superficial masses and/or placement of interstitial metallic markers during biopsy for selected cases requiring better eventual CT localization. MR-guidance has little clinical benefit or cost-efficacy. For safety, cases will be considered for choosing the most amenable approach for a wide variety of anatomic locations. Imaging outcomes of complications and their avoidance will be shown. For optimal efficacy, tumor size in relation to number and size of cryoprobes emphasize the 1-2 Rule of at least 1 cryoprobe per cm of tumor diameter and no further than 1 cm from tumor margin, as well as cryoprobe spacing of

### VSI041-17 • When Should I Be Using that Specialized Device: IRE

**Stephen B Solomon MD (Presenter) \***

#### LEARNING OBJECTIVES

View learning objectives under main course title.

### VSI041-18 • When Should I Be Using that Specialized Device: HIFU

**David C Gianfelice MD (Presenter)**

#### LEARNING OBJECTIVES

1) Introduction to technology of focused ultrasound ablation. 2) Review of thermal monitoring as an aid to treatment. 3) Review of FDA approved treatment protocols to date, uterine fibroids and bone metastases. 4) Update on research protocols in progress. 5) Future applications.

### VSI041-19 • RF Ablation: Still the Preferred Ablation Technology in Practice!

**Alison R Gillams MBChB (Presenter) \***

#### LEARNING OBJECTIVES

1) To learn the relative merits of radiofrequency ablation over other ablation technologies. 2) To understand the limitations of radiofrequency and how to overcome them.

### VSI041-20 • Panel Discussion

#### LEARNING OBJECTIVES

View learning objectives under main course title.

---

## Cardiac Radiology Series: Cardiac Dual Energy CT

Thursday, 08:30 AM - 12:00 PM • S404CD

QA CT CA

[Back to Top](#)

VSCA51 • AMA PRA Category 1 Credit™:3.75 • ARRT Category A+ Credit:4

Moderator

U. Joseph Schoepf, MD \*

Moderator

James P Earls, MD \*

VSCA51-01 • Technique

#### LEARNING OBJECTIVES

1) To learn about the basic principles and data acquisition strategies of dual energy CT. 2) To understand the different acquisition strategies for cardiac CT. 3) To learn about dose implications in cardiac dual energy CT.

#### ABSTRACT

Dual-energy cardiac CT represents the combination of two of the most demanding CT applications; special hardware, scan protocols and dedicated data processing algorithms are demanded for both, high scan speed is an additional prerequisite.

Dual energy CT (DECT) data acquisition can be achieved by taking two separate scans at different voltages, by rapid kV-switching, or by using dual-source CT operating with different voltages and pre-filtrations. These concepts and the resulting options to determine tissue parameters will be explained.

Cardiac CT requires data acquisition in time intervals as short as possible based on either prospective triggering or retrospective gating. The technical options available allow either single or dual source spiral CT or stepwise sequential acquisition and will also be explained. Dose levels for cardiac dual energy CT are moderate in general. Details and examples are given in the following lectures.

### **VSCA51-02 • Dose Levels and Image Quality of Second-generation 128-slice Dual-source Coronary CT Angiography - Comparison of High-pitch Spiral, Sequential, Retrospectively ECG-gated Spiral and Dual-energy Acquisition Mode**

**Julian L Wichmann** MD (Presenter) ; **Xiaohan Hu** MD ; **Alexander Engler** MD ; **Ralf W Bauer** MD \* ; **Claudia Frellesen** ; **Boris Bodelle** MD ; **Thomas Lehnert** MD ; **Martin Beeres** MD ; **Thomas J Vogl** MD, PhD ; **Josef Matthias Kerl** MD \*

#### PURPOSE

To compare the radiation exposure and image quality of coronary CT angiography (cCTA) protocols on a second generation 128-slice dual-source CT (DSCT) scanner.

#### METHOD AND MATERIALS

We prospectively included 100 patients referred for cCTA. Patients with a heart rate below 65 bpm were randomized between prospectively ECG-gated high-pitch spiral (group 1) and narrow-window sequential (group 2) acquisition. Patients with a heart rate above 65 bpm were randomly assigned to a retrospectively ECG-gated spiral acquisition protocol in either dual-source (group 3) or dual-energy (group 4) mode. CT dose index volume, dose length product, effective dose, contrast-to-noise and signal-to-noise ratio were compared. Subjective image quality was rated by two observers blinded to the used protocol.

#### RESULTS

High-pitch spiral cCTA showed a mean estimated radiation dose of  $1.27 \pm 0.64$  mSv, significantly ( $p < 0.05$ ), ranging from  $16.03 \pm 6.3$  (group 1) to  $19.3 \pm 9.5$  (group 4) and  $20.1 \pm 16.5$  (group 2) up to  $26.4 \pm 23.0$  (group 3). Each protocol showed diagnostic image quality in at least 98.4% of evaluated coronary segments.

#### CONCLUSION

Prospectively ECG-gated DSCT protocols allow cCTA with significant dose reduction. High-pitch spiral mode generates less than 1/2 of the estimated radiation exposure of sequential acquisition mode. In patients with a heart rate above 65 bpm, dual-energy mode should be preferred over spiral DSCT as it significantly decreases estimated dose without compromising diagnostic image quality.

#### CLINICAL RELEVANCE/APPLICATION

Second-generation DSCT scanners allow cCTA in patients with normo- or arrhythmia that result in significant dose reduction while maintaining diagnostic image quality.

### **VSCA51-03 • Diagnostic Performance of Dual Energy Computed Tomography Stress Myocardial Perfusion Imaging: A Direct Comparison to Cardiac Magnetic Resonance**

**Sung Min Ko** (Presenter) ; **Jin-Woo Choi** ; **Hweung Kgon Hwang** ; **Meong Gun Song**

#### PURPOSE

This study aimed to determine the diagnostic performance of stress testing by dual-energy computed tomography (DECT) for identification and exclusion of hemodynamically significant stenoses when compared to combined conventional coronary angiography (CCA) and stress perfusion cardiac magnetic resonance (SP-CMR) as reference standards.

#### METHOD AND MATERIALS

One hundred patients without prior known coronary artery disease without chronic myocardial infarction detected by coronary CT angiography (CCTA) were included and underwent SP-DECT, SP-CMR, and CCA. All CT examinations were performed using a Somatom Definition scanner. DECT-based iodine maps were used for detecting myocardial perfusion defects (MPDs) (per-vessel and per-segment) and compared with SP-CMR. The assessment of MPDs was based on visual analysis instead of quantitative analysis because DECT-based iodine map highlights areas of decreased iodine in the left ventricular myocardium. SP-CMR exams were performed on a Signa HDxt 1.5-T system with an 8-element phased array surface coil or a Magnetom Skyra 3.0-T system with a 32-channel body coil after SP-DECT. Diagnostic values of CCTA for detecting hemodynamically significant stenosis were assessed before and after SP-DECT on a per-vessel basis compared with CCA/SP-CMR as the reference standard.

#### RESULTS

The performance of SP-DECT for detecting MPDs compared with SP-CMR was sensitivity, 89%; specificity, 74%; positive predictive value (PPV), 73%; negative predictive value (NPV), 90% (per-vessel). Compared to the combined CCA/SP-CMR for identifying hemodynamically significant stenosis, per-vessel territory sensitivity, specificity, PPV, and NPV of CCTA were 95%, 61%, 61%, and 95%, respectively, those by using SP-DECT were 92%, 72%, 68%, and 94%, respectively, and those by using CCTA/SP-DECT were 88%, 79%, 73%, and 91%, respectively. The area under the receiver operating characteristic curve increased from 0.78 to 0.84 ( $p = 0.02$ ) using CCTA/SP-DECT compared with CCTA.

#### CONCLUSION

SP-DECT can play a complimentary role to enhance the accuracy of CCTA for identifying hemodynamically significant stenosis.

#### CLINICAL RELEVANCE/APPLICATION

SP-DECT has the potential to become a robust clinical tool for the detection of myocardial ischemia and can be used as an alternative to other perfusion imaging techniques such as SP-CMR and SPECT.

### **VSCA51-04 • Diagnostic Value of Dual-energy Computed Tomography (DECT) Combined CT Perfusion and CT Angiography in Patients after Coronary Stent Implantation**

**Lingyan Kong** MD (Presenter) ; **Zhengyu Jin** MD ; **Yining Wang** MD

#### PURPOSE

To evaluate the diagnostic value of dual-energy computed tomography (DECT) combined CT perfusion (CTP) and CT angiography (CTA) in patients after coronary stent implantation, in compare with quantitative coronary angiography (QCA).

#### METHOD AND MATERIALS

#### RESULTS

Using QCA as a reference standard, the sensitivity and specificity of DE-CTA for detecting in-stent stenosis was 75.0% and 100%, respectively. The accuracy was 94.3%. For detecting non-stent stenosis on the vessel-based analysis, DE-CTA showed sensitivity of 87.5%, specificity of 100%, and accuracy of 93.3%, while the combination of CTA and CTP showed accuracy of 100%.

## CONCLUSION

DECT has a high diagnostic accuracy for the detection of in-stent restenosis. CTA combined with CTP may improve the diagnostic accuracy for detecting non-stent significant coronary stenosis.

## CLINICAL RELEVANCE/APPLICATION

DECT may evaluate both stenosis of coronary artery and myocardial perfusion in the assessment of coronary artery disease, and shows value in follow up of coronary stent implantation.

### VSCA51-05 • Reduced Contrast Medium in 100kVp Coronary Artery Angiography with Dual-source CT

**Dan Han MD (Presenter) ; Jun Zhang**

#### PURPOSE

To evaluate the image quality of 100kVp dual-source CT coronary angiography using three different contrast media (CM) injection protocols.

#### METHOD AND MATERIALS

In this IRB approved study, dual-source CT coronary angiography scans were performed in 120 patients, who were randomly divided into three groups using contrast medium with concentration of 370 mg I/mL, 320 mg I/mL and 270 mg I/mL at the same injection rate (5.0 mL/s, 14 s). The CT scan protocol was the same in three groups (prospective scan, 100kVp, reference mAs: 400 mAs) with automatic tube current modulation activated. Two observers evaluated the visibility of 4 main branches of coronary arteries. The mean CT values in coronary artery, image noise, signal-to-noise ratio (SNR), contrast-to-noise ratio (CNR), radiation dose, patient BMI were recorded and compared using one way ANOVA test among three groups.

#### RESULTS

The three groups all had an average body mass index (BMI) value of 22 kg/m<sup>2</sup>. The assigned CM volume was 60 mL in 370 group, 65 mL in 320 group and 65 mL in 270 group. The visibility of 4 main branches of coronary arteries are all 100% in three groups by two observers. The mean CT value in 270 group (390.65 +/- 50.34 HU) was lower than 320 group (466.76 +/- 45.65 HU) and 370 group (710.32 +/- 45.65 HU), where the difference was statistically significant (p < 0.05). The SNRs and CNRs were 27.42 +/- 4.21 and 21.7 +/- 4.4 for 370 group; 27.68 +/- 4.09 and 20.1 +/- 5.2 for 320 group; 26.12 +/- 4.13 and 21.2 +/- 5.7 for 270 group. There was no statistical difference were found in image noise, SNR, CNR and radiation dose (p > 0.05).

#### CONCLUSION

Using 270 mg I/mL iodine Contrast Medium and 100 kVp tube voltage scan protocol with dual-source CT coronary angiography is feasible in patients with normal BMI. This scan protocol can substantially reduce iodine intakes for patients while preserve good diagnostic image quality.

#### CLINICAL RELEVANCE/APPLICATION

Using 270 mg I/mL iodine Contrast Medium with dual-source CT coronary angiography is equal to 370 mg I/mL in detecting plaque of coronary.

### VSCA51-06 • Multiple Vulnerable Plaque Characteristic Factors Co-existing in Single Non-obstructive Non Calcified or Mixed Plaques in Coronary Arteries are Higher Risk Predictors of Major Cardiac Events on CT

**Hiroyuki Takaoka MD, PhD (Presenter) ; Nobusada Funabashi MD, PhD ; Masae Uehara MD ; Koya Ozawa MD ; Yoshihide Fujimoto ; Yoshio Kobayashi**

#### PURPOSE

To evaluate significance of presence of three vulnerable plaque characteristics (VPC) co-existing in single non calcified plaques (NCP) or mixed plaques (MP) in non obstructed coronary arteries on CT: 1) low attenuation (LA) (< 30HU), 2) positive remodeling (PR) and 3) spotty calcification (SC), for the risk of major adverse cardiac events (MACE).

#### METHOD AND MATERIALS

166 consecutive subjects with suspected coronary artery disease (81 male; 62 ± 13 years; hypertension, 61%; diabetes mellitus, 21%; dyslipidemia, 56%; smokers, 45%; obese, 49%) underwent cardiac CT (Light speed Ultra 16, GE Healthcare) from 2003 to 2004. On CT no significant stenosis (> 50%) of coronary arteries was observed; subjects were retrospectively followed for a median of 103 months after CT and incidence of MACE was compared. Subjects with old myocardial infarction or myocardial diseases were excluded from the analysis. MACE included cardiac death, acute coronary syndromes, new onset of angina pectoris, and cardiac failure.

#### RESULTS

39 subjects had NCP (17) or MP (22), of whom 8, 29, and 14 subjects had LA, PR, and SC in NCP or MP, respectively. These were classified into 4 groups, 1) 128 who did not have NCP or MP with any VPCs, 2) 20 who had NCP or MP with one VPC, 3) 14 who had NCP or MP with two VPCs and 4) 2 who had NCP or MP with three VPCs. 6 subjects (4%) had MACE. Subjects who had NCP or MP with = two VPCs (n=16) had a higher risk of MACE than subjects with = one VPC (n=150) (P < 0.05) during the observation period. Significant differences between subjects with NCP or MP with = two VPCs and others (zero, one VPC groups) were observed at each time point when the whole period of follow-up was compared by Kaplan Meier analysis and log rank test (P < 0.001). A Cox proportional hazard model revealed that presence of NCP or MP with = two VPCs on coronary arteries on CT was a greater predictor of MACE (Hazard ratio 7.5, 95% confidential interval 1.0-55.4, P < 0.05 than other factors).

#### CONCLUSION

Presence of NCP or MP with = two VPCs in non obstructed coronary arteries on CT were critical factors for the prediction of MACE in subjects with normal myocardium on follow-up for a median of 103 months.

#### CLINICAL RELEVANCE/APPLICATION

Even in subjects without significant stenosis in coronary arteries on CT, if NCP or MP with = two VPCs are observed on CT, careful follow-up with control of risk factors is desired.

### VSCA51-07 • Radiation Dose

**James P Earls MD (Presenter) \***

#### LEARNING OBJECTIVES

1) Understand how the use of dual energy technique affects radiation dose from CT exams. 2) Identify which parameters can be changed to reduce the dose of dual energy exams. 3) Discuss the relative differences in radiation dose of dual energy and single energy CT exams.

#### ABSTRACT

Dual energy techniques have been developed and are now available for imaging the heart with CT. This course will discuss how different techniques, dual source and single source fast kV switching, can effect the dose of the exams. We will review how the scan protocols can be manipulated to minimize the dose to the patient. We will also compare doses from dual energy and single energy exams.

### VSCA51-08 • Dual Energy versus Single Energy CT in the Evaluation of Myocardial Perfusion in Correlation with SPECT Studies

**Patricia M Carrascosa MD (Presenter) \* ; Carlos Capunay MD ; Alejandro Deviggiano MD ; Javier Vallejos MD ; Roxana Campisi ; Maria Munain ; Carlos Tajer ; Jorge M Carrascosa MD**

#### PURPOSE

A main challenge of myocardial CT perfusion (CTP) is beam hardening. With the developments of dual-energy CT (DECT) scanning, the beam hardening artifact could be reduced with the generation of monochromatic images. The objective of this paper is to determine the usefulness of Stress-Rest DECT versus Single Energy CT (SECT) in the evaluation of myocardial perfusion in correlation with SPECT findings.

#### METHOD AND MATERIALS

Forty patients with known or suspected coronary artery disease who had a positive stress test for ischemia or had an indication of SPECT study were included. Twenty patients were scanned using a DECT scanner and the other 20 using a SECT scanner. Demographic data was similar in both groups. In all patients, a stress CT scan was carried out first, and 30 minutes later a rest CT scan was complemented. Dipyridamol was used for stress myocardial perfusion imaging in both CT and SPECT studies.

A 17 segmental-model analysis was done to determine myocardial segments with perfusion defects. Monochromatic images at different keV from the DECT data and SECT images were evaluated for the detection of myocardial perfusion defects based on Hounsfield units. CT analysis was carried out blinded to SPECT results, considered as the gold standard. Statistical analysis: The 95% confidence interval of the proportions was calculated by the exact binomial method to determine the presence of myocardial perfusion defects. Correlation between DECT, SECT and SPECT studies was measured by the kappa coefficient.

#### RESULTS

The mean radiation dose for each patient was 7.1 +/- 1.2 mSv on DECT exams and 8.1 +/- 1.1 mSv on SECT scans. For detection of the presence of myocardial perfusion defects, DECT showed a sensitivity of 82.1%; specificity 96.7%; PPV 85.5%; NPV 96%, with a k=0.77. SECT showed a sensitivity of 70.3%; specificity 90.7%; PPV 79.3%; NPV 85.7%, with a k=0.62.

#### CONCLUSION

Stress-Rest DECT myocardial perfusion demonstrated higher sensitivity and specificity than SECT in correlation with SPECT for the detection of myocardial perfusion defects using similar radiation dose. More studies have to be done to validate these results.

#### CLINICAL RELEVANCE/APPLICATION

Quantitative myocardial CT perfusion for the assessment of coronary artery disease may have a significant effect on patient care, giving a functional significance to a coronary stenosis.

### **VSCA51-09 • One-step Dual-energy Cardiac CT Scan for Diagnostic and Prognostic Evaluation of Coronary Artery Disease**

**Patricia M Carrascosa MD (Presenter) \* ; Carlos Capunay MD ; Alejandro Deviggiano MD ; Javier Vallejos MD ; Jorge M Carrascosa MD**

#### PURPOSE

Coronary artery calcium score (CCS) is used for risk stratification and early detection of coronary atherosclerosis. It is well known that CCS is an independent predictor of cardiovascular events and it adds value to the Framingham risk score. The objective of this study is to evaluate the possibility of obtaining the information given by CCS from a contrast enhanced dual energy coronary CT angiography (DE-CCTA).

#### METHOD AND MATERIALS

Twenty five patients were evaluated with a 128 slice CT scanner (Discovery CT750 HD; GE Medical Systems). All patients underwent a non-contrast calcium score and then a contrast enhanced DE-CCTA. First the non contrast CCS scan was evaluated with a dedicated special software (Smart score; GE Medical Systems) in order to quantify the calcium score of each patient. Additionally, mass and volume of burden calcium plaque were obtained from the same software.

The contrast enhanced DE-CCTA data was decomposed into monochromatic images at 140 keV obtaining a virtual non-contrast serie and calcium [iodine] material images. The volume of burden calcium plaque was obtained by using a 3-D voxel quantification method. Correlation between results of calcium volumes from CCS software and DE-CCTA data was performed by the intra-class correlation coefficient.

#### RESULTS

By coronary calcium score software, the median of Agatston score was 208 (range: 0-2045), the median coronary calcium mass was 36 mg (range: 0-264 mg), and the median of calcium plaque volume was 92 mm<sup>3</sup> (range: 0-778 mm<sup>3</sup>), while the median of calcium volume by 3-D quantification from the DE-CCTA data was 98 mm<sup>3</sup> (range: 0-771 mm<sup>3</sup>), without significant differences between both methods (p >0.05). Correlation between CCS and DE-CCTA in calcium volume quantification was r: 0.98.

#### CONCLUSION

There was a linear relationship with excellent correlation between the amounts of calcium measured by coronary calcium score software and those by the 3-D quantification obtained from contrast enhanced DE-CCTA. In this way, prognostic as well diagnostic information could be obtained from a single scan reducing the total radiation dose and costs.

#### CLINICAL RELEVANCE/APPLICATION

Coronary artery is an independent predictor of cardiovascular events and it adds value to the Framingham risk score. Having its information from a dual energy coronary CT angiography is feasible.

### **VSCA51-10 • A Randomized Trial of Low Contrast Volume vs. Standard Contrast Volume CT Angiography Using Rapid kVp Switching Dual Energy CT**

**Sasi R Gangaraju MBChB (Presenter) ; Angus G Thompson PhD, MBBS ; Kristy Lee MD ; Giang Nguyen MD ; Carolyn Taylor MD ; Jonathan A Leipsic MD \* ; Brett Heilbron MD, FRCPC ; Tae-Hyun Yang ; James P Earls MD \* ; James K Min \* ; Jennifer D Ellis MD ; Cameron J Hague MD**

#### PURPOSE

CCTA is a robust tool for evaluating CAD. Its application is limited in those with borderline renal function out of concern for contrast-induced nephropathy (CIN). We evaluated qualitative and quantitative measures of image quality and diagnostic efficacy of a reduced iodine contrast volume Dual Energy CCTA(DE) vs the standard iodine contrast volume CCTA(STD).

#### METHOD AND MATERIALS

A prospective single centre double-blind trial recruited 77 consecutive outpatients who were then randomised to 2 cohorts; STD with BMI based tube potential selection (100-120 kVp)(n=41) or DE with rapid kVp switching (n=35). STD protocol used 110cc iodinated contrast via a triple phase injection and the DE protocol used 55cc of iodinated contrast with the reduced volume being substituted with saline. Demographics and cardiac history was obtained via a questionnaire at the time of CCTA. 2 readers measured signal and noise in the left main, left anterior descending, circumflex and right coronary artery, and SNR and CNR was calculated. A 5-point Likert scale subjectively evaluated vascular enhancement, noise and overall image quality (5:excellent, 1:non-diagnostic, scores

#### RESULTS

#### CONCLUSION

DE CCTA results in inferior image quality scores, but demonstrates comparable SNR and CNR and rate of diagnostic interpretability with no radiation dose penalty, while allowing for a 50% reduction in contrast volume compared to standard CCTA.

#### CLINICAL RELEVANCE/APPLICATION

DE reduced contrast volume CCTA may be considered a viable imaging option in patients at higher risk for CIN.

### **VSCA51-11 • Feasibility of Low Concentration Contrast Medium in Dual Energy Spectral Coronary CT Angiography**

**Xinhui Wu (Presenter) ; Wei Han ; Junliang Lu**

## PURPOSE

To investigate the utility of low concentration contrast medium in coronary CT angiography with dual energy spectral imaging mode for overweight patient.

## METHOD AND MATERIALS

## RESULTS

The mean CT values of LAD, LCX and RCA (389.6±54.3, 421±61.3, 415.3±58.4) in group B had no significant difference with those in group A (LAD (379.4±48.3, 356.7±55.8, 402.9±77.2) (each p>0.05). The image noise of group A (21.43±7.69) was lower than that of group B (27.28±7.14). The mean CNR of LAD, LCX and RCA in group B (23.44±8.23) was higher than that in group A (17.69±7.95) (p=0.023). Effective radiation dose was similar between group A and group B (2.75±0.43 mSv vs 2.49±0.57mSv, p=0.17)

## CONCLUSION

Dual energy spectral CCTA (70keV monochromatic images) provides better image quality than conventional CCTA and reduces the contrast medium demand.

## CLINICAL RELEVANCE/APPLICATION

Dual energy spectral CCTA provides better image quality, and should be a better choice for elderly patients who have impaired renal function.

### **VSCA51-12 • Applications**

**U. Joseph Schoepf MD (Presenter) \***

## LEARNING OBJECTIVES

1) To select suitable clinical image acquisition protocols for cardiac dual-energy CT. 2) To discuss the role of pharmacological stress for dual-energy CT imaging of myocardial ischemia. 3) To identify potential future applications of cardiac dual-energy CT in the diagnostic algorithm of coronary heart disease.

### **VSCA51-13 • Dual Energy Subtraction Radiography in the Evaluation of Calcific Valve Disease**

**Calen Frolkis BA (Presenter) ; Robert C Gilkeson MD \* ; Alan H Markowitz MD**

## PURPOSE

This retrospective study investigates the diagnostic implications of Dual Energy Subtraction Radiography (DES) in the work up of cardiovascular disease.

## METHOD AND MATERIALS

Four hundred patients who underwent Aortic and/or Mitral valve replacement and/or repair from February 2010 to November 2012 were identified. Of those, 222 patients met inclusion criteria: record of both pre-operative DES chest radiography, and Chest CT or CT Angiography. Dual Energy Subtraction protocol included an initial 60kV acquisition, 150msec delay, followed by 140kV acquisition. The subtracted low energy bone algorithm was evaluated, and compared to standard 140kV CXR for visualization of cardiovascular calcification. Those cases where cardiovascular disease was better visualized on bone window were then further screened, and disease confirmed with correlative CT images. Primary findings were coronary artery calcification (CAC), valvular calcification (both mitral and aortic), Mitral annular calcification (MAC), and aortic arch or descending aorta disease. The final patient cohort was 47, with 29 women (61.7%), and 18 men (38.2%). The age range was 38-92, with an average age of 74.4yrs. Of these patients, 21 underwent subsequent AVR. Twelve patients underwent Aortic Root Reconstruction with valve conduit enlargement. Eight patients underwent AVR and MVR. Three patients underwent subsequent MVR, 2 patients underwent AV-repair with MVR, and 1 patient had AV-repair with MVR

## RESULTS

Of the 47 patients with significant findings on DES radiography, the most common finding was Mitral Annular Calcification with 31 cases (65.9%). Coronary Artery Calcification was the next most common finding, seen in 23 cases (48.9%). Calcific aortic valve (CAV) was seen in 22 patients (46.8%). MV disease was seen in 8 cases, and aortic disease in 5 patients.

## CONCLUSION

Dual Energy Subtraction improves visualization of calcified cardiovascular structures. The use of both CT and DES offers an intriguing clinical correlation in the evaluation of cardiovascular calcification. Further prospective studies are warranted.

## CLINICAL RELEVANCE/APPLICATION

Dual Energy Radiography enables an enhanced detection of cardiovascular disease compared to standard radiographic techniques.

### **VSCA51-15 • Direct Comparison of Stress- and Rest-dual-Energy Computed Tomography with Cardiac Magnetic Resonance for Detection of Myocardial Perfusion Defect**

**Sung Min Ko (Presenter) ; Jin-Woo Choi ; Hweung Kgon Hwang ; Meong Gun Song**

## PURPOSE

We assessed the diagnostic performance of stress- and rest-dual-energy computed tomography (DECT) and their incremental value when used with coronary CT angiography (CCTA) for detecting hemodynamically significant stenosis causing myocardial perfusion defect (MPD) compared with combined conventional coronary angiography (CCA)/cardiac magnetic resonance (CMR).

## METHOD AND MATERIALS

Seventy-one patients with known coronary artery disease (CAD) detected by CCTA underwent stress-DECT followed by rest-DECT. Among those, 46 patients underwent CMR and 62 underwent CCA. DECT-based iodine maps were compared with CMR. Diagnostic value of CCTA for detecting hemodynamically significant stenosis was assessed before and after stress- and rest-DECT, respectively, on a per-vessel basis, compared with CCA/CMR.

## RESULTS

Forty (56%) patients completed all the protocol. Compared to CMR (n=46), sensitivity, specificity, positive predictive value (PPV), and negative predictive value (NPV) of stress-DECT for detecting segment (vessel)-based MPDs were 73 (94)%, 85 (78)%, 70(72)%, and 87 (96)%, respectively, and those by using rest-DECT were 29 (47)%, 89 (80)%, 54 (59)%, and 74 (72)%, respectively. There was moderate (?=0.45) agreement between stress- and rest-DECT iodine maps in identifying segments with MPDs. Compared with the CCA/CMR (n=40) for identifying hemodynamically significant stenosis, per-vessel territory sensitivity, specificity, PPV, and NPV of CCTA were 91%, 56%, 55%, and 91%, respectively, those by using CCTA/stress-DECT were 87%, 79%, 71%, and 91%, respectively, and those by using CCTA/rest-DECT were 42%, 83%, 59%, and 70%, respectively. The area under the receiver operating characteristic curve increased from 0.74 to 0.83 (p=0.02) but decreased to 0.62 (p=0.06), respectively, if using CCTA/stress-DECT and CCTA/rest-DECT, respectively.

## CONCLUSION

Stress-DECT has superior performance for detection of MPDs and incremental value when used with CCTA for detecting hemodynamically significant stenoses compared with rest-DECT.

## CLINICAL RELEVANCE/APPLICATION

The use of combined coronary CT angiography and stress-dual-energy CT may provide accurate assessment of hemodynamically significant coronary stenosis inducing myocardial perfusion defect.

### **VSCA51-16 • Relation between Stenosis Severity, CT-derived Myocardial Blood Flow, and CT-derived Myocardial Flow Reserve in**

## Patients with Stable Chest Pain

**Alexia Rossi MD (Presenter) ; Andrew Wragg ; Ernst Klotz DiplPhys \* ; Maria A Cova MD ; Steffen E Petersen ; Francesca Pugliese MD, PhD**

### PURPOSE

The functional significance of coronary stenosis of intermediate severity is often difficult to determine from anatomical information alone derived from coronary angiography. Therefore, the aim of our study was to assess the relationship between hyperaemic myocardial blood flow (MBF) and flow reserve measured by dynamic CT perfusion imaging and stenosis severity on invasive coronary angiography (ICA) in patients with stable chest pain.

### METHOD AND MATERIALS

Forty-seven patients with stable chest pain referred to ICA and invasive fractional flow reserve (FFR) were included in the study. All patients underwent stress and rest dynamic CT perfusion imaging using a second generation dual source CT. Hyperaemic stress was induced by continuous infusion of adenosine (140 µg/kg body weight) for 3 to 5 minutes. Hyperaemic and rest MBF (ml/100ml/min) were computed using a model-based parametric deconvolution method. Hyperaemic and rest MBF were obtained from regions of interest following a standard 16-segment model. Individual myocardial segments supplied by the same coronary vessel were considered as parts of the same territory. Myocardial flow reserve was calculated as the ratio of hyperaemic MBF and rest MBF. Stenosis severity in each coronary vessel was classified from ICA as mild (=30% lumen narrowing), intermediate non-functionally significant (INFS, 30%-85% and FFR>0.80), intermediate functionally significant (IFS, 30%-85% and FFR=0.80), and severe (=85%).

### RESULTS

A total of 133 coronary vessels and myocardial territories were analysed. Rest MBF was similar in all groups of coronary stenosis ( $p>0.05$ ). Hyperaemic MBF and myocardial flow reserve progressively decreased with increasing coronary stenosis severity following a non-linear relationship (all  $p$ -values

### CONCLUSION

CT-derived hyperaemic MBF and myocardial flow reserve are inversely and non-linearly related to stenosis severity as defined by ICA and FFR. In intermediate lesions, hyperaemic MBF can discriminate IFS from INFS coronary stenoses.

### CLINICAL RELEVANCE/APPLICATION

CT-derived measurements of hyperaemic MBF and myocardial flow reserve provide functional characterization of anatomically defined coronary stenoses.

## VSCA51-17 • Comparison of ECG-gated Coronary CT Angiography with Stress Nuclear Imaging for Evaluation of Myocardial Perfusion

**Jacob P Deutsch ; Ethan J Halpern MD (Presenter)**

### PURPOSE

To compare myocardial perfusion data obtained during coronary CT angiography (cCTA) with stress nuclear imaging.

### METHOD AND MATERIALS

We retrospectively identified 53 patients with ECG-gated cCTA and stress nuclear perfusion imaging performed within 30 days. Among these patients, 37 had helical cCTA with both diastolic and systolic imaging; 16 had only diastolic imaging. cCTA was performed with the iCT 256 slice scanner (Philips Medical Systems), and myocardial perfusion was evaluated with the comprehensive cardiac analysis application (Philips Intellispace Portal version 5.0). Areas of perfusion abnormality were identified by subjective evaluation of a binary polar map based upon the American Heart Association standardized 16 myocardial segment model. cCTA perfusion abnormalities were also identified automatically by quantitative analysis of a defect probability map using a cutoff probability of 15%.

### RESULTS

Fifteen of 53 patients demonstrated perfusion defects on nuclear imaging, including 11 fixed defects and 15 reversible defects. There was complete agreement between the subjective assessment of cCTA polar maps and the automated quantitative cCTA analysis on location of defects, although the size of one defect was larger by subjective assessment while two defects were judged to be larger by quantitative assessment. Eleven of these 15 patients had cCTA imaging in both systole and diastole. In a by-patient analysis, true positive perfusion defects were identified on cCTA in 10/15 (67%) by diastolic imaging and in 9/11(82%) by systolic imaging ( $p=0.17$ ). False positive perfusion defects were identified in 37/53 (70%) of patients by diastolic cCTA imaging and in 36/37 (97%) of patients by systolic cCTA imaging. Furthermore, among true positive cases, cCTA overestimated defect size in 10/10 (100%) of cases.

### CONCLUSION

Systolic phase cCTA imaging of the myocardium may be more sensitive for detection of perfusion defects as compared to diastolic phase imaging. Although the majority of myocardial perfusion defects found by nuclear imaging are detected on cCTA with the comprehensive cardiac analysis application, this technique is unlikely to be clinically useful, given the high rate of false positive perfusion cCTA defects.

### CLINICAL RELEVANCE/APPLICATION

A majority of myocardial perfusion can be identified by cCTA, but many of the apparent myocardial defects found during cCTA do not correspond with perfusion defects on nuclear imaging.

## VSCA51-18 • Prognostic Value of SYNTAX Score Based on Coronary Computed Tomography Angiography

**Young Joo Suh MD (Presenter) ; Sae Rom Hong MD ; Yoo Jin Hong MD ; Hye-Jeong Lee MD ; Jin Hur MD ; Young Jin Kim MD ; Byoung Wook Choi MD**

### PURPOSE

The SYNTAX score is an angiographic score to quantify the complexity of coronary artery disease (CAD). It has been reported as an independent predictor of major adverse cardiac events (MACEs) in populations with a varying extent of CAD. Computed tomography angiography (CTA) can be a useful modality to score non-invasively estimate SYNTAX score. The aim of our study was to investigate the prognostic value of CT-based SYNTAX for prediction of MACEs.

### METHOD AND MATERIALS

Institutional review board approval was obtained. We included 375 patients (mean age, 60.9 years; 224 men and 151 women) with a suspicion of CAD who underwent coronary CTA. The SYNTAX scores were obtained based on CTA. Follow-up clinical outcome data regarding composite MACEs were procured. Cumulative event rates were obtained by using the Kaplan-Meier method for coronary CTA-diagnosed CAD and CT-based SYNTAX score (threshold level >22), respectively. Cox proportional hazards model was developed to predict MACE.

### RESULTS

During the mean follow-up of 1070 days  $\pm$  121, there were 12 MACEs, for and event rate of 3.2%. The presence of obstructive CAD at coronary CTA showed a positive correlation with CT-based SYNTAX score ( $P$

### CONCLUSION

The SYNTAX score based on coronary CTA can be a useful method for noninvasively predicting MACEs.

### CLINICAL RELEVANCE/APPLICATION

The SYNTAX score based on coronary CTA can be a useful method for noninvasively predicting MACEs.

CT	BQ	CH
----	----	----

**VSCH51** • AMA PRA Category 1 Credit™:3.25 • ARRT Category A+ Credit:3.75

**Moderator**

**Jonathan G Goldin**, MBChB, PhD

**Moderator**

**Jens Bremerich**, MD

### **VSCH51-01 • Quantitative Imaging: Lung Nodule Analysis**

**Jane P Ko** MD (Presenter)

#### LEARNING OBJECTIVES

1) To increase understanding of the advancements in computer-assisted quantification of lung nodule size and features. 2) To enhance knowledge of the challenges pertaining to nodule evaluation techniques and their clinical applications.

#### ABSTRACT

### **VSCH51-02 • Quantitative Imaging: COPD and Airways**

**Alexander A Bankier** MD, PhD (Presenter) \*

#### LEARNING OBJECTIVES

1) To present up-to-date imaging techniques for assessing airways and lung parenchyma in patients with COPD. 2) To present quantitative imaging approaches to COPD. 3) To discuss the clinical impact of quantitative imaging, notably for phenotyping patients with COPD.

#### ABSTRACT

This presentation will present current imaging techniques used to assess changes in lung parenchyma and airways in patients with COPD. It will discuss the importance of a quantitative approach to imaging COPD, notably as to phenotyping patients with this disease. Finally, potential future trends in imaging COPD will be discussed.

### **VSCH51-03 • Reproducibility of Automated Three-dimensional Airway Wall Thickness Measurements in Thoracic Computed Tomography and Influence of Inspiration Depth**

**Michael Schmidt** MSc ; **Eva M Van Rikxoort** PhD ; **Onno M Mets** MD ; **Pim A De Jong** MD, PhD ; **Jan-Martin Kuhnigk** PhD, MS (Presenter) ; **Matthys Oudkerk** MD, PhD ; **Harry De Koning** \* ; **Bram Van Ginneken** PhD

#### PURPOSE

Pathological changes of the airways are strongly associated with lung function impairment in chronic obstructive pulmonary disease (COPD). We investigate the reproducibility of CT-based airway dimension measurements and their dependence on the level of inspiration.

#### METHOD AND MATERIALS

We analyzed 740 pairs of low-dose chest CT scans of male (former) smokers who were recalled for a three-month follow up scan in the NELSON lung cancer screening trial. Given the slow progression of COPD, we expect that no significant COPD-related changes in airway dimensions should exist between baseline and three month follow-up. Each scan was analyzed fully automatic using CIRRUS Lung 13.03 and airway wall thickness (Pi10) and lung volume were recorded. Subjects where processing failed for any of the two scans were excluded for analysis (n=32). First, we analyzed the differences in airway wall thickness measurements for all scan pairs. Next, we determined reproducibility in absence of significant changes in inspiration depth by repeating the analysis for the subset of scans where the difference in lung volume between baseline and follow-up was less than 200ml (n=312). Finally, we investigated the correlation between difference in inspiration depth and airway wall thickness measurements, established a linear correction model for the airway measurements and analyzed differences for corrected measurements.

#### RESULTS

#### CONCLUSION

Changes in level of inspiration are significantly associated to changes of airway wall thickness and accounted for approximately 25% of the total differences between baseline and follow-up measurements.

#### CLINICAL RELEVANCE/APPLICATION

Inspiration depth should be controlled or linear correction should be applied for monitoring of airway wall thickness. This may help to better differentiate COPD subtypes in chest CT scans.

### **VSCH51-04 • Quantitative Imaging: Interstitial Lung Disease**

**Jonathan G Goldin** MBChB, PhD (Presenter)

#### PURPOSE

The learning objectives are the following: Approaches to Quantitative Imaging in ICD, Quantitative Imaging in Clinical Trials as a Biomarker and Quantitative Imaging in Clinical Practices.

### **VSCH51-05 • Phenotypes of Pulmonary Fibrosis in the MUC5B Promoter Site Polymorphism (SNP)**

**Jonathan H Chung** MD (Presenter) \* ; **Ashish Chawla** MD, MBBS ; **David Mckean** ; **Janet Talbert** ; **Anna Peljto** ; **David A Lynch** MBBCh \* ; **Marvin I Schwarz** MD ; **David Schwartz**

#### PURPOSE

The purpose of this study was to determine the variation of phenotypic manifestations of pulmonary fibrosis with regard to the MUC5B promoter site (rs35705950) polymorphism, which has been strongly associated with IPF and familial pulmonary fibrosis.

#### METHOD AND MATERIALS

HRCT scans of 1,764 subjects were scored as part of a genome-wide association study. Two thoracic radiologists independently evaluated the HRCT scans. Discrepancies were resolved by a third thoracic radiologist. All patients were genotyped specifically for the rs35705950 SNP. Two-tailed Fisher exact or Chi-square tests and t-test or one-way ANOVA tests were used to compare proportions and means, respectively. A p-value of 0.05 was considered statistically significant.

#### RESULTS

The major and minor alleles at the rs35705950 SNP are guanine (G) and thymine (T), respectively. There were 670 GG, 958 GT, and 136 TT subjects. This distribution showed significant departure from Hardy-Weinberg equilibrium (p

#### CONCLUSION

Polymorphisms at the MUC5B promoter site are associated with different phenotypes of lung fibrosis on chest CT.

#### CLINICAL RELEVANCE/APPLICATION

Integration of imaging and genotypic information may provide valuable information regarding patient prognosis and optimal treatment in



fibrotic lung disease.

## **VSCH51-06 • Dual Energy CT: Emerging Applications**

**Ioannis Vlahos** MRCP, FRCR (Presenter) \*

### **LEARNING OBJECTIVES**

1) To understand the current potential for dual energy CT in thoracic imaging. 2) To review select current literature supporting the use of dual energy imaging. 3) To highlight emerging areas of clinical evaluation.

## **VSCH51-07 • Dual-energy CT with Reduced Iodine Load: A New Option for Standard Chest CTA in Patients with Superior Vena Cava Syndrome**

**Sofiane Bendaoud** MD (Presenter) ; **Olivier Vanaerde** MD ; **Francesco Molinari** MD ; **Arianna Simeone** MD ; **Emanuela Algeri** MD ; **Martine J Remy-Jardin** MD, PhD \*

### **PURPOSE**

To evaluate the interpretive conditions for analysis of all thoracic circulations on a chest CT angiographic examination optimized for suspicion of superior vena cava syndrome (SVCS).

### **METHOD AND MATERIALS**

41 patients with suspected SVCS underwent a dual-source, dual-energy CT angiographic examination of the chest with bi-brachial administration of a low-concentration contrast agent (160 mg iodine /mL). From each data set, 3 series of images were systematically reconstructed: (a) the 2 polychromatic series acquired at 80 and 140 kV; and (b) the fused images from both tubes, with a weighting factor of 0.6 (i.e., averaged images equivalent to images acquired at 120 kV). On each series of images, a quantitative and qualitative analysis of 3 anatomical compartments was performed, including the: (a) superior vena cava; (b) pulmonary arteries; and (c) aorta. In the quantitative evaluation: (a) ROIs were placed in each vessel-of-interest to measure mean  $\pm$ SD attenuation; (b) the signal-to-noise (SNR) and contrast-to-noise (CNR) ratios were calculated. Qualitative analysis evaluated the presence and severity of streak artifacts at the level of 3 nodal stations (i.e., 2R, 4R, 10R). On a patient-by-patient basis, the number of series to-be-interpreted for optimal analysis of all anatomical regions was then assessed.

### **RESULTS**

Averaged images provided (a) a good to excellent level of opacification within the SVC (n=40 ; 98%) without artifacts at the level of 2R (n=26 ; 63%), 4R (n=40 ; 98%) and 10 R (n=41 ; 100%) ; (b) analyzability of pulmonary arteries down to the subsegmental level (n=31 ; 76%) ; and (c) a good to excellent opacification of the aorta (n=35; 85%). In 29 patients (29/41; 71%), averaged images alone provided optimal evaluation of all vascular compartments; in 12 patients (12/41; 29%), they had to be completed by images at 140 kV (n=6) to suppress artifacts at the level of the nodal station 2R and/or images at 80 kV (n=10) to improve the CNR at the level of subsegmental pulmonary arteries and/or the aorta.

### **CONCLUSION**

Dual-energy CT enables combination of optimal evaluation of SVCS and diagnostic image quality at the level of the other thoracic circulations.

### **CLINICAL RELEVANCE/APPLICATION**

On dual-energy CT angiograms obtained with low-concentration contrast material, an optimal analysis of all thoracic vessels requires the reading of a single series of images in the majority of cases.

## **VSCH51-08 • CT Innovations for Radiation Dose Reduction**

**John R Mayo** MD (Presenter) \*

### **LEARNING OBJECTIVES**

1) To identify the patient factors that increase CT radiation dose risk. 2) To describe current CT radiation dose reduction techniques. 3) To outline the relationship between CT image noise and the detection of abnormalities. 4) To evaluate the impact of iterative reconstruction on CT radiation dose reduction.

## **VSCH51-09 • Incidental Findings Detection on CT Pulmonary Angiography Images with Low kVp Techniques**

**Kanako K Kumamaru** MD, PhD (Presenter) ; **Rachna Madan** MD ; **Ritu R Gill** MBBS \* ; **Nicole Wake** MS ; **Frank J Rybicki** MD, PhD \* ; **Andetta R Hunsaker** MD

### **PURPOSE**

To evaluate the effect of reduced kVp on detection of incidental findings in the lungs and mediastinum in patients who underwent CT Pulmonary Angiography (CTPA) for suspected acute pulmonary embolism.

### **METHOD AND MATERIALS**

This IRB-approved HIPAA-compliant study included consecutive CTPA studies performed from January 2008 to April 2010 which used low kVp technique (80kVp for patients weighing

### **RESULTS**

Compared with standard kVp settings, objective/subjective noise scores were significantly greater at lower kVp, while the SNR/CNR/contrast opacification scores were not significantly different, in both weight cohorts. Confidence level of clinical interpretation tended to be lower at low kVp, with a significant decrease for mediastinal lesions interpreted by one of two readers (coefficient=-2.35, 95%CI=-2.89 to -1.82, p0.1). Multivariate analysis did not show a significant correlation between accuracy of interpretation and kVp settings for lung nodules and mediastinal nodal detection (adjusted odds ratio=0.67-1.22, p-values >0.2).

### **CONCLUSION**

Despite the increased image noise, lower kVp techniques in CTPA studies in patients suspected of acute pulmonary embolism does not adversely affect the detection of lung nodules or mediastinal nodes.

### **CLINICAL RELEVANCE/APPLICATION**

Lower kVp does not adversely affect the detection of lung nodules or mediastinal nodes on CTPA studies, despite the increased noise and decreased confidence in the interpretation.

## **VSCH51-10 • Hyperpolarized Gas MR Imaging**

**Talissa A Altes** MD (Presenter) \*

### **LEARNING OBJECTIVES**

1) Understand the limitations of proton lung MRI and the strengths and weaknesses of hyperpolarized gas MRI of the lung. 2) Learn about potential research and clinical applications of hyperpolarized gas lung MRI in lung diseases such as CF, asthma, and COPD.

### **ABSTRACT**

## **VSCH51-11 • Are Hyperpolarized <sup>3</sup>He Magnetic Resonance Imaging Ventilation Defects Clinically Relevant in Ex-smokers without Airflow Limitation?**

**Damien Pike** BSC (Presenter) ; **Miranda Kirby** PhD ; **Sarah Svenningsen** BSC ; **Harvey O Coxson** PhD \* ; **David McCormack** MD

#### PURPOSE

In early or mild chronic obstructive pulmonary disease (COPD), spirometry measurements are relatively insensitive to changes in the **silent zones** of the lung in the small airways (1). However, hyperpolarized  $^3\text{He}$  magnetic resonance imaging (MRI) has provided evidence of early or very mild emphysema in never-smokers with exposure to second hand smoke (2) as well as early emphysema (3) and airways abnormalities (4) in asymptomatic ex-smokers. We recently evaluated 160 ex-smokers and 71/160 (44%) did not have spirometry measurements diagnostic for COPD. We hypothesized that  $^3\text{He}$  MRI and computed tomography (CT) measurements of airways disease and emphysema would detect a subgroup of ex-smokers without airflow limitation but with clinically relevant structure-function pulmonary abnormalities.

#### METHOD AND MATERIALS

Seventy-one ex-smokers ( $69 \pm 10$ yr, FEV1/FVC = .70) underwent spirometry,  $^3\text{He}$  MRI, thoracic CT and the St. George's Respiratory Questionnaire (SGRQ). CT-derived measurements were generated for wall area percent (WA%) and lumen area (LA) of the sub-segmental lower right (RB8) airway and the relative area at -950 Hounsfield units of the CT density histogram (RA950). Hyperpolarized  $^3\text{He}$  MRI ventilation defect percent (VDP), a surrogate of airways and bullous disease, and apparent diffusion coefficients (ADC), a surrogate of emphysema was generated for whole lung (WL) and lower right lobe (LRL) pulmonary measurements.

#### RESULTS

Subjects were classified into two sub-groups: ex-smokers with a LRL  $^3\text{He}$  MRI defect (Defect, n=9) and ex-smokers with no LRL defect (No Defect, n=62). Subjects with a defect had significantly greater VDP, RB8 WA%, smaller RB8 LA and worse symptoms than subjects without a LRL defect.

#### CONCLUSION

In 9/71 (13%) ex-smokers without airflow limitation and a LRL ventilation defect, symptoms were worse and  $^3\text{He}$  MRI and CT measurements showed abnormal airway structure and function that was significantly worse than in a subgroup of ex-smokers without an LRL ventilation defect.

#### CLINICAL RELEVANCE/APPLICATION

In ex-smokers without airflow limitation and previously undetected but clinically relevant symptoms, lung imaging provided evidence of structure-function abnormalities that require clinical follow-up.

### **VSCH51-12 • MR Imaging: Recent Advances for Chest Imaging**

**Jens Bremerich MD** (Presenter)

#### LEARNING OBJECTIVES

1) Understand physical limitations specific to the chest and how to improve image quality. 2) Current applications of MR for imaging pulmonary morphology and function. 3) Oversee emerging techniques for MR imaging of the entire chest.

#### ABSTRACT

##### Introduction:

Magnetic Resonance is an attractive tool for imaging of morphology and function of the chest with ionizing radiation. Magnetic properties of the chest, however, remain unfavourable for MR because of low water proton density and considerable magnetic field inhomogeneities. Recently new imaging protocols and sequences became available that may overcome these limitations. This abstract reviews current applications and recent advances of MR of the chest. Methods:

Fast imaging techniques such as turbo spin echo or segmented gradient echo can reduce susceptibility artefacts and enable breath held acquisitions. Free breathing respiratory gated sequences may be used alternatively. Standard imaging protocols comprise T1 and T2 weighted images for morphology assessment and edema detection. Diffusion weighted MR may be added to identify diffusion restriction which may indicate malignancy. Pleural infiltration of peripheral masses may be assessed by means of cine imaging during in- and expiration. For further characterisation of masses and inflammatory diseases T1 weighted images pre and post gadolinium may be used. Emerging techniques based on fourier decomposition for assessment of perfusion and ventilation are currently under investigation. Results: Magnetic Resonance may be used to identify and characterise pulmonary masses, monitor pulmonary perfusion and ventilation, assess chest wall motion, identify involvement of chest wall in peripheral lung tumors and to identify pulmonary embolism. Fourier decomposition may enable assessment of perfusion and ventilation and is currently under investigation. Conclusion: Today, MR is a useful tool for assessment of pulmonary morphology, function and tissue characterisation. Recent advances in MR of the chest include fourier decomposition techniques which may enable assessment of perfusion and ventilation without injection of contrast material.

### **VSCH51-13 • SUVmax Correlation between PET/MRI and PET/CT in FDG Avid Lesions of the Chest Using a Three Segment Model Attenuation Correction**

**Andres Kohan MD** (Presenter) \* ; **Christian Rubbert MD** \* ; **Jose L Vercher-Conejero MD** \* ; **Sasan Partovi BS** \* ; **Karin A Herrmann MD** ; **Luis A Landeras MD** ; **Peter F Faulhaber MD** \*

#### PURPOSE

PET/MRI combines the superior tissue resolution and multiparametric capabilities of the MRI with the functional capabilities of PET. It is theorized to improve oncologic imaging in multiple areas of the body, specially: brain, liver, pelvis and bone. Nonetheless other areas are bound to benefit from this technology.

However, SUVs obtained from FDG avid lesions in PET/MRI remains a concern, mainly due to the migration from CT attenuation correction to MRI attenuation correction (MRAC). One area of major concern is the chest, where two critical tissue interfaces with very different attenuation coefficients can be found.

We studied FDG avid lesions in the chest to determine the correlation between the SUVmax from PET/MRI and PET/CT using a three segment model MRAC.

#### METHOD AND MATERIALS

First 47 oncologic consecutive patients from a research protocol were included. Final n was 19 due to 6 failed MRAC and 22 patients without chest lesions to analyze. All patients underwent PET/CT (Gemini TF) and PET/MRI (Ingenuity TF) with a single FDG injection. Lesions were identified by direct comparison and sub-classified as mediastinal, lung or chest wall lesions. SUVmax was determined with a spherical ROI including the lesion. Spearman Ranked correlation was performed.

#### RESULTS

Out of all patients (5 male, 14 female): 9 had lung cancer, 3 breast cancer, 2 head and neck cancer, 2 lymphoma, 1 melanoma, 1 pancreas and 1 colon cancer. Seventy six lesions were analyzed: 21 in the lung, 14 in the chest wall and 41 in the mediastinum. Mean exam scan time:  $18 \pm 4$ min (PET/CT) and  $21 \pm 3$  (PET/MRI). Mean time from FDG injection:  $66 \pm 8$ min (PET/CT) and  $105 \pm 20$ min (PET/MRI). Spearman for SUVmax was 0.93, 0.95, 0.84 and 0.96 for overall, lung, chest wall and mediastinal lesions respectively (p

#### CONCLUSION

Chest wall lesions had a somewhat lower correlation (0.84) than the others ( $>0.90$ ), probably related to more than half of the lesions being in vertebrae and ribs, whereas the MRAC cannot identify bone tissue. Nonetheless, correlation between SUVmax was very strong ( $\rho > 0.8$ ) for all lesions in all areas which raises the question whether there is any clinical relevance to the findings seen in the chest wall.

#### CLINICAL RELEVANCE/APPLICATION

Reliability of SUVs in an area with air/soft tissue boundaries is vital for PET/MR to succeed in chest oncologic imaging. The high correlation to PET/CT SUVs seen here is a step into that direction.

### **VSCH51-14 • Innovations in Chest Radiography**

**Heber Macmahon MD (Presenter) \***

**LEARNING OBJECTIVES**

1) Understand the newer enhancements that have become available for digital chest radiography. 2) Learn how these techniques may improve diagnostic accuracy. 3) Appreciate the benefits and limitations of dual energy radiography, bone suppression, computer-aided nodule detection in clinical practice.

**VSCH51-15 • Digital Chest Tomosynthesis**

**Ase A Johnsson MD, PhD (Presenter)**

**LEARNING OBJECTIVES**

1) The benefits of chest tomosynthesis in comparison to chest radiography. 2) The limitations of chest tomosynthesis in comparison to computed tomography. 3) The role of chest tomosynthesis as a problem solver in daily clinical practice.

ABSTRACT

---

**Interventional Radiology Series: Non-Vascular Interventions**

---

**Thursday, 08:30 AM - 12:00 PM • E352**

[Back to Top](#)



**VSIR51 • AMA PRA Category 1 Credit™:3.25 • ARRT Category A+ Credit:4**

**Moderator**

**Peter R Mueller, MD \***

**Moderator**

**Jonathan M Lorenz, MD**

**LEARNING OBJECTIVES**

1) Describe evidence concerning timing emergent abscess drainage. 2) Explain the use of celiac plexus block. 3) Describe two techniques to safely perform dangerous biopsies. 4) Outline 3 controversies in non-vascular intervention. 5) List two catastrophic complications of non-vascular intervention. 6) Describe two techniques to facilitate difficult abscess drainage.

**VSIR51-01 • Dangerous Biopsy - Spleen, Mediastinum, Capsular Lesions, Cavitory Lung Lesions**

**William W Mayo-Smith MD (Presenter) \***

**LEARNING OBJECTIVES**

View learning objectives under main course title.

**VSIR51-02 • CT-guided Biopsy of Pulmonary Nodules: Risk Factor Analysis for Pneumothorax in 650 Patients**

**Ahmed F Emam MBBCh (Presenter) ; Thomas J Vogl MD, PhD ; Nagy N Nagib MSc ; Mohammed A Alsubhi BMBS ; Nour-Eldin A Nour-Eldin MD, MSc**

**PURPOSE**

To evaluate the significant risk factors involved in the development of Pneumothorax during CT-guided Lung of pulmonary Nodules.

**METHOD AND MATERIALS**

Institutional board approval for the current retrospective study. Patients provided an informed consent for CT-guided biopsy and the anonymous use of the data for research purposes. The study included 650 patients (221 females and 429 males with mean age 56.2 years SD: 5.2) who underwent CT-guided biopsy of pulmonary lesions in the period between January 2008 and January 2013. Factors associated with the development of pneumothorax were analyzed including: Age, emphysema, lesion size, lesion position, coaxial versus non coaxial system, fine needle vs trucut needle. Univariate analysis was performed. P value of < 0.05 was considered as statistically significant.

**RESULTS**

Significant risk factors involved in the development of pneumothorax were: patients age > 60 years (p=0.04), emphysema (p=0.035), lesion size < 1 cm (p=0.023), central lesions (5 cm (p=0.022), basal pulmonary lesions versus apical lesions (p=0.03). No significant correlation for development of pneumothorax was detected in coaxial versus no-coaxial technique, as well as and fine needle versus tru-cut needle (p > 0.08). The incidence of pneumothorax was 12% (78 out of 650). Manual evacuation was performed in 25 out of 78 patients (32.1%) and the need for intercostal chest tube was 6 out of 78 (7.7%).

**CONCLUSION**

Significant risk factors involved in the development of pneumothorax were old age, emphysema, subcentimeteric lesions, central or basal lesions, and long intrapulmonary needle track.

**CLINICAL RELEVANCE/APPLICATION**

The incidence of pneumothorax is rather unpredictable and it is associated with certain factors that make certain cases of higher risk for the emergence of pneumothorax.

**VSIR51-03 • US-guided Transhepatic Core Biopsy of Right Renal or Adrenal Masses: Safety and Short Term Follow Up**

**Moon Young Kim MD (Presenter) ; Byung Kwan Park MD ; Sung Yoon Park ; Chan Kyo Kim MD, PhD ; So Yoon Park**

**PURPOSE**

To retrospectively evaluate the accuracy and safety of ultrasound (US)-guided trans-hepatic biopsy of right upper renal or adrenal masses.

**METHOD AND MATERIALS**

Ten US-guided trans-hepatic biopsies were performed in ten patients with six right upper renal masses and four right adrenal masses which were invisible or inaccessible via an extra-hepatic route. The control population comprised of 19 US-guided extra-hepatic biopsies that were performed in 19 patients with 18 right upper renal masses and one right adrenal mass. Trans-hepatic and extra-hepatic biopsies were compared with respect to the diagnostic or complication rates. The size of the mass, biopsy distance, number and length of cores as well as biopsy duration were also compared.

**RESULTS**

The diagnostic rates of trans-hepatic and extra-hepatic biopsies were 90% (9/10) and 89% (17/19), respectively (p=1.000). The complication rates of trans-hepatic and extra-hepatic biopsies were 10% (1/10) and 21% (4/19), respectively (p=1.000). None of these biopsies resulted in major complications. The sizes (mean ± standard deviation) of the mass, biopsy distances and number of cores for trans-hepatic and extra-hepatic biopsies were 33.0 ± 14.3 mm and 46.9 ± 18.5 mm, 100.5 ± 17.9 mm and 76.5 ± 9.9 mm, and 2.7 ± 0.9 and 4.0 ± 0.7, respectively (p=0.001-0.046). However, the length of cores and biopsy durations were not significantly different between these biopsies (p=0.077-0.91).

#### CONCLUSION

US-guided trans-hepatic core biopsy appears to be feasible and safe procedure for the histologic diagnosis of right upper renal or adrenal masses which are either invisible or inaccessible via an extra-hepatic route.

#### CLINICAL RELEVANCE/APPLICATION

Trans-hepatic core biopsy allows for better sampling of right renal or adrenal masses due to excellent US penetration of normal hepatic parenchyma compared to an extra-hepatic core biopsy.

### **VSIR51-04 • Computer Assisted Electromagnetic Navigation Improves Accuracy in CT Guided Interventions: A Prospective Randomized Clinical Trial**

**Pierre Durand MD, MSc (Presenter) ; Alexandre Moreau-Gaudry MD, PhD ; Julien Frandon MD ; Emilie Chipon PhD ; Maud Medici MSc ; Ivan Bricault PhD \***

#### PURPOSE

To assess the accuracy and usability of a novel electromagnetic navigation system designed to assist CT guided interventions.

#### METHOD AND MATERIALS

The tested navigation system prototype uses an electromagnetic localizer in order to track the position and orientation of a needle holder; it can display the needle path in real-time on 2D reconstructed CT-images extracted from the 3D CT volume. This study was approved by the regional ethics committee and all patients gave written informed consent. From June 2010 to January 2012, 120 patients undergoing a routine percutaneous CT procedure (drainage, biopsy, tumor ablation, infiltration, sympathectomy) were randomized between the conventional procedure (CT group) and a navigation-assisted procedure (NAV group). The main outcome was the distance between the planned trajectory and the actual needle trajectory after a first attempt at placement.

#### RESULTS

N=120 patients were analyzable in intention-to-treat analysis (CT: 60; NAV: 60). Nineteen radiologists participated in the study; their satisfaction score (0-10) shows that the help provided by the navigation system was favorably appreciated: CT=8[7; 9]; NAV=9[8; 9.5] (p=0.025). The accuracy was improved when the navigation system was used: distance error (mm) with CT=8.86[4.86; 15.09], vs. with NAV=4.07[2.7; 9.14] (p

#### CONCLUSION

Electromagnetic navigation, as compared with conventional CT procedures, provides significant improvement in accuracy. Usability in a real clinical setting is established.

#### CLINICAL RELEVANCE/APPLICATION

Improvements in accuracy and ability for the radiologist to plan optimal trajectories in any plane can lead to a security benefit for the patient, particularly in case of complicated targets.

### **VSIR51-05 • Controversies in Non-Vascular Interventions**

**George I Getrajdman MD (Presenter)**

#### LEARNING OBJECTIVES

Three controversies will be discussed. The participants will learn about lymphocele drainage- ETOH vs iodine sclerosis vs none. Pre procedural antibiotics for chest wall ports- always, never, or sometimes. They will also learn about current management of pneumothorax in outpatients undergo lung or mediastinal biopsies.

### **VSIR51-06 • Tough Abscess Drainage**

**Ronald S Arellano MD (Presenter)**

#### LEARNING OBJECTIVES

1) Review anatomic consideration that impose challenges for image-guided percutaneous abscess drainage. 2) Discuss techniques that can be used to facilitate image-guided percutaneous drainage of technically challenging abscesses.

#### ABSTRACT

Image-guided percutaneous abscess drainage is one of the most commonly performed procedures in Interventional Radiology. Facility with the various techniques and modalities used for drainage is essential. While most abdominal abscess are readily accessible for image-guided percutaneous drainage, there can be situations when drainage is challenging due to anatomic or patient factors. The purpose of this refresher course is to discuss techniques, by way of case examples, that can be used to successfully drain challenging abdominal abscesses.

### **VSIR51-07 • Drainage Catheter Flow Rate Related to the Number and Location of Sideholes: Does It Matter?**

**David H Ballard MS (Presenter) ; Jeffery A Weisman JD ; Mackenzie A Orchard ; Jason T Williams MPH ; Jonathan S Alexander PhD ; Horacio R D'Agostino MD**

#### PURPOSE

Currently, there is no evidence suggesting that the number or position of sideholes within drainage catheters has been based on fluid dynamics or clinical principles. The purpose of our study was to investigate the effect of varying catheter sidehole number and position on fluid flow rates in an in vitro model.

#### METHOD AND MATERIALS

Ad hoc customized drainage catheters were constructed with various numbers of sideholes (1 to 6). To optimize flow, each sidehole was created with the same diameter as the lumen of the catheter (15 Fr). Drainage catheters were constructed with sideholes on one side (single-sided model), or pairs of sideholes on opposite sides of the shaft (double-sided model). The drainage reservoir consisted of a cylindrical container filled with water. The cylinder was constructed to maintain a constant pressure independent of catheter fluid evacuation. This constant pressure outflow system was established in the reservoir with a 500 mL pressure head using a fixed fluid inflow with a flow/overflow valve. After the catheters were inserted and the pressure gradient was established, fluid evacuation was evaluated using 10-second intervals by draining the fluid into a collection vessel and recording the volume. A total of 5 trials were performed for each catheter to account for measurement error.

#### RESULTS

Our data shows that flow rate is maximized at 3 sideholes in the single-sided model catheters. Single-sided model catheters with more than 3 sideholes showed no significant improvement in flow rate. All the double-sided model catheters had significantly better flow rates than their single-sided counterparts. Flow rate was maximal in the double-sided model catheter with 2 holes (one on each side) and there was no significant improvement in the catheters with more bilateral sideholes.

#### CONCLUSION

Our results suggest that optimal flow in drainage catheters can be achieved through a design consisting of a single pair of sideholes arranged opposite of each other and inclusion of additional sideholes does not significantly improve flow. These in vitro results illustrate that using fluid dynamics principles to redesign drainage catheters could serve to improve catheter performance.

#### CLINICAL RELEVANCE/APPLICATION

Clinical observations reveal that drainage catheter distal sideholes are often filled with debris that could be a source of sepsis. Our data suggests catheters with few sideholes achieve optimal flow.

## **VSIR51-08 • Percutaneous Interventions for Management of Post-surgical Pelvic Abscesses in Patients with Rectal Cancer: Does Neo-adjuvant Chemo-radiation Impact Clinical Outcome?**

**Avinash R Kambadakone MD, FRCR (Presenter) ; Ashraf Thabet MD ; Diane Alagno ; Kara P Stasko MS ; Ronald S Arellano MD ; Debra A Gervais MD \* ; Peter R Mueller MD \***

### **PURPOSE**

The purpose of this study was to evaluate the impact of peri-operative chemo radiation on the clinical outcome of percutaneous interventions for management of post surgical pelvic abscesses in patients with rectal cancer.

### **METHOD AND MATERIALS**

In this retrospective study we included 54 patients (M: F-33: 21, mean age-65yrs, age range: 29-91yrs) with rectal cancer who underwent CT guided percutaneous drainage of pelvic abscesses developing after low anterior or abdomino-perineal resection. In this cohort, thirty-three patients (M: F-20: 13, mean age -65 yrs) had received neoadjuvant chemoradiation either prior to or after surgical resection (Group A) and 21 patients (12M:9F, mean age-65yrs) did not receive any chemoradiation (Group B). The electronic medical records and imaging studies in these patients were retrospectively evaluated to record the surgical details, chemo radiation details and details of abscess drainage. The technical success, primary and secondary success and treatment failure rates were compared between the two groups.

### **RESULTS**

A total of 80 CT-guided percutaneous abscess drainage procedures were performed on the 54 patients (Group A, n=57 and Group B, n=33). The mean surgery to abscess drainage period was longer in Group A compared to Group B (210 days vs 39 days, p=0.02). The technical success rate was comparable between the two groups (96.5% vs 95.5%). The primary success was higher in Group B as compared to Group A (83.3% vs 54.5%). The total period of catheter drainage was higher in patients who received chemo-radiation (105 days vs 26 days, p=0.02). The abscess recurrence rate (re-accumulation) and catheter malposition was also higher in patients with chemo-radiation (p=0.01). Enteric fistulas complicating drainage of pelvic abscesses were also more common in chemo-radiation group [A: 42% (21/50), B: 21% (4/19)].

### **CONCLUSION**

Peri-operative chemoradiation adversely impacts outcome after percutaneous drainage of post surgical abscess in patients with rectal cancer necessitating prolonged drainage, frequent recurrences and multiple catheter manipulations.

### **CLINICAL RELEVANCE/APPLICATION**

Percutaneous management of post surgical abscesses in patients with rectal cancer can be challenging particularly in patients receiving chemoradiation and therefore needs multidisciplinary management.

## **VSIR51-09 • Debate - Emergent Abscess Drainage - Can It Wait Until Morning?**

**Ronald S Arellano MD (Presenter) ; Jonathan M Lorenz MD (Presenter)**

### **LEARNING OBJECTIVES**

The urgency of percutaneous catheter drainage depends on a number of factors such as the type of fluid collection, complications related to the fluid collection, and the clinical presentation. This interactive session reviews those factors in a point-counterpoint format.

### **ABSTRACT**

An old surgical adage states: " Do not let the sun go down or rise on an abscess." Such is no longer the case. While all patients with abscesses will benefit from percutaneous drainage, not all abscesses require urgent or emergent drainage. Both anatomic as well as clinical scenarios factor into the decision making in how to appropriately triage abdominal abscesses. This workshop will present cases that illustrate examples of abscesses that require urgent drainage.

## **VSIR51-10 • Celiac Plexus Block**

**Peter R Mueller MD (Presenter) \***

### **LEARNING OBJECTIVES**

View learning objectives under main course title.

## **VSIR51-11 • Controversies in Non-Vascular Interventions II**

**Jonathan M Lorenz MD (Presenter)**

### **LEARNING OBJECTIVES**

Controversies and solutions regarding triaging patients toward appropriate multidisciplinary therapeutic options will be addressed. In addition, decisions regarding the appropriate application, performance, and follow-up of therapeutic options offered by interventional radiology will be discussed in the context of appropriate supportive literature and expert opinion.

## **VSIR51-12 • Catastrophic Complications of Non-Vascular Intervention**

**Thomas B Kinney MD (Presenter) \***

### **LEARNING OBJECTIVES**

View learning objectives under main course title.

## **VSIR51-13 • Wrap Up and Discussion**

### **LEARNING OBJECTIVES**

View learning objectives under main course title.

## **Musculoskeletal Radiology Series: Pelvis and Hip Imaging**

**Thursday, 08:30 AM - 12:00 PM • E451B**



**VSMK51 • AMA PRA Category 1 Credit™:3.25 • ARRT Category A+ Credit:3.5**

**Moderator**

**Donna G Blankenbaker , MD**

**Moderator**

**Christian W Pfirrmann , MD, MBA \***

## **VSMK51-01 • Developmental Hip Dysplasia in the Child and Adult**

**Donna G Blankenbaker MD (Presenter)**

[Back to Top](#)

## LEARNING OBJECTIVES

1) Review the imaging features of hip dysplasia. 2) Know the potential complications seen in the dysplastic hip.

### **VSMK51-02 • Foveal Acetabular Impingement: Is Perifoveal Chondral Damage a Marker of Hip Dysplasia on Delayed Gadolinium Enhanced MRI of Cartilage (dGEMRIC)?**

**Luis S Beltran MD (Presenter) ; Riccardo Lattanzi PhD ; Soterios Gyftopoulos MD ; Zehava S Rosenberg MD ; Jenny T Bencardino MD**

#### PURPOSE

To evaluate if fovea alta is associated with perifoveal chondral damage in hip dysplasia.

#### METHOD AND MATERIALS

#### RESULTS

Results: 3 dysplastic, 3 borderline, and 3 non-dysplastic hips were present (4 M, 5 F; 15-66 years, mean=39 years). Fovea alta was found in all dysplastic, 67% of borderline and 0% of non-dysplastic hips. Average FA score was 1.8 (dysplastic), 1.3 (borderline), and 1.1 (non-dysplastic). Average dGEMRIC index was 476 (dysplastic), 895 (borderline dysplastic), and 927 (non-dysplastic). A significant ( $p=0.042$ ) negative correlation of  $r = -0.69$  between FA score and dGEMRIC index was found.

#### CONCLUSION

Fovea alta is associated with perifoveal cartilage injury on dGEMRIC.

#### CLINICAL RELEVANCE/APPLICATION

Perifoveal cartilage injury in fovea alta evaluated on dGEMRIC may be an important marker of foveal acetabular impingement in hip dysplasia.

### **VSMK51-03 • Prevalence and Pattern of Gluteus Tendon Pathology and Muscle Atrophy in Older Individuals**

**Andrew S Chi MD, MS (Presenter) ; Suzanne S Long MD ; Adam C Zoga MD ; Paul J Read MD ; Diane M Deely MD ; William B Morrison MD \***

#### PURPOSE

To evaluate gluteus medius and minimus tendon pathology and muscle atrophy in older individuals.

#### METHOD AND MATERIALS

A retrospective study of MR imaging of 184 individuals was performed to evaluate for gluteus pathology. Inclusion criteria: age=50. Exclusion criteria: hip surgery, fracture, infection or tumor, or inadequate image quality. Both hips were evaluated for each individual. Greater trochanteric bursitis was graded as none, mild, moderate, or severe. Gluteus medius, gluteus minimus, and iliopsoas tendon pathology was graded as normal, tendinosis, low grade partial tear, high grade partial tear, or full tear. Gluteus medius, gluteus minimus, and iliopsoas muscle fatty atrophy was scored using the Goutallier scale (0=no atrophy to 4=complete atrophy). Insertion of tendon pathology and anterior/posterior location of muscle atrophy was also analyzed.

#### RESULTS

184 subjects were stratified by age as follows: n=63(50-59 y.o.), 64(60-69 y.o.), 38(70-79 y.o.), 17(80-89 y.o.), 2(90-99 y.o.). Percentage of gluteus medius tendon abnormalities were: 34.9%(50-59 y.o.), 53.9%(60-69 y.o.), 82.9%(70-79 y.o.), 73.5% (80-89 y.o.), 100%(90-99 y.o.). For the gluteus medius, tendinosis accounted for 68.2% of tendon pathology in 50-59 y.o., low grade tears accounted for 42.0% in 60-69 y.o., and high grade tears accounted for 17.5% in 70-79 y.o.. Average gluteus medius atrophy scores were as follows: 0.3(50-59 y.o.), 0.6(60-69 y.o.), 1.2(70-79 y.o.), 1.6(80-89 y.o.), and 3.0(90-99 y.o.). Percentage of gluteus minimus tendon abnormalities were: 30.2%(50-59 y.o.), 50.0%(60-69 y.o.), 86.8%(70-79 y.o.), 79.4%(80-89 y.o.), and 100%(90-99 y.o.). For the gluteus minimus, tendinosis accounted for 73.7% of tendon pathology in 50-59 y.o., low grade tears accounted for 53.1% in 60-69 y.o., and high grade tears accounted for 7.6% in 70-79 y.o.. Average gluteus minimus atrophy scores were as follows: 0.4(50-59 y.o.), 0.9(60-69 y.o.), 1.7(70-79 y.o.), 2.4(80-89 y.o.), and 3.8(90-99 y.o.).

#### CONCLUSION

Gluteus medius and minimus tendon pathology and muscle atrophy increase with age above 50 years. There appears to be progression from tendinosis to tendon tears with advancing age with an associated progression in muscle atrophy.

#### CLINICAL RELEVANCE/APPLICATION

Given tendon tear may prelude atrophy and atrophy is greater in fall-related hip fractures, more aggressive therapy could be useful to prevent subsequent falls in patients with gluteus tendon tears.

### **VSMK51-04 • Intraarticular Hip Pathology**

**Kawan S Rakhra MD (Presenter)**

#### LEARNING OBJECTIVES

1) Review MRI techniques and protocols for investigating intraarticular causes of hip pain. 2) Recognize the common internal derangements of the hip joint.

#### ABSTRACT

### **VSMK51-05 • Ischiofemoral Impingement. Do You Want to Believe?**

**Roque Oca MD (Presenter) ; Raquel Prada MD ; Maria Gonzalez Vazquez ; Maria Costas Alvarez ; Gonzalo Tardaguila de la Fuente MD ; Ana Fernandez Del Valle MD ; Alex Grande Astorquiza MD ; Ariana C Bustos Fiore MD**

#### PURPOSE

To find out if there are anatomic and MRI criteria to diagnose ischiofemoral impingement.

#### METHOD AND MATERIALS

290 MRIs of the hip were retrospectively reviewed from June 2012 to January 2013. A total of 9 ischiofemoral impingement were diagnosed and 20 normal patients were included as control. Ischiofemoral space, quadratus femoris space and femoral inclination angle were measured independently by two blinded radiologists. The degree of oedema and fatty infiltration in the quadratus femoris muscle were also assessed visually. Differences in ischiofemoral space, quadratus femoris space and femoral inclination angle were studied between pathological and control cases. The interobserver reliability was obtained for quantitative variables.

#### RESULTS

#### CONCLUSION

Ischiofemoral impingement can be accurately diagnosed following **anatomic** and **MRI** criteria.

#### CLINICAL RELEVANCE/APPLICATION

Ischiofemoral impingement is a not very well known syndrome, only referred in a few articles in the trauma and radiological literature. Being aware of it turns diagnosis faster and more accurate.

## VSMK51-06 • Psoas Muscle Atrophy in Patients with Ipsilateral Groin Pain: Is there an Association with Prior Hip Surgery and Why?

**Adam C Zoga** MD (Presenter) ; **George P Hobbs** MD ; **Andrew S Chi** MD, MS ; **Suzanne S Long** MD ; **William C Meyers** MD ; **William B Morrison** MD \*

### PURPOSE

We sought to establish the incidence of unilateral or asymmetric psoas muscle atrophy in subject group with groin pain and a history of ipsilateral hip or lower abdominal surgery, and then correlate with the prevalence of psoas atrophy in a population without prior surgery.

### METHOD AND MATERIALS

A database of patients with pelvic MR for hip/groin pain was queried for a history of prior hip or abdominal surgery, generating 109 subjects; demographics, surgical history, and pain situs were recorded. 2 MSK radiologists independently reviewed MR exams retrospectively for the presence and degree of psoas muscle atrophy (mild = intramuscular signal abnormality, moderate = 50% loss), atrophy within other core muscles, postsurgical lesions and native muscle, tendon or intrinsic hip injuries. A control group of 180 subjects with MR for groin pain but no history of regional surgery was reviewed for asymmetric psoas muscle atrophy. Potential causes of this phenomenon were then explored.

### RESULTS

Asymmetric psoas atrophy was present in 24/109(22%) study subjects with reader consensus but only 5/180(2.7%) control subjects (p

### CONCLUSION

We have documented a significant incidence of asymmetric psoas muscle atrophy at MR patients with hip/groin pain after ipsilateral hip or abdominal surgery. The majority of these subjects had hip arthroscopy and preoperative MRs showed normal psoas bulk when available.

### CLINICAL RELEVANCE/APPLICATION

The cause and significance of postoperative psoas atrophy warrants further investigation. Potential contributors include traction during arthroscopy, surgical exposure and perioperative trauma.

## VSMK51-07 • Imaging of Sports Pubalgia

**Lawrence M White** MD (Presenter) \*

### LEARNING OBJECTIVES

1) Review the causes of acute and chronic athletic pubalgia. 2) Understand the etiologic theories as to origin of chronic athletic pubalgia. 3) Review the spectrum of imaging findings observed in the setting of athletic pubalgia. 4) Understand the value and limitations of imaging findings in guiding clinical management of patients with athletic pubalgia.

### ABSTRACT

## VSMK51-08 • Arthroplasties - What You Need to Know

**Jonelle M Petscavage-Thomas** MD, MPH (Presenter) \*

### LEARNING OBJECTIVES

1) Review different types and techniques of hip replacement. 2) Discuss new designs in hip replacement. 3) Review normal radiographic appearances and measurements. 4) Illustrate the imaging appearance of complications of hip arthroplasty and revisions. 5) Understand the role of cross-sectional imaging. 6) Learn techniques to optimize MR and CT imaging of hip replacement.

### ABSTRACT

## VSMK51-09 • Evaluation of Metal Artifact Reduction MRI in Patients with Total Hip Arthroplasty

**Lorenzo Nardo** MD (Presenter) ; **Roland Krug** PhD ; **Misung Han** ; **Craig Sam** ; **Kevin Koch** PhD \* ; **Andrew Lai** ; **Pia M Jungmann** MD ; **Hans Liebl** MD ; **Ursula R Heilmeier** MD ; **Thomas M Link** MD, PhD \*

### PURPOSE

The goal of our study was to assess whether adding a multiacquisition variable-resonance image combination (MAVRIC) sequence to the standard hip MRI post total hip replacement (THR) protocol improved the characterization of pathological findings.

### METHOD AND MATERIALS

In fifty-five patients with symptoms of hip pain (30 males, 25 females, aged 57-75) hip MRI at 3.0 T was performed with an eight-channel phased-array cardiac coil. The sequence protocol included: MAVRIC PD (coronal), MAVRIC STIR (axial), 2D-FSE T1 (axial and coronal), 2D-FSE PD (axial and coronal), STIR fat suppression (axial and coronal). Each sequence was assessed by two radiologists, independently, for joint effusion and synovitis including findings of aseptic lymphocyte dominated vasculitis-associated lesions (ALVAL), bone marrow edema pattern, osteolysis and insertion tendinopathy at the greater trochanter using a four-point scale (absent (0), probably absent (1), probably present (2), present (3)). Furthermore the extent of the metal artifacts was measured. Wilcoxon signed rank test was used to compare the data from standard FSE sequences to data from MAVRIC sequences. Agreement between the two readers was determined by calculation of kappa values.

### RESULTS

Osteolysis, joint effusion and synovitis were characterized on MAVRIC images with higher confidence (p<0.05). The size of metal artifacts was significantly reduced with the MAVRIC (p

### CONCLUSION

MAVRIC significantly reduced metal artifacts and added important diagnostic information to standard FSE images in patients status post total hip arthroplasty, particularly, when there was concern for ALVAL or osteolysis.

### CLINICAL RELEVANCE/APPLICATION

Multiacquisition variable-resonance image combination (MAVRIC) sequence adds significant diagnostic information to evaluation of Total Hip Replacement.

## VSMK51-10 • Metal-on-Metal Hip Complications

**Christian W Pfirrmann** MD, MBA (Presenter) \*

### LEARNING OBJECTIVES

1) To understand the causes of complications in patients with Metal-on-Metal hip implants. 2) Understand the role of imaging in the workup of patients with Metal-on-Metal hip implants. 3) Review the spectrum of imaging findings observed in the setting of Metal-on-Metal hip complications.

## VSMK51-11 • Investigating the Painful Metal-on-Metal Hip Arthroplasty: Is 3DCT a Suitable Substitute for MARS MRI?

**Elizabeth Robinson** (Presenter) ; **Shiraz Sabah** BSc ; **Johann Henckel** MD ; **Keshthra Satchithananda** MBBS \* ; **Thomas Parsons** ; **Michael Khoo** MRCP, FRCP ; **John A Skinner** MBBS ; **Alister Hart** MBBS

### PURPOSE

To compare the imaging findings of 3DCT against the gold-standard, MARS MRI.  
To demonstrate the role of 3DCT and MARS MRI in the evaluation of the painful MOM hip arthroplasty.

#### METHOD AND MATERIALS

We conducted a cohort study to determine the diagnostic accuracy of 3-dimensional computed tomography compared with metal artifact reduction sequence MRI for detection of pathologies associated with MOM hip replacements. 20 patients with painful prostheses were consecutively recruited. MARS MRI images were acquired with a 1.5T scanner and CT images with a 64-slice scanner, according to published protocols. Imaging was reported according to objective criteria by two MSK radiologists blinded to clinical data. Soft tissue lesions, muscle atrophy, osteolysis and tendon avulsion were evaluated. Diagnostic test characteristics were calculated.

#### RESULTS

#### CONCLUSION

3DCT was an unsuitable substitute for MARS MRI to image soft tissues around MOM hips. 3DCT showed poor ability to detect pseudotumor and provided inadequate information to permit lesion classification.

3DCT was not a reliable assessment tool for muscle atrophy and provided no information on tendinous pathologies.

However, 3DCT is a useful modality for detecting periprosthetic osteolysis.

#### CLINICAL RELEVANCE/APPLICATION

MARS MRI should be used for the diagnosis of painful MOM hip arthroplasties. Where MARS MRI is contraindicated or unavailable 3DCT is an unsuitable substitute and other modalities should be considered

### VSMK51-12 • Post-operative Muscle Atrophy on MARS MRI: Clinical-radiological Correlation for 80 Metal-on-Metal Hips

**Thomas Parsons** (Presenter) ; **Shiraz Sabah** BSc ; **Johann Henckel** MD ; **Elizabeth Robinson** ; **Michael Khoo** MRCP, FRCP ; **Keshthra Satchithananda** MBBS \* ; **John A Skinner** MBBS ; **Alister Hart** MBBS

#### PURPOSE

- ◆ To assess the reliability of hip abductor muscle atrophy seen on MARS MRI as an indicator of hip function.
- ◆ To estimate the prevalence of hip abductor muscle atrophy in a metal-on-metal hip cohort.

#### METHOD AND MATERIALS

179 patients (200 hips) were referred to a tertiary centre with problematic metal-on-metal hips. 80 patients with unilateral implants, an Oxford hip score (scored 0-48) and a MARS MRI scan of the pelvis were retrospectively selected. Peri-prosthetic muscles were graded 0-3 using MARS MRI according to the Bal and Lowe system (0=normal, 1=not exceeding 30% decrease in mass, 2=30-70% fatty change with decreased mass, 3=greater than 70% fatty change with 80% loss in muscle). A linear regression model was used to quantify the value of grading abductor atrophy as a predictor of hip function.

#### RESULTS

80 patients (40 male, 40 female) underwent primary surgery (64 resurfacing, 16 modular) at a median age of 54 years (range 25-83). All patients had a MARS MRI scan and Oxford hip score performed between December 2007 and February 2012, a median of 32 months (range 1-129) after primary implantation. Grade 2 or higher atrophy was observed in either gluteus medius or minimus in 35 cases (43.75%). Grade 2 or higher atrophy in both abductor muscles was seen in 25 cases (31.25%). A linear regression model showed that an increase in hip abductor group atrophy grade was associated with a 2.47 (95% CI 1.09-3.85) point decrease in Oxford hip score (p

#### CONCLUSION

Grading of hip abductor atrophy on MARS MRI is a significant predictor of hip function. However, the low R-square value indicates that a large unexplained variance is present and therefore makes this an unreliable method of assessing function.

#### CLINICAL RELEVANCE/APPLICATION

MARS MRI provides a non-invasive aid to pre-operative planning of revision surgery but should not be used as a substitute for clinical evaluation of hip function.

### VSMK51-13 • Hip Tumor Imaging and Mimics

**Mark J Kransdorf** MD (Presenter)

#### LEARNING OBJECTIVES

- 1) Identify the common bone and soft tissue lesions in and around the hip joint.
- 2) Recognize the tumor and tumor-like lesions associated with hip arthroplasty.
- 3) Identify differentiating features.

#### ABSTRACT

There are a wide variety of bone and soft tissue tumors, as well as tumor-like conditions, which have a predilection for the hip. Rather than a complete review, this session will highlight the common lesions in and around the hip, emphasizing imaging and diagnosis. The imaging evaluation of a suspected tumor always begins with radiographs. For osseous lesions, radiographs can be highly specific and accurately characterize biological activity. In the assessment of suspected soft tissue lesions, they can depict characteristic calcifications or ossifications, as well as secondary osseous changes, such as remodeling or invasion. MR imaging has emerged as the preferred imaging modality for evaluating osseous and soft tissue masses of the hip by providing information for diagnosis and staging. The MR imaging signal characteristics and enhancement patterns of malignant and benign hip tumors permit specific diagnoses in the majority of cases. This presentation will review the imaging of common tumors in and around the hip, highlighting those lesions with a characteristic imaging appearance.

### Vascular Imaging Series: CT Angiography-New Techniques and Their Application

Thursday, 08:30 AM - 12:00 PM • S502AB



[Back to Top](#)

**VSA51** • AMA PRA Category 1 Credit™:3.25 • ARRT Category A+ Credit:4

#### Moderator

**Dominik Fleischmann**, MD \*

#### LEARNING OBJECTIVES

- 1) To describe and illustrate new techniques for CT angiography.
- 2) To show present and future clinical applications of these methods.

### VSA51-01 • Iterative Reconstruction for CTA

**Sandra S Halliburton** PhD (Presenter) \*

#### LEARNING OBJECTIVES

- 1) Understand the basic principles of iterative reconstruction for CT.
- 2) Describe commercially available iterative reconstruction techniques.
- 3) Review the advantages and disadvantages of iterative reconstruction.
- 4) Discuss the incorporation of iterative reconstruction algorithms into clinical protocols for CT angiography.

#### ABSTRACT

### VSA51-02 • Model-based Iterative Image Reconstruction (MBIR) in CT Angiography of the Chest - A Dose Finding Cadaver Study



**Stefan Wirth MD (Presenter) \* ; Fabian Mueck ; Zsuzsanna Deak MD ; Sonja Kirchhoff MD ; Oliver Peschel ; Maximilian F Reiser MD ; Michael K Scherr MD**

#### PURPOSE

To compare image quality (IQ) of 64-row CT angiography of the chest, respectively acquired at varying dose levels and reconstructed with model based iterative reconstruction (MBIR), to standard baseline examinations at full dose and using adaptive statistical iterative image reconstruction (ASIR).

#### METHOD AND MATERIALS

8 male and 3 female cadavers were included (79±18.5kg; 72.5±17.2y/o; BMI 26.3±5.1). Following injection of contrast media (Angiofil-Macro: Arterial=800ml; Venous=1200ml; Virtangio, Fumedica, Muri; Switzerland) a full-dose baseline reference (FBR) was acquired (CT HD750; GE Healthcare, Waukesha, IL) using a standard-of-care protocol (0.625mm helical, 0.984 pitch, 120kV, 10-400mA modulation, noise index NI=39 VS=0.625; NI = allowed procentual level of noise in a water phantom in virtual slices of varying thickness (VS) in mm; raw data were reconstructed in soft tissue kernel using ASIR 50%). These baseline raw data were also reconstructed with MBIR (D0). Additionally, each cadaver was scanned with varying dose levels D1-D5 by changing NI and VS (D1: NI=35, VS=2.5; D2: NI=70, VS=0.625; D3: NI=35, VS=5; D4: NI=70, VS=2.5; D5: NI=70, VS=5; all reconstructed with MBIR). Except for NI, VS and MBIR, all other parameters were identical to the FBR, all series reformatted in 3mm axial, coronal and sagittal slices. Two radiologists, blinded to the dose level, independently compared IQ for CT angiography of D0-D5 to the full-dose FBR (IQ: -2:diagnostically inferior, -1:inferior, 0:equal, +1:superior, +2:diagnostically superior; respectively). For statistical analysis ICC and Wilcoxon test were used.

#### RESULTS

Mean values were (CTDIvol in mGy: D0 = 10.4±0.9, D1 = 7.4±2.6, D2 = 6.6±2.5, D3 = 4.3±1.8, D4 = 2.1±0.9, D5 = 1.1±0.5); (IQ: D0 = +1.0±0.3, D1 = +0.9±0.3, D2 = +0.7±0.3, D3 = +0.5±0.3, D4 = +0.2±0.3, D5 = -0.5±0.6). All values were significant different from one another; p

#### CONCLUSION

Data reconstruction with MBIR instead of ASIR allows for significant dose reduction of 80% in CT angiography of the chest without impairment of the image quality, resulting in a calculated mean effective dose of 0.94±0.66 mSv.

#### CLINICAL RELEVANCE/APPLICATION

For standard CT angiography, MBIR allows for diagnostic imaging of the chest below 1mSv without loss of image quality (overall, vessel wall, thrombus material, calcifications).

### **VSVA51-03 • Evaluation of Diagnostic Quality and Image Adequacy of Low Dose CT Angiography with Model Based Iterative Reconstruction in Follow Up of Endovascular Aortic Aneurysm Repair**

**Neil Hansen MD (Presenter) ; Ravi K Kaza MD ; Katherine E Maturen MD ; Peter S Liu MD ; Joel F Platt MD**

#### PURPOSE

To evaluate the image quality and overall adequacy of low dose Computed Tomographic Angiography (LD-CTA) with model based iterative reconstruction (MBIR) in patients evaluated following endovascular aortic aneurysm repair (EVAR) in comparison to standard dose CTA (SD-CTA) with Adaptive Statistical Iterative Reconstruction (ASIR).

#### METHOD AND MATERIALS

30 patients who had LD-CTA with MBIR and a prior SD-CTA with ASIR following EVAR were included. Two radiologists independently evaluated 60 CTAs in a random blinded fashion. Image quality for evaluation of stent configuration, stent lumen, aneurysm outline, vessel outline, and overall vascular and solid organ imaging adequacy were graded on a scale of 1 to 5 (1=poor, 2=acceptable, 3=good, 4=very good, 5=excellent). Maximal aneurysm sac diameter was measured, and the presence or absence of an endoleak was recorded. Image noise and contrast to noise ratio (CNR) were measured for all CTs. Scanner generated CT dose index (CTDI vol) and Dose Length Product (DLP) were recorded for the arterial and delayed phases.

#### RESULTS

Mean qualitative image score for LD-CTA averaged in the good to very good range in all categories. There was no significant difference between LD-CTA and SD-CTA in evaluation of stent lumen (4.1 vs. 3.9; p = .077). There was a significantly (p < .0001) higher score for the SD-CTA in the following categories: stent configuration (4.5 vs. 3.6), aneurysm outline (4.8 vs. 3.8), vessel outline (4.7 vs. 3.3), overall vascular adequacy (4.6 vs. 4.1), and overall solid organ imaging adequacy (4.6 vs. 3.3). Interobserver evaluation for endoleak detection was good for both groups, but higher for the LD-CTA (kappa = .92 vs .77). There was no significant difference in the mean aneurysm diameter between the two readers on LD-CTA and SD-CTA. The effective radiation dose for the LD-CTA was significantly (p < .0001) lower than SD-CTA during both the arterial (4.4 vs 16.2 mSv) and the venous (2.4 vs 6.7mSv) phases. As compared to SD-CTA with ASIR, the measured image noise was significantly lower (14.7 vs. 19.3; p < .001) and CNR was higher (25.6 vs. 17.1; p < .001) on the LD-CTA.

#### CONCLUSION

In patients being followed up after EVAR, low dose CTA with MBIR produces diagnostically acceptable image quality with significant radiation dose reduction.

#### CLINICAL RELEVANCE/APPLICATION

Low dose CTA with MBIR after EVAR produces diagnostic image quality with significant patient radiation dose reduction.

### **VSVA51-04 • CT Angiography of the Chest and Abdomen: Image Quality, Interobserver Variability, and Diagnostic Accuracy for Iterative versus Filtered Back Projection Reconstruction**

**Elizabeth George MBBS (Presenter) ; Kanako K Kumamaru MD, PhD ; Pamela M Deaver MD ; Katherine Mullen MD ; Sachin S Saboo FRCR, MD ; Frank J Rybicki MD, PhD \* ; Kurt Schultz RT \* ; Ashish R Khandelwal MD ; Michael L Steigner MD \* ; Dimitris Mitsouras PhD**

#### PURPOSE

To test the hypothesis that CT angiography (CTA) images reconstructed with iterative method (AIDR3D) have superior image quality, lower interobserver variability in anatomical measurements, and higher diagnostic accuracy when compared to the same raw data reconstructed with filtered back projection (FBP).

#### METHOD AND MATERIALS

All 157 clinical chest and abdominal CTA (Table) acquisitions (320x0.5 mm CT) over 5 months (6/12-10/12) were performed at a reduced radiation dose (compared to standard at our institution) and the raw data was reconstructed with both AIDR3D and FBP. Quality of arterial phase images was assessed by two independent readers (4-point scale) for both reconstructions. For 1/3 of patients (n=53, randomly chosen), signal-to-noise ratio (SNR) and contrast-to-noise ratio (CNR) was measured at the artery of interest. For renal donors (n=10), kidney size and renal artery length were measured by two readers for both reconstructions, and interobserver variability determined. For coronary CTA with reference standard catheter angiography (n=15), degree of coronary stenosis and level of confidence (3-point scale) in assessment was determined by two readers for both reconstructions, interobserver agreement and diagnostic accuracy was assessed.

#### RESULTS

Image quality score had good interobserver agreement (weighted  $\kappa=0.67$ ) and was higher (p

#### CONCLUSION

Reduced radiation exposure CTA images reconstructed with AIDR3D have higher objective and subjective image quality when compared to FBP, with a tendency towards lower interobserver variability among the CTA clinical indications tested.

**V5VA51-05 • Dual-Energy and Low kVp CTA****Sachio Kuribayashi MD (Presenter) \***

## LEARNING OBJECTIVES

1) Understand the basic principles and technical basics of dual energy CTA. 2) Describe two components of dual energy imaging including material decomposition and virtual monochromatic spectral imaging. 3) Review the experimental studies and discuss the potential clinical application to vascular systems.

**V5VA51-06 • Reduced Radiation Dose and Improved Diagnostic Image Quality at Cardiovascular CT Angiography by Automated, Individualized X-ray Tube Voltage Selection: Intra-individual Comparisons****Aleksander Krazinski (Presenter) ; U. Joseph Schoepf MD \* ; Justin R Silverman ; Christian Canstein \* ; Robin Brothers RT ; Lucas L Geyer MD \* ; Felix G Meinel MD**

## PURPOSE

To evaluate radiation dose and image quality at cardiovascular CT angiography (CTA) with an automated x-ray tube voltage adjustment application by intra-individual comparison in patients undergoing CTA of the heart or aorta.

## METHOD AND MATERIALS

The study was IRB approved and HIPAA compliant. We retrospectively analyzed paired studies in 64 patients (35 male, 60±16 years), who had undergone two 2<sup>nd</sup> generation dual-source CTA acquisitions of the heart or aorta before and after the implementation of an automated x-ray tube voltage adjustment application. Each study pair consisted of a baseline scan (scan1) where tube voltage was operator selected based on the patient's body mass index and a follow up scan (scan2) where tube voltage was automatically selected based on the anatomical attenuation of the topogram (scout) acquisition. Other parameters were kept identical between the two scans: 2x64x0.6mm collimation; 320mAs modulated reference tube current-time product. Subjective image quality (IQ) was rated and objective IQ was measured by mean arterial attenuation, image noise, signal-to-noise ratio (SNR) and contrast-to-noise ratio (CNR). To adjust for differences in radiation exposure, a figure of merit (FOM) was calculated. Effective radiation dose equivalents were compared. All values are given as mean±standard deviation (SD) and were tested for significance using the Wilcoxon signed-rank test.

## RESULTS

All studies were considered diagnostic. A different kV level between scan1 and scan2 was automatically selected in 18 patients (28%). Overall subjective IQ (3.30±0.87, 3.56±0.85, p=0.02), SNR (14.6±5.93, 16.65±5.90, p=0.005), CNR (12.13±5.34, 14.08±5.30, p=0.007), and FOM (20.9±24.3, 44.0±44.7, p

## CONCLUSION

Patient specific protocol adjustment by automated x-ray tube voltage selection can operator-independently optimize cardiovascular CTA image acquisition parameters with improved objective and subjective image quality.

## CLINICAL RELEVANCE/APPLICATION

At cardiovascular CTA, patient specific protocol adjustment by automated voltage selection offers significant radiation reduction across an identical patient population while image quality is enhanced

**V5VA51-07 • Utility of Iodine Extracted Images from Single Source Dual-energy CTA to Evaluate the Success of Endovascular Repair of Abdominal Aortic Aneurysm****Mukta D Agrawal MBBS, MD (Presenter) \* ; Sanjeeva P Kalva MD \* ; George R Oliveira MD ; Jorge M Fuentes MD ; Yasir Andrabi MD, MPH ; Koichi Hayano MD ; Dushyant V Sahani MD**

## PURPOSE

To investigate if the iodine-extracted (IE) images from DE-CTA can enable confident assessment of stent patency and endoleak following endovascular repair of abdominal aortic aneurysm (EVAR).

## METHOD AND MATERIALS

In this IRB approved prospective study, 51 consecutive patients with EVAR had follow-up CTA exam using ssDECT (GE discovery CT750 HD). The arterial (25-30 sec) and delayed phase (60 sec) DECT datasets were processed to create material density iodine extracted images (IE) and virtual monochromatic (VMC) images at 50 and 70 keV. Three-experienced radiologist independently evaluated only the IE images to assess stent patency and endoleak detection. The diagnostic evaluation based on combined unenhanced, multiphase enhanced and processed VMC images served as the reference standard for comparison of performance and interpretation time. Number of endoleak detected on IE images were compared to that detected on all other images.

## RESULTS

All readers made their interpretations in 51 cases using IE except in 4 cases for R1 and 2 cases for R2, review of other image datasets was demanded but their interpretations remained unchanged. 15 endoleaks were confidently detected on IE images by all readers including those in 4 patients with Onyx embolization for type 2 endoleaks. Although arterial phase IE images detected all 15 leaks, in 3 patients delayed phase IE images were helpful. Average time spent per case was 5.34 minutes for IE images alone in comparison to 21.30 minutes for the entire processed DECT dataset.

## CONCLUSION

Review of ssDE-CTA rendered IE images alone can enable confident assessment of stent patency and endoleak detection in patients with EVAR.

## CLINICAL RELEVANCE/APPLICATION

ssDECT benefit vascular imaging but has introduced workflow challenge to process and interpret multiple dataset. IE combine the unique features to efficiently yield pertinent information for EVAR exam

**V5VA51-08 • Implications for Contrast Medium Delivery****Hans-Christoph R Becker MD (Presenter)**

## LEARNING OBJECTIVES

1) Understand the basic principles and technical basics of dual energy CTA. 2) Describe two components of dual energy imaging including material decomposition and virtual monochromatic spectral imaging. 3) Review the experimental studies and discuss the potential clinical application to vascular systems.

**V5VA51-09 • Utility of Dual Energy Spectral CT for Reducing Contrast Medium Dose in Abdominal CT Angiography: Initial Clinical Experience****Xin Lei (Presenter) ; Yang Xiaotang ; Gao Jinfang ; Zhao Zhikai ; Chang Chao ; Fan Lin**

## PURPOSE

To investigate the utility of dual energy spectral CT (DEsCT) for reducing contrast medium in abdominal CT angiography.

## METHOD AND MATERIALS

This prospective study was approved by the institutional review board with patient informed consent. 22 consecutive patients (BMI>=24,

13men, 9 women; mean age, 45.4±12.6 years) with suspected abdominal occupied lesions underwent either conventional CTA with 120kVp and iodixanol (Visipaque, 270mg/ml) (n=12) or spectral CTA with iohexol (Omnipaque, 350mg/ml) (n=10). The injection rate and amount for two groups were 3.5 ml/s and 1ml/kg. Images of both groups had 0.625mm slice thickness. Monochromatic images (40-140keV) were generated from the spectral CTA, and from which an optimal energy level was selected for obtaining the best contrast-noise-ratio (CNR) for the abdominal aorta at the renal artery level relative to the erector spine muscle. The CT value and noise of the abdominal aorta and muscle at the optimal monochromatic image set of spectral CTA group and at conventional CTA group were measured. Two radiologists assessed all images with 5-points scale. CTDIVol was recorded. Data were analyzed using student T-test.

## RESULTS

### CONCLUSION

With 29% contrast medium reduce and similar radiation dose, spectral CTA provided better image quality than conventional CTA.

### CLINICAL RELEVANCE/APPLICATION

Low-keV monochromatic CTA should be an optional choice for patients who have underlying renal function impairment.

## **VSVA51-10 • CT Venography with Dual Energy CT: Dose Reduction of Contrast Material with Low Tube Voltage**

**Shintaro Ichikawa** MD (Presenter) ; **Utaroh Motosugi** MD ; **Masato Imaizumi** ; **Katsuhiko Sano** MD ; **Hiroyuki Morisaka** MD ; **Tomoaki Ichikawa** MD, PhD \*

### PURPOSE

To assess whether dose of contrast material can be reduced in CT venography with low tube voltage (80 kVp) CT.

### METHOD AND MATERIALS

This prospective study included 63 patients. They were randomly divided into 3 groups that were administered different doses of contrast material (600, 500, and 400 mg I/kg). We used an area-detector CT scanner (Aquilion ONE; Toshiba Medical Systems, Japan) and iopamiroI (Iopamiron®; Bayer Yakuhin, Ltd., Japan). All patients underwent dual energy CT at 80 and 135 kVp. Conventional image (120kVp) was made from them and 80 and 120 kVp were compared. We measured the average CT value of 4 regions of interests, namely, the left and right femoral and popliteal veins, and a value of =80 HU was considered sufficient contrast for detecting deep vein thrombosis (Goodman, et al. Radiology 2005). Two radiologists evaluated the contrast of veins and muscles with a 3-point confidence scale, and scores within =5 points of the total score were considered adequate.

### RESULTS

The mean CT value of images taken at 80 kVp was significantly higher than that taken at 120 kVp (600 mg I/kg, 150.1 ± 19.9 HU vs. 121.8 ± 14.2 HU; 500 mg I/kg, 134.4 ± 19.4 HU vs. 108.7 ± 14.3 HU; and 400 mg I/kg, 115.9 ± 15.8 HU vs. 91.6 ± 12.2 HU, respectively). The mean CT value was lowest for the image at 120 kVp after administration of 400 mg I/kg of contrast material. The proportion of patients with scores over 80 HU of 400 mg I/kg and at 120 kVp (15/21 [71.4%]) was significantly lower than that of the control group (600 mg I/kg at 120 kVp; 21/21 [100%]). The proportion of patients with scores 5 points higher than the total score of 400 mg I/kg of contrast material and at 120 kVp (12/21 [57.1%]) was significantly lower than that of the control group (600 mg I/kg at 120 kVp; 20/21 [95.2%]). There was no significant difference between the images obtained after administration of 400 mg I/kg of contrast material at 80 kVp and the control images (600 mg I/kg at 120 kVp). Moreover, in this study, the use of 80 kVp rather than 120 kVp showed a 30% reduction in radiation exposure (CTDI VOL [10.4 vs. 14.9 mGy], respectively).

### CONCLUSION

By using low tube voltage (80 kVp), the dose of contrast material can be reduced to at least 400 mg I/kg, while keeping sufficient contrast to diagnose deep venous thrombosis.

### CLINICAL RELEVANCE/APPLICATION

This study showed that low tube voltage (80 kVp) CT can help reduce the dose of contrast material and radiation exposure.

## **VSVA51-11 • Feasibility of Low kV Settings CT-angiography with Ultra Low Contrast Medium Volume for the Assessment of Thoracic and Abdominal Aorta Disease**

**Cammillo R Talei Franzesi** (Presenter) ; **Davide Ippolito** MD ; **Pietro A Bonaffini** MD ; **Davide Fior** MD ; **Orazio Minutolo** MD ; **Sandro Sironi** MD

### PURPOSE

To evaluate the image quality, the diagnostic performance and the radiation dose exposure of low-kV CT angiography (CTA) protocol (100 kV) with ultra low-contrast medium volume (40 mL) in the assessment of thoracic and abdominal aorta disease.

### METHOD AND MATERIALS

From July 2011 to February 2013, 76 patients (28 women; mean age 65.4 years; range, 35-83 years; BMI

### RESULTS

In all the CT studies we could correctly visualize and evaluate main branches of thoracic and abdominal aorta. No significant difference of density measurements was achieved between the low-kV protocol (mean attenuation value of thoracic aorta 304HU, abdominal aorta 343HU and renal arteries 331HU) and the control group (mean value of thoracic aorta 320HU, abdominal aorta 339HU and renal arteries 303HU). The radiation dose exposure was significantly lower (p

### CONCLUSION

Low-kV protocol provides a diagnostic performance comparable to standard protocol, decreasing significantly the radiation dose exposure (particularly in the abdomen) and with a significant reduction of contrast material volume.

### CLINICAL RELEVANCE/APPLICATION

Low-kV and low-contrast volume CT-angiography provides a significant reduction of radiation exposure, maintaining good image quality, also allowing evaluation of patients with renal dysfunction.

## **VSVA51-12 • A Novel CT-based Calcium Scoring System of the Lower Extremity Arteries: Impact on Luminal Assessment with CT Angiography**

**Stacey Schriber** (Presenter) ; **Waleska M Pabon-Ramos** MD ; **Holly L Nichols** BS ; **Mark L Lessne** MD ; **Charles Y Kim** MD \*

### PURPOSE

Calcification of the lower extremity arteries can hinder luminal visualization on CT angiography. However, not all types and degrees of calcification are problematic. The purpose of this project is to utilize a novel calcium scoring system to correlate calcification characteristics with luminal visibility and diagnostic accuracy.

### METHOD AND MATERIALS

The study population consisted of 99 legs in 57 patients (31 male, mean age 65 years) that underwent both CT and conventional angiography of the lower extremities within 3 months of each other. The arteries of each leg were divided into 9 segments. A single axial image was chosen from the CTA in each arterial segment for evaluation. The degree of stenosis (

### RESULTS

371 of 514 arterial segments analyzed had some degree of calcification. Both calcium morphology and circumference scores demonstrated a strong inverse correlation with diagnostic confidence for the infrainguinal arteries but moderate in the iliac arteries (p

### CONCLUSION

The proposed calcification scoring system based on calcium morphology and circumference correlated well with diagnostic confidence and accuracy of luminal assessment on CTA.

## CLINICAL RELEVANCE/APPLICATION

Characterization of the calcium morphology and circumference on CTA can provide a method for quantifying the diagnostic accuracy of interpretation of luminal patency and stenosis

### VSVA51-14 • Post Processing, Workflow and Interpretation

**Karin E Dill MD** (Presenter)

#### LEARNING OBJECTIVES

1) To illustrate steps in image post-processing for the interpretation of CTA images. 2) To highlight elements that can be used to optimize workflow for multiplanar reformatted images, maximum intensity projections, and three-dimensional volumes.

ABSTRACT

## Interventional Oncology Series: Liver Metastases and Bone

Thursday, 01:30 PM - 06:00 PM • S405AB

[RO](#) [OI](#) [IR](#) [GI](#)

[Back to Top](#)

**VSI051** • AMA PRA Category 1 Credit™:4.25 • ARRT Category A+ Credit:5

#### Moderator

**Matthew R Callstrom**, MD, PhD \*

#### LEARNING OBJECTIVES

1) Describe the characteristics of liver metastases and bone tumors amenable to interventional oncologic treatment. 2) Describe new techniques for the percutaneous treatment of liver metastases and bone tumors. 3) Describe the role of percutaneous ablation for liver metastases and bone tumors in the context of other treatments including surgery and radiation oncology.

ABSTRACT

### VSI051-01 • Which Ablation - Where and Why

**Riccardo A Lencioni MD** (Presenter)

#### LEARNING OBJECTIVES

1) To describe the different methods and techniques used for image-guided tumor ablation. 2) To understand the use of image-guided ablation in focal cancer therapy. 3) To understand the role of image-guided ablation with respect to surgical and medical treatments.

### VSI051-02 • IRE for Liver Metastases

**Govindarajan Narayanan MD** (Presenter) \*

#### LEARNING OBJECTIVES

View learning objectives under main course title.

### VSI051-03 • Chemo ± RFA; Does RFA Provide a Benefit?

**Alison R Gillams MBChB** (Presenter) \*

#### LEARNING OBJECTIVES

1) To learn the survival results for patients treated with ablation, chemotherapy and combinations of ablation and chemotherapy. 2) To learn the optimal timing of ablation and chemotherapy in different clinical situations.

#### ABSTRACT

Chemotherapy regimes in the 80;s and early 90;s using 5 fluorouracil (5FU) based regimens did not improve survival. They did result in a morphologic response on imaging in just 30% of patients. Median survival was about 9 months. It was not until the late 90;s with the introduction of irinotecan and oxaliplatin that a change in survival was seen. Response rates increased to 50% and the use of sequential oxaliplatin and irinotecan produced a further small increase in survival. The introduction of Cetuximab and Bevacizumab saw a further increase in response rates to approximately 75% and a further increase in survival. This improvement was further honed with the realisation that only Kras wild type patients responded and Kras testing is now routine prior to Cetuximab administration. Kras status may differ between the primary lesion and the metastatic disease but the difference is small. Median survival for patients who receive all the possible chemotherapeutic options is now approximately 21 months, 5 year survival remains exceptional. Ablation is generally used in small volume, liver only disease in inoperable patients. The median survival is of the order of 36 months with 5 year survival of 30%. This is better than has been achieved with any chemotherapy regime and so ablation should be offered to all suitable patients. Adjuvant chemotherapy has been shown to be useful in post resection patients and there is some anecdotal evidence that it is useful post ablation. Neo adjuvant chemotherapy is used to downsize metastases in patients who are not initially resectable or ablatable in the hope that they will become suitable for definitive treatment. Although some tumours will disappear on imaging, the chances of recurrence are very high (96%) and therefore treatment should be aimed to encompass all the original sites of disease.

### VSI051-04 • Microwave Ablation (MWA) Therapy of Liver Metastases from Colorectal Carcinoma Post Systemic Chemotherapy

**Nour-Eldin A Nour-Eldin MD, MSc** (Presenter) ; **Nagy N Naguib MSc** ; **Tatjana Gruber-Rouh** ; **Thomas Lehnert MD** ; **Thomas J Vogl MD, PhD**

#### PURPOSE

to evaluate the safety, efficiency, effectiveness, and overall outcome in patients treated with microwave thermal ablation of colorectal metastases post systemic chemotherapy.

#### METHOD AND MATERIALS

An institutional review board-approval was obtained with informed consent of all patients. Retrospective analysis of prospective intention to treat study was performed from January 2008 to January 2013, and included 92 patients (mean age 56 years SD: 2.6) with 132 liver metastases measuring 0.7-5.0cm, who were treated with microwave ablation (MWA). Local tumor control, complications, and long-term survival were analyzed.

#### RESULTS

The mean follow-up period was 32.5 months. Complete ablation was achieved in 117 of 132 (88.6%) nodules. Seventeen of the 117 (14.5%) successfully treated nodules developed local recurrence. Univariate analysis showed that tumor size of < 3 cm is a significant risk factor (P = 0.04). Multivariate analysis showed that number of cycles of chemotherapy (FOLFOX) was a significant prognostic factor for overall recurrence (P=0.03), whereas disease-free interval was the significant prognostic factor for distant recurrence (P=0.03). Major complications occurred in 1.1% of patients. No procedure-related mortalities were observed. The 1, 2, 3, and 5-year overall survival rates after the initial ablation were 82, 61.2, 51.2, and 38.3%, respectively. The main cause of death was systemic tumor progression in 65.3% of the patients.

#### CONCLUSION

MWA is a safe and effective treatment therapeutic option for patients with liver metastases from Colorectal Carcinoma post systemic

chemotherapy.

#### CLINICAL RELEVANCE/APPLICATION

Thermal ablative techniques such as MWA are safe and effective minimally invasive therapeutic option in the management of patients with hepatic metastasis, especially after systemic chemotherapy.

### VSI051-05 • Surgery for CRC Liver Mets - When Is Ablation Indicated?

**Yuman Fong MD (Presenter) \***

#### LEARNING OBJECTIVES

1) To understand the available ablative options for metastatic colorectal cancer. 2) To understand the determinants of success and failure for ablative treatment for colorectal metastases. 3) To understand the use of ablative therapy as an adjunct to surgery in the care of patients. 4) To understand the use of ablative therapy in the treatment of recurrent liver metastases.

### VSI051-06 • Treatment of Difficult Liver Metastases

**Thierry J De Baere MD (Presenter) \***

#### LEARNING OBJECTIVES

1) To know what are the most difficult situations when treating liver metastasis with percutaneous ablation techniques. 2) To know tips and tricks that can help to improve quality of targeting during percutaneous ablation of liver metastases. 3) To know what are the limitations of different ablation technologies of percutaneous ablation according to tumor size and location.

#### ABSTRACT

Percutaneous ablation of liver metastases allows for complete ablation in approximately 90% in well selected indications. Some metastases are more difficult to ablate due to either difficulty in targeting, or their location close to large vessels, close to fragile neighboring organs, or in proximity to the liver hilum. Difficulties in targeting are often due to poor visualization of the targeted tumor with image guidance. We will present possible benefit of fusion imaging between US and enhanced CT and discuss accuracy of such technique. We will describe technique and results of tumor tagging with either percutaneously inserted metallic coils or tagging with intra-arterial injection of Lipiodol. Location close to large vessels favors convective tissue cooling and is responsible for lower rate of complete ablation with RFA for such tumor. Combining RFA with percutaneous balloon occlusion of hepatic or portal veins can improve results and the technique will be presented. Other ablative technologies can improve results of ablation close to large vessels and will be discussed namely with regards to microwaves ablation and irreversible electroporation. Neighboring organ can be preserved from any damage by using aerodissection (air or carbon dioxide) or hydrodissection (dextrose, G5%, G10%) for shielding, and tips and tricks to achieve such dissection will be presented.

### VSI051-07 • Assessing Geometric RF Ablation Accuracy and Predicting Outcome within 24h after Treatment by Mapping the Preprocedure Liver Lesion to the Postprocedure Ablation Zone

**Frederik Vandenbroucke MD (Presenter) ; Jef Vandemeulebroucke PhD, MSc ; Nico Buls DSc, PhD \* ; Pablo R Ros MD, PhD \* ; Johan De Mey \***

#### PURPOSE

In RF ablation, complete coverage of the lesion by the ablation zone, is considered the primary indicator for treatment success. The purpose of this study was to evaluate the predictive value of early assessment of the geometrical accuracy of the procedure by using contrast enhanced CT images acquired before and within 24h after ablation.

#### METHOD AND MATERIALS

Twenty-three patients, with a total of 45 liver lesions, received a CT scan before and 24 hours after RF ablation. Follow up PET/CT scans were performed every 2-3 months after the intervention. Pre- and post-ablation CT images were aligned using commercial registration software. Lesion and ablation zone were semi-automatically segmented and masked during registration. A global, rigid registration based on mutual information was performed. If required, this was followed by an interactive local registration based on a smaller region of interest. Using the registered images, we verified the geometrical accuracy of the RF ablation treatment by measuring the minimal distance between the lesion and the outer edge of the ablation zone, and correlated this to local tumor progression (LTP) as recorded during follow up.

#### RESULTS

Eleven lesions (24.4%) showed LTP during a mean follow up of 62 weeks. Registration was successful for all lesions, although 5 were perceived as challenging. Based on the registered images, 29 lesions were completely covered by the ablation zone, while 10 were not. For 6 lesions, the edge was found to coincide with the edge of the ablation zone. Incomplete coverage of the lesion was found to be a powerful predictor for LTP (Se = 100%, Sp = 85%, PVV = 69%, NPV = 100%). Interestingly, two lesions only showed LTP after 5-6 months, and both belonged to the group where the edges of lesion and ablation zone coincided.

#### CONCLUSION

Verifying the coverage of liver metastases by an ablation zone through registration of pre- and early post-ablation CT images is feasible and has a strong predictive power for treatment outcome. Increasing the robustness and degree of automation of the procedure could further improve the accuracy and reproducibility of the method.

#### CLINICAL RELEVANCE/APPLICATION

Early and accurate detection of RF ablation failure may allow for reablation and will ultimately improve the efficacy of this minimally invasive procedure.

### VSI051-08 • Liver Metastases Tumor Board

**Matthew R Callstrom MD, PhD (Presenter) \***

#### LEARNING OBJECTIVES

1) Describe the characteristics of liver metastases amenable to interventional oncologic treatment. 2) Describe new techniques for the percutaneous treatment of liver metastases. 3) Understand the role of percutaneous ablation for treatment of liver metastases in the context of other treatments including surgery and radiation oncology.

#### ABSTRACT

### VSI051-09 • Surgery vs Ablation for Bone Tumors

**Peter Rose MD (Presenter)**

#### LEARNING OBJECTIVES

1) To understand the factors that decide whether a lesion is best treated with surgery or ablation.'

### VSI051-10 • SBRT for Bone and Soft Tissue Metastases

**Kenneth R Olivier MD (Presenter)**

#### LEARNING OBJECTIVES

1) Review the technique of Stereotactic Body Radiotherapy. 2) Discuss cases where SBRT has been used in soft tissue and non-spine

bone metastases. 3) Review literature and Mayo Clinic experience with SBRT in these situations. 4) Discuss opportunities for collaboration with Interventional Radiology in complex patients.

#### ABSTRACT

Stereotactic Body Radiotherapy (SBRT) is a useful treatment modality for solitary metastases in many locations. SBRT has been used more recently for spinal metastases with good results. The use of SBRT for non-spine bone metastases is not as widely reported, but can be useful in certain situations. Mayo Clinic has been treating select patients with SBRT and the experience will be discussed.

### VSI051-11 • Soft Tissue Cryoablation Is Crucial for Patients with Oligometastatic Disease

**Peter J Littrup MD (Presenter) \*** ; **Hussein D Aoun MD** ; **Barbara A Adam MSN** ; **Evan N Fletcher MS, BA** ; **Mark J Krycia BS**

#### PURPOSE

To assess whether diverse tumor location(s) show differences in local cryoablation outcomes of cancer control, morbidity, and ablation volume reduction for many soft tissue tumor types. We hypothesize that non-organ cryoablation locations respond similarly in terms of recurrence, complication and/or healing rates, regardless of anatomic location and tumor type.

#### METHOD AND MATERIALS

220 CT and/or US-guided, percutaneous cryotherapy procedures were performed for 251 oligometastatic tumors from multiple primary cancers in 126 patients. Tumor location was grouped according to regional sites: retroperitoneal, superficial, intraperitoneal, bone, and head and neck. PCA complications were graded according to Common Terminology Criteria for Adverse Events Version 4.0 (CTCAE). Local tumor recurrence and resorption was calculated from ablation zone measurements, grouped into 1-, 3-, 6-, 12-, 18- and ≥24-month statistical bins.

#### RESULTS

Tumor and procedure numbers for each site are: 75, 69 - retroperitoneal; 76, 62 - superficial; 39, 32 - intraperitoneal; 34, 34 ♦ bone; and 27, 26 - head and neck. Average diameters of tumor and visible ice during ablation were 3.4 and 5.5 cm, respectively. Major complications (CTCAE Grade >3) occurred after 7 procedures (3.2%). At 11 months average follow-up (range: 0-82), 10% local recurrence rates (26/251) were noted, of which 3 occurred within the ablation zone for a PCA procedural failure rate of 1.2%. Average time to recurrence was 4.9 months. At 21 months following the procedure, the initial ablation zone had reduced in volume by 93%.

#### CONCLUSION

CT-guided PCA is a broadly safe, effective local cancer control option for oligo-metastatic patients with soft tissue tumors in most anatomic sites. Other than bowel and nerve proximity, PCA also shows good healing if proper visualization and precautions are followed. Cryoablation thus allows highly successful tumor control with minimal morbidity and healing, especially near skin, subcutaneous and osseous locations that would not be readily amenable for heat-based ablations.

#### CLINICAL RELEVANCE/APPLICATION

Oligometastatic disease is becoming widely recognized with improved systemic treatments. Soft tissue cryoablation contributes to improved cancer-specific survival for many tumor types, despite location

### VSI051-12 • Mid-term Outcome of Percutaneous Image-guided Cryoablation on Inoperable Extra-abdominal Desmoid Tumors

**Marion Havez (Presenter)** ; **Francois Cornelis MD** ; **Paul Sargos** ; **Sultan Al Ammari** ; **Agnes Neuville** ; **Eberhard Stoeckle** ; **Michele Kind MD** ; **Antoine Italiano MD**

#### PURPOSE

To report the effectiveness and mid-term outcome of percutaneous image-guided cryoablation on extra-abdominal desmoid tumors.

#### METHOD AND MATERIALS

The institutional review board approved this study and informed consent was waived. Between 2011 and 2012, 13 patients (17 tumors), with a median age of 39.3 years (15♦74), consecutively treated with cryoablation under ultrasound (n=8), computed tomography (n=1) or both (n=8) guidance for extra-abdominal desmoid tumors were retrospectively selected and prospectively followed until 2013. The study included 2 patients with Gardner syndrome and 12 recurrences on ablative site after initial surgical treatment. Maximal tumor volumes were between 0.8 to 127.2 mm<sup>3</sup> (median: 28 mm<sup>3</sup>). Disease free survival (DFS) and local control were calculated on clinical (pain evaluation) and imaging (according to RECIST criteria) follow-up, respectively. The Kaplan-Meier method was used for calculation of DFS.

#### RESULTS

Cryoablation was technically possible for all lesions under general (n=15) or local (n=2) anesthesia. Two probes were used in mean (range: 1-4) per procedure. Mean follow-up was 14.1 months (4♦27 months). The disease-free survival rates based on clinical evaluation were 100%, 92% and 73% at 6, 12 and 24 months, respectively. The rates of local tumour progression based on RECIST criteria were 0% at 6, 12 or 24 months. However, 10 patients (59%) presented asymptomatic residual tumors surrounding the ablative site on imaging follow-up. The major complications rate was 5.8% per session (1/17).

#### CONCLUSION

Despite high rate of partial ablation, percutaneous image-guided cryoablation appears to be safe and effective for mid-term local control in case of inoperable extra-abdominal desmoid tumors.

#### CLINICAL RELEVANCE/APPLICATION

Cryoablation is a well-tolerated technique according to mid-term results. Mid-term efficacy of cryoablation was close to that of formal conservative surgery

### VSI051-13 • MRgFUS for Palliation of Painful Metastatic Disease

**Mark D Hurwitz MD (Presenter)**

#### LEARNING OBJECTIVES

View learning objectives under main course title.

### VSI051-14 • Cementoplasty Beyond the Spine

**Giovanni Carlo Anselmetti MD (Presenter) \***

#### LEARNING OBJECTIVES

1) To learn indications and contra-indications to cementoplasty beyond the spine. 2) To learn the optimal technique, regarding materials and image guiding systems, in performing percutaneous cementoplasty.

#### ABSTRACT

Bone is one of the most frequent sites of spread for many common cancers. In such case, when appropriate systemic treatment for the underlying cancer fails, patients should be considered for specific treatment, the principal modalities being radiotherapy and bisphosphonates. These therapies leave approximately one third of cases with inadequate pain control. This failure prompted the search for other strategies aimed at bone pain control through local bone augmentation such as percutaneous cementoplasty (PC). PC can be performed under combined Computed Tomography (CT) and Fluoroscopic guidance; flat panel angiographic suite with integrated CT can also be used. Both systems allow precise positioning of the needle within the bone lesion. Most frequently PC is executed in sacrum, hip and femur but this procedure is also successful and feasible in fingers, astragalus, calcaneus, ribs, sternum, etc. Local anesthesia is employed in most cases.

Bone lesions are localized on CT and the most adequate access point is identified. A dedicated vertebroplasty beveled needle is then advanced into the bone lesion.  
Bone cement is injected under continuous fluoroscopic control. After PC a CT scan of the treated region is carried out to assess the extent of lesion filling and to visualize possible PMMA leaks.  
Patients are discharged the same procedural day.  
In our experience PC was technically successful in all cases with no immediate severe complications. In lesions with lost integrity of the cortical bone, asymptomatic leakage of PMMA in the soft tissues can occur but, normally, it not requires any treatment.  
Delayed complications such as fractures in metastases of the femoral diaphysis can occur; lytic lesions of the long bones shaft cannot be treated with PC due to high risk of fracture during ambulation.  
PC, in our opinion, should be proposed in all patients with painful or invalidating bone lesions when conventional therapies fail or surgery is not feasible.

### **VSI051-15 • Chondrolysis and Femoral Head Osteonecrosis: A Complication of Periacetabular Cryoablation**

**Michael V Friedman MD (Presenter) ; Jack W Jennings MD ; Travis J Hillen MD \* ; Daniel E Wessell MD, PhD \***

#### **PURPOSE**

Cryoablation is an emerging alternative in the treatment of primary osseous malignancies or metastatic diseases that are not amenable to more conventional therapies. As experience compounds with this newer, less-invasive technique, associated complications will be continually defined. We describe a novel complication associated with percutaneous cryoablation of periacetabular bone tumors.

#### **METHOD AND MATERIALS**

Between 2008 and 2013, 41 patients with a total of 100 musculoskeletal lesions were treated by cryoablation at our institution. 12 patients were referred to our department specifically for treatment of periacetabular osseous malignancies. There were a total of 15 lesions, with 3 of the 12 patients having bilateral lesions. Follow-up clinical notes and imaging of the patients were retrospectively reviewed for a minimum of 2 months. Generalized estimating equations were performed to assess the effect that patient demographics and treatment parameters (including ablation time, cycle distribution, and probe proximity to the femoral head and fovea) had on development of chondrolysis and osteonecrosis.

#### **RESULTS**

Chondrolysis or femoral head osteonecrosis developed in 31% (4 of 13) of periacetabular lesions. Of the remaining patients with non-periacetabular lesions that underwent cryoablation, none subsequently developed osteonecrosis. Patients who developed chondrolysis or osteonecrosis had ablation zones closer to the joint. There was no difference in ablation times or cycle distribution. Chondrolysis or osteonecrosis developed within a 5 month period, with a mean of 89 days. 3 of the 4 patients who developed chondrolysis have undergone total joint replacement.

#### **CONCLUSION**

Chondrolysis or femoral head osteonecrosis developed in 31% of periacetabular malignancies treated by cryoablation, ultimately requiring joint replacement in 3 of 4 patients. Careful pre-ablation planning and risk/benefit analysis should be considered before performing periarticular cryoablation, and patients should subsequently be monitored for developing chondrolysis.

#### **CLINICAL RELEVANCE/APPLICATION**

Periarticular cryoablation can be associated with osteonecrosis and chondrolysis, and therefore, careful pre-ablation planning and risk/benefit analysis should be performed prior to proceeding.

### **VSI051-16 • Percutaneous Image-guided Ablation of Metastatic Renal Cell Carcinoma**

**Brian T Welch MD (Presenter) ; Matthew R Callstrom MD, PhD \* ; Jonathan M Morris MD ; Anil N Kurup MD ; Grant D Schmit MD ; Thomas D Atwell MD ; Adam J Weisbrod MD ; Manish Kohli MD ; Brian Costello MD ; Christine Lohse ; Stephen Boorjian ; Robert Thompson MD**

#### **PURPOSE**

Over 65,000 new cases of RCC will be diagnosed this year in the United States. Approximately 50% of RCC patients will present with or subsequently develop metastases after primary treatment. Our purpose is to assess the safety, local control, complications, and adjunctive survival of ablation in treatment of mRCC in this selected cohort.

#### **METHOD AND MATERIALS**

A retrospective review was performed of 61 patients who underwent 74 ablation procedures to treat 82 mRCC lesions with intent of local control (i.e. not palliative). Technical success, safety, local control, complications, and survival were analyzed according to standard criteria.

#### **RESULTS**

Four (4.9%) technical failures were observed. Time to recurrence was assessed for the subset of 76 (93%) tumors that were followed past ablation. Six (7.9%) tumors recurred at a mean of 1.6 years following ablation (median 1.4; range 0.6 -2.9). The mean duration of follow-up for the 70 tumors that did not recur was 1.9 years (median 1.2; range 10 days - 7.5 years). Estimated local recurrence-free survival rates (95% CI; number still at risk) at 1, 2, 3, 5, and 7 years following ablation were 94% (88 ♦ 100; 41), 94% (88 ♦ 100; 32), 83% (70 ♦ 97; 17), 83% (70 ♦ 97; 5), and 83% (70 ♦ 97; 3), respectively. Estimated overall survival rates (95% CI; number still at risk) at 1, 2, 3, 5, and 7 years following ablation were 87% (79 ♦ 97; 42), 83% (73 ♦ 94; 31), 76% (63 ♦ 90; 19), 52% (35 ♦ 76; 6), and 52% (35 ♦ 76; 2), respectively. Recognizing this highly selected patient population and additional concurrent or subsequent treatment, estimated cancer-specific survival rates (95% CI; number still at risk) at 1, 2, 3, 5, and 7 years following ablation were 91% (83 ♦ 99; 42), 86% (76 ♦ 96; 31), 82% (71 ♦ 95; 19), 62% (46 ♦ 85; 6), and 62% (46 ♦ 85; 2), respectively. Four (5%) CTCAE grade 3 or greater complications were observed; there were no deaths related to the ablation.

#### **CONCLUSION**

Image guided ablation of mRCC is a relatively safe procedure with acceptable local control rates. In carefully selected patients, adjunct ablation with systemic therapy, radiation, and surgery may confer a survival benefit, although further follow-up and validation are needed.

#### **CLINICAL RELEVANCE/APPLICATION**

In carefully selected patients, adjunct ablation with systemic therapy, radiation, and surgery may confer a survival benefit, although further follow-up and validation are needed.

### **VSI051-17 • Bone Metastases Tumor Board**

**Matthew R Callstrom MD, PhD (Presenter) \***

#### **LEARNING OBJECTIVES**

1) Describe the characteristics of bone tumors amenable to interventional oncologic treatment in the context of other treatments including surgery and radiation oncology. 2) Describe the techniques to avoid complications in the percutaneous treatment of metastatic bone tumors. 3) Describe characteristics of metastatic bone tumors that benefit from combination treatments.

**VSIR61** • AMA PRA Category 1 Credit™:3.25 • ARRT Category A+ Credit:3.75

**Moderator**

**Charles E Ray**, MD, PhD \*

LEARNING OBJECTIVES

1) List 2 important recent publications in interventional oncology. 2) Explain the mechanism of one complication related to thermal ablation. 3) Describe pros and cons of chemoembolization versus radioembolization of hepatocellular carcinoma with portal vein thrombosis. 4) Outline 3 complications in combination therapy for hepatocellular carcinoma. 5) List three complications of chemo-embolization. 6) Describe rationale for and against interventional oncology as a distinct specialty.

**VSIR61-02 • Chemo-Embolization Cxs**

**Charles E Ray** MD, PhD (Presenter) \*

LEARNING OBJECTIVES

View learning objectives under main course title.

**VSIR61-03 • Tc-99m Macroaggregated Albumine Lung Shunt Calculation Overestimates the Lung Dose in Radioembolization**

**Mattijs Elschot** MSc ; **Jip F Prince** MSc (Presenter) ; **Maarten L Smits** ; **Marnix G Lam** MD ; **Johannes F Nijsen** PhD ; **Bernard A Zonnenberg** MD ; **Max A Viergever** \* ; **Maurice A Van Den Bosch** MD, PhD ; **Hugo W De Jong** PhD

PURPOSE

Hepatic radioembolization is preceded by a safety procedure in which a scout dose of <sup>99m</sup>Tc-MAA is infused in the hepatic artery for assessment of lung shunting. If the lung shunt is substantial, the treatment dose is reduced to minimize the risk of radiation pneumonitis, which may lead to inadequate absorbed doses to tumors. The purpose of this study was to assess the accuracy of <sup>99m</sup>Tc-MAA lung shunt calculations

METHOD AND MATERIALS

Fourteen patients were treated with radioembolization using holmium-166-loaded microspheres (<sup>166</sup>Ho). These particles can be quantified with SPECT and can be used for scout dose and treatment. During preparatory angiography, <sup>99m</sup>Tc-MAA (150 MBq) was injected, followed by (planar) scintigraphy and SPECT-CT. At the day of treatment, a scout dose of <sup>166</sup>Ho-microspheres (250 MBq) was first injected, followed by SPECT-CT imaging. Subsequently, a treatment dose of <sup>166</sup>Ho-microspheres was injected and imaged with SPECT-CT. Lung shunting was calculated on <sup>99m</sup>Tc-MAA scintigraphy. Mean lung doses were calculated on quantitative SPECT images for all three procedures and also on scintigraphy for <sup>99m</sup>Tc-MAA. The activity in the lungs was converted into absorbed dose (Gy) corresponding to the net injected treatment dose. The pre-treatment estimations were compared to the lung dose after actual treatment, as measured with post-treatment SPECT.

RESULTS

No signs of radiation pneumonitis were seen in any patient during three months follow up. The median lung shunt based on <sup>99m</sup>Tc-MAA scintigraphy was 4.1% (range 2.2 ♦ 11.3%). The median lung dose after <sup>166</sup>Ho-radioembolization was 0.2 Gy (range 0 ♦ 0.7 Gy), based on quantitative SPECT. This lung dose was significantly overestimated by <sup>99m</sup>Tc-MAA scintigraphy (median difference (?) 5.1 Gy, range 1.4 ♦ 17.1 Gy, p < 0.001) and by <sup>99m</sup>Tc-MAA SPECT (? 2.3 Gy, range 0.5 ♦ 11.8 Gy, p < 0.001). The estimations on SPECT images of the <sup>166</sup>Ho-scout dose did not differ significantly from treatment (? 0.0 Gy, range -0.7 ♦ 0.3 Gy, p = 0.542).

CONCLUSION

<sup>99m</sup>Tc-MAA lung shunt calculations significantly overestimate the mean lung dose after radioembolization with <sup>166</sup>Ho microspheres. In contrast, a scout dose of <sup>166</sup>Ho-microspheres accurately predicts the mean lung dose after treatment.

CLINICAL RELEVANCE/APPLICATION

The mean absorbed dose to lung parenchyma of patients treated with <sup>166</sup>Ho radioembolization is significantly overestimated by <sup>99m</sup>Tc-MAA planar scintigraphy and SPECT-based lung dose calculations.

**VSIR61-05 • Y-90 Cxs**

**Robert J Lewandowski** MD (Presenter) \*

LEARNING OBJECTIVES

View learning objectives under main course title.

**VSIR61-06 • Trans-arterial Radioembolization (TARE) of Intermediate-advanced HCC: Does Portal Vein Thrombosis Affect Survival ?**

**Francesco Fiore** MD (Presenter) ; **Francesco Somma** MD ; **Roberto D'Angelo** MD ; **Rosa Ambrosio** MD ; **Sergio Setola** ; **Francesco Izzo** MD

PURPOSE

Our purpose is to assess and compare the survival of patients with portal vein thrombosis (PVT) and patients without PVT after a TARE using Y-90 microspheres of unresectable HCC, not responsive to other loco-regional treatments.

METHOD AND MATERIALS

Between November 2005 and February 2013, 81 TARE were performed in 74 patients (43% male; 57% female; range of age 28-84years) with unresectable HCC (size of lesions 1.1 to 5.5cm) and bilirubine values up to 2.6 mg/dl, 21 with PVT. Every patient was studied with Multislice Computed Tomography (MSCT) scans and angiography while just 12 of them underwent the embolization of the Gastro-duodenal artery, using micro-coils. In these cases, a previous study was performed with the injection of TC-99MAA through a 3F microcatheter. Proton-Pump Inhibitors (PPI) were administered to prevent gastritis and ulcers.

RESULTS

The average dose administered was 1.7GBq. After the treatment, fever and abdominal pain were found in 29 and 19 patients, respectively. No other side-effect was observed. According to the mRECIST criteria at least a partial response was found in 70% of patient three months after the procedure and in 90.5% at nine months. The mean survival of patients with PVT was similar to those without thrombosis. Moreover, a regression of PVT was registered in more than 50% of patients.

CONCLUSION

TARE using Y-90 microspheres showed to be a safe and effective technique even in patients with PVT. Among the loco-regional treatments of intermediate-advanced HCC, TARE is extremely useful in case of relapse after trans-arterial embolization (TAE) or chemoembolization (TACE) in improving the survival of these patients.

CLINICAL RELEVANCE/APPLICATION

Portal vein thrombosis does not affect survival of patients who undergo the Y-90 TARE of intermediate-advanced HCC not responsive to other loco-regional

**VSIR61-07 • Debate: HCC With Portal Vein Thrombosis**

**Charles E Ray** MD, PhD (Presenter) \* ; **Robert J Lewandowski** MD (Presenter) \*



#### LEARNING OBJECTIVES

1) Discern the impact of transcatheter intra-arterial embolotherapy in patients with hepatocellular carcinoma and portal vein thrombosis. 2) Understand the microembolic effects of radioembolization, and the potential advantages of this treatment over other intra-arterial embolotherapies. 3) Become familiar with the current literature regarding radioembolization of patients with unresectable hepatocellular carcinoma with portal vein thrombosis.

#### VSIR61-08 • Thermal Ablation Cxs

**Daniel B Brown MD (Presenter) \***

#### LEARNING OBJECTIVES

1) Techniques to avoid complications with thermal ablation. 2) How to manage complications of thermal ablation.

#### ABSTRACT

Complications are unusual with thermal ablation but can be severe. This presentation is designed to avoid complications as well as identify untoward events early after therapy to optimize management.

#### VSIR61-09 • Evaluation of Thrombotic Risk in Hepatic Vessels during Microwave Tumor Ablations: Does Size Really Matter?

**Jason Chiang BS (Presenter) ; Bridgett J Willey \* ; Alejandro Munoz Del Rio PhD ; Christopher L Brace PhD \***

#### PURPOSE

Microwave tumor ablation is a powerful tool that can more effectively overcome the  $\diamond$ heat-sink $\diamond$  effect of nearby vasculatures. Such power may also increase the risk of thrombosing larger vessels, which can have devastating consequences for a patient whose liver is already compromised. The goal of this study is to correlate the risk of vascular thrombosis with vessel size, blood velocity and proximity to heating zone during microwave ablations.

#### METHOD AND MATERIALS

Microwave antennas were placed in-vivo, 5-20 mm away from a portal vein, hepatic vein and hepatic artery in a porcine liver (n=6). Vessel sizes, flow velocities and distance from antenna were measured under Doppler and ultrasound imaging. Microwave ablations were then created at 100 W for 5 minutes. Post-ablation ultrasound was used to determine presence of thrombus in each vessel. Uni- and multivariable logistic regressions were fitted to model the relationship predictors to thrombotic events in each kind of vessel. Fitted models were compared to each other using the area under the receiver operator characteristic curves (AUC); 95% confidence intervals for AUC were also obtained.

#### RESULTS

Thrombus formation was detected in 53.3% of portal veins (8/15), 13.3% of hepatic veins (2/15) and 0.0% in hepatic arteries (0/15). The hepatic vein AUC of velocity, spacing and diameter were 0.885 [95% CI: 0.617-0.989], 0.923 [0.667-0.997] and 0.904 [0.641-0.994], respectively. Portal vein AUC of velocity, spacing and diameter were 0.509 [0.163-0.853], 0.643 [0.340-0.946] and 0.536 [0.168-0.814], respectively. Multivariate prediction models of both hepatic and portal veins did not show significant increase in AUC over their respective individual univariate models.

#### CONCLUSION

The risk of thrombosis decreased with increasing vessel velocity, size and spacing in hepatic veins. Portal veins thrombosed at a rate four times higher than hepatic veins, but our analysis was not able to discriminate which factors were most relevant. Further study is required to elucidate the physical and biochemical mechanisms behind this discrepancy in thrombotic rates.

#### CLINICAL RELEVANCE/APPLICATION

Portal veins have greater, but less predictable risk for thrombosis compared to hepatic veins in microwave tumor ablation procedures.

#### VSIR61-10 • The Effect on Renal Function Following Image Guided Radiofrequency Ablation (RFA) of Renal Tumors

**Tze M Wah MBChB, FRCR (Presenter) ; Walter Gregory PhD ; Henry C Irving MBBS ; Jon Cartledge MD ; Adrian D Joyce MD ; Peter J Selby MD, DSc**

#### PURPOSE

To analyse changes in GFR in patients who had image-guided RFA of their renal tumors and to correlate the percentage GFR change (% GFR change) with tumor size, polar position, tumor treatment location, the total size of the tumor treated per ablation session, number of tumors treated, and solitary kidney status.

#### METHOD AND MATERIALS

From June 2004-2012, a total of 165 patients (109 men, 56 women; mean age 67.7 years) had image-guided RFA of 200 renal tumors with size ranging from 1-5.6cm (mean= 2.9cm). The position of the renal tumors was: upper (n=63), middle (n=86) and lower (n=51). The tumor location was: exophytic (n=43), mixed (n=100), parenchymal (n=41) and central (n=16). All patients had renal function measured immediately before and at 24 hours post-RFA. Multivariate logistic regression analysis was performed to determine any association between % GFR change with the tumor size, polar position (upper, middle and lower pole of the kidney), tumor treatment location (exophytic, mixed, parenchymal and central), the total size of the tumor treated per ablation session, number of tumors treated and solitary kidney status.

#### RESULTS

The mean GFR pre- and post-renal RFA were: 54.7 ml/min/1.73m<sup>2</sup> (+/- SD 18.2 ml/min/1.73m<sup>2</sup>) vs. 52.7 ml/min/1.73m<sup>2</sup> (+/- SD 18.5 ml/min/1.73m<sup>2</sup>). There is a significant difference between the pre- and post-RFA GFR measurements (p 25% decrease in GFR) whilst in the majority (98%) of the patients renal function was preserved. The mean % change of GFR pre- and post-RFA was  $\diamond$  3.1% (+/- SD 15.2%). However, using multivariate logistic regression analysis there is no association between the % of GFR change with tumor size, polar position, tumor treatment location, the total size of the tumor treated per ablation session, number of tumors treated and solitary kidney status.

#### CONCLUSION

Preservation of the renal function can be achieved following image-guided RFA of renal tumors and the percentage of GFR change was not influenced by tumor factors or solitary kidney status.

#### CLINICAL RELEVANCE/APPLICATION

Any change in renal function following image-guided renal RFA is not influenced by tumors factors (size, polar position, treatment location, number of tumors treated) or solitary kidney status.

#### VSIR61-11 • Combination Therapy Cxs

**Thuong G Van Ha MD (Presenter) \***

#### LEARNING OBJECTIVES

View learning objective under main course title.

#### ABSTRACT

Combination therapy utilizing both transarterial chemoembolization and thermal ablation will be discussed with an emphasis on complications. Different techniques of TACE will be shown, in combination with either radiofrequency ablation or microwave ablation. Management of complications will also be discussed.

## **VSIR61-12 • Debate: Interventional Oncology - A Distinct Specialty/Interventional Oncology - We Are Radiologists, Not Oncologists**

**Daniel B Brown** MD (Presenter) \* ; **Charles E Ray** MD, PhD (Presenter) \*

### LEARNING OBJECTIVES

View learning objectives under main course title.

## **VSIR61-13 • Literature Review: The Most Important IO Papers from 2012-13**

**Charles E Ray** MD, PhD (Presenter) \*

### LEARNING OBJECTIVES

View learning objectives under main course title.

## **VSIR61-14 • Panel Discussion: Unknown Case Presentation**

### LEARNING OBJECTIVES

View learning objectives under main course title.

## **VSIR61-15 • Wrap Up and Discussion**

### LEARNING OBJECTIVES

View learning objectives under main course title.

## **Musculoskeletal Radiology Series: Elbow, Hand and Wrist Imaging**

**Friday, 08:30 AM - 12:00 PM • N228**

[Back to Top](#)

**MK**

**VSMK61 • AMA PRA Category 1 Credit™:3.25 • ARRT Category A+ Credit:3.5**

### **Moderator**

**Bruce B Forster**, MD \*

### **Moderator**

**Mark D Murphey**, MD

## **VSMK61-01 • Sports Related Injuries of the Elbow**

**Bruce B Forster** MD (Presenter) \*

### LEARNING OBJECTIVES

1) Demonstrate an understanding of the technical and procedure-related considerations in MR imaging of the elbow. 2) Identify the normal anatomic structures and variants within the four compartments of the elbow. 3) Diagnose common sports injuries of the elbow, using this compartmental approach.

### ABSTRACT

## **VSMK61-02 • Accuracy of 3 Tesla MR Arthrography versus Conventional 3 Tesla MR Imaging of the Elbow as Compared with Arthroscopy**

**Thomas H Magee** MD (Presenter)

### PURPOSE

MR arthrography of the elbow has been found to be useful in the diagnosis of full versus partial thickness tears of the collateral ligaments. MR arthrography is also useful for characterization of chondral defects. We assess the accuracy of 3 Tesla MR arthrography of the elbow versus conventional 3 Tesla MR imaging of the elbow as compared with arthroscopy.

### METHOD AND MATERIALS

43 consecutive conventional elbow MR and MR arthrography exams performed on the same patients who went on to arthroscopy were reviewed retrospectively by consensus reading of two musculoskeletal radiologists. Full or partial thickness tears of the collateral ligaments, full or partial thickness tears of the extensor and flexor tendons, chondral defects and loose bodies in the joint space were assessed.

### RESULTS

In thirty one patients, the diagnoses made on MR and MR arthrogram exams were the same. In seven patients MR arthrogram exams demonstrated additional findings that were not clearly demonstrated on conventional MR exams. There were three full thickness extensor tendon tears, three radial collateral ligament tears and one ulnar collateral ligament tear seen on MR arthrography exam that were not well seen on conventional MR exam. In five patients MR arthrogram demonstrated ligaments and tendons to be intact that appeared torn on conventional MR exam. There were three ulnar collateral ligaments and two common flexor tendons demonstrated to be intact on MR arthrography exam that appeared torn on conventional MR exam. All MR arthrography findings were confirmed at arthroscopy.

### CONCLUSION

MR arthrography of the elbow is more accurate than conventional MR imaging of the elbow at three tesla. In seven cases MR arthrography demonstrated tendons and ligaments to be torn that appeared intact on conventional MR exam. In five cases MR arthrography demonstrated intact tendons and ligaments that appeared torn on conventional MR exam. These five cases are most likely due to the tears healing with fibrous tissue allowing the tendon and ligament tissues to coapt.

### CLINICAL RELEVANCE/APPLICATION

MR arthrography is more accurate in detection of intact or torn tendons and ligaments than conventional MR imaging of the elbow at three tesla. This is useful in pre surgical planning.

## **VSMK61-03 • Entrapment Neuropathies of the Upper Extremity**

**Ali M Naraghi** (Presenter)

### LEARNING OBJECTIVES

1) Identify the common sites of nerve entrapment in the upper extremity. 2) Describe the normal peripheral nerve anatomy and muscle innervation in the upper extremity with an emphasis on sites of compression. 3) Recognize the imaging features peripheral nerve entrapment in the upper extremity.

### ABSTRACT

## VSMK61-04 • T2 Mapping of the Median Nerve in the Wrist Joints: Preliminary Study in Patients with Carpal Tunnel Syndrome and Healthy Volunteers

Ji Eun Lee MD (Presenter) ; Jang Gyu Cha MD ; Jong Kyu Han MD, PhD ; Soo Bin Im ; Sung Byung Kim

### PURPOSE

To perform a prospective quantitative analysis of median nerve T2 values and cross-sectional area (CSA) in patients with carpal tunnel syndrome (CTS) and in asymptomatic volunteers.

### METHOD AND MATERIALS

Twelve CTS patients with positive nerve conduction results and 12 healthy volunteers (controls) were enrolled and underwent axial T2 mapping of the wrist joints. Median nerve T2 values and CSAs at the distal radioulnar joint, pisiform, and hook of hamate levels were compared between the groups.

### RESULTS

The T2 values at the proximal and distal carpal tunnel were higher in the CTS patients than in the controls ( $p < 0.05$ ). The T2 values at the distal radioulnar joint did not differ between the groups ( $p = 0.99$ ). The CSAs of the median nerve at all levels of the carpal tunnel were significantly larger in the CTS patients than in the controls ( $p < 0.05$ ).

### CONCLUSION

It is feasible to use T2 mapping to measure an increase of the median nerve T2 value in CTS patients. Quantitative measurements of T2 values can complement measurements of the median nerve CSA in the evaluation of CTS.

### CLINICAL RELEVANCE/APPLICATION

T2 mapping can be useful for measuring an increase in the median nerve T2 values. Quantitative measurements of T2 values can complement measurements of the median nerve CSA in the evaluation of CTS.

## VSMK61-05 • Comparison of Various 3D and 2D MR Imaging Sequences of the Wrist at 3 Tesla

Christoph Rehnitz MD (Presenter) ; Bastian Klaan ; Falko Stillfried ; Erick Amarteifio MD ; Hans-Ulrich Kauczor MD \* ; Marc-Andre Weber MD \*

### PURPOSE

To quantitatively and qualitatively compare both image quality and diagnostic performance of 2D and 3D sequences for dedicated wrist imaging.

### METHOD AND MATERIALS

16 healthy volunteers (mean age, 26.4 years) and 18 patients (mean age, 36.2 years) with wrist pain were examined using an 8-channel wrist-coil at 3 Tesla MRI. The imaging protocol consisted of 2D-proton-density fat-saturated (PDFs), isotropic 3D MEDIC, 3D-TrueFISP and 3D-PDFs-SPACE sequences. Signal-to-noise-ratios (SNR) and contrast-to-noise-ratios (CNR) of cartilage/bone/muscle/fluid and mean overall SNR/CNR were calculated using region-of-interest analysis. Qualitative analysis included overall image quality (OIQ), visibility of important structures and degree of artifacts rated on a five-point scale (0-4). ANOVA and adjusted Wilcoxon-signed-rank tests were applied. The study was approved by the institutional review board and all patients gave informed consent prior to inclusion.

### RESULTS

Mean overall SNR/CNR for 2dPDFs; 3D-PDFs-SPACE; 3D-TrueFISP; 3D-MEDIC was 96/73; 43/28; 61/53; 77/45. SNR and CNR were higher ( $p$

### CONCLUSION

Standard 2D-PDFs sequence provides high SNR/CNR, image quality and robustness when compared to 3D sequences. Isotropic 3D-TrueFISP (cartilage) and 3D-MEDIC (ligaments/TFCC) exhibit additional advantages, while 3D-PDFs-SPACE is currently not advantageous.

### CLINICAL RELEVANCE/APPLICATION

When imaging the wrist at 3 Tesla, the sequence protocol should include 2D-PDFs. An additional 3D-TrueFISP sequence can be recommended for assessing cartilage and a 3D-MEDIC for ligaments and TFCC.

## VSMK61-06 • Magnetic Resonance Microscopy of the Triangular Fibrocartilage Complex at 11.7T

Paul A DiCamillo MD, PhD (Presenter) ; Sheronda Statum ; Christine B Chung MD ; Graeme M Bydder MBChB \*

### PURPOSE

Anatomic studies of the Triangular Fibrocartilage Complex (TFCC) have been performed on clinical systems at field strengths up to 7T. In our study, we assessed the use of an 11.7T small bore system with high performance gradients and micro-array coils for detailed imaging of the TFCC.

### METHOD AND MATERIALS

Human wrist samples were collected per institutional policy, and imaged on an 11.7T Bruker BioSpec 117/16USR system (Bruker BioSpin, Billerica, MA) fitted with a 750 mT/m gradient system, using solenoidal and four element semi-circular array coils. Both gradient and spin echo sequences were used (FLASH: 90-120um<sup>2</sup> isotropic resolution, TE 6ms, TR 25ms, fat sat, NEX 9-25, 4-6 hour scans; Multislice Spin Echo: 80x80x400um resolution, TE 7-14ms, TR 5000ms, 2 echoes, fat sat, NEX 5-15, 4-6 hour scans).

### RESULTS

Detailed visualization of the TFCC was achieved at a spatial resolution well over 10 times greater than previously reported. Instead of the low signal, low contrast appearance seen in the TFCC with clinical T2 weighted images, with our acquisitions parameters and high performance system, the TFCC tissues displayed relatively high signal. Fiber structure in the upper and lower laminae, magic angle effects, entheses and the lamella layer of the disc were observed.

### CONCLUSION

Unprecedented spatial resolution and contrast were achieved, with clear demonstration of detail in structures not previously not well visualized or seen at all. These results are likely to help in the recognition of injury and disease of the TFCC as stronger field strength systems become clinically available.

### CLINICAL RELEVANCE/APPLICATION

High resolution 11.7T MR images of the TFCC were generated. These results may indicate what will be achievable on higher field clinical systems.

## VSMK61-07 • Sports Related Injuries of the Wrist

Catherine N Petchprapa MD (Presenter)

### LEARNING OBJECTIVES

1) Review multiple common injuries of the wrist, as demonstrated on multiple imaging modalities.

## VSMK61-08 • Common Tumors in the Hand and Wrist

Mark D Murphy MD (Presenter)

## LEARNING OBJECTIVES

1) Identify common tumors that affect the hand/wrist including giant cell tumor of tendon sheath, ganglion, enchondroma and synovial sarcoma. 2) Recognize the imaging appearance and spectrum of these common tumors of the hand/wrist. 3) Understand the pathologic basis of the imaging appearances that may allow differentiation of these lesions.

## VSMK61-09 • 11.7T Magnetic Resonance Microscopy of the Pulleys and Plates of the Fingers and Thumb

**Paul A DiCamillo MD, PhD (Presenter) ; Sheronda Statum ; Christine B Chung MD ; Graeme M Bydder MBChB \***

### PURPOSE

Excellent anatomical studies on clinical systems have been done to demonstrate the detail of the digital pulleys and plates at fields up to 7T. In our study, using an 11.7T system with high-performance gradients and micro-array coils, we attempted to visualize details of these structures which have previously been refractory to MR imaging.

### METHOD AND MATERIALS

Human fingers and thumbs were collected per institutional policy, firmly immobilized, and placed into the bore of an 11.7T Bruker BioSpec 117/16USR system (Bruker BioSpin, Billerica, MA) fitted with a 750 mT/m gradient system. Ten fields of view (**finger**: proximal, middle, distal phalanx, PIP, DIP and MCP; **thumb**: proximal, distal phalanx, IP and MCP) were independently imaged with both gradient and spin echo sequences (FLASH: 90-120um<sup>3</sup> isotropic resolution, TE 6ms, TR 25ms, fat sat, NEX 9-25, 4-6 hour scans; Multislice Spin Echo: 35x35x250um to 60x60x500um resolution, TE 7-14ms, TR 5000ms, 2 echoes, fat sat, NEX 5-15, 4-6 hour scans).

### RESULTS

Detailed visualization of fibers in tendons, ligaments, pulleys, plates, and entheses of the fingers and thumb was achieved. A series of structures that correlate with anatomic descriptions of entities which have not previously been captured in detail in imaging studies was visualized. A partial list includes the cruciate pulleys of the finger; finger pulleys A<sub>1</sub> and A<sub>5</sub>; thumb pulleys A<sub>1</sub>, A<sub>V</sub>, A<sub>2</sub>; the oblique thumb pulley; and the fibrous structure of the palmar plates.

### CONCLUSION

Unprecedented spatial resolution and contrast was achieved, with well over 10 times greater spatial resolution than previously reported. This allowed clear demonstration of the fiber direction in structures, as well as production of the first MR images of structures such as the cruciate pulleys of the finger. A high performance MR system together with coil repositioning for each of the 10 target locations was instrumental in meeting our resolution and contrast goals. These results are likely to help in the recognition of injury and disease of the pulleys and plates as stronger field strengths become clinically available.

### CLINICAL RELEVANCE/APPLICATION

High resolution 11.7T MR images of the pulleys and plates of the finger were generated. These may facilitate the interpretation of normal anatomy as higher field clinical systems become available.

## VSMK61-10 • MR Findings in Avulsion Injuries at the Extensor Carpi Radialis Brevis Insertion and the Os Styloideum: A Case Series of Lesions in Hockey Players and Other 'Stick Swinging' Athletes

**Pranshu Sharma MD (Presenter) ; Adam C Zoga MD ; William B Morrison MD \* ; Diane M Deely MD ; Randall W Culp MD**

### PURPOSE

To detail initial and follow-up imaging findings in athletes with avulsion injuries at the insertion of the Extensor Carpi Radialis Brevis (ECRB) tendon, and its relation to the os styloideum and carpal boss, with operative and 'return-to-play' correlation.

### METHOD AND MATERIALS

A database of wrist MR exams over 18 months was searched for athletes with avulsion injuries at the dorsal wrist in the region of the extensor carpi radialis brevis (ECRB) insertion. 6 subjects were identified and demographics, athletic activity, and trauma vs. overuse were documented. The initial MR was reviewed by two MSK radiologists in consensus and the presence of an os styloideum or carpal boss, any synchondrosis or synostosis between the os and the base of third metacarpal were recorded. Bone marrow edema and displaced or nondisplaced fractures as well as fracture extension proximal or distal were noted. The insertion site of the ECRB was observed as directly on the os, directly on the base of third metacarpal, or both. MR findings and surgical findings when applicable were reviewed with a single hand surgeon. Any follow-up imaging to monitor healing was reviewed, and the interval to 'return-to-play' was documented.

### RESULTS

3 were pro hockey players with forceful extension injuries. 1 was a collegiate golfer and the other 2 sustained falls on flexed wrists. 6 of 6 had os styloidea with bone marrow edema at the os. The ECRB inserted on the metacarpal base in 2, on the os in 2, and on both in 2. 3/6 had displacement of the os with a fracture extending to the metacarpal base at initial MR. No high grade tendon tear was observed. 3 went to surgery for os resection and cast immobilization and 1 for screw/plate fixation of the fracture and the os. The fixation subject was monitored for healing with CT and was able to return to hockey in 4 weeks, while 2 hockey players post os resection missed the remainder of the season but returned the following Spring (9 and 11 weeks).

### CONCLUSION

There is an anatomical and injury spectrum in athletes with avulsion lesions at the ECRB insertion. The ECRB can insert on the os styloideum, the base of the metacarpal, or both. These injuries can be encountered in athletic activities involving repetitive wrist extension against resistance while holding a stick, such as hockey and golf.

### CLINICAL RELEVANCE/APPLICATION

Location of the insertion of the ECRB and any fusion of the os to the metacarpal base should be noted to optimize treatment.

## VSMK61-11 • Eponyms to Know in Hand and Wrist Imaging

**Wilfred C. G Peh MD (Presenter)**

### LEARNING OBJECTIVES

1) Review the imaging appearance of a variety of hand and wrist injuries that are named after physicians.

## VSMK61-12 • Flexor Carpi Radialis Tendinopathy and its Association with Scapho-trapezio-trapezoid and First Carpometacarpal Osteoarthritis

**Waseem K Khan MD (Presenter) ; Andrew R Palisch MD ; Suzanne S Long MD ; Adam C Zoga MD ; William B Morrison MD \***

### PURPOSE

We sought to establish a potential association between flexor carpi radialis (FCR) tendinosis and/or tears and osteoarthritis of either the scapho-trapezio-trapezoid (STT) or first carpometacarpal (CMC) joints, as identified by magnetic resonance imaging (MRI).

### METHOD AND MATERIALS

A retrospective analysis was performed by searching a database from a single institution for MRI exams of the wrist performed over a 15 month period with reports including the term **flexor carpi radialis**. Exams with reports describing the tendon as 'normal' were excluded. Two MSK radiologists evaluated images and confirmed the presence of FCR tendinosis and/or FCR tears. The STT and first CMC joints were then evaluated for evidence of osteoarthritis at MR including eburnation, subchondral cysts/marrow edema, osteophytes and joint space narrowing. FCR tendinosis/tears were then correlated with findings of STT and 1st CMC osteoarthritis.

## RESULTS

There were 26 wrists with FCR tendinosis and/or tear. M/F= 10/16, with a mean age of 57.8 years (14  $\diamond$  80 years). The majority (24/26, 92%) had either STT (20/26, 77%) and/or first CMC (21/26, 81%) osteoarthritis. The two patients with no appreciable STT or first CMC osteoarthritis demonstrated only mild FCR tendinosis at MRI. 14/26 (54%) subjects had either partial (11) or complete (3) FCR tendon tears. 12/14 patients (86%) had tears positioned adjacent to the STT joint, including all three complete tears. The other 2 patients (14%) had tears located adjacent to the first CMC joint. In all FCR tears, volar spurs were noted extending from the affected joint and appeared to impinge upon the FCR.

## CONCLUSION

This retrospective series suggests that there may be an association between FCR tendinosis or tear and osteoarthritis at the scapho-trapezio-trapezoid and first carpal-metacarpal joints. Further, partial or complete FCR tendon tears appear to be more often positioned near an STT joint with osteoarthritis. Potential etiologies of this association include osseous productive changes at the STT and 1st CMC joints impinging the FCR during dynamic activities.

## CLINICAL RELEVANCE/APPLICATION

FCR tendinosis and tearing should be suspected and observed at MR if there are findings of osteoarthritis at either the STT or first CMC joints associated with volar/radial sided pain.

## VSMK61-13 • Arthritides-What's Hot in the Rheumatology Literature

**Eric Y Chang MD** (Presenter)

### LEARNING OBJECTIVES

1) Discuss the roles of the radiologist in diagnosis and management of arthropathies. 2) Identify the various categories of disease modifying therapies (DMOADs and DMARDs). 3) Describe the imaging findings of rheumatoid arthritis and spondyloarthritis based on current literature.

## Vascular Imaging Series: MR Angiography-Principles and Technique Optimization

Friday, 08:30 AM - 12:00 PM • E352



[Back to Top](#)

**VSVA61** • AMA PRA Category 1 Credit <sup>TM</sup>:3.25 • ARRT Category A+ Credit:4

## VSVA61-01 • Contrast-enhanced and Time-resolved MRA

**Stefan G Ruehm MD** (Presenter) \*

### LEARNING OBJECTIVES

1) Understand the general principles of contrast-enhanced and time-resolved MR Angiography. 2) Be familiar with sample clinical applications for time-resolved MR Angiography in several vascular beds. 3) Be aware of the major caveats in contrast enhanced MR Angiography at 1.5T and 3.0T and how to avoid them.

## VSVA61-02 • Whole Body Cardiovascular Magnetic Resonance Imaging in the Detection of Occult Disease in Diabetes Mellitus

**Graeme Houston MD, FRCR \*** ; **Jonathan Weir-McCall MBBCh, FRCR** (Presenter) ; **Suzanne L Duce PhD** ; **Shona Matthew BSc, PhD \*** ; **Stephen Gandy** ; **Helen Colhoun** ; **Deirdre Cassidy** ; **Gill Reekie** ; **Jil J Belch** ; **Patricia Martin**

### PURPOSE

The IMI-SUMMIT MRI study assessed whole body cardiovascular MR (WBCVMR) to provide surrogate markers of macrovascular disease in patients with diabetes mellitus. WBCVMR combines whole body contrast enhanced magnetic resonance angiography (WBCE-MRA) and cardiac MR(CMR) in a single examination. We compared WBCVMR in type 2 diabetic and non-diabetic patients, with and without symptomatic cardiovascular disease(CVD).

### METHOD AND MATERIALS

156 subjects were divided into 4 groups: diabetics with (group 1, n=31) or without (group 2, n=55) CVD, and non-diabetics with (group 3, n=28) or without (group 4, n=29) CVD. WBCVMR was performed on 3T MRI (Siemens Trio, Erlangen, DE). WBCE-MRA was performed from skull vertex to feet following intravenous gadoterate meglumine (Dotarem, Guerbet, FR). The subtracted data were divided into 31 anatomical arterial segments. Each segment was scored according to degree of luminal narrowing: 0=normal, 1=

### RESULTS

143 datasets were included, of which 87(60%) were male (13 excluded due to incomplete scan/inadequate image quality),. The mean age was 63.9 $\pm$ 8.1 years. Mean WBAS were 0.41 $\pm$ 0.45 (group 1), 0.17 $\pm$ 0.17 (group 2), 0.49 $\pm$ 0.4 (group 3), and 0.15 $\pm$ 0.18 (group 4). Mean LVM(g) were: 61.6  $\pm$ 9.7 (group 1), 55.6 $\pm$ 10.5 (group 2), 60.4 $\pm$ 10.6 (group 3), and 52.6 $\pm$ 8.7 (group 4). WBAS correlated with LVM (r=0.41; p

### CONCLUSION

WBCVMR offers a robust investigation for detecting and quantitating whole body atheroma burden. Extensive arterial disease and silent myocardial scarring can be visualised in asymptomatic diabetic patients.

### CLINICAL RELEVANCE/APPLICATION

Type 2 diabetics have an elevated risk of cardiovascular events which can occur in apparently healthy patients. Screening with WBCVMR may identify those at increased risk of future events.

## VSVA61-03 • Feasibility Study of MR-tricks Sequence in Evaluation of the Dorsalis Pedis Artery and the First Dorsal Metatarsal Artery

**Bo Sun** (Presenter) ; **Yue Dong** ; **Dianxiu Ning** ; **Qingwei Song BS, BEng** ; **Meiyu Sun**

### PURPOSE

To study the feasibility of MR angiography of the dorsalis pedis artery and the first dorsal metatarsal artery ( FDMA) by three-dimensional time-resolved imaging of contrast kinetics (TRICKS) sequences.

### METHOD AND MATERIALS

43 cases with suspected or known soft tissue diseases of the ankle and foot were examined retrospectively by conventional MR sequences and TRICKS sequence on GE signa 1.5T HD echospeed MRI . MIP reconstruction was done to evaluate the image quality of arterial branches on ADW4.4 workstation and the evaluated criteria was divided into 4 grades according to the visualization of dorsalis pedis artery( grade 1 $\diamond$ 2), FDMA and toe web network(grade3 $\diamond$ 4). FDMA was dissected and categorized according to its location(superficial, intramuscular, inframuscular, absent), diameter[large( > 1.5mm ) , medium( 1.0 $\diamond$ 1.5mm ) , and small( second toe =Dfirst toe),main trunk type(Dsecond toe>Dfirst toe),fine small branch(Dsecond toe first toe)]

### RESULTS

8 cases(18.6%,8/43)in grade 4, 22(51.16%,22/43)in grade 3,8(18.6%,8/43) in grade 2 and 5(11.62%,5/43) in grade 1. In the grade 1 group, the dorsalis pedis arteries of 2 cases were absent and images of the other 3 cases were not clear because of severe venous contamination.

The TRICKS images of 38 cases(arterial scales=2 point) showed location and diameter of FDMA ,and the TRICKS images of 30

cases(arterial scales=3 point) showed branching pattern at the toe web of FDMA:( 1)Location:superficial (8), intramuscular(22 cases), inframuscular (8 cases), absent(0 cases);(2)Diameter: large(2 cases) , medium(25 cases) , and small(11 cases);(3)Branching pattern at the toe web:ramifying type(11 cases),main trunk type(5 cases),fine small branch(14 cases).

#### CONCLUSION

MR angiography of the dorsalis pedis artery and FDMA was achievable with MR TRICKS sequences, and it was useful for clinical evaluation of FDMA.

#### CLINICAL RELEVANCE/APPLICATION

MR angiography of the dorsalis pedis artery and FDMA with MR TRICKS sequences is available in preoperative evaluation for rebuilding thumb and finger by dissociating toe transplant.

### **VSVA61-04 • Renal MRA at 7T: How Much Gadolinium Do We Need?**

**Lale Umutlu MD (Presenter) \*** ; **Karsten J Beiderwellen MD** ; **Michael Forsting MD** ; **Mark E Ladd PhD** ; **Oliver Kraff MSc** ; **Thomas C Lauenstein MD**

#### PURPOSE

Renal impairment displays a relative contraindication to the application of Gadolinium- based contrast-agents. Hence, contrast dose reduction has become an important issue in the clinical setting. The aim of this trial was to determine whether contrast agent (CA) dose reduction to one-half and one-quarter of the standardized dosage allows for preserved image quality of renal MR angiography at 7T.

#### METHOD AND MATERIALS

12 healthy subjects underwent renal MR angiographic examinations on a 7T MR system (Magnetom 7T), utilizing a custom-built 8-channel RF body coil. Dynamic 3D FLASH data sets were obtained pre contrast and in arterial phase after the application of contrast agent. Examinations were performed at three different time points for injection of three dosages of CA (Gadobutrol, Bayer Healthcare): (1) 0.1 mmol/kg body weight (BW), (2) 0.05 mmol/kg BW and (3) 0.025 mmol/kg BW. Contrast ratios (CR) were measured pre and post contrast in the aorta and both renal arteries in correlation to adjacent psoas major muscle. Qualitative analysis with regard to delineation of the pre-contrast and post-contrast renal arterial vasculature was performed by two radiologists using a five-point-scale (5=excellent to 1= non diagnostic).

#### RESULTS

Non-enhanced T1w MRI provided an inherently high signal intensity of vasculature, yielding a good overall pre-contrast arterial delineation (mean 3.65). The application of contrast agent showed improved vessel delineation in subjective ratings of qualitative analysis for all three dosages, yielding comparable results with only minor improvement associated to increased dosage (mean aorta: 0.025Gd 4.4; mean0.05Gd 4.6; mean0.1Gd mean 4.80). Accordingly, quantitative analysis of contrast ratios showed minor increase of mean values with increasing Gadolinium dosage (mean right renal artery: 0.025Gd 0.36; mean0.05Gd 0.38; mean0.1Gd mean 0.42).

#### CONCLUSION

Our results demonstrate the successful facilitation of a significant dose reduction to one-quarter of the standardized dosage, while maintaining high image quality.

#### CLINICAL RELEVANCE/APPLICATION

The facilitation of a significant dose reduction to one-quarter while maintaining high image quality, may be of high diagnostic value for MRA examinations in patients with renal impairment.

### **VSVA61-05 • MR Contrast Agents for Vascular Imaging**

**Tim Leiner MD, PhD (Presenter) \***

#### LEARNING OBJECTIVES

1) To understand the different classes of contrast agents available for vascular imaging as well as their strengths and weaknesses. 2) To understand both acute and delayed safety concerns associated with administration of MR contrast agents for vascular imaging. 3) To understand proper contrast agent dosing for vascular MR imaging. 4) To understand basic principles underlying successful contrast injection.

#### ABSTRACT

### **VSVA61-06 • Gadofosveset-enhanced MR Venography of the Lower Extremities for Evaluation of Venous Reflux Disease: Feasibility and Comparison of Perforator Vein Imaging with Duplex Ultrasound**

**Andrew R Lewis MD (Presenter) ; Daniele Marin MD ; Holly L Nichols BS ; Daniel Geersen ; Cynthia K Shortell MD ; Charles Y Kim MD \***

#### PURPOSE

Duplex ultrasound (U/S) is the gold standard for imaging of venous reflux disease. CT and direct MR venography (MRV) have shown promising results, but are limited in the degree and extent of superficial vein opacification. Gadofosveset, a blood-pool agent, is uniquely well suited for venous imaging. The purpose of this study is to assess the feasibility of MRV of the deep and superficial venous system and to determine its accuracy in detection of perforator veins.

#### METHOD AND MATERIALS

Retrospective review of our imaging database from 9/2010 to 9/2012 yielded 58 patients (40 females, mean age 54) who underwent MRV of the abdomen, pelvis, and lower extremities as well as dedicated U/S evaluation of venous reflux disease of one or both legs. Axial MRV images were acquired during the equilibrium phase, approximately 5 minutes after IV gadofosveset injection. The lower extremity deep, superficial, and perforator veins were divided into 11 segments for evaluation. Two radiologists independently rated the visualization score of each venous segment on a scale of 1-4 with 4 being highest. Signal and contrast-to-noise ratios were calculated for the venous segments. The detection of enlarged perforator veins was assessed and compared to sonography.

#### RESULTS

Analysis was performed on 80 legs that underwent both MRV and U/S. The mean visualization scores for all analyzed venous segments were excellent (3.8-3.9 on a scale of 1-4). The SNR/CNR values were 280/165 for the femoral vein, 230/144 for the above-knee GSV, 394/237 for the below-knee GSV, 303/177 for the small saphenous vein, and 385/240 for superficial varices. 100% of pathologic perforator veins identified on dedicated U/S were detected on MRV. Additional occult enlarged perforator veins were identified on MRV measuring up to 6mm in diameter.

#### CONCLUSION

MRV with gadofosveset allowed excellent visualization of varices, superficial, and perforator veins of the legs with a high SNR and CNR that was not previously possible with other contrast agents. The exceptional sensitivity for detection of perforator veins may enable improved treatment of venous reflux disease. Additional studies are warranted to correlate MRV findings with disease characterization and treatment outcomes.

#### CLINICAL RELEVANCE/APPLICATION

The excellent imaging quality of the entire venous system of the lower extremities with gadofosveset-enhanced MR venography may enable a new system for evaluation of venous reflux disease.

### **VSVA61-07 • MRA at 3T in Peripheral Arterial Occlusive Disease: Comparison of Gadoterate Meglumine - to Gadobutrol-MRA Using DSA as a Standard of Reference: A Randomized European Multicenter Trial**

**Christian Loewe MD (Presenter) \* ; Javier Arnaiz Garcia MD ; Denis Krause MD ; Luis Marti-Bonmati MD, PhD ; Manuela Aschauer MD ; Armando Tartaro MD ; Massimo Lombardi MD \* ; Marta Burrel MD, PhD ; Reynald Izzillo ; Michael M Lell MD \***

#### PURPOSE

To assess the diagnostic value of two contrast agents in CE-MRA at 3T in peripheral arterial occlusive disease (PAOD).

#### METHOD AND MATERIALS

189 patients were included in this double-blind trial. Patients randomly underwent peripheral CE-MRA with 0.1mmol/kg of either gadoterate meglumine (Dotarem) or gadobutrol (Gadavist). The primary endpoint was degree of agreement to DSA in stenosis detection and grading of both CE-MRA examinations. A non-inferiority analysis was performed based on two independent centralized readings. Secondary endpoints were specificity, sensitivity, positive/negative predictive values, diagnostic confidence, stenosis length, vessel diameter, signal-to-noise ratio and contrast-to-noise ratio. Safety and treatment recommendation were also recorded.

#### RESULTS

The non-inferiority was demonstrated for the primary endpoint. The sensitivity in the detection of significant stenosis for Reader 1 was 69.9% in gadoterate meglumine group compared to 71.0% in gadobutrol group ( $p=0.72$ ), whereas the specificities were 85.0% and 85.2% ( $p=0.84$ ), respectively. For Reader 2, sensitivities were 61.5% and 62.0% ( $p=0.77$ ) and specificities were 91.4% and 91.2% ( $p=0.51$ ). No difference in SNR and CNR was found between both groups ( $p = 0.72$  and  $p=0.73$ ), respectively as well as regarding the other secondary endpoints. There were no serious adverse events.

#### CONCLUSION

Contrast media with higher T1 relaxivity have been proposed to be advantageous as far as efficacy is concerned. However, the present study demonstrated the feasibility of PAOD evaluation at 3T and the lack of superiority of gadobutrol over gadoterate meglumine in terms of diagnostic accuracy despite the different Gd-concentrations and T1 relaxivities exhibited by the two contrast agents.

#### CLINICAL RELEVANCE/APPLICATION

Our study has demonstrated that there is no significant difference in terms of diagnostic accuracy when comparing Gd-DOTA-enhanced MRA and gadobutrol-enhanced MRA in an equimolar manner..

### **VSVA61-08 • Non-contrast MRA: TOF and SSFP Based Techniques**

**James C Carr MD (Presenter) \***

#### LEARNING OBJECTIVES

1) Understand the technical issues underlying non contrast MRA based on TOF and SSFP. 2) Become familiar indications and guidelines for using non contrast MRA. 3) Illustrate applicability of non contrast MRA in a variety of relevant clinical scenarios.

### **VSVA61-09 • Comparison of Non-contrast Enhanced SSFP MRA with Gadolinium Enhanced MRA in the Evaluation of the Post-operative Ascending Aorta**

**Emily Pang MD (Presenter) ; Gregory P King MD ; Simin Jeddian MD ; Anna E Zavodni MD, MPH**

#### PURPOSE

The objective of this study was to evaluate the comparability of non-contrast SSFP and gadolinium enhanced MRA sequences in the quantitative and qualitative assessment of the post-operative ascending aorta.

#### METHOD AND MATERIALS

After obtaining Research Ethics Board approval, we conducted a single center retrospective review of the 59 consecutive patients sent for MRI follow-up post ascending aortic replacement surgery between 2007 and 2012. Our analysis included 51 patients (mean age 67 +/- 3 years) with both non-contrast SSFP and gadolinium enhanced MRA sequences (8 patients were excluded due to not having one or both sequences performed). The images were independently evaluated by two cardiovascular fellowship trained radiologists with at least 2 years of experience, who measured the diameter of the thoracic aorta at several points including the root, ascending aorta, arch and descending aorta, as well as assessed for qualitative abnormalities. The datasets were compared using paired T-test, Bland-Altman, and kappa coefficient analysis (statistical significance was determined using a Bonferroni correction for multiple comparisons). Intra and inter-observer variability was also determined.

#### RESULTS

There was no statistically significant difference in measurements between non-contrast SSFP and gadolinium sequences, with the exception of the aortic annulus in patients who did not have valve replacement ( $p < 0.001$ ). We postulate that this finding was because the 3D gadolinium sequences allowed for measurements of the normally ovoid annulus in more than one dimension. Kappa analysis also demonstrated good agreement with regards to the quantitative observations. Inter and intra-observer variability was excellent (ICC >0.8).

#### CONCLUSION

Our results suggest that using an unenhanced SSFP MRA sequence is comparable to gadolinium enhanced MRA in the quantitative and qualitative evaluation of the post-operative ascending aorta. Adequate and accurate information is obtained from the non-contrast SSFP sequence such that intravenous gadolinium may be rendered unnecessary for surgical follow-up imaging, reducing the risk and inconvenience to the patient, as well as health care costs.

#### CLINICAL RELEVANCE/APPLICATION

Using unenhanced SSFP MRA may be sufficient in the post-operative MR imaging follow up of ascending aorta replacements, omitting the risks and costs associated with IV gadolinium administration.

### **VSVA61-10 • Performance of Non-enhanced ECG-gated Quiescent-interval Single Shot MRA (QISS-MRA) at 3 Tesla. A Comparison with Contrast-enhanced MRA and DSA**

**Jan Hansmann MD (Presenter) ; John N Morelli MD ; Henrik J Michaely MD \* ; Thomas Riestler MD ; Johannes Budjan MD ; Stefan O Schoenberg MD, PhD \* ; Ulrike I Attenberger MD \***

#### PURPOSE

To evaluate the diagnostic accuracy of a non-enhanced ECG-gated quiescent-interval single shot MR-Angiography (QISS-MRA) at 3T with contrast-enhanced MRA (CE-MRA) and digital subtraction angiography (DSA) serving as the standard of reference.

#### METHOD AND MATERIALS

16 consecutive patients (9 male, 7 female, mean age 70±12 years) with peripheral arterial disease stages II-IV underwent a combined peripheral MRA protocol consisting of a large field-of-view QISS-MRA (acquisition time 18 min), continuous-table-movement MRA (acquisition time 62 sec), and an additional time-resolved MRA (acquisition time 96 sec) of the calves. DSA correlation was available in 8 patients. Image quality and degree of stenosis was assessed. Sensitivity and specificity of QISS-MRA was evaluated with CE-MRA and DSA serving as the standards of reference by two readers.

#### RESULTS

328 total segments were assessed. Overall sensitivity and specificity were, respectively, 81.1% and 83.5% for QISS-MRA vs CE-MRA. Relative to DSA, sensitivity for QISS-MRA was high (100% versus 91.2% for CE-MRA) in the evaluated segments; however, specificity was substantially less than that of CE-MRA (76.5% vs 94.6%,  $p$  There was no significant difference in image quality between QISS-MRA and CE-MRA at the calf station ( $p=0.17$ ). For the vasculature of the pelvis and thigh QISS-MRA was rated significantly lower compared to

CE-MRA ( $\kappa$  interreader agreement was very good for both QISS-MRA and CE-MRA ( $\kappa=0.83$  and  $0.96$  respectively).

#### CONCLUSION

Overall image quality and specificity of QISS-MRA at 3T are diminished relative to CE-MRA, potentially due to long acquisition times. However, when image quality is adequate, the high sensitivity of QISS-MRA may render it useful as a screening examination in patients with contraindications to gadolinium chelate administration.

#### CLINICAL RELEVANCE/APPLICATION

Due to its high sensitivity at 3 Tesla, QISS might serve as screening tool to rule out significant stenoses in patients with impaired renal function.

### **VSVA61-11 • Performance of Unenhanced MRA Using Spatial Labeling with Multiple Inversion Pulses Sequence to Depict Transplant Renal Vascular Anatomy and Complications**

**Hao Tang** (Presenter) ; **Daoyu Hu** MD, PhD ; **Zi Wang**

#### PURPOSE

To prospectively evaluate the performance of a new unenhanced magnetic resonance angiography (Unenhanced MRA) sequence, spatial labeling with multiple inversion pulses (SLEEK), to depict transplant renal vascular anatomy and complications in comparison to color doppler ultrasonography (CDUS) , digital subtraction angiography (DSA) and intraoperative findings.

#### METHOD AND MATERIALS

75 patients with renal transplant were examined with Unenhanced MRA using SLEEK and CDUS. DSA was performed in 14 patients. Surgery was performed for 7 patients. The ability to present transplant renal vascular anatomy and complications with SLEEK were evaluated by two experienced radiologists, and to correlate the results with CDUS, DSA and intraoperative findings.

#### RESULTS

#### CONCLUSION

Unenhanced MRA using SLEEK is a reliable diagnostic method for depicting transplant renal vascular anatomy and complications. It is relatively inexpensive and is not associated with renal complications. It can be as a good choice for screening renal vascular anatomy and complications, especially in patients with renal insufficiency.

#### CLINICAL RELEVANCE/APPLICATION

Unenhanced MRA using SLEEK is a reliable diagnostic method for depicting transplant renal vascular anatomy and complications, especially in patients with renal insufficiency.

### **VSVA61-12 • Hemodynamic Outcome Following Aortic Root Replacement with or without Hemiarch Replacement Assessed by 4D Flow MRI**

**Edouard Semaan** (Presenter) ; **Michael Markl** PhD ; **Chris Malaisrie** \* ; **Alex Barker** ; **Bradley D Allen** MD ; **Zoran Stankovic** MD ; **Patrick McCarthy** ; **James C Carr** MD \* ; **Jeremy D Collins** MD \*

#### PURPOSE

To evaluate aortic hemodynamics using 4D flow MRI following aortic root replacement (AR) or aortic root and hemiarch replacement (AR+HA), comparing to patients following non-mechanical aortic valve replacement (AVR) alone.

#### METHOD AND MATERIALS

IRB approval was obtained. 31 patients were recruited following open AVR (group 1: AR, n=16,  $51\pm 13$  yrs; group 2: AR+HA, n=4,  $60\pm 10$  yrs; group 3: AVR alone, n=11,  $69\pm 11$  yrs). Aortic blood flow was measured using ECG and respiration synchronized 4D flow MRI (3-directional  $venc = 150\text{cm/s}$ ,  $2.0\text{-}2.8\text{mm}^3$ , temp res 40-44msec) at 1.5 or 3T (Aera, Avanto, or Skyra, Siemens, Erlangen, GE) post-contrast administration. Data analysis included 3D blood flow visualization (EnSight, CEI, USA) based on time-resolved 3D pathlines and systolic 3D streamlines. Helical flow was assessed in the Ascending aorta (AAo), arch, and descending aorta on a 3-point Likert scale (360°). 3D pathlines qualitatively identified the existence of flow jets and the quadrant of flow impingement in the proximal, mid, and distal AAo. Flow uniformity was analyzed by quadrant dichotomizing systolic peak velocities at  $1\text{m/s}$ . Peak systolic velocities and acceleration were quantified in 9 planes distributed throughout the thoracic aorta. Groups were compared using the student's t-test.

#### RESULTS

4D flow MRI revealed similar helical flow across groups ( $p>0.05$ ). 72 % (8 of 11) of patients in group 3 demonstrated outflow jets impinging on the right anterior proximal aortic wall. Jet flow was seen in 52% (10 of 20) of patients in groups 1 and 2 and was preferentially directed towards the anterior wall. Flow profiles were asymmetric in 62%, 100%, and 72% of groups 1-3, respectively. There were significant differences between groups 1 and 2 compared to group 3 for peak acceleration and significant differences between groups 1 and 3 for peak velocities (p

#### CONCLUSION

4D flow MRI characterized flow in AVR patients. Our preliminary findings demonstrate elevated peak systolic velocities and acceleration in patients with aortic grafts compared to patients with AVR alone. Follow-up studies are warranted to investigate the influence of these findings on ventricular loading and patient outcome.

#### CLINICAL RELEVANCE/APPLICATION

4D flow MRI demonstrates increased aortic peak velocities and acceleration status-post aortic replacement with graft material, suggesting increased ventricular loading with altered aortic compliance.

### **VSVA61-13 • 3D Cine PC VIPR as a Sensitive Indicator of Post-prandial Hyperemia with an Added Value of Avoiding Vortex and Helical Flow Portions**

**Masataka Sugiyama** (Presenter) ; **Yasuo Takehara** MD ; **Kevin M Johnson** \* ; **Oliver Wieben** PhD ; **Tetsuya Wakayama** PhD \* ; **Hiroyuki Kabasawa** ; **Shuhei Yamashita** MD ; **Harumi Sakahara** MD ; **Atsushi Nozaki** ; **Naoki Ooishi**

#### PURPOSE

3D cine PC with vastly undersampled isotropic projection steady-state free precession imaging (VIPR) is a recently developed MR method that can cover full spatial and temporal data of the blood flow velocity. The purpose of our study is two folds i.e., 1) to test if 3D PC VIPR can be used for dietary stress test in detecting the post-prandial hyperemia of the SMA, and 2) to assess the flow patterns within SMA with streamline analysis for finding out the optimum plane to measure correct blood flow.

#### METHOD AND MATERIALS

All studies were conducted on a 3.0T MR imager with phased array coil. Five healthy volunteers (23 to 53 y.o.) were enrolled. Under 8 hr fasting , 2D cine PC and 3D cine PC VIPR were repeated before and after the intake of 400 Kcal supplementary diet. The measuring planes for the 2D cine PC were placed at the proximal portion, mid curved portion and the distal straight portion of the main trunk of SMA. With 3D cine PC VIPR, retrospective measurements at the corresponding planes were performed and the values were compared.

#### RESULTS

#### CONCLUSION

Newly developed 3D cine PC VIPR can be used for dietary stressed SMA flow measurement with an added value of delineating the vortex and helical flow portions in the SMA where the measurement should be avoided.

#### CLINICAL RELEVANCE/APPLICATION



## VSPA61-14 • Non-contrast MRA: Phase-contrast MRA

**Scott B Reeder MD, PhD (Presenter)**

### LEARNING OBJECTIVES

1) Understand the underlying principles of phase velocity MRA. 2) Be familiar with the currently available methods for phase velocity MRA. 3) Be familiar with important applications and examples of phase velocity MRA. 4) Understand current limitations and pitfalls associated with phase velocity MRA.

## Disclosure Index

### A

**Abbara, S.** - Consultant, Perceptive Informatics, Inc Author with royalties, Reed Elsevier Author with royalties, Amirsys, Inc  
**Abujudeh, H. H.** - Research Grant, Bracco Group Consultant, RCG HealthCare Consulting  
**Agrawal, M. D.** - Advisor, Bayer AG  
**Aguirre, S.** - Founder, EchoPixel, Inc Shareholder, EchoPixel, Inc  
**Altes, T. A.** - Research Grant, Vertex Pharmaceuticals Incorporated Research Grant, Novartis AG Research support, Siemens AG  
**Altman, A.** - Employee, Koninklijke Philips Electronics NV  
**Anselmetti, G.** - Research Consultant, Medtronic, Inc  
**Antoch, G.** - Speaker, Siemens AG Speaker, Bayer AG  
**Arai, Y.** - Royalties, FUJIFILM Holdings Corporation Royalties, Sumitomo Bakelite Co, Ltd Medical Advisory Board, Otsuka Holdings Co, Ltd Medical Advisory Board, Sumitomo Bakelite Co, Ltd Medical Advisory Board, Sumitomo Bakelite Co, Ltd Research support, Otsuka Holdings Co, Ltd Research support, Nippon Kayaku Co, Ltd  
**Attenberger, U. I.** - Research Consultant, Bayer AG  
**Awai, K.** - Research Grant, Toshiba Medical Sysmtes Research Grant, Hitachi Medical Corporation Research Grant, Bayer AG Research Consultant, DAIICHI SANKYO Group Research Grant, Eisai Ltd

### B

**Bamberg, F.** - Speakers Bureau, Bayer AG Speakers Bureau, Siemens AG Research Grant, Bayer AG Research Grant, Siemens AG  
**Bankier, A. A.** - Author with royalties, Reed Elsevier Consultant, Olympus Corporation  
**Barboriak, D. P.** - Research support, Eisai Co, Ltd Advisory Board, General Electric Company  
**Barth, R. A.** - Research Consultant, General Electric Company  
**Bauer, R. W.** - Research Consultant, Siemens AG Speakers Bureau, Siemens AG  
**Beaule, P. E.** - Consultant, Wright Medical Group, Inc Consultant, Getinge AB  
**Bedi, D. G.** - Consultant, Koninklijke Philips Electronics NV  
**Bilhim, T.** - Research Consultant, Cook Group Incorporated  
**Binkert, C. A.** - Consultant, Merit Medical Systems, Inc Consultant, Johnson & Johnson  
**Bluemke, D. A.** - Research support, Siemens AG  
**Brace, C. L.** - Shareholder, NeuWave Medical Inc Consultant, NeuWave Medical Inc  
**Bresnahan, B. W.** - Stockholder, Johnson & Johnson Investigator, General Electric Company Consultant, General Electric Company Consultant, Johnson and Johnson Consultant, Novartis AG  
**Bricault, I.** - Medical Advisory Board, IMACTIS  
**Bronowicki, J.** - Research Consultant, Bayer AG Speakers Bureau, Bayer AG  
**Brook, A. L.** - Speakers Bureau, Johnson & Johnson Speakers Bureau, CareFusion Corporation  
**Brown, D. B.** - Consultant, Cook Group Incorporated Consultant, Biocompatibles International plc  
**Buls, N.** - Medical Advisory Board, General Electric Company  
**Buurman, J.** - Employee, Koninklijke Philips Electronics NV  
**Bydder, G. M.** - Research Grant, General Electric Company

### C

**Callstrom, M. R.** - Research Grant, Endocare, Inc Research Grant, Siemens AG  
**Canstein, C.** - Employee, Siemens AG  
**Carr, J. C.** - Speaker, Lantheus Medical Imaging, Inc  
**Carrascosa, P. M.** - Research Consultant, General Electric Company  
**Carrino, J. A.** - Research Grant, Siemens AG Research Grant, Carestream Health, Inc Research Consultant, General Electric Company  
**Chan, F. P.** - Research collaboration, Siemens AG Research collaboration, Echopixel, Inc  
**Chang, P. J.** - Co-founder, Stentor/Koninklijke Philips Electronics NV Technical Advisory Board, Amirsys, Inc Medical Advisory Board, Koninklijke Philips Electronics NV Medical Advisory Board, MModal Inc Medical Advisory Board, lifeIMAGE Medical Advisory Board, Merge Healthcare Incorporated  
**Chen, G.** - Research funded, General Electric Company Research funded, Siemens AG Research funded, Varian Medical Systems, Inc Research funded, Hologic, Inc  
**Chen, J. Y.** - Research Consultant, EBM Technologies, Inc  
**Chernyak, V.** - Speakers Bureau, Lantheus Medical Imaging, Inc  
**Cho, S.** - Research support, Amgen Inc Research support, Peregrine Pharmaceuticals, Inc Research support, Algeta ASA  
**Choi, B.** - Research Consultant, Samsung Electronics Co Ltd  
**Chou, C.** - Research funded, Hologic, Inc  
**Choyke, P. L.** - Researcher, Koninklijke Philips Electronics NV Researcher, General Electric Company Researcher, Siemens AG Researcher, F. Hoffmann-La Roche Ltd Researcher, iCAD, Inc  
**Chung, J.** - Grant, BTG International Ltd  
**Chung, J. H.** - Research Grant, Siemens AG  
**Cloft, H. J.** - Researcher, Johnson & Johnson  
**Cloughesy, T. F.** - Speakers Bureau, Merck & Co, Inc Consultant, F. Hoffmann-La Roche Ltd Consultant, Merck KGaA Consultant, Novartis AG Consultant, Celgene Corporation  
**Collins, B. T.** - Speakers Bureau, Accuray Incorporated  
**Collins, J. D.** - Consultant, C. R. Bard, Inc  
**Collins, J. M.** - Researcher, General Electric Company  
**Coxson, H. O.** - Research Grant, GlaxoSmithKline plc Contract, GlaxoSmithKline plc Contract, Olympus Corporation Steering Committee, GlaxoSmithKline plc  
**Czernin, J.** - Stockholder, Sofie Biosciences

### D

**Dale, B. M.** - Employee, Siemens AG  
**Darcy, M. D.** - Advisory Board Member, AngioDynamics, Inc Speakers Bureau, W. L. Gore & Associates Speaker Bureau, Argon Medical Devices, Inc Consultant, Boston Scientific Corporation  
**De Baere, T. J.** - Consultant, Terumo Corporation Speaker, Covidien AG Speaker, Terumo Corporation Speaker, General Electric Company Consultant, General Electric Company Consultant, Guerbet SA Speaker, Guerbet SA  
**De Koning, H.** - Research Grant, F. Hoffman-La Roche Ltd Equipment support, Siemens AG Medical Advisory Board, F. Hoffman-La Roche Ltd  
**De Mey, J.** - Research Grant, General Electric Company  
**Demartini, W. B.** - Research Grant, Koninklijke Philips Electronics NV Research Grant, General Electric Company

**Deshpande, V.** - Researcher, Siemens AG  
**Diekmann, F.** - Research Grant, Bayer AG Research Grant, Koninklijke Philips Electronics NV

## E

**Earls, J. P.** - Consultant, General Electric Company Speakers Bureau, General Electric Company  
**Eben, E. B.** - Support, Hologic, Inc  
**Ekseth, U.** - Support, Hologic, Inc  
**Ellingson, B. M.** - Research Consultant, MedQIA Imaging CRO Research Consultant, F. Hoffman-La Roche Ltd Research Consultant, Tocagen Inc Research Consultant, Boston Scientific Corporation Research Consultant, Amgen Inc

## F

**Fahey, M.** - Stockholder, Sigma Pharmaceuticals, LLC Advisor, Actelion Ltd  
**Fallenberg, E. M.** - Research Grant, Bayer AG Research Grant, Siemens AG Research Grant, General Electric Company Speaker, Siemens AG Speaker, General Electric Company Speaker, Bayer AG Speaker, Guerbet SA Travel support, Bayer AG  
**Faulhaber, P. F.** - Speaker, Koninklijke Philips Electronics NV Grant, Koninklijke Philips Electronics NV Medical Advisor, MIM Software, Inc  
**Fenster, A.** - License agreement, Eigen  
**Feuchtner, G.** - Advisory Board, Covidien AG Research Consultant, Medtronic, Inc  
**Finlayson, C.** - Consultant, Fixes 4 Kids Inc  
**Fischman, A. M.** - Consultant, Surefire Medical, Inc Consultant, Terumo Corporation Speakers Bureau, Koninklijke Philips Electronics NV  
**Fleischmann, D.** - Research support, Siemens AG Research support, General Electric Company  
**Fletcher, J. G.** - Grant, Siemens AG  
**Fong, Y.** - Consultant, Covidien AG Consultant, Johnson & Johnson Consultant, AngioDynamics, Inc Consultant, Perfint Healthcare Pvt. Ltd  
**Forster, B. B.** - Beneficial trust, Doyen Medical, Inc  
**Fritsch, J.** - Officer, M\*Modal Inc

## G

**Geppert, C.** - Employee, Siemens AG  
**Gervais, D. A.** - Research Grant, Covidien AG  
**Geschwind, J. H.** - Consultant, Biocompatibles International plc Consultant, Bayer AG Consultant, Guerbet SA Consultant, Nordion, Inc Grant, Biocompatibles International plc Grant, F. Hoffmann-La Roche Ltd, Inc Grant, Bayer AG Grant, Koninklijke Philips Electronics NV Grant, Nordion, Inc Grant, ContextVision AB Grant, CeloNova BioSciences, Inc Founder, PreScience Labs, LLC CEO, PreScience Labs, LLC  
**Geyer, L. L.** - Speaker, General Electric Company  
**Gilkeson, R. C.** - Research consultant, Riverain Technologies, LLC Research support, Koninklijke Philips Electronics NV  
**Gill, R. R.** - Scientific Advisory Board, F. Hoffmann-La Roche Ltd  
**Gillams, A. R.** - Speaker, Covidien AG  
**Glielmi, C.** - Employee, Siemens AG  
**Goldberg, S.** - Consultant, AngioDynamics, Inc Research support, AngioDynamics, Inc Research support, Cosman Medical, Inc Consultant, Cosman Medical, Inc  
**Goldstein, J.** - Consultant, CSL Limited  
**Goodman, M. M.** - Royalties, Nihon Medi-Physics Co, Ltd  
**Goyal, M.** - Shareholder, Calgary Scientific, Inc Research Grant, Covidien AG Consultant, Covidien AG Shareholder, NoNO Inc Investigator, Covidien AG  
**Grainger, A. J.** - Speaker, General Electric Company  
**Groves, A. M.** - Investigator, GlaxoSmithKline plc Investigator, General Electric Company Investigator, Siemens AG Advisory Board, Merck & Co, Inc  
**Guimaraes, M.** - Consultant, Cook Group Incorporated Consultant, Terumo Corporation Consultant, Bayer AG Consultant, Baylis Medical Patent holder, Cook Group Incorporated Research Grant, Terumo Corporation  
**Gullien, R.** - Support, Hologic Inc Travel support, Hologic, Inc

## H

**Haakenaasen, U.** - Support, Hologic, Inc  
**Hagemeister, N.** - Research collaboration, Emovi Inc Research collaboration, EOS imaging SA  
**Haider, M. A.** - Consultant, Bayer AG  
**Halkar, R. K.** - Research Grant, General Electric Company Research Grant, Gilead Sciences, Inc Royalties, General Electric Company  
**Halliburton, S. S.** - Research Grant, Koninklijke Philips Electronics NV Research Grant, Bayer AG  
**Halpern, E. F.** - Research Consultant, Hologic, Inc  
**Hara, A. K.** - License agreement, General Electric Company Researcher, General Electric Company  
**Haramati, L. B.** - Investor, OrthoSpace Ltd Investor, Kryon Systems Ltd Spouse, Board Member, Bio Protect Ltd Spouse, Board Member, OrthoSpace Ltd Spouse, Board Member, Kryon Systems Ltd  
**Heberlein, K.** - Employee, Siemens AG  
**Helbich, T. H.** - Research Consultant, Siemens AG Research Consultant, Hologic, Inc Research Grant, Siemens AG  
**Helvie, M. A.** - Institutional Grant, General Electric Company  
**Heverhagen, J. T.** - Speaker, Bracco Group  
**Hillen, T. J.** - Consultant, Biomedical Systems Consultant, Vidacare Corporation  
**Hinshaw, J.** - Stockholder, NeuWave Medical, Inc Medical Advisory Board, NeuWave Medical, Inc Stockholder, Novelos Therapeutics, Inc  
**Holodny, A. I.** - Member, fMRI Consultants LLC  
**Houston, G.** - Director, Vascular Flow Technologies Ltd Shareholder, Vascular Flow Technologies Ltd Grant, Guerbet SA  
**Huisman, H.** - Stockholder, QView Medical, Inc

## I

**Ichikawa, T.** - Consultant, DAIICHI SANKYO Group

## J

**Jacobson, J. A.** - Consultant, BioClinica, Inc Royalties, Reed Elsevier Equipment support, Terumo Corporation Equipment support, Arthrex, Inc  
**Jarvik, J. G.** - Stockholder, PhysioSonics, Inc Consultant, HealthHelp  
**Jebsen, I. N.** - Support, Hologic, Inc  
**Johnson, K. M.** - Research support, General Electric Company

## K

**Kalender, W. A.** - Consultant, Siemens AG Consultant, Bayer AG Founder, CT Imaging GmbH Scientific Advisor, CT Imaging GmbH CEO, CT Imaging GmbH  
**Kallmes, D. F.** - Research support, Terumo Corporation Research support, Covidien AG Research support, Sequent Medical, Inc Research support, Benvenue Medical, Inc Consultant, General Electric Company Consultant, Covidien AG Consultant, Johnson & Johnson  
**Kalra, M. K.** - Faculty, General Electric Company  
**Kalva, S. P.** - Proctor, Sirtex Medical Ltd Consultant, Celonova Biosciences Inc  
**Kamalian, S.** - Research support, General Electric Company  
**Kamel, I. R.** - Research support, Bracco Group Research support, Bayer AG  
**Kaminski, M. S.** - Consultant, GlaxoSmithKline plc Royalties, GlaxoSmithKline plc  
**Karssemeijer, N.** - Shareholder, Matakina International Limited Scientific Board, Matakina International Limited Shareholder, QView Medical, Inc Research Grant, Riverain Medical

**Kashef, E.** - Consultant, W. L. Gore & Associates, Inc  
**Kauczor, H.** - Research Grant, Boehringer Ingelheim GmbH Research Grant, Siemens AG Speakers Bureau, Boehringer Ingelheim GmbH Speakers Bureau, Bayer AG Speakers Bureau, Siemens AG  
**Kaufman, J. A.** - Consultant, Bio2 Technologies, Inc Consultant, Cook Group Incorporated Consultant, Covidien AG Consultant, W. L. Gore & Associates, Inc Consultant, Guerbet SA Stockholder, Hatch Medical LLC Stockholder, VuMedi, Inc Stockholder, Veniti, Inc Royalties, Reed Elsevier Advisory Board, Delcath Systems, Inc Researcher, W. L. Gore & Associates, Inc Researcher, Guerbet SA  
**Kerl, J.** - Research Consultant, Siemens AG Speakers Bureau, Siemens AG  
**Kessler, L. G.** - Consultant, General Electric Company  
**Khorasani, R.** - Stockholder, Medialis Corp Royalties, Medialis Corp Advisory Board, General Electric Company  
**Kim, C. Y.** - Research Grant, Bayer Inc Research Grant, Lantheus Medical Imaging, Inc Consultant, Lantheus Medical Imaging, Inc  
**Kim, D. H.** - Consultant, Viatronix, Inc Co-founder, VirtuoCTC, LLC Medical Advisory Board, Digital ArtForms, Inc  
**Kinney, T. B.** - Data Monitoring Safety Board, Crux Biomedical, Inc Data Monitoring Safety Board, Bio2 Medical  
**Klotz, E.** - Employee, Siemens AG  
**Koch, K.** - Employee, General Electric Company  
**Kohan, A.** - Research support, Koninklijke Philips Electronics NV  
**Kooijman, H.** - Employee, Koninklijke Philips Electronics NV  
**Krager, M.** - Support, Hologic, Inc  
**Krishnamurthy, R.** - Research Consultant, Eisai Co, Ltd Research support, Koninklijke Philips Electronics NV  
**Kruskal, J. B.** - Author, UpToDate, Inc  
**Kuribayashi, S.** - Research Grant, General Electric Company

## L

**Ladron De Guevara, L.** - Consultant, Bayer AG Speaker, Bayer AG  
**Lambert, M.** - Director, Vascular Flow Technologies Ltd Shareholder, Vascular Flow Technologies Ltd  
**Lammer, J.** - Scientific Advisory Board, W. L. Gore & Associates Scientific Advisory Board, Abbott Laboratories Scientific Advisory Board, Boston Scientific Corporation  
**Langlotz, C. P.** - Shareholder, Montage Healthcare Solutions, Inc Advisory Board, General Electric Company Advisory Board, Reed Elsevier Advisory Board, Activate Networks, Inc Spouse, Consultant, Amgen Inc Spouse, Consultant, Novartis AG Spouse, Consultant, Johnson & Johnson  
**Larson, A. C.** - Research Consultant, DuNing Inc Research Consultant, PhaseRx, Inc  
**Law, E.** - Speakers Bureau, Toshiba Corporation Medical Advisory Board, Bayer AG Medical Advisory Board, Bracco Group Medical Advisory Board, FUJIFILM Holdings Corporation  
**Lee, F. T. JR.** - Stockholder, NeuWave Medical, Inc Patent holder, NeuWave Medical, Inc Board of Directors, NeuWave Medical, Inc Patent holder, Covidien AG Inventor, Covidien AG Royalties, Covidien AG  
**Lee, J.** - Advisory Board, Bayer AG  
**Lee, K. S.** - Research Consultant, SuperSonic Imagine Speakers Bureau, Medical Technology Management Institute  
**Lee, Y. Z.** - Research Grant, Carestream Health, Inc  
**Lehman, C. D.** - Consultant, Bayer AG Consultant, General Electric Company Research Grant, General Electric Company  
**Leiner, T.** - Speakers Bureau, Koninklijke Philips Electronics NV Consultant, Bayer AG Research Grant, Bracco Group  
**Leipsic, J. A.** - Speakers Bureau, General Electric Company Speakers Bureau, Edwards Lifesciences Corporation Medical Advisory Board, General Electric Company Medical Advisory Board, Edwards Lifesciences Corporation Research Grant, Heartflow, Inc  
**Lell, M. M.** - Research Grant, Siemens AG Speakers Bureau, Siemens AG Research Grant, Bayer AG Speakers Bureau, Bayer AG Research Consultant, Bracco Group  
**Lev, M. H.** - Consultant, General Electric Company Consultant, Takeda Pharmaceutical Company Limited Research support, General Electric Company Stockholder, General Electric Company  
**Levin, D. C.** - Consultant, HealthHelp Board of Directors, Outpatient Imaging Affiliates, LLC  
**Lewandowski, R. J.** - Scientific Advisory Board, Surefire Medical, Inc Consultant, PhaseRx, Inc Advisory Board, Nordion, Inc Advisory Board, Boston Scientific Corporation  
**Lewin, J. M.** - Medical Advisory Board, Koninklijke Philips Electronics NV Scientific Advisory Board, Hologic Inc Research Grant, Hologic Inc  
**Link, T. M.** - Research Grant, General Electric Company Research Grant, InSightec Ltd  
**Littrup, P. J.** - Founder, CryoMedix, LLC Research Grant, Galil Medical Ltd Research Grant, Endo Health Solutions Inc Officer, Delphinus Medical Technologies, Inc  
**Loewe, C.** - Speaker, Bracco Group Speaker, Guerbet SA Speaker, General Electric Company Speaker, Covidien AG Speaker, Bayer AG  
**Lombardi, M.** - Research Grant, Novartis AG Research Grant, Chiesi Farmaceutici SpA Research Grant, Apotex, Inc  
**Lubner, M. G.** - Grant funding, GE-AUR Radiology Research Academic Fellowship  
**Lynch, D. A.** - Research support, Siemens AG Scientific Advisor, Perceptive Informatics, Inc Consultant, Actelion Ltd Consultant, InterMune, Inc Consultant, Gilead Sciences, Inc Consultant, F. Hoffmann-La Roche Ltd

## M

**Machan, L. S.** - Medical Advisory Board, Boston Scientific Corporation Steering Committee, Cook Group Incorporated Medical Advisory Board, Calgary Scientific, Inc Medical Advisory Board, Ultrasonix Inc Medical Advisory Board, Endologix, Inc Consultant, Ikon Medical Inc. Stockholder, Nitinol Devices and Components, Inc  
**Macmahon, H.** - Shareholder, Hologic, Inc Consultant, Riverain Technologies, LLC Royalties, UCTech  
**Macura, K. J.** - Research Grant, Siemens AG  
**Maisel, J.** - Chairman, Zydoc.com Shareholder, Zydoc.com  
**Malaisrie, C.** - Consultant, Edwards Lifesciences Corporation Research Grant, Medtronic, Inc  
**Manduca, A.** - Royalties, General Electric Company  
**Mann, R. M.** - Speakers Bureau, Bayer AG  
**Margolis, D. J.** - Research Grant, Siemens AG  
**Marks, L. S.** - Speaker, Avero Diagnostics Investigator, Watson Pharmaceuticals, Inc Investigator, Indevus Pharmaceuticals Inc Investigator, Light Sciences Corporation Investigator, Hologic, Inc Investigator, Beckman Coulter, Inc Investigator, GlaxoSmithKline plc Investigator, Allergan, Inc Investigator, GTX, Inc Advisor, Indevus Pharmaceuticals Inc Advisor, Hologic, Inc Advisor, GlaxoSmithKline plc Advisor, GTX, Inc  
**Marrero, J.** - Consultant, Bayer AG Consultant, Onyx Pharmaceuticals, Inc Speaker, Bayer AG Research funded, Bayer AG  
**Martincich, L.** - Speaker, Bracco Group Consultant, Bayer AG Speaker, ABC Medical Imaging  
**Matthew, S.** - Research funded, Guerbet SA  
**Mayo, J. R.** - Speaker, Siemens AG  
**Mayo-Smith, W. W.** - Royalties, Reed Elsevier Royalties, Cambridge University Press  
**McCollough, C. H.** - Research Grant, Siemens AG  
**McConathy, J. E.** - Research Consultant, GLG Consulting Speakers Bureau, Eli Lilly and Company Research Consultant, General Electric Company  
**Megibow, A. J.** - Consultant, Bracco Group  
**Michaely, H. J.** - Speakers Bureau, Siemens AG Speakers Bureau, Bayer AG Speakers Bureau, Guerbet SA  
**Middleton, M. S.** - Research Consultant, Siemens AG Research Grant, General Electric Company Stockholder, General Electric Company Research Grant, Bayer AG Research Consultant, Merck & Co, Inc Contract, Gilead Sciences, Inc Contract, sanofi-aventis Group Contract, Isis Pharmaceuticals, Inc  
**Min, J.** - Medical Advisory Board, General Electric Company Research support, General Electric Company Speakers Bureau, General Electric Company Medical Advisory Board, Arineta Ltd Research support, Koninklijke Philips Electronics NV Research support, Toshiba Corporation Medical Advisory Board, AstraZeneca PLC Medical Advisory Board, Bristol-Myers Squibb Company Consultant, HeartFlow, Inc Stockholder, TC3 Health, Inc Stockholder, MDDX Medical Solutions  
**Min, J. K.** - Speakers Bureau, General Electric Company Advisory Board, General Electric Company Stockholder, General Electric Company  
**Minn, H. R.** - Support, Bayer AG  
**Moore, W. H.** - Research Grant, EDDA Technology, Inc Medical Board, EDDA Technology, Inc Research Grant, Galil Medical Ltd Research Grant, Endo Health Solutions Inc  
**Morgan, D. E.** - Research support, Bracco Group Research Support, Koninklijke Philips Electronics NV  
**Morgan, R. A.** - Consultant, Cook Group Incorporated Consultant, AngioDynamics, Inc Proctor, Covidien AG  
**Morrison, W. B.** - Consultant, General Electric Company Consultant, AprioMed AB Patent agreement, AprioMed AB  
**Mueller, P. R.** - Consultant, Cook Group Incorporated  
**Muthupillai, R.** - Research support, Koninklijke Philips Electronics NV

## N

**Nakajima, K.** - Stockholder, Bayer AG Employee, Bayer AG  
**Narayanan, G.** - Consultant, Biocompatibles International plc Consultant, AngioDynamics, Inc Consultant, Boston Scientific Corporation  
**Nelson, R. C.** - Consultant, General Electric Company Research support, Nemoto Kyorindo Co, Ltd Research support, Bracco Group Research support, Becton, Dickinson and Company Speakers Bureau, Siemens AG Royalties, Lippincott, Williams & Wilkins  
**Nemcek, A. A. JR** - Consultant, B. Braun Melsungen AG

## O

**Ohno, Y.** - Research Grant, Toshiba Coporation Research Grant, Koninklijke Philips Electronics NV Research Grant, Bayer AG Research Grant, DAIICHI SANKYO Group Research Grant, Eisai Co, Ltd Research Grant, Terumo Corporation Research Grant, Covidien AG Research Grant, FUJIFILM Holdings Corporation  
**Omary, R. A.** - Founder, IORAD LLC

## P

**Padhani, A. R.** - Consultant, IXICO Limited Advisory Board, Acutus Medical Ltd Advisory board, Siemens AG  
**Papandreou, C.** - Consultant, Bayer AG  
**Partovi, S.** - Research Grant, Koninklijke Philips Electronics NV  
**Partridge, S. C.** - Research Grant, Koninklijke Philips Electronics NV  
**Pednekar, A.** - Employee, Koninklijke Philips Electronics NV  
**Petscavage-Thomas, J. M.** - Consultant, Medical Metrics, Inc  
**Pfirrmann, C. W.** - Advisory Board, Siemens AG Scientific Consultant, Medtronic, Inc  
**Pickhardt, P. J.** - Research Consultant, Bracco Group Research Consultant, Check-Cap Ltd Co-founder, VirtuoCTC, LLC  
**Podberesky, D. J.** - Author, Amirsys, Inc Speakers Bureau, Toshiba Corporation Travel support, General Electric Company Travel support, Koninklijke Philips Electronics NV  
**Pomerantz, S. R.** - Research Grant, General Electric Company  
**Pope, W. B.** - Research Consultant, F. Hoffmann-La Roche Ltd Research Consultant, Amgen Inc Research Consultant, Tocagen Inc

## R

**Rafferty, E. A.** - Research Grant, Hologic, Inc  
**Raja, A.** - Medical Advisor, Diagnostion, LLC  
**Rajan, D. K.** - Consultant, TVA Medical, Inc  
**Ray, C. E. JR** - Therasphere Advisory Board, Nordion, Inc  
**Remy-Jardin, M. J.** - Research Grant, Siemens AG  
**Rio Tinto, H. A.** - Speaker, Cook Group Incorporated Consultant, Cook Group Incorporated  
**Robbin, M. L.** - Consultant, Koninklijke Philips Electronics NV Investigator, Bracco Group  
**Romman, Z.** - Employee, Koninklijke Philips Electronics NV  
**Ros, P. R.** - Radiology Advisory Committee, Koninklijke Philips Electronics NV Institutional research collaboration, Siemens AG Institutional research collaboration, Koninklijke Philips Electronics NV Institutional research collaboration, Toshiba Corporation Institutional research collaboration, Sectra AB  
**Rubbert, C.** - Fellowship funded, Koninklijke Philips Electronics NV  
**Ruehm, S. G.** - Research Grant, Siemens AG  
**Rybicki, F. J. III** - Research Grant, Toshiba Corporation Research Grant, Bracco Group

## S

**Safriel, Y.** - Principal, PharmaScan Clinical Trials  
**Salem, R.** - Consultant, Bayer AG Consultant, Nordion, Inc Consultant, BioSphere Medical, Inc Advisory Board, Sirtex Medical Ltd Consultant, Merit Medical Systems, Inc  
**Sardanelli, F.** - Speakers Bureau, Bracco Group Research Grant, Bracco Group Speakers Bureau, Bayer AG Research Grant, Bayer AG Research Grant, IMS International Medical Scientific  
**Satchithananda, K.** - Committee member, Johnson & Johnson  
**Schoenherg, S. O.** - Institutional research agreement, Siemens AG  
**Schoepf, U.** - Research Grant, Bracco Group Research Grant, General Electric Company Research Consultant, Siemens AG Research Grant, Siemens AG  
**Schultz, K.** - Employee, Toshiba Corporation  
**Schweiger, B.** - Speaker, Guerbet SA  
**Seethamraju, R. T.** - Employee, Siemens AG Stockholder, Siemens AG  
**Seri, I.** - Grant, Covidien AG  
**Sevenster, M.** - Employee, Koninklijke Philips Electronics NV  
**Shepard, J. O.** - Consultant, Agfa-Gevaert Group  
**Shih, G. L.** - Consultant, Image Safely, Inc Stockholder, Image Safely, Inc Consultant, Vitesso, LLC Stockholder, Vitesso, LLC Consultant, Angular Health, Inc Stockholder, Angular Health, Inc Consultant, Merge Healthcare Incorporated  
**Siegel, E. L.** - Research Grant, General Electric Company Speakers Bureau, Siemens AG Board of Directors, Carestream Health, Inc Research Grant, XYBIX Systems, Inc Research Grant, Steelcase, Inc Research Grant, Anthro Corp Research Grant, RedRick Technologies Inc Research Grant, Evolved Technologies Corporation Research Grant, Barco nv Research Grant, Intel Corporation Research Grant, Dell Inc Research Grant, Herman Miller, Inc Research Grant, Virtual Radiology Research Grant, Anatomical Travelogue, Inc Medical Advisory Board, Fovia, Inc Medical Advisory Board, Vital Images Medical Advisory Board, McKesson Corporation Medical Advisory Board, Carestream Health, Inc Medical Advisory Board, Bayer AG Research, TeraRecon, Inc Medical Advisory Board, Bracco Group Researcher, Bracco Group Medical Advisory Board, Merge Healthcare Incorporated Medical Advisory Board, Microsoft Corporation Researcher, Microsoft Corporation  
**Silverman, S. G.** - Author, Lippincott Williams & Wilkins  
**Skaane, P.** - Equipment support, Hologic, Inc Support, Hologic, Inc  
**Solomon, S. B.** - Research Grant, General Electric Company Research Grant, AngioDynamics, Inc Consultant, Johnson & Johnson Consultant, Covidien AG Director, Devicor Medical Products, Inc Director, Aspire Bariatrics, Inc  
**Sosna, J.** - Consultant, ActiViews Ltd Research Grant, Koninklijke Philips Electronics NV  
**Spottiswoode, B.** - Employee, Siemens AG  
**Stavropoulos, S.** - Advisory Board, Teleflex Incorporated Research, W. L. Gore & Associates, Inc Research, B. Braun Melsungen AG Research, C. R. Bard, Inc  
**Stavros, A.** - Advisor, Devicor Medical Products, Inc Advisor, General Electric Company Advisor, SonoCine, Inc Owner, Ikonopedia, LLC Medical Director, Seno Medical Instruments, Inc  
**Steigner, M. L.** - Speaker, Toshiba Corporation  
**Sumkin, J. H.** - Scientific Advisory Board, Hologic, Inc

## T

**Takahashi, N.** - Research Grant, Siemens AG  
**Taneja, S. S.** - Consultant, Eigen Consultant, GTX, Inc Consultant, Bayer AG Consultant, Healthtronics, Inc Speaker, Johnson & Johnson Investigator, STEBA Biotech Royalties, Reed Elsevier  
**Tanenbaum, L. N.** - Speakers Bureau, General Electric Company Speakers Bureau, Bracco Group Speakers Bureau, Vital Images, Inc Speakers Bureau, Bayer AG  
**Thomas, G.** - Consultant, Acorda Therapeutics, Inc Consultant, Bayer AG Consultant, Biogen Idec Inc Consultant, sanofi-aventis Group Consultant, Novartis AG Consultant, Merck KGaA Consultant, Pfizer Inc Consultant, Teva Pharmaceutical Industries Ltd Speaker, Acorda Therapeutics, Inc Speaker, Bayer AG Speaker, Biogen Idec Inc Speaker, sanofi-aventis Group Speaker, Novartis AG Speaker, Merck KGaA Speaker, Pfizer Inc Speaker, Teva Pharmaceutical Industries Ltd  
**Togashi, K.** - Research Grant, Bayer AG Research Grant, DAIICHI SANKYO Group Research Grant, Eisai Co, Ltd Research Grant, FUJIFILM Holdings Corporation Research Grant, Nihon Medi-Physics Co, Ltd Research Grant, Shimadzu Corporation Research Grant, Toshiba Corporation Research Grant, Covidien AG  
**Topalian, S.** - Consultant, Bristol-Myers Squibb Company Research Grant, Bristol-Myers Squibb Company  
**Trerotola, S. O.** - Royalties, Cook Group Incorporated Consultant, Medical Components, Inc Consultant, C. R. Bard, Inc Consultant, Teleflex Incorporated Consultant, W. L. Gore & Associates, Inc Consultant, B. Braun Melsungen AG Consultant, Medical Components, Inc Royalties, Teleflex Incorporated Research Grant, Vascular Pathways, Inc  
**Turk, A. S. III** - Scientific Advisory Board, Nfocus Consulting Inc Scientific Advisory Board, Pulsar Vascular, Inc Consultant, Stryker Corporation Consultant, Nfocus Consulting Inc Consultant, Pulsar Vascular, Inc Consultant, Johnson & Johnson Consultant, Penumbra, Inc Researcher, MindFrame, Inc Researcher, Pulsar Vascular,

**U**

**Umutlu, L.** - Consultant, Bayer AG

**V**

**Van Ha, T. G.** - Investigator, C. R. Bard, Inc

**Van Herwerden, L.** - Research Consultant, St. Jude Medical, Inc

**Van Holsbeeck, M. T.** - Consultant, General Electric Company Consultant, Koninklijke Philips Electronics NV Stockholder, Koninklijke Philips Electronics NV

Stockholder, General Electric Company Grant, Reed Elsevier Grant, Siemens AG

**van Rensburg, L. J.** - Speaker, Mallinckrodt plc

**Vasanawala, S. S.** - Research collaboration, General Electric Company Stockholder, Morpheus Medical, Inc

**Veltri, A.** - Speakers Bureau, Eli Lilly and Company Speakers Bureau, Bayer AG

**Venook, A. P.** - Researcher, Bayer AG Researcher, Onyx Pharmaceuticals, Inc

**Vercher-Conejero, J. L.** - Research Grant, Koninklijke Philips Electronics NV

**Viergever, M. A.** - Research Grant, Koninklijke Philips Electronics NV Research Grant, Pie Medical Imaging BV

**Vlahos, I.** - Consultant, Siemens AG Consultant, General Electric Company

**Von Falck, C.** - Grant, Siemens AG Grant, Pro Medicus Limited

**Von Tengg-Kobligk, H.** - Research Grant, W. L. Gore & Associates, Inc

**W**

**Wacker, F. K.** - Research Grant, Siemens AG Research Grant, Pro Medicus Limited

**Wahl, R. L.** - Patents, Naviscan, Inc Patents, GlaxoSmithKline plc Patents, Spectrum Pharmaceuticals, Inc Research Consultant, GlaxoSmithKline plc Research Consultant, Nihon Medi-Physics Co, Ltd Research support, General Electric Company Research support, Molecular Insight Pharmaceuticals, Inc Research support, Cell Point LLC

**Wakayama, T.** - Employee, General Electric Company

**Wang, D.** - Employee, Siemens AG

**Webb, J.** - Consultant, Edwards Lifesciences Corporation

**Weber, M.** - Research Grant, Bayer AG Research Grant, Guerbet SA Research Grant, Bracco Group Research Grant, Siemens AG

**Wen, P. Y.** - Research Consultant, F. Hoffmann-La Roche Ltd

**Werner, J.** - Grant, AngioDynamics, Inc

**Wessell, D. E.** - Research Consultant, Biomedical Systems

**West, O.** - Speaker, Siemens AG Travel support, Siemens AG

**Whelehan, P.** - Consultant, General Electric Company

**White, L. M.** - Advisory Board, Siemens AG

**Willey, B. J.** - Consultant, NeuWave Medical Inc

**Winalski, C. S.** - Institutional research contract, Smith & Nephew plc Contract, Smith & Nephew plc Contract, Johnson & Johnson Contract, sanofi-aventis Group Contract, Bioclinica, Inc Contrast, Axio Research Research Grant, The Procter & Gamble Company Shareholder, NitroSci Pharmaceuticals, LLC Shareholder, Pfizer Inc Shareholder, General Electric Company

**Wintermark, M.** - Research Grant, General Electric Company Research Grant, Koninklijke Philips Electronics NV

**Wirth, S.** - Speaker, General Electric Company

**Wong, T. Z.** - Advisory Board, Eli Lilly and Company Consultant, Bayer AG

**Wood, B. J.** - Grant, Koninklijke Philips Electronics NV Grant, Celsion Corporation Grant, Biocompatibles International plc Grant, W. L. Gore & Associates, Inc

**Wood, D.** - Consultant, Edwards Lifesciences Corporation Consultant, St. Jude Medical, Inc

**Y**

**Yamashita, Y.** - Consultant, DAIICHI SANKYO Group

**Yeh, B. M.** - Research Grant, General Electric Company Consultant, General Electric Company

**Young, G. S.** - Consultant, Pioneer Diagnostics & Research Corporation Stockholder, Pioneer Diagnostics & Research Corporation Consultant, Thimble Inc Stockholder, Thimble Inc Researcher, Amgen Inc Researcher, AstraZeneca PLC Researcher, Bracco Group Researcher, Celldex Therapeutics, Inc Researcher, F. Hoffmann-La Roche Ltd Researcher, GlaxoSmithKline plc Researcher, Novartis AG Researcher, Siemens AG Research support, Siemens AG Research support, Toshiba Corporation

**Z**

**Zaharchuk, G.** - Research Grant, General Electric Company

**Zalis, M. E.** - Co-founder, QPID Inc Stockholder, QPID Inc

**Zulliger, M. A.** - Former Employee, SCANCO Medical AG